



**WORLD METEOROLOGICAL ORGANIZATION**  
**COMMISSION FOR INSTRUMENTS AND METHODS OF OBSERVATION**

---

INSTRUMENTS AND OBSERVING METHODS – REPORT No. 82 – WMO/TD-No. 1265

PART I - PAPERS

PART II - POSTERS

WMO Technical Conference on Meteorological and Environmental  
Instruments and Methods of Observation

(TECO-2005)

Bucharest, Romania, 4-7 May 2005

CONFERENCE THEME

*The Role of Instruments in the Earth Observation Systems*

---

## **World Meteorological Organization**

### **NOTE**

The designations employed and the presentation of material in this publication do not imply the expression of any opinion whatsoever on the part of the Secretariat of the World Meteorological Organization concerning the legal status of any country, territory, city or area, or of its authorities, or concerning the delimitation of its frontiers or boundaries.

This report has been produced without editorial revision by the WMO Secretariat. It is not an official WMO publication and its distribution in this form does not imply endorsement by the Organization of the ideas expressed.

**INSTRUMENTS AND OBSERVING METHODS — REPORT No. 82**

**WMO/TD-No. 1265**

**TABLE OF CONTENTS**

PART I - PAPERS

PART II - POSTERS

**PART II - POSTERS**

**SESSION 1 - NEW DEVELOPMENTS AND OPERATIONAL EXPERIENCE WITH  
SURFACE OBSERVATION TECHNOLOGY**

***Session 1 - Poster Presentations:***

- P1(1) Meteorological monitoring system for NPP-Kozloduy  
*by Branzov, H. (Bulgaria)*
- P1(2) Research on Lightning warning with SAFIR lightning observation and meteorological detection data in Beijing-Hebei areas  
*by Meng, Q. (China), et al.*
- P1(3) Observations of stormy zone hourly study in Kinshasa *(not available)*  
*by Tagisabo, A. (Dem. Rep. of Congo), et al.*
- P1(4) New developments and operational experience with surface observation technology  
*by Refaie, E. (Egypt)*
- P1(5) Next generation all weather precipitation gauge  
*by Räisänen, E. (Finland), et al.*
- P1(6) Météo France Network Supervision *(not available)*  
*by Vogt, V. (France).*
- P1(7) The new synoptic-climatological station AMDA in the DWD primary network  
*by Klapheck, K. (Germany), et al.*
- P1(8) Visibility measurement technique and its application in aviation services at international airports in India  
*by Mali, R. (India), et al.*
- P1(9) Present status of surface meteorological measurements in India  
*by Vashistha, R. (India), et al.*
- P1(10) Modernization of radiation network  
*by Vashistha, R. (India), et al.*
- P1(11) Rain intensity gauge with no moving parts  
*by Yassky, D. (Israel), et al.*

- P1(12) Chemical analysis of meteoric wet atmospheric deposition. Comparison between daily and weekly precipitation samples  
*by Casu, G. (Italy), et al.*
- P1(13) Automatic cloud-coverage evaluation by a ground-based Total-Sky Camera  
*by Rafanelli, C. (Italy), et al.*
- P1(14) Surface energy balance investigations using scintillation measurements  
*by Sciortino, M. (Italy), et al.*
- P1(15) A method to estimate sunshine duration from global irradiance measurements  
*(not available)*  
*by Benschop, H. (Netherlands)*
- P1(16) Cost effective 1-minute network data collection: A new paradigm  
*by Hartley, B. (New Zealand)*
- P1(17) Cost efficient data transport with GSM from weather stations in Norway  
*by van Nes, A. (Norway)*
- P1(18) Surface meteorological measurements and meteorological services in Pakistan  
*by Mir, H. (Pakistan), et al.*
- P1(19) Technical and operational aspects of setting-up an AWS network in Romania  
*(not available)*  
*by Lucaschi, B. (Romania), et al.*
- P1(20) The low cost radio frequency rain meter  
*by Koldaev, A. (Russian Federation), et al.*
- P1(21) The new capillary surface microlayer sampler for monitoring of the transboundary source of coastal ecosystems' pollution *(not available)*  
*by Syroeskhin, A. (Russian Federation), et al.*
- P1(22) Design and development of a low cost and reliable automatic weather station.  
*by Kumarasinghe, E. (Sri Lanka)*
- P1(23) The flood forecasting and precipitation measurement by using radar system  
*by Eroglu, H. (Turkey)*
- P1(24) The man-made satellite; an instrument of opportunity  
*by Mudenda, O. (Zambia), et al.*
- P1(25) A comparison of Beaufort, Vaisala and radiosonde wind measuring systems in the course of migration  
*by Ngenda, Ch. (Zambia)*
- P1(26) Mass and energy fluxes monitoring using eddy covariance techniques  
By Mendicino, G. (Italy), et al.
- P1(27) TOA - Advanced Lightning Positioning System (ALPS)  
*by Geitz, W. (USA)*
- P1(28) The ozone influence risk assessment on population health: Optical instrument of ozone concentration measurement

by Naumenko, T. (Belarus), et al.

- P1(29) OTT Parsivel® - Enhanced precipitation identifier and new generation of present weather sensor by OTT Messtechnik, Germany  
by Nemeth, K. (Germany), et al.

## **SESSION 2 - NEW DEVELOPMENTS AND OPERATIONAL EXPERIENCE WITH UPPER-AIR OBSERVATION TECHNOLOGY**

### **Session 2 - Poster Presentations:**

- P2(1) Some results from atmospheric sounding in cases with foehn in Sofia valley  
by Videnov, P.(Bulgaria), et al.
- P2(2) Applying working knowledge for well managing the upper air stations network in order to preserve its historical achievements and work on continuing its development and prosperity  
by Amer, M.(Egypt)
- P2(3) A round the clock observation technology to measure vertical profiles of visibility and spectral transmission in the mixing layer  
by Weller, M.(Germany), et al.
- P2(4) Radiosounding: Impact on aerological measurements due to instrumentation transition (*not available*)  
by Casu, G.(Italy), et al.
- P2(5) Use of doppler radar in Romania for nowcasting and warning  
by Stan-Sion, A.(Romania), et al.
- P2(6) Time-lag correction of operational RS80-A radiosonde humidity  
by Kats, A.(Russian Federation), et al.
- P2(7) The impact of new RF95 radiosonde introduction on upper-air data quality in the North-West region of Russia  
by Kats, A.(Russian Federation), et al.
- P2(8) The field and laboratory intercomparison test between two different types of the sondes and the ground systems  
by Borštnik, A.(Slovenia), et al.
- P2(9) On board processing capability for radiosonde platforms using low-cost processors mixed signal ICs and semi-conductor sensors  
by Kumarasinghe, N.(Sri Lanka)
- P2(10) Upper air observations in Turkey  
by Erdem, M.(Turkey), et al.
- P2(11) Observing fog and low cloud with a combination of 78 GHz cloud radar and laser ceilometer  
by Nash, J.(UK, et al.)

- P2(12) Demonstration of the new InterMet radiosondes system installed at the Tanzania Meteorological Agency, Dar es Salaam  
*by Smout, R.(UK), et al.*
- P2(13) Maturation and application of operational doppler lidar for meteorological applications  
*by Hannon, S.(USA), et al.*
- P2(14) Recent application of the accurate temperature measuring radiosonde  
*by Schmidlin, F.(USA).*
- P2(15) Improved forecast skill with ground-based radiometric profiling (*not available*)  
*by Ware, R.(USA), et al.*
- P2(16) InterMet 403 MHz radiosonde system  
*by Wierenga, R.(USA), et al.*
- P2(17) Quantitative assessment of improved spectral moments selection algorithms on an operational 64 MHz clear-air doppler wind profiler (*not available*)  
*by Winston, H.(USA), et al.*
- P2(18) Polarization diversity for the National Weather Service, WSR-88D radars  
*by Zrnica, D.(USA)*
- P2(19) Radar technique for the study of structure and dynamics of the hail-storm process  
*by Imamdjanov, K.(Uzbekistan)*
- P2(20) Radar techniques of meteorological events detection by polarization characteristics of signal  
*by Imamdjanov, K.(Uzbekistan), et al.*
- P2(21) Development of a mean intensity radiometer for GRAW radiosondes  
*By Schmidmer, F. (Germany)*

### **SESSION 3 - QUALITY MANAGEMENT, CALIBRATION, TESTING AND COMPARISON OF INSTRUMENTS AND OBSERVING SYSTEMS**

#### **Session 3 - Poster Presentations**

- P3(1) Intercomparison of ground-based water vapour radiometer measurements and radiosonde measurements with the integrated water vapour from numerical models (*not available*)  
*by Vukovic, Z. (Canada)*
- P3(2) The experiment and analysis on available data rate of wind profiler radar  
*by He, P. (China), et al.*
- P3(3) Performance evaluation for net pyrradiometers  
*by Lu, W. (China), et al.*
- P3(4) Some step of quality control of upper-air network data in China  
*by Zhao, Z. (China), et al.*
- P3(5) The in Situ Pressure Calibration System in Météo-France  
*by Duvernoy, J. (France), et al.*

- P3(6) ISO 9001 Quality Certification in the Area of Surface Observing Systems  
*(not available)*  
by Leroy, M. (France)
- P3(7) Uncertainties of Measurements in Météo France's Monitoring of the Chemical Composition of Precipitation  
by Mezdour, A. (France), et al.
- P3(8) A Quality Control Program for Radiation Data *(not available)*  
by Behrens, K. (Germany), et al.
- P3(9) Measuring air temperature by using an ultrasonic anemometer  
by Lanzinger, E. (Germany), et al.
- P3(10) Automatic technical self check system for the DWD weather radar network  
by Mammen, T. (Germany), et al.
- P3(11) Fast-response, open path optical hygrometer for long-term measurements - experiences, results, future requirements  
by Weisensee, U. (Germany), et al.
- P3(12) Quality management and quality control of the long-term observing system "ZUZI" a provider of the WMO World Data Centre for Aerosols (WDCA)  
by Weller, M. (Germany), et al.
- P3(13) Temperature measurement *(not available)*  
by Traore, F. (Guinea)
- P3(14) Intensity of precipitation and comparison among different measuring instruments  
by Casu, G. (Italy), et al.
- P3(15) Influence of rain gauge calibration on data series at Re. S.M.A. station in Vigna di Valle (Italy)  
by Lanza, L. (Italy), et al.
- P3(16) Dealing with uncertainty in rainfall gauges calibration: The QM-RIM metrological validation  
by Molini, A. (Italy), et al.
- P3(17) The new automatic weather system  
by Zahari, A. (Malaysia)
- P3(18) Quality and representativity of wind measurements  
by Benschop, H. (Netherlands)
- P3(19) A test of the precipitation amount and intensity measurements with the OTT Pluvio  
by Wauben, W. (Netherlands)
- P3(20) Wind tunnel and field test of three 2D sonic anemometers  
by Wauben, W. (Netherlands)
- P3(21) Testing of wind sensors and the usefulness of video technology at marine stations  
by Larre, M. (Norway)

- P3(22) Comparison of manual precipitation observations with automatic observations in Oslo and Utsira  
*by Mathisen, T. (Norway), et al.*
- P3(23) Variation in precipitation measurement through different instrumentation  
*(not available)*  
*by Awan, S. (Pakistan)*
- P3(24) Preliminary results obtained following the intercomparison of the meteorological parameters provided by automatic and classical stations in Romania  
*by Baciu, M. (Romania), et al.*
- P3(25) Review of the Dobson 121 spectrophotometer accuracy as a result of the international intercomparison sessions  
*by Manea, L. (Romania), et al.*
- P3(26) The meteorological data quality management of Romanian national surface observation network  
*by Ralita, I. (Romania), et al.*
- P3(27) Advanced atmospheric boundary layer temperature profiling with MTP-5HE microwave system.  
*by Kadygrov, E. (Russian Federation), et al.*
- P3(28) The operational web-based presentation of the Russian Federation upper-air network performance monitoring  
*by Kats, A. (Russian Federation), et al.*
- P3(29) Intercomparison measurements of recording precipitation gauges in Slovakia  
*by Chvila, B. (Slovakia), et al.*
- P3(30) Calibration of relative humidity measuring instruments at EARS  
*by Groselj, D. (Slovenia), et al.*
- P3(31) Accredited calibration laboratory service as a subject of an integral QA system at EARS  
*by Groselj, D. (Slovenia), et al.*
- P3(32) The effect of the relative humidity on sunshine duration measurements during the last eclipse in Turkey *(not available)*  
*by Aksoy, B. (Turkey)*
- P3(33) Data quality management  
*by Karatas, S. (Turkey), et al.*
- P3(34) Detection of Zdr abnormalities on operational polarimetric radar in Turkish weather radar network  
*by Sireci, O. (Turkey), et al.*
- P3(35) The United States National Weather Service in-situ radiation temperature correction for radiosonde replacement system GPS radiosondes  
*by Bower, C. (USA)*
- P3(36) Wind tunnel tests of some low-cost sonic anemometers  
*by Sturgeon, B. (USA)*



**SESSION 4 - TECHNOLOGY TRANSFER, CAPACITY BUILDING, TRAINING AND DEVELOPMENT OF RICs**

***Session 4 - Poster Presentations:***

- P4(1) Technology, training, development, testing and calibration at the ReSMA  
*by Casu, G. (Italy), et al.*
- P4(2) Modernization of Observation Network in Turkey  
*by Büyükbas, E. (Turkey), et al.*
- P4(3) U.S. support for the global climate observing system (GCOS) and associated support for international, regional, and bi-lateral GCOS activities  
*by Diamond, H. (USA)*
- P4(4) Revitalization of the GCOS surface and upper-air network stations  
*by Thigpen, R. (USA)*
-

## PART II - POSTERS

## SESSION 1

### NEW DEVELOPMENTS AND OPERATIONAL EXPERIENCE WITH SURFACE OBSERVATION TECHNOLOGY

Session 1

POSTERS

# Meteorological monitoring system for NPP “Kozloduy”

**Hristomir Branzov**

**National Institute of Meteorology and Hydrology  
66 Tzarigradsko schaussee, Sofia 1784 , Bulgaria  
Tel. (+359 2) 975 35 91, E-mail: Hristomir.Branzov@meteo.bg**

## **Abstract**

This work presents the features of the system providing meteorological monitoring of the Bulgarian NPP “Kozloduy”. It discusses the choice of representative for the particular region sites for location of meteorological stations, characteristics of measurement and telecommunication means, structure and operative algorithms of the system as a whole and use of diffusion atmospheric models. Spatial variation of wind characteristics over the Kozloduy region is demonstrated, showing the necessity to preprocess meteorological data when using Gaussian diffusion model.

## **1. Introduction**

Yet in normal operation Nuclear Power Plants (NPP) release differing by kind and composition pollutants which, although in quantities considerably lower than the maximum admissible concentration (MAC), should be monitored. In case of accident the amount of released radionuclides could considerably exceed MAC. Measuring only radioactive substances’ concentration and deposition at certain points of the region merely gives a snapshot of the situation. It couldn’t give any suggestion for pollution spatial characteristics, not to mention its time variations. It is because there is no information about the condition of the environment in which pollution takes place – Earth atmosphere. Such approach doesn’t yield good results in obtaining realistic assessment of NPP impact on the environment. For these considerations, International Atomic Energy Agency (IAEA) imposed the requirement for obligatory equipment of NPP with meteorological monitoring systems. Nowadays these are automated systems for meteorological monitoring (ASMM), operating on-line. Such ASMM shall provide the measurement of the basic metrological parameters, pollution fields modeling, assessment of concentrations and depositions of pollutants of different kind, and forecasting of their time and spatial variation. Here the ASMM of operating NPP “Kozloduy” will be described. The system is designed by the National Institute of Hydrology and Meteorology with the Bulgarian Academy of Sciences and produced by the Consortium “MS&E” – Bulgaria. ASMM meets the Safety Standards Series requirements of International Atomic Energy Agency (IAEA) and those of the national Nuclear Regulatory Agency..

## **2. Automated meteorological monitoring system for NPP Kozloduy.**

ASMM for NPP Kozloduy meets all requirements of the existing national and international regulations, that is:

- ◆ provides, in normal operation and in accident, real-time weather data, for:
  - wind speed and direction at 10 m height, averaged for 10 min period;
  - precipitation intensity and amount;
  - variance of wind direction;
  - Pasquill stability categories;
  - air temperature and relative humidity;
  - atmospheric pressure.
- ◆ provides, in case of accident in NPP Kozloduy, real-time data for:
  - atmospheric mixing layer height over the station area;
  - main flow velocity and direction.

- ◆ archives and stores on technical carrier whole meteorological information for NPP Kozloduy site for the entire period of its operation;
- ◆ has reliably verified numerical dispersion model for calculation of diffusion in the atmosphere of radioactive substances, concentrations, depositions, and doses in NPP zones of responsibility;
- ◆ ASMM is protected, maintained and serviced, and calibrated within the regulated terms; it provides at least 90% of annual data.

### **2.1. Accounting for terrain influence when determining the number and location of measuring devices**

ASMM for NPP Kozloduy is designed in 1992 and implemented in 1995. The choice of the number and location of measuring instruments takes into account terrain features, the requirements of reliable digital information transfer via VHF radio channel and existing infrastructure. Three automated meteorological stations *MS&E-3RD* (AMS) are located at three sites, typical for the area:

- ◆ AMS1 is located on the plateau south of NPP Kozloduy, elevated +90 m compared to NPP site. This place is typical for the greater part of the area around NPP Kozloduy;
- ◆ AMS2 is located in the low part, close to the Danube river and is 15 m lower of the NPP site. This AMS is representative of the wind in case of calm weather over the region, as it registers the channel effect of the big river;
- ◆ AMS3 is situated in the area where rivers Skat and Ogosta flow into the Danube and is elevated by +20 m over the NOO site. This AMS registers the effect of the two deep river beds on the wind..

This siting of AMS allows correct wind field retrieval over the whole monitored area, on data from the three local measurements. Besides the standard meteorological variables - air temperature, relative humidity, wind velocity and direction, precipitation amount and intensity, AMS *MS&E-3RD* determine also Pasquill stability category, using the method of horizontal wind direction variance.

Automated system for aerological sounding (ASAS) is used to obtain necessary data for main flow direction and speed and mixing layer height. ASAS is situated to the west of NPP Kozloduy, accounting for the prevailing flow in the region. Digital DFM-98 radiosondes with GPS positioning and GK90C ground station are employed. A model is integrated to ASAS for automated determination of main flow speed and direction and mixing layer height according to the obtained air temperature, relative humidity, and wind vertical profiles. ASAS is integrated informationally in ASMM and its data are automatically included into the common radio exchange. Location of measuring instruments is shown in Fig. 1.

### **2.2. Choice of appropriate dispersion model**

Major requirements to dispersion models for assessment of radioactive substance transport in the atmosphere are formulated in IAEA normative documents and WMO regulations concerning meteorological aspects at normal run of the NPP and at emergency state. The are:

- ◆ To allow assessment of the short-term (a few hours) normalized concentrations and depositions, as well as the probability of occurrence of high values and pollution levels;
- ◆ To allow assessment of long-term (a year or more) summary (time integrated) normalized concentrations and depositions;
- ◆ To account for the change of source effective height due to the difference between the temperature of released gases or aerosols and environmental air, as well as the flow variation due to the presence of obstacles like buildings and other structures;

When describing released radionuclides, besides transport and diffusion processes, have to account for the following accompanying ones:

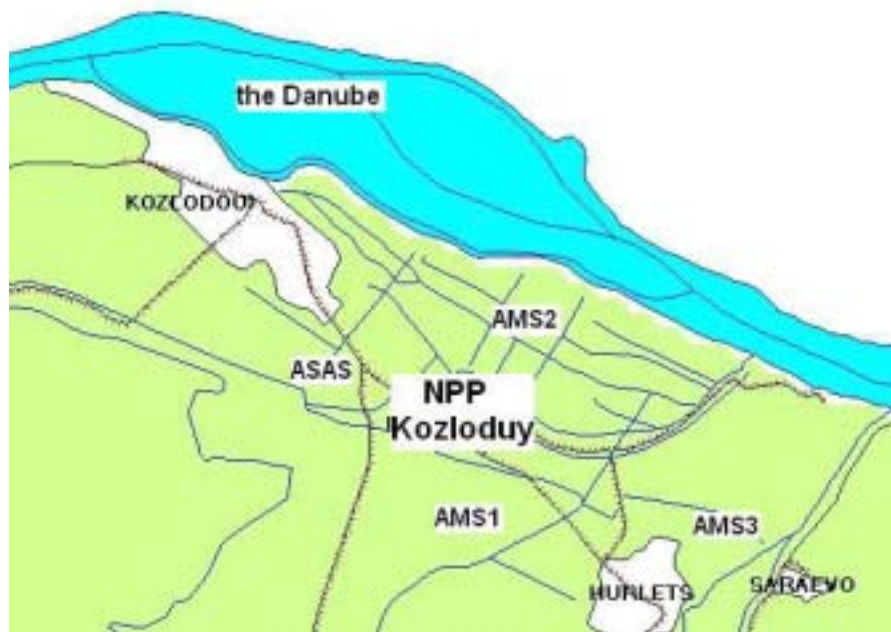


Figure 1. Location of measuring instruments of ASMM – NPP Kozloduy

- Radioactive decay and daughter products;
- Wet deposition:
  - In-cloud rain or snow;
  - Aerosol wash-out by the sub-cloud precipitation;
  - Aerosol capture in fog;
- Dry deposition;
  - aerosol deposition or gravitational precipitation (of particles with dimension greater than 10  $\mu\text{m}$ );
  - Capture of aerosols and adsorption of gases in the presence of obstacles to the wind;
  - Formation of aerosols;
  - Accounting for resuspension by the Earth surface.
- ◆ The used mathematical models for the atmosphere dispersion shall be selected in compliance with the requirements of the study purposes, hopefully taking into account also the peculiarities of the source location.

It is important to know the limitations of the corresponding model, as in different applications depending on the task and the results looked for, the appropriate model could be selected. E.g., actually the most used models for assessment of the dose load to distances up to 10 km from the source, are Gaussian models. In some specific situations, e.g. complex orography, littoral zones and large rivers, very high chimneys, accounting for mesoscale transformations, etc., Gaussian models are not suitable. Then the more complex Eulerian and Lagrangian models are used.

ASMM of Kozloduy NPP still uses the numerical realization of a classical Gaussian for the dose load assessment.

In 2005 integration of a version of EMAP model (Eulerian Model for Air Pollution) / Syrakov (2002)/ is to be integrated. This is an Eulerian dispersion 3-D model for assessment of radionuclide concentration and deposition in the NPP Kozloduy, in normal and in possible accident state. The model uses Cartesian coordinate system with uniform discretization along the horizontal axis and non-uniform one along the vertical one. Horizontal coordinate surfaces which follow the terrain shape are denser near the Earth surface and become rarer with height, which corresponds to

the characteristic profiles of meteorological elements in the atmospheric boundary layer – rapid changes at the ground and more smooth in height.

Diffusion schemes in EMAP are different. An explicit “open boundary” scheme is applied along the horizontal axis. Along the vertical one an implicit scheme with open upper boundary is used. The reason to apply implicit scheme is the non-uniformity of the network along the vertical. At the lower boundary a Neuman boundary condition is set, reflecting the process of dry deposition of pollutants when interacting with the Earth’s surface. The wet deposition in EMAP is taken into account by a formula, similar to this for radioactive decay. Instead of half-life period (more precisely its reciprocal value) the exponent uses a coefficient consisting of the product of the rain intensity and the so called “wash-out” coefficient, dependent on the type of pollutant and the type of precipitation intensity as well..

The version used in ASMM of NPP Kozloduy differs from Syrakov D. (1997) by the addition of pre-processing for the wind and precipitation and obtaining assessments of doze loads as output. EMAP is verified in the framework of the ETEX experiment and in two intercallibrations carried out by the Meteorological Synthesizing Centre-East of EMEP in 1997 и 2000.

### 2.3. Functional scheme of ASMM in NPP Kozloduy

The means for ground meteorological measurements AMS1, AMS2 and AMS3 operate on-line and are connected in a common network.. ASAS operates only in accident state. The overall management of the measurement of vertical profiles of meteorological elements, archiving of row data and automatic running of the meteorological models for determination of mixing layer height and the velocity and direction of the main flow is performed by the ASAS computer. On turning on ASAS is automatically recognized and integrated into ASAS.

The principal meteorological computer is situated in the environment control center, It is provided with special software for management of operating mode of the devices for measurement, control and diagnostics of the ASMM operation, controlling of telecommunications, data visualization and archiving. Meteorological models for preprocessing of meteorological elements are also installed on this computer. The specialized software should automate to the highest degree all processes of data acquisition, screening, processing and submission of results, as the NPP operating staff usually possesses basic training in meteorology. Therefore, all necessary knowledge should be algorithmized and set up in this specialized software. .

Wind preprocessing is required because diffusion models operate with generalized wind data at the emission point. In case of a complex relief like at NPP Kozloduy, wind parameters at the site area often are different. Figures 2, 3 and 4 show the wind rose for speed (in m/s) for the three AMS on 23.11.2003.

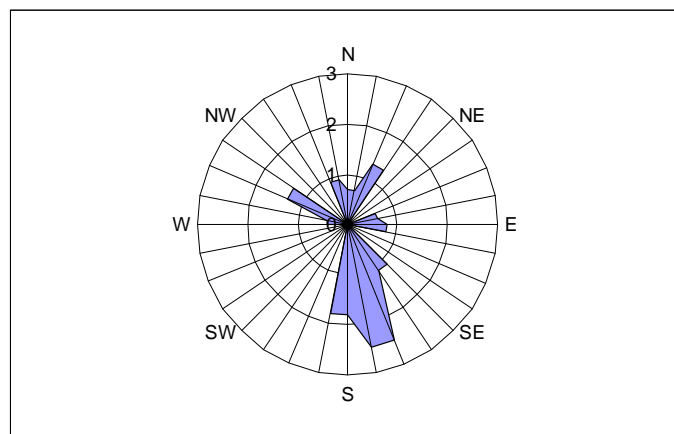


Fig.2 Wind rose plot for speed on 23.11.2003 at AMS1.



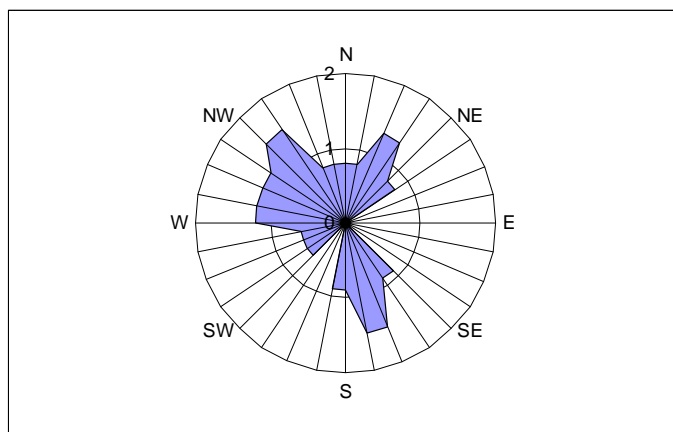


Fig.3 Wind rose plot for speed on 23.11.2003 at AMS2.

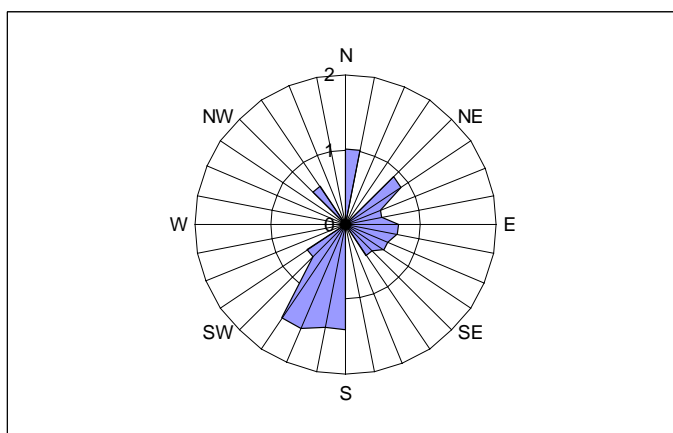


Fig.4 Wind rose plot for speed on 23.11.2003 at AMS3.

Differences in wind characteristics in the three measuring sites are a function, simultaneously depending on wind velocity and its direction. The preprocessing is based on empirical statistical model which transforms wind data from the three points into a generalized for the region value, used by diffusion models.

The situation concerning precipitation is analogous. Here main spatial differences are related to the precipitation type – continuous or shower and thus basic predictors in the statistical model are precipitation intensity and the spatial differences of its amount.

Additionally a second meteorological computer is installed in the Accident Control Centre taking control of ASMM in case of accident. Connection between ASMM measuring devices and the main meteorological computer is via UHF channel, and between the two meteorological computers at NPP Kozloduy – via internal network.

General functional scheme of ASMM – NPP Kozloduy is shown in Fig. 5.

**ASMM  
NPP "Kozloduy"**

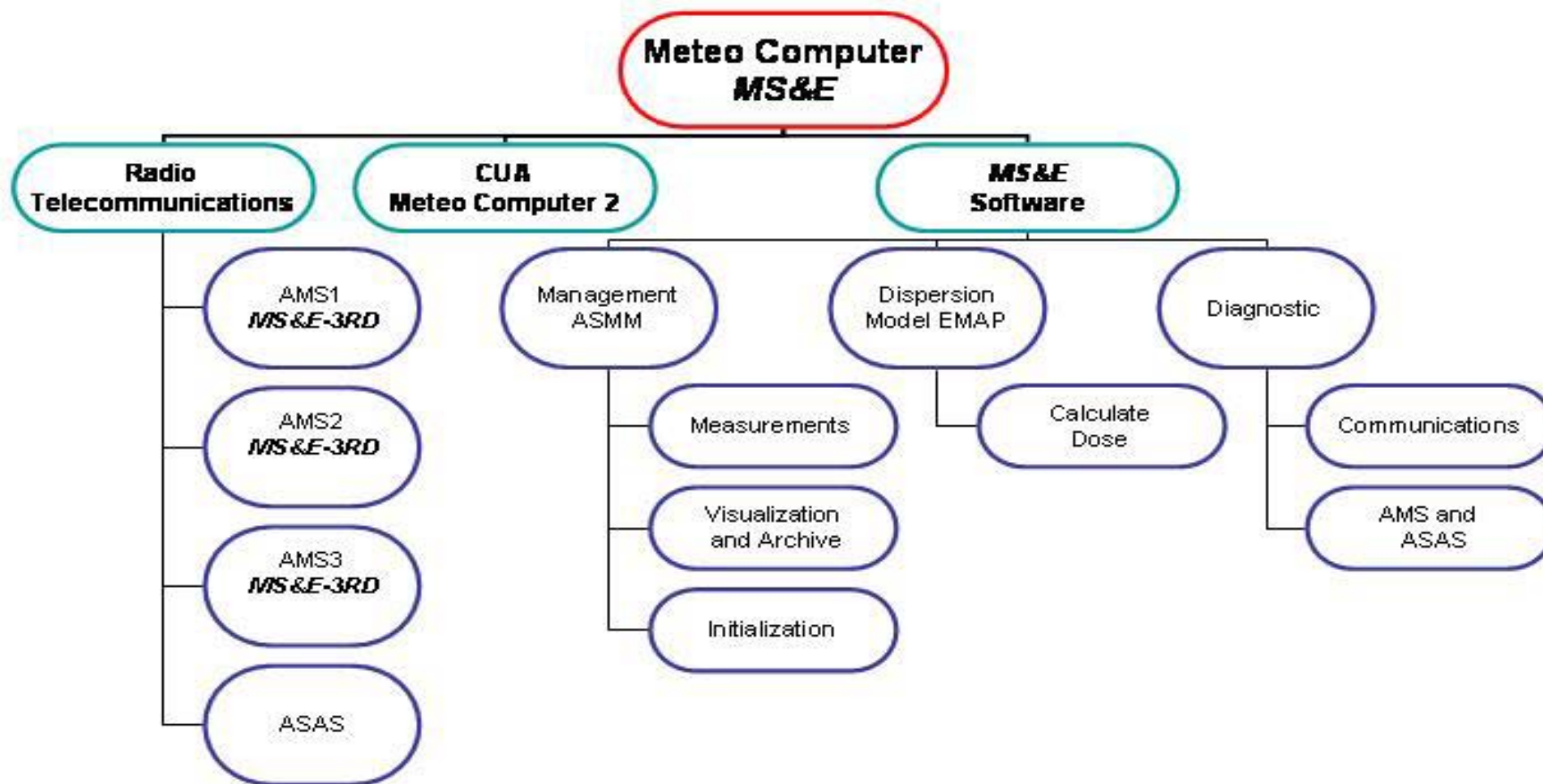


Figure 5. Functional scheme of ASMM in NPP Kozloduy

## Conclusion

Many-sided aspects of a well-run up-to-date NPP meteorological monitoring system are shown. The need for a preliminary micrometeorological study is indicated, aimed at determining the smallest number of measurement means and their installation at proper sites in the monitored region, so that to retrieve with maximum reliability the fields of the meteorological elements. Selection of appropriate means of measurement and their management and information integration. Selection of appropriate dispersion model adequate to the conditions in the monitored region and development of empirical meteorological models for wind and precipitation data preprocessing. Creation of appropriate communication environment, adequate to NPP operation in normal and in accident state. Development of applied meteorological software, automating to the highest degree the entire process of acquisition, processing and visualization of meteorological information, in order that operating personnel could take the necessary decision.

All this is demonstrated on a particular automated meteorological monitoring system –of the Bulgarian NPP “Kozloduy”, and shows the complexity of the meteorological task to design and develop such a system

## References

- Syrakov D. and m Prodanova, (1997) Bulgarian Long-range Transport Models - Simulation of ETEX First Release. In *Proc. of ETEX Symposium on Long-range Atmospheric Transport, Model. Verification and Emergency Response, 13-16 May 1997, Vienna (Austria)*, ed. K. Nodop, pp. 141-144, Office for Official Publications of the European Communities, Luxembourg, ISBN 92-828-0669-3.
- Syrakov D., m Prodanova, (2002): A system for interpretation and short range forecast of the radioactive background in North-West Bulgaria (RINFOR), *NATO Advanced Workshop “Air Pollution Processes in Regional Scale”, 13-15 June 2002, Kallithea, Greece*, (ще бъде публикуван от Kluwer Publissers)

# Research on Lightning Warning with SAFIR Lightning Observation and Meteorological detection Data in Beijing-Hebei Areas

Meng Qing<sup>1</sup> Zhang Yijun<sup>1</sup> Yao Wen<sup>1</sup> Zhu Xiaoyan<sup>1</sup> He Ping<sup>1</sup> Lv Weitao<sup>1</sup>

Ding Haifang<sup>2</sup> Xu XiaoFeng<sup>2</sup>

1.Chinese Academy of Meteorological Sciences

2.China Meteorological Administration

46 Zhongguancun Nandajie, Beijing, 100081, P.R. China

Direct: 86 10 68408146

Fax: 86 10 68408941

E\_mail:mengqing@cams.cma.gov.cn

## ABSTRACT

A field experiment with SAFIR system during summer seasons in 2003-2004 is organized by China Meteorological Administration. Meanwhile we will put up the research on method of lightning warning for severe weather through lightning observation with SAFIR system.

The correlation coefficient with time sequence of radar echo data, the distribution map of lightning discharges and the typical lightning characteristics have been analyzed based on the data detected by SAFIR 3000 system, the pattern of meteorological radar echo, and other parameter changes in meteorological detection data from a few strong thunderstorm. The results indicate that good correlation between radar echo data and SAFIR 3000 location distribution, SAFIR 3000 system own the capability of lightning warning with the moving trace of thunderstorm cell and detection three dimension distribution of lightning discharge. It is also shown that SAFIR 3000 location data is important parameters of lightning warning and study on the method of severe weather forecasting, lightning protection and weather modification etc.

**Keywords:** Lightning warning, SAFIR3000, Radar echo

### 1. Introduction

In order to meet the need of the development for automatization of atmospheric detection and sensing, standardize the establishment of operational National Lightning Detection Network (NLDN) and expand its applications on disastrous weather forecasting, lightning protection and weather modification etc., China Meteorological Administration (CMA) organize the field experiment with SAFIR 3000 lightning detection system in different experimental areas in China.

The field experiment with SAFIR system formally started from June 23, 2003 to Oct 1, 2004 in Beijing-Hebei areas. The localization principles of SAFIR network are based on the VHF interferometric technique<sup>[1]-[2]</sup>. The Long rang localization of all lightning discharges (CG and CC lightning flashes) is obtained by triangulation performed on GPS time synchronized direction of arrival provided by interferometric sensor of two different detection station in a SAFIR network. In Beijing-Hebei area spot, three interferometric antennas were installed at Huairou in Beijing suburb , Fengrun and Yongqing in Hebei area via survey and selection.

The strong convection, precipitation and lightning activities are often produced in thunderstorms. A lot of significant research results on the relationship among them have been revealed with the applications of lightning location system. There are a significant relationship between severe weathers such as hail, heavy precipitation and tornado, which often occur in supercell thunderstorms, and temporal and spatial characteristics of lightning discharges<sup>[3-4]</sup>.

In this paper, the observed data of strong thunderstorms are analyzed and typical lightning characteristics at beginning, mature and dissipation stage of thunderstorm and the relationship between lightning and convection are discussed.

## **2. Observation and analysis**

Figure1 shows the operational coverage of SAFIR 3000. Three sites places respectively situate at Huairou, Fengrun, and Yongring Meteorological station. The city zone of Beijing almost nears the center of detection areas.

Nowadays the SAFIR network have operated and observed several thunderstorms in the filed experiment. More than 200 days lightning location data, echo pattern data of Doppler weather radar and the normal meteorological detection data in 2003-2004 summer season are obtained.

Figure2 shown an example of severe weather passed over the edge Beijing region on June 23,2004. From Figure2(a) and (b), it is seen that Beijing-HeibeI areas are located in the trough region. There are two Radar echo which had strongest intensity echo of more than 45dBz during 07:41-08:23, the northwest one moved down to south and the southwest one moved up to north. From Figure2(c) and (d), it is also noticed that lightning discharges location record are associated with storms distribution along southwest-northwest frontal disturbance which the two independency cells moved separately toward north and south with time. Figure2(e) and (f) shown the general trend in variation of lightning flashes rate with the peak of flashes rate of about 30/min during 08:00 to 09:00 (UTC). Compared with Figure2(a)-(f), activity of lightning sources is associated with the radar echo on temporal and spatial characteristics in strong

storm updraft region. According the meteorological observation, it appeared hailstone caused by the northwest echo which created strong echo center with 90 km<sup>2</sup> areas at YanQing in north of Beijing. At the meanwhile, there are a lot intro-cloud lightning discharges location detection by SAFIR 3000 at YanQing (figure2(d)). After 08:40(UTC), intro-cloud lightning discharges decreased dissipation stage of thunderstorm. These lightning discharge sources are a good indicator for variation of strong convection at the beginning, mature and dissipation stage of thunderstorm.

Figure 3 shows another example of location which were recorded on September 23, 2003. SAFIR 3000 system may gave us warning of thunderstorm activity almost 30 minutes advance. Figure 3(a) and (b) shows Lightning warning of moving trace of thunderstorm cell for 10 minutes and 30 minutes advance at 22:59. It clearly indicates SAFIR 3000 may provide the information of lightning warning on the spatial and temporal development of thunderstorm.

Figure 3(c) and (d) shows the comparison between lightning discharges and radar echo. The thunderstorm had a band echo that started to develop in the southwest and moved to the northeast of the observation area from 20:00(UTC) to 0:30(UTC) on September 24, 2003, lasting for about 5 hours. The storm produced more than 8,000 lightning radiation events for 4hours. It was seen the lightning data (pink dots) superimposition on a radar echo map at 21:56 and 23:38 (UTC) on September 23<sup>th</sup>. To get each superimposition map, Radar echo is overlapped with lightning data by forward 10 minute of time radar observation. From Figure3(c) and (d), it can be observed that there are several storm cells in the band echo, which had strongest intensity echo over 45dBz. Compare with (a)-(b) and (c)-(d), it is believed that the echo may corresponded lightning data during respective time period and SAFIR network may be meet the basic needs of lightning monitor and warning in Beijing region.

The figure3(e) and (f) shows this thunderstorm with lightning discharges locations on temporal and spatial characteristics from 21:00 (UTC) to 23:59. In figure3(f), lightning discharges lightning location are presented by different colors to shows the movement of lightning activity on a 3D distribution map. From figure3(f), it was seen that lightning radiation sources started(blue), at about 21:30(UTC), moving to northeastward, distributed vertically at two altitude of 5-10km and 10-15km. Comparing Figure3(e) and (f), at maturity period, the height of lightning discharges became more and more low with the development of storm. At last some lightning radiation events distributed vertically under 5km. The figure2(f) also present most of lightning radiation sources appeared at 9-10km. The movement of storm shows variation of structure on electric charge and lightning characteristics.

### **3.Lightning Warning**

Through compare and analysis of the distribution map of lightning discharges detected by SAFIR, the pattern of meteorological radar echo, and the parameter changes in meteorological detection data from thunderstorm, we find the important parameters of lightning warning and study on the method of model and arithmetic for lightning warning.

Figure4 shows the method and steps of lightning warning. The process of lightning warning consist 3 steps, which represented by the red circle .

Setp1: Data collection and analysis. This part is the base of lightning warning, it includes new data detection, as electric field on the ground <sup>[5]</sup>, sounding, satellite and other lightning location data and the data analysis for the use of research on lightning warning, as draw lightning characteristic, calculation the statistic data etc.

Setp2: Lightning warning methods. This key part includes getting the characteristic synthesize diagnosis arithmetic through parameter recovering base on the numerical forecasting analysis products, in order to get the lightning warning product.

Step3: Data display interface. This last step is necessary for user. The software may own two basic functions. One is for represent the lightning warning product, as the moving trace, occurring probability and danger scale of lightning activity. Another is the tool for meteorological detection data analysis on lightning data application. All warning and display product will be sent to any user terminal.

#### **4.Discussions and Conclusion**

Based on the observation data analyzed above, we may get the relation between thunderstorm and lightning radiation:

- (1) SAFIR 3000 system can locate the lightning discharge including CG and IC lightning which distribute on 3-dimensional in high temporal and spatial resolution for thunderstorms and provide lightning warning of moving trace of thunderstorm cell almost 30 minutes advance.
- (2) With comparison of relationship between radar echo and variation of lightning characteristics during summer 2003-2004 in Beijing-Hebei, The lightning radiation sources normally appeared at 9-10km and its vertical altitude normally changes from 10-15km to less 5km with the development of thunderstorms, typical lightning characteristics in the characteristics of lightning were associated with the charges structure in thunderstorm. Lightning discharge sources are a good indicator for variation of strong convection.
- (3) Further study of lightning warning has been improvement in Project on lightning detection, warning and forecasting for Beijing 2008's Olympic Games base on the other new data detection and SAFIR

3000 undergoing performance evaluation <sup>[6]- [7]</sup> at Beijing--Hebei in 2005 summer season.

The lightning parameter is one of important factors in warning and forecasting severe weathers. Especially, the results are of general significance and can be referred in morning and forecasting severe weathers. However, further researches and observations are needed.

### **Acknowledgment**

Vaisala Company and Beijing Meteorological Bureau were gracious to supply us with many data observation. This work was supported by Ministry of Science and Technology of the People's Republic of China under contract 2003BA904B10.

### **References**

- [1] Richard P, 1985: "*Auffray G VHF-UHF interferometric measurements, applications to lightning discharge mapping*", Radio Science, 20(2),171~192.
- [2]Richard P, Delannoy A, Labaune G, et al., 1986: "*Results of spatial and temporal characterization of the VHF-UHF radiation of lightning*", J Geophys. Res.91(D1),91(D1),1248~1260.
- [3]MacGorman, D. R., Rust, W. D., 1998,:*The electrical nature of storms*, New York: Oxford University Press, 49-75.
- [4] Zhang, Y., Krehbiel, P. R., Liu, X., 2002: "*Polarity inverted intracloud discharges and electric charge structure of thunderstorm, Chinese Science Bulletin*", Vol.47, No.20,1725-1729.
- [5] Jacobson, E. A., and E. P. Krider, 1976:" *Electrostatic field changes produced by Florida lightning.*" J. Atmos. Sci., 33,103-117.
- [6] Z-I Kawasaki,K.Yamamoto,K.Matsuura, et al., 1994: "*SAFIR operation and evaluation of it's performance*", Geophysical Research Letters , 21(12), 21(12),1133-1136.
- [7] Vladislav Mazur, Earle Williams, Robert Boldi, et al., 1997: "*Initial comparison of lightning mapping with operational Time-Of-Arrival and Interferometric systems*", J Geophys. Res. 102(D10),11071~11085.



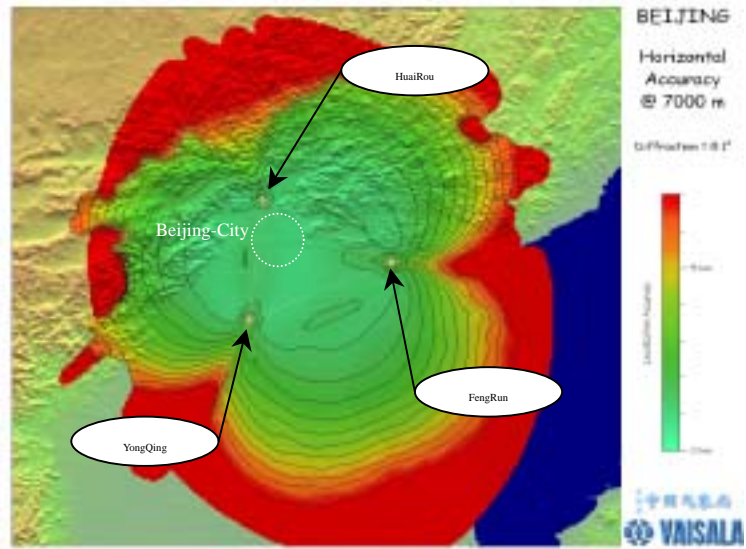


Figure 1:Operational coverage of SAFIR system in Beijing

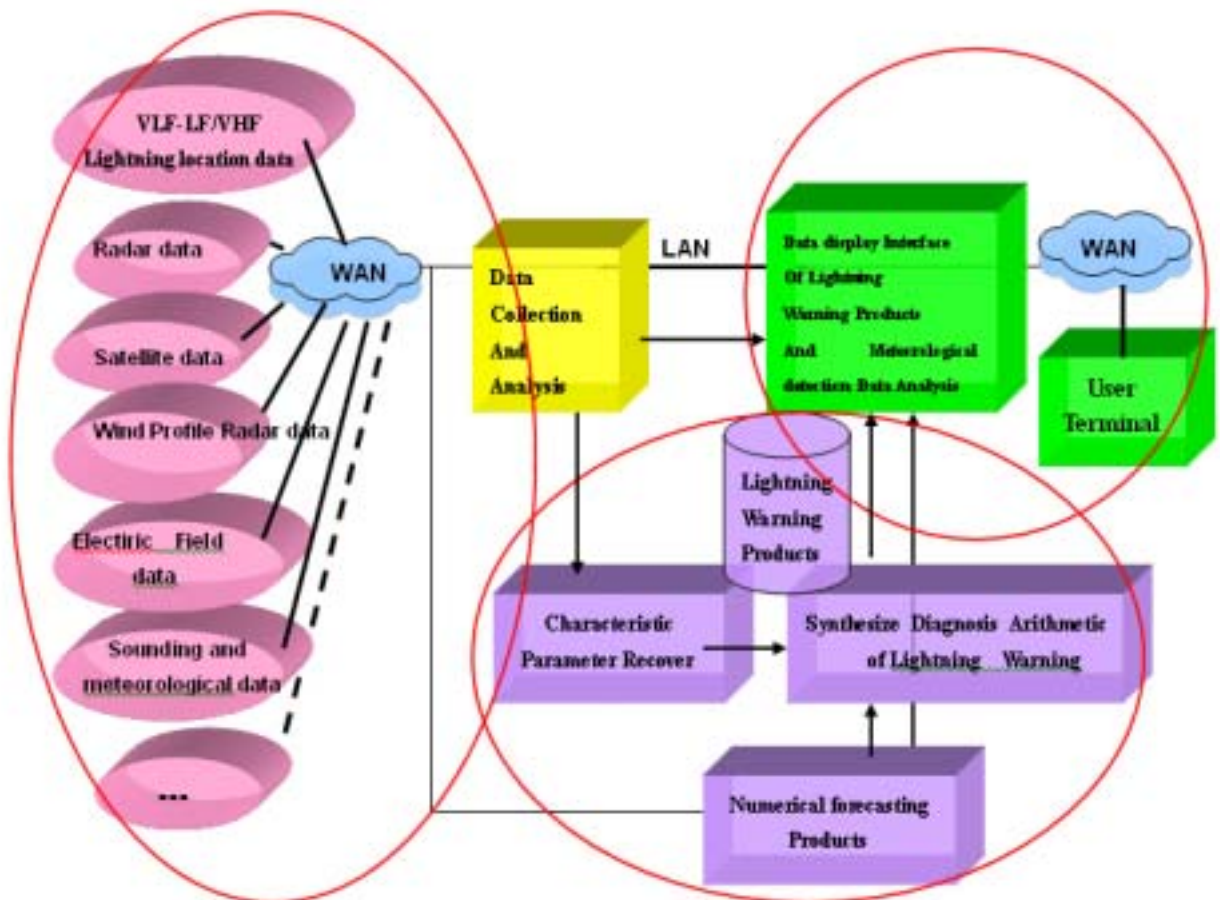
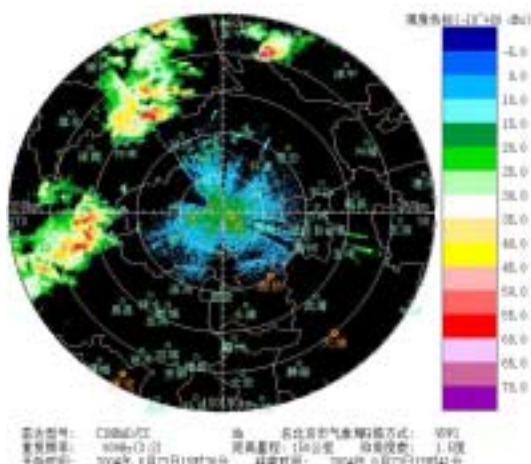
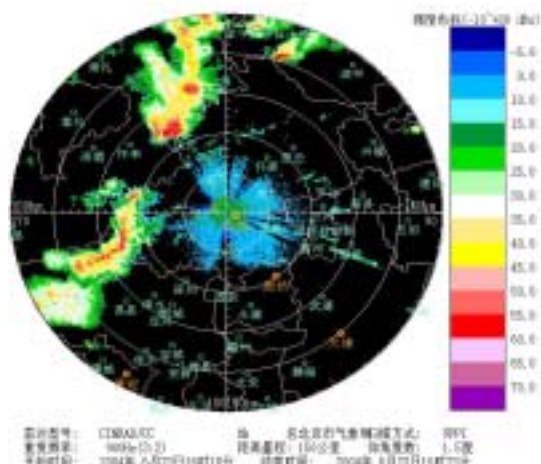


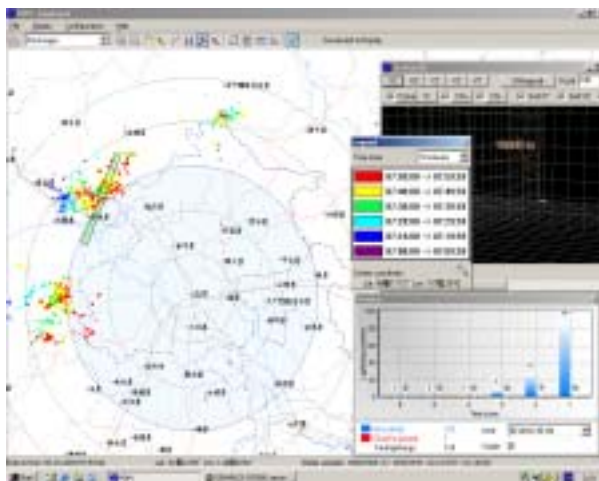
Fig4. Sketch map of lightning warning method and steps



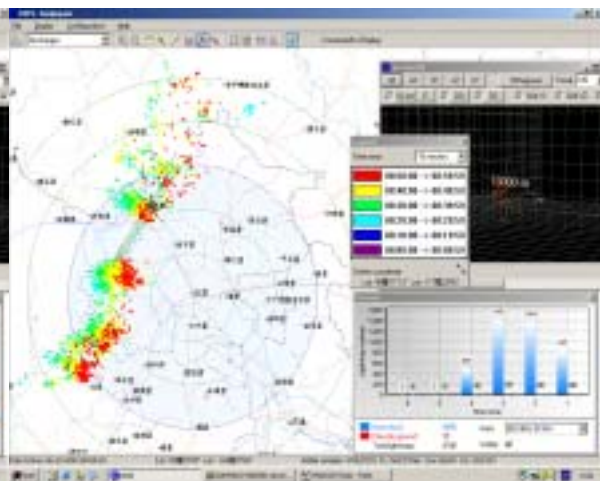
(a) Radar data at 07:41(UTC)



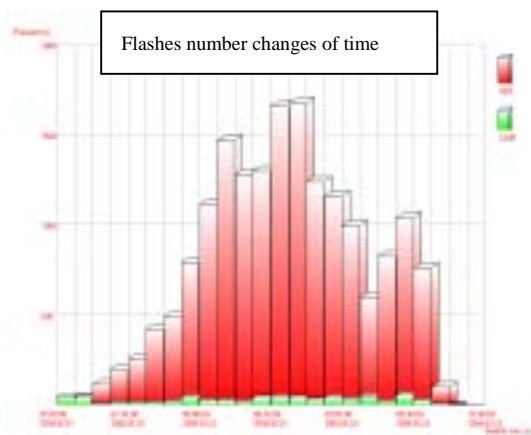
(b) Radar data at 08:23(UTC)



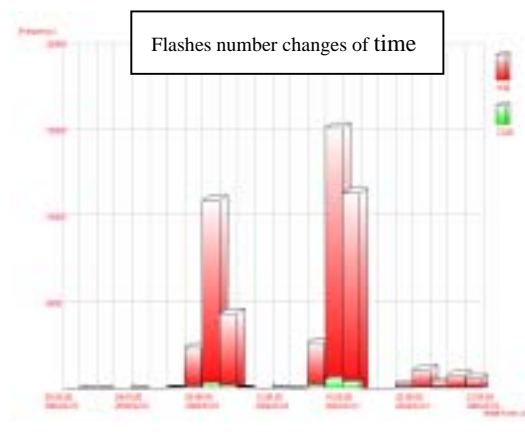
(c) Lightning discharge data at 07:00-08:00(UTC)



(d) Lightning discharge data at 08:00-09:00(UTC)

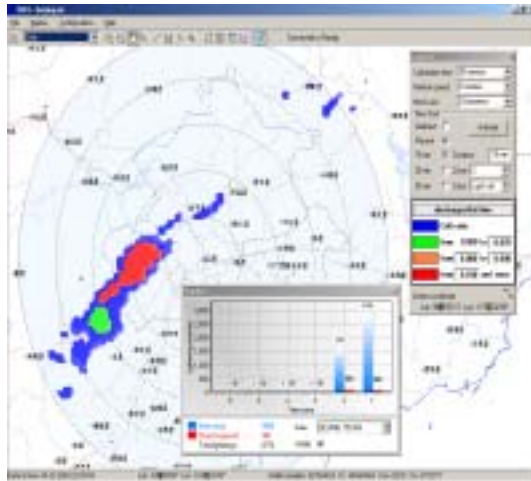


(e) Flashes number changes at 07:00-10:00(UTC)

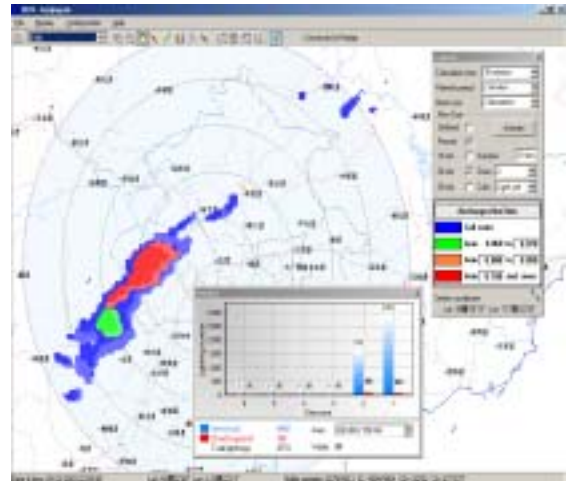


(f) Flashes number changes on daily

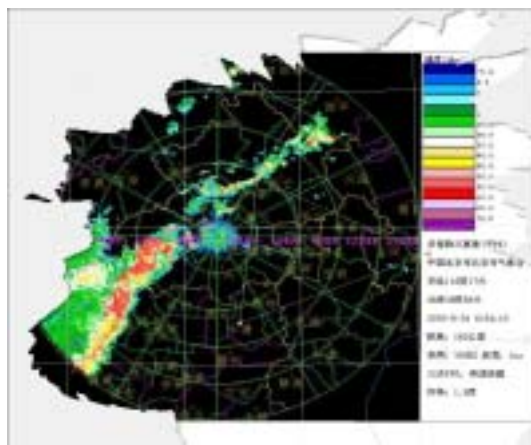
**Figure 2: Observation data sample. Meteorological Radar data , Locations of lightning discharges and Flashes number changes of time detected by SAFIR 3000 network from 07:00 to 09:00 (UTC) on June 23<sup>th</sup> in Beijing**



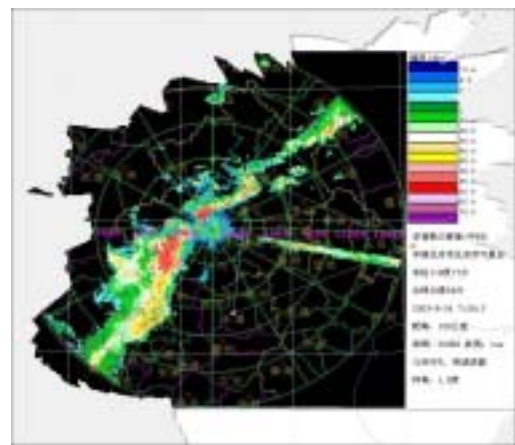
(a) Lightning warning 10 minutes in advance



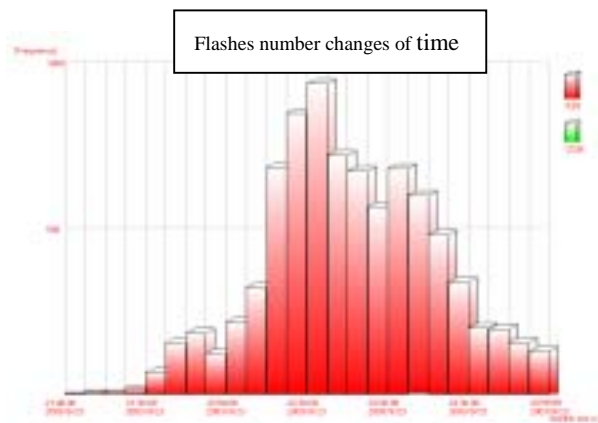
(b) Lightning warning 30 minutes in advance



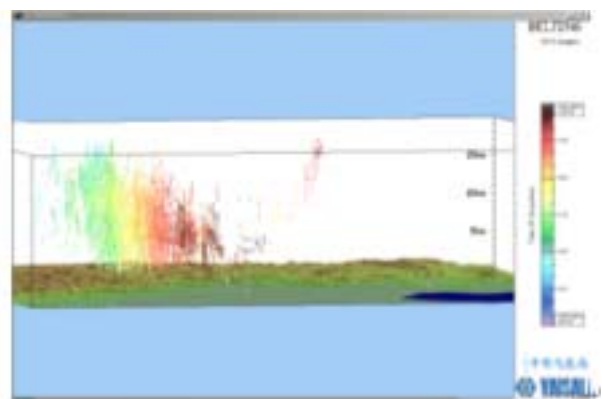
(c) Lightning superimposition on radar at 22:56 (UTC)



(d) Lightning superimposition on rada at 23:38 UTC



(e) Flashes number changes of time



(f) Locations of lightning discharges on 3D spatial

**Figure3: comparison of relationship between of lightning distribution and Radar echo data.(a) and (b) Lightning warning of moving trace of thunderstorm cell Lightning warning 10 minutes and 30 minutes in advance at 22:59 (UTC) estimated by SAFIR 3000 network. (c) and (d) Lightning data superimposition on a radar echo map, Lightning data (red dots) are gathered on a 10 minutes time frame centered around radar scan time. (e) and (f), Flashes number changes of time, Locations of lightning discharges on 3D spatial distribution at 21:00-23:59 (UTC) on September 23<sup>rd</sup> in Beijing.**

# *New Developments and Operational Experience With Surface Observation Technology*

By M.I.Refaie

E Mail [ref\\_1952@yahoo.com](mailto:ref_1952@yahoo.com)

Egyptian Meteorological Authority

TECO – 2005 Bucharest Romania , 4 -7 May 2005

## **1-Introduction**

The presence of \*Automatic Weather Observing Systems (AWOS) was commissioned in EMA 25 years ago and since that time EMA installed many of AWOS in a lot of surface stations .So the new technology become reliable. Modifications have been made with the view of maintaining.

High availability of AWOS can be achieved either through high Mean Time To Failure (MTTF) or low Mean Time To Repair (MTTR) .System designers have focused on maximizing MTTF as a way of providing high availability. However recent work in recovery oriented computing systems has emphasized recovery from failures -rather than failure avoidance.

The Reliability, Availability, and Maintainability, through the operational experience with surface observations as a new development technology will be discussed in this paper. The results obtained were based on the experiments of maintenance of 25 AWOS during the period 1997 -2002.

## **2-Reliability**

The reliability is the probability of a given system to perform its required function under specified condition for a specified period of time

Possible methods to increase reliability

- 1- Reduce system complexity
- 2- Parallel redundancy
- 3- Standby redundancy
- 4- Repair preventative maintenance
- 5- Increase reliability of system components
- 6- Quality control during manufacturing

A primary component of reliability analysis is referred to as failure rate , or the number of failures expected during a certain period of time . Calculation of equipment failure rate and its inverse –The Mean Time Between Failures (MTBF) is the basic of reliability predication

### **3-Mean Time Between Failures (MTBF)**

MTBF is the basic measure of reliability for repairable items .It can be described as the number of hours that pass before a component , assembly , or system fails it is d commonly used variable in reliability and maintainability analysis .

MTBF can be calculated as the inverse of the failure rate for constant failure rate systems. For example if a component has a failure rate of 2 failure per 3 years (12720 hours), the MTBF would be the inverse of that failure rate

$$MTBF = 12720/2=6360 \text{ hours}$$

MTTF is the basic measure of reliability for non repairable systems .It is the mean time expected until the first failure of a piece of equipment .MTTF is a statistical value and is meant to be the mean over a long period of time and large number of units . For constant failure rate systems MTTF is the inverse of failure rate

Technically MTBF should be used only in the reference to repairable items While MTTF should be used for non repairable items .However MTBF is commonly used for both repairable and non repairable items.

#### **3-1 MTBF calculation**

Calculated MTBF values are used during the design phase of systems and sensors. However it has been found that statistical analysis from a statistically relevant sample shows that calculated values are too pessimistic. Therefore statistical values are used for realistic MTBF calculation purposes and evaluate the reliability and availability of the systems .

#### **3-2 MTBF based on statistical values**

The statistical MTBF calculations are the ratio of total normal operation time of all the systems to the number of failure so from our experience and documents which trace repairs to the installed base of sensors and systems in 5 major airports and 20 surface stations The systems are assumed to be regularly and correctly maintained. consumable items are not regarded as part of the statistical analysis for the MTBF.

The statistical MTBF is calculated as a function of:

- The number of installed systems
- The average time since installation of the sensors
- The number of repairs to systems.

Due to the number of AWOS and sensors involved as well as the close co operation with department of the instrument, who's responsibility it is to maintain the systems, it is considered that the sample volume is statistically relevant for the purposes of MTBF calculation.

MTTR includes time for identification of failure, assembling of spares and tools and transportation to sensor/system position. This time may vary corresponding to local facilities. Pure repair time will normally not exceed 2h per sensor

Device	QTY	#of failure	MTBF(hours)	MTTR(hours)	Availability
Visibility (forward scatter)	10	32	13687.5	6	0.999561836
Wind	50	60	36500	5	0.999863032
Temp	25	53	20660.37736	3	0.999854816
Humidity	25	50	21900	3	0.999863032
Pressure	25	65	16846.15385	4	0.999762613
DCP	25	43	25465.11628	5	0.999803692
Data bus	25	15	73000	7	0.999904119

The resulting availability (Av) is calculated to be 0.999801877

### Central Processing Unit (CPU)

If the Central Computers are fully independent duplicated units it is assumed that the MTBF is limited by that of the data lines or power supply or the probability that two Workstations are down at the same time. The probability of the secondary Central Processing Unit failing during the repair period of the primary is calculated to be less than 1:10 Million. It is assumed that spare parts are available either on site or within 24 hours of registration of failure.

Device	MTBF (hours)	MTTR (hours)	Availability
CPU	10900	3,00	0.9997

DPU MTBF > 15000 hours

Critical failure DPU > 35000 hours

Other Workstations and Display Units

It is assumed that a single workstation failure does not mean a critical system failure has occurred. It is assumed that spare parts are available either on site or within 24 hours of registration of failure. MTTR covers time to set up a new computer and loading of relevant software. Workstations and Display Units are assumed to be exchanged as complete unit.

### 4- Maintenance Costs

There will be no additional maintenance costs except consumables and spare parts. After the factory training course, our experts able to perform maintenance and replacement of defect components by themselves. Under normal conditions no external assistance from the supplier necessary.

## 5-Conclusion

1. If there are two units or more of one sensor or component are included in the system, these lead to lower MTBF values. Therefore spare parts are recommended which would not be necessary for the 2 years period if only one system would be installed.

For example:

A system has a MTBF of 24,000 h. If two units of the same system are installed, MTBF of the 2 systems will be 12,000 h and relevant spares have to be foreseen for the 2 years period, If 3 units are installed, even a doubled number of spares might be necessary.

2. A general periodic Maintenance four times a year, is recommended. All sensors should be cleaned and performance shall be evaluated. Bearings of wind sensors shall be checked for smooth rotation.

Cleaning of sensor optics may be necessary in between, depending on contamination caused by environmental phenomena. Cleaning requests will automatically be generated by the system and displayed on CPU Workstation.

3. There are averaged yearly costs that may occur after warranty period for maintenance and repair, assuming that parts are repaired in factory or by authorized and trained personnel but if there is a professionals persons these costs will be few \$.and we well keep our system in high availability

4. The experience and documents for all the systems including failure diagnostic and fault isolation and how you fixed these fault all these items are very important to reduce the MTTR and increase availability of the systems

## References

- 1 – Dr. A. Hafez. Lecture in electronics faculty of engineer – Cairo- University Egypt
- 2 – Hchmat others . Operational Experience with the cern Hadram Geneva – Switzerland.
- 3 – Yee Jiun sang & others . is MTTR more important than MTTF for imparting user perceived availability Stanford university . CA- USA
- 4- MTBF and MTTF calculation Relex – Software website
- 5 – Maintaince time table . for AWOS in Egypt –EMA – instrument department period 1997 – 2002

## NEXT GENERATION ALL WEATHER PRECIPITATION GAUGE

Heikki Turtiainen and Samuli Räisänen  
Vaisala Oyj, P.O.Box 26, FIN-00421 Helsinki, Finland  
Tel. +358 9 89491, fax + 358 9 8949 2227  
e-mail: heikki.turtiainen@vaisala.com

Anu Petäjä  
Finnish Meteorological Institute, Sahaajankatu 20E, FIN-00810 Helsinki, Finland  
Tel. +358 9 1929 5718, fax +358 9 1929 5703  
e-mail: anu.petaja@fmi.fi

### ABSTRACT

The new Vaisala weighing precipitation gauge features technical innovations providing high quality measurements in all weather conditions and low life-cycle cost. Highlights of the gauge design and operation are presented, as well as first results obtained in the field tests at the Finnish Meteorological Institute's test field in Jokioinen.

### 1. INTRODUCTION

Accurate measurement of precipitation has been a challenge, especially in climatic conditions where both liquid and solid precipitation (snow, sleet) occur. In principle weighing gauges are the most suitable point precipitation gauges for these conditions due to the fact that melting of snow is not required for the measurement.

However, conventional weighing precipitation gauges are impaired by a multitude of errors. These include the error sources common to all point precipitation gauges - wind, evaporation and wetting errors - which all tend to cause systematic deficits. In winter conditions instrumental errors related to accumulation of snow and ice on rim and funnel parts of the gauge, as well as complete filling of the gauge with snow may result in severe underestimation. These problems are only partially solved using antifreeze solution in the container and applying rim heating.

The new Vaisala all weather precipitation gauge features technical innovations providing higher quality of measurement and lower life-cycle cost in all weather conditions. The design of the gauge is based on Vaisala's long experience of precipitation measurements and sensor design for meteorological applications.

This paper highlights the gauge operation and the aspect of lower life-cycle cost. It also presents preliminary results obtained at the Finnish Meteorological Institute's test field in Jokioinen.

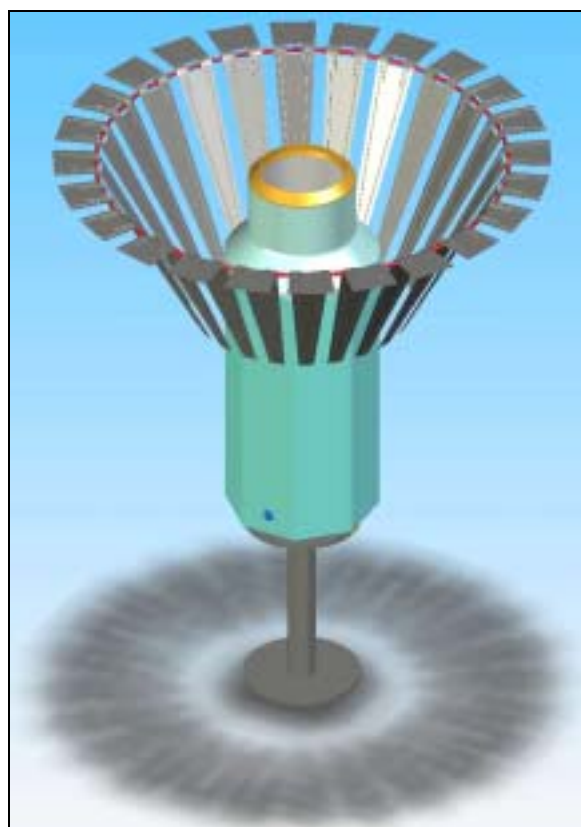


**Fig. 1.** Vaisala all weather precipitation gauge with wind shield.



## 2 TECHNICAL HIGHLIGHTS

### 2.1 Weighing method

The gauge utilizes latest high-accuracy, temperature-compensated load cell technology. The single point - type load cell is designed for direct mounting of the weighing platform. Eliminating levers and flexures, this allows simple, robust and low cost mechanics.

The load cell is insensitive to eccentric loading. Therefore, unlike some other types of weighing gauges, unsymmetrical distribution of snow in the collecting bucket (typical for winter conditions) does not introduce measurement errors.

Another error source which is eliminated by enhanced mechanics is the deficit caused by water and snow sticking on the inner surfaces of the gauge inlet funnel. In conventional designs this mass is not measured and eventually evaporates. In Vaisala's design the funnel element is resting on the collector container. All water and snow on it's surface will be included in the measured mass.

### 2.2 Gauge heating

Optional rim heating is recommended whenever solid precipitation measurement is needed. Heating prevents accumulation of snow and ice on the rim and collecting funnel. To prevent extraneous evaporation error caused by heating, as well as to minimize power consumption, the heating is controlled by the gauge software. The control algorithm is based on ambient temperature and precipitation status.

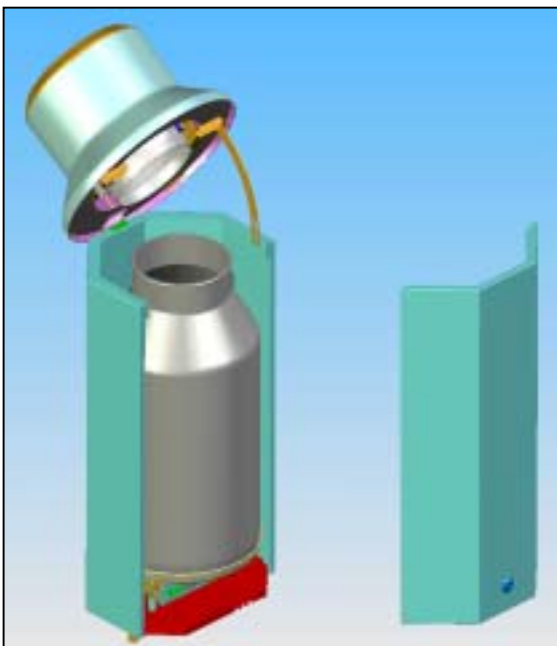


**Fig. 2.** The gauge with enclosure opened.

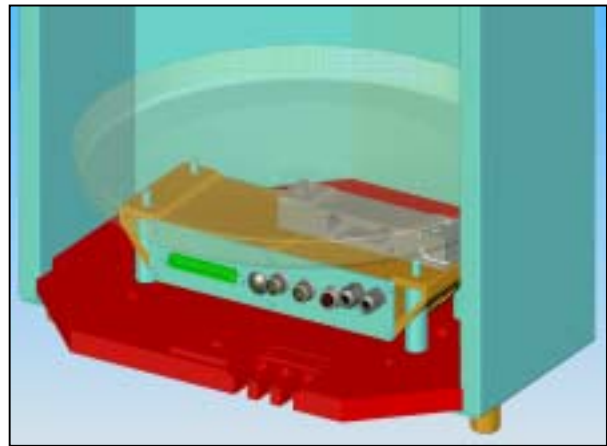


**Fig. 3.** Electronics unit and load cell are situated under the weighing platform.

### 2.3 Ease of maintenance

In the design special emphasis has been put on easy maintenance and extended service interval.

The hinged upper part (rim and collecting funnel) and detachable enclosure door allow smooth access for performing maintenance or adding antifreeze agent, as well as easy removal of the collector container (see fig. 2)

The electronics unit, including the load cell is field-removable (fig. 3). Replacement of the electronics is straightforward and quick causing minimal data loss, i.e. there is no need to transport the whole gauge to the laboratory for calibration. If needed, field calibration can be done using calibration weights.

Selection of optional features enhance performance and extend service interval.

## 3. TEST RESULTS

The gauge was tested at the Finnish Meteorological Institute's (FMI) test field in Jokioinen in Southwestern part of Finland. The test field is a grass-covered field about 60m x 100m in size (fig.4). For comparison the unit under test was installed in the middle of the field with it's orifice at 1.5 m height (fig. 6). Wind shield was not used in the first tests.

The Vaisala gauge was compared with the FMI's double fence intercomparison reference (DFIR): a high accuracy weighing gauge with orifice at 3 m height, surrounded by an octagonal vertical double fence. The reference is located at the north-west corner of the field, the distance between the gauges being approximately 50 meters.



**Fig. 4.** Jokioinen test field

The comparison started on 20.8.2004 and it will be continued until spring 2005. Rainfall data as well as temperature, humidity, wind speed and direction at the height of the gauges orifices was collected with 1-min intervals. Using the 1-min dataset daily totals of precipitation were calculated. In this poster the first preliminary results from liquid precipitation, obtained in autumn 2004 are presented.

Table 1 shows daily total values divided in three categories (slight rain, rain and heavy rain). Additionally it shows that Vaisala gauge's catch ratio was highest in slight rain and decreased with increasing rainfall rate.

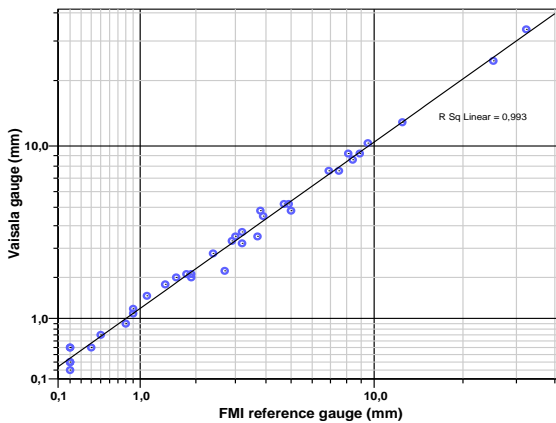


**Fig. 5.** Daily totals, Vaisala gauge versus FMI reference gauge (DFIR)

Since the end of August and throughout November 2004 the total precipitation measured was 176.9 mm. Daily total values varied from 0.2 mm to 32.3 mm.

Overall, the Vaisala gauge caught 6 % more precipitation compared to the FMI reference gauge (DFIR). The catch ratio ranged from 80%



to 150 % in a single rainfall, being highest in slight rains.

**Fig. 6.** The Vaisala gauge installed on the FMI Jokioinen test field.

The observed differences between values obtained with the Vaisala gauge and the FMI reference gauge (DFIR) are possibly due to different construction of the gauges. The Vaisala gauge has a larger catchment area (400 cm<sup>2</sup> versus 200cm<sup>2</sup>). Additionally, the inlet funnel of the the Vaisala gauge is a part of the instrument weighing system, whereas this is not the case for the reference gauge. Therefore water droplets

caught on the surface of the inlet of the reference gauge cause a loss in rain totals.

Table 1. Summation of daily precipitation

	Number of events (Days)	FMI reference gauge (DFIR)	Vaisala gauge
TOTAL	37	176.9 mm 100 %	188.1 mm 106 %
RDay < 1 mm	10	4.5 mm 100 %	6.2 mm 137 %
RDay 1-4,4 mm	15	38.5 mm 100 %	43.0 mm 112 %
RDay > 4,4 mm	12	133.9 mm 100 %	138.9 mm 104 %

#### 4. CONCLUSIONS

The Vaisala all weather gauge represents a new generation of weighing precipitation gauges. Simple and robust mechanics, large collecting area, latest high-accuracy load cell technology and advanced measurement and heating control algorithms ensure high performance, both in liquid and solid precipitation and in all weather conditions.

Preliminary test results from liquid precipitation show that undercatchment of the Vaisala gauge is very low - in fact it measured few percent more precipitation than the FMI reference gauge at the Jokioinen Observatory. The tests will be continued. More results, including solid precipitation data and a more thorough analysis of the observed differences will be presented at the conference.



Fig. 7. The gauge on the Vaisala test field with wind shield.

# ***The new synoptic-climatological station AMDA in the DWD primary network***

K. Klapheck and K. Wolff

*Deutscher Wetterdienst Frahmredder 95 D-22393 Hamburg*

e-mail: [Karl-Heinz.Klapheck@dwd.de](mailto:Karl-Heinz.Klapheck@dwd.de)

[Karsten.Wolff@dwd.de](mailto:Karsten.Wolff@dwd.de)

## **Abstract:**

The German Meteorological Service is currently modernizing its ground based and upper-air observing networks. Part of these networks are 160 synoptic weather stations. They will be equipped with a new measurement technique during the years 2005 to 2007. Their sensor equipment and possible modes of operation are explained. They can work fully automatically or by including observer information. Also monitoring and administration of the stations, data communication and archiving of data, alarm handling and quality control of the measurements are discussed.

The paper presents station design, data flow and network functions and some results of the operational test phase.

## **Introduction**

The primary network is the backbone of ground based observations made by Deutscher Wetterdienst (DWD). At present it includes about 80 stations with full-time observers resp. observers at times and 80 automatical stations, whose number is trending upwards. A secondary network with voluntary observers and a reduced amount of data is supplementary [1] and in operation.

In DWD the objective is to increase the data of ground based observation in time and space as well as to improve the quality of data in both networks. So forecasters' as well as climatologists' requirements will be fulfilled. Additionally the operation of the network shall be strongly automated and the maintenance shall have less expenditure. Therefore now the primary network will be equipped with modern measurement systems called 'Automatische Meteorologische Datenerfassungs-Anlage' AMDA in DWD-jargon, type I for manned operation and type II for unmanned operation. The system was designed and is produced as 'Meteodea E100' by Ernst Basler + Partner, a German meteorological software company. The company also develops most units of the network centre.

The secondary network has already been equipped to the most part with a technique called AMDA III, developed by another manufacturer with a different design.

This paper concentrates on the properties of AMDA I / II. It shortly introduces the sensors actually coupled, the data communication components and the functions of the central network control. Finally the state of instalment and the future tasks are mentioned.

## **Sensors**

The sensors are installed in a standardized field covering an area of 25 m x 25 m. In special cases the wind sensors can be far outside this area, then they are coupled wirelessly to the system. Also radiation sensors can be mounted outside the field to avoid shading. The pressure sensor is installed near the system computer (inside a building or a container). Generally the same types of sensors are used at all stations in both networks except at certain mountain stations, where due to the extreme climate the wind measurement is better done by a sonic anemometer than by a conventional wind vane / rotating anemometer. There also the temperature / humidity measurement with a heated dew point mirror will probably remove the iced radiation shields.

For a number of meteorological quantities intelligent sensors with integrated computing components are developed for automatic operation. These sensors transfer data in data telegrams

via a digital intersection. One of them is the Present Weather Sensor (PWS), an important step in automating eye observations. It generates a weather code as well as particle size distributions. PWS will be installed at fully automatic stations.

Radiation is measured with the first class instruments pyranometers and pyrgeometers only at certain manned stations. At unmanned stations a second class instrument called Scanning-Pyranometer-Pyrheliometer (SCAPP), a development based on the sunshine indicator, will be used. It is planned to measure the state of soil too, but no sensor is selected till now. In table 1 the meteorological parameters together with the accompanying measurement principles and sensor types are listed.

Cameras installed at some stations are not integrated in AMDA but represent a separate system resp. network [2].

## **Data acquisition and data processing**

The essential characteristics of the AMDA system are

- completely modular design of hardware and software
- all sensors connected via PROFIBUS, Europe's most common industrial field bus
- high reliability due to redundant subsystems
- flexible adjustment and extension of measurement data processing by configuration
- standardized internal communication via CORBA protocol
- standardized external communication via XML protocol
- comfortable input and visualization of data by the observer or service personnel
- usage of Open Source Software

### **Hardware**

According to the hardware concept an industrial server-PC works as the station computer. It is equipped with redundant hard disks and power supplies, with an integrated PROFIBUS controller and a multi-channel RS485 serial interface card. Buffering of supply voltage by batteries is added.

The system operates reliably, is capable of further extensions and is equipped with remote monitoring functions by a web interface independent of the PC. The system is mounted in a 19" rack and works at a monitored temperature range of  $-5^{\circ}$  to  $+50^{\circ}\text{C}$ . It is placed either in a building (manned station, AMDA I) or a container (unmanned station, AMDA II). At manned stations the observer uses a separate standard PC as an AMDA client for data input, visualization and maintenance. The AMDA-LAN is connected by a router over a DSL or ISDN line to the headquarter.

All sensors in the sensor field are connected to the AMDA system via the PROFIBUS field bus, see also figure 1.

Components of the PROFIBUS are a controller card in the PC (the master), bus modules (the slaves) on the field and the connecting cable (two wire serial RS485). A maximum of 126 slaves can be placed over a length of up to 600 m. Repeaters allow further extension up to 10 km.

The AMDA system uses not more than three different types of bus modules for converting analogue and digital signals, which are electrical resistance, voltages as well as digital status levels and pulse frequencies. An additional type of bus modules is used to transfer all data telegrams from the intelligent sensors to the PROFIBUS. These modules are standard components from industrial automation technique with high reliability and conformability.

A concept of overload voltages protection is realized.

### **Software**

The AMDA application system is designed as a set of independent components, see figure 2.

The component Data Acquisition is responsible for the data input from the sensors in fixed, configurable periods, depending on the sensor in a range from 4/s up to 1/min. Further data processing is done in the resp. component. It includes the computation of sums, averages, extreme values etc. An integrated formula language allows also complex calculations, in which the arithmetic expressions are part of the configuration.

The AMDA Client serves as an interface for observer and service personnel. At AMDA I visual observations of cloud type and amount, visibility, present weather, state of soil and other special

weather phenomena can be entered in comfortable dialogs, in regular intervals or arbitrary. The visualization allows numerical display of actual measured and computed values as well as status of sensors and components. Missing, erroneous and questionable values are attributed in different colours. (x,t)-diagrams with selectable scales show the courses of one or several parameters in one diagram. (x,y)-diagrams can be chosen to see two parameters in relation. Also polar diagrams are possible. Several diagrams can be placed on the screen. Of course tables of numerical values are possible.

Data and configuration exchange between AMDA and headquarter is done by the standardized XML (Extensible Markup Language) protocol. XML is a simple, very flexible text format derived from SGML (ISO 8879) for the exchange of data on the Web and elsewhere.

Additionally local or remote users can be connected over serial lines. Amount and format of the transmitted data are freely configurable.

Except for the Data Acquisition, which is coded in C++, the complete system is based on Java. The internal communication between all components uses the CORBA (Common Object Request Broker Architecture) protocol.

The Open Source database system postgresSQL is used by AMDA for local archiving of data and configurations. One of our objectives was to use Open Source Software whenever possible. Therefore DWD chose LINUX as operating system for AMDA.

## **Quality assurance**

A central design principle of AMDA is to achieve high availability, plausibility and accuracy of data. Air temperature and humidity sensors are doubled. Status of all sensors and modules is regularly controlled, if necessary, alarms are triggered. The allocation of sensors and their technical specifications follow national and international rules. Recalibration of sensors and modules are part of the quality management plan.

Data processing includes algorithms to test the data values on plausibility. To each value in the output a quality byte is added. It classifies data quality and status of sensors and modules. A second phase of off-line quality management is done in the central database by the Quality Control and Monitoring System QualiMET [3].

## **Central control**

Ernst Basler + Partner is developing a Network Control and Monitoring System, see figure 3. Essential server functions are calling the stations by a configurable schedule, storing all data in databases, administration of configurations, alarm handling and distribution of software-updates . Clients allow a comfortable survey and configuration of the stations. Geographical maps provide a quick overview of the status of all AMDA I / II stations, as it is already realized for the AMDA III network. AMDA III will be integrated into the new central control system too. Clients are installed in the DWD headquarter and in local service branches, access should be possible at any location in the DWD intranet. Reports like SYNOP, MREP etc. are generated in the Report & Product Generator. External users get access to the DWD database via a Gateway, which is separated from the intranet by a firewall.

## **Final remarks**

Modern hardware and software technique enable us to increase the degree of automated observations as well as the amount of measured and computed data. The quality of data is improved and the maintenance of stations will be simplified.

A prototype test has been started in autumn 2004 and will be finished at the end of 2005. The installation of 160 regular station systems will start in summer 2005.

The operational prototype test includes a sample of 6 AMDA stations located in areas with different climatic conditions together with a prototype of the Network Control and Monitoring System. First

results confirm the reliability of the AMDA stations, of data transfer and of storage in the database. Quality of all data measurements is excellent.

## Literature

- [1] Klapheck, K. and Alsen, S.: Aufbau eines neuen Stationsnetzes für Klimatologie und Hydrologie. Proc. Deutsch-Österreichische-Schweizerische Meteorologen-Tagung, Karlsruhe, Sept. 2004
- [2] Mammen, T. et al.: Digital video technique as a new part of the DWD observing network. To be published in Proc. WMO Techn. Conf. on Meteorol. and Environm. Instrum. and Methods of Observ., Bucharest, 2005
- [3] Spengler, R.: The new quality control and monitoring system of the Deutscher Wetterdienst, Proc. WMO Techn. Conf. on Meteorol. and Environm. Instrum. and Methods of Observ., Bratislava, 2002

**Table 1:** List of sensors connected to AMDA

parameter	sensor principle	Sensor type / manufacturer	intersection
air temperature 2m	pt100 resistance	1/3 DIN class B / Friedrichs	analogue
relative humidity 2m	capacitive sensor multi-plate radiation shield	HMP45 A / Vaisala ,DWD' / Eigenbrodt	analogue
air temperature 5cm	pt100 resistance	1/3 DIN class B / Friedrichs	analogue
soil temperature: 5, 10, 20, 50, 100 cm	pt100 resistance	1/3 DIN class B / Ketterer	analogue
precipitation vol./int.	electronic weighing	Pluvio / Ott	RS485
precipitation duration	IR-light barrier	Precip. monitor / Thies	relay contact
sun shine duration	Photoel. sunshine indicator	SONIe / Siggelkow	RS422
(alternative)	SCAPP (scanning pyranometer pyrliometer)	,DWD' / Siggelkow	RS422
global radiation	Pyranometer	CM11 / Kipp&Zonen	analogue
(alternative)	SCAPP		
diffuse radiation	Pyranometer	CM11 / Kipp&Zonen	analogue
(alternative)	SCAPP		
direct radiation	SCAPP		
atmosph. radiation	pyrgeometer incl. pt100	CG4 / Kipp & Zonen	analogue
wind direction	wind vane	Standard / Thies	Gray-Code
wind speed	cup anemometer	Standard / Thies	Pulses
wind (mountain st.)	ultra sonic anemometer	2D / Thies	RS485
snow height	ultra sonic device	SR50 / Campbell	RS485
cloud height	laser radar	LD40 / Vaisala	RS485
visibility	forward scatter instr.	DF20 / Degreane	RS485
present weather	laser disdrometer	Disdrometer / Thies	RS485
air pressure	capacitive sensor	PTB220 / Vaisala	RS485
state of soil			

Figure 1: AMDA hardware components

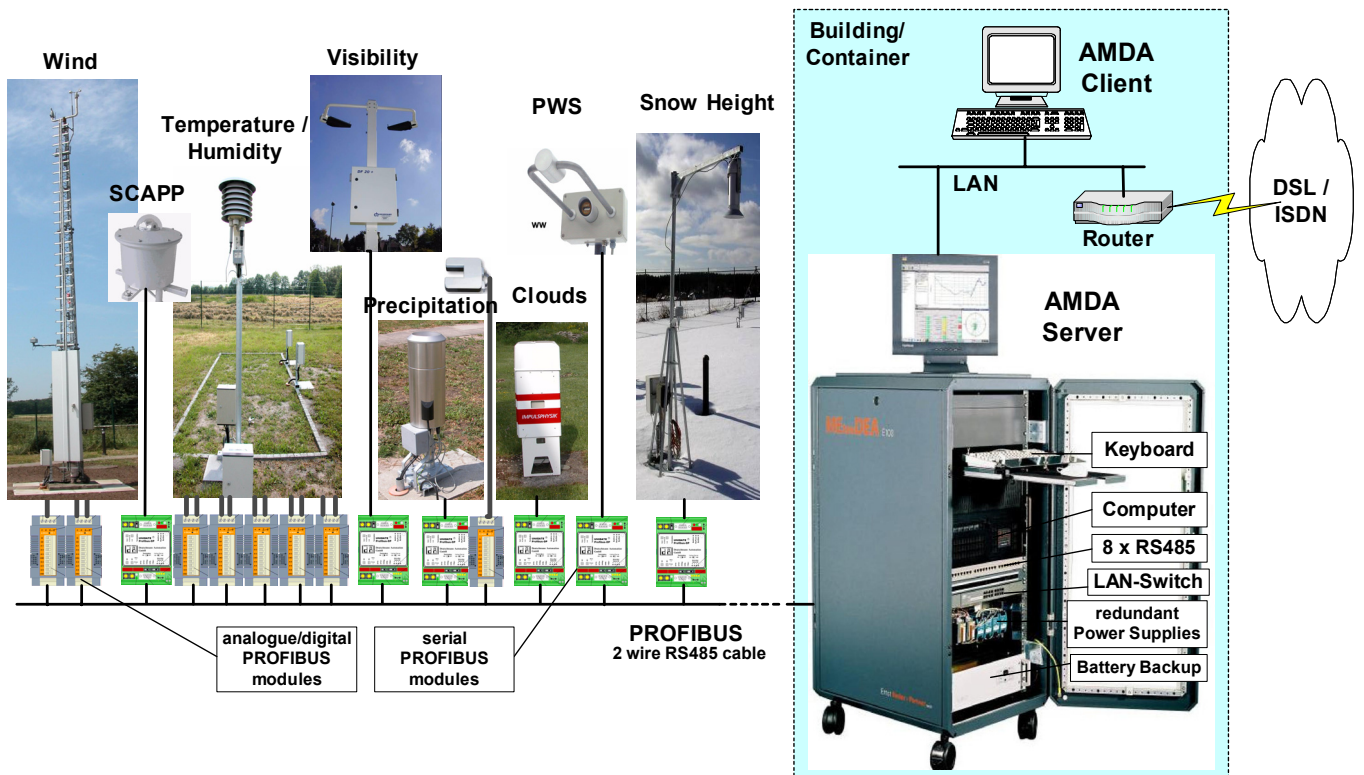


Figure 2: AMDA software components

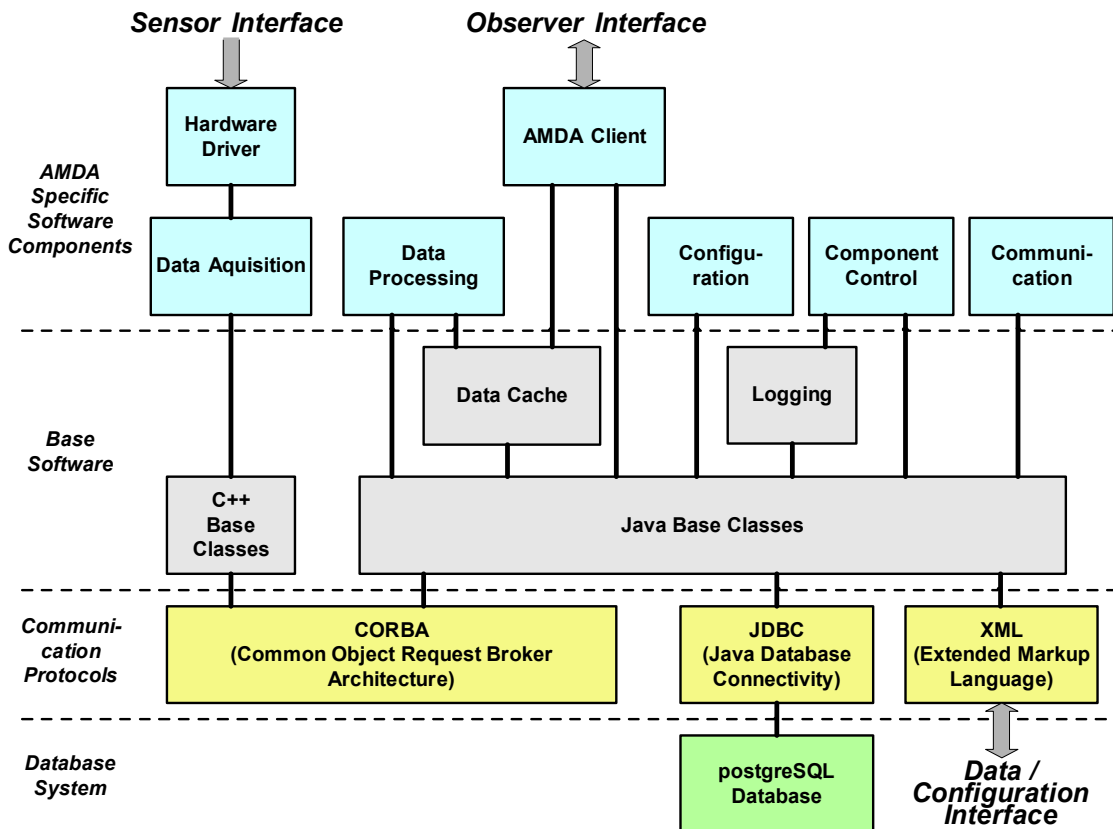
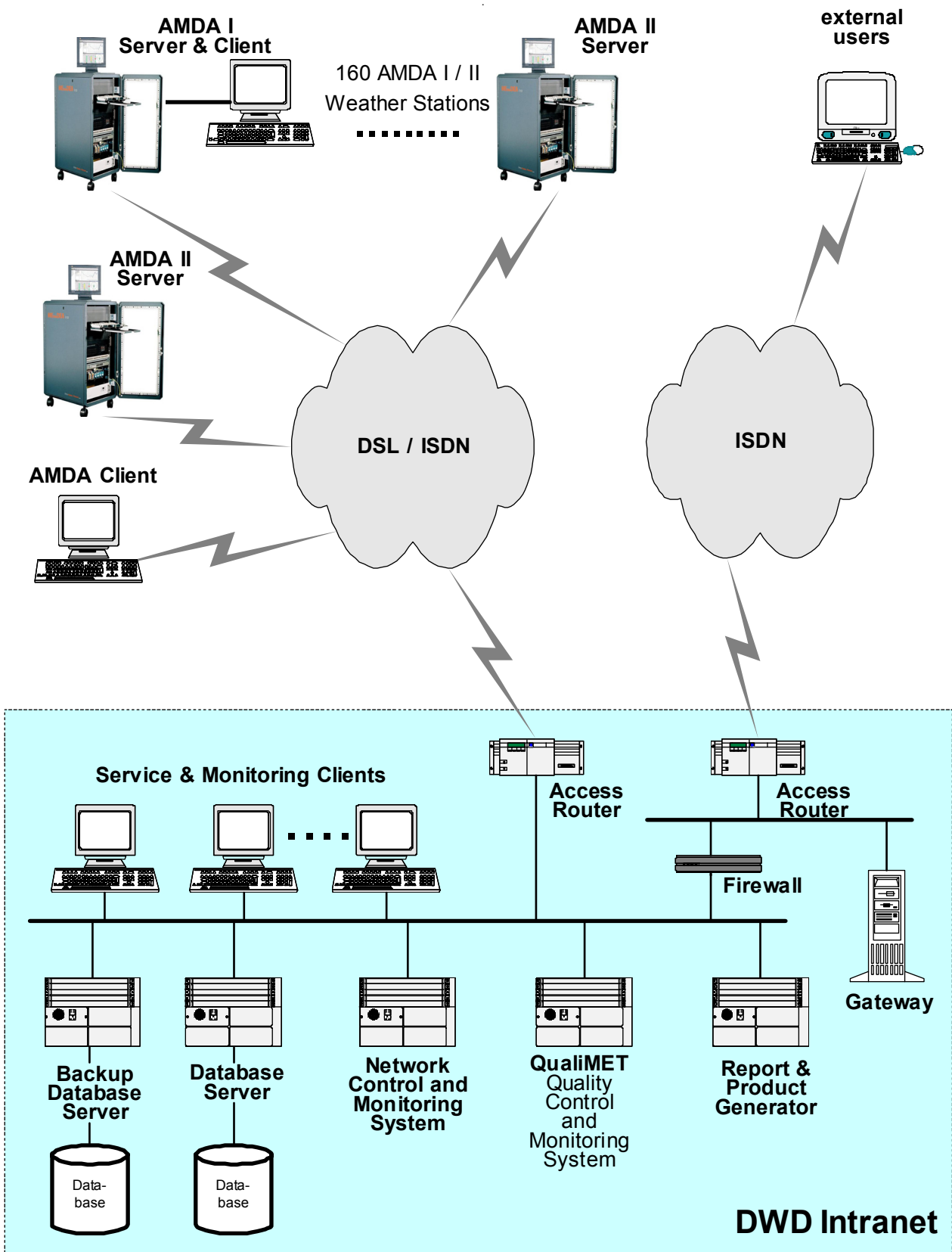




Figure 3: AMDA network components



# VISIBILITY MEASUREMENT TECHNIQUE AND ITS APPLICATION IN AVIATION SERVICES AT INTERNATIONAL AIRPORTS IN INDIA

By

***R.R. Mali & R.D. Vashistha***

Instruments Division, India Meteorological Department, Pune – 411 005, INDIA.

Tel: +91-20-25535411 :: Fax: +91-20-25521529

E-mail: [rajesh132002@yahoo.com](mailto:rajesh132002@yahoo.com) ; [ramdhanv@hotmail.com](mailto:ramdhanv@hotmail.com)

## A B S T R A C T

The term ‘visibility’ is variously defined, but generally indicates the distance to which human visual perception is limited by atmospheric conditions. The physical mechanisms that influence visual perception during the night in distinguishing lights differ from those in the day time in distinguishing objects illuminated by daylight. Basically, however, visibility describes the transparency of the air in the horizontal direction and represents the maximum distance that one can see in the atmosphere at any given time.

Provision of this visibility within specified accuracy to the pilots and air-traffic controllers has assumed great importance with the advent of high speed high altitude jet and supersonic aircrafts. Meteorological visibility concerns the transparency of the atmosphere as related to human vision. The transparency of the atmosphere is affected by the presence of hydrometeors (rain, snow, mist, fog) or litho meteors (dust, smoke etc.).

A transmissometer is used for measuring the atmospheric transmittance at visibility deterioration (fog, rain etc.). This instrument is mainly installed at the runways of airports in order to determine the visual range for the flight control safety service. The double baseline unit is new generation equipment especially suited to render exact visual range data for flight operation at CAT-II to CAT-III(b) type airports.

In India, New Delhi and Kolkata are equipped with three and two dual baseline transmissometers respectively, catering to CAT-IIIB ILS requirement at these airports.

Continuous data obtained from these transmissometers during 2001-2003 are analysed and presented in this paper.

## 1. INTRODUCTION

Aviation activities have increased tremendously in the recent decade in volume and diversity and will continue to do so in future. India Meteorological Department caters to the needs of aviation services through a network of 4 meteorological watch offices (MWOs) – Chennai, Delhi, Kolkata and Mumbai - 18 Class-I Meteorological Offices and 52 Class-III Meteorological Offices.

With increased operating costs and lower operating minima, a much higher degree of precision sophistication and timeliness are needed in meteorological observations and processed information feeding the aviation sector. The meteorological systems are required to be installed near the runway as per ICAO recommendations and the data obtained from these systems are to be acquisitioned, processed and displayed on line as per the requirements in an airport. These systems are crucial for the determination of the operation characteristics in an airport.

The visibility should be measured and observed by reference objects or lights whose distance from the point of observation is known. Since, in practice the runway visual range (RVR) can not be measured directly on the runway, it is the best possible assessment of the range over which the pilot of an aircraft on the centre line of runway can see the runway surface markings or the lights delineating the runway or identifying its centre line. RVR observations should be representative of the touchdown zone and depending on the category of operation for which the runway is intended and the length of the runway.

## **2. VISIBILITY**

### **2.1 Visual Range:**

Visual range is determined by an observer and defined as the maximum distance at which an object or low intensity light can be distinguished. Visual range and visibility are used here interchangeably.

### **2.2 Runway Visual Range (RVR):**

Runway Visual Range is defined as an instrumentally derived value, based on standard calibrations, that represents the horizontal distance a pilot will see down the runway from the approach end by observing runway lights or runway markers, from a specified height, i.e. 2.5m above ground level, whichever yields the greater visual range.

RVR is normally obtained from transmissometers, located along side the runway. Conversion from atmospheric transmittance along the baseline of the transmissometers to RVR is made using Allard's Law for various runway light settings.

## **3. VISIBILITY MONITORING SYSTEM**

The Transmissometer system is used for measuring the visual range at visibility deterioration (e.g. fog). This system is generally installed along the runways of airports in order to determine the visual range for the flight control safety service. The double baseline unit of this system is installed at both New Delhi and Kolkata, to render exact visual range data for flight operation at CAT-II & CAT-III B.

For the double base-line system, two receivers and one transmitter are installed. In this type of arrangement visibility measuring range of 10m to 3000m and an RVR range from 50m to 3000m are obtained at a baseline of 15 m and 75 m.

The basic equipment of the system consists of a transmitter, receiver and a registration control unit. The optical axes of the transmitter and the receivers are precisely aligned with each other (Fig. 1).

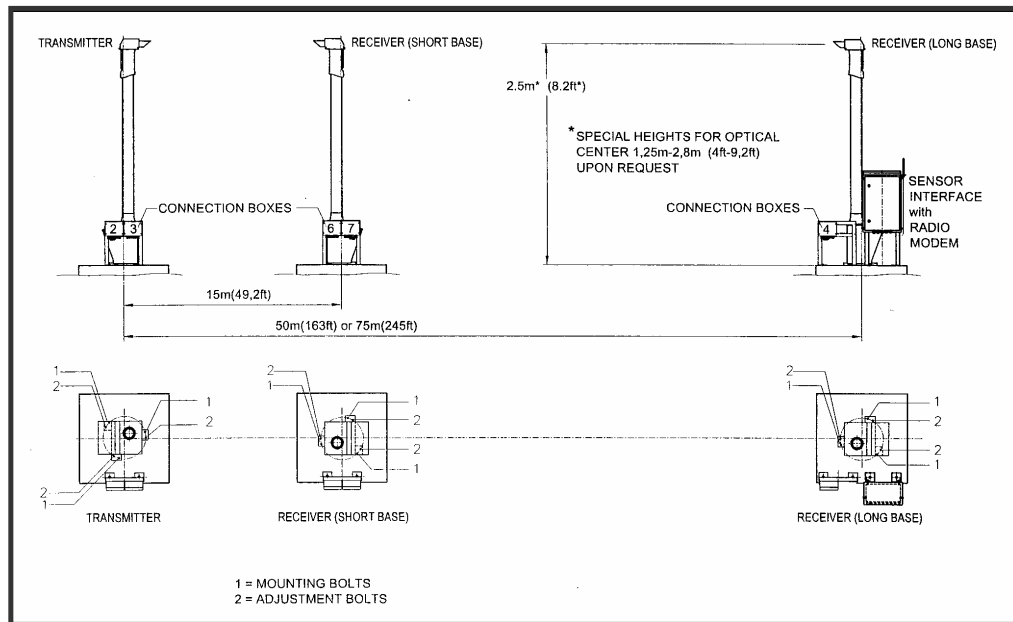


**Fig. 1: Dual Baseline Transmissometer**

### 3.1 Measuring procedure:

The transmissometer measures light transmittance of the atmosphere. The transmitter and the two receivers are optically aligned to each other and located within a precisely determined measuring distance (baseline). The transmitter radiates short light power light pulses with a frequency of approximately 180 flashes/minute. The Intensity of the light pulse i.e. the average of several light pulses is constant. The receiver responds only to these short light pulses and measures their intensity. Increasing visibility deterioration within the baseline causes the light radiated by the transmitter intensity to decrease as it reaches the receiver. A registration and control unit (STATION) indicates this decreasing light transmittance of the atmosphere by showing lower visual range values.

The “Visual range” of the runway lights (RVR – runway visual range at night) can be calculated from the Allard Law :

$$E_t = \frac{I x T^{R/B}}{R^2}$$

where,  $E_t$  - representing the pilot’s sensitivity to the illumination intensity,

$I$  - The effective intensity (towards the pilot) of the most distant but still recognizable runway lights.

Using the above equation, the RVR can be determined from the indicated transmissometer data (T), by inserting the respective values for light intensity of the runway lights (I) and the visual threshold of illumination ( $E_t$ ). The letter is related to the luminance of the background ( $L_v$ ) against which the light is viewed. This brightness from the background can be determined by a luminance sensor, called Background Luminance Monitor (STILBUS).

#### 4. VISIBILITY CRITERIA FOR INSTRUMENT LANDING OPERATIONS

Measurement of RVR is critical in determining whether or not a pilot can make an approach to the runway. Landing criteria for instrument landing system runways are based on the operational performance categories listed in Table-1 below:

TABLE -1

CATEGORY	RVR LIMIT (m)
I	550 +
II	300 – 550
III(A)	200 – 300
III(B)	50 – 200
III(C)	0 - 50

#### 5. SYSTEM DESCRIPTION

The basic components of a double base line transmissometer system are:

- ❖ transmitter
- ❖ receiver
- ❖ data control unit
- ❖ communication equipment

##### 5.1 Transmitter:

The transmitter basically consists of a xenon flash lamp with a flash frequency of 2.5-3.5 Hz. The optics basically consists of an achromatic, 46mm diameter lens with a focal length of 120mm. This system works on 220 V ac, 50 Hz and the total power demand is 100 VA.

##### 5.2 Receiver:

Receiver consists of a photodiode (OSD-100) which converts the received light signal into proportionate electrical values. It also has an optical system consisting of an achromatic lens of 46mm diameter with a focal length of 200mm. It also has a provision to receive the data in 0 - 5 mA range from STILBUS, which monitors the ambient light. The data output is selectable RS232/RS422/RS485/MODEM form. Interface for the test purpose is made available in 0 – 1 mA range corresponding to 0 – 100% transmission. Serial data transmission RS232C is having ASC11 format with 8 data bits, 1 stop bit, no parity and transmitted at 9600 baud maximum.

##### 5.2.1 STILBUS:

STILBUS is a background luminance sensor. The luminance of the background has a strong influence on the observer's perception of lighting element. The STILBUS provides stepless measuring range of 1 – 10000 Cd/m<sup>2</sup> on a decadic logarithmic scale. The measuring range includes important decision thresholds for calculations.

Ambient Conditions	Background Luminance
Night	< 40 Cd/m <sup>2</sup>
Twilight	50 – 1,000 Cd/m <sup>2</sup>
Day	1,000 – 12,000 Cd/m <sup>2</sup>
Bright Day	> 12,000 Cd/m <sup>2</sup>

These four illuminance values have proven effective in the calculation of RVR.

The transmitter and the two receivers with communication interface unit are installed in the field, whereas data control unit and slave display units are located in Meteorological Briefing Room (MBR) and ATC which are generally 5-10 km away from the field sensors. The data communication between the sensor output and data control unit is achieved via 4-core underground armoured cables as a serial transmission over a distance of about 10 km through cable modem. The wireless data communication system between the sensor and

data control unit is achieved via radio modems operating at different frequencies in UHF modem, in the range 433-434 MHz, as given in Fig 2. Furthermore, a background luminance sensor is connected for monitoring ambient light condition, the status of which is included in the data transmission telegram (message).

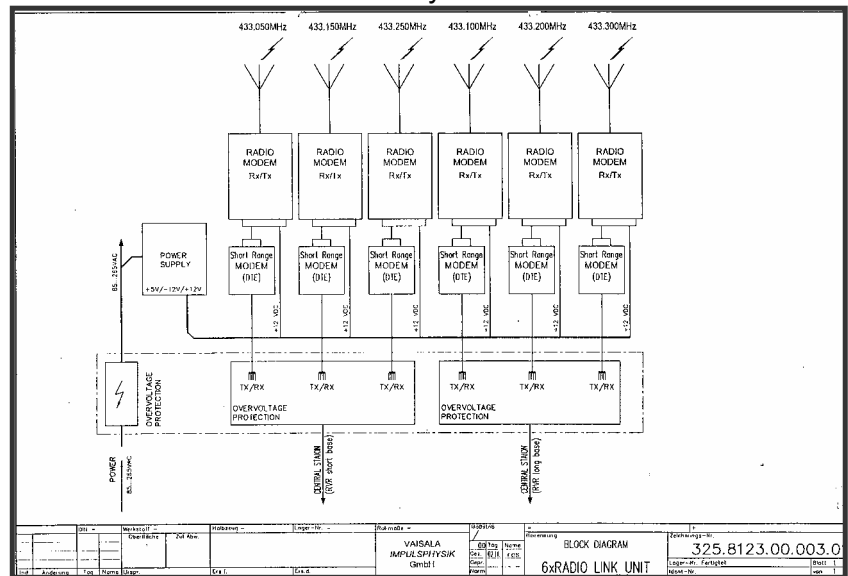


Fig. 2: Wireless communication system.

A typical transmissometer installation fulfilling CAT-III RVR requirements at New Delhi airport is presented in Fig. 3. The processed data and on line display output of MOR and RVR in graphical form is presented in Fig. 4. The slave display output in front of ATC controller is presented in Fig. 5.

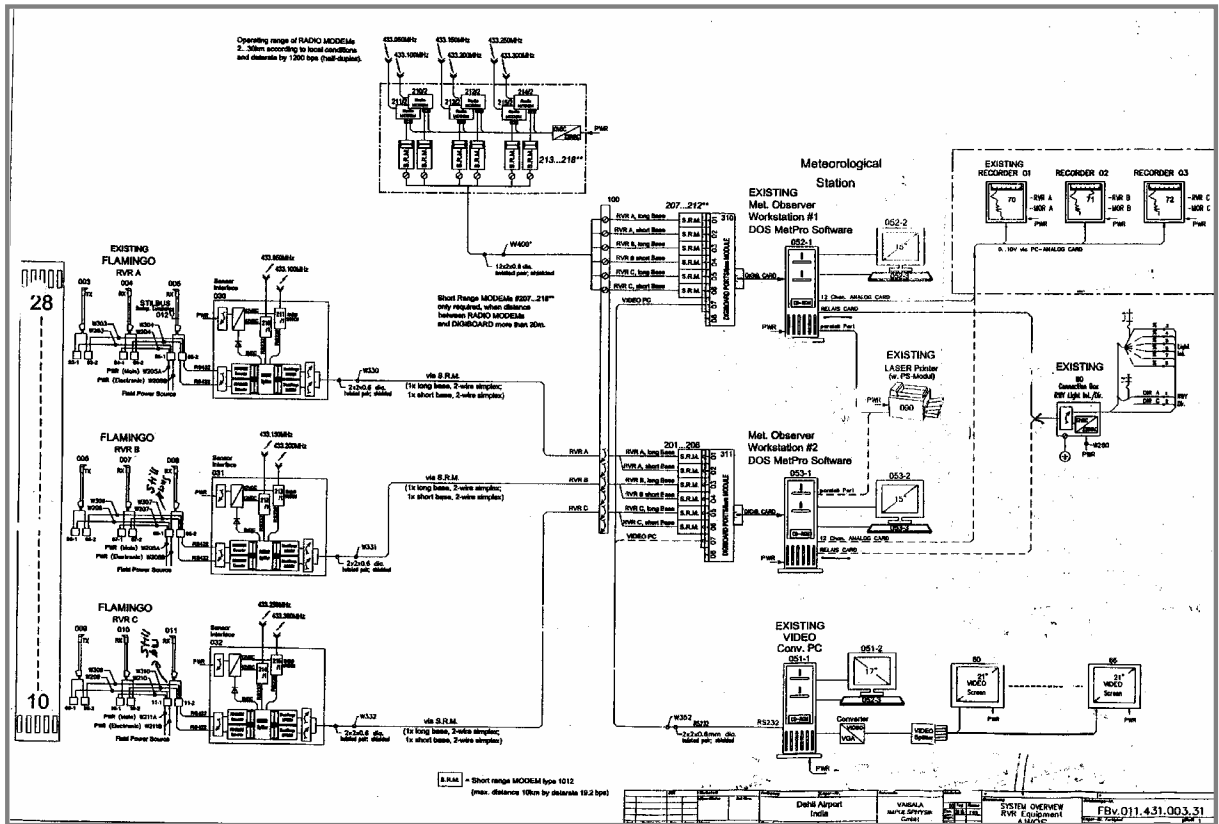


Fig. 3: Complete installation at Delhi airport.

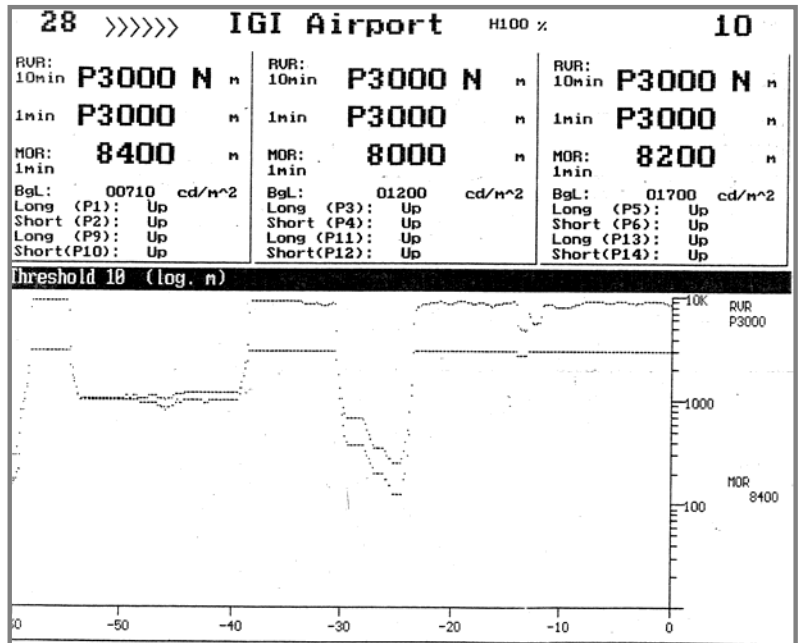


Fig. 4: Processed on-line data presentation

VIDP	24 JUL 01	07 46 18
28	>>>>>	mid 10
RVR:	P3000	P3000 P3000
Trend:	N	N N
MOR:	7900	7700 8400

**Fig. 5: Slave Display – in front of ATC Controller.**

## 6. DATA PRESENTATION

The data used for the presentation is obtained from the transmissometers installed at New Delhi and Kolkata airports for the period December 2000 to January 2004. The hourly average RVR values are used for presentation. The critical months when air-traffic is affected due to low visibility condition at both the airports is observed to be in December and January. Hence, sample data for both the months at these airports have been analyzed and presented in the graphical form.

**Graph-1:** Variations in RVR with respect to time, due to low visibility condition (fog) on 24 Dec., 2003 at Delhi airport.

**Graph-2:** Variations in RVR with respect to time, due to low visibility condition (fog) on 06 Jan., 2004 at Delhi airport.

**Graph-3:** Variations in RVR with respect to time, due to low visibility condition (fog) on 20 Dec., 2001 at Kolkata airport.

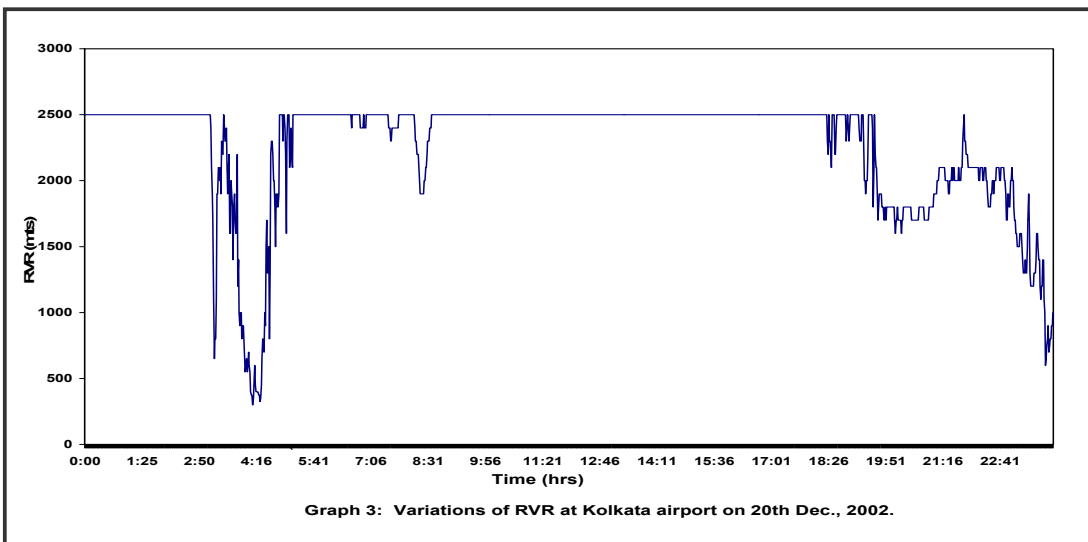
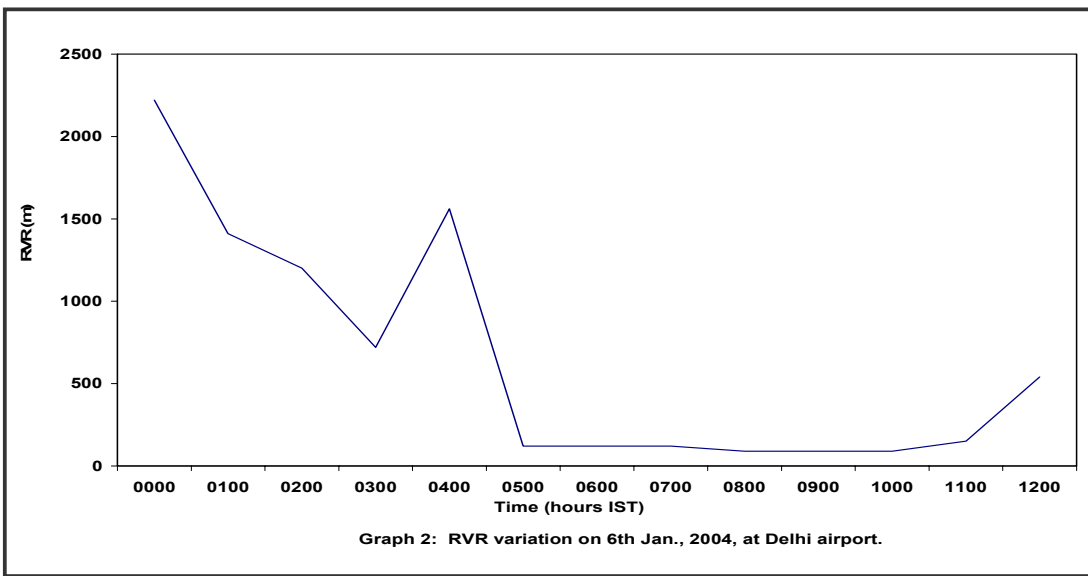
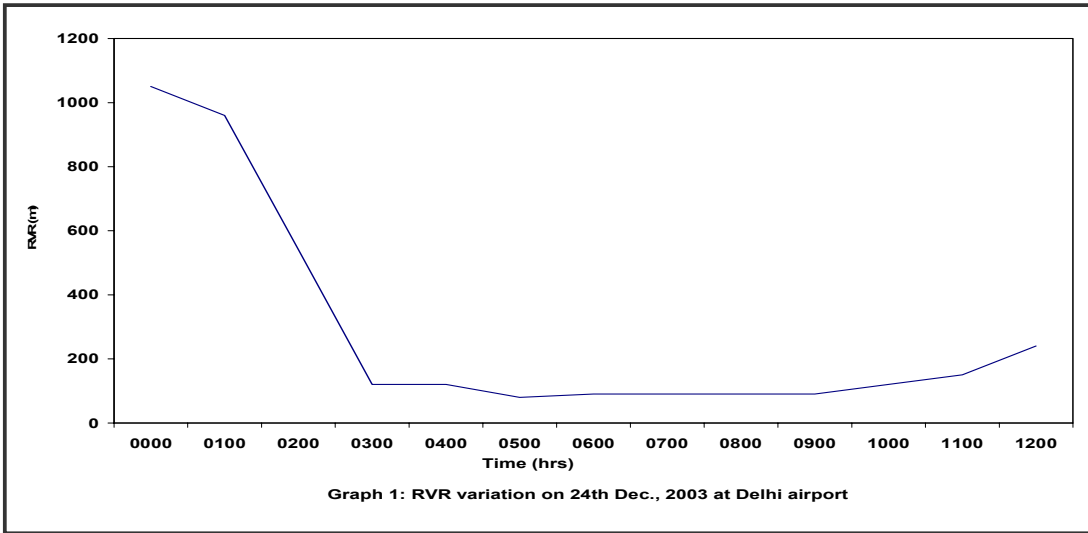
**Graph-4:** Variations in RVR with respect to time, due to low visibility condition (fog) on 16 Jan., 2002 at Kolkata airport.

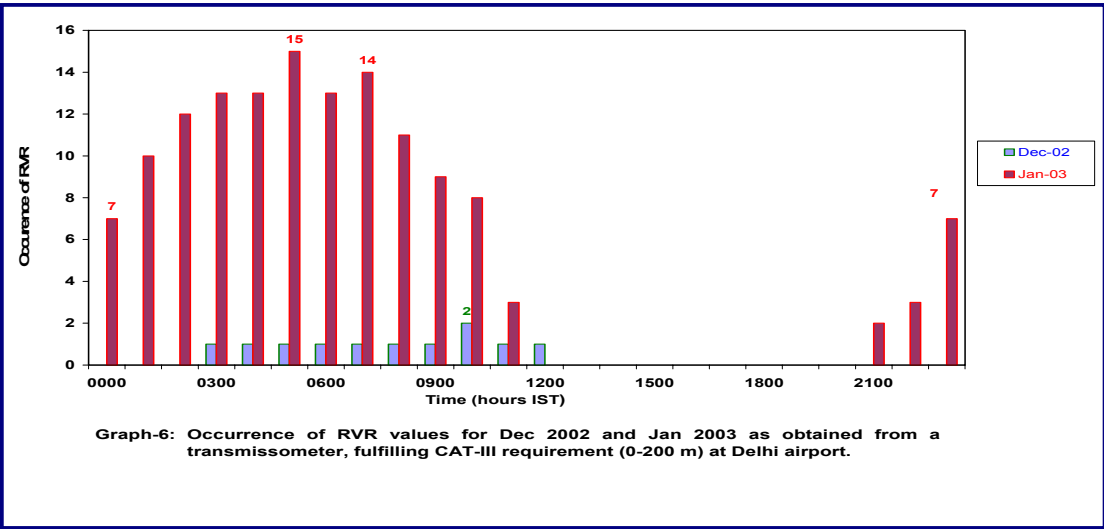
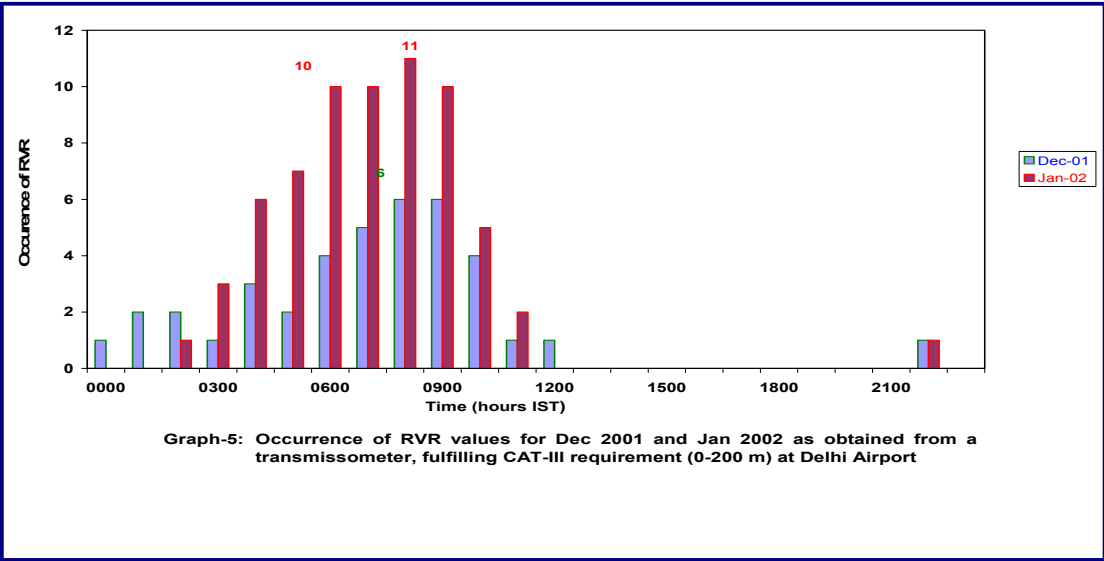
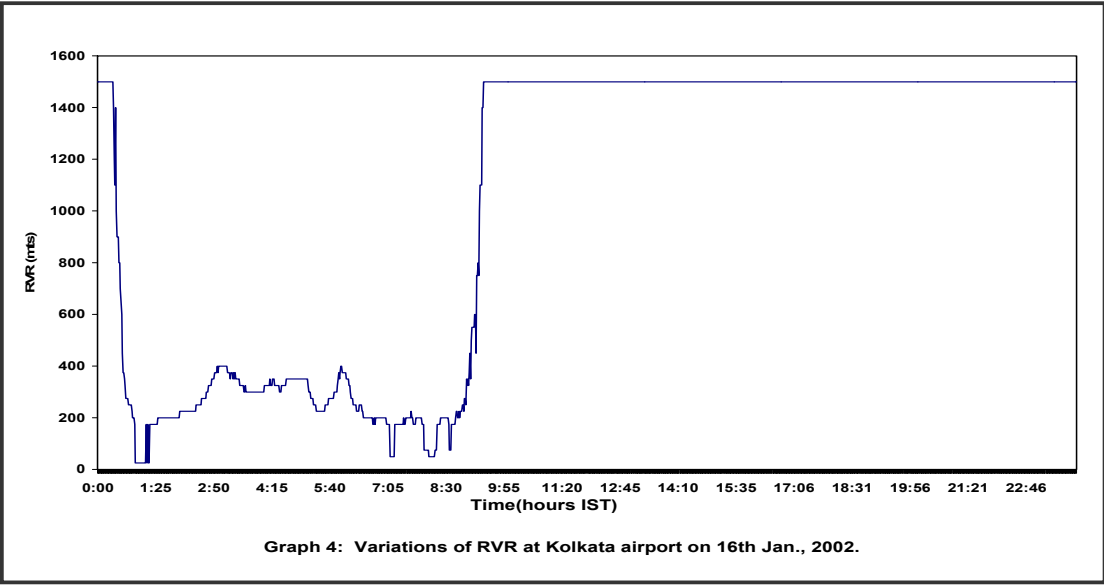
**Graph-5:** Occurrence of RVR values, based on hourly average for Dec. 2001 and Jan.2002 as obtained from Transmissometer fulfilling ILS CAT-III requirements (50 to 200 m) at Delhi airport.

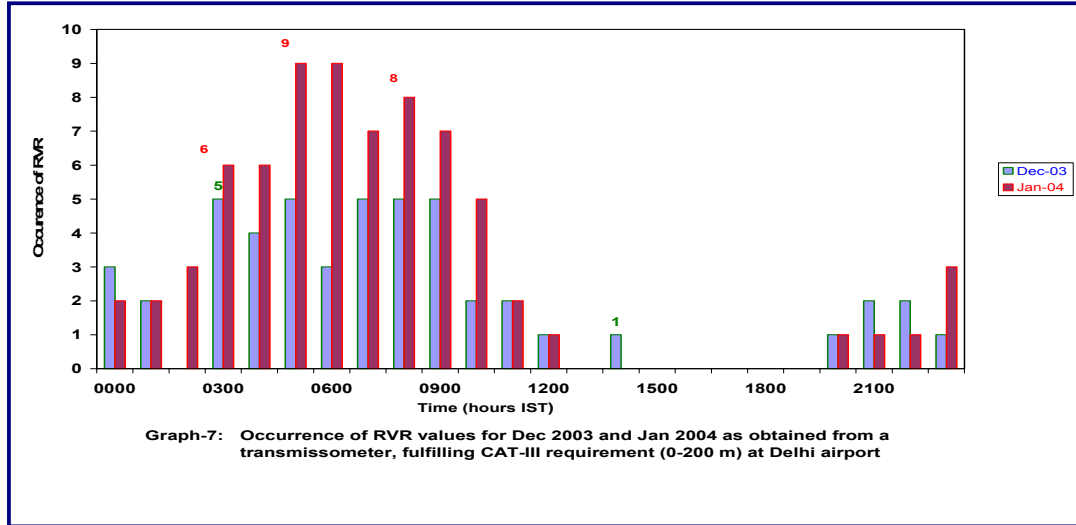
**Graph-6:** Occurrence of RVR values, based on hourly average for Dec. 2002 and Jan. 2003 as obtained from Transmissometer fulfilling ILS CAT-III requirements (50 to 200 m).

**Graph-7:** Occurrence of RVR values based on hourly average for December 2003 and January 2004 as obtained from Transmissometer fulfilling ILS CAT-III requirements (50 to 200 m) at Delhi airport.









## 7. CONCLUSIONS

Measurements of RVR are critical in determining whether a pilot can make an approach to an instrument runway. Landing criteria for instrument runways are based on operational performance of the system under each category.

The operational performance of the transmissometer system, fulfilling all the requirements up to ILS Cat-IIIB is satisfactory, since their installation at Delhi and Kolkata airports. It has been observed that the RVR values reported by the instruments are well within the accuracy limits as recommended by ICAO.

## REFERENCES

1. 'Guide of Meteorological Instruments and methods of observations'. WMO No. 8 [2001].
2. ICAO Annex 3, Meteorological Services for International Air Navigation, 2001.
3. Manual of Runway Visual Range Observing & Reporting Practices, March 2001.



# PRESENT STATUS OF SURFACE METEOROLOGICAL MEASUREMENTS IN INDIA

*R.D. Vashistha, B. Amudha & Rudra Pratap*

Instruments Division, India Meteorological Department, Pune – 411 005, India

Tel: +91-020-2553 5411 :: Fax:: +91-020-2552 1529

E-mail: [ramdhanvashistha@yahoo.co.in](mailto:ramdhanvashistha@yahoo.co.in); [ramdhanv@hotmail.com](mailto:ramdhanv@hotmail.com)

## ABSTRACT

After the launch of INSAT-1B, India Meteorological Department installed 100 automatic Weather Stations (AWS) during 1984-85. Status of operational Automatic Weather Stations was above 60 per cent. After ten years, when life span of Automatic Weather Stations was completed, 15 state-of-art Automatic Weather Stations were procured and installed during 1996-1997. The operational status of these Automatic Weather Stations after seven years of operation is above 90 per cent.

India Meteorological Department is shortly procuring 100 state-of-art Automatic Weather Stations and they will be installed in uninhabited, remote, inaccessible areas from where data for weather forecasting, cyclone forecasting are of paramount importance. The AWS data was compared with surface observatory data, standard deviation, deviation, scattered diagrams and correlation coefficient for few stations are plotted and data quality was found within WMO accuracy limits.

Under the augmentation of surface meteorological measurements in India, it is proposed to install 500 Automatic Weather Stations in different parts of India.

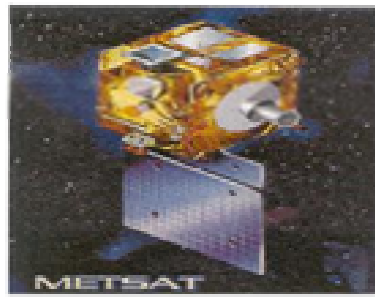
## Introduction

India Meteorological Department has been operating a network of 100 Automatic Weather Stations in India since 1984. The technology had become obsolete and after ten years of operation the old Data Collection Platforms (DCPs) now renamed as Automatic Weather Stations (AWS) were replaced with state-of-art AWS systems during 1997-98. Various meteorological parameters such as dry bulb temperature, wind speed, wind direction, relative humidity, barometric pressure and rainfall are being measured. AWS Receiving Earth Station is also located in Pune and the quality of data received from the AWS are being evaluated. The quality of data has been found to be very encouraging.

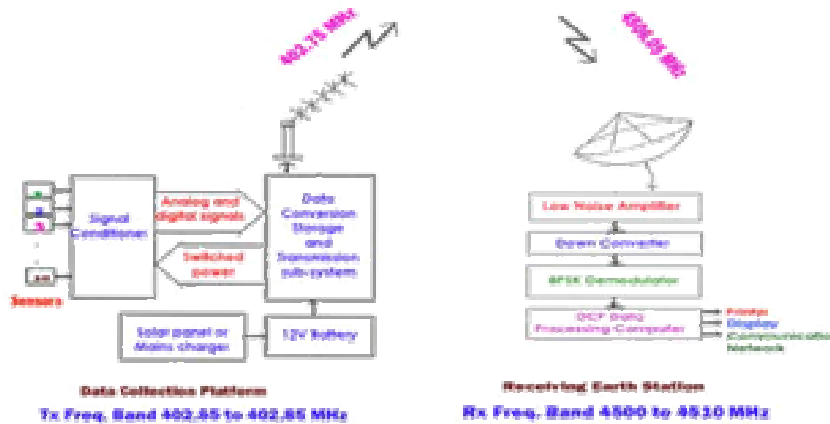
The performance of three such automatic weather stations has been evaluated in this paper by comparing the data with co-located observatory data and the results are discussed here. The overall accuracy of the data received from the AWS is found to be mostly well within the required limits specified by WMO for acceptance of data from an AWS.

## INSAT-AWS System

A typical INSAT-AWS system configuration is depicted in Fig.1. INSAT-AWS system consists of field unit, space segment and the ground segment consisting of data receiving, processing and dissemination system. Automatic Weather Station includes sensors, signal conditioning unit, digital system, transmitter and antenna unit. AWS unit is housed in a weather-proof housing.



**METSAT  
74°E RHCP**



## INSAT DATA COLLECTION SYSTEM

Fig.1 INSAT AWS System Configuration

The space segment METSAT(Kalpana-1) consists of UHF receiving antenna for 402.75 MHz, down converter (402.75 MHz to 28 MHz), filter, upconverter, amplifier and transmitting antenna. The receiving earth station at Pune consists of 3.8 meter parabolic dish antenna, low noise amplifier, down converter, Digital Direct Read Out Ground Station (DDRGS) and data processing computer.

AWS field stations automatically take environmental observations and transmit weather data at every full hour UTC at an uplink frequency of 402.75 MHz which is received by METSAT(Kalpana-1). The received signals are downconverted to 28 MHz at the satellite and then amplified and upconverted and transmitted back to Pune receiving earth station at down link frequency of 4506.05 MHz. The dish antenna of the receiving earth station receives the signal transmitted by METSAT and is amplified by low noise amplifier and downconverted to 140.95 MHz by downconverter and fed to DDRGS demodulator. The raw data is processed by the computer and hourly data of the meteorological parameters are made available and archived for further use for climatological purpose. It is also used for data validation. The weather parameters measured are air temperature, wind speed, wind direction, atmospheric pressure, relative humidity and rainfall. The data is made available to the forecasters and other users in real time through GTS network of IMD in WMO format.

### Data and methodology

AWS and surface data for 03 UTC and 12 UTC observations for two stations Dwarka and Ratnagiri along the west coast of India for the period Jan-Nov 2004 has been taken for analysis. The meteorological parameters dry bulb temperature, station level pressure and relative humidity have been taken for preparation of scatter diagrams and calculation of correlation coefficient and

standard deviation. The monthly standard deviations for the dry bulb temperature and station level pressure for the same period Jan-Nov 2004 for 03 and 12 UTC have also been compared for the stations Dwarka and Ratnagiri. AWS and Surface data for the station Chennai on the east coast of India has been compared for dry bulb temperature and station level pressure for Jan-Nov 2004 for both 03 and 12 UTC. The results have been analysed and discussed.

## Results and discussions

### a) Dwarka

Fig.2 shows the scatter diagram in respect of Dwarka for 03 and 12 UTC for dry bulb temperature, station level pressure and relative humidity for the period Jan-Nov 2004. Figs. 2(a) & (b) show the existence of a high degree of correlation between AWS Dry bulb data and surface observatory data for 03 and 12 UTC. The correlation coefficient (CC) for 03 UTC is 0.98 with a standard deviation of 0.59 °C. The CC for 12 UTC is 0.98 with a standard deviation of 0.44 °C.

Scatter diagrams for 03 UTC and 12 UTC Station Level Pressure (SLP) of Dwarka AWS site shown in Fig.2(c) & (d) also show a correlation coefficient equal to nearly 1 (0.99). Standard deviation between AWS data series and surface data series for Dwarka (Jan-Nov 2004) for 3 UTC & 12 UTC is 0.20 hPa which depict the higher dependability of pressure sensor measurements. Figs. 2(e) & (f) show the relative humidity scatter between AWS Dwarka and surface observatory data of 03 & 12 UTC for the same period. The CC for 03 UTC is 0.96 with a standard deviation of 2.59% and CC for 12 UTC is 0.98 with a standard deviation of 2.77%. The standard deviations are well within WMO accuracy limits.

### b) Ratnagiri

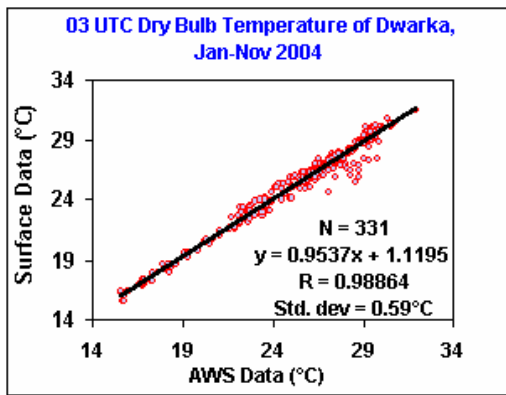
Fig. 3 shows the scatter diagrams of 03 UTC and 12 UTC of Ratnagiri AWS data and surface observatory data for period Jan-Nov 2004. The Correlation Coefficient for 03 UTC dry bulb temperature data is 0.96 with a standard deviation of 0.66 °C and CC for 12 UTC is 0.97 with a standard deviation of 0.36 °C which has been shown in Figs.3(a) & (b).

Fig.3(c) & (d) are the scatter diagrams for Ratnagiri station level pressure(SLP) which depict a near perfect correlation with a CC of 0.99 at both 03 UTC and 12 UTC. The standard deviations are 0.38 hPa and 0.25 hPa respectively for 03 & 12 UTC. Figs.3(e) & (f) for relative humidity values show a CC of 0.97 for 03 UTC & 0.98 for 12 UTC with standard deviations of 3.28% and 2.61% respectively for 03 & 12 UTC.

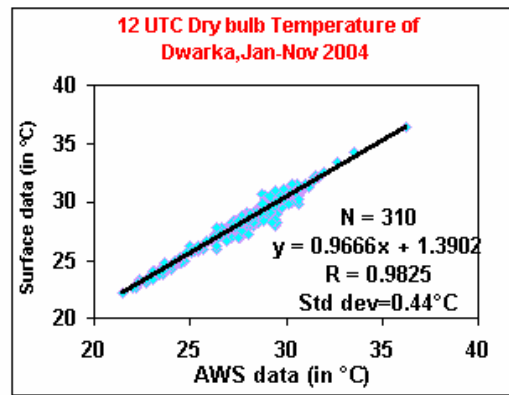
### c) Chennai

The scatter diagrams for 03 & 12 UTC station level pressure (SLP) and dry bulb temperature values have been shown in Figure 4. CC for dry bulb temperature is 0.98 and 0.99 for 03 & 12 UTC with standard deviations of 0.55 °C & 0.43 °C respectively as shown in fig 4(a) & (b). Correlation coefficient(CC) R=0.99 for both 03 & 12 UTC SLP values with standard deviations of 0.44 hPa and 0.61 hPa respectively as seen in Fig. 4(c) & (d).

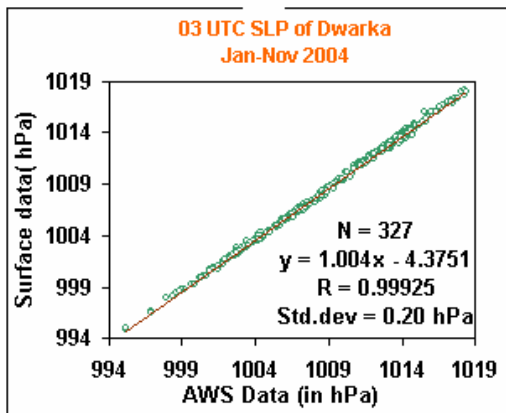
The effect of diurnal variation can be seen from the monthwise standard deviations calculated from the deviation between AWS values and surface observatory values for 03 and 12 UTC. This analysis has been done for Dwarka and Ratnagiri for the period Jan-Nov 04 and is shown in Fig.5. It is seen from fig.5(a) & (c) that 03 UTC dry bulb temperature deviations for Ratnagiri are more than 12 UTC for the entire period. In the case of Dwarka 03 UTC similar trend is observed except in the months of May-Aug where the deviations are less than 12 UTC. In the case of station level pressure the trend is shown in fig.5(b) & (d).



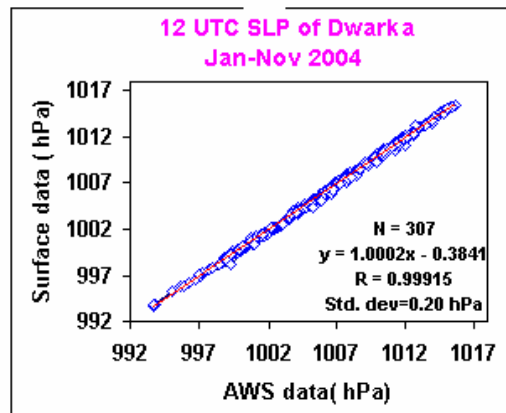
(a)



(b)



(c)



(d)

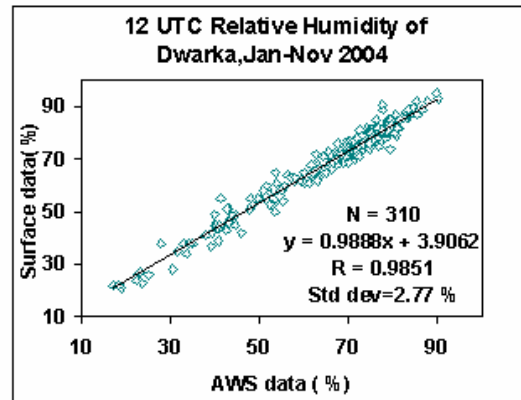
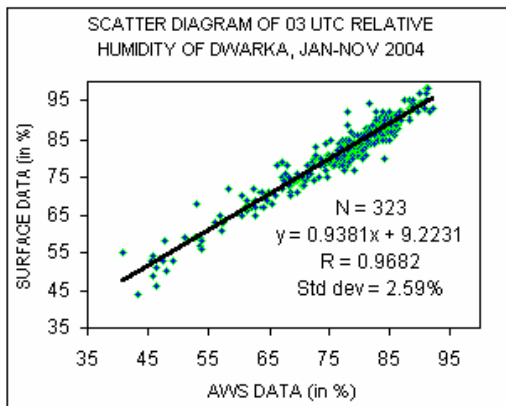


**Fig.2 Scatter diagrams of Dwarka, 03 & 12 UTC for Jan-Nov 2004**

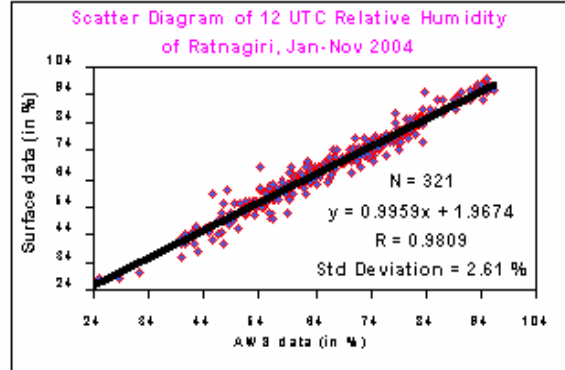
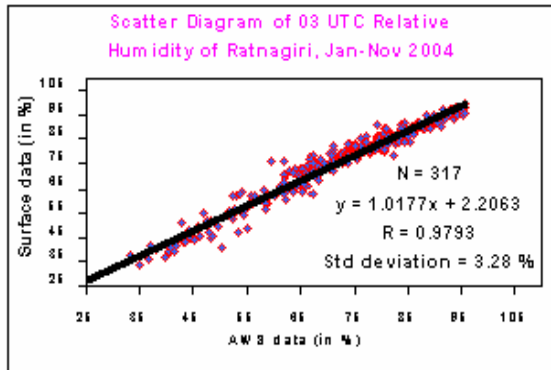
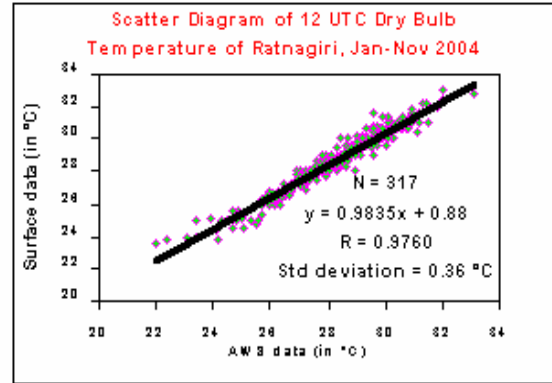
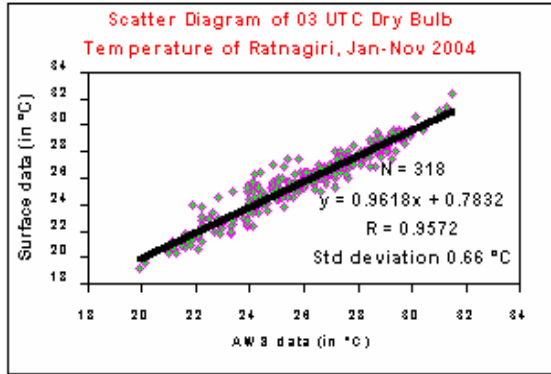
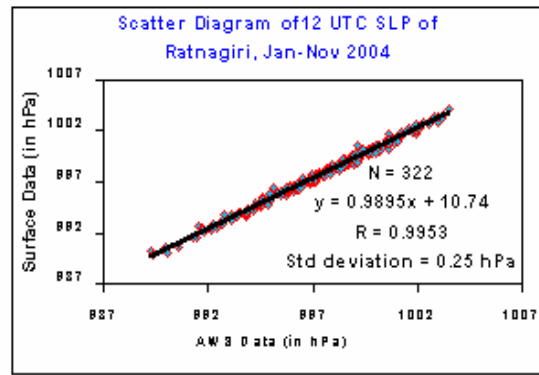
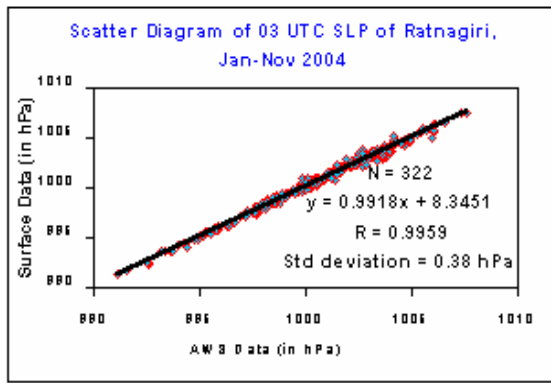
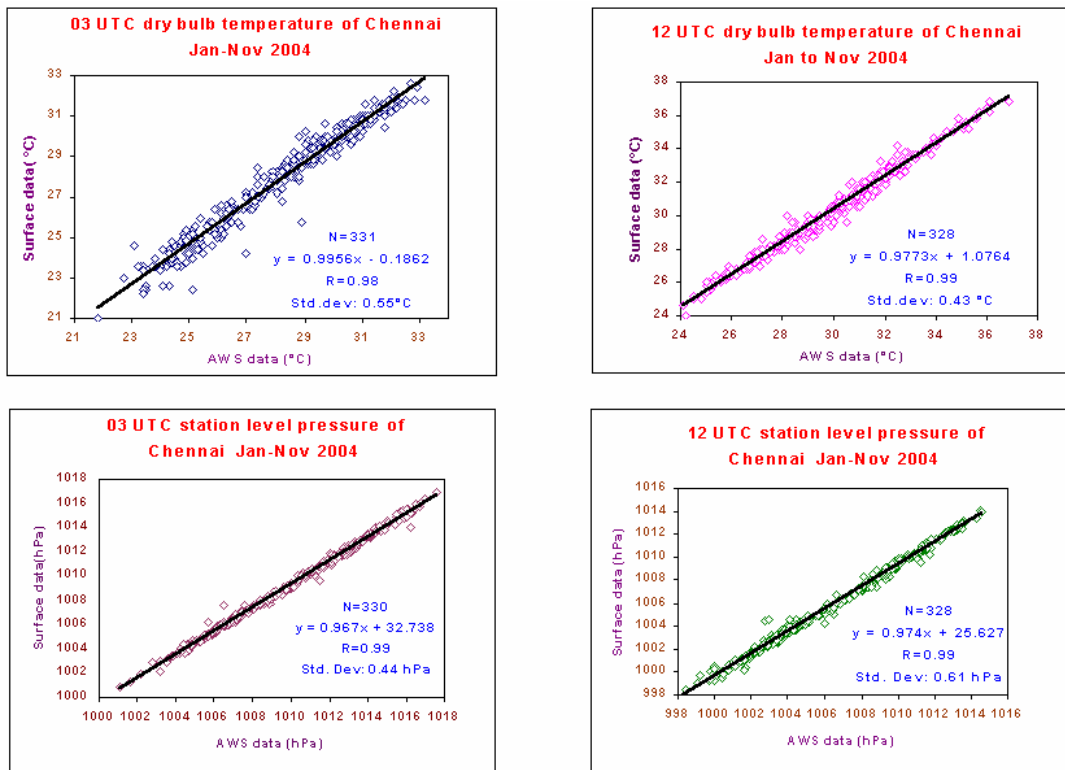
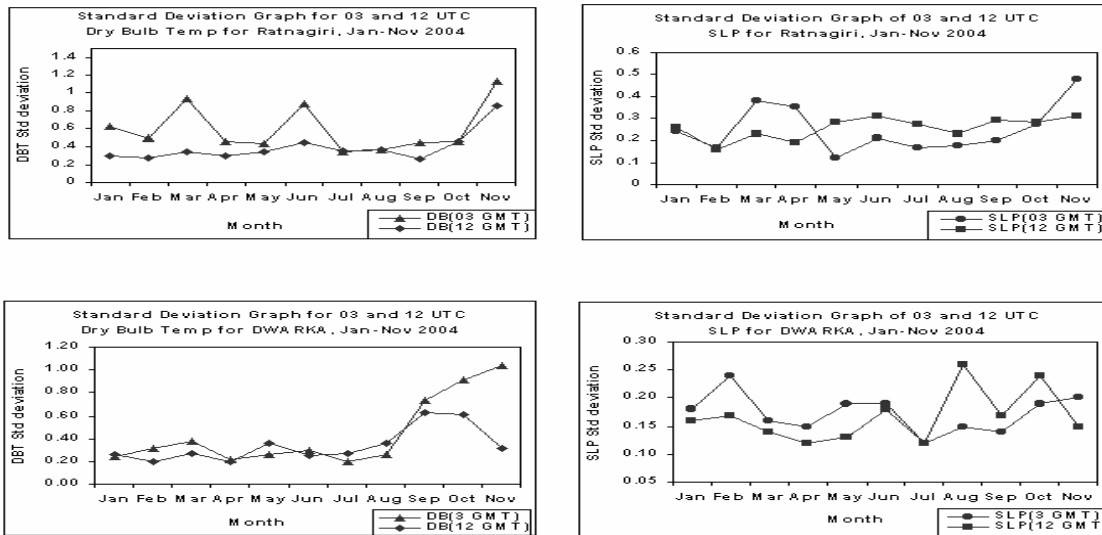


Fig.3 Scatter diagrams of Ratnagiri for 03 & 12 UTC, Jan-Nov 2004





**Fig.4 Scatter diagrams for Chennai 03 & 12 UTC, Jan-Nov 2004**



**Fig.5 Monthwise standard deviation graphs for Dwarka & Ratnagiri 03 & 12 UTC**

## Conclusion

The values of statistical parameters for series of differences are within WMO accuracy limits for automatic weather stations. Rigorous checking of data for quality control and preventive maintenance of the automatic weather stations have ensured that the data received from the AWS are of highly comparable and dependable quality. Monitoring of the data is required because of the probability of instrumental uncertainty. Corrective maintenance is required for sensor failures. The presence of a satellite based AWS data receiving earth station which monitors data from AWS at

real time plays a very important role in monitoring the network of AWS and undertaking preventive measures in the case of non-functioning of a station.

It has been also noticed that the differences in the values of meteorological parameters is due to the difference in the time of observation between a manual observation and an automatic measurement. The time of observation in a surface observatory for the entire network could never be set exactly at full hour UTC against an automatic sampling which records the values automatically at that hour without any human intervention.

All these factors have been taken into consideration and from the experience gained it is strongly felt that, AWS systems will provide accurate and timely surface meteorological data because of the full range of sophisticated sensors available, data communications options and remote maintenance monitoring capabilities. Hence it is planned to establish a wider network of automatic weather stations and automatic raingauge stations to get data from unrepresented areas of the country. This will aid in better forecasting of weather occurrences.

## References

1. Ranju Madan, M.K. Gupta and R.D. Vashistha. "Automation in measurements of surface meteorological parameters", Proceedings of TROPMET-95.
2. Vashistha R.D., M.S. Rawat and R. Pratap, "Field experiences in unmanned meteorological Data Collection Platforms". WMO Technical Conference on Instruments and Methods of observation (TECO-94).
3. WMO, 1998, "Instruments and Observing Methods", Report No. 68.
4. Vashistha R.D., and S.K. Srivastava, "Automatic Weather Stations for Collecting Meteorological Data for Urban Areas". WMO Technical Conference on Instruments and Methods of Observation (TECO-2000).
5. Vashistha R.D., S. Balachandran, R. Pratap and S.K. Dikshit, "Data Comparison between AWS and Conventional Method of Observations". Proceedings of TROPMET-2000.



# **Modernisation of Radiation Network**

by

**R.D. Vashistha & M.K. Gupta**

India Meteorological Department, Pune, India

E-mail : [ramdhanv@hotmail.com](mailto:ramdhanv@hotmail.com)

**ABSTRACT:** The network activity on radiation measurements was initiated during IGY in July, 1957 with the commissioning of 4 stations. The density of the network was gradually increased to the present level of 45 stations. The parameters measured vary from station to station, through global solar radiation is the common parameter monitored at almost all the stations. The very important components like the direct solar irradiance, diffuse solar irradiance and the net terrestrial radiant energy are not measured at many of the stations. Direct solar irradiation is measured at 21 stations whereas the diffuse irradiances are monitored at 23 locations. The net terrestrial radiant energy is measured at 12 stations only. There is no UV measurement.

With increased industrialization and its associated urbanization, the skies get increasingly loaded with both particulate matter and radiatively active gaseous matter. They have deleterious effect on radiation and thermal energy. Hence a need was felt to expand radiation measurement activities quantitatively and qualitatively.

IMD has thus drawn a very extensive plan to bring about uniform measurement of various radiation parameters through out the network. The basic parameters like direct and diffuse radiations, wherever not measured, will be introduced. Net terrestrial radiation will be uniformly recorded round the clock using latest pyrgeometers. UV-A, UV-B and UV-Total measurement will also be introduced at all the station to study the impact of climate on human health, agriculture productivity, ozone depletion etc. State-of-the-art sky scanning radiometers and sunphotometers with suitable filters will also be introduced to determine particle size distribution in the atmosphere. The data thus gathered will fill the existing gap of information in radiation measurement.

## **Introduction:**

To begin with, India started radiation measurements on a network scale from July, 1957 with a modest number of four stations viz. New Delhi, Pune, Kolkata and Chennai. All the four stations made continuous recording of global solar irradiances and instantaneous observations two times a day in the night of net terrestrial radiant energy. Besides these, New Delhi and Pune recorded the diffuse solar irradiances continuously and instantaneous direct solar irradiances in selected band pass spectral regions at the four synoptic hours during the day time (at 03, 06, 09 and 12h UT). The density of the radiation network was gradually increased over the next three decades to the present 45 stations. The increase in the network density was however not necessarily on any climatological requirements; they were started mainly to meet the requirements of different disciplines like agricultural meteorology and environmental (atmospheric pollution) studies.

## Present Status of Radiation Network

The present distribution of stations in the radiation network is given in Fig. 1. There are 21 principal and 22 ordinary stations in the network. A principal station makes continuous recording of global and diffuse solar irradiances (radiant exposure) and duration of bright hours of sunshine besides measurements of direct solar irradiances either at specified times or continuously using a solar tracker. An ordinary station has to record continuous global solar irradiation and duration of bright hours of sunshine. In the Indian radiation network there are other parameters which are also monitored. Table I gives the various parameters being recorded at different locations in the network.

### Instruments in use at the network stations:

Different types of instruments are in use in the network stations. They are:

(i)	Thermoelectric pyranometers	For global solar irradiances
(ii)	Thermoelectric pyranometers with Schüepf model shadow band	For diffuse solar irradiances
(iii)	Ångström pyr heliometer	For direct solar irradiances (including spectral)
(iv)	Thermoelectric pyr heliometer on solar tracker	For direct solar irradiances
(v)	Ångström pyrgeometer	For net terrestrial radiant energy in the nights
(vi)	Funk type net pyr radiometer	For net total radiant energy
(vii)	Sunphotometer	For optical depth
(viii)	Bimetallic pyranograph (SIAP model)	For global solar irradiances
(ix)	Bellani spherical pyranometer	For global solar irradiances
(x)	Campbell-Stokes sunshine recorder	For duration of sunshine
(xi)	Thermoelectric pyranometer	For reflected solar irradiance

### The network has the following measurements distribution:

(i)	Global solar irradiation	43 stations 38 stations use pyranometer 2 stations use bimetallic pyranograph 3 stations use Bellani pyranometer
(ii)	Diffuse solar irradiation	24 stations
(iii)	Direct solar irradiation	14 stations six times a day
(iv)	Direct solar irradiation	10 stations using solar trackers
(v)	Reflected solar irradiation	1 station
(vi)	Global solar irradiation inclined at 45° and facing south	1 station
(vii)	Net terrestrial radiant energy	12 stations
(viii)	Net total radiant energy	6 stations
(ix)	Optical depth	12 stations

Besides, several stations compute the turbidity parameters from direct solar irradiance measurements. They are:

- (i) Linke turbidity factor  $T$  – 22 stations
- (ii) Ångström turbidity coefficient  $\beta$  - 14 stations.

Fig 2 gives typical installation at one station.

Besides these 45 stations, India maintains one weather monitoring station at Maitri, Antarctica with measurements of global and diffuse solar radiation using pyranometers and of optical depth using a sunphotometer.

### **Maintenance of Network:**

The Central Radiation Laboratory of Instruments Division at Pune of India Meteorological Department has been designated as the National Radiation Centre by Government of India. It is also one of the two designated Regional Radiation Centres for Asian Region of WMO. This Laboratory maintains an hierarchy of radiation standards to ensure the reliability in the performance of the field radiation instruments. It maintains three primary standard cavity radiometers (PACRAD, HF and PMO-6) which are inter-compared regularly to ensure the stability of these instruments performances. At least one of the three participates in the 5 yearly International Pyrheliometer Comparisons held at Davos, the World Radiation Centre and also in the regional comparisons whenever they are conducted. There are transfer and working standard pyrheliometers to calibrate other pyrheliometers and all other types of instruments like pyranometers. Reference and working standard pyranometers are also maintained here and used to standardize the pyranometers which are made in the Instruments Division at Pune and which come for repairs and calibrations. Working standard pyrheliometers and pyranometers are taken out to field stations for *in situ* standardization of field instruments. The laboratory also maintains standard electrical equipment for calibrating the recording and other auxiliary equipment used in the network.

The data collected at the field stations are sent to the Climatology Division at Pune where they are subjected to 100 per cent scrutiny and then archived. Thus all efforts are being made to ensure that the data generated in the network are well within the accuracy limits specified by WMO. The data are available on payment of relevant charges. Since the majority of data are evaluated manually they are also scrutinized in the same way. This however necessitates an unavoidable delay in archival timings.

### **Limitations in the present network:**

- (i) Since the measurement programme was started to cater to the needs of different users, the parameters measured and even the instruments used for the same parameter are not necessarily uniform. Thus instruments with lower accuracy like a bimetallic pyranograph and a Bellani spherical pyranometer are still in use. The measurement of the more important parameters like direct solar irradiances and diffuse solar irradiances are made in only about half the number of network stations. The need for the use of indigenously manufactured recording equipment has also introduced different types of recorders with differing performance characteristics.
- (ii) The use of Ångström pyrheliometer limits the data to selected optical air masses, six times in a day. The use of thermopile pyrheliometers on solar trackers enables the collection of hourly and daily totals of direct solar irradiation which in turn enables the monitoring of variations in the atmospheric turbidity conditions during a day. It also enables the computation of the attenuation effected by transparent and translucent cloudy and hazy sky conditions. But pyrheliometers on solar

trackers are available at ten stations only. Further Ångström pyrhemometers can be used under cloudless sky conditions only. In addition hourly or even shorter interval atmospheric transparency conditions can not be deduced from these Ångström pyrhemometers.

- (iii) The measurement of net terrestrial radiant energy is of vital requirement as all living beings are permanently immersed in the field of terrestrial radiant energy. Further it is the immediate trigger in the physics of the atmosphere in the boundary layer, causing changes in the weather conditions at the place. This important parameter is measured only instantaneously two times, that too in the night time only because of the use of Ångström pyrhemometers. This instrument, by construction principles can not be used during the day. And this measurement is made at 12 stations only.
- (iv) The atmospheric turbidity parameter, viz. the optical depth is measured using a sunphotometer at 12 stations. The sunphotometer used for the purpose is of an early technology using only a microammeter. The stations which use them are background air pollution monitoring stations. Of these Pune, Nagpur and Visakhapatnam no more qualify to serve as reference stations due to high incidence of atmospheric pollution over these stations.
- (v) A very vital part of the electromagnetic spectrum viz. ultra violet irradiances are not being measured in the network. This is a major lacuna in the network programme. Another important parameter not measured is the daylight illumination, though it is a difficult parameter to monitor.
- (vi) Two parameters, reflected solar irradiance and net total radiant energy are measured at one and six stations respectively. These are extremely important for any study involving albedo and in agricultural sciences. However, these measurements need open spaces at ground level and hence it may not be feasible within the scope of the present network.
- (vii) The radiation data are being collected on potentiometric recorders and extracted by manual evaluation. This introduces a certain subjectivity in the estimated values from the recorded charts. Though the data thus extracted undergo a hundred per cent scrutiny at the station itself and again in the Climatology Division before they are archived, the subjectivity element can not be eschewed totally.

### **Perspective plans for modernization:**

The need for modernization of the network measurement methodology requires no stress. Fig. 3 gives the futuristic network proposals. Some of the salient features will be:

1. The sensors for global, diffuse or reflected irradiances will be made uniform by the use of same detector principles. All the bimetallic pyranographs and spherical pyranometers are to be replaced by thermoelectric pyranometers preferably with provisions for temperature compensation.
2. The present Schüepf model or for that matter, any diffuse shading band (ring device) are made using a basic assumption, viz. the scattering processes is isotropic. It is well known that the scattering process is anisotropic even on cloud

free sky conditions. The process becomes more complicated in the presence of clouds. The diffuse irradiances are therefore to be monitored using a shading disc. Then there is no need for the computation of corrections in the irradiances based on assumptions.

3. Ångström pyrheliometers are capable of very high accuracy and actually they are treated as secondary standards. They can not however be used for continuous measurements of direct solar irradiances. The network Ångström pyrheliometers are therefore being replaced by the use of thermoelectric pyrheliometers which can be mounted on suitable solar trackers as is being done at present at ten stations. This would also ensure the continuous monitoring of direct solar irradiances and enable the computations of hourly turbidity parameters for the entire network stations.
4. The net terrestrial radiant energy is being measured only two times instantaneously during the night times. This parameter is of utmost importance. Modern solar blind pyrgeometers are to be installed at each of the 45 stations and continuous recording of the parameter is to be made. Unlike net pyrradiometers these do not need installations in the open field and hence can be installed at the pyranometer site itself.
5. The single filter sunphotometers would be replaced by narrow band multispectral sunphotometers with necessary self-computing software. They are to be provided at 24 stations which need not be background stations. Thus the optical depth measurements due to some of the important attenuating constituents of the atmosphere can be monitored with great ease and accuracy.
6. State of the art sky scanning radiometers with dedicated software would be introduced at selected 21 stations so the variations in the particle size distribution in the atmosphere can be studied and used in the environmental control applications.
7. One of the most important parameters to be monitored is the ultra violet irradiance which have far reaching consequences on the health of all living beings including the humans. With the industrial developments and consequent urbanization taking place, the possibility of damages to the delicate balance of the ozone concentrations is great, which may result in higher dosages of the incident ultraviolet radiant energy. Besides, their applications in physiological, biological, dyeing and textile fields are great. It is proposed to measure total UV, UV-A and UV-B at all the radiation stations.
8. At present, the recording of radiation data is generally being made using potentiometric recorders. At some places the galvanometric recorders are still in use. These recorders are being phased out with the latest designs of data loggers. The use of data loggers also ensures a better objectivity in data collection and higher reliability.
9. It is also envisaged to utilize satellite link facilities so that the data can be made available at the National Radiation Centre without any delay. It will also ensure to keep a check on the health of every instrument at each station from Pune by the Central Radiation Laboratory.

10. Central Radiation Laboratory also has to undergo modifications to meet the above needs.
- (a) A data acquisition system is being planned for the intercomparison of standard pyrheliometers and for the calibration of field pyrheliometers.
  - (b) A Laboratory calibration facility for the calibration of pyranometers for their characteristics is being organized. With this established, it would be possible to determine the cosine error, tilt error, temperature and spectral responses and linearity of pyranometers in the Laboratory.
  - (c) The installation of the UV-VIS-NIR spectrophotometer and another of IR spectrophotometer is to be done for carrying out various checks on filters, painted surfaces etc.
  - (d) A good and reliable calibration facility in infrared wavelengths for pyrgeometers and net pyrradiometers is to be established.
  - (e) Establishing a photometric calibration facility for illumination measurements is also being planned.
  - (f) Similarly the calibration of UV measuring instruments using double monochromators and if possible a Brewer Spectrophotometer is to be planned and organized.

It is envisaged that the entire activity of radiation data collection in India will be completely modernized in the next 3 to 4 years.



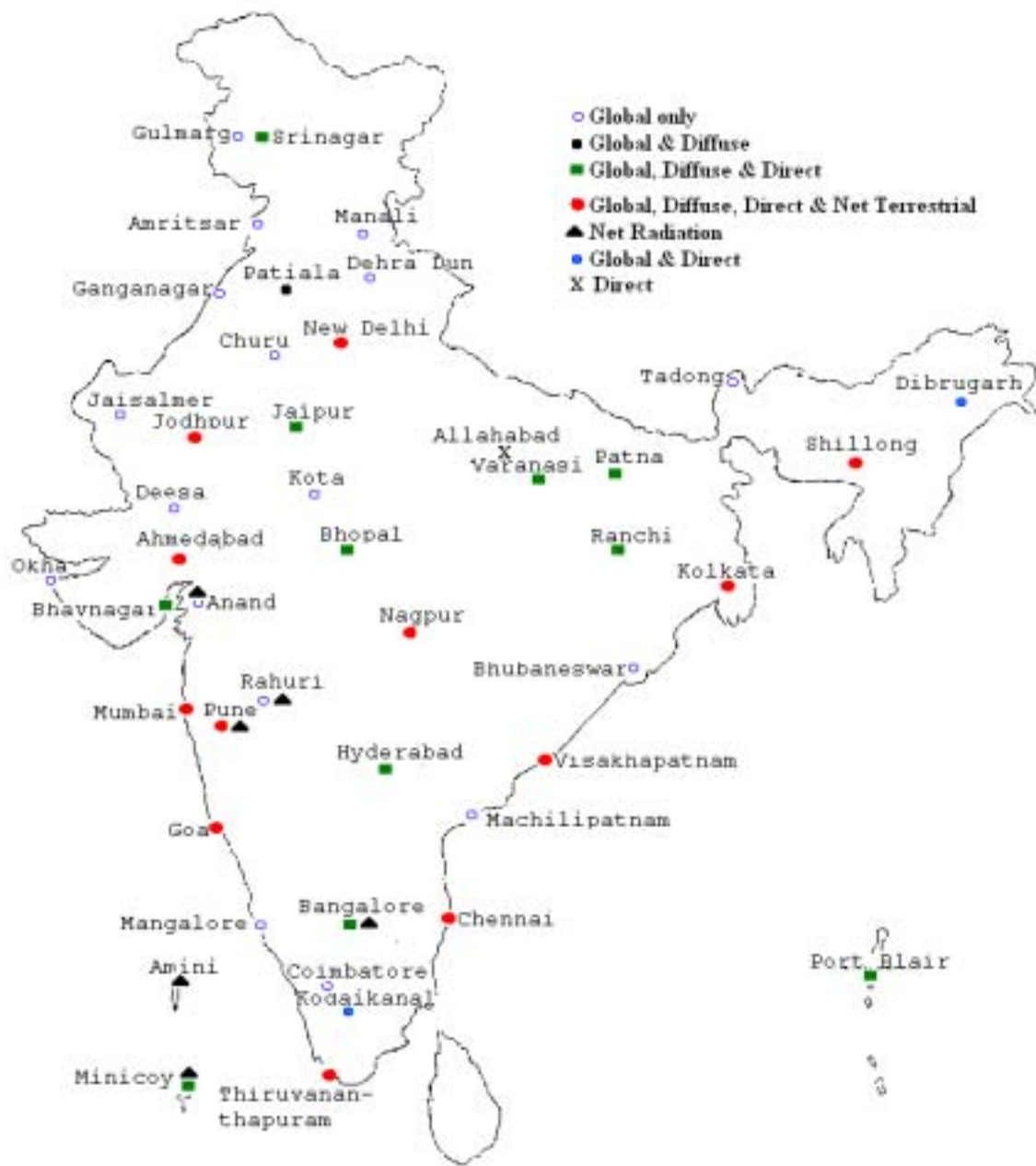


**Fig 1: Existing radiation network**



**Fig 2: Radiation site at Varanasi**

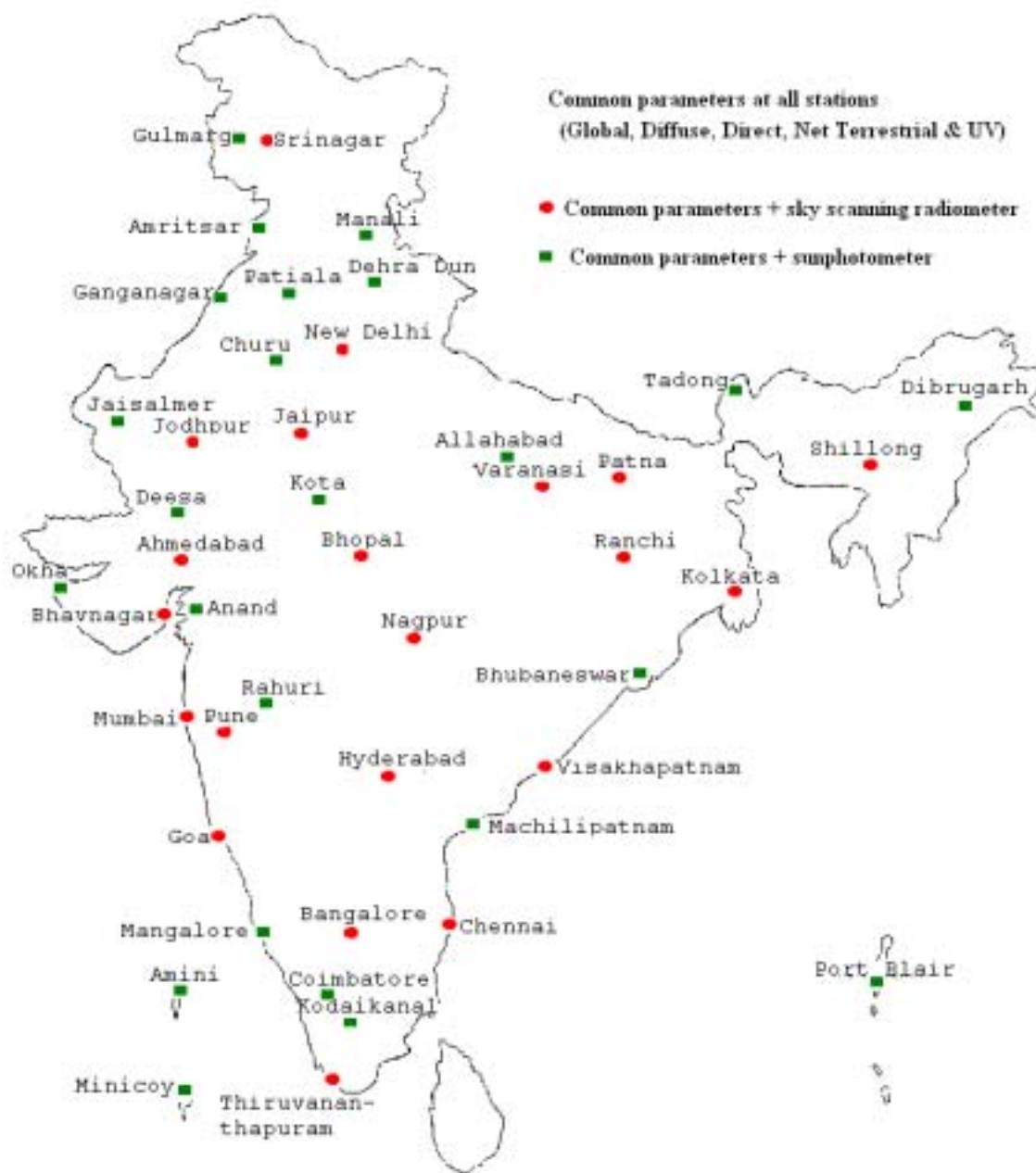


**Fig. 3: Futuristic radiation network**

**Table 1. Details of radiation measurements at the existing network stations of IMD**

S.No.	Station Name	Global Irradiance (Pyranometer)	Diffuse Irradiance (Pyranometer)	Direct Irradiance (Pyrheliometer)	Optical Depth (Sun photometer)	Net Terrestrial radiation (Ångström Pyrgeometer)	Net radiant energy (Net Pyradiometer)	Upper air net radiant energy
<b>Principal Station</b>								
1	Ahmedabad	✓	✓	Ångström		✓		
2	Bangalore	✓	✓	Thermopile				
3	Bhavnagar							
4	Bhopal	✓	✓	Thermopile				
5	Mumbai	✓	✓	Ångström		✓		
6	Kolkata	✓	✓	Ångström		✓		✓
7	Goa	✓	✓	Ångström		✓		
8	Hyderabad	✓	✓	Thermopile				
9	Jaipur	✓	✓	Thermopile				
10	Jodhpur	✓	✓	Ångström	✓	✓		✓
11	Chennai	✓	✓	Ångström		✓		
12	Nagpur	✓	✓	Ångström	✓	✓		✓
13	New Delhi	✓	✓	Ångström & Thermopile	✓	✓		✓
14	Patna	✓	✓	Thermopile				
15	Pune	✓	✓	Ångström	✓	✓	✓	✓
16	Ranchi	✓	✓	Thermopile				
17	Shillong	✓	✓	Ångström		✓		
18	Srinagar	✓	✓	Thermopile	✓			✓
19	Thiruvananthapuram	✓	✓	Ångström & Thermopile		✓		✓
20	Varanasi	✓	✓	Thermopile	✓			
21	Visakhapatnam	✓	✓	Ångström	✓	✓		
22	Amritsar	✓						

S.No.	Station Name	Global Irradiance (Pyranometer)	Diffuse Irradiance (Pyranometer)	Direct Irradiance (Pyrheliometer)	Optical Depth (Sun photometer)	Net Terrestrial radiation (Ångström Pyrgeometer)	Net radiant energy (Net Pyradiometer)	Upper air net radiant energy
23	Anand	✓					✓	
24	Bangalore A.R.U.	✓					✓	
25	Bhubaneshwer	✓						✓
26	Dehradun	✓						
27	Gulmarg							
28	Jaisalmer	✓						
29	Kodaikanal	✓		Ångström	✓			
30	Kota	✓						
31	Machilipatnam	✓						
32	Manali	✓						
33	Mangalore	✓						
34	Minicoy	✓	✓		✓		✓	
35	Mohan Bari	✓			✓			
36	Okha	✓						
37	Patiala	✓	✓					
38	Port Blair	✓	✓		✓			
39	Rahuri	✓					✓	
40	Tadong	✓						
41	Allahabad				✓			
42	Amini						✓	
43	Churu							
44	Coimbatore	✓						
45	Deesa	✓						
46	Sri Ganganagar	✓						

# RAIN INTENSITY GAUGE WITH NO MOVING PARTS

## NEW NEEDS

- Global warming causes changes in distribution of rainfall
- Arid, irrigated, agriculture needs more data on available rain
- Municipal authorities need rain-information for drainage management
- Flood control authorities need quickly available rain data
- Manual servicing of meteorological stations has become expensive

## NEW POSSIBILITIES

- Embedded controllers have become very competent
- Solid state sensors have become less expensive

## MODERN RAIN INTENSITY GAUGES SHOULD BE:

- Inexpensive
- Robust
- Easily maintainable
- Connectible to any logger

## THE MAD-MET LTD. NEW RAIN INTENSITY GAUGE (PATENT APPLIED FOR) EASILY COMPLIES WITH THESE NEEDS.

Field instrumentation for measuring rain intensity should minimize dependence on sensitive components. Moving parts, such as tipping buckets, very often necessitate periodic calibration at least and also removal of debris, colonizing insects and dust accumulation whenever regular functioning is hampered. Manpower suitable for periodic checks of deployed instrumentation is getting more and more scarce and expensive.

On the other hand, data flow patterns and output types have gradually become standardized in order to fit data acquisition systems such as loggers and other computerized data transmission and backup setups.

We therefore propose a novel rain intensity gauge (patent applied for), which has no moving parts. Its response is linear over a range of rain intensities wider than that of the best tipping bucket instruments, its resolution is better than

the usual and its output is a regular pulse train with frequency proportional to rain intensity.

For special purposes our instrument's characteristics can be changed, using software only, without electrical or mechanical manipulation, in order to accommodate especially high or very low rain intensities.

Our instrument's prototype has been extensively tested in the laboratory using a precision peristaltic pump water-delivery system and a computerized pulse-recording setup. It has also been field-tested and has clearly outperformed 2 different commercial tipping bucket gauges.

The size of our gauge is determined largely by WMO recommendations concerning input funnel sizes and proportions. Space needed for other components is relatively small.

**Electrical consumption:**  
8-12V at < 50mA

**Output**

> 10msec, 5V pulse train (software adjustable)

**Sensitivity**

> 0.2mm rain per pulse (software adjustable)

**Connections**

> 3 conductor cable

8-12V

(input)

Ground

(common)

Signal

(output)

## THIS RAIN INTENSITY GAUGE IS OFFERED FOR EITHER:


- Purchase of full manufacturing rights
- Distribution agreement for manufactured units.

## CONTACT ↘

Mad-Met Ltd. / 13, Sderot Chen / Tel Aviv 64071 / Israel

Voice: +972 3 620 9031 / +972 3 540 7765 / Fax: +972 3 620 9098 / +972 3 549 2533

Email: dovy@bezeqint.net




Balnea Aer Rome Centre of  
Atmospheric Experimentation

## Chemical analysis of meteoric wet atmospheric deposition. Comparison between daily and weekly precipitation samples.

**G. CASU, L. FALASCONI, F. FOTI, R. LAMAGNA, F. MALASPINA, E. VUERICH**

**R.S.M.A., Vigna di Valle, Rome, Italy**



Italian Air Force

### Introduction

In the work of the Meteorological Centre of Vigna di Valle (Italy), site of the R.S.M.A., 20 years' experience in meteorological measurement has been enriched by "atmospheric wet deposition collection", of which one working from 1995 and dedicated to the collection of weekly precipitation samples and the other working from 2007 to collect daily precipitation samples.

In the same Centre is located a Chemical Laboratory that carries out the chemical analysis of meteoric wet atmospheric precipitation, within an international group of the IAGI (International Association of Geographical and Meteorological Observations) called I.A.M. (Italian Association of Meteorological Observations) and that includes, between the others, the previous program called BALNEO AER (Bologna, Monitoring Network, started from 1975 and then the G.A.M. for the main goal to realize quantification of patterns and trends in the composition of atmospheric precipitation at global and regional scales, to identify global processes of acid-deposition and to establish long-range transport from remote source areas and to provide the information for modelling effect of acid deposition on forest vegetation and for developing countermeasures).

The comparison of such activity, from July 2007, a limited period of experimentation begins to evaluate the practical data characteristic in the two types of sampling and to measure the differences found in terms of acidity and other chemical parameters and to use the wetting period as the precipitation.

Based on a simple model, with a pH of around 5.4. This model is a result of laboratory studies on the  $\text{CO}_2$  which describes the water vapour in the atmosphere.

$$\text{CO}_2 + \text{H}_2\text{O} \rightleftharpoons \text{H}_2\text{CO}_3 \rightleftharpoons \text{HCO}_3^- + \text{H}^+$$

So, when the pH level of meteoric precipitation is considered and one:

Because acidity is due to the sum of total acids in water drops, result as the release of sulfur dioxide ( $\text{SO}_2$ ) and nitrous oxide ( $\text{NO}_2$ ), also the presence of these "strong acids" can be due to the decrease of alkalinity before coming back down to earth in the form of dry particles and precipitation.



Underneath is the interaction  $\text{CO}_2$  and  $\text{H}_2\text{O}$ , that only water vapour forms and, presence of water and without acid.

$$\text{pH}_1 + \text{pH}_2 = \text{pH}_{\text{TOT}}$$

$$\text{pH}_1 + \text{pH}_2 = \text{pH}_{\text{TOT}}$$

### Sample collection, storage and analytical procedures

The daily sampling (weekly samples) has been carried out in the meteorological station (770 gpa @ Vigna di Valle - Lat. 42° 41' - Long 12° 17' - Sea level 100 m) in the mountain forest (the forest area is about 400 ha) and the forest is a highly wooded mountain forest (the forest area is about 400 ha).



The two METEOROLOGICAL stations weekly precipitation collectors are placed approximately 1000 meters apart and collect the rain in different directions.

Work procedures in sample collection: collected each 10 minutes starting at 08:00. The collected water samples are placed in clean plastic bottles (100 ml) and daily acid precipitation is collected in the same bottles. The bottles are placed in the open field at the time of precipitation. For an acid, to reduce the possibility of contamination of samples in the laboratory, immediately after receipt of the samples, they have to be stored in a refrigerator (4°C) until the analysis. The bottles and acid samples were stored in the analytical laboratory of the R.S.M.A. of Vigna di Valle.

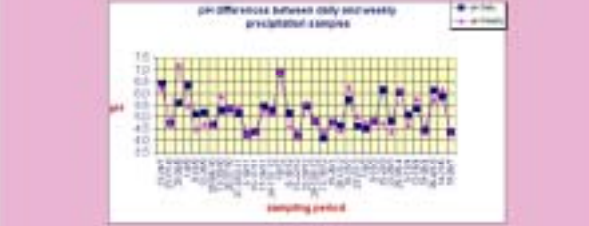


ANALYTICAL LABORATORY OF R.S.M.A. The analytical laboratory is equipped with the following instruments: pH-meter, titration apparatus, spectrophotometer, etc. The laboratory is located in the R.S.M.A. of Vigna di Valle.

ANALYTICAL LABORATORY OF R.S.M.A. The analytical laboratory is equipped with the following instruments: pH-meter, titration apparatus, spectrophotometer, etc. The laboratory is located in the R.S.M.A. of Vigna di Valle.

Parameter/Parameter	Method	Equipment
pH	Titrimetric	glass electrode
Sulfate	Turbidimetric	turbidimeter
Nitrate	Titrimetric	titration apparatus
$\text{SO}_4^{2-} + \text{NO}_3^-$	As above	titration apparatus
$\text{NO}_2^- + \text{NO}_3^-$	As above	titration apparatus
$\text{NO}_2^-$	Spectrophotometric	spectrophotometer

### Results



### Conclusions

In the work the meteorological and chemical data of an about a period of experimentation (started in July 2007) at the meteorological station of Vigna di Valle are shown. They're focused to comparison of analysis of chemical data carried out by meteoric precipitation samples, collected weekly and daily. When the experimentation will be concluded, this work would have to compare the two sampling data and to discriminate every event that have brought acidity from those that have done with "acid effect" acid, at the same time, to be able to associate these phenomena at a meteorological specific situation.

This study comes from the opportunity of having in the same site two complete meteorological stations: the chemical laboratory is responsible of collected samples analysis, of successive daily analytical calibration and statistic elaboration.

It has to be noted in the context of atmospheric pollution monitoring activity and therefore also of analysis carried out by "OSVP", which the A.M. is member of since 1977, managing a net of collection stations, that also comprises the site of Vigna di Valle (from 1996). Finally, through pH diagnosis and other chemical-physical parameters, it's possible to represent a first indication emerged from the analysis of two different kind of samples collected, and also it's possible make a relation about differences and future perspectives of this experimentation.

\*Consiglio Nazionale delle Ricerche  
\*\*Università Europea di Roma  
\*\*\*Aeronautica Militare Italiana, ReSMA



## Automatic Cloud-Coverage Evaluation by a Ground Based, Total-Sky Camera

C.Rafanelli<sup>o</sup>, G. Casagrande<sup>o\*\*o</sup>, E. Piervitali<sup>o</sup>  
G.Casu<sup>o\*</sup>, F. Malaspina<sup>o\*\*</sup>, F. Foti<sup>o\*\*</sup>, E. Vuerich<sup>o\*\*</sup>

<sup>\*</sup> Consiglio Nazionale delle Ricerche <sup>\*\*</sup> Università Europea di Roma <sup>\*\*</sup> Aeronautica Militare Italiana, ReSMA

### Introduction

We have developed an image-processing procedure to obtain an automatic cloud-coverage evaluation. Images to be analyzed are captured by a ground-based digital camera, equipped with fish-eye lenses. The images are in the visible-light spectrum; the cloud-coverage evaluation is performed taking into account RGB and Hue parameters. By setting appropriate RGB values the algorithm provides for the discrimination of different colors, separating typical cloud palettes from those of the clear-sky. When a solar flare is present in the picture, it can be recognized and isolated by setting an appropriate Hue demarcation value.

This algorithm has been implemented in a JAVA program, which was then tested against a series of 502 images. The program output, expressed in octaves of coverage, was verified by comparison with cloud coverage evaluations made by three, independent human observers on the same images set. The automatic system accuracy proved higher than the human operators' one throughout the entire image series.

### Method

The system is composed of software algorithms that to a computer when software should periodically "capture" images of the entire sky area. The main software module is the so-called Local Cloud Module (LCM), which is designed to manage other modules by which the system is operated. The software modules which constitute the main sky camera will capture an image. Despite its recording time, appropriate frame acquisition (frame capture) is achieved.

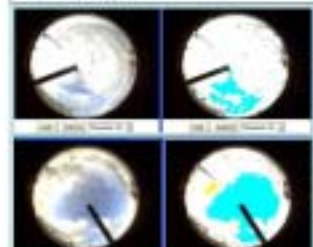
The file is then opened by the Image Processing Module (IPM), which performs the evaluation of cloud coverage. The resulting values are given as a percentage of coverage. The system also provides for the recognition of solar flares, i.e. of images captured when the Sun has also been observed through appropriate interface modules, as called "Flare Image Module" (FIM). This can be implemented by remote control of another by user information dissemination system.



**Image File (IF)**  
The image file (IF) is a 24-bit color image (24-bit color) with a resolution of 1024x1024 pixels. The image is captured by the camera and stored in a file format compatible with the operating system.

**Image File Conversion (IFC)**  
The image file (IF) is converted into a format compatible with the operating system. The conversion is performed by the IFC module, which also performs the necessary operations to ensure the correct functioning of the system.

**Image File Processing (IFP)**  
The image file (IF) is processed by the IPM module, which performs the evaluation of cloud coverage. The resulting values are given as a percentage of coverage. The system also provides for the recognition of solar flares, i.e. of images captured when the Sun has also been observed through appropriate interface modules, as called "Flare Image Module" (FIM). This can be implemented by remote control of another by user information dissemination system.



**Cloud Coverage Evaluation**  
The cloud coverage evaluation is performed by the IPM module, which uses the RGB and Hue parameters to discriminate between different cloud types. The resulting values are given as a percentage of coverage.

**Solar Flare Detection**  
The solar flare detection is performed by the FIM module, which uses the Hue parameter to identify the presence of a solar flare in the image. The resulting values are given as a percentage of coverage.

### Conclusions

The purpose of the experiment was to verify the feasibility of an automatic cloud-coverage evaluation system which could replace a human operator for continuous observations in marginal environments. Such a system could have several applications in meteorology and in environmental sciences as well: a measure of cloud coverage could indeed be correlated with solar radiation assessment in local area expedition analysis. The tested device can be coupled with traditional instruments, either as a stand-alone system or as part of a wider network, for wider-area-data-processing.

The performed tests have shown that not only the system itself is feasible, but also that it can be more reliable, under normal conditions, than standard routine observations made by operators.

### Results

**Measurements**

Timing image (00:00:00) to (00:00:01)  
Size: 1024 x 1024 pixels  
Format: RGB

Alt: 40.78 N  
Lon: 12.12 E  
Az: 279.6

**Tested image (00:00:00) to (00:00:01)**

Cloud coverage: 100%

**Tested image (00:00:01) to (00:00:02)**

Cloud coverage: 100%

**Tested image (00:00:02) to (00:00:03)**

Cloud coverage: 100%

**Tested image (00:00:03) to (00:00:04)**

Cloud coverage: 100%

**Tested image (00:00:04) to (00:00:05)**

Cloud coverage: 100%

**Tested image (00:00:05) to (00:00:06)**

Cloud coverage: 100%

**Tested image (00:00:06) to (00:00:07)**

Cloud coverage: 100%

**Tested image (00:00:07) to (00:00:08)**

Cloud coverage: 100%

**Tested image (00:00:08) to (00:00:09)**

Cloud coverage: 100%

**Tested image (00:00:09) to (00:00:10)**

Cloud coverage: 100%

**Tested image (00:00:10) to (00:00:11)**

Cloud coverage: 100%

**Tested image (00:00:11) to (00:00:12)**

Cloud coverage: 100%

**Tested image (00:00:12) to (00:00:13)**

Cloud coverage: 100%

**Tested image (00:00:13) to (00:00:14)**

Cloud coverage: 100%

**Tested image (00:00:14) to (00:00:15)**

Cloud coverage: 100%

**Tested image (00:00:15) to (00:00:16)**

Cloud coverage: 100%

**Tested image (00:00:16) to (00:00:17)**

Cloud coverage: 100%

**Tested image (00:00:17) to (00:00:18)**

Cloud coverage: 100%

**Tested image (00:00:18) to (00:00:19)**

Cloud coverage: 100%

**Tested image (00:00:19) to (00:00:20)**

Cloud coverage: 100%

**Tested image (00:00:20) to (00:00:21)**

Cloud coverage: 100%

**Tested image (00:00:21) to (00:00:22)**

Cloud coverage: 100%

**Tested image (00:00:22) to (00:00:23)**

Cloud coverage: 100%

**Tested image (00:00:23) to (00:00:24)**

Cloud coverage: 100%

**Tested image (00:00:24) to (00:00:25)**

Cloud coverage: 100%

**Tested image (00:00:25) to (00:00:26)**

Cloud coverage: 100%

**Tested image (00:00:26) to (00:00:27)**

Cloud coverage: 100%

**Tested image (00:00:27) to (00:00:28)**

Cloud coverage: 100%

**Tested image (00:00:28) to (00:00:29)**

Cloud coverage: 100%

**Tested image (00:00:29) to (00:00:30)**

Cloud coverage: 100%

**Tested image (00:00:30) to (00:00:31)**

Cloud coverage: 100%

**Tested image (00:00:31) to (00:00:32)**

Cloud coverage: 100%

**Tested image (00:00:32) to (00:00:33)**

Cloud coverage: 100%

**Tested image (00:00:33) to (00:00:34)**

Cloud coverage: 100%

**Tested image (00:00:34) to (00:00:35)**

Cloud coverage: 100%

**Tested image (00:00:35) to (00:00:36)**

Cloud coverage: 100%

**Tested image (00:00:36) to (00:00:37)**

Cloud coverage: 100%

**Tested image (00:00:37) to (00:00:38)**

Cloud coverage: 100%

**Tested image (00:00:38) to (00:00:39)**

Cloud coverage: 100%

**Tested image (00:00:39) to (00:00:40)**

Cloud coverage: 100%

**Tested image (00:00:40) to (00:00:41)**

Cloud coverage: 100%

**Tested image (00:00:41) to (00:00:42)**

Cloud coverage: 100%

**Tested image (00:00:42) to (00:00:43)**

Cloud coverage: 100%

**Tested image (00:00:43) to (00:00:44)**

Cloud coverage: 100%

**Tested image (00:00:44) to (00:00:45)**

Cloud coverage: 100%

**Tested image (00:00:45) to (00:00:46)**

Cloud coverage: 100%

**Tested image (00:00:46) to (00:00:47)**

Cloud coverage: 100%

**Tested image (00:00:47) to (00:00:48)**

Cloud coverage: 100%

**Tested image (00:00:48) to (00:00:49)**

Cloud coverage: 100%

**Tested image (00:00:49) to (00:00:50)**

Cloud coverage: 100%

**Tested image (00:00:50) to (00:00:51)**

Cloud coverage: 100%

**Tested image (00:00:51) to (00:00:52)**

Cloud coverage: 100%

**Tested image (00:00:52) to (00:00:53)**

Cloud coverage: 100%

**Tested image (00:00:53) to (00:00:54)**

Cloud coverage: 100%

**Tested image (00:00:54) to (00:00:55)**

Cloud coverage: 100%

**Tested image (00:00:55) to (00:00:56)**

Cloud coverage: 100%

**Tested image (00:00:56) to (00:00:57)**

Cloud coverage: 100%

**Tested image (00:00:57) to (00:00:58)**

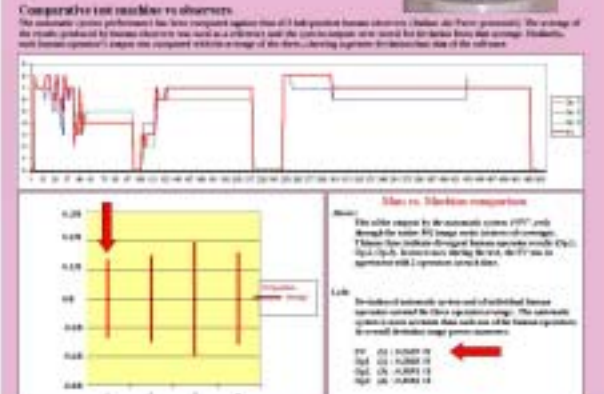
Cloud coverage: 100%

**Tested image (00:00:58) to (00:00:59)**

Cloud coverage: 100%

**Tested image (00:00:59) to (00:01:00)**

Cloud coverage: 100%



**Automatic System Results**

The purpose of the experiment was to verify the feasibility of an automatic cloud-coverage evaluation system which could replace a human operator for continuous observations in marginal environments. Such a system could have several applications in meteorology and in environmental sciences as well: a measure of cloud coverage could indeed be correlated with solar radiation assessment in local area expedition analysis. The tested device can be coupled with traditional instruments, either as a stand-alone system or as part of a wider network, for wider-area-data-processing.

The performed tests have shown that not only the system itself is feasible, but also that it can be more reliable, under normal conditions, than standard routine observations made by operators.

**Automatic System Results**

Type of Value	By cloud
Time (00:00:00) to (00:00:01)	+100,000,000
Time (00:00:01) to (00:00:02)	+100,000,000
Time (00:00:02) to (00:00:03)	+100,000,000
Time (00:00:03) to (00:00:04)	+100,000,000
Time (00:00:04) to (00:00:05)	+100,000,000
Time (00:00:05) to (00:00:06)	+100,000,000
Time (00:00:06) to (00:00:07)	+100,000,000
Time (00:00:07) to (00:00:08)	+100,000,000
Time (00:00:08) to (00:00:09)	+100,000,000
Time (00:00:09) to (00:00:10)	+100,000,000
Time (00:00:10) to (00:00:11)	+100,000,000
Time (00:00:11) to (00:00:12)	+100,000,000
Time (00:00:12) to (00:00:13)	+100,000,000
Time (00:00:13) to (00:00:14)	+100,000,000
Time (00:00:14) to (00:00:15)	+100,000,000
Time (00:00:15) to (00:00:16)	+100,000,000
Time (00:00:16) to (00:00:17)	+100,000,000
Time (00:00:17) to (00:00:18)	+100,000,000
Time (00:00:18) to (00:00:19)	+100,000,000
Time (00:00:19) to (00:00:20)	+100,000,000
Time (00:00:20) to (00:00:21)	+100,000,000
Time (00:00:21) to (00:00:22)	+100,000,000
Time (00:00:22) to (00:00:23)	+100,000,000
Time (00:00:23) to (00:00:24)	+100,000,000
Time (00:00:24) to (00:00:25)	+100,000,000
Time (00:00:25) to (00:00:26)	+100,000,000
Time (00:00:26) to (00:00:27)	+100,000,000
Time (00:00:27) to (00:00:28)	+100,000,000
Time (00:00:28) to (00:00:29)	+100,000,000
Time (00:00:29) to (00:00:30)	+100,000,000
Time (00:00:30) to (00:00:31)	+100,000,000
Time (00:00:31) to (00:00:32)	+100,000,000
Time (00:00:32) to (00:00:33)	+100,000,000
Time (00:00:33) to (00:00:34)	+100,000,000
Time (00:00:34) to (00:00:35)	+100,000,000
Time (00:00:35) to (00:00:36)	+100,000,000
Time (00:00:36) to (00:00:37)	+100,000,000
Time (00:00:37) to (00:00:38)	+100,000,000
Time (00:00:38) to (00:00:39)	+100,000,000
Time (00:00:39) to (00:00:40)	+100,000,000
Time (00:00:40) to (00:00:41)	+100,000,000
Time (00:00:41) to (00:00:42)	+100,000,000
Time (00:00:42) to (00:00:43)	+100,000,000
Time (00:00:43) to (00:00:44)	+100,000,000
Time (00:00:44) to (00:00:45)	+100,000,000
Time (00:00:45) to (00:00:46)	+100,000,000
Time (00:00:46) to (00:00:47)	+100,000,000
Time (00:00:47) to (00:00:48)	+100,000,000
Time (00:00:48) to (00:00:49)	+100,000,000
Time (00:00:49) to (00:00:50)	+100,000,000
Time (00:00:50) to (00:00:51)	+100,000,000
Time (00:00:51) to (00:00:52)	+100,000,000
Time (00:00:52) to (00:00:53)	+100,000,000
Time (00:00:53) to (00:00:54)	+100,000,000
Time (00:00:54) to (00:00:55)	+100,000,000
Time (00:00:55) to (00:00:56)	+100,000,000
Time (00:00:56) to (00:00:57)	+100,000,000
Time (00:00:57) to (00:00:58)	+100,000,000
Time (00:00:58) to (00:00:59)	+100,000,000
Time (00:00:59) to (00:01:00)	+100,000,000



## Surface energy balance investigations using scintillation measurements.

M. Sciortino\*, G. Salvetti\*,  
G. Casu\*\*, F. Malaspina\*\*, F. Foti\*\* and E. Vuerich\*\*

\*ENEA, C.R.Casaccia, Rome, Italy

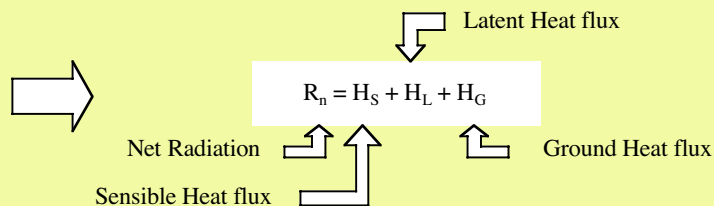
\*\*Aeronautica Militare, R.S.M.A., Vigna di Valle, Rome, Italy

### 1. Introduction

- ENEA is conducting, in collaboration with Aeronautica Militare and other institutions, scientific investigations within the RIADE project. Major aim of these investigations is to assess and mitigate the impacts of desertification in Italy.
- Water is increasingly becoming a scarce natural resource in Southern Italy drylands and agriculture demands increasing quantities of fresh water. Therefore there is a need for new tools to support the efficient management of water used for irrigation. An important component of the surface water and energy balance is the Latent Heat flux (EvapoTranspiration  $H_L$ ). Current methods to estimate EvapoTranspiration are based on point data and do not provide good estimation for large areas. Scintillometer can provide reliable measurement of  $H_L$  to validate model and assessments made for large areas.

#### Energy balance

Energy Balance Equation

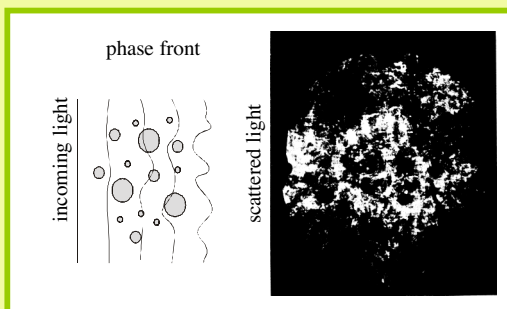


The latent heat flux  $H_L$  represents the EvapoTranspiration fraction of the surface energy balance equation. Usually it is not directly measured but it can be derived from the energy balance equation if all other components are known:

- $R_n$  and  $H_G$  can be measured or estimated from climatic parameters
- $H_S$  can be measured using two different method: one is Eddy Covariance, the other is Scintillometry

#### Scintillometry

- A scintillometer directs a light beam between a transmitter and a receiver and the receiver records and analyses fluctuations in the turbulent intensity of the air refractive index caused by changes in temperature and humidity due to heat and moisture eddies.
- In practice, scintillometers measure the structure parameter of the air refractive index,  $C_n^2$ , that in the visible and near-IR is mainly dependent on the air temperature fluctuations.
- $C_n^2$  data together with additional data on surface air temperature, pressure and humidity allow to derive the sensible heat flux.



#### Advantages of Scintillometers

- spatially averaging: representative data
- no statistical noise: high temporal resolution
- no flow distortion: highest accuracy
- remote access: over water, across valleys etc.
- easy operation

## 2. Method

The instrument utilized in this work for measuring Sensible Heat flux is a **Coherent Scintillometer** \*

Laser scintillometers with their collimated, narrow light beams, respond to smaller eddies, those whose size define the **'inner scale,  $l_0$** .

In fact, the most effective eddies at creating intensity fluctuation are those of sizes comparable with the scale of diffraction spreading of the laser radiation, given by the **First Fresnel zone**.

Comparable sizes can be found for path lengths up to 50-150 m.



Consequently, coherent scintillometers allow to measure

- The structure parameter of the refractive index,  $C_n^2$
- The inner scale,  $l_0$ , using a displaced-beam technique



$l_0$  data supplement  $C_n^2$  data, obtained through undisplaced-beam measurements, for determining sensible heat flux using an iterative procedure fed with additional pressure and temperature data.

When the light source is a **laser** the instrument is a **coherent** (or **laser**) **scintillometer**

**Inner scale** : spatial scale characterizing the transition between inertial-convective and dissipation ranges of the refractive index spatial power spectrum.  
Typical inner scale range is 1-10 mm.

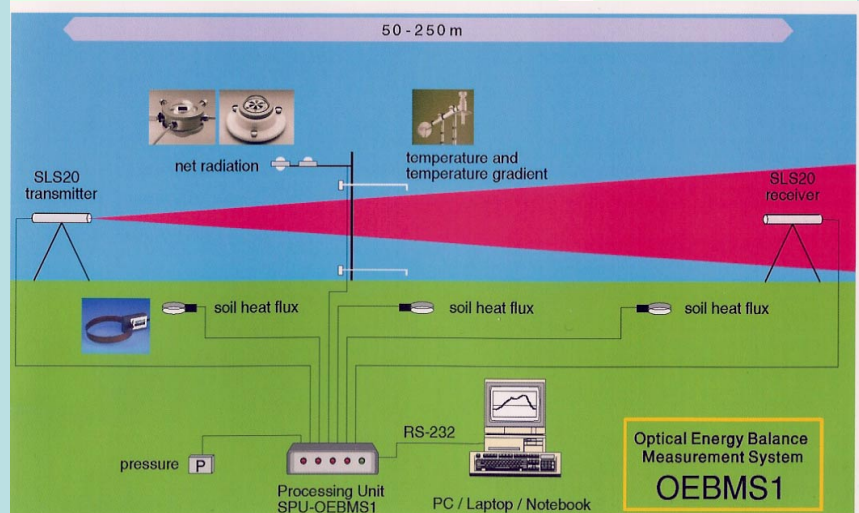
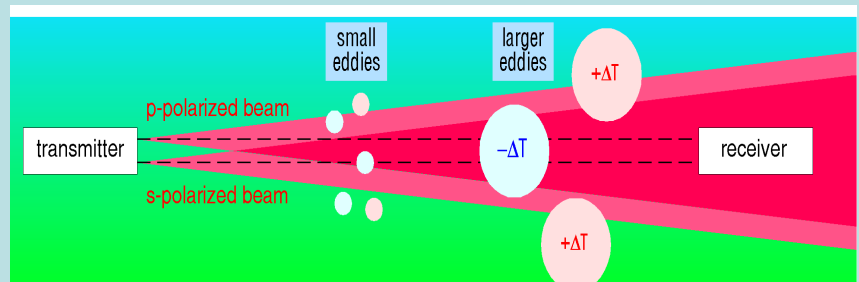
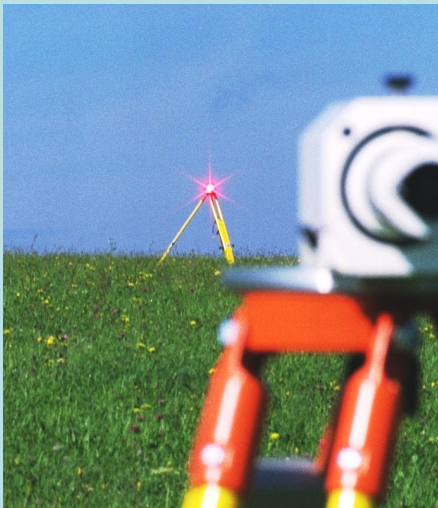
First Fresnel zone =  $(\text{wavelength} \times \text{optical path})^{1/2}$

Optical path	$\lambda$		
	330 nm	670 nm	10.6 $\mu\text{m}$
50 m	4 mm	6 mm	28 mm
250 m	9 mm	13 mm	63 mm
1000 m	18 mm	26 mm	126 mm

\* **Scintec SLS20**

**Surface Layer Scintillometer:**

- Light source: diode laser
- Operating wavelength: 670 nm
- Number of sources: 2



### Directly measured data

Pressure  
Temperature  
Thermal gradient  
Global and net Radiation  
Soil Heat flux

### Derived output data

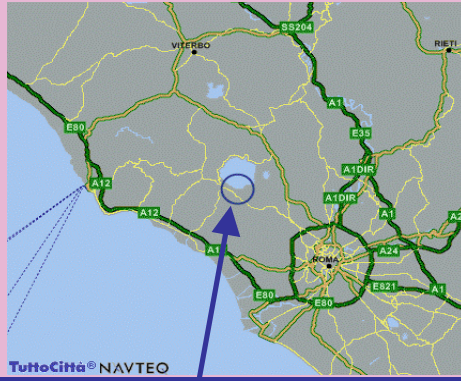
Monin-Obukhof length  
 $C_T^2$ ,  $C_n^2$  and  $l_0$   
Sensible and Latent Heat fluxes



### 3. Results

#### Measurements site

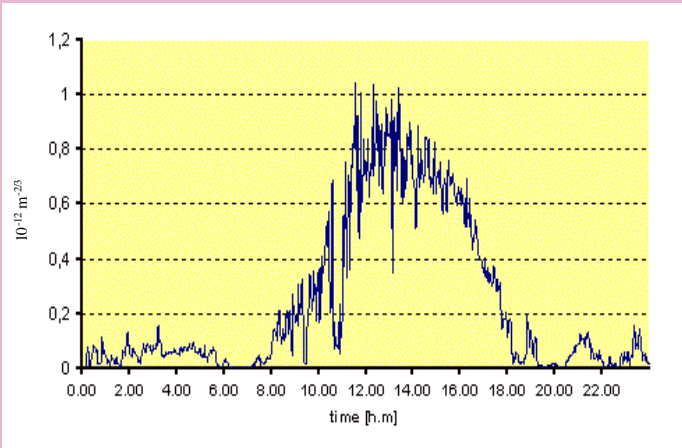
Preliminary measurements were performed in collaboration with R.S.M.A., *Reparto Sperimentazioni Meteorologia Aeronautica*, at Vigna di Valle in close proximity to the lake of Bracciano



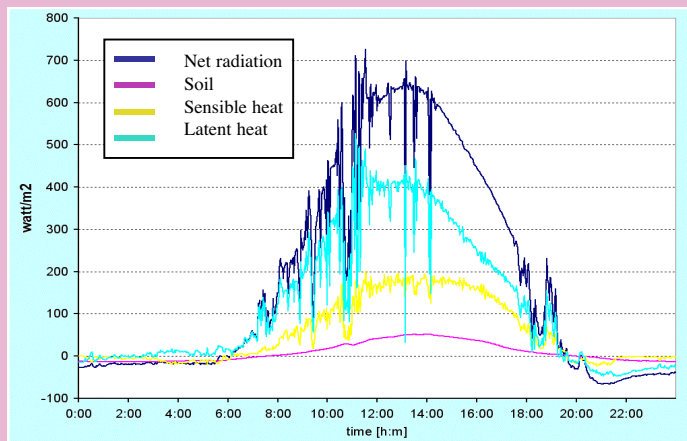
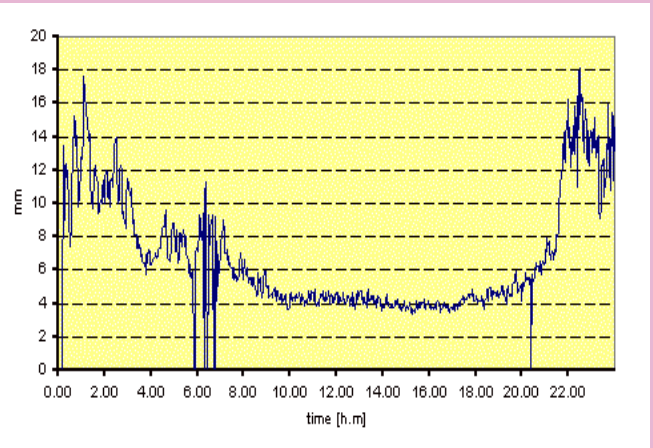
- Lat 42.08 N
- Lon 12.22 E
- Hi 270 m

#### Typical results obtained at the site on the 25.06.2004

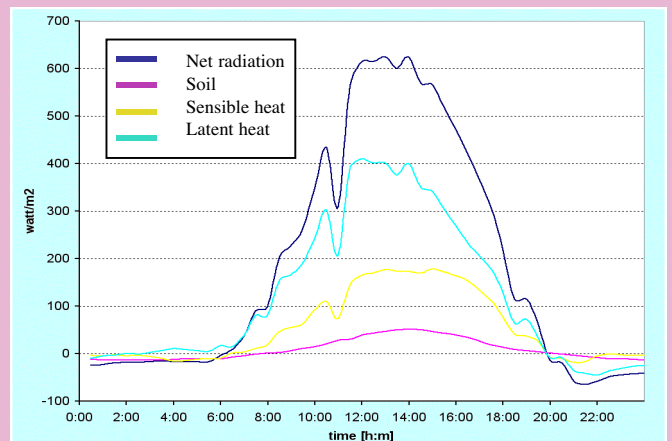
Fluctuations of the refractive index structure coefficient  $C_n^2$



Inner scale  $l_0$



Surface energy fluxes (2 min aver.)



Surface energy fluxes (30 min aver.)

## 4. Conclusions

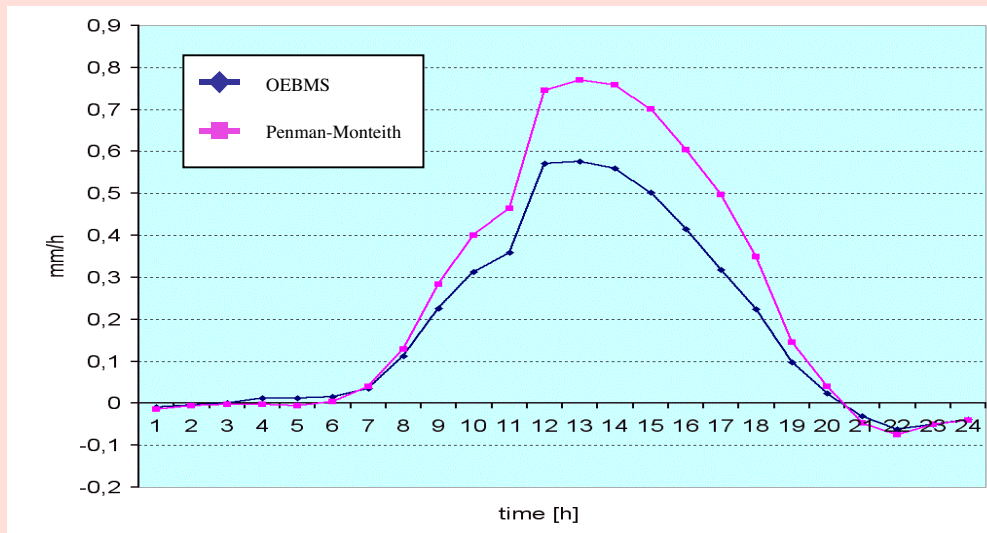
- Aim of the ongoing investigation is to provide reliable experimental measurements of EvapoTranspiration in order to validate different methods for its estimation.
- A preliminary comparison of the experimental and theoretical evaluation of EvapoTranspiration for hourly time steps shows a difference of up to 30%.

### Comparison of theoretical and experimental data

$$ET_o = \frac{0.408\Delta(R_n - G) + \gamma \frac{37}{T_{hr} + 273} u_2 (e^s(T_{hr}) - e_a)}{\Delta + \gamma(1 + 0.34u_2)}$$

#### FAO56 Penman-Monteith equation for hourly time step

$ET_o$  reference evapotranspiration [mm hour<sup>-1</sup>],  
 $R_n$  net radiation at the grass surface [MJ m<sup>-2</sup> hour<sup>-1</sup>],  
 $G$  soil heat flux density [MJ m<sup>-2</sup> hour<sup>-1</sup>],  
 $T_{hr}$  mean hourly air temperature [°C],  
 $\Delta$  saturation slope vapour pressure curve at  $T_{hr}$  [kPa °C<sup>-1</sup>],  
 $\gamma$  psychrometric constant [kPa °C<sup>-1</sup>],  
 $e^s(T_{hr})$  saturation vapour pressure at air temperature  $T_{hr}$  [kPa],  
 $e_a$  average hourly actual vapour pressure [kPa]  
 $u_2$  average hourly wind speed [m s<sup>-1</sup>].



- The field measurements available until now are too limited to draw any conclusion of practical interest but the methodology seems to be promising.
- Further measurements will be performed in different geographical contexts, e.g. at Castelvetro in the Belice River Basin in Sicily, with the ultimate purpose of improving the management of irrigated agriculture in dryland areas.

# Cost Effective 1 Minute Network Data Collection:

## A New Paradigm

Bruce Hartley

Meteorological Service of New Zealand Ltd.

P.O.Box 722, Wellington, New Zealand.

Phone +64-4-4729379, Facsimile +64-4-4700772

bruce.hartley@metSERVICE.com, www.metSERVICE.com

13 January 2005

### Abstract:

A **new paradigm** is emerging in the method, timeliness and frequency of data collection. New Internet Protocol (IP) based networks and communication technologies have made it possible for **cost effective 1 minute network data collection** from remote stations. Message intervals as frequent as once per minute are possible nationally and internationally at costs comparable to methods used for traditional 1 to 6 hour communications.

Messaging at 1 minute intervals can provide network and equipment operating benefits. Some statistical and derived data processing can be moved from stations to the central data server. Most IP network Data Link Layers include error detection and correction which alleviates the need for user level detection of message corruption. These benefits mean: Message sizes can be smaller thereby minimising communications costs; Frequency and complexity of remote equipment software updates are reduced in deference to single software updates on a local server; Processing overhead at stations is reduced thereby reducing their complexity, capital cost and maintenance.

One minute near real time data collection creates new opportunities. Weather forecast accuracy may be improved with more timely data or by triggering forecast reviews from appropriate changes in conditions. Fine detail weather forecasting and climatology research can be performed on a day-by-day basis or in hind sight after an event. Creation of commercial products with fine time resolution and near real time delivery are possible. In areas with cellular IP coverage rapid deployment stations are possible.

For AWS that do not fall within direct coverage of IP communication technologies alternative methods need to be considered when implementing new networks or upgrading existing ones.

This paper describes the design considerations and implementation steps taken during upgrade and expansion of MetService's network using 1 minute messaging and GPRS cellular IP data communications.

### Key Phrases

- The world is undergoing a data revolution.
- High rate data can be provided at excellent value for money.
- People love watching the weather and now they can do it real time.

### Acronyms

- ATIS            Automatic Terminal Information Service
- AWS             Automatic Weather Station
- CDMA          Code Division Multiple Access - IP cellular network operated by Telecom NZ
- GPRS          General Packet Radio Service - IP cellular network operated by Vodafone NZ
- MetService    Meteorological Service of New Zealand Limited
- NZ              New Zealand
- PacNet        Packet Switch Network - X25 packet switch network operated by Telecom NZ
- POTS          Plain Old Telephone System
- SIM            Subscriber Identity Module - Small circuit module used in Vodafone modems and phones
- TCP            Transmission Control Protocol - An IP network information transfer protocol
- UDP            User Datagram Protocol - An IP network information transfer protocol
- VPN            Virtual Private Network

## Introduction

The author works for the MetService which is the official NZ public weather service provider (www.metservice.com). The author's area of expertise is automated surface observation and so the discussions and illustrations presented in this paper are focused towards this area, however the principles employed can readily be applied to other areas.

Changes in cellular communications technology that have been implemented in NZ by the two major telecommunications network operators has presented a relatively low cost cellular GPRS communications infrastructure and MetService is currently implementing network changes to take advantage of this. To begin with MetService has chosen to use the Vodafone NZ GPRS network however this does not exclude the CDMA network from being used in the near future, particularly where some AWS do not have GPRS coverage but do have CDMA coverage, and the use of both networks can provide diversity in the unlikely event that either network provider suffers a major network failure.

## Network Features and Operating Considerations

The following are some of the features to be considered when deciding whether to invest in using a Cellular IP network.

- ❑ Network coverage - Areas with cellular coverage are also areas with high commercial opportunities for real time data. i.e. The areas where data is valuable as a commercial commodity is generally where there are higher population densities (where people live, congregate and travel), and for the same reason (higher population density) these are the areas where cellular network operators ensure good coverage e.g. cities and large towns, main highways, airports, marine ports, high density industry, popular leisure areas. Cellular networks use radio communications and due to the inherent limitations of the technology there will always be locations that do not have coverage. Some sites may need to be re-located nearby or use a radio modem or dedicated land-line link to a site where there is cellular coverage. Some sites may be completely outside coverage and therefore require an alternative means of communication. It should not be assumed that a new cellular network will provide a total replacement solution for an existing communications network.
- ❑ Network availability - The quality of service provided by the network operator should be investigated. This will include the network availability (up-time), mean time between failure and mean time to repair. The Vodafone NZ GPRS network has maintained an availability of better than 99.9% over the 12 months to December 2004
- ❑ Network Support - The level of support to be provided by the network operator should be considered. This will include demarcation points, the fault reporting process (help desk), and the expected time to respond. Support should also include notification by the network operator of scheduled maintenance well in advance, faults that have been reported and are under action, and when faults are cleared.
- ❑ Network Security - Some network providers can implement a VPN, normally for a routine management cost. This allows secure data transfer from the AWS to the central data processor, and fixed remote modem IP addressing which makes communication with a remote modem easier.
- ❑ Message transfer protocol - With IP communications messages are broken into packets and then communicated over a physical medium (e.g. an ethernet network, the internet) to a pre-defined destination. There is a protocol layer between IP and the user application that controls the way that messages are packetised, sent, received and handshaked. Different communications modems may implement one or several of the available protocols. For the NZ cellular modems the two main protocols are UDP and TCP.

UDP messages are split into packets of several hundred characters in size (512 characters for Vodafone NZ) and then the packets are individually sent like a letter or an email to the destination. After the packet is sent the sender does not know how long the packet takes to reach the destination or in fact whether the packet even reaches the destination. Each packet can travel by a different route so multiple packets from the same message or even different messages can arrive in a different order at the receiving system. Due to the relatively large time difference between messages (typically 1 minute) compared to the time between packets from the same message (typically milliseconds) it is very unlikely that packets from different messages will become mixed. The receiving system software is therefore required to sort and reconstitute messages that have been split before they are passed to the message decoding process. This problem can be avoided by keeping individual message sizes below the packet size. UDP packet overheads are less than TCP.

TCP messages are split in a similar way to UDP however this protocol includes the re-ordering and stitching process at the receiver as well as packet resend requests when they are corrupted or lost. The process is a like a two-way radio conversation in that the sender knows whether the message gets through from the responses sent back from the receiving system and the information can be resent if required. As long as there is some connectivity within the protocol timeouts, the message is more likely to get through, and if it does not the sender is notified. TCP packet overheads are higher than UDP, and the characters transmitted per message will be higher, particularly if there are retries.

- ❑ Message transfer parameters- Cellular IP networks are normally relatively high speed (tens to hundreds of kilobits per second) and the time to transmit simple data messages is typically less than a second. Latency (the average time taken for message to travel from an AWS to the central data processor) is typically a few seconds. Jitter (the variation in the latency) is typically hundreds of milli-seconds. It is worth noting that when a VPN is employed the latency for the first packet in a burst of packets is increased by several seconds due to the overhead in setting up the virtual "tunnel".
- ❑ Billing regiem (volume plans) - Message communications costs are usually based on volume with minimal connect time and/or SIM management charges. Network providers normally provide a selection of data communication plans and the plan that best fits you network will need to be determined (see Network volume usage). Available plans may include: Intermittent transmission or "telemetry" (suitable for event reporting); Moderate usage 10s of MegaBytes per month (suitable for single stations); 100s of MegaBytes per month (suitable for AWS networks). Some network operators may support special negotiated volume rate, plans based on your special requirements, but take note of any special conditions like minimum volume per transmission, or minimum volume per event and time period. Typical monthly charges can be as follows (in NZ currency):
  - Network management fee - per network - hundreds of dollars
  - Virtual private network management fee - per network - hundreds of dollars
  - Data volume plan - per network - hundreds of dollars for 100s of MegaBytes
  - Excess usage over the volume plan - per network - dollars for MegaByte
  - Telemetry plan - per station - tens of dollars for kiloBytes
  - SIM management fee - per station - few dollars
- ❑ Network volume usage - The calculation to determine the volume of characters transmitted from each remote station per time interval will include:
  - Message size (including spaces and line terminators);
  - Network overheads per message (e.g. 32 characters per message for network transport);
  - AWS minimum volume per transmission per time interval (billing requirement) i.e. if a message is sent then a minimum volume charge will be made for the billing time interval starting from the send time.
  - Any user initiated communications with remote stations (normally small or 0);
- ❑ Network setup costs - To support cellular IP messaging the central data processor will need to interface to the Internet or the network provider servers. Whether a VPN is implemented or not, the communications pathway to the central data processor may at some point use the public Internet. This may provide an access point for outsiders to try and connect into or disrupt the integrity of the central data processor. Security measures must be put in place and these should include at least setup of the Internet gateway (switch) to accept only messages from valid IP source addresses and ports, and firewall software on a separate processor that only allows in messages with valid formats. The costs to be considered will include:
  - Network connection (hardware/firmware) - hundreds to thousands of dollars
  - Virtual private network setup - hundreds of dollars
  - Network switch setup - staff or contractor time, and documentation
  - Network firewall software - staff or contractor time, and documentation
- ❑ Central data processing - New software will be required on the central data processor to receive and process messages, and to store and provide access to the new data for the creation of products. Where a network is being progressively upgraded the central data processor will need to support the existing and new message delivery and processing systems in parallel. This will require a software switch that defines, for each AWS, how messages are received and processed. For the new communications system the following software modules will be required:
  - Message ingest, decoding, validation and control (software switch to turn the station on/off)
  - Station data element control (software switches to turn each data parameter acceptance on/off)
  - Data storage for online real time product creation and long term archival
  - Processing to create longer period data values i.e. averages, maxima, minima, accumulated totals. This processing will need to allow for missing data values e.g. Allow 1 missing minute for 2 minute derived values; 2 missing minutes for 10 minute derived values; 6 missing minutes for 1 hour derived values; 6 sequential and 60 non-sequential missing minutes for 24 hour derived values.
  - Create existing message formats and input these to their existing processes
  - Create new products and delivery mechanisms
  - Automated monitoring and alarms (see Monitoring)
- ❑ Monitoring - Although the communications network provider normally performs their own monitoring it is also useful to have a separate full network traffic monitor at the central data processor ingest server. To monitor the

correct operation of each station requires information to be extracted at various stages in the message ingest process, and due to the large volumes of high rate data involved this process must be automated. It may be useful to modularise this process so that statistics and fault information is placed in files that are read by a separate program which raises warnings and alarms when appropriate. Software implementation could be as follows:

- Server - Volume monitoring of the main pipe for network wide faults and billing.
  - Firewall - Volume monitoring per modem IP number for station communications faults (stream volume too high or low) and billing.
  - Message ingest - Message statistics per AWS for missing station and missing/corrupted messages.
  - Message decoding - Extraction of AWS house keeping data (e.g. power supply, equipment temperature) and sensor status (alarms, missing sensor, missing data, data quality indicators).
  - Alerting - Read all status files, check for fault conditions, raise warnings and alarms (on screen, emails, cellular text, pagers), and produce routine performance summaries.
- ❑ Network Tools - Tools to allow technicians to perform remote diagnostics and maintenance should be considered.
- PING - An IP network tool that can be used to establish that a remote modem is operating and is contactable (the network provider must support the PING protocol and the modem should use fixed IP addressing).
  - Some form of station remote access, particularly for more complex stations that incorporate aviation sensors.
- ❑ AWS upgrade costs - To upgrade existing AWS the following will need to be considered:
- Cellular IP modem and cables - several hundred dollars
  - SIM activation (per modem) - 0 to tens of dollars
  - AWS software upgrade - staff or contractor time, and documentation
  - AWS software and hardware installation - staff or contractor time, and documentation
- ❑ GPRS modem setup and control - A GPRS modem must be pre-programmed with the appropriate cellular IP network provider access information and the message destination IP address and port number. Once the modem is powered on and the initial connection is established with the IP network then the connection (or context) is always available (provided the link is physically available) i.e. there is no further need for modem control or dialling whenever a message is sent.

The required network operator information is: *Internet or VPN APN* (e.g. Internet); *Username* if required (e.g. aname); *Password* if required (e.g. thepassword); *message source IP addressing* (this will be a fixed address range for modems on a VPN, and a range for dynamic modem IP addressing, e.g. 123.45.67.890/123).

The required receiving system information is, (web facing server) information is: *destination IP address* (e.g. 123.45.67.890); *destination IP port number* (e.g. 123456).

- ❑ Backup System - At first glance it would seem beneficial to have a hot backup system in place e.g. POTS toll calls to a backup computer system or POTS dial up to Internet Service Provider and then email or UDP, etc. The decision whether to implement such a backup system is based on the cost to risk benefit. The cellular IP network reliability and network operator track record will need to be considered compared to the cost of installing a dual but hardly ever used communications system. An alternative method is to build diversity into the network by strategically spreading AWS between physically different cellular networks (in NZ the options would be Vodafone GPRS and Telecom CDMA).
- ❑ Options where there is No Cellular Coverage - There will be areas where there will be no cellular IP coverage even when using high gain antenna so alternatives will be required. These can be categorised as follows:
- Extend the existing network coverage by: Talking to the network operator about cell site pattern enhancement or mini-cell sites; Use a radio modem link to the nearest coverage point (extends coverage by up to 50 km).
  - Alternatives for 1 minute interval messages: On-line hard wire or wireless Internet access; Third party Internet access (tap into an existing local network); Leased lines and dedicated on-line modems.
  - Alternatives for greater than 1 minute interval messages: Retain existing communications (if not being phased out); Dial-up internet access with Email, UDP, TCP, etc.; Dial up POTS; Satellite; HF packet radio.

## Whether to Upgrade or Not

Upgrading any network can involve significant infrastructure costs which need to be justified before the project to upgrade proceeds and the new method needs to satisfy some or all of the following: alleviate threats; save money; generate new revenue. The pros (benefits) and cons of upgrading the existing MetService network to cellular IP communications were considered during the early planning phases and the following points were considered:



## Pros (Benefits)

- ❑ Limited life of PacNet - The communications system used by most of the MetService network of AWS is a dial up POTS to a PacNet gateway. The PacNet service provider in NZ has signalled that this network has a limited life in the order of only a few years. This posed a threat to MetService's data collection operations and so alternative communications methods had to be found. The GPRS network alleviates this threat at all sites where there is coverage.
- ❑ Reduction in communications costs - The monthly cost of 1 minute message delivery via GPRS is about half the cost of a POTS circuit rental plus message volume costs of PacNet so it will be possible to reduce communications costs at most sites.
- ❑ Reduction in AWS complexity - First, as the GPRS modem operation is simpler from the AWS point of view, the AWS can be a simpler in design and therefore lower cost and easier to operate i.e. closer to a plug-and-play type system. Second, more frequent messaging, and ideally real time (once per minute), means a small and simple data set can be implemented at the AWS with post processing to produce more complicated data sets and codes being performed at the central data collection centre. This has the flow on effect that it is easier to implement and manage software upgrades for coding changes, for fixing bugs, and to produce new data products because these are performed at the central data collection centre.
- ❑ Improvements in forecast accuracy and timeliness - The availability of real time data to forecasters and numerical models may make it possible to produce better trending, event timing and provide data closer to the time of forecast issue, therefore improving forecast accuracy and timeliness. Higher time resolution data may provide a better understanding during post forecast analyses thereby paving the way to improve future forecasts.
- ❑ New real time data products - Real time data communication to a central data collection centre means data products can be created and delivered to multiple clients in real time. The Internet can be used for real time data delivery and therefore there are minimal limitations on client geographical location i.e. The Internet is normally accessible from most places using either dial-up, dedicated wire of fibre optic, cellular and wireless, or satellite. Some typical applications of real time data collection and delivery include:
  - Aviation - Air Traffic Control and ATIS, pilot briefing
  - Coast guard (voice to speech radio broadcast of conditions)
  - Port operations (current conditions and alarms)
  - Television (up-to-the-minute weather conditions)
  - Road weather (current conditions and alarms)
  - Horticulture (current conditions and alarms)
  - Consumer weather (up-to-the-minute weather conditions via phone, cell phone, internet)
- ❑ New archived data products - Archived real time data provides more useful event timeliness information that can be used for insurance, accident and forensic investigations.
- ❑ New portable rapid deployment AWS - In places where there is cellular IP coverage it becomes very cost effective (in terms of installation time and infrastructure setup) to perform short term installations for items such as: Research projects; Recreational events (land, marine and aviation sports events); Environmental accidents (chemical spills, fires); Search and rescue; Structural construction projects.

## Cons

- ❑ No remote on-line dial in" access for UDP - The ability to remotely access remote stations is more difficult and requires additional communications protocol software. The ability to remotely call into AWS to get current data is however not really a loss because the delivery of real time data means this facility is not required. The ability to remotely call into AWS for technical access to perform detailed diagnostics and control is however a loss. The loss of this feature is however balanced by the availability of diagnostics information in real time, and that as the AWS equipment and operation is simplified there is less need for remote control. For those sites where remote technical access is still required an option is to retain the POTS connection for maintenance purposes.
- ❑ Higher volume "pipe" required for central data collection - To handle the increased volume of message traffic at the central data processor more bandwidth (a bigger "pipe") may be required. This must be considered when evaluating the per AWS operating costs. The size of the "pipe" may need to be reviewed periodically as the number of stations changes.
- ❑ Security of data - When the public Internet is used for message communication then the data is insecure (can be listened to by others). Due to the perishability of the data with age (i.e. the data has less value as it time increases) this may not be an issue, however where it is an issue the use of a VPN or encryption of messages can be employed. A VPN will incur a network provider routine management cost and data encryption will require additional AWS and central data processor software complexity.

- ❑ New message formats - The requirements of a real time data stream are not the same as for much less frequent message reporting. As the new data stream costs are normally based on volumes of traffic it is more cost effective to minimise the size of messages (down to any billing thresholds) and this can be done by sending a base set of 1 minute data that can be further processed at the central data processor. This is not traditionally the way data has been communicated so a new messages code will most likely need to be defined.
- ❑ Increased complexity of central data processing software - The central data processing software will need to perform additional tasks compared to traditional hourly or less frequent data collection. This will include: decoding the likely new message code; performing data quality control; deriving additional time period data values; creating tradition message codes.
- ❑ Coverage not always available - Not all AWS may have coverage so alternative communications methods (dial up Internet, radio link, satellite) will still be required.

## MetService Implementation



MetService's new low cost mSTAR system that sends CSD messages once a minute using cellular GPRS communications. mSTAR (Standard or Pro version) supports the measurement of:

- ❑ Wind Speed
- ❑ Wind Direction
- ❑ Air Temperature
- ❑ Relative humidity
- ❑ Pressure
- ❑ Precipitation
- ❑ Solar Radiation
- ❑ Soil Moisture and Earth Temperature
- ❑ 3 Additional Temperatures (any location)
- ❑ System battery voltage and cabinet temperature

The Harvest SPE GPRS modem with internal antenna (pointing down) is located in the top half of the equipment cabinet and on the very left side.

## GPRS Modem

MetService uses a modem manufactured by company in NZ called Harvest Electronics ([www.harvest.com](http://www.harvest.com)). The modem is called a "GSM/GPRS Serial Port Extender" or Harvest SPE for short.

- ❑ SIM Card - The modem requires a SIM card to be installed that has been programmed by the local GPRS network provider with GPRS communications enabled and the modem IP number.
- ❑ Power consumption - The modem operates from a dc power supply voltage of 6 to 30 volts DC. This allows the modem to be powered directly from backup batteries or solar power supplies. After power up and establishment of a context the modem consumes 29mA during no message transfer and 90 mA during a message transmission.
- ❑ Antenna options - There are 3 standard modem antenna options. For good signal coverage an indoor antenna may be used; Where coverage is marginal or an external antenna must be used a vandal resistant wire rope with ground plane antenna may be used; Where coverage is even lower a high gain yagi antenna can be used.
- ❑ RS232 Connectivity - The modem is fully configurable/controllable using an extended Hayes AT command set. The modem is configured before installation so that at power on it automatically establishes a context with the

GPRS network so that all messages sent to the modem serial port are automatically forwarded to the central data processor without any control or handshaking from the AWS.

## Message Codes

Before upgrading: METAR, SYNOP, 01HRx, ENGxx, DDBT

After upgrading: CSD, DDBT

- ❑ METAR, SYNOP - Designed many years ago and managed by ICAO and WMO. These codes were primarily designed for hourly or less frequent manual observations within the meteorological and aviation communities.
- ❑ DDBT - Display Data Binary Transfer (MetService NZ 1990). This code was primarily designed for passing data from AWS to on site display and ATIS systems. The communications was by hard wire or radio circuit with no routine communications costs so optimising message size was not required. A typical message size for an aviation AWS with a full compliment of sensors is 500 to 600 characters. The code was designed to be transmitted once every minute but includes pre-processed information e.g. 2 minute and 10 minute wind averages, gusts, lulls, counter-clockwise and clockwise direction variability to allow display on simple terminals.
- ❑ 01HRx - 01 Hour reported Data (MetService 1992), DLYCL - Daily Climatological Data (MetService 1992), ENGLx - Engineering Data (MetService 1999). These codes enable the passing data and engineering information not catered for in the METAR and SYNOP codes and normally included in the remarks sections.
- ❑ CSD - Comma Separated Data (MetService 2004). This code was designed with optimal message size in mind but still using simple ASCII characters for ease of interpretation and maintenance. A typical message size for an aviation AWS with a full compliment of sensors and 1 minute messaging is 200 to 250 characters. The code includes the minimum data set required to generate all post processed data values i.e. post processing to generate longer time interval data values is performed by the receiving system. The code was primarily designed for 1 minute message sending of 1 minute data values, but the code has the capability of being used for other message communication intervals such as 2, 5 or 10 minutes by including additional data items that can be used by the receiving system to calculate all traditional data values including continuous climatological records.
- ❑ BUFR, CREX - These WMO codes were primarily designed for the international exchange of observational data. They were considered but were not implemented due to: Table descriptor overhead is high for small and frequent messages; Additional processing is required at the site; Not easily read by humans.
- ❑ Message Volumes - For Vodafone NZ GPRS UDP 1 minute interval messaging the optimum message size is determined from the minimum volume per time interval of 5 kB per 20 minutes as follows...

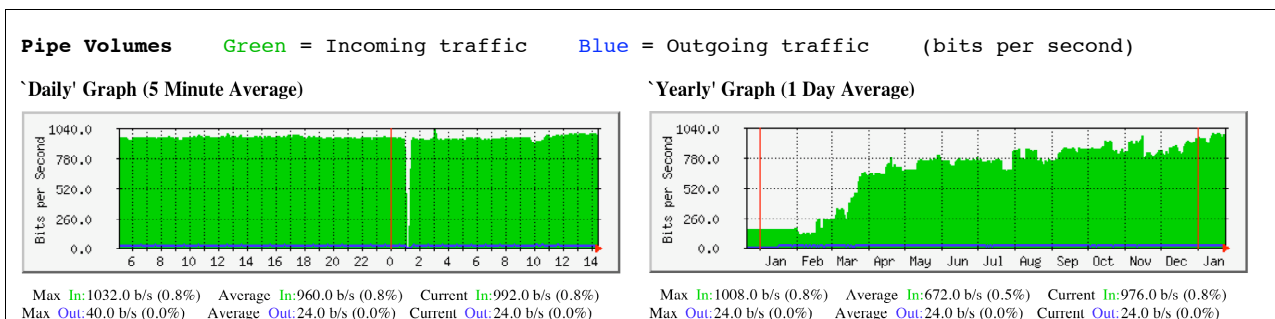
Optimum message size =  $(5000 / 20) - 32 = 218$  characters (32 is the network provider message overhead)

There is no saving for sending messages of less than 218 characters. Messages larger than this will use up part of a bulk volume plan that could be used for other AWS so the CSD message code is the most cost effective.

The minimum billed volume for a month =  $5 \text{ kB} \times 3 \times 24 \times 30 / 1000 \text{ MB} = 10.800 \text{ MB}$

## Monitoring and Network Tools

The whole "pipe" is monitored using network software (a scheduled network maintenance can be seen at 1am in the Daily graph and the expansion of the number of stations can be seen in the yearly graph).



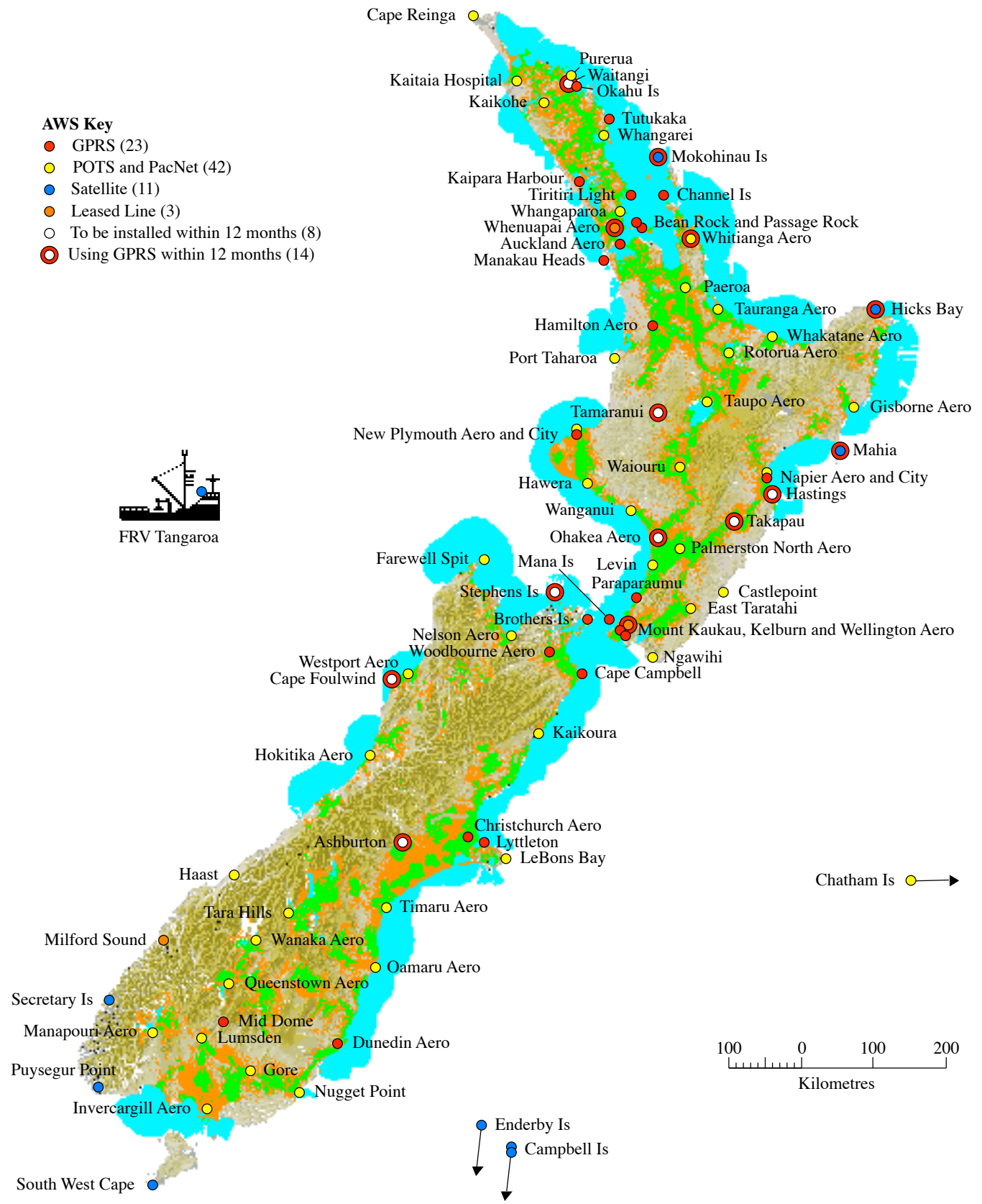
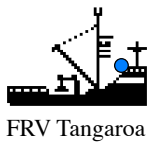
Ingest software counts characters from each modem IP address, and counts messages from each AWS and produces hourly and daily message counts. Message housekeeping and sensor statistics are extracted and placed in files and a separate program called "Fault Monitor" analyses all monitor files and produces email alarms when appropriate.

The Vodafone VPN supports PING. For aviation sites with ceilometers, present weather and/or visibility sensors, the POTS is retained for remote maintenance. The POTS is not used for any message sending.

Raoul Is

**AWS Key**

- GPRS (23)
- POTS and PacNet (42)
- Satellite (11)
- Leased Line (3)
- To be installed within 12 months (8)
- Using GPRS within 12 months (14)



GSM Primary Land Coverage
  GSM Secondary Land Coverage
  GSM Marine Coverage

**MetService New Zealand AWS Network and Vodafone GPRS Coverage**

January 2005

# Cost efficient data transport with GSM from weather stations in Norway

Poster presentation TECO 2005

Aslaug M. van Nes, Norwegian Meteorological Institute.

## Motivation:

In the entrance of a new century most of the weather stations in the Norwegian network where manned stations reporting their observations by phone to centrals. Stations not reporting in real time sent their observations weekly or monthly by mail. Again observations had to be punched into the collecting system. The aim was to get a faster data collecting and to get an end to the centralized registration. This could be achieved by digitalizing the data flow all the way from the station.

The station network in Norway is build up in such a way that manned stations still are cheaper than fully automatic stations. The automation process is more motivated by receiving more accurate data at a higher frequency, and to receive data form remote areas where observers are hard to find.

## SMS in data transport from weather stations:

In 2002 the Norwegian Meteorological Institute started to use SMS and the GSM network to collect data from weather stations to get a faster data collecting at a lower cost. The stations do not send a ready coded synop. The synop for a station is produced first when the SMS messages made at the station reach the National Meteorological Service (NMS).

This has given the opportunity to split stations in modules.

Example: A station can have an automatic part (AWS) observing temperature (T), humidity (U), pressure (p), precipitation and wind data. Another part is an observer observing clouds, visibility and weather, parameters that are usually difficult and expensive to collect by automatic instruments. The AWS and the observer send 2 separate SMS-messages (with the same identification-number for the station). When the 2 messages are received at the NSM the synop is generated for the station.

Different SMS message types are developed to improve the dataflow from different types of stations. Message types so far developed for the Norwegian weather station network are:

1. Precipitation: Manned stations where 24 hour precipitation is reported. Traditional these stations send their observations by mail once a week. Now the observation is reported by using a mobile phone. The measurements are collected inn in real time and can now with little cost be used as additional information in the daily weather analysis.
2. Visual observations: Manual reported observations of clouds, visibility, weather and past weather. These parameters are still easiest observed by human. This module is always connected to an AWS or Airport-station. In the message type lays also the possibility to report manual precipitation and snow measurements. The observation can be reported by using a mobile phone or a computer connected to a GSM modem.
3. Traditional stations and climate stations: Manned stations where the observer punches the observation in a computer connected to a GMS modem. These are stations where classical instruments still are in use and must be read and reported by an observer.
4. Automatic station (AWS): Data from instruments are sent as a sms message every hour.

The parameters reported by the AWS (T, U, p and vind) are normally better observed in accuracy and time than by observers. In this module it is also possible to auto-report snow depth and precipitation.

5. Airport station: A computer is collecting observations from airport instruments and sending one SMS message every hour.
  6. Message: This format is made for observers who want to send a message to the NMS.
- New synoptic stations in the Norwegian network mainly consist of modules 2 and 4, or 2 and 5.

Results and benefits:

- The data-collecting rate has improved. With GSM the data collecting system can receive data from 500 stations per minute. By experience the data from all the sms reporting stations in Norway are received within less than 10 minutes.
- More data is collected in real time without higher costs.
- It's easier to find persons to take visual observations since the work is less and easier to share with others.
- The observer is less bound and the teaching is easier. Because of the AWS module we are less vulnerable to data loss when observers can't observe.
- We can benefit both the qualities of manual observations and automatic observations at one station. The AWS can be placed at a good spot without considering the access for the observer.
- Data from Climate stations and precipitation stations are reported in real time with little extra costs.

Future development: GPRS (General Packet Radio Service) can improve the cost benefit and the data rate from weather stations. A lot more data can be transported at a very low cost. GPRS makes it also possible to be online with the equipment all time. It leaves the possibility for a very flexible observation system.

SURFACE METEOROLOGICAL MEASUREMENTS AND  
METEOROLOGICAL SERVICES IN PAKISTAN



By

H. Mir & ZAHID RAFI

Pakistan Meteorological Department

P.O.Box Number 1214, Sector, H-8/2

Islamabad.

**PAKISTAN**

Telephone Number 92-51-9257313

Fax Number 92-51-4432588

Email: [hazratmir2000@yahoo.com](mailto:hazratmir2000@yahoo.com)

# **SURFACE METEOROLOGICAL MEASUREMENTS AND METEOROLOGICAL SERVICES IN PAKISTAN**

By  
H. Mir & ZAHID RAFI

## **Abstract:**

In this study, effort has been made to examine the observations of the meteorological elements, near the surface of the earth with the aid of sensors such as Thermometers, Barometers, weather Surveillance Radar and Remote sensing units. The information's regarding the Atmospheric Pressure, Air temperature, Humidity, Wind speed & Direction, Rainfall, Visibility used operationally in day-to-day weather analysis and forecasting is discussed here. Some observations like a solar radiation; Soil & Grass Temperature and Potential Evaporation are essential for studies in the fields of climatology, Hydrology and Agro meteorology. The main objective of this study is to assess the function of instruments installed in Pakistan meteorological Department before 1980s and the new development in instrumentations after 1980s. In view of the changes, some suitable adaptation strategies have been proposed. A brief about the meteorological services provided by Pakistan meteorological department (PMD) to different agencies is also mentioned in this paper.

## **1. Introduction**

For day today weather analysis and forecasting, surface observations like an atmospheric pressure, air temperature, humidity wind speed & direction, rainfall and visibility are the basic tools. Without instruments, observations are impossible. The surface Meteorological observation Instruments (SMOI) mostly uses Conventional in Site Sensors to obtain 1-minuts and 30 minutes average of the surface wind speed, wind direction, air temperature, reletive humidity barometric presser and precipitation.

Routine surface Meteorological observation begins at Pakistan observation in 1947. The atmospheric presser, Clouds, Temperature, amounts and direction of movement, rainfall amount recorded, Relative humidity. Air temperature, observations were made by observer at synoptic hours. The brief of instruments installed before 1980s and some develop instruments after 1980s are explained (Byers, 1959). Recent advancement in technology has allowed a significant expansion in remote weather sensing capability during the past 10 years. The state of see was calculates by the Jinnah international Airport met office Karachi (Pakistan), based on the costal winds. Agro meteorological stations normal meteorological parameters are measured on daily bases and the data is conveyed to the national Agro meteorological center Islamabad, after every 10 days. Flood forecasting division collected the observation from the catchments areas and issued a flood forecast. Weather services are compasses a wide range of forecast, warning and information services to the general public, national and international shipping and aviation, the Department of Defence and other users (A.Bureau, Met, Report,).

## **2- Observing stations in Pakistan**

The following types of meteorological station/ offices established in the country, shown in table –1.



Table-1.

S.NO	OBSERVATORIES	NUMBERS
1	Surface observatories	45
2	Pilot Balloon	28
3	Aero-met	32
4	Atmospheric	04
5	Marine	01
6	Main Meteorological offices	04
7	Dependant Meteorological offices	02
8	Regional agro met center	04
9	Solar radiation stations	12
	TOTAL	145

The role of the a national Meteorological services starts from the establishment of a network of meteorological Observatories where real time World Meteorological Organization (WMO) Meteorological Observations are recorded all over the world at an interval of three hours, starting from 0000 UTC. For the recording of various types of Meteorological data, different types of Meteorological stations set up, detailed as below.

### Main five types of surface Meteorological stations

#### i-Surface synoptic Meteorological station.

Three hourly observations are taken about the mentioned weather parameters beside the past weather during the previous three hours. Minimum Temperature and total rainfall during previous 24 hours is noted at 0300 UTC and Maximum is recorded at 1200 UTC.

#### ii-Aeronautical stations

Hourly/half hourly Met. Observations are recorded regarding Atmospheric pressure, Air temperature, Prevailing wind speed / direction, cloud types/amount, visibility and present weather. Climatologically stations.

**iii-Climatological stations:** Those, which record meteorological observations at selected synoptic hours for climatological purposes and submit their records to Regional centers by post at the end of the month.

#### iv- Rain gauge stations ions or Hydro meteorological stations:

Those which record only rainfall or snowfall once a day or more often at synoptic hours and send their data by post to the authorities maintaining them.

**V-Ships observatory:** Ships observatories that record synoptic weather observations while out at sea and report them in coded messages by wireless to the nearest coast radio stations for weather forecasting and warning purposes.

### 3-Metrological instruments

i) List of the Instruments Installed in PMD before 1980s:

Different types of surface observation instruments used before 1980s are in Appendix (i).

ii) List of the Instruments Installed in PMD after 1980s:

Different types of surface observation instrument used after 1980s are in Appendix (ii). The instruments that are normally installed in the observatory are shown in table-2 as well as in appendix (iii).

Table-2

S.NO.	INSTRUMENTS	PAMETER MEASURED
1	Rain gauge	Rainfall
2	Cup counter Anemometer	Wind run
3	Sun shine recorder	Sun shine hours
4	Evaporation pen	Evaporation
5	Stephenson screen	Housing for instruments
6	Dry & wet bulb thermometer	Dry & Wet bulb temperature
7	Grass Minimum	Grass minimum temperature
8	Soil minimum	Soil Temperature in different depth
9	Thermograph	Temperature & Humidity.
10	Mercury Barometer	Pressure

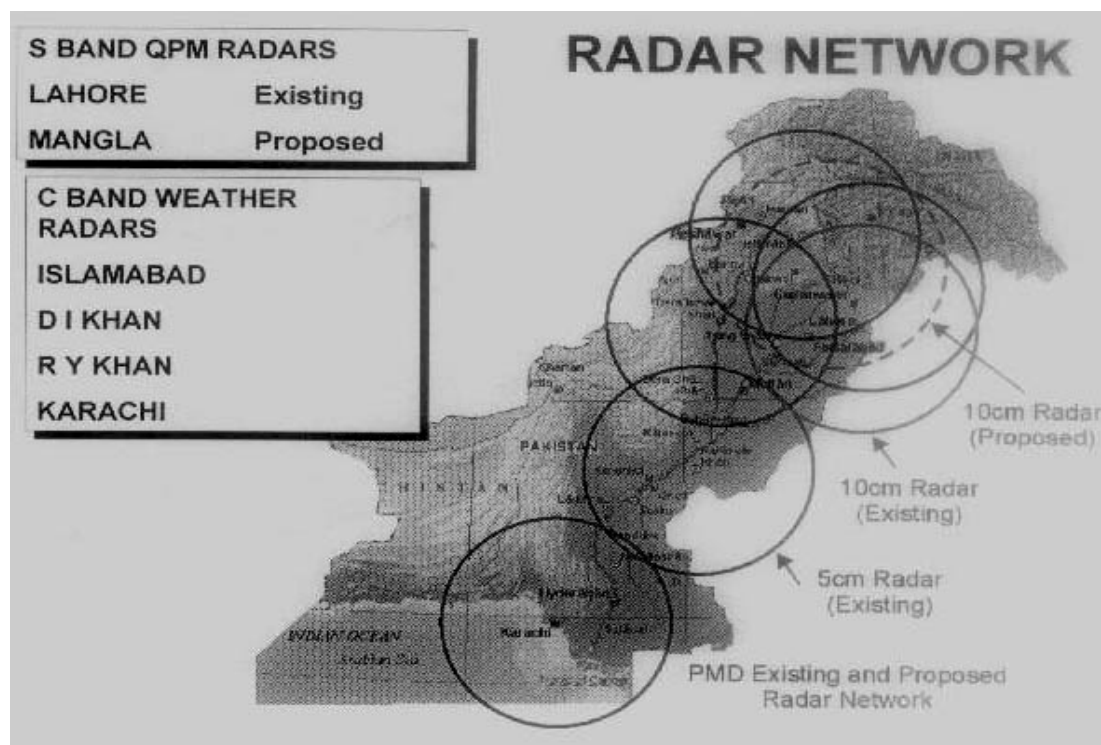
#### 4. Surface Observations

The following observations, instrumental and non-instrumental, are recorded at the Surface Meteorological Stations (A. Miller.et.al).

- (i) Direction and speed of the wind: The direction from which the wind is blowing is recorded with the help of a wind vane in tens of degrees or according to the points of the compass. The speed of wind is measured by means of an anemometer and is expressed in nautical miles per hour or knots, a knot being about 2km or about 1.25 miles per hour.
- (ii) Barometric Pressure: The pressure of the air is measured in millibars with the help of a barometer. A millibar is one-thousandth part of a bar, which is the meteorological unit of atmospheric pressure in the GGS system, and is equivalent to a force of 1000 dynes acting on a surface of one sq.cm. Dyne is the unit of force and stands for the force, which produces a unit acceleration in one gram. A column of 29.92 inches of mercury in a barometer represents 1013.2 mb.
- (iii) Temperature of the air: It is measured in degrees Fahrenheit or Centigrade by means of a thermometer exposed to air in shade in a Stevenson screen, which has double louvred sides for free ventilation.
- (iv) Wet Bulb temperature: If the bulb of thermometer containing mercury is wrapped up in muslin and is kept wet, the temperature recorded by such a thermometer is generally lower than that recorded by an ordinary thermometer whose bulb is dry. This is called wet bulb temperature. The lowering of the wet bulb thermometer reading depends upon amount of water vapor present in the atmosphere.
- (v) Dew point temperature: this is the temperature at which the water vapor present in the atmosphere would begin to form dew. The drier the air the lower will be the dew point temperature as compared to the dry bulb temperature. It thus gives a measure of the water vapor content of the atmosphere. In air saturated with water vapor the dry bulb, wet bulb and dew point temperatures are all equal.
- (vi) Humidity: When the amount of water vapor actually present in the atmosphere at the time of observation is expressed as a percentage of the amount that is needed to saturate it at its dry bulb temperature, it is called relative humidity.
- (vii) Rainfall: Rainfall is measured by a rain gauge. One inch of rainfall means that if the rain that falls on a horizontal surface is collected there, its depth would be one inch.

- (viii) **Visibility:** It represents the maximum horizontal distance at which objects can be seen distinctly at the time of observation, and is estimated by experienced observers by observing known landmarks at known distances. This is also measured precisely by electronic equipment wherever available.
- (ix) **Present weather and past weather:** The weather phenomena like haze, mist, fog, sandstorm or dust storm, drizzle, rain, shower, snow, thunderstorms, etc., along with an indication of their intensity and time of occurrence are divided into 10 main groups and 100 categories. The phenomena experienced within one hour of the time of observation are termed present weather and those experienced since last observation or within the last 24 hours as past weather.
- (x) **Amount and type of cloud cover:** The clouds are classified into three main categories—high, medium and low—depending on the level of their formations and under each category ten sub-divisions are made (I.C. Atlas, WMO.1956). For the purpose of observation, the whole sky as observed from an open observing position, is considered as consisting of eight parts. The amount of sky covered by each category of cloud is estimated by mentally combining the clouds present in different parts of the sky and recorded in terms of the eight parts of the sky (oktas). The kind of the cloud is determined and the amount of the sky covered by the clouds of each of the three categories is estimated and reported.
- (xi) **Height of base of clouds:** This is determined by observers with the help of a small hydrogen filled balloon, called ceiling balloon, or by a search-light or by electronic equipment. At observing stations not having any of the above equipment the height of base of cloud is obtained by estimation (I.C. Atlas, volume, 1987).
- (xii) **Sea and Swell:** At coastal stations, as well as on ships, observations are also recorded on the state of sea and swell and the direction of swell.
- (xiii) **Weather Warning radar Stations:** Weather warning radar station is a high powered, land-fixed radar designed to locate the cyclones, fronts, thunderstorms and areas of precipitation and their movement within a radius of 150 to 200 miles by means of the reflection of radar beams by the suspended obstructions. This equipment has been provided at Karachi, Sargodha and Cherat and is of great use for weather warning service with a high degree of accuracy and confidence. Storm warning radar networking after 980s in Pakistan is shown in the maps I.

Map-1.



Automatic Weather stations and Lightning Detectors are also installed at few stations in Pakistan recently.

### **5- Meteorological communication system/services.**

The role of the media in a successful public weather services programme is thus crucial and every effort should be made to build a cooperative and trusting relationship between the national meteorological services (NMS) and the media. PMD are used four main communication systems.

- i) GTS system
- ii) SADIS system
- iii) AFTN system.
- iv) V set system

To collect & transmit the Met data's from these systems, the products are prepared and the following services are provided to the clients.

#### **Meteorological services:**

Weather services are compasses a wide range of forecast, warning and information services to the general public, national and international shipping and aviation, the Department of Defence and other users. It consists of the following six individual outputs.

#### **i) Aviation meteorological services**

Aviation Weather services continued to enhance the safety, regularity and efficiency of national and international aviation operations. Services are provided within the international technical and regulatory framework of the International Civil Aviation Organization (ICAO) and the World Meteorological Organization (WMO).

Products supplied for aviation users are as under.

- Upper level wind charts
- Significant Weather prognostic charts
- METAR (current weather)
- SPACI (special weather report)
- TAFOR (Terminal Aerodrome Forecast)
- ROFER Route Forecast)
- SIGMET (significant Meteorological information)
- VOLMET broadcast

#### **ii) Hydro meteorological services and flood forecasting**

Hydro-Meteorological services encompass aspects of water resources assessment, the provision of flood forecasting and warning services and Hydrological and Hydro meteorological advice for design. These services depend on the information collected through the Pakistan Meteorological Department net works of Meteorological Observatories.

The flood warning services also operate a special purposes network of rainfall and river level station in cooperation with state and Local Government agencies.

Flood Forecasting Center in Pakistan provides the following main products.

- i) Flood forecasting.
- ii) River stream flow forecasting.

iii) Water management at Dam s especially in South West Monsoon.

### iii) Agro meteorological services

The PMD continued to provide the Agro-met services, Included the provision of Rain predictions Frost predictions, Soil Moisture information, Time of crop sowing/ Harvesting, Spring of pesticides on crops, Water requirement of crops, Heat and cold waves forecast, Special Weather Advisories for farmers, Monthly Agro met bulletin of Pakistan, Research on regional Basis in collaboration with Agriculture research institutions.

### iv) Climatological services

Long-term climatic data obtained from both basic and special observatories networks and store in the Computer data center (CDPC) Karachi, Pakistan. These are published in the form of climate summaries and normal, and made available in both hard copy and computer computable form for use in research. Climatic services are also under pointed by the month-to-month and year to year monitoring of climatic fluctuation including extremes such as Drought and Flood rain. The Prediction of climate anomalies and trends likely to effects the Environment, Agriculture and other Weather and climatic sensitive are of the economy (A. Bureau, Met, Report.

Climatological information for national Developmental projects (e.g. Tunnel in the northern Area, water level in lake & Rivers, Design For Dams Motorways, Roads), and for Environment Pollution, and Ozone monitoring are used.

### v) Marine Meteorological services

PMD- Areas of responsibilities under GMDSS (Global Maritime Distress& safety system).

Forecast is issued twice daily through INMARSAT Coastal station Perth, Australia for the ship already in sea.

Issued warning when the port is threatened & issued sea bulletin for fisheries broadcast by Radio.

### vi) Weather forecasting services to publics.

The PMD provides a wide range of weather information and forecasting services in the public interest for the benefit of the community at large in all states. Public weather services are distributed through mass media, the Internet, and telephone information systems. A few products are as under.

- i) Next t 24 hours weather forecast.
- ii) Next 2-3 days forecast for farmers.
- iii) Weekly weather forecast.
- iv) Seasonal weather prediction for planning.

### Others services

PMD are provided the following other services.

- i) Astronomical information for public e.g. Sunrise/sunset timing, Moon rising/moonset timings,

Information for moon sighting,  
ii) Geophysical and seismological services e.g. Earth quakes monitoring, Monitoring of nuclear Explosion in the region, Building sector.

## **6-ACHIEVEMENTS**

The Pakistan Meteorological Department, at the time of its establishment in 1947, inherited only 15 Meteorological Observatories from the Central Meteorological Organization then operating in the Subcontinent. The Department with its continuous efforts has improved weather forecasting capabilities by expanding the network of meteorological observatories, developing methods of observation, improving telecommunication facilities and forecasting techniques.

The major achievements of the Department are introduction of modern flood forecasting system, earthquake and nuclear explosion detection system, radar, satellite, computer technology, flight safety consultancy services in seismic design of dams, buildings and other development and disaster relief schemes.

The Department has also played vital role in research work and its scientists have made valuable contribution. More than 300 scientific papers have been written and published in both national and international scientific journals. Major emphasis in the research has been laid on the field of artificial rain making, ground water detection, arid zone research, ozone measurements, solar energy, wind power potential, oceanographic and space research.

Many of the Research Organizations such as Arid Zone Research Institute (AZRI), Space and Upper Atmospheric Research Corporation (SUPARCO), and Pakistan Atomic Energy Commission (PAEC) started their functioning with the initial assistance of the Pakistan Meteorological Department. Meteorological services are extended on regular basis to Civil Aviation Authority (CAA), Federal Flood Commission (FFC), Pakistan Agriculture Research Council (PARC), Ministry of Environment and Ministry of Food & Agriculture.

## **7-Future program**

The present trend of automation in meteorological measurements, real time data processing and recording on computer compatible media will continue into the future. The existing work of automatic stations will be expanded to further improve special coverage. Weather stations will be set up at Pakistan & this will provide valuable information on the weather system affecting Pakistan from various directions.

## **TO UP GRADE AND EQUIP THE DEPARTMENT**

A National Center for "Drought / Environment Monitoring and Early Warning" has been set-up in Islamabad as part of PMD.

Instruments will be installed to measure the Green House Gases, Soil Moisture data, River & Stream Flow Data, and Sub-surface water situation. The details are shown in table-3.

Table-3

S.NO	Item	Quantity	Area
1	AWS with Soil Moisture Sensors	50	Southern half of country
2	Self Recording Rain gauges	30	Catchments areas of Dams
3	Ordinary rain gauges	350	Southern half of country
4	Remote Sensing & GIS.	1	Whole Country.

## 8-Recommendation

To control the natural disaster, the author personally recommended and suggested to provide the technical supports including training and equipments to reduce the disaster and saved the human life. e.g. Tsunami Warnings could have saved thousands Peoples. A warning center such as those used around the Pacific could have saved thousands of people in Asia who were killed by the earthquake and tsunamis (Tidal waves).

## 9-References

- 1-Albert Miller & J.C.Thompson, CHARLESS E MERRILL PB.CO. A.B. Howell, Atmospheric measurements, Page 23-50.
- 2-Australian Govt: Bureau of Meteorology Annual report 2002-2003. Weather services Page 78-95.
- 3-H.R.Byers, General meteorology (1959) Third edition- Mc Graw-Hill book company, INC, Observation and station instruments Page-61.  
Haleh Kootval Regional Training
- 4-International cloud Atlas, WMO, 1956, Page 8-13.
- 5-International cloud Atlas, WMO, 1987, volume 2.

### Appendix i Instruments Installed in PMD before 1980s

S.No	Name of Instrument	Company Name	Received Date & Year
1	Minimum Thermometer -35C° to +40 C°	G.H.Zeal Ltd London	10-6-1965
2	Gran Minimum Thermometer -35C° to +40C°	M/s.C.F.cassella and Co Ltd London	17-10-1965
3	Minimum Thermometer sheath pattern -35C°to +40C°	Associated Instrument Casella standered	23-4-1963
4	Minimum Thermometer -30C° to 50C°	G.H.Zeal Ltd London	10-6-1965
5	Minimum Thermometer -30C°to 50C°	C.F.Casetter C.O. ltd London	17-6-1965
6	Minimum thermometer -20C°to 55C°	Associated Instrument Po Box - 4800 Karachi	19-11-1964
7	Grass Minimum Thermometer -35C° to 40C°	DO	16-1-1972
8	Minimum Thermometer Wooden From -25C° to 50C°	Salmul Co Karachi Casseter London	30-6-1971
9	Minimum Thermometer -25C°to 50C° Mugni Fram with N.P.L.	Assicuated Instrument Karachi canella london	7-3-1972
10	Slandered Thermometer -30C° to 50C°	Sermina Ltd Karachi Tunuya &Co Japan	17-8-1976
11	Sea Temperature Thermometer with Shild & Convas Buket -10C° to +42C°	Samina Ltd Karachi Tanuya &Co Ltd Tokeyo Japan	17-8-1976
15	Maximum Thermometer -10C° to 50C°	Associated International Po Box No 4800 West <b>Wahorf</b> Road Karachi	19-11-1964
16	Maximum Thermometer -10C°to 50C°	G.H.Zeal ltd London	10-06-1965
17	Electrical Anemograph	R.W. Munro Ltd	10-12-1964



	Velocity & Direction Recorder	London	
18	DO	Are Kos Karachi	29-10-1965
19	W.T. Bathy Thermograph depth Range 0-900ft or 0-275m	Nazer & Co Bender Road Karachi )2-04-1964	02-04-1964
20	Rain Recorder Hilmas 200 cm receiving surface	KARAL Kolb Thranfunt /Main Hum burg (Runtimes Naki 34	10-12-1964
21	Halifax weather Chart Transmenting Scanner TYP WF-204	Samina &Co Karachi	23-2-1965
22	PBO Theodolite Day& Night	Hilgen & Watts London	15-10-1952
23	PBO Theodolite Day & Night	Modem Trading & Co Vielona Road Karachi	15-10-1961
24	DO	Associated Instruments Pak Karachi	29-11-1965
25	Barograph BMO Range, 950 to 1050 Small Pattern	Associated Insh Karachi	25-3-1972
26	Fortin Barometer 670 to 1100 Mbs	Ahmed international Equipment Karachi	25-3-1972
27	Nephi scop	Fraucis Barker & Sons London	21-1-1949
28	DO	J.S. Industries Bundir Road Karachi	10-6-1965
29	Pocket Watches Assoted 15/16	Luntion Watch & Co Karachi	6-2-1966
30	<b>Soil</b> Thermograph Mercury remote type with three Recording system	International Commissariat Agencies Karachi	4-1-1973
31	Thermograph Temperature Range 15C° to 40C°	Selwel Corporation Bambino Chambers Golden Road Karachi	19-5-1973
32	Kp Marine Barometer Range <b>25" to 32"</b>	F. Darton London	18-7-1955
33	Barograph Weekly 940-1045 Mbs	Selewel Corporation Karachi	5-9-1973
34	Barograph Daily 940-1045Mbs	DO	10-11-1973
35	Micro Barograph	DO	1-611974

	Weekly 990-1020Mbs		
36	Thermometer Ordinary Range 0° to 130F°	Nagrethi & Zombra London	16-9-1958
37	Thermometer Ordinary Hill Range - 30° to 120F°	S.M.London	19-1-1953
38	Thermometer Ordinary Hill Range -30° to 120F°	DO	19-1-1953
39	Thermometer low Temperature -30° to 80F°	In Assets Fram I.M.D PONA	12-10-1954
40	Low Temperature Thermometer Range 0° to 550C°	Short & Mason Ltd Aneroid Works 280 wood welth abstias London	
41	High temperature Thermometer Range 0° to 110C°	Bird & thad London	20-2-1952
42	Thermometer Comical range 0° to 110C°	Griffin & Tat lock London	20-2-1952
43	Comical Thermometer range 0° to 200C°	DO	DO
44	Comical Thermometer range 0° to 360C°	DO	DO
45	Test Thermometer in C° & F° Scale -40° to 140F°	S.M.London	14-5-1955
46	Inspector thermometer standard range +10° to 140F°	In asset fram I.M.D. PONA	12-10-1949
47	Standard thermometer range -20° to 120F°	George Backer London	20-10-1955
48	Standard Thermometer +30° to 400F°	DO	DO
49	Standard Thermometer -90° to 30C°	DO	DO
50	Standard Thermometer -90° to 30C°	Bird & Tat lack London	17-1-1962
51	Standard (assorted dacoratui Thermometer -20° to 20F°	In asscts fram Imd PONA	12-10-1949
52	Thermometer Boiling Point -95° to 105C°	S.M.London	3-6-1958
53	Distance Thermometer	Do	15-901952

	Murcury in steet Air Temperature recorder - 36°to 56C°		
54	Thermograph Daily (Dry) Casella	C.F.Cessella London	6-11-1957
55	Thermograph Dry And Wet Daily	S.M.London	13-6-1962
56	Hygrograph wet dry daily	Associated International Karachi	13-3-1962
57	Hygrometer type 5635 daily clade	DO	1-2-1963
58	Thermograph Wet & Dry Daily	Arkos Cowan Road Karachi	23-4-1963
59	Recording Dry Wet Thermograph S.M. Type	S.M. London	1-6-1961
60	Hygrothermograph Daily	C.F.Cessella & CO London	6-11-1957
61	Earth Temperature	M/S with leمبر re-utgottijam Germany	6-July-59
63	Galvanometer range 12/0/12	M/S Cambridgeing LTD London	07-July-59
64	Gelavanometer (Micro Amp)	M/S Associated Inst. Mnfg Karachi	21-May-60
65	Air Meter Casella	M/S C&FCasella LTD London	20-Dec-60
66	Earth ThermometerNo, 1001	M/S N&Z London	11-Feb-61
67	Psychrometer Range 10 to 00 DG (ASSMAM)	M/S Reliance Pak Corp Khi	11-Feb-61
68	Sunshine Recorder Card No 1603	M/S C&F Casela London	11-FEB-61
69	Psychrometer Range 10 To 00 Dg (Assmam)	M/S Associated Inst Mnfg Karachi	11-SEP-61
70	Aspiration Psychrometer -10 to 00 C(Assmam)	M/S Modern Trading Comp Khi	4-DEC-62
71	Soil Thermometer-10 TO 40 C Depth 10 CM	M/S Jaylam Short & Masion Ltd London	4-DEC-62
72	Soil Thermometer-10 TO 40 C Depth 10 CM 20CM	DO	4-DEC-62
73	Soil Thermometer-10 TO 40 C Depth 10 CM 50CM	DO	4-DEC-62
74	Soil Thermometer-10 TO 40 C Depth 10 CM 100CM	M/S S & M LONDON	4-DEC-62

75	SUNSHINE RECORDER	M/S WLLH Lember Re-Utgottijom Germany	4-DEC-62
76	Solar Radioation Thermometer Range - 10 TO 70 C	M/S N& Z LONDON	5-MAR-62
77	Dew Guage Equipment	M/S Associated Inst Mnfg, Karachi	10-May-62
78	Suushine Recordedr Card No 1603	M/S C & F Casella &Co Ltd London	10-MAY-62
79	Whirling Psychrometer 5 To 50 C	M/S Associated Inst Mnfg Karachi	10-MAY-62
80	Solar Radioation Thermometer Range - 10TO 70 C	M/S Modern Trading Comp Khi	10-NOV-62
81	Preshmatic Copass Th Stand	M/S C & F Casella & Co Ltd London	15-MAY-63
82	Ordinary Thermometer -5 To 55 C W Th Npl	M/S Associated Inst Mnfg Karachi	17-JUL-63
83	Whrling Hygrometer -5 To 50c	M/S Associated Inst Mnfg Karachi	17-JUL-63
84	Galvanometer 8.00c Pi No A2003	M/S General Agencies Ltd Khi	5-DEC-64
85	Galvanometer Upper Suspention	M/S General Agencies Ltd Khi	5-DEC-64
86	Galvanometer Lower Suspention	M/S General Agencies Ltd Khi	5-DEC-64
87	Soil Maxture Meter Completer	M/S Lodhi & Co Khi	5-DEC-64
88	Ordinary thermometer range -20 to 55 c	M/S Associated Inst Mnfg Karachi	19-NOV-64
89	Whirling Hygrometer T-0724 Range 5 To 50 C	M/S Associated Instrument Ltd Khi	19-NOV-64
90	Rain Recorder Hlmon	M/S Kasl Kolb Main Nka Hamburg	12-OCT-64
91	Micro Galvanometer	M/S Ins Trading Comp Khi	14-DEC-64
92	Hair Hygrograph	M/S G.Luff Metell Barometer Hambur	20-DEC-64
93	Ceilo Graph Brand Celometer	M/S Ahmed Inst Equipment Khi	23-FEB-65
94	Sun Shine Recorder	M/S With Lember Re-Utgottijam Germany	17-MAR-65
95	Lolar Rdiation Thermometer -10to 95 C	M/S G.H Zeal London	06 OCT-65
96	Goto model 303 ginch equetorial refractor	M/S Inst Trading Comp Khi	10-DEC-66

	Telescope complete		
97	Ceilograph Brand Ceilometer Const Meter Recorder Only	M/S Ahmed Inst Equipment Khi	21-OCT-66
98	Micro Barograph Daily 580-670 Mbs	M/S Arkos Come Saddar Khi	14-DEC-66
99	Hair Hygrograph Fig 5 Eos08	M/S Ahmed Inst Equipment Khi	23-JUN-67
100	Micro Barograph Type 524451 Daily	DO	27-SEP-69
101	Whirling Psychrometer Model 520550 Range 30 To 40 C	DO	27-SEP-69
102	Hand Anemometer Tyse 52	DO	27-SEP-69
103	Natural Siphone Rainfall Recorder 203mm	M/S Associated Instrument Khi	30-MAY-70
104	Measuring Jar	DO	30-MAY-70
105	Sunshine Recorder	DO	30-MAY-70
106	Glass Measuring Jar 10mm	DO	30-MAY-70
107	Magnometer Typ 592/N	M/S Mslittle More Scientific Engineering Co Paching Chine	30-MAR-71
108	5335 Binifellicinet & Dry Hygrometer Range 15 TO 40	M/S Cosmo Polition Treders Karachi	1-JAN-72
109	Hair Hygrograph Compleat	M/S Associated Inst Mnfg Karachi	1-JAN-72
110	Whirling Hygrometer -5 TO 50 C	DO	1-JAN-72
112	Natural Siphone Recorder	DO	1-JAN-72
113	Solar Radiation Therometer -10 To 95 C	M/S G.H Zeal london	7-MAR-72
114	Hair Hygrograph	M/S Selwel Corp Khi	19/5/73
115	Hand Anemometer Osk 756	M/S Associated Mechine Tool Makers	1/12/73
116	Temp Indicator Model No 5500102-1-01-02	M/S Zelin Ltd Khi	17/10/74
117	Ken Pattern Barometer E 430	M/S Azam Trading Corporation Khi	5/4/75
118	Fortin Barometer Be 380	DO	5/4/75
119	Sea Temp Thermometer -10to 42 C	M/S Samina Ltd Karachi	17/8/76

120	Temp Indicator Telex Model T Range -20 To 50c	M/S Samina Ltd Karachi	31/11/77
121	Apt Equipment	Donate By French Met Service Free Of Cost	31/8/78
122	Murihead Automatic Compositive 198,230 Am/Fm Weather Recorder	M/S Ial Pvt Ltd Khi	13/4/78
123	Thermograph Daily 0250 C	M/S G.R Trading Comp Karachi	28/8/78
124	Self Recording Raiuage Daily 0.10	DO	28/8/78
125	Hair Hygrograph Daily Range 0-100%	DO	28/8/78
126	Rain Measuring Glass 5 Inch Ordinary	DO	28/8/76
127	Micro Barograph Daily 950 To 1050	M/S G.R. Trading Comp Karachi	13/10/79
128	Micro Barograph Weekly Range 950 To 1050	M/S G.R. Trading Comp karachi	13/10/79

Appendix(ii).List of the Instruments Installed in PMD after 1980s

S.No	Name of Instrument	Company Name	Received Date & Year
1	Maximum Thermometer -20C°to 55C°	G.R.Trading Fida Chambers Karachi Cassella London	8-9-1986
2	P.B.O. Theodolite TAMYA TYP E0 Cat No 1940 Japan	Samina Ltd Nalson Chambers 4th floor I.I.Chundrigals road karachi	10-5-1983
3	Digital Barometer Pt.No –M 2236A Range 800-1050Mbs plus minus 0.4Mbs	Mayyar International Karachi M/sNegrte &zambra (Aviation) Ltd England.	21-8-1983
4	Fortin Barometer range, 700-1050Mbs	Schwet Corporation Abdullah Haroon Road Karachi	24-10-1984
5	K.P. Barometer (station Barometer) Range 700-1100Mbs	DO	24-10-1984
6	Hair Hygrograph (Hygrometer T2-16)	Azam Internationl Shahe- de- Millat Road Karachi	24-10-1986
7	Thermograph T2-16	DO	24-10-1986
8	Thermograph daily	Rizvi & Co Ghulshan Center S.B –B Block 130, Ghulshan-e-Iqbal Karachi	9-2-1988
9	Thermograph T2-18	Azam & Co International Shahe-de-Millat Road Karachi	29-10-1984
10	Barpgra[j TZ-20	DO	29-10-1984
11	Fortin Barometer Range, 700-1100 Mbs	G.R.Trading & Co Fida Chambers M.A. Jenah Road Karachi	29-10-1984
12	Kew Pattern Barometer 700-1100Mbs	DO	DO
13	Prexision aneroid Barometer 850-1100Mbs	Arkos Pakistan Ltd 307 Mehboob chambers Victoria Road Karachi	31-12-1986
14	Precision Aneroid Berometer 750-1020 Mbs	DO	DO
15	Precisan Aneroid 650-1050Mbs	DO	DO
16	OMS-10 Combined Wind speed and Direction trams	Internaional Aeradio Pak (privat) Ltd Po. Box -3160	21-2-1987
17	OMC-170 Digital Display units	DO	21-2-1987
18	Two channel Rushtak Recorder For Wind Speed & direction	DO	DO
19	PBO Thedolite SMI/MK-5	Samanters Street No-25 F- 8/2 Islamabad	23-12-1987
20	Hair Hygrograph daily &	Rizvi & Co Gulshan centre	9-2-1988

	Weekly	SB-B, Block 130,ghulshan-e-Iqbal Karachi	
21	Electrical Anemometer to Measure Wind & Velocity & wind direction to <b>Briths</b> IM-146 Without Recorder	R.W.Munro Ltd London	24-7-1997
22	Barograph Daily Range, 950-1050Mbs	3A Corporation MF.26 <sup>th</sup> Street <b>Phax V</b> Defance Housing authority Karachi	19-1-1994
23	Prismatic Compass (Breithaupt) No 3010	M/S Electronic <b>Business</b> System Karachi	25/6/81
24	Precision Aneroid Barometer Pressure Range 900 to 1050 Mbs	m/s W.M.O Free Of Cost	27/8/81
25	Set Of Inspector Kit	M/S W.M.O Free Of Cost	27/8/81
26	JV 728 Hygograph	M/S Razvi & Co Khi	24/11/81
27	JV748 Actinograph	DO	24/11/81
28	Earth Thermometer Range 1058c Tcm 10cm,20cm,30cm,50cm &100cm	M/S Associate Instrument Ltd Khi	10/12/81
29	Observatory Type Triple Compound Visual Recorder Wpen Driv	M/S Samakos Trading Pechs Khi	1/11/82
30	Natural Siphon Rainfall Recorder 203mm	M/S Associated Instrument Ltd Khi	19 <sup>th</sup> May-83
31	Digital Barometer 2236 800,1050MBS	M/S Mayyar Instrument Khi	21/8/83
32	T16324 Portable Anemometer range 50 to 1000 M/M/N	do	08-Nov-84
33	Inspection kit special traveling carrying case	M/S chavs instruments khi	26-Nov-84
34	Vs/ model 80A recorder for 230 v 50 hz	M/ ray trading company khi	26-Dec -84
35	Takamisana model str-300 seismometer	M/S instruments trading corp khi	25-Apr84
36	Dew balance recording type daily hillier type	M/S Alkos Pakistan Ltd khi	08-Sep 85
37	Platinum resistance thermometer shield	.....do.....	08-Sep 85
38	Foster Cambridge p-130 thermometers range 30 to 5c 50 cycle	M/S commercial instruments khi	08-Sep 85
39	Uhf fm handheld Transceiver 335 -512 Mhz 6 channel	M/s Magnum pak khi	30 Nov 86
40	OMC-170 combined wind speed and direction	M/s IAL pak Ltd khi	21-Feb 87
41	Transmitter		
42	OMC-174 digital display unit	M/s IAL pak Ltd khi	21-Feb 87
43	2 channel ultrasonic recorder for wind speed and direction	M/s IAL pak Ltd khi	21-Feb 87



44	Solar power Automatic weather station Equipment (spares)	M/s Associated instrument Ltd khi	13 Apr 87
45	Solar power system consisting of G- 12- 1336 standard arrays 50	M/s Electronic Business system khi	28 Nov 87
46	Alpha 6121 oMhz walki talki sets	M/s interhome Ltd khi	28 Nov 87
47	Automatic weather station	M/s Associated instrument Ltd khi	19 Mar 88
48	APT system Model- MSG-20	M/s Magnum pak khi	26 Jun.89
49	Hostion instrument DMP29 TG-10H	M/S AWB, UNDP	19 Jul 89
50	Solar arrays system	U N D P	30 Apr 90
51	Radio sound R80-15	M/s I A L pak Ltd khi	15 Jul 1979 20th Dec 1990
52	Liquid damped prismatic compass patted punch	M/s Avionic society int khi	03 June 99
53	Yaesu sys-600 Transceiver	M/S East west khi	17 Oct 00
54	Satellite system pc/sat sadisi/nt	M/s Techno dyngrnic Pakistan	20 Nov 00
55	Automatic plotting system	M/s 3A corp. khi	18 Oct 01
56	Complete Remote seismic station	M/s 3A corp. khi	16 .Nov – 02
57	Ultra sonic Anemometer	M/s Associated instrument Ltd khi	12- Aug-03
58	Seismic. Meters e component	M/s 3A corp.. Khi	25- May –03
59	IMC seismic Montoring system	M/s Associated instrument Ltd khi	20 –May-03

Appendix (iii).

The following instruments are normally found in the observation compound:

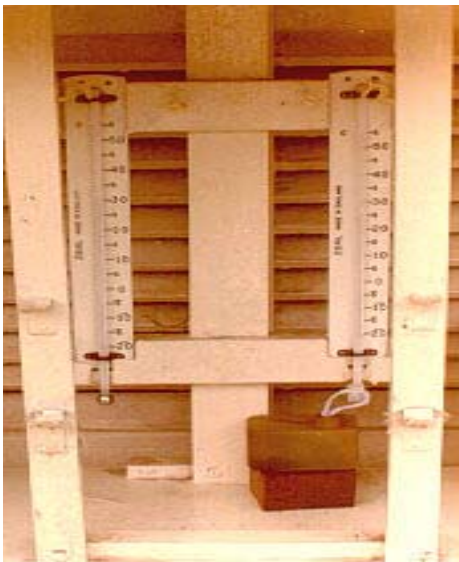
- Stevenson Screens
- Evaporation Pan
- Rain Gauge
- Rain Recorder
- Sunshine Recorder
- Theorize (Tracking Balloon)



The following instruments are kept inside the Stevenson screen:

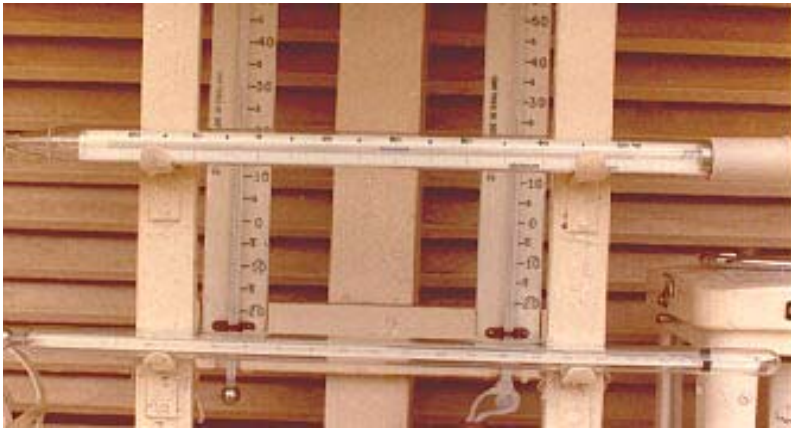
- Dry and Wet Bulb Thermometers
- Maximum Thermometer
- Minimum Thermometer
- Thermograph
- Hygrograph

### ***Dry and Wet Bulb Thermometers***



The dry and wet bulb thermometers are placed vertically on supports inside the Stevenson screen. The bulb of the wet bulb thermometer is wrapped with muslin and is tied up with a wick. The wick is then dipped inside a container, which contains distilled water.

### ***Maximum and Minimum Thermometers***



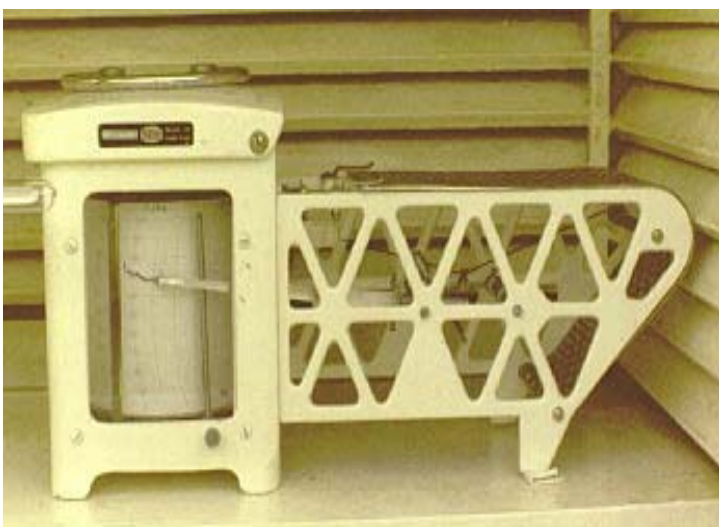
The Maximum and Minimum thermometers are mounted horizontally inside the Stevenson Screen. With the minimum thermometer slightly tilted.

### ***Thermograph***



Thermograph records air temperature continuously on a chart. Two metals of different alloys are welded together in a coil form. The different in the coefficient of expansions will uncoil or tighten the coil when subjected to temperature changes. The movement is then magnified by a lever system to a horizontal pen, which is attached to the coil with a pen nib slightly rested on a chart. The scaled chart is wrapped around a drum. A clock is built inside the drum.

### ***Hygrograph***



The hygrograph is an automatic instrument for measuring relative humidity.

### ***Check Gauge***



The Check gauge is used to measure amount of rainfall.

### ***Rain Recorder***

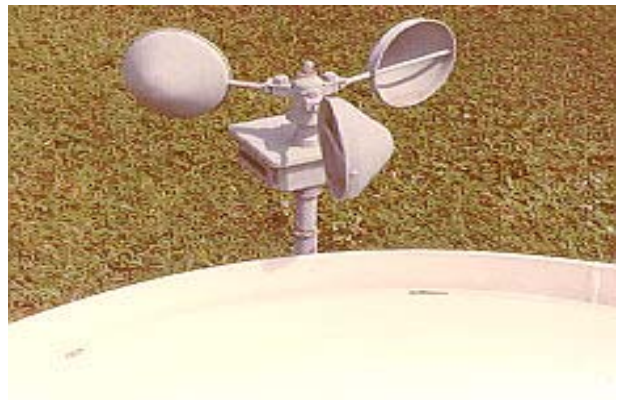
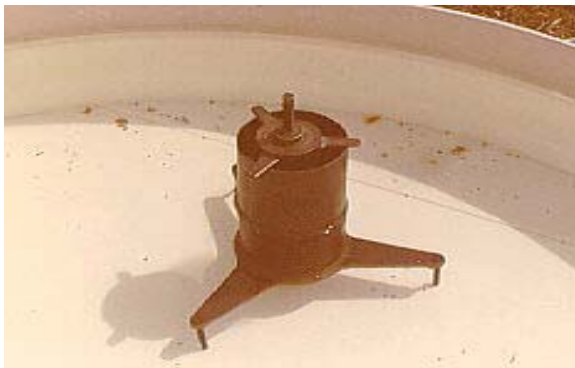


The rain recorder is the instrument for measuring rainfall over a period of time (daily , weekly or monthly depending on the type of recorder and also the chart used)

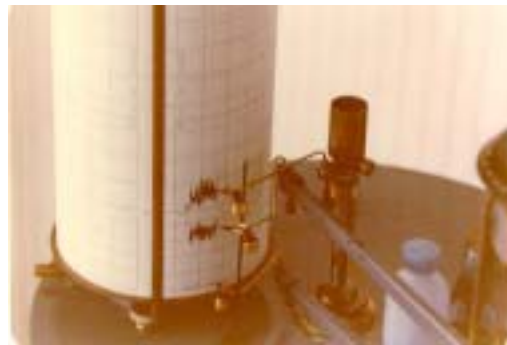
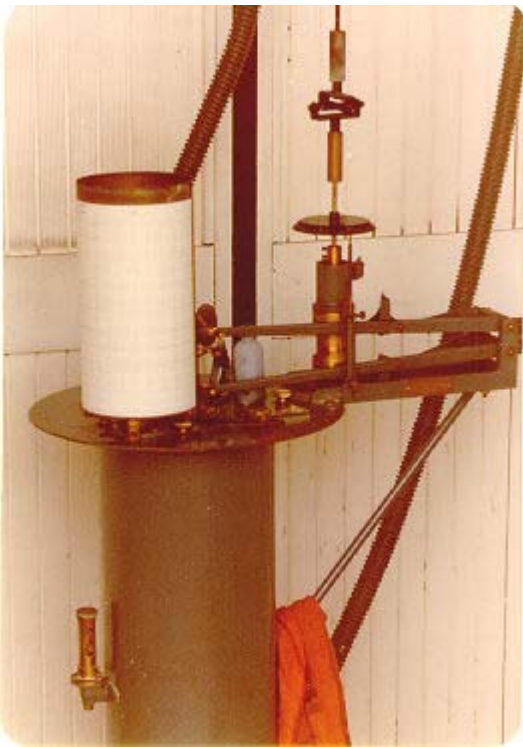
## **US Class A " Evaporation Pan**



"US class A" pan is used to measure the rate of evaporation. A hook gauge is used to measure the water level inside the pan and A cups anemometer is placed beside the pan to measure the surface wind blow over it.



## **Anemometer**



The anemometer is used to measure wind direction and speed and Sunshine recorder measured the sunshine hour of the day.

# The Low Cost Radio Frequency Rain Meter

A.Koldaev\*, A. Kutarov\*, D.Konovalov\*\*, A.Mironov\*

\*Central Aerological Observatory, State Hydro Meteorological Service of Russian Federation.

\*\* Main Hydrological Institute, State Hydro Meteorological Service of Russian Federation.

## Abstract

The low cost radio frequency rain meter was developed and constructed. The principle for operation is in measurements of Doppler spectra of raindrops in the vicinity of the sensor. The low cost of the sensor is achieved by employment of serially produced microwave unit (generator + detector), which is ordinary used for home security systems. The microwave unit is accomplished with amplifier and microprocessor board. The microprocessor board pre-programmed for: executing of FFP, integration of the retrieved spectra within 10min, transforming of average Furies spectra into Drop Size Distribution (DSD), and translating of this data via RS232 port. The main advantage of the sensor is in its small size dimensions (10sm x 10sm x 20sm) and small weight (less then 1kg), so the sensor can be easy added to the current meteorological musts. Power consumption can be provided by accumulator battery and data transmission can be made via GSM modem. With these two options, the sensor is ideal for unmanned meteorological stations. The comparisons of the radio rain meter with the standard rain gage were carried out within summer 2004 at the Valday State Hydro Meteorological Experimental Site, Russia.

## 1. Introduction

The measurement of atmospheric precipitation is a routine job for any meteorological observations worldwide. The most common applications of the data are: floating warning, agriculture, draying warning, global climate change. Most recent applications are in Weather Radar validation/calibration procedure as well as in validation experiments for Satellite Meteorology. The Tretyakov precipitation bucket O-1 was accepted as the first common device on the whole territory of former USSR. The principle is very simple: just collection of precipitation and measuring of the accumulated amount within definite period of time. The problems are basic: wind, evaporation, and losses on damping. The disadvantage cannot be overlapped: any autoimmunization is impossible. The next step: self recorded rain gage P-2: the accumulating amount of precipitation pushes the pen, which record the current level on the tape of mechanical recorder. The disadvantage stills the same as for O-1.

Most recent developments are based on Doppler type micro radars, which allow retrieving Drop Size Distribution (DSD) in the vicinity of the installation of the system. There are a lot of companies, who produce Doppler radio technical gages now. But the first one (POSS) was developed in Canada in the beginning of 90th and is widely used in Canada up to current days.

The presented development LCR-11 (Low Cost Rainsensor, operating at frequency 11GHz) was focused on accumulation of all advantages provided by Doppler radar gages, but the main goal was in reduction the price up to bottom level for such type of sensors. The original algorithm for Doppler spectra processing was proposed and tested to decrease impact of wind into the errors of rain intensity measurements. The comparisons prove that the accuracy of the new radio rain meter corresponds to the Russian State Standard for rain precipitation measurements. The results of the comparisons, including the rains with different nature and intensity are discussed in the paper.

## 2. Theoretical Background

The basic physical principle is that the drops of rain have sustainable (constant for each size of drops) velocity of sedimentation, and thus the Doppler spectra is "one-to-one" corresponded to the DSD. It is well know [1] that back scattering cross-section of the falling rain drop with time correlation is:

$$\mathbf{s}_B(r, \mathbf{l}, \mathbf{t}) = \mathbf{s}_B(r, \mathbf{l}) \mathbf{c}(\bar{k}, \mathbf{t}) \exp(i, \bar{k}, \bar{U}, \mathbf{t})$$

$\bar{k}$  - wave vector;  $\mathbf{s}_B(r, \mathbf{l})$  - stationary back scattering cross-section;  $\mathbf{c}(\bar{k}, \mathbf{t})$  - drop velocity fluctuation function;  $\exp(i, \bar{k}, \bar{U}, \mathbf{t})$  - wave phase factor which is changed by the drop velocity U.

The spectrum of that back scattering cross-section can be written as:

$$W_{SB}(\mathbf{w}) = \int_{-\infty}^{\infty} \mathbf{s}_B(\mathbf{t}) \exp(i\mathbf{w}\mathbf{t}) dt \quad \text{where} \quad W_{SB}(\mathbf{w}) = W_{SB}(\mathbf{w}, r)$$

If to take into account that rain contains the assemble of particles with DSD described as  $n(r)$ , the Doppler power spectrum can be written as:

$$P(\mathbf{w}) = \int_{r_{\min}}^{r_{\max}} n(r) W_{wB}(\mathbf{w}, r) dr \quad P_i = P(\mathbf{w}_i) \otimes \bar{P} \quad W_{SB}(\mathbf{w}) \rightarrow \mathbf{A} \quad \text{where}$$

$$A_{ij} = W_{SB}(\mathbf{w}_i, r_j)$$

$$n_j = n(r_j) dr_j \rightarrow \bar{n}$$

$$\bar{P} = \mathbf{A} \bar{n} \quad (1)$$

If to suppose that the drop with the radius  $r$  is moving with the constant speed  $U$ , the power  $P(\mathbf{w}_j)$  in the Doppler spectra will correspond to  $\mathbf{w}_j = 2kU(r_j)$ . Thus:

$$P(\mathbf{w}_j) \Delta \mathbf{w}_j = \mathbf{s}_B(r_j) n(r_j) \Delta r_j \quad \Delta \mathbf{w}_j = -2k \left. \frac{\partial U(r)}{\partial r} \right|_{r=r_j}$$



$$P(\mathbf{w}_j) = \mathbf{s}_B(r_j) n(r_j) \left( -2k \frac{\partial U}{\partial r} \Big|_{r=r_j} \right)^{-1}$$

From where we can retrieve the matrix for the task (1) in the strait form as:

$$A_{i,j} = -\frac{\mathbf{s}_B(r_j)}{2r \frac{\partial U}{\partial r} \Big|_{r=r_j}}; A_{i,j} = 0 \quad i \neq j$$

As far the n(d0 is determined from (1), we can determine the intensity of precipitation as:

$$p = t * \frac{4}{3} \rho \int_0^{\infty} U(r) n(r) r^3 dr$$

Where: p- rain intensity, t- time of measurements.

### 3. Principle of operation and block diagram

The principle of operation is based on measurements of vertical velocities of rain drops by means of micro power Doppler radar working in continuous mode of radiation at frequency 11GHz.

The system is consist with:

- Microwave receiver/transmitter working through the same horn antenna (Microwave Module)
- Low Frequency Amplifier (LFA)
- The Digital Processor, which performs FFT algorithm and all digital exchange functions.

The block diagram is presented on the fig.1.

Micro power Microwave transceiver works according to the principle of homodyne continuous-wave radar. Major portion of the energy of non-modulated microwave oscillations, produced by the open wave-guide section with build in Gun diode, is emitted into the space by horn antenna. The part of the energy, due to the uncontrolled connection, passes directly into the wave-guide mixing section and is used as the signal of heterodyne.

It is known that the uniform velocities of the raindrops are within the range 1 to 10 m/s. Thus, at the frequency of transmitter of approximately 11 GHz value  $F_d$  will be found within the range 60 to 700 Hz. Further, the signal, detected on mixer diode, is amplified by Low Frequency Amplifier and transferred to digital processing board. The digital processing board converts the analog signal by means of low frequency ADC and, using the algorithm of digital Fourier Processing transforms it into the spectrum. Then, the spectral data are accumulated in the working storage during the assigned period of time. The averaged spectra is used for retrieving of DSD and thus for further calculation of the current precipitation intensity.

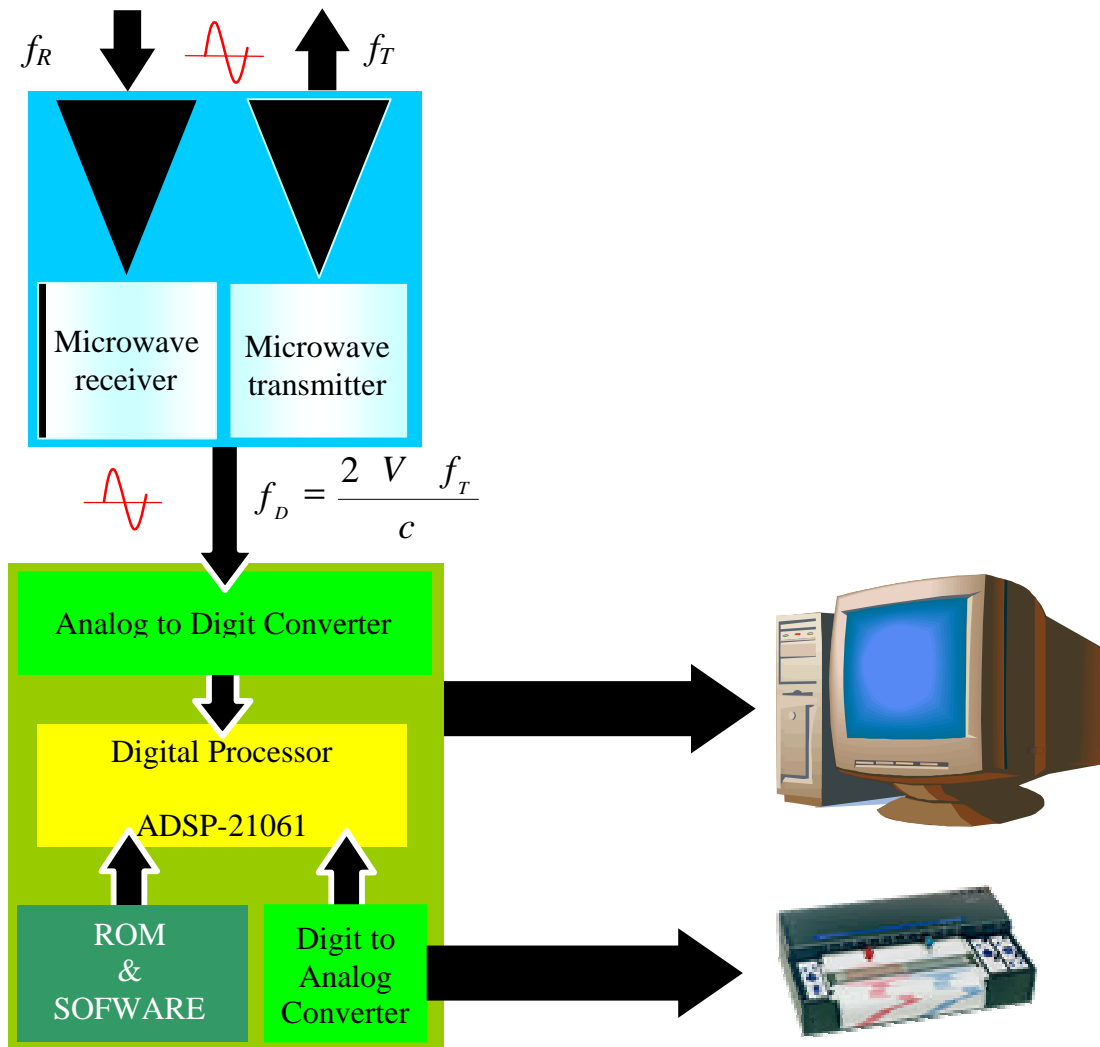


**Figure 1.**

The main advantage of proposed and realized in LCR-11 technical solution is that the Microwave Module (MM) is the same as MM industrially produced in large series for microwave alarm systems for common life. Thus the price of this part of the system is extremely cheap. It is executed as a solid part composed with two wave-guide sections: mixing and generator, and common horn antenna. Horn antenna is equipped with the shielding radio-transparent cap of conical shape, made from glass-fiber-reinforced plastic and intended for the protection from the meteorological effects and the pollution. The conical shape of cap is caused by the need for avoiding the accumulation of precipitation layer on its surface and preventing destruction of the instrument by birds.

Horn antenna is connected to the output of wave-guide section and has various forms of antenna pattern for the transmitting and receiving section. In this case the acting radiation pattern is determined by the intersection of the diagrams of receiver and transmitter. This feature makes it possible (without using large-dimension antenna) to create narrow "effective" antenna beam.

The specialized signal processor of firm Analog Devices Inc ADSP of 21061 "Sharc" is used in the system. This processor has the built-in working storage and the arithmetic-logical device, intended for the work with 32- bits discharge words with the floating point. The architecture of this processor is adapted for its effective application in the devices, which use different algorithms of digital processing of signals, in

particular the translation algorithms of Fourier. Moreover, the application of arithmetic with the floating point makes it possible to qualitatively increase the accuracy of processing signals. The presence of the built-in the processor device of direct access to the memory (Direct Memory Access - DMA) makes it possible to organize the continuous processing of signals. It means that, the processes of the accumulation of the data from ADC and processing of the previously accumulated data are performed in parallel mode. The transmitting of data to the external terminals does not interrupt the calculations also. Great possibilities for the subsequent modernization and the expansion are placed in the computational part of the instrument. There is a possibility of the performance of instrument for the work in the autonomous regime with the transmission of information along the existing contemporary communication systems.

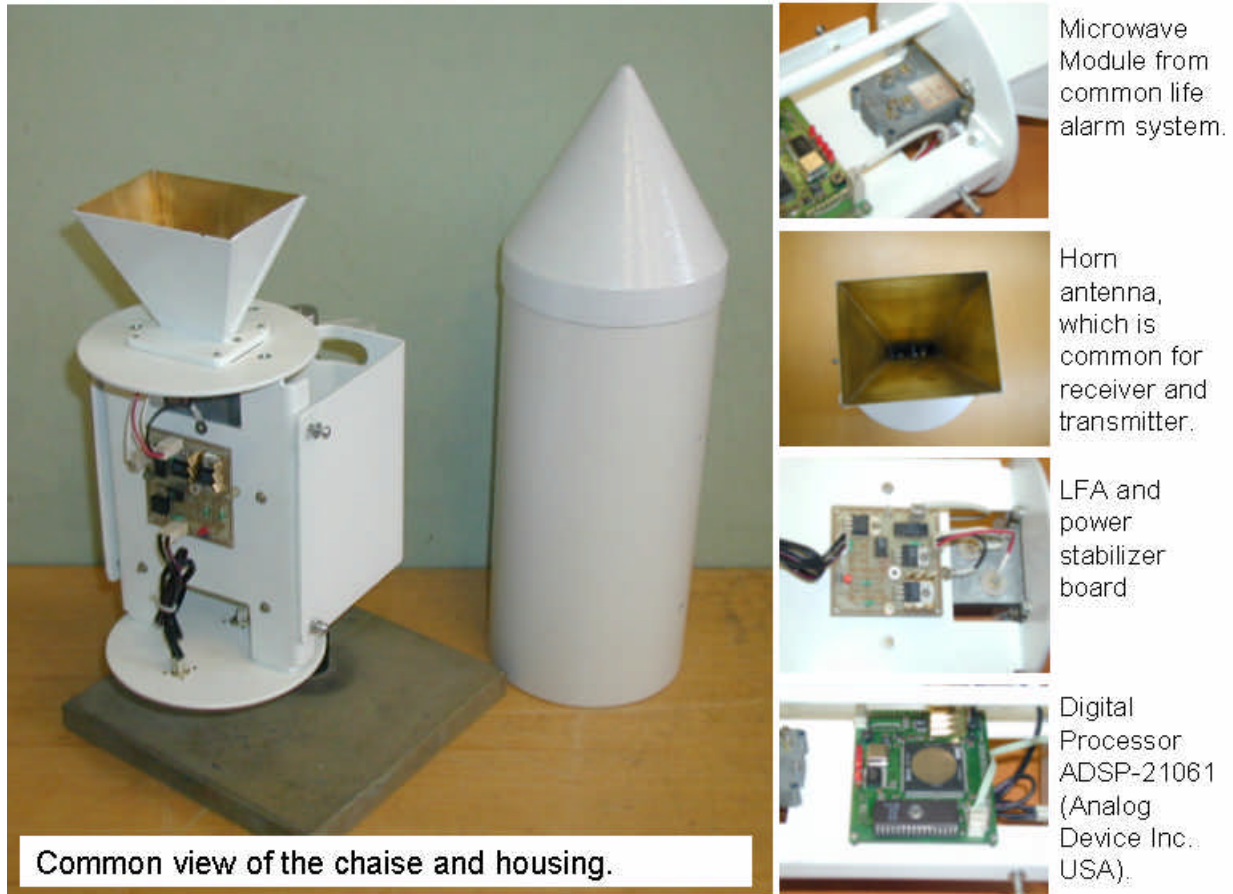


**Figure 2.**

The housing of instrument is made from weather proof plastic and is intended for the protection of instrument from the mechanical and meteorological actions. The aluminum chassis, which ensures the hardness of construction and fastening all knots and instrument units, is located inside the housing. For fastening of instrument on the vertical supports is provided the aluminum bracket rigidly connected with the chassis. The common view of the LCR-11 device and their parts is presented on the Fig.2

#### **4.Laboratory and field tests**

The laboratory tests were conducted in the Central Aerological Observatory, Dolgoprudny, Moscow Reg. The tests included the measurements with LCR-11, weight type precipitation gage and 3D wind measurements. The comparisons were performed within fall 2003 –spring 2004 period. The results of this

comparisons were very promising, that allow us to schedule and conduct field comparisons on the territory of State Hydrological Experimental site in Valday , Novgorod Region. The main feature of the State Hydrological Experimental side is that it is equipped with Russian Federation State Standard of Rain Precipitation. This standard is just a composition of three (3) Tretykov type precipitation gages, which located in special environment.



**Figure 3.** Comparisons of LSR –11 with the Russian Federation State Standard of Rain Precipitation on the experimental site of State Hydrological Institute. Valday, Novgorod Reg. May-September 2004.

The State Hydrological Experimental site is a unique place not only because of State Rain Standard. On the territory of the Experimental site there are more then 20 rain gages of different type. In accomplishment to the rain gages, the Experimental site is equipped with a set of evaporation pools, meteorological stations and special wind sensors. The wind sensors were actively used in our work, because the influence of a side wind as well as a vertical wind is one of the main source of errors for the Doppler type precipitation gages. We have used three mechanical wind sensors installed on three different standard heights and one ultrasonic wind sensor , which was installed immediately in vicinity of LCR-11. The field tests were conducted within May-September 2004. The picture with common view of the installation is presented on the Fig.3.

## 5. Results of comparisons

It was recorded about 60-e rain events of different nature, intensity and duration. The results were presented in three grope of plots: The first grope is the plots for “case study” which describes the time series of accumulated precipitation for each individual rain. The example of such direct comparisons of LCR-11 with the Rain recorder P-2. is presented on the Fig. 4. The graphs presented the precipitation accumulation within about 7 hours. (Valday, 28 August 2004).

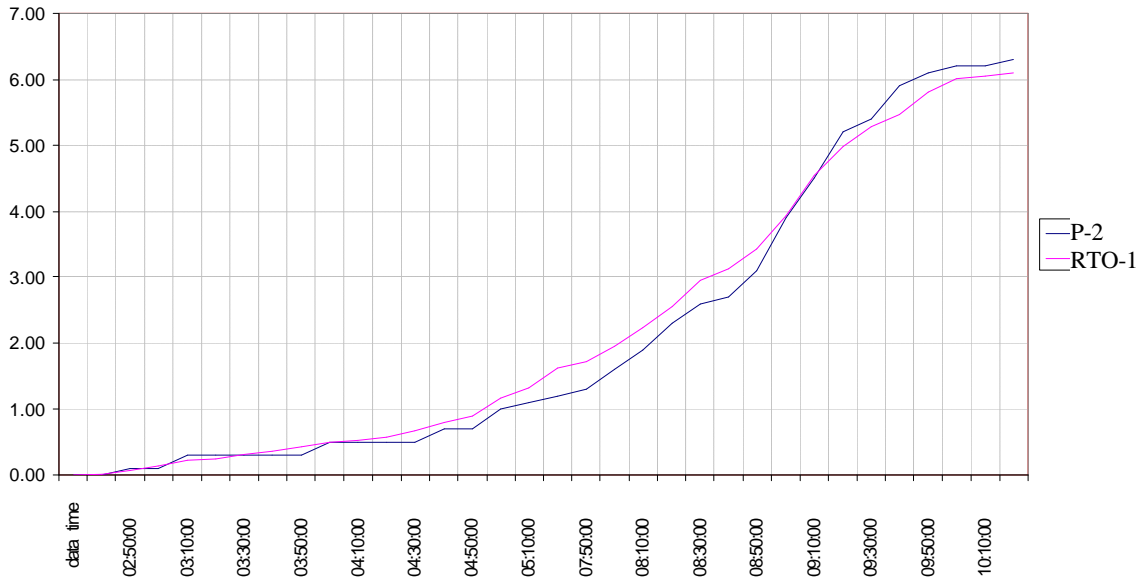


**Figure 4.** The results of direct comparisons of LCR-11 with the Rain recorder P-2. The graphs of precipitation accumulation within about 7 hours. Valday, 28 August 2004.

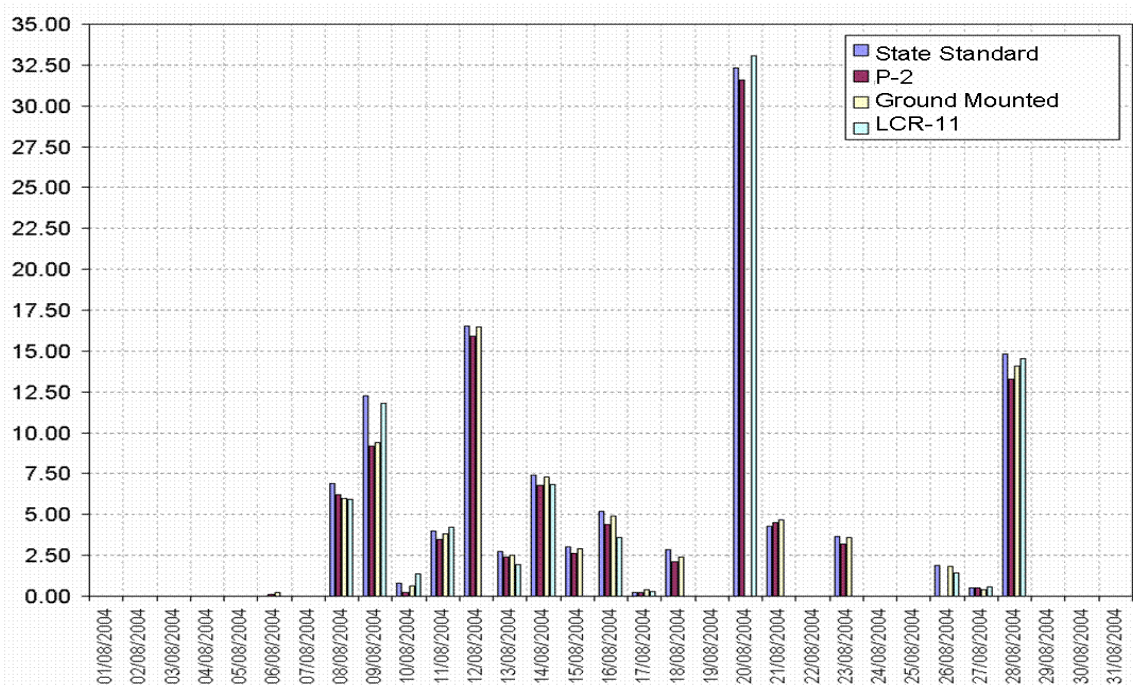


**Figure 5.** The results of comparisons with State Standard and Ground Mounted Standard within a whole month. (Valday, 1-31 August 2004). On the plot the 24 hours accumulated values are presented. P-2 data are presented also for reference only

The second group is the plots with histogram presentation of accumulated precipitation within 24 hours by different type of precipitation gages. The example of such histogram obtained within August 2004 is presented on the Fig. 5.

And the third type of the plots is the scatter plot of LCR-11 versus State Standard in Log scale with division of the results for the different range of precipitation accumulation within 24 hours. The example of that plot for August 2004 is presented on the Fig.6.

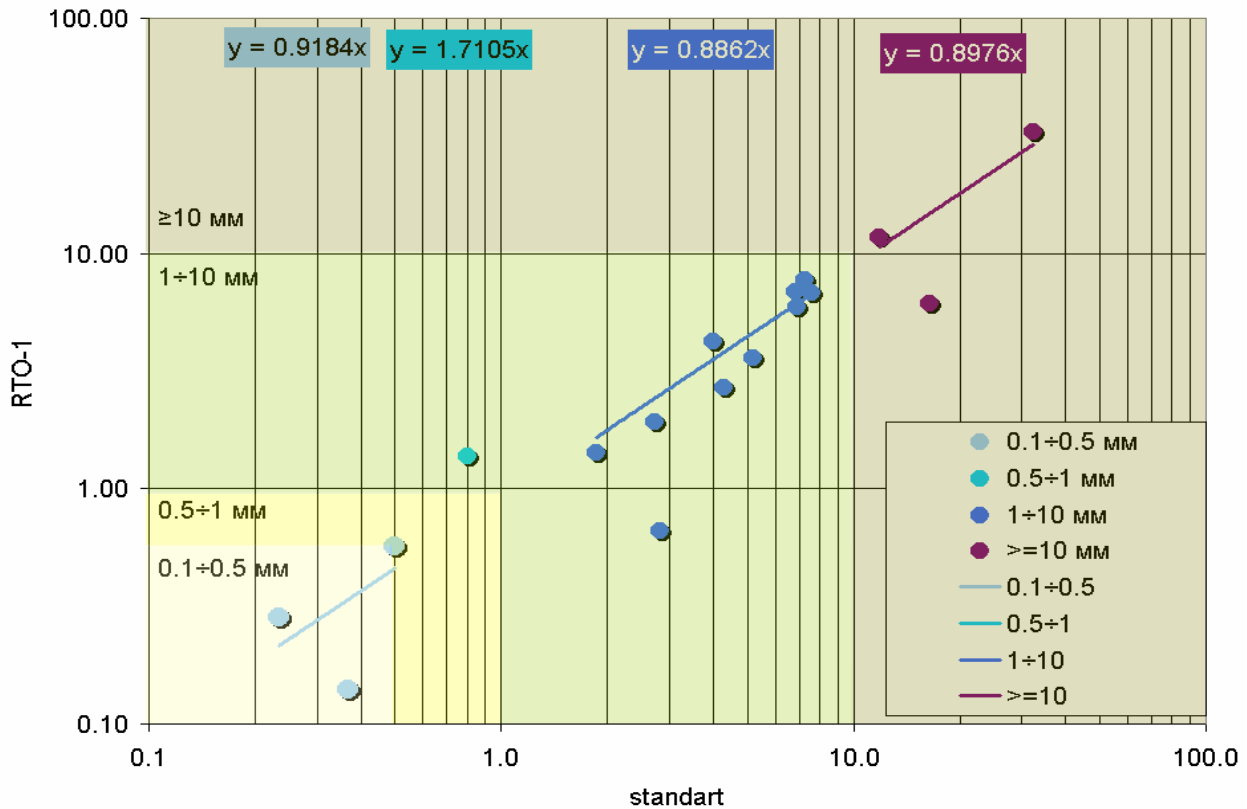


**Figure 6.** Scatter plot of comparisons with State Standard in Log scale with division of the results for the different range of precipitation accumulation within 24 hours

As a result of field tests the big volume of experimental data was obtained. This information allows to improve the parts and whole construction of the device and to start the production of signal series of LCR-11. The influence of wind was investigated also, and it was experimentally proven that wind not decrease the accuracy, which is found in good agreement with the accuracy of State Standard.

## Conclusions

1. As the result of field tests all disadvantages of the LCR-11 “alpha” sample were reviled. This allows improving the construction and starting serial production of the devices.
2. The performed comparisons prove the accuracy of measurements of 24 hours accumulated rain within the range of accuracy of Russian Federation State Standard. The influence of horizontal wind is found negligible small.
3. The improvements of the devices made on the basis of field tests have not increased its price, but sufficiently increase its reliability and Customer oriented properties.

# DESIGN AND DEVELOPMENT OF A LOW COST AUTOMATIC WEATHER STATION

By: Nuwan Kumarasinghe

Department of Meteorology, Bauddhaloka Mawatha, Colombo 07, Sri Lanka.

Telephone: 94-11-2681039, Fax: 94-11-2698311, e-mail: [nuwan1960@yahoo.com](mailto:nuwan1960@yahoo.com)

## ABSTRACT

Observation of weather data plays a major role in the field of meteorology. The Automatic Weather Systems (AWS) provide meteorological observations to users in real-time basis by gathering data from a network of automatic weather stations through various communication channels. Availability of real-time meteorological data is an essential tool for daily weather forecasting. The reliability of weather forecasting mainly depends on the amount of data received for analysis. Setting up of a manned meteorological station is relatively costly exercise. With the advancement of information technology and electronics and also the growing demand for meteorological information, it becomes more popular to disseminate the meteorological information through network means to meteorological community.

Main objective of the design of AWS is to have more user friendly and flexible network of instrument which is made by incorporating locally developed low cost and reliable sensors such as wind direction sensor for weather observation.

Rabbit 2000 8-bit core module micro-controller is used as the main processor. It handles data acquisition, field processing, data storage and data transmission and it can also handle both analog and digital signals. Assembly and C programming languages are used for Rabbit micro-controller. Both application and communication software are user friendly and flexible. IC based sensors are used for temperature, humidity and atmospheric pressure and are compatible with WMO standards.

### 1. Introduction

The Automatic Weather Systems (AWS) provide meteorological observations to users in real-time by gathering data from a network of automatic weather stations through various communication channels. Design and development of an low cost automatic weather station (AWS) is a challenging task because the data obtained from the device should be compatible with WMO standards and also be accurate. This paper describes the design and development of a low cost AWS which can use in meteorological and environmental applications. The state of the art technology was used for the design. The results were compared with the thermograph, barograph and other recording devices to verify the accuracy of the AWS.

### 2. Methodology

The following meteorological sensors were used for the design.

- i. Sensirion SHT75 sensor provides - unlike other sensor elements - a combined relative humidity and temperature measurement. This would help for both temperature and relative humidity measurements.
- ii. Pulse type wind anemometer for wind speed measurements.
- iii. Motorola MPX 5100 pressure sensor.
- iv. Tipping bucket type rain gauge for rainfall measurement.
- v. New sensor with digital output was designed for wind direction measurement.

Output data of meteorological sensors were stored in the internal memory of the processor and could be accessed from data modem of the central location through one of the ports of the micro-processor Rabbit RCM 2020. Output data were being saved in a Microsoft Access data base.

Rabbit RCM 2020 micro-controller was used as the main processor. The Rabbit is an 8-bit processor with an 8-bit external data bus and an 8-bit internal data bus. Because the Rabbit makes the most of its external 8-bit bus and because it has a compact instruction set, its performance is as good as many 16-bit processors. Thus the Rabbit can handle many 16-bit operations. There are four serial ports designated ports A, B, C, and D. All four serial ports can operate in an asynchronous mode up to the baud rate of the system clock divided by 32. The asynchronous ports can handle 7 or 8 data bits. A 9th bit address scheme, where an additional bit is sent to mark the first byte of a message, is also supported.

In case of an analog output, a signal conditioned circuit and analog to digital converter were used. In this particular case of atmospheric pressure measurements, a signal conditioner circuit was used as the output of the pressure sensor was too small. After that all digital outputs were coupled to port D and port B of the Rabbit RCM 2020 processor. Output signal from the Port was connected to the external modem as shown in the Fig. 1.

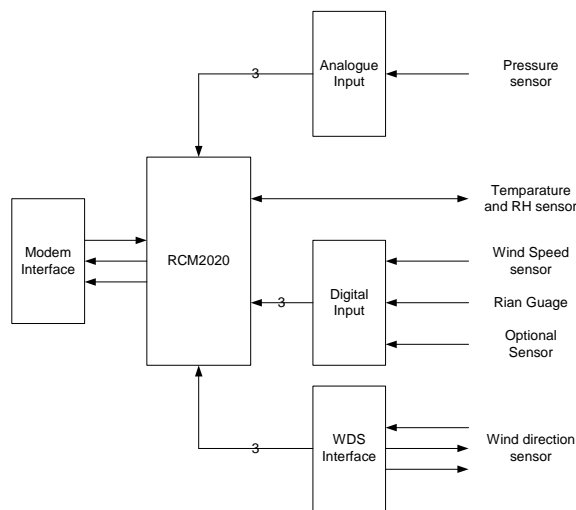


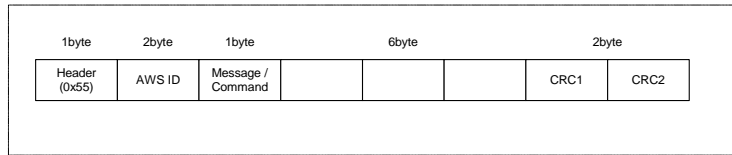
**Fig. 1**

Sampling periods of temperature, relative humidity and pressure sensors were taken as 10 seconds whereas sampling period of wind direction sensor was taken as 1 second. As the type of wind speed and rainfall sensors were pulse type, their respective sampling periods were calculated when a pulse occurred. Recording interval was taken as 10 minute for all data. In this recording period you can get average meteorological data for 10-minutes. Data, message or command formats are given in Fig. 2.

All firmware was written in Dynamic C and the application software was written in Visual Basic. Graphical representation of meteorological data was done in Microsoft Excel. The layout of the main PCB is shown in Fig. 3.



**Message / Command packet**



**Data packet**

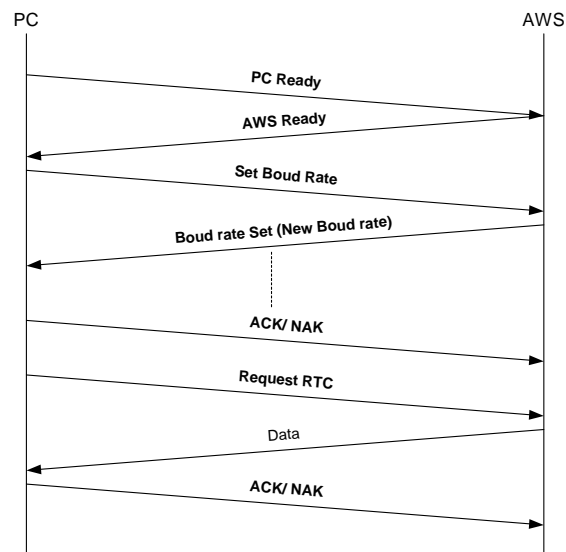
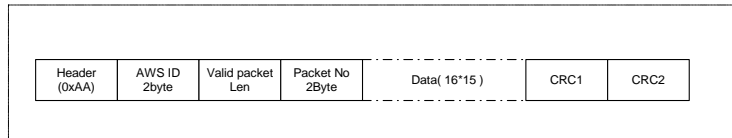


**Fig. 2**

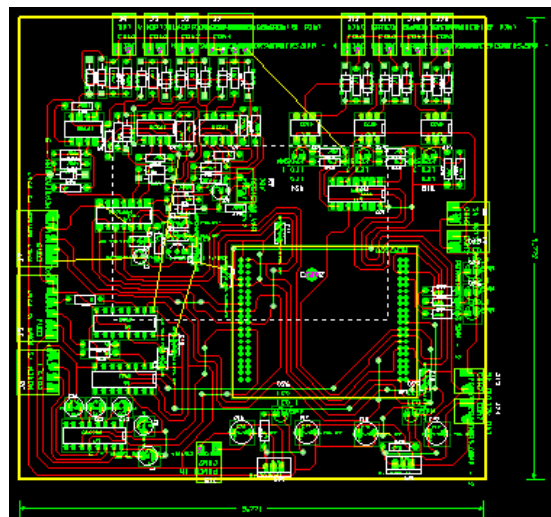


**Fig. 3 Main PCB of the AWS**

### 3. Results and Discussion

The AWS was tested in various weather conditions. The data obtained from the AWS was acceptable and its accuracy match with the WMO standards. Data were being recorded with the corresponded time. Comparison of the temperature data obtained from the AWS and thermograph is shown in Fig. 4, and it clearly shows the behavior of the AWS is acceptable.

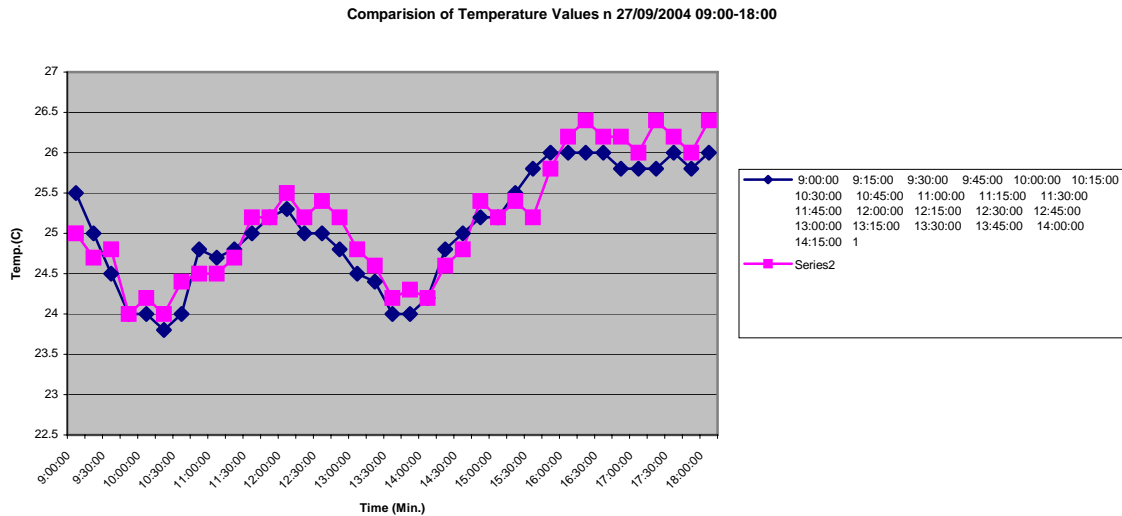


Fig. 4

### 4. Conclusions

This type of a low cost AWS can be developed with the state of art technology sensors which are easy to calibrate. As these sensors are at comparably low price and their output values are within the WMO standards. One can get remote meteorological parameters through a data modem. Its maintenance is fairly user friendly therefore a normal person also can attend its day today maintenance.

### 5. References

1. RabbitCore RCM 2000 C-Programmable Module Getting Started Manual.
2. Technical Notes – TN 231 Rabbit 2000 Features and Their Use in Board-Level Products.
3. Technical Notes – TN 232 Rabbit 2000 C Release.  
Sensirion Data Sheet SHT75/71.

**THE FLOOD FORECASTING  
AND PRECIPITATION MEASUREMENT  
BY USING RADAR SYSTEM  
TEFER PROJECT IN TURKEY**

Hikmet EROĞLU\*  
Meteorological Engineer

# **THE FLOOD FORECASTING AND PRECIPITATION MEASUREMENT BY USING RADAR SYSTEM**

## **TEFER PROJECT IN TURKEY**

Hikmet EROĞLU\*

Meteorological Engineer

### **ABSTRACT**

Until 1998, Turkey carried out the flood related activities, generally as structural measures in the river basins so as to reduce or eliminate long-term risk in the sensitive areas to the floods and water erosion. DSI has built dams, reservoirs, dykes, drop structures, weirs and channel improvements to minimize the adverse affects of floods on people.

The experiences gained from the floods of last decade show that structural measures implemented in the basin-wide are effective but too costly in reducing the risk of flood damages. Therefore, within the framework of Integrated Flood Management concept, after 1998 floods, more importance was given to non-structural measures, including flood proofing, early warning system, land use control especially at floodplains, flood disaster awareness creation, initiation of the concept of flood insurance, and timely and effective emergency management to be more effective for flood hazard management in the country

---

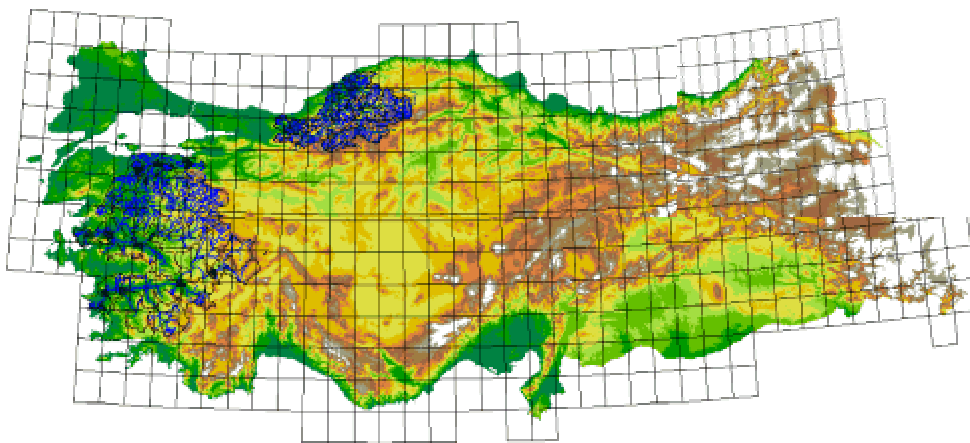
\* The General Directorate of State Hydraulic Works , TURKEY

### **INTRODUCTION**

In response to 1998 floods at western Black Sea region, the Government of Turkey with the assistance from the World Bank has identified an Integrated Flood Management programme, named TEFER (Turkey Earthquake and Flood Emergency Recovery) Project to develop flood management and to reduce or eliminate long-term risk and damage to people and their property from natural hazards. With TEFER, the urgent need in the flood prone area; which has been presented as case study from Turkey; the establishment of all kinds of structural and non-structural measures as flood control alternatives are being realized.

The project provides technical assistance to perform hydrometric network review and design and automated weather and hydrometric system design. In addition, the project supported the installation of about 129 automatic real-time hydrometric, 206 automatic real-time meteorological and 5 Doppler radar stations so that real-time data be available in order to run the operational flood forecasting models. Data integration is one of the highest concerns. The integration of the rainfall-runoff routing model to incorporate hydrometric and automatic weather data, and real-time quantitative radar data, in real time, is required

### **Turkey Emergency Flood and Earthquake Recovery (TEFER) Flood Forecasting and Model Development**



The contract for the Turkey Emergency Flood and Earthquake Recovery (TEFER), Flood Forecasting Model Development project was signed between the General Directorate of

State Hydraulic Works (DSI) and DHI Water and Environment, Denmark on 30th November 2001. Subconsultants to DHI for the project are einfalt & hydrotec GbR, Germany, and from Turkey Arti Proje Ltd and UBM United International Consultants Inc.

DSI has selected four pilot catchments for the establishment of the forecasting system: West Black Sea, Susurluk, Gediz and Buyuk Menderes, with catchment areas ranging from 18,000 to 30,000km<sup>2</sup>

### **Flood Forecasting System**

The Flood Forecasting System developed under this TEFER component takes real time monitoring data of the catchment status and produces forecasts of the flood state of the catchment. The forecasting process is automated, with the possibility for manual inspection and intervention. Below figure shows an overview of the Flood Forecasting Model System

The flood forecasting system takes real time monitoring data of the regional meteorology and the catchment status, and produces forecasts of the flood state of the catchment. The forecasting system is based on FLOOD WATCH and SCOUT. FLOOD WATCH is a GIS based decision support system for flood management, with MIKE 11 at its core. SCOUT integrates real time numerical weather prediction, radar and raingauge data to produce rainfall forecasts. The system combines the compilation of real time data with rainfall and flood forecasting and presentations of the information and results.

### **Forecasting Operations**

The TEFER Flood Forecasting Model has an interface to the telemetry system through the DSI central data server. This server is the ground station of the VSAT system at DSI. In addition to the computers and the VSAT ground station, a meteorological workstation from the TEFER Radar project will be included in the LAN of the flood forecasting centre.

A diagram of the data flow is shown in figure below. The overall data communication context is as follows:

- measured hydrometric field data are delivered either via VSAT (satellite communication) or via GSM/modem connection to DSI
- AWOS (Automated Weather Station) data are provided by DMI (State Meteorology Organization) via a dedicated data line to DSI
- the arriving hydrometric and AWOS data are transformed from their original formats to the format specified for the Flood Forecasting Model

radar and NWP (Numerical Weather Prediction) data are provided by DMI via a dedicated data line to DSI

## **SCOUT**

The SCOUT module produces rainfall forecasts in real time from an integration of the radar data, the Numerical Weather Prediction (NWP) data, and the point raingauge data from the real time networks of DSI and DMI. The raw data are preprocessed, including quality control. The forecasts are transferred in real time to FLOOD WATCH as time series for each model sub-catchment.

SCOUT carries out the following functions:

- Import of radar and raingauge data
- Quality control and adjustment of data
- Forecasts computed from the integration of catchment topography and NWP data
- Presentation of measured radar images, individual and composite, raingauge data and rainfall forecasts
- E-mail reports of system performance

## **FLOOD WATCH**

The flood forecasting and warning system is set up within FLOOD WATCH, a decision support system for flood management, developed by DHI Water and Environment.

FLOOD WATCH combines the compilation of real time data with rainfall and flood forecasting and presentations of the information and results. FLOOD WATCH has a customised ArcView graphical user interface and includes the following facilities, with “push button” operations:

- Real time data management with preprocessing and quality controls
- An automatic interface with the real time rainfall and water level data provided by the hydrometric network
- An automatic interface with precipitation fields predicted and measured
- Operation of the flood forecasting system
- Graphical and tabular presentation of the monitored data and the flood forecasts, with direct broadcast to the Internet
- Preparation of flood warnings, in textual, tabular, graphical and map based formats, with direct broadcast to the Internet

FLOOD WATCH operates within the environment of a Geographic Information System, and has an automatic interface with the data in the hydrometeorologic and hydrometric network database. All the thematic maps and information from GIS are available within FLOOD WATCH. The setup of the FLOOD WATCH time series database is prepared from the thematic maps with the locations of the stations in the real time network.

At the core of the FLOOD WATCH system is MIKE 11. MIKE 11 incorporates hydrologic and hydraulic modelling and is set up for the catchment area and the river network. MIKE 11 has a unique self-correcting updating procedure, automatically minimising deviations between the real time observed and simulated discharges and water levels. Updating is transparent to the user and by compensating for errors and uncertainties, particularly in the rainfall forecasts, greatly enhances the accuracy of the forecasts.

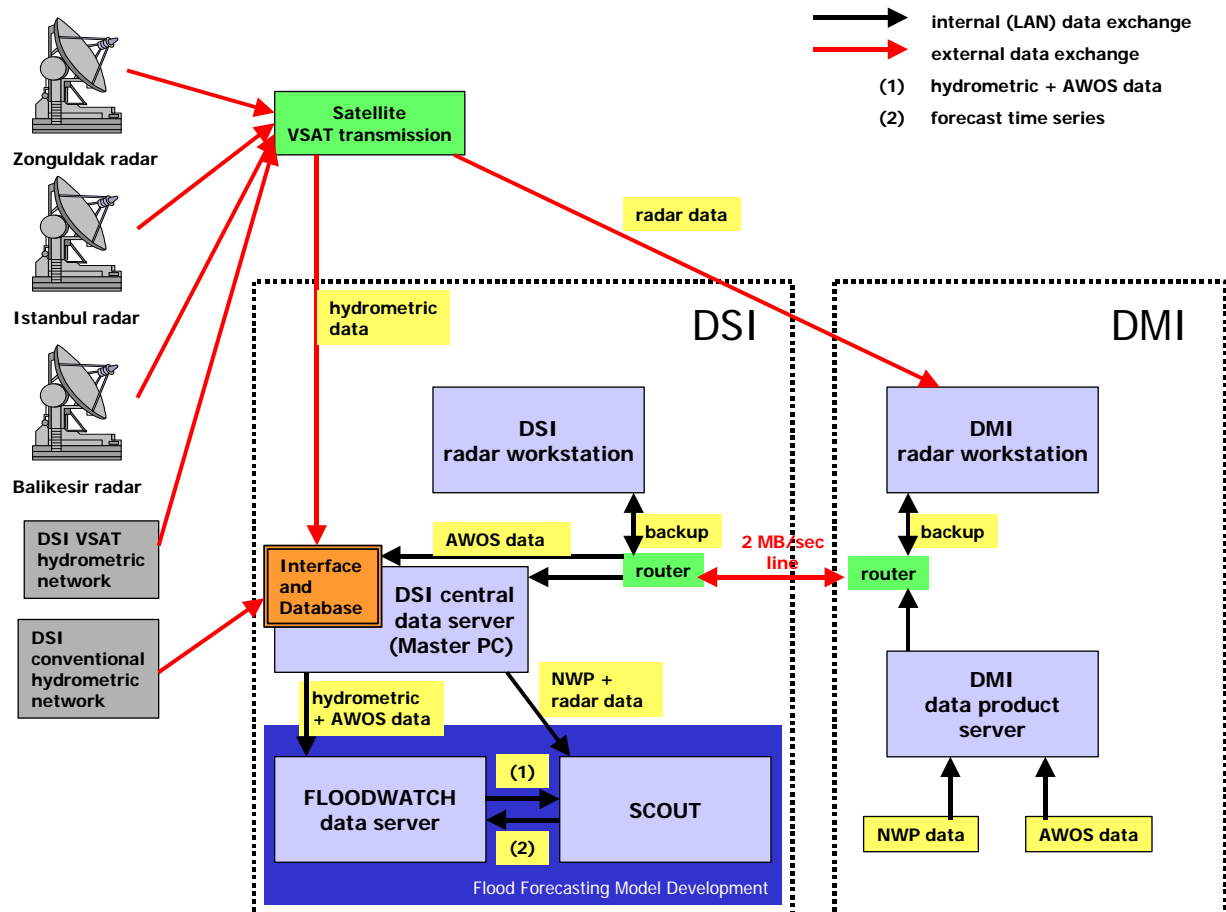
### **TEFER Flood Forecasting Model Interface Specification**

This document describes the assumptions and definitions made in order to provide an interface between the TEFER Flood Forecasting Model and the telemetry system through the



DSI central data server. This server is the ground station of the VSAT system at DSI (see figure 2, TEFER Final Report Component 2, Hydrometric Network Review). In addition to the TEFER computers and the VSAT ground station, a meteorological workstation from the TEFER RADAR project will be included in the LAN of the flood forecasting centre.

A diagram of the data flow is shown below. The exact configuration of this scheme outside



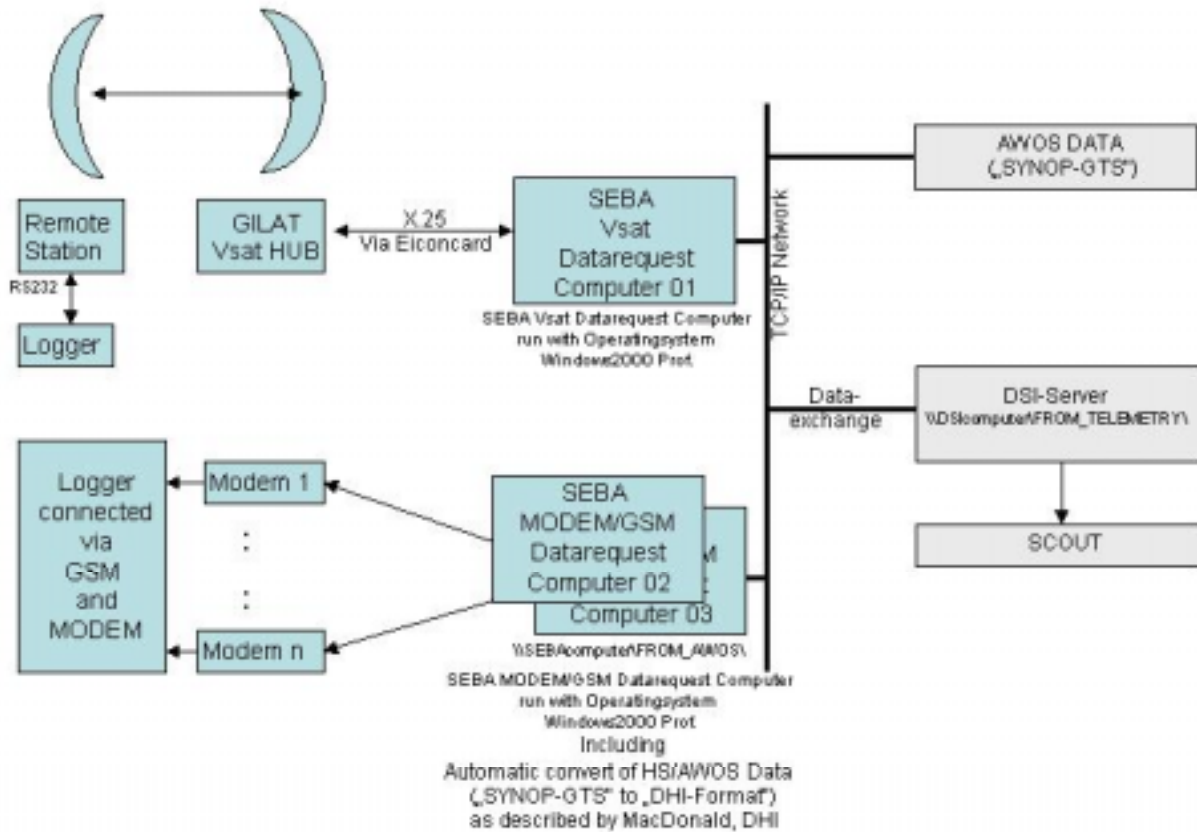
the Flood Forecasting Model Development should be verified with DSI, DMI and the individual component suppliers.

**Data Flow Scheme relative to TEFER Flood Forecasting Components**

The overall data communication context is as follows (see interface scheme below):

- measured hydrometric field data are delivered either via VSAT (satellite communication) or via GSM/modem connection to DSI
- AWOS data are provided by DMI via a dedicated data line to DSI
- the arriving data are transformed from their original formats to the format specified for the TEFER Flood Forecasting Model below
- radar and NWP data are *not* part of this interface

All incoming data will be written to an Oracle database in a format to be prepared by the supplier and approved by DSI. The database is for storage, and not a part of the interface specification.

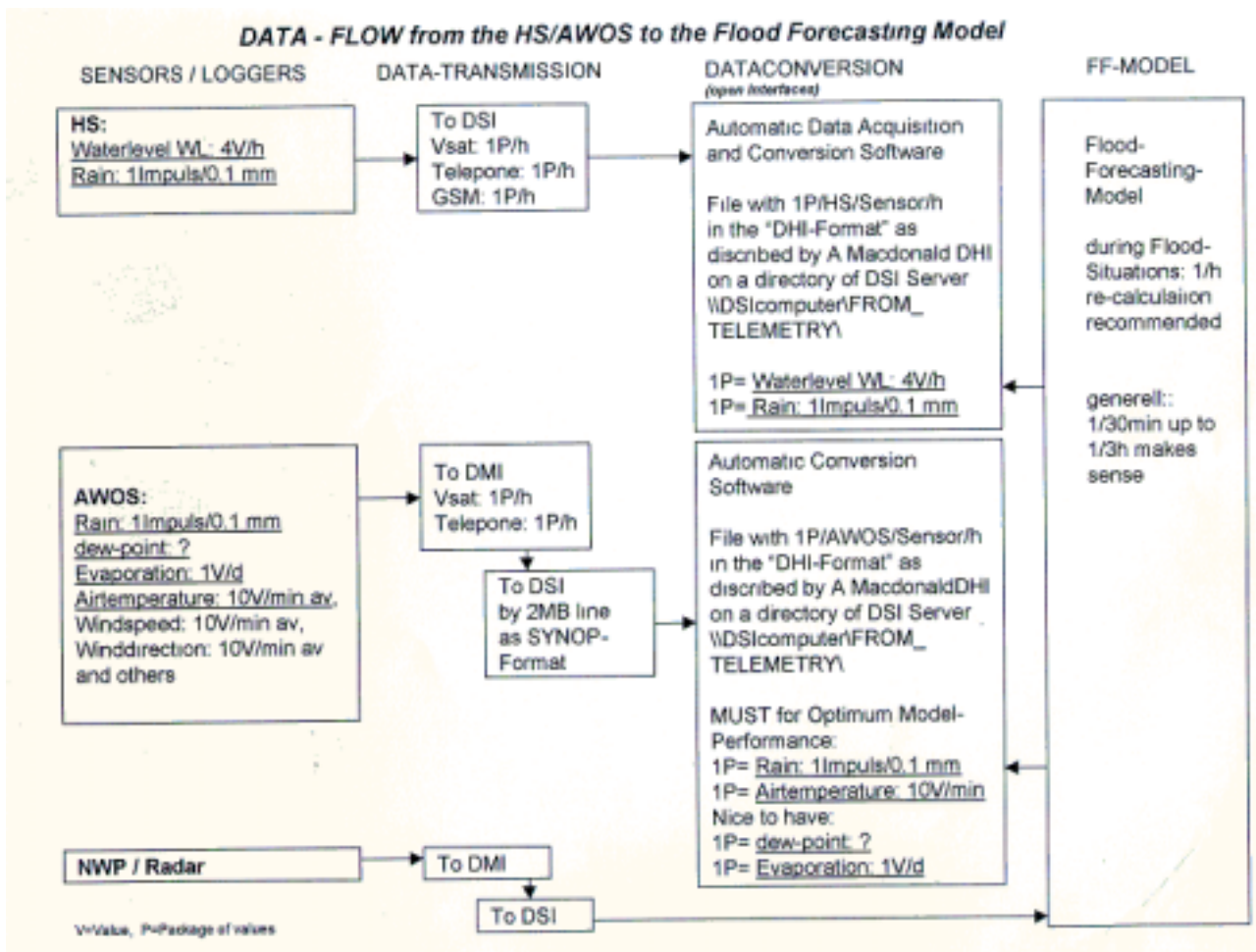


### ***Interface Scheme relative to Communication Components (prepared by SEBA)***

#### ***Interface Specification***

FLOOD WATCH is the central module for data exchange on the Flood Forecasting side. It resides on a computer which is connected via LAN to the DSI central data server. The following components are required by FLOOD WATCH:

1. An indicator file in a specified directory for FLOOD WATCH to monitor. The existence of this file tells FLOOD WATCH that new data have arrived.
2. Incoming data automatically output in an export file located in a specified directory. Once the indicator file is produced any new data will be written in a new export file. The indicator file contains the names of the accompanying export files.



*Interface Scheme relative to Information Flow Components (prepared by SEBA and DHI)*

Thus FLOOD WATCH needs two items as specified below:

1. An indication that new data has arrived in the system. These files will have the following names, content and location:

File name: **VSAT\_BATCH\_yyyymmddhhmmss.TXT** (telemetry data) and

**AWOS\_BATCH\_yyyymmddhhmmss.TXT** (AWOS data)

Content: A list of the export files produced since the previous indicator file was made.

Location: a shared folder in the DSI computer,

[\\<DSIcomputer>\FROM TELEMETRY\](#)

2. The new data, see file format below.

The data will be provided automatically and the data exchanged in the form of files in predefined formats and locations. FLOOD WATCH will have no direct communication with VSAT, but act as a receptor of the incoming data.

### ***Data Streams***

FLOOD WATCH assumes all incoming station data will be available on a central DSI server, which is in charge of communicating with external systems providing data for the flood forecasting model. The radar data and NWP data are supplied through the meteorological workstation situated at DSI through the TEFER RADAR project. These data are directly taken over by SCOUT (the rainfall forecasting module) and are not an item in this specification.

Telemetry data and AWOS data are placed on the DSI server in a specified directory at regular intervals or when data are ready. FLOOD WATCH will normally run models hourly and should receive observations accordingly - it will use whatever data are available. A defined naming standard of files, directory structure and file layout will be observed (see below).

In the FLOOD WATCH database server a process monitors the DSI server directories. When new data are ready, the files are treated as follows:

- Telemetry and AWOS data are received and stored in the FLOOD WATCH database. Quality control procedures and processing are performed on data as they arrive. A batch of files is processed into the FLOOD WATCH database and once received the files will be removed from the DSI server.

### ***Specification for Telemetry Data Interface***

Telemetry data will be received in ASCII file format (see also the following section on AWOS data). Every transmission of data (batch) consists of a set of files - one for each sensor plus one file describing the files in the batch. This will allow a new batch to be created during the processing of a batch.

The batch description file will be named **VSAT\_BATCH\_yyyymmddhhmmss.TXT** where yyyymmddhhmmss gives the time of the batch to the second. An example of the file name is:

## VSAT\_BATCH\_20020501172745.TXT

The content of the batch is all the file names in the batch, one file name per line. Each data file in the batch is named with the the parameter identifier, the station identifier and the time of the batch:

**<parameter>\_<station>\_yyyymmddhhmmss.DAT**

Valid parameter IDs are:

- r: rainfall [mm]
- w: water level [cm]

Valid station IDs comprise a number of characters between two underscores. This means that underscore ('\_') cannot be part of a station name. Examples of such file names are:

w\_27853\_20020501172745.DAT  
r\_13-14\_20020501172745.DAT

Each file contains one reading per line, with no header. Readings are in the form:  
**yyyy mm dd hh mm ss value**

Example of content:

2001 12 27 14 05 00 123.456  
2001 12 27 14 15 00 23.756  
2001 12 27 14 25 00 123.245

### ***Specification for AWOS Data Interface***

The radar data processing and forecasting software SCOUT requires data from radar, NWP and raingauges. Measurements of temperature and, if available, dew point temperature or evaporation are used for the flood forecasting part of the models in the TEFER Flood Forecasting Model Development project.

AWOS data will be available on the central server at DSI (DSI central data server), from which the flood forecasting system may retrieve the data. The setup will be:

- AWOS data will be received in ASCII file format
- Every transmission of data (batch) consists of a set of files - one for each parameter plus one file describing the files in the batch. This will allow a new batch to be created during the processing of a batch.

- The batch description file will be named:

**AWOS\_BATCH\_YYYYMMDDHHMMSS.TXT**

where YYYYMMDDHHMMSS give the time of the batch to the second, eg

**AWOS\_BATCH\_20020501172745.TXT**

The content of the batch file is all the file names in the batch, one file name per line. Each data file in the batch is named with the parameter identifier, the station identifier and the time of the batch:

**<parameter>\_<station>\_YYYYMMDDHHMMSS.DAT**

Valid parameter IDs are:

- r: rainfall [mm]
- t: temperature [°Celsius]
- d: dew point temperature [°Celsius]
- e: evapotranspiration [mm]
- s: snow depth [cm]

Valid station IDs consist a number of characters between the underscores. This means that underscore ('\_') cannot be part of a station name.

Examples of such file names are:

e\_27853\_20020501172745.DAT

r\_13-14\_20020501172745.DAT

t\_27853\_20020501172745.DAT

Each file contains readings in the form:

**YYYY MM DD HH MM SS value**

One reading per line, no header.

Example of content:

2001 12 27 14 05 00 123.456

2001 12 27 14 15 00 23.756

2001 12 27 14 25 00 123.245

2001 12 27 14 35 00 111.999

# **THE MAN-MADE SATELLITE; AN INSTRUMENT OF OPPORTUNITY.**

**O.S.Mudenda and E.Nkonde**

Zambia Meteorological Department, P.o. Box 30200, Lusaka, Zambia

Tel: 260-1-271100, Fax: 260-1-271312,

Email: [zmd@zamnent.zm](mailto:zmd@zamnent.zm)

## **ABSTRACT**

With the advent of space-based remote sensing techniques, the data requirements for Environmental, Meteorological and Hydrological applications are being met through the combined use of the surface based and space based systems. This paper is a case study based on operational experience with surface observation from space using the satellite, space based sensor, as an instrument. The analysis was done at the National Meteorological Center (NMC) on products that employ an overhead perspective that is maps; aerial photographs including many that are based on radiation not visible to the human eye. In particular the paper displays several Meteosat/NOAA products and images in the last fifteen years intended for operational meteorology and climate studies from the wide and diverse satellite services at the Zambia Meteorological Department. In Meteorological terms, a product means a parameter which is extracted and processed from the image data and which can be used in everyday applications. The man-made satellite as an instrument is one of the most comprehensive observation instruments. Its product has multi-disciplinary science applications for science and society. It is an instrument of opportunity.

## **1. INTRODUCTION**

A picture is worth a thousand words. Each picture therefore can truthfully be said to distill the meaning of thousands of words. With the advent of space-based remote sensing techniques, the data requirements for Environmental, Meteorological and Hydrological applications are being met through the combined use of the surface based and space based systems. This paper is a case study based on operational experience with Zambian analysis of products that employ an overhead perspective that is maps; aerial photographs including many that are based on radiation not visible to the human eye. The emphasis is on the man made satellite as an instrument. In particular the paper displays several Meteosat/NOAA products and images intended for operational meteorology and climate studies from the wide and diverse satellite services at the Zambia Meteorological Department. The main advantage of the satellite as an instrument of surface observation from space is that the product has a multi-disciplinary science application for both science and society. The products cover a wide range of atmospheric, oceanographic and land cover geophysical parameters.

In Meteorological terms, a product means a parameter which is extracted and processed from the image data and which can be used in everyday applications. Some typical examples of these products are wind and land cover data, water body location, atmospheric trace gas monitoring, meteorological parameters, text and graphical products. The man-made satellite as an instrument is one of the new most comprehensive observation instrument of the Earth from space.

## **2. OBJECTIVES**

The main objective of this paper was to do a case study based on operational experience with surface observation from space. In particular the paper displays several Meteosat/NOAA operational products and images in the last fifteen years from the Zambia National Meteorological Center.

## **3. DATA AND METHODOLOGY**

The study involved collection of all the available and accessible Meteosat/NOAA remote sensed products in the last fifteen years of the satellite technology at the National Meteorological Center. Part of the knowledge on new developments with surface observation from space was acquired from literature materials and International satellite conferences attended by the lead author.

## **4. RESULTS**

In current and previous satellite programmes, Zambia National Meteorological Center (NMC) has been able to access the following services using the satellite (space based sensors) as an instrument:

High Resolution Images (HRI)  
Meteorological Products Extraction Facility (MPEF)  
Indian Ocean Data Coverage (IODC)  
Data collection and Retransmission (DCP)  
Meteorological Data Display (MDD)  
Satellite Application Facility (SAF)  
Numerical weather Prediction (NWP)  
Regional services in surveying, mapping and remote sensing (RSSMRS)  
Geo-information services (GIS)  
Satellite Distribution (SADIS)

Among the processed products from these services are the following:

- Meteorological parameters- temperature, wind, precipitation, relative humidity and sea-surface temperature.
- Land cover data and surface analysis- Normalized Difference Vegetation Index (NDVI), Cold Cloud duration (CCD), Surface albedo.
- Water body location- rivers, lakes, flooded areas, severe storms, clouds and oceans.
- Atmospheric trace gas monitoring- Air pollution (Dust, Smoke), and aerosol indicators.
- Text and graphical formats- Aviation forecast charts, numerical forecast models, images, map views, weather analysis and displays.



- General geoinformation technology products in the assessing and management of - Agriculture and forestry, Soil, geology, water resources, Biodiversity, Rural and urban, Coastal and marine resources, Disasters, Climate change and variability.
- World area forecast system (WAFS) products- significant weather charts.

## 5. CONCLUSION

The satellite is a fully fledged meteorological, hydrological and environmental instrument covering all aspects from image processing to weather analysis, now casting, forecasting and the automatic production of high quality weather graphics for end users- the scientist and society. It is an instrument designed to operate in the complex data processing environment of modern meteorological services. It represents a flexible and user-friendly approach to the whole concept of earth observation from space to a larger user community. The man-made satellite is an instrument of opportunity.

---

## ACKNOWLEDGEMENTS

We are very grateful to the Zambia National Meteorological Center (ZNMC) for the various archived products and images. We also acknowledge EUMETSAT, NOAA and ECMWF for some of the operational satellite data used in this research.

## REFERENCES

- Zambia Meteorological Department, crop weather bulletins, 1990-2004.
- Glenn R McGregor 2004. International Journal of Climatology, vol.24 #1
- The 2004 EUMETSAT, Meteorological satellite conference Abstract brochure.
- The EUMETSAT 2004, Meteosat transition programme ((MTP), reliable weather data for Europe.

Footnote: *The opinion and views presented in this paper do **not in** any way reflect the official representation of the Zambia Meteorological Department. They are solely by the individual authors.*

# **A COMPARISON OF BEAUFORT, VAISALA AND RADIOSONDE WIND MEASURING SYSTEMS IN THE COURSE OF MIGRATION**

BY

CHARLES NGENDA.  
METEOROLOGICAL DEPARTMENT,  
P.O BOX 30200 ,LUSAKA-ZAMBIA.  
E-mail: [mwilola2004@yahoo.com](mailto:mwilola2004@yahoo.com)

## **Abstract.**

Estimation of wind speed has passed through different measuring systems. One of the initial systems being the Beaufort Scale originally devised by Admiral Beaufort for use at sea but has been modified for use on land as well. The beaufort scale bases the speed of the wind on effects it has on common objects around us.

Vaisala wind measuring system is one of the current systems in use. The system is a remote-indicating wind instrument based on the utilization of a two wire connection between the measurement site and the display site operating to distance of up to 10km. It consists of sensors, control units, display units and recording units designed to perform different functions.

To have an effective socio-economic application of the wind resource it is important to accurately estimate wind speed. In view of this, a comparison of Beaufort, Vaisala and Radiosonde measuring systems with respect to Wind speed measurement has been done and results have revealed that Vaisala is the most reliable system.

## **INTRODUCTION**

Wind is one of the renewable energy resources being pursued to reduce the dependence on fossil-based fuels. However the usefulness of this form of energy is severely restricted by its measurement and variability amongst other concerns. To measure this highly variable resource there is need to have reliable wind measuring systems. Wind has been measured using different systems ranging from Beaufort scale to Vaisala measuring system. This migration has resulted into some benefits being gained by some end-users of these systems. Some of the main applications are in the fields of water pumping and electricity generation. It is critically important that wind measurements by these systems be as accurate estimates as possible to be usefully applied in the designing of wind energy technologies for example. The study therefore attempts to show some systems and their usefulness by comparing the different systems during the course of migration.

## **METHODS OF COMPARISON**

Many methods are presently available through which mean wind speed can be estimated for developmental applications. The three wind measuring systems that are considered in this study are; the **Beaufort scale**, the **Vaisala** and the **Radiosonde**.

**Beaufort scale wind measuring system.**

FORCE	DESCRIPTION	SPECIFICATION FOR USE ON LAND	KNOTS MEAN LIMITS	
0	CALM	CALM; SMOKE RISES VERTICALLY	0	< 0
1	LIGHT AIR	DIRECTION OF WIND SHOWN BY SMOKE DRIFT, BUT NOT BY WIND VANES	2	1-3
2	LIGHT BREEZE	WIND FELT ON FACE, LEAVES RUSTLE, ORDINARY VANE MOVED BY WIND	5	4-6
3	GENTLE BREEZE	LEAVES AND SMALL TWIGS IN CONSTANT MOTION, WIND EXTENDS LIGHT FLAG	9	7-10
4	MODERATE BREEZE	RAISES DUST AND LOOSE PAPER, SMALL BRANCHES ARE MOVED	13	11-16
5	FRESH BREEZE	SMALL TREES IN LEAF BEGIN TO SWAY; CRESTED WAVELETS FORM ON INLAND WATERS	19	17-21
6	STRONG BREEZE	LARGE BRANCHES IN MOTION; WHISTLING HEARD IN TELEGRAPH WIRES; UMBRELLAS USED WITH DIFFICULTY	24	22-27
7	NEAR GALE	WHOLE TREE IN MOTION; INCONVENIENCE FELT WHEN WALKING AGAINST WIND	30	28-33
8	GALE	BREAKS TWIGS OFF TREES; GENERALLY IMPEDES PROGRESS	37	34-40
9	STRONG GALE	SLIGHT STRUCTURAL DAMAGE OCCURS (CHIMNEY POTS AND SLATES REMOVED)	44	41-47
10	STORM	SELDOM EXPERIENCED INLAND; TREES UPROOTED; CONSIDERABLE STRUCTURAL DAMAGE	52	48-55
11	VIOLENT STORM	VERY RARELY EXPERIENCED; ACCOMPANIED BY WIDESPREAD DAMAGE	60	56-63
12	HURICANE	—	—	>64

**Table 1: BEAUFORT SCALE: Specifications and Equivalent Speeds**

Wind force is estimated on a numerical scale ranging from 0 for calm to 12 for hurricane (Table 1). This method is based on the empirical relationship between estimated number and measured wind speed,  $U = \sqrt{1.87 B}$ , where

U represents the wind speed and B is the corresponding Beaufort number.

## **VAISALA WIND MEASURING SYSTEM METHOD**

The basic units for Vaisala wind measuring system are: **Sensors**-Anemometer WAA 12, Windvane WAV 12, **Control**-Wind sensor control unit WAT 11, **Display**-Analog wind display unit WAD 11, Analog slave display unit WAD 12, Digital wind display unit WAD 13, Averaging wind display unit WAD 21, **Recording**-Analog wind recorder WAR13. The system is intended for weather stations, Airports and other meteorological, environmental, research and industrial applications.

The system is based on the utilization of a two wire connection between the measurement site and the display site operating to distances of up to 10km. The wind sensor control unit samples the speed and direction sensor's data, converts the values into serial digital format and transmits the data along a serial line. Both the sensors and control unit operate from DC power supply which is supplied by the averaging display unit through the same line.

No supply is needed at the sensor site, and the connection can be made via a standard telephorepair. The sensor control unit operates at -40 to 55 Deg/C temps and is installed to the wind mast near the sensors.

An optional AC powered sensor heating power supply is available for low temperature conditions.

The averaging display unit WAD 21 performs the functions of both the computer and the display device. The instantaneous data transmitted by the wind sensor control unit is received in real time by the display unit (WAD 21) which performs averaging, minimum and maximum calculations and other required data processing and displays the instantaneous and computed values by means of a compact display panel. The display unit is AC powered and feeds the sensors via the two conductor lines. Multiple averaging display unit can be connected to the same current loop line, enabling the information from the same site of sensors to be displayed in several locations.

Only two-conductor cable is still needed and the link operates to the same distances. Also multiple sensor control unit may be connected to the same loop, thus enabling wind information from several locations to be displayed. In that case a switch option is used on the display unit for data source selection. With no need of a sensor control unit the digital display unit WAD 13 is straight connected to the sensor signal line. It is thus obligated to be installed near the sensor. WAD 13 performs no data processing and shows only instantaneous wind values. Several display units can be connected to display information from a small per of sensors. The display units have to be powered.

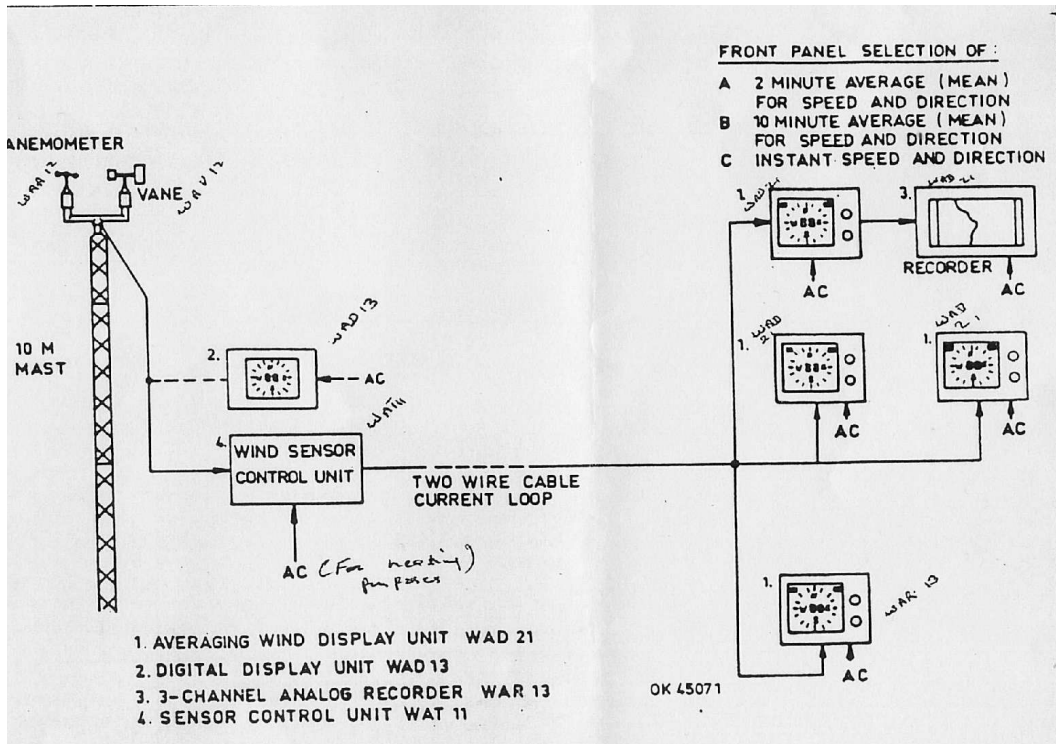


Fig 1: A Configuration scheme of Vaisala system

### RADIOSONDE WIND MEASURING METHOD

A small radio transmitter, by means of which observations usually of temperature and wind amongst other parameters are obtained during an ascent. This is done by radar reflections from a sonde (target) carried by the balloon. The major difference between the Radiosonde and the Vaisala system is that the later is a remote instrument while the former is not but has a radio transmitter attached to it.

### DATA and COMPARISONS

In order to assess the quality, reliability and consistency of Beaufort, Radiosonde and Vaisala methods employed in this study, wind speed values have been compared.

- **Beaufort scale method:** measurements for the month of August were estimated at about 10m height above the ground at Chelstone station in Lusaka as shown in table 2.

	1994	1995	1996	1997	1998	1999	2000	2001	2002	2003	
01	07	05	00	00	11	03	07	21	18	04	
02	09	12	00	00	10	01	01	13	11	03	
03	10	17	09	02	10	10	03	10	00	00	
04	06	06	00	02	00	03	05	00	03	00	
05	08	08	00	00	00	06	08	01	08	06	
06	04	05	10	00	01	10	03	05	10	06	
07	01	06	06	03	10	11	00	08	10	06	
08	07	06	13	09	16	10	08	11	03	09	
09	08	10	11	06	09	01	07	10	13	00	
10	05	07	00	00	13	00	00	03	15	00	
11	11	08	12	03	09	08	00	05	03	00	
12	06	07	07	03	00	09	04	04	03	06	
13	04	00	00	07	00	09	09	02	00	03	
14	00	08	00	08	00	13	11	00	00	01	
15	08	06	15	13	03	11	14	00	00	02	
16	12	05	09	11	03	07	17	04	09	00	
17	07	04	04	06	07	08	01	00	11	05	
18	00	08	03	00	10	02	11	00	12	04	
19	03	05	06	00	10	06	08	08	07	04	
20	06	07	07	00	13	09	05	07	11	07	
21	04	04	00	03	12	05	05	00	14	10	
22	15	01	00	14	00	07	00	01	03	07	
23	07	00	00	04	13	02	01	09	04	05	
24	10	02	06	06	16	00	10	09	03	01	
25	08	09	04	08	15	00	13	10	04	05	
26	13	00	06	01	06	10	00	17	01	06	
27	11	04	00	06	06	07	00	18	00	05	
28	05	11	01	00	00	06	08	13	01	11	
29	06	04	07	09	09	03	09	05	03	11	
30	08	06	05	01	10	03	03	07	11	06	
31	04	14	03	11	18	00	00	05	05	01	
August mean windspeed	6.9	6.3	4.6	4.4	7.7	5.8	5.5	6.6	6.3	4.3	

**Table 2:** The daily August wind-speed estimates.

- **The Vaisala method:** wind speed values for the month of August were estimated at 10m height above the ground at Lusaka International Airport station as shown in table 3 below.

	1994	1995	1996	1997	1998	1999	2000	2001	2002	2003	
01	04	02	03	01	07	05	03	09	09	00	
02	05	05	01	00	05	05	03	03	05	03	
03	06	09	06	05	05	07	03	05	02	02	
04	05	02	02	03	03	03	05	02	05	02	
05	05	02	03	02	03	03	08	04	04	04	
06	05	03	05	01	04	07	03	07	05	04	
07	05	05	04	03	05	09	01	06	06	02	
08	06	06	08	07	07	05	04	06	05	05	
09	09	06	07	05	06	03	03	05	07	02	
10	06	00	01	01	05	03	00	05	07	02	
11	04	06	03	05	05	05	03	00	04	02	
12	00	07	05	05	04	04	05	00	03	03	
13	03	02	02	04	01	05	08	02	02	03	
14	03	06	04	05	03	08	06	00	00	02	
15	05	05	09	07	04	07	09	02	03	04	
16	07	05	05	05	05	07	07	03	03	01	
17	05	06	06	04	04	06	03	00	07	03	
18	03	07	04	03	07	06	06	02	05	02	
19	06	06	05	02	05	06	07	03	05	00	
20	02	02	05	02	07	08	05	03	07	01	
21	05	02	03	05	05	02	05	00	05	06	
22	09	03	01	07	01	03	03	03	04	05	
23	05	00	02	04	07	01	04	05	04	02	
24	05	05	04	06	07	01	08	04	03	02	
25	06	06	04	04	07	03	06	05	04	03	
26	07	03	02	03	04	06	03	05	03	04	
27	07	05	03	02	05	03	01	07	03	02	
28	03	06	06	01	03	04	06	07	01	06	
29	05	05	05	05	03	02	07	05	03	05	
30	08	05	07	03	06	03	05	04	06	03	
31	03	08	05	06	09	04	01	05	05	04	
August mean Wind-speed	5.1	4.6	4.3	3.8	4.9	4.6	4.5	3.8	4.3	2.9	

**Table 3:** The daily August wind speed estimates

- **Radiosonde method**:-wind speed values for the month of August were estimated at about 10m height above the ground at Lusaka City Airport station. This data was extracted from Temp messages(TTAA) and translated into monthly wind speed means as shown in table 4 below under **Lusaka city Airport for example**.

	<b>Chelstone station(Beaufort)</b>	<b>Lusaka International Airport (Vaisala)</b>	<b>Lusaka city Airport (Radiosonde)</b>
<b>1994</b>	<b>6.9</b>	<b>5.1</b>	<b>4.9</b>
<b>1995</b>	<b>6.3</b>	<b>4.6</b>	<b>5.1</b>
<b>1996</b>	<b>4.6</b>	<b>4.3</b>	<b>4.1</b>
<b>1997</b>	<b>4.4</b>	<b>3.8</b>	<b>4.6</b>
<b>1998</b>	<b>7.7</b>	<b>4.9</b>	<b>6.7</b>
<b>1999</b>	<b>5.8</b>	<b>4.6</b>	<b>4.9</b>
<b>2000</b>	<b>5.5</b>	<b>4.5</b>	<b>5.0</b>
<b>2001</b>	<b>6.6</b>	<b>3.8</b>	<b>5.2</b>
<b>2002</b>	<b>6.3</b>	<b>4.3</b>	<b>4.8</b>
<b>2003</b>	<b>4.3</b>	<b>2.9</b>	<b>3.3</b>

**Table 4:** The August mean wind-speed with respect to Beaufort, Vaisala and Radiosonde systems.



- **Specific wind power** (numerical application).

The monthly average energy input per unit area for a wind pump is determined by the monthly average wind speed and follows from the equation.

$$P_{av,wind} = \frac{1}{2} \rho_a V_{av}^3 \text{ in which}$$

$P_{av,wind}$  = monthly average specific wind power ( $W/m^2$ )

$\rho_a$  = Specific air density ( $Kg/m^3$ )

$U_{av}$  = monthly average wind speed (m/s)

Variable	Beaufort	Vaisala	Radiosonde
$\rho_a$ ( $kg/m^3$ )	1.2	1.2	1.2
$U_{av}$ (m/s)	5.81	4.28	4.86
<b>P (<math>W/m^2</math>)</b>	<b>117.6</b>	<b>47.0</b>	<b>68.9</b>

**Table 5:** wind power with respect to Beaufort, Vaisala and Radiosonde systems.

	Mean(Beaufort)	Mean(Vaisala)	Average	Diff	STD	
1994	6.900	5.100	6.000	1.800	1.273	
1995	6.300	4.600	5.450	1.700	1.202	
1996	4.600	4.300	4.450	0.300	0.212	
1997	4.400	3.800	4.100	0.600	0.424	
1998	7.700	4.900	6.300	2.800	1.980	
1999	5.800	4.600	5.200	1.200	0.849	
2000	5.500	4.500	5.000	1.000	0.707	
2001	6.600	3.800	5.200	2.800	1.980	
2002	6.300	4.300	5.300	2.000	1.414	
2003	4.300	2.900	3.600	1.400	0.990	

**Table 6:** wind speed means, standard deviations, averages and differences with respect to Beaufort and Vaisala wind measuring systems.

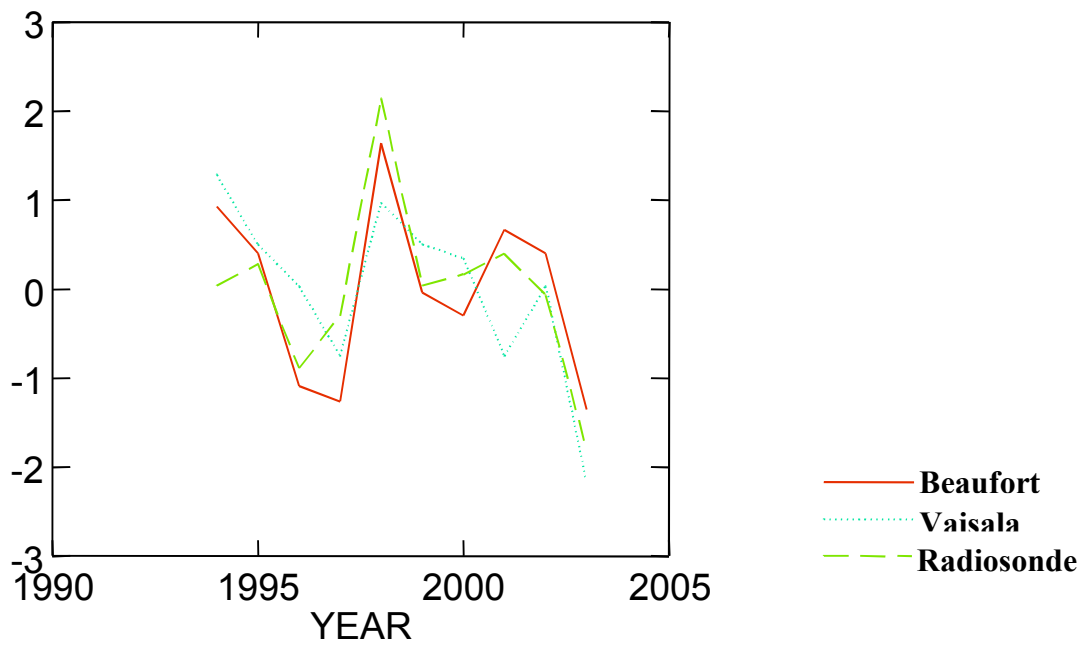


**Fig 2:** The anomaly pattern for August 1994 to 2003 wind speed estimates.

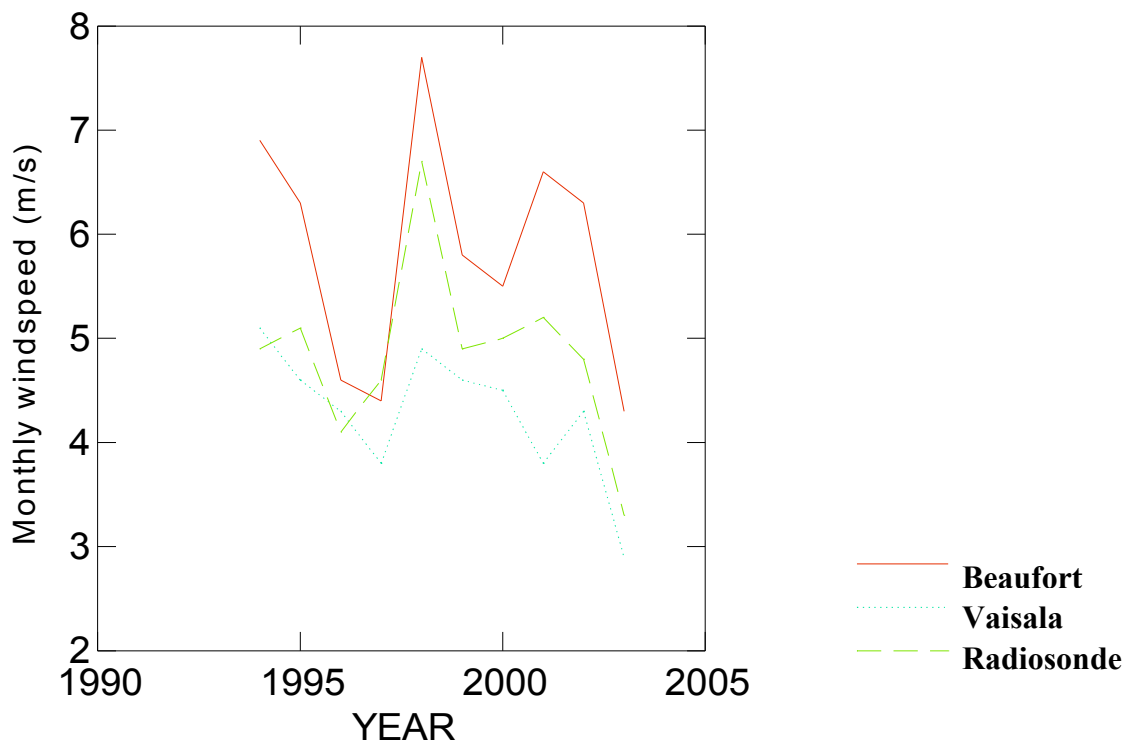


**Fig 3:** The 12utc August mean wind speed estimates from 1994 to 2003.

When comparing the August (monthly) wind speed values from the Beaufort, Radiosonde and Vaisala systems-the maximum difference found actually amounts to 2.8m/s in 1998 and 2001 with Beaufort system reading higher. The minimum difference being 0.3m/s with Vaisala system having a lower reading. Also comparison results given in table 6 show that the Beaufort and Vaisala systems are consistent and in agreement in 1996 and 1997. The agreement is only and in general at about 4m/s. The highest standard deviation of 1.98 occurred in 1998 and 2001 while the lowest standard deviation of 0.2 occurred in 1996. The Beaufort system values are offset by several meters per second.

The monthly wind speed values from the Beaufort, Radiosonde and Vaisala systems when applied in the formulae for specific wind power-show that the Beaufort system reads higher than the other two systems in most cases (refer to table 5)

### **DISCUSSION AND CONCLUSION**

The variations by Beaufort system are large and abrupt while those variations from the Vaisala system are smooth and consistent/gradual. Respective variations or discrepancies might be due to differences in location, technology and parallax error but some unexplained variations such as those anomalies depicted by Radiosonde system in fig 2 remain not yet understood and need further investigations. The need for accurate measurement of wind speed is highlighted in the results for specific wind power for use in water pumping and electricity generation (for example). Which value should we use needs further investigation.

From the analysis and assessments done the results show that Vaisala wind measuring system is the most suitable system/method.

### **ACKNOWLEDGEMENTS**

The author is indebted to the Zambia Meteorological Department staff for the provision of data and constructive guidance.

### **REFERENCES**

Seth Gutman and Stanley G. Benjamin-The role of ground based GPS meteorological observations in NWP.

Van Meel-Assessment of wind resources-The Netherlands, 1984

Golding, E.W-The generation of electricity by wind power, SPON LTD, London, 1955&1976.

SADC PROJECT AAA 5.17



**WMO Technical Conference on Meteorological and Environmental Instruments and Methods of Observation**  
4 – 7 May 2005, Bucharest, Romania

## MASS AND ENERGY FLUXES MONITORING USING EDDY COVARIANCE TECHNIQUES

Giuseppe MENDICINO<sup>(1)</sup>, Giuseppina MONACELLI<sup>(2)</sup>, Alfonso SENATORE<sup>(1)</sup>

- (1) Department of Soil Conservation, University of Calabria, Ponte Pietro Bucci, Cubo 41 b - 87036 Arcavacata di Rende (CS), Italy, [menjoe@dds.unical.it](mailto:menjoe@dds.unical.it), [senatore@dds.unical.it](mailto:senatore@dds.unical.it)
- (2) APAT - Agenzia per la Protezione dell'Ambiente ed i Servizi Tecnici - Servizio Idrologico, Via Curtatone, 3 - 00185 Roma, Italy, [giuseppina.monacelli@apat.it](mailto:giuseppina.monacelli@apat.it)

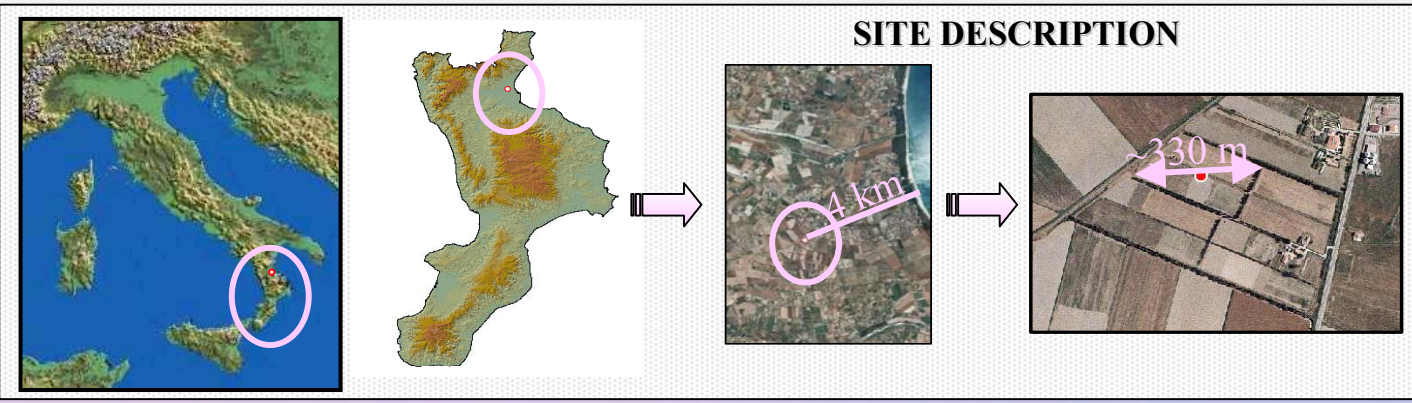
Climatic changes observed in last decades have made even more critical the surface water and the groundwater availability in southern Italy affected by recurrent and severe droughts. The use of adequate drought monitoring techniques represents a fundamental aspect to catch in time signals forecasting non ordinary drought events, in order to correctly manage the emergency.

The eddy covariance (EC) method is one of the most reliable approaches for measuring the vertical turbulent fluxes of heat, water vapor and CO<sub>2</sub> from the surface to the atmosphere, but the data collected in a number of field campaigns has revealed that the sum of sensible and latent fluxes estimated by the EC method is often less than the difference between the net radiation and the soil heat flux. The reasons for the energy imbalance problem are numerous and can be related both to uncertainties in observational conditions such as sites and instruments and to flow and turbulent structures in the atmospheric boundary layer (Kanda et al., 2004; Wilson et al., 2002).

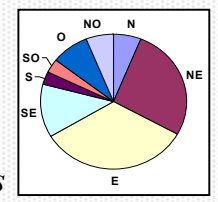
The EC technique needs some restrictive conditions (Foken and Wichura, 1996; Göckede et al., 2004), generally fulfilled by large homogeneous flat sites, with a representative fetch (fetch to height ratio of 100 are usually considered adequate but longer fetches are desirable, Wieringa, 1993). These sites are seldom available in regions with few plain areas, intensively exploited by agriculture, such as those in southern Italy. In the present study data collected in a non-ideal site are analyzed, with the aim of verifying turbulence effects on the energy balance closure.

# MASS AND ENERGY FLUXES MONITORING USING EDDY COVARIANCE TECHNIQUES

G. MENDICINO, G. MONACELLI, A. SENATORE



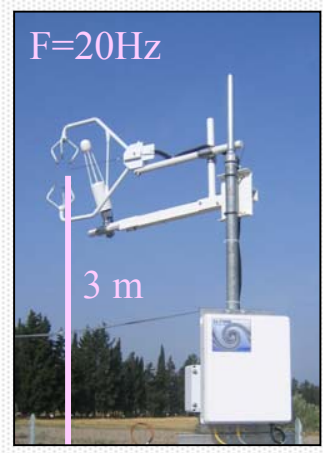
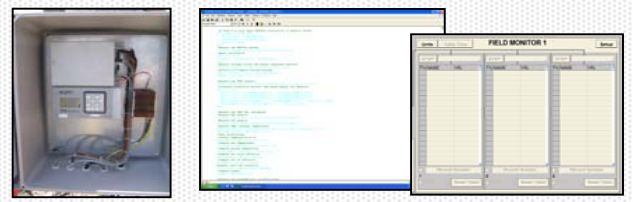
The study was carried out in the Sibari Plain (Calabria - southern Italy) in a field characterized by low vegetation surrounded by rows of cypresses, with prevalent winds from sea.



## MATERIALS AND METHODS

### Measures of turbulent fluxes

- CSAT3-3D sonic anemometer and FW05 Thermocouples for CSAT3, Campbell Sci.
- LI-7500 CO<sub>2</sub>/H<sub>2</sub>O Analyzer, Li-Cor, Inc.
- CR5000 Datalogger, Campbell Sci., with personalized code for PC9000 software



### Supporting meteorological and energy balance measurements

- CNRI Net Radiometer, Kipp & Zonen
- 2 Self Calibrating Heat Flux Sensors HFP01SC, Hukseflux, with 4 107 thermistors

- Furthermore:
- 2 InfraRed Temperature Sensors (IRTS-P, Campbell Sci.)
  - Soil volumetric water content probe EasyAG50



Data has been collected from 08.11.2004 to 12.07.2004 averaging every 30 minutes the raw data acquired with a 20 Hz frequency, and tested for stationarity and integral turbulence statistics using the methods described by Foken and Wichura (1996) and Thomas and Foken (2002). The presence of obstacles in the footprint led to a not fully developed and unperturbed turbulence and to low values of friction velocity  $u^*$ .

# MASS AND ENERGY FLUXES MONITORING USING EDDY COVARIANCE TECHNIQUES

G. MENDICINO, G. MONACELLI, A. SENATORE

## RESULTS

### Overall energy balance closure

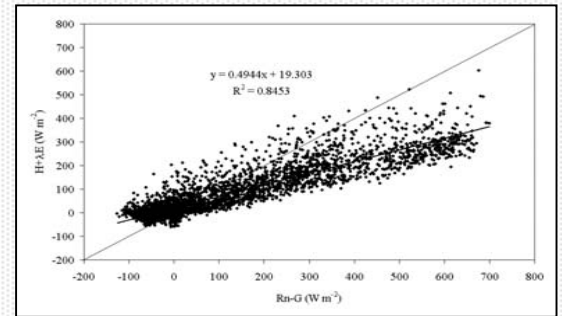


Fig. 1

The OLS slope of  $\lambda E+H$  against  $Rn-G$  on all the about 5200 data (Fig. 1) is less than 0.5, indicating a considerable 'closure gap'. The mean coefficient of determination ( $R^2$ ) is comparable to literature data (e.g. Wilson et al., 2002).

### Effects of turbulent mixing

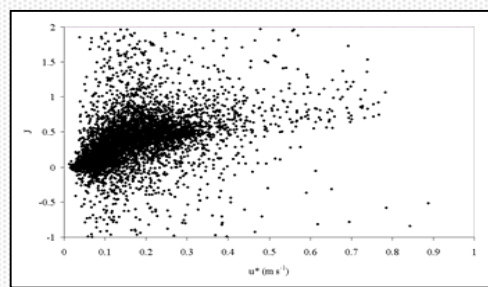


Fig. 4

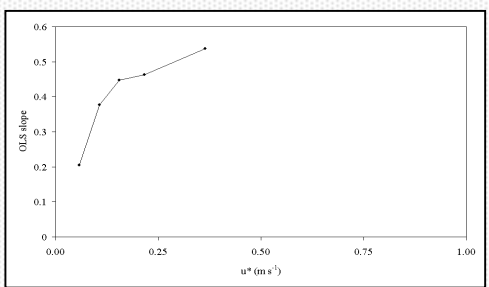


Fig. 5

A more evident correlation exists between  $J$  and  $u^*$  (Fig. 4). The graph of OLS slope against mean friction velocity of 5 20-percentile data groups sorted by  $u^*$  (Fig. 5) shows an higher closure increasing  $u^*$ . Specifically, data with  $u^*$  greater than  $0.4 m s^{-1}$  has shown a 0.6232 OLS slope.

### Diurnal and stability variations in closure

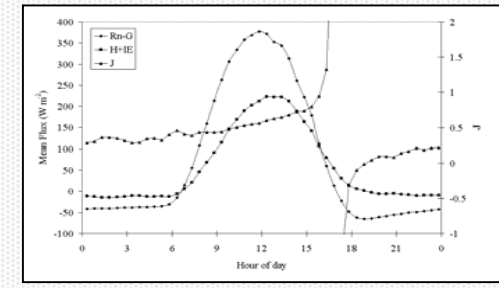


Fig. 2

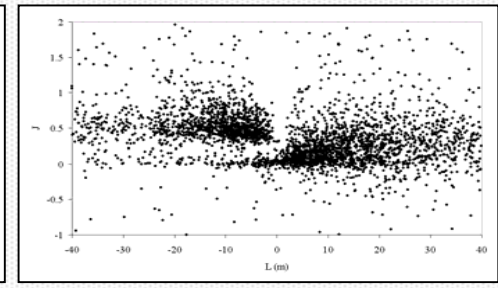


Fig. 3

Mean daily data were combined to compute the diurnal course of  $J=(\lambda E+H)/(Rn-G)$  (Fig. 2), showing not significant values during evening transition periods, and greater  $J$  in the afternoon. The analysis of  $J$  against Obukhov length  $L$  (Fig. 3) showed a correlation between  $J$  and stability conditions, even if not marked.

### Wind directions/footprint analysis

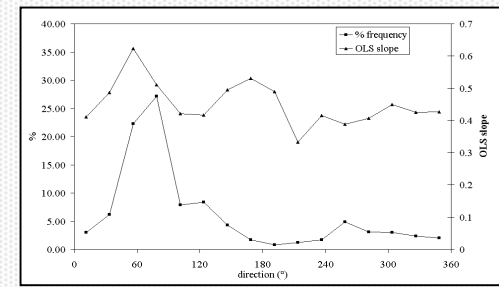


Fig. 6

An analysis of OLS slope against wind directions (Fig. 6) shows that winds coming from sea, which represent the major direction, have the biggest OLS slope. The analysis was made considering 16 different directions, with a  $22.5^\circ$  width. The class with the biggest OLS slope ( $45^\circ-67.5^\circ$ ) has shown the highest mean  $u^*$ .

## RESULTS

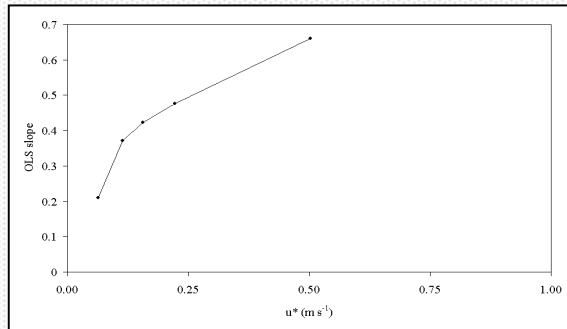


Fig. 7

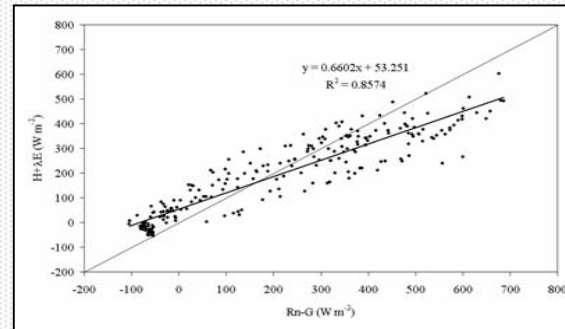


Fig. 8

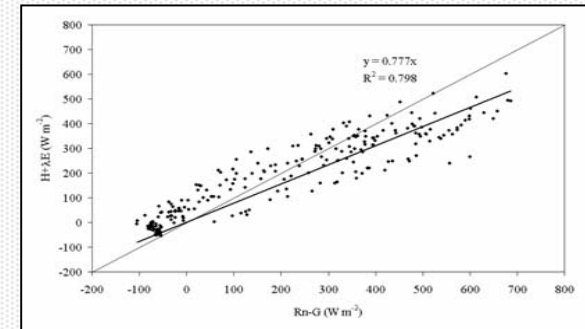


Fig. 9

The graph of OLS slope against mean friction velocity of 5 20-percentile data groups sorted by  $u^*$  for the  $45^\circ$ - $67.5^\circ$  wind direction (Fig. 7) shows an higher closure when  $u^*$  increases. The best results are obtained with a mean  $u^*$  equal to 0.50 with an OLS slope value of 0.66 and  $R^2$  equal to 0.8574 (Fig. 8). Forcing intercept equal to 0 the OLS slope increase to 0.778 (Fig. 9).

## DISCUSSION AND CONCLUSIONS

The best energy balance closures are obtained for the sea-direction characterized by highest  $u^*$  values. Better closures are obtained selecting the highest  $u^*$  values in this direction. Greatest  $u^*$  values for the sea-direction are not only due to the major wind frequency and intensity (typically in this area daytime winds blow from seaside), but also to the fact that in this direction the rows of cypresses surrounding the site are quite far from the EC system (about 150 m), allowing a better developed turbulence. Great problems in balance closure arise for other directions, especially during nighttime, when stable conditions occur.

The main variable in any case seems to be the friction velocity: not considering direction and other factors (that can be related to  $u^*$ ), energy balance closure becomes to be acceptable for  $u^*$  values greater than  $0.4 \text{ m s}^{-1}$ . The dependence of the energy balance closure from  $u^*$  will be further investigated, together with the spectral and co-spectral characteristics of the EC measurements.

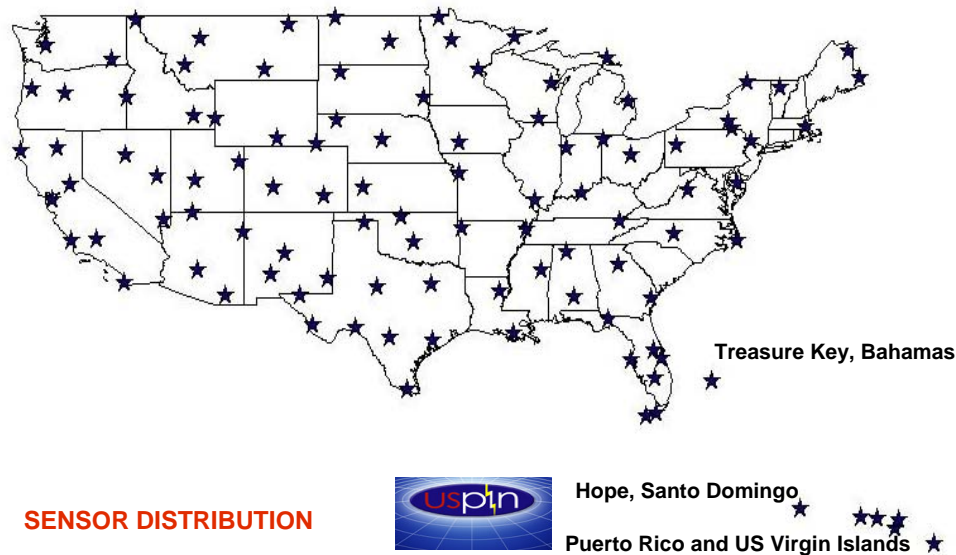
## BIBLIOGRAPHY

1. Foken and Wichura, 1996. Tools for quality assessment of surface-based flux measurements. *Agr. For. Met.* 78, 83-105.
2. Göckede et al., 2004. A combination of quality assessment tools for eddy covariance measurements with footprint modelling for the characterisation of complex sites. *Agr. For. Met.* 127, 175-188.
3. Kanda et al., 2004. LES study of the energy imbalance problem with eddy covariance fluxes. *Bound.-Lay. Met.* 110, 381-404.
4. Thomas and Foken, 2002. Re-evaluation of integral turbulence characteristics and their parameterisations. In: *Proceedings of the 15th Symposium on Boundary Layers and Turbulence*. Am. Met. Soc, Wageningen, The Netherlands, pp. 129-132.
5. Wieringa, 1993. Representative roughness parameters for homogeneous terrain. *Bound.-Lay. Met.* 63(4), 323-363.
6. Wilson et al., 2002. Energy balance closure at FLUXNET sites. *Agr. For. Met.* 113, 223-243.

TOA Advanced Lightning Positioning System (ALPS™) “Covering N. America with real-time stroke detection and mapping.”

William Geitz, TOA International, Arlington, VA 22207 USA. Tel +1 703 533 3190 ext. 299 Telefax + 1 703 533 3190 E-mail [worldsales@toasystems.com](mailto:worldsales@toasystems.com)

## ALPS™ USPLN SENSOR DISTRIBUTION (106 SENSORS)



SENSOR DISTRIBUTION



Hope, Santo Domingo

Puerto Rico and US Virgin Islands



GPS Antenna



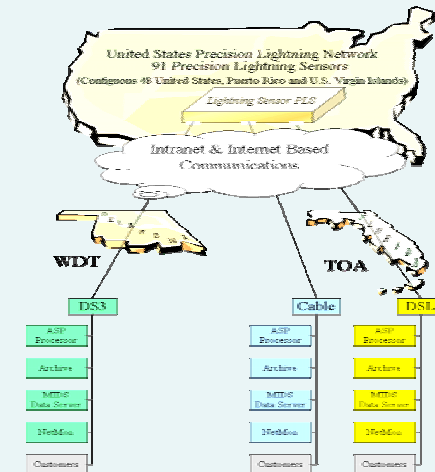
PLS Receiver

(Comm-interface, waveform digitizer, high-resolution timing device, processors and self test)

Stroke Detection Antenna (Capacitive Probe)



## USPLN COMMUNICATIONS, PROCESSING, REAL-TIME MONITORING, QUALITY CONTROL & ARCHIVE



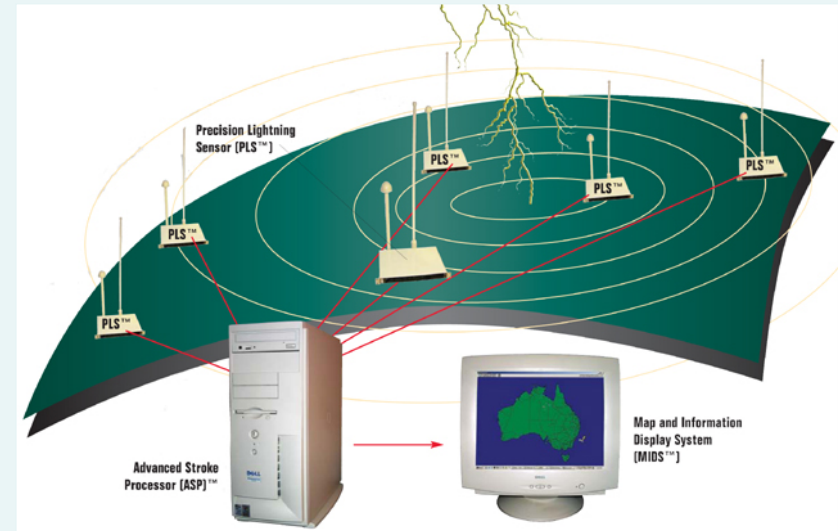
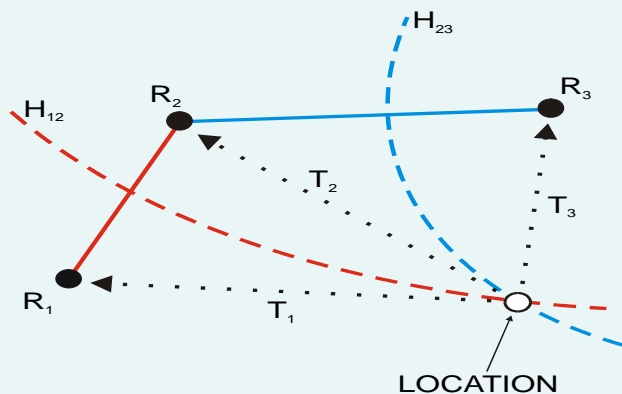
## USPLN INTERNET COMMUNICATIONS (SENSORS TO MULTIPLE NCCs)

- In most cases, Virtual Personal Networks are employed.
- During network design, tracer studies defined internet paths from individual PLS sites to each of the NCC locations.
- Almost all sensors are connected to separate internet back-bones and as such, paths used to deliver data to all NCC's are very different.
- Time to deliver data from PLS sensor to the front-end of the NCC processors is typically less than one second.
- NCC's operated by WDT and TOA provide for at least 8 different direct connections to the Internet.



## SOME NOTEWORTHY FEATURES OF THE PRECISION LIGHTNING SENSOR (PLS™)

- **Proprietary Sensor design, for enhanced signal-to-noise characteristics**
  - The PLS sensor provides the best lightning signal-to-noise characteristics of any lightning sensor available on the market today.
  - High sensitivity permits the monitoring of large areas with fewer sensors.
- **Point-of-Impact Stroke Location**
  - The PLS sensor utilizes proprietary low frequency detection methods and waveform discrimination in the sensor to enable the system to calculate and display the location where the stroke actually hits the ground.
- **Improved Timing Accuracy and Resolution**
  - The PLS timing resolution is 25 nsec. with an accuracy of about 40 nsecs.
  - The dead time can be as low as 200 microseconds.
  - Timing is constantly monitored & corrected/adjusted automatically for temperature/aging effects
- **Remote Maintenance Design**
  - Diagnosis and repair of software problems.
  - Adjustment of sensor operating parameters can be made via land line or the Internet.
  - Remote downloading of software
  - Re-configuration of hardware via the Internet through use of the Advanced Stroke Processor.
- **Greater Sensitivity Than Old LPATS Technology**
  - High sensitivity permits the monitoring of large areas with fewer sensors.
- **Lightning Event Detection and Analysis**
  - PLS analyze the radio wave produced by each lightning stroke and digitize the signal @ a rate of forty (40) nanoseconds.
  - PLS accurately monitors the precise time of the received signals, especially certain time sensitive characteristics such as rise time and fall time.



**ALPS™ Lightning System** Locates lightning over very long ranges (1000's of kms) using ionospheric sky wave propagation.

### **Advanced Stroke Processor (ASP™)**

- Provides Lightning Analysis & Location Processing
- Programmed with site data mathematical & physical coefficients.
- Using all data, the ASP computes a position for each lightning strike or rejects it as noise
- Solution data is output in both binary and ASCII text format
- ALPS™ lightning system can also locate lightning over a great distance (1000's of km) using ionospheric sky wave propagation.
- **ALDA™ Lightning Data Base Functions**
- An SQL Database subsystem, the ALDA will archive the USPLN data plus allow for automatic offline archiving to CD or DVD ROM.

### **ASMS™ Performance Monitoring and Maintenance**

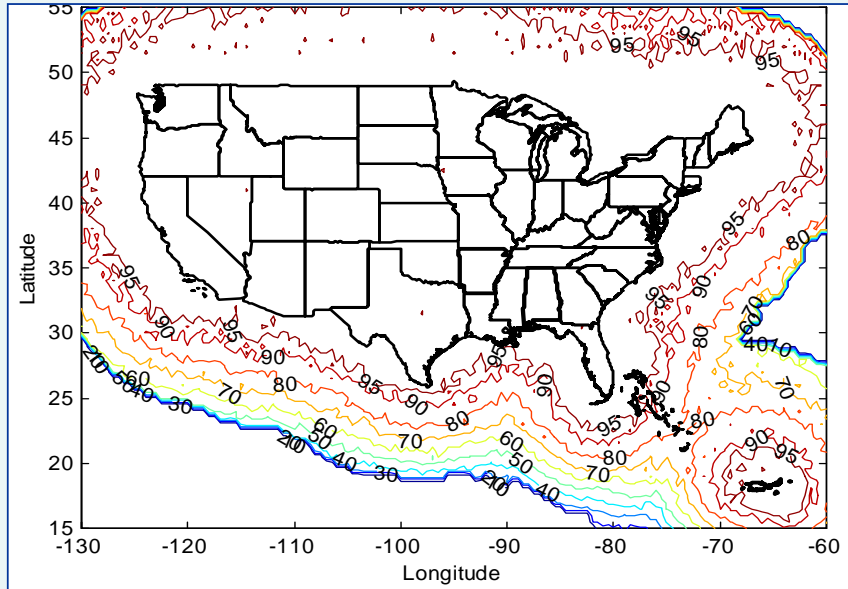
- The central data processing system includes comprehensive system performance monitoring and maintenance tools called ASMS. These applications run on separate processors and support the following functions:

#### **NetMon™ Network Monitor**

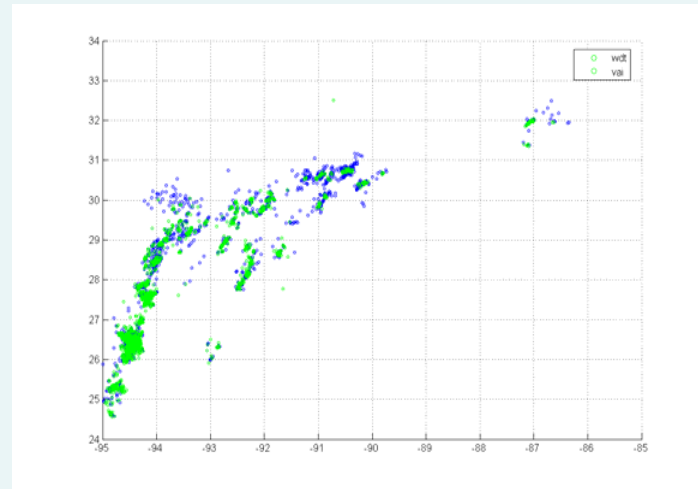
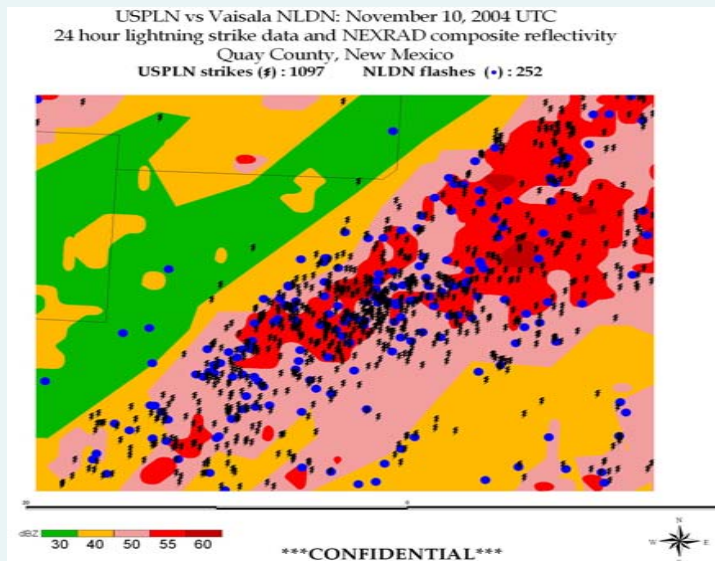
- NetMon displays real time information on the status of all network sensors.
- Data includes # of times each sensor reports activity & takes part in a solution.
- NetMon can also access the database server for historical analysis.

#### **RSD™ Remote Sensor Diagnostics**

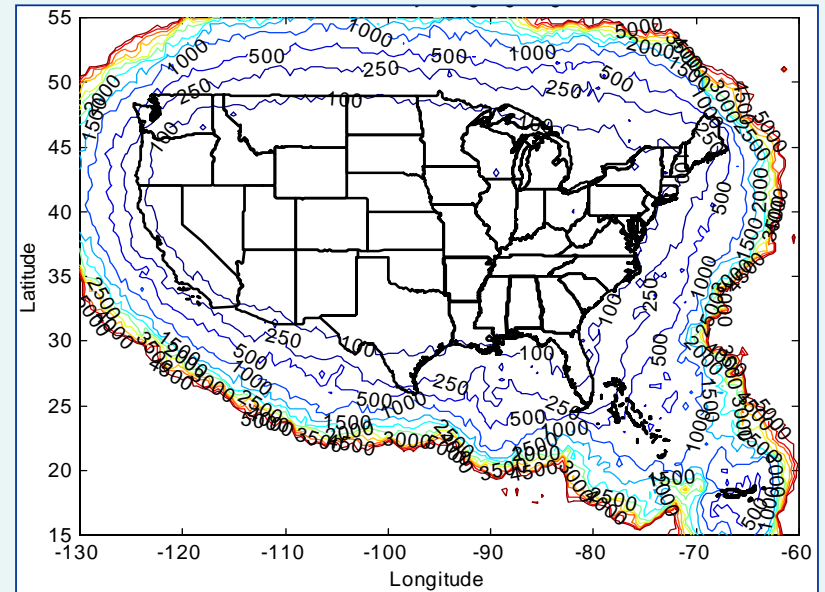
- RSD allows access to the complete system via a communications link to the ASP to communicate directly with any of the active sensors.
- Download software & firmware, monitor oscillator frequency, power supply levels, read the sensor internal temperature and scores of other parameters.



**Cloud-to-Ground Detection Efficiency ( $\geq 95\%$ )**  
Contiguous 48 United States, Puerto Rico, and the U. S. Virgin Islands

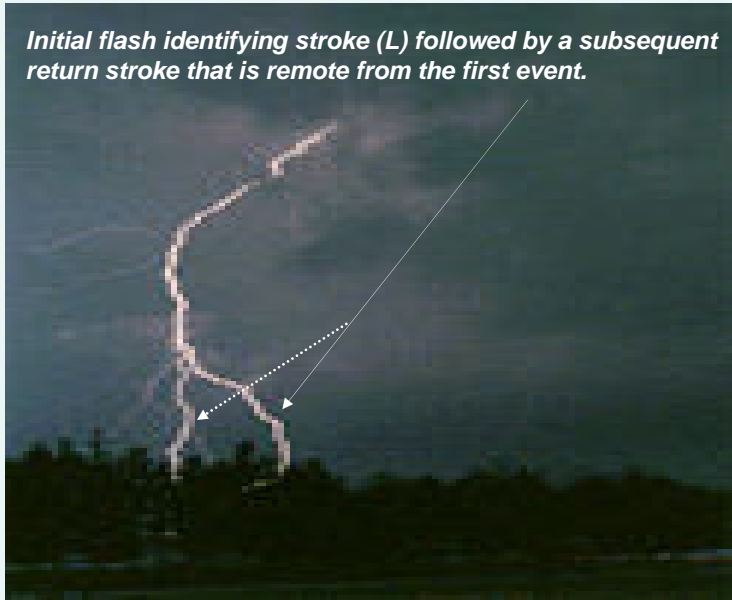


**Note: USPLN detected strokes (green) are tightly clustered due to better location accuracy, whereas NLDN flash data (blue) are more dispersed. Analysis performed by The Weather Channel.**



**Cloud-to-Ground Location Accuracy (Contours are in meters RMS)**

Initial flash identifying stroke (L) followed by a subsequent return stroke that is remote from the first event.



## Why Stroke Data

- Stroke data provides a clearer and concise view of the CG lightning distribution as it relates to the storm.
- CG stroke reports are ideally suited to define the presence of a thunderstorm within both synoptic and METAR operations in a timely fashion.
- Stroke data provides a clearer picture of the overall cycle of air mass thunderstorms and also serve as an early indicator of storm decay.
- Lack of stroke data can have a major impact on safety & sensitive ops. Research by Dr. Martin Uman of the University of Florida has shown that on occasion a return stroke can be initiated at a point remote to the initial point of attachment and that such events can occur up to 7 km from such point within a half-second time. In situations such as this, the INPACT could be a misinterpretation of the extent of the storm and possibly the premature or unnecessary delays in setting local warnings or to return to normal operations.
- In areas where radar coverage is rather sparse access to cloud stroke data, as well as a reasonable number of cloud reports, can provides sufficient coverage of the area as well as define the extent of thunderstorm activity as well effectively gauge their trajectory and speed of movement.

### Flash #1

Date	Time (UCT)	Lat	Long
6/10/2004	01:04:30.880	034.0828	-100.0382
6/10/2004	01:04:30.915	034.0849	-100.0393
6/10/2004	01:04:30.944	034.0850	-100.0383
6/10/2004	01:04:30.967	034.0851	-100.0388
6/10/2004	01:04:31.098	034.0852	-100.0387
6/10/2004	01:04:31.198	034.0851	-100.0396

### Flash #2

Date	Time (UCT)	Lat	Long
6/10/2004	01:04:38.073	030.8194	-096.8339
6/10/2004	01:04:38.436	030.8178	-096.8327
6/10/2004	01:04:38.540	030.8178	-096.8329

### Flash #3

Date	Time (UCT)	Lat	Long
6/10/2004	01:09:03.109	030.8652	-096.8507
6/10/2004	01:09:03.158	030.8665	-096.8497
6/10/2004	01:09:03.247	030.8670	-096.8529
6/10/2004	01:09:03.295	030.8694	-096.8513
6/10/2004	01:09:03.422	030.8660	-096.8559
6/10/2004	01:09:03.763	030.8697	-096.8516
6/10/2004	01:09:04.028	030.8696	-096.8514

• The consistency and accuracy of the individual calculations produced by the APST™ for each of the strokes within a flash is essential to the effective & efficient application of such data.

• Research has shown that most CG flashes contain 1 to 3 return strokes. Why limit yourself to looking at only 25% of the picture when you can see the whole thing with access to individual stroke data from ALPS™

• If this flash defining event was missed by a system that used directional technology as an essential part of its operating scheme, then for all intent and purposes, the IMPACT would be that the event and possibly the presence of lightning would not have been reported

• When your operations are lightning sensitive, whether they involve personnel, facilities or productivity, there can be no margin of error when it comes to making the right decision in a timely fashion. Why limit yourself to a subjective solution answer, when you can have a number of objective ones..

• If ALPS™ technology was in use, and even if the first event was missed, the system would still report the location of the other 6 CG strikes and the presence of the storm.

• If forestry is your business, why spend time and money to investigate a lightning flash with a multiplicity value of 6 that is based on the assumption that they all occurred in the same location. By using the ALPS™ technology, you can view the location of each stroke and as such, base your decision on fact not fiction.

**THE OZONE INFLUENCE  
RISK ASSESSMENT ON POPULATION HEALTH:  
OPTICAL INSTRUMENT OF OZONE CONCENTRATION MEASUREMENT**

\*Naumenko T., \*Sokolov S., \*\*Filinov V. \*\*\*Krasowski A.

\* The Republican Scientific - Practical Centre of Hygiene,  
\*\* The Republican Center of Hygiene, Epidemiology & Public Health  
\*\*\* The National Ozone Monitoring Research Center  
Academic St. 8  
BEL220012, Minsk  
Belarus

Phone: 375 17 284 13 70; Fax: 375 17 284 03 45;  
E-mail [rspch@rspch.by](mailto:rspch@rspch.by)

**ABSTRACT**

The ozone monitoring in Belarus is not conducted. The European guideline value for ozone differed from accepted in Belarus. We've established the new threshold level of ozone (maximum permissible concentration) and developed "The Optical Route Instrument Of Ozone Concentration Measurement - Trio", which is established for the control at Ozone Monitoring Minsk's Station №354 of European networks in the beginning of 2004. The purpose of measurement: definition of ozone concentration in ambient air in natural conditions (without selection of tests). The software for automatic mode is developed. A range of concentration is 0-200 ppb (0-400 мкг/м3). Limits of the basic absolute error + 1.45 ppb. The validation of the technique have been made by using TEI49C ozone analyzer with internal ozone calibrator. The data proved to be true by means of comparative measurements with use of the transportable industrial UV photometric O<sub>3</sub> analyzer (model 49C, Thermo Environmental Instruments - USA). Similar optical Trio is entered into operation at station of background monitoring Berezinsk's Bio Sphere Park.

The Ministry of Health of the Republic of Belarus are responsible for the Social-Hygienic Monitoring (SHM) according to the Law "About Sanitary-Epidemic Well-being of Population". For this purpose we have the Hygiene&Epidemiology Centers, where the environment quality and population health is observed and supervised. We prepare the State Annual Report "Sanitary-Epidemic Situation at Belarus", which is the global official document with objective information about sanitary-epidemic situation in regions, conditions and factors of population health formation, accepted and necessary actions on a population health protection for the state management.

**TEXT**

As is known, hygienic estimation of a regional exposition ozone, the assessment of zones and agglomerations, in which the levels of ozone in ambient air are higher than the target values or higher than the maximum permissible concentration are very important for Environmental Health Information System according to Declaration of the Fourth Ministerial Conference on Environment and Health, Budapest, Hungary, 23–25 June 2004.

The adverse effects of air pollutants such as nitrogen dioxide, sulfur dioxide, particulate matter, carbon monoxide and specific substances such as formaldehyde, phenol, PAH, H<sub>2</sub>S, NH<sub>3</sub>,

etc. Besides, really more than 200 organic chemicals have been detected by chromat-mass-spectrometric analysis, most part of them are alkanes and aldehyde, aromatic hydrocarbons (derivatives of benzene), cycloalkanes

The hygienic estimation of the air pollution danger was conducted according to the maximum permissible concentration, quantity chemicals and class of danger, bioequivalent effect, the long-time average. We have Y degrees: 0 - permissible, I - weak, II - moderate, III - strong, IV - dangerous.

**TABLE 1.** The hygienic estimation of the air pollution danger

City	Air pollution levels		Danger degree	
	$M \pm m; \delta$	$y = a \pm bx; r; p$	fact	prognosis
Brest	$3.250 \pm 0.54$ $\delta = 2.15$	$y = 0.49 + 0.32x; r = 0.72; P \leq 0.01$	moderate	strong
Vytebsk	$4.65 \pm 0.71$ $\delta = 2.86$	$y = 2.18 + 0.29x; r = 0.48; P \geq 0.05$	moderate,	moderate
Gomel	$4.11 \pm 0.41$ $\delta = 1.65$	$y = 2.04 + 0.24x; r = 0.70; P \leq 0.01$	moderate,	сильная
Grodno	$1.58 \pm 0.27$ $\delta = 1.10$	$y = 1.11 + 0.05x; r = 0.24; P \geq 0.05$	permissible	слабая
Minsk	$3.28 \pm 0.32$ $\delta = 1.29$	$y = 3.21 + 0.08x; r = 0.30; P \geq 0.05$	moderate	moderate
Mogilev	$6.45 \pm 0.84$ $\delta = 3.37$	$y = 7.54 - 0.13x; r = 0.18; P \geq 0.05$	strong	strong

Also, we carried out the retrospective epidemiological analysis of primary morbidity some diseases: respiratory disease, pneumonia, bronchitis, asthma.

**TABLE 2.** The asthma morbidity levels. Cases on 100 thousand adult population.

City	Average level $M \pm m \sigma$	Trend $y = f(x)$	Prospect level (min-max)
Brest	$10.02 \pm 0.91$ $\sigma = 3.41$	$\delta = 7.64 + 0.32\delta; r = 0.39; p \geq 0.05$	8.02 - 11.98
Vytebsk	$20.14 \pm 3.89$ $\sigma = 14.58$	$y = 0.33 + 2.64x; r = 0.76; p \leq 0.01$	11.74 - 28.5
Gomel	$11.68 \pm 1.79$ $\sigma = 6.69$	$y = 1.63 + 1.34x; r = 0.84; p \leq 0.01$	7.88 - 15.52
Grodno	$23.57 \pm 1.66$ $\sigma = 6.22$	$y = 17.63 + 0.79x; r = 0.53; p \leq 0.05$	19.97 - 27.14
Minsk	$12.11 \pm 1.59$ $\sigma = 5.96$	$y = 2.28 + 1.31x; r = 0.92; p \leq 0.01$	8.71 - 15.53
Mogilev	$16.21 \pm 1.78$ $\sigma = 6.66$	$y = 6.08 + 1.35x; r = 0.85; p \leq 0.01$	12.41 - 20.04

We develop the risk assessment medical questionnaire on acute influence exposition of concentration ozone on a children health. It is represented important to analyze peaks asthma at children during a maximum daily 8 hour mean of 120  $\mu\text{g}/\text{m}^3$  ozone concentration.

The National Ozone Monitoring Research Center has developed the device "The Optical Route Instrument Of Ozone Concentration Measurement - Trio" and has received the Certificate N1905 at February 06, 2004. "Trio" which is established for the control at Ozone Monitoring Minsk's Station №354 of European networks. The purpose of measurement: definition of ozone concentration in ambient air in natural conditions (without selection of tests).

The software for automatic mode is developed. A range of concentration is 0-200 ppb (0-400  $\text{MKГ}/\text{M}^3$ ). Limits of the basic absolute error + 1.45 ppb. The validation of the technique have been made by using TEI49C ozone analyzer with internal ozone calibrator. The data proved to be true by means of comparative measurements with use of the transportable industrial UV photometric  $\text{O}_3$  analyzer (model 49C, Thermo Environmental Instruments - USA). Similar optical Trio is entered into operation at station of background monitoring Berezinsk's Bio Sphere Park.

Since July 21 and up to the end of month the ozone concentration close to a maximum permissible concentration (60 ppb = 120  $\text{MKГ}/\text{M}^3$ ) were observed. Let's notice, that the maximal concentration per solar days are achieved by 15-16 to hours, July 21 by 15 hours, for example, the concentration ozone has achieved 82 ppb. From August 16 till August 21 as the greatest concentration ozone were observed. In the first 10 days of September the ozone concentration at a level 20-30 ppb were registered. For statistical processing of the information about frequency distribution of man-days depending on concentration ozone (for each interval of concentration) the software is developed.

Also, we carried out the retrospective epidemiological analysis of primary morbidity level of some diseases: respiratory illnesses, pneumonia, bronchitis, asthma. We establish the children morbidity tendencies and prognoses in 5 region of Minsk, which contrast on air pollution (nitrogen dioxide, carbon monoxide, formaldehyde, phenol, VOC, aldehyde, aromatic hydrocarbons, etc.).

In one of 5 areas the regular monitoring ozone is carried out.

# OTT Parsivel® - Enhanced precipitation identifier and new generation of present weather sensor by OTT Messtechnik, Germany

Author: Kurt Nemeth

Co-Author: Jens-Michael Hahn

**OTT PARSIVEL®:** Laser-based optical Disdrometer for simultaneous measurement of **PART**icle **S**ize and **VEL**ocity of all liquid and solid precipitation

## Background and design requirements:

The design requirements for the instrument lead to a universal Commercial Off-The-Shelf (COTS) equipment which meets substantially the meteorological and hydrological requirements of the sensor specification according to WMO and NWS regulation as an enhanced precipitation identifier and present weather sensor.

The patented extinction method for simultaneous measurements of particle size and velocity of all liquid and solid precipitation performs the direct physical measuring principle and classification of hydrometeors.

The instrument provides a full picture of the precipitation event in all weather phenomena and provides accurate reporting of precipitation types and intensities without degradation of performance in severe outdoor environments. Parsivel® operates in any climate weather regime and the incorporated heating device minimizes the negative effect of freezing and frozen precipitation accreting critical surfaces on the instrument.

This piece of equipment detects and identifies 8 different precipitation types as drizzle, mixed drizzle/rain, rain, mixed rain/snow, snow, snow grains, freezing rain and hail.

The output data - consisting of raw data, classification related to size and velocity of particles, rain accumulation and intensity, present weather reports and housekeeping data - make the instrument suitable to any kind of meteorological and hydrological application.



OTT Parsivel® - Enhanced Precipitation Identification Sensor

Parsivel® can be integrated into an Automated Surface/Weather Observing System (ASOS/AWOS) as part of the sensor suite. The derived data can be processed and included into the transmitted weather observation report and messages (WMO, SYNOP, METAR and NWS codes).

The new generation of Parsivel® disdrometer provides the latest state of the art laser optical technology. The data performance has been tested successfully in comparison with a meteorological observer with a distinction rate better than 97%.

Due to modern and high speed DSP technology the wide spectrum of precipitation from drizzle to tropical rain with extreme intensities up to 20 mm/min can be acquired and processed without limitation regarding influence of wind and

effecting catching orifice problems concerning conventional rain gauges.

The instrument supports meteorological observer missions in general and weather service missions for improving severe winter weather warnings for snow and ice conditions, flood forecast and warnings, support to aviation and road traffic, and severe thunderstorm forecast and warnings.

The derived radar reflectivity coefficient together with ground based precipitation data improves essentially the performance of the spatial weather radar information, improves the regional weather forecasts and high water early warning system by combination and correlation of precise and overall precipitation network data.

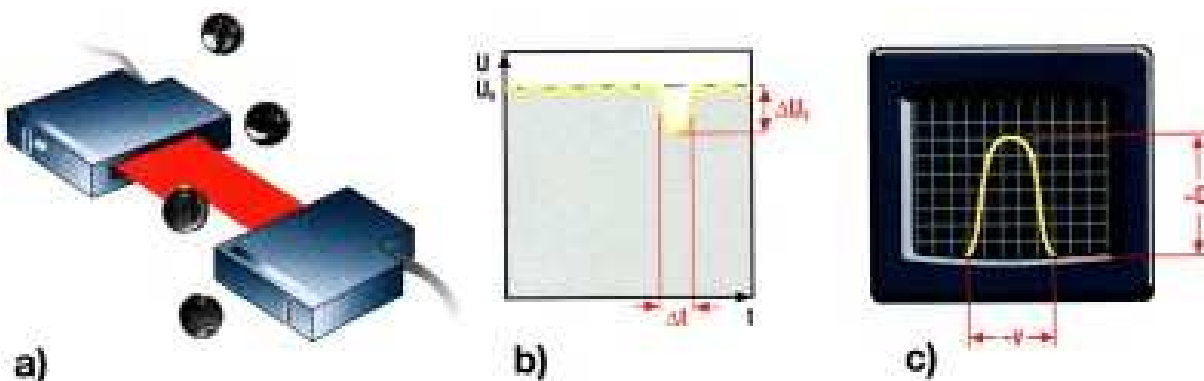
**Parsivel® feature unique performance**

- Patented extinction measurement procedure
- Unattended and reliable operation, using maintenance-free laser technology
- Operable in all environmental and weather conditions (lightning protection and self-regulated heating)

- Low power and heating operation by software commands
- Identification of all precipitation types, including mixed precipitation in the melting layer
- Comprehensive precipitation analysis using 2-dimensional distribution of size and velocity
- Special measuring head prevents secondary spectra caused by drops splashing on the sensor head
- Transmitter and receiver head in perfect design with no obstacles for precipitation catching

**Extinction measuring principle**

The new generation of enhanced precipitation identifier measures directly each single hydrometeor and performs a revolutionary change compared to forward scattered laser optical systems which needs additional sensors onboard and is based on experimental and proofed algorithm to determine the rain rate and identification of precipitation types.



A) The sensor's transmitter unit generates a flat, horizontal beam of light, which the receiver unit converts into an electric signal.

B) This signal changes whenever a hydrometeor falls through the beam anywhere within the measurement area

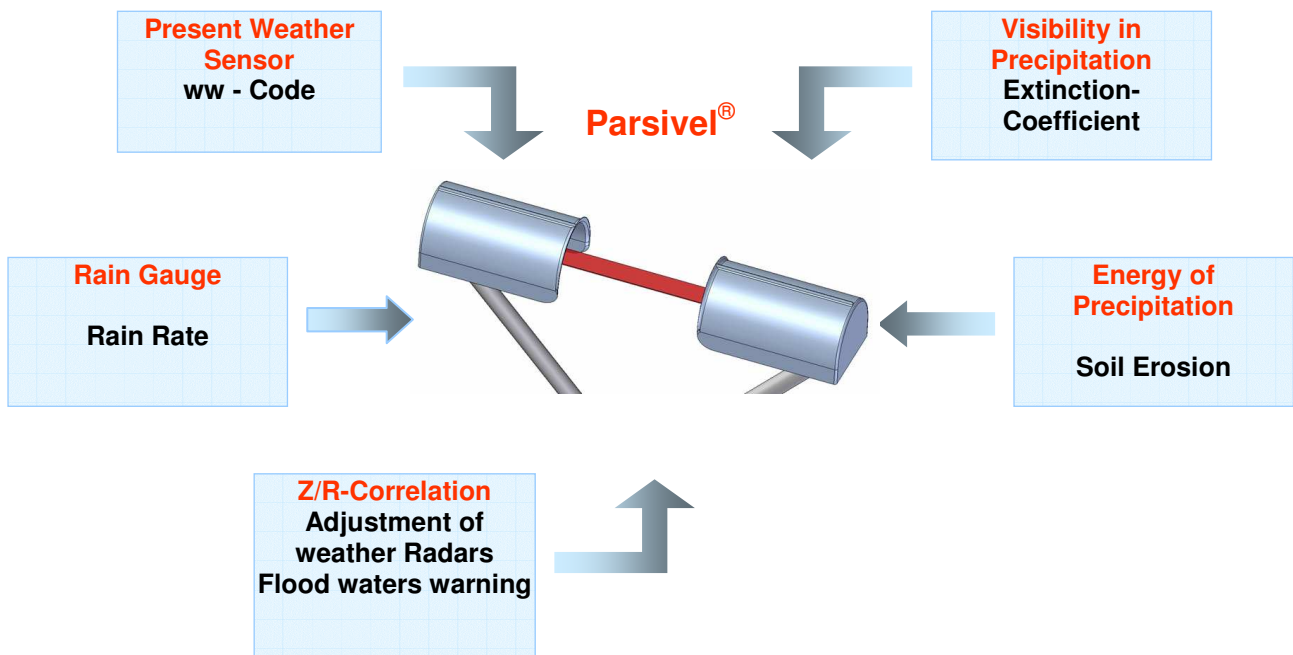
C) The degree of dimming is a measure of the hydrometeor's size, and together with duration of the signal, the fall velocity can be derived.



**Multipurpose instrument featuring enhanced precipitation measurements:**

The full data output of precipitation is accomplished with additional algorithm and the derived data make the instrument

suitable for the use in various meteorological and hydrological applications featuring five single instruments in one unique unit:



The different Features of the Parsivel®

**Precipitation**

Measurements designed for determining the distribution and amount of precipitation can be carried out maintenance-free with Parsivel®, regardless of the intensity, duration or type of precipitation. Additionally, its composition – i. e. the distribution of particles with respect to their type – is obtained directly from the measured sizes and velocities of each single particle and is recorded statistically.

**Present Weather Sensor (PWS)**

The present weather and the types of precipitation (rain, drizzle, snow, hail and sleet) are classified in accordance with a weather code established by the WMO. Unmanned weather stations require automatic detection, reliably and unambiguously. Parsivel® can ascertain the type, quantity and composition of the

hydrometeor and the atmospheric visibility – in every kind of weather!

**Monitoring of disposal sites**

The functions of precipitation kinetic energy distribution and precipitation measurement are utilised by Parsivel® to record the effect of rain on the condition of the disposal sites in conjunction with other sensors, e. g. ground-condition probes.

**Monitoring road conditions**

Local intense precipitation can lead to aquaplaning or packed snow on roads. Therefore, rapid traffic warning and control systems are necessary in order to prevent accidents. Precipitation measurement, hydrometeor composition and atmospheric visibility are of considerable importance in such systems. Parsivel® is an integrated instrument that

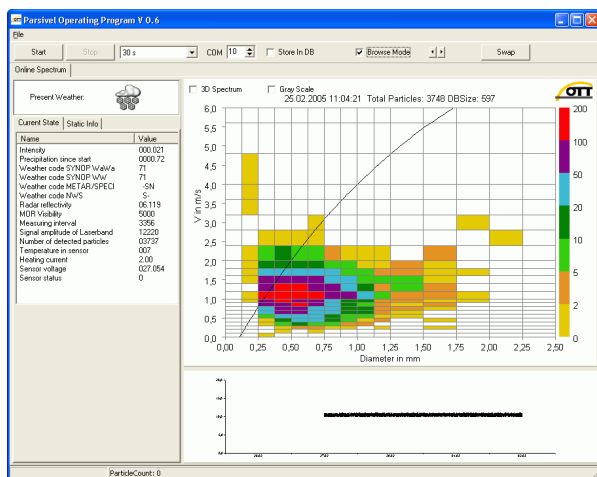
measures all required parameters in accurate quality and performance.

### Flood early warning

To assure a timely warning of impending high water it is necessary to measure the amount and spatial distribution of precipitation rapidly and accurately. This goal can be achieved by combining weather radar measurements (spatial information with reduced accuracy) and ground based disdrometer measurements: Parsivel® provides drop size distributions on the ground and a function to derive a local Z/R relation – ready to be used to adjust the radar data. In combination with water level sensors and drainage modelling, a high-performance regional flood early warning system can be erected.

### Expert Software ASDO

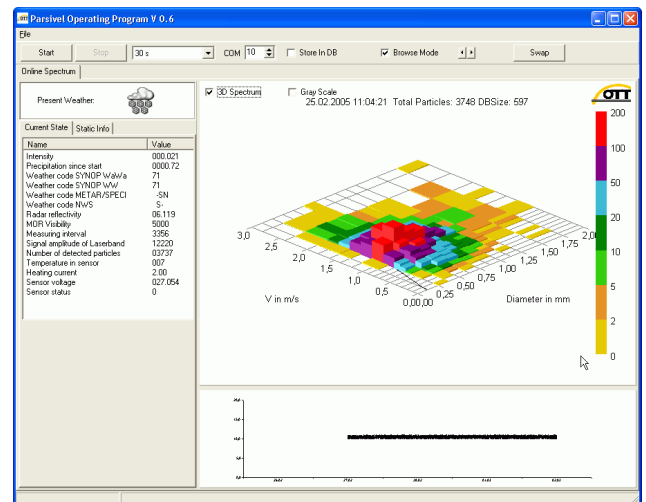
The corresponding Software ASDO monitors the outdoor precipitation event to comfortable indoor evaluation with windows performance.



Screenshot ASDO – Tabular view and 2D Mode

The sensor transmits all data to a PC and supports the observer with full information

of present weather and precipitation and provides a history of precipitation falls stored in a data base. Present weather icon, all derived precipitation data and weather codes as well as housekeeping data like supply, voltage laser output energy and firmware related information are displayed as digital information.



Screenshot ASDO- 3D Mode

The precipitation spectrum can be evaluated as graphical displays and spectrum distribution in 2 and 3 dimensional mode.

All data are stored in a powerful data base and can be retrieved by browser with related date and time and displayed in equal form as online display.

All configuration tasks like time interval from 10 sec to 120 minutes, baud rate and size of telegram and others can be selected and stored as configured variables.



OTT MESSTECHNIK GmbH & Co. KG  
 Postfach 2140 D - 87411 Kempten  
 Ludwigstraße 16 D - 87437 Kempten  
 GERMANY  
 Tel. 0831/5617-0  
 Fax 0831/5617-209  
 E-Mail: [info@ott-hydrometry.de](mailto:info@ott-hydrometry.de)  
[www.ott-hydrometry.com](http://www.ott-hydrometry.com)

## SESSION 2

NEW DEVELOPMENTS AND OPERATIONAL EXPERIENCE WITH  
UPPER-AIR OBSERVATION TECHNOLOGY

Session 2

POSTERS

# **SOME RESULTS FROM ATMOSPHERIC SOUNDING IN CASES WITH FOEHN IN SOFIA VALLEY**

**P. Videnov, A. Tzenkova, A. Gamanov**

National Institute of Meteorology and Hydrology, Bulgarian Academy of Science  
66 Tzarigradsko Shoussee, Sofia, Bulgaria, plamen.videnov@meteo.bg

## **ABSTRACT**

Sofia Valley is surrounded by Vitosha Mountain from the South. One of the typical characteristics of local climate in Sofia Valley is the manifestation of foehn in some specific synoptically situations. In accordance of the power and depth of the foehn in some cases the temperature increased and the balloon is going down. In these situations the process of the sounding has problems in determination of the beginning and the end of foehn.

In the presented paper some soundings with a foehn are analyzed. The obtained results show problems, which have to be, solved in future development of the software of the data processing.

## **INTRODUCTION**

Sofia, the capital of Bulgaria, is situated in the valley of the same name. The highest surrounding mountains are the Balkans to the North, and Vitosha and Ljulin to the South. Sofia aerological observatory is located near the northern slope of Vitosha mountain. Station's altitude is 590 m and this of the highest Vitosha peak – Cherni vrh – 2290 m. In case of southerly winds passing over the mountain in Sofia occurs foehn wind. Foehn situations in Sofia are observed when Mediterranean cyclones pass along the line Belgrade – Carpathians towards Bessarabia [1].

Foehns are descending strong winds from the mountains, accompanied by increase of air temperature and decrease of air humidity. Foehn is one of characteristic winds in the Sofia valley, blowing usually from south-southwest and displays most strongly over the southern city parts, where NIMH is situated. Foehn formation is related to the transformation of air flow by the orography. Foehn over Sofia is usually generated when south or southwest flow passes over Vitosha and Ljulin mountains and downslopes on the lee side (towards Sofia valley), experiencing adiabatic warming and drying. A massive lenticular cloud develops along the southern part of Vitosha crest.

Foehn situations are observed about 30 times a year on the average [2]. Table 1 shows the monthly frequency of foehn.

Table 1. Mean frequency of foehn in Sofia

I	II	III	IV	V	VI	VII	VIII	IX	X	XI	XII	year
2.6	2.6	4.3	3.6	2	1.3	0.5	1.1	1.9	3.8	3.8	2.5	30

The average surface wind velocity in case of foehn is 15-20 m/s, and in some cases it is gusty strong wind blowing at speed of 25-30 m/s. In December 1970, for instance, it reached 35 m/sec, and 40 m/s at Cherni vrah. In such clearly pronounced situation in December 1979 the temperature in Sofia reached 17.3 °C. While overflowing the Vitosha mountain, on the lee side arises a big rotor, comprising the Sofia Aerological observatory. Particularities of the radiosounding in foehn situations over Sofia valley are poorly studied. [3].

### ANALYSIS OF SOME CASES OF ATMOSPHERIC SOUNDING UNDER THE FOEHN CONDITIONS

It has been found that when radiosounding is carried out in such cases, after the start the radiosonde, following the wind direction, turns to Vitosha and at some height enters the strong “jet” of the descending air (Fig. 1). Its further behaviour depends on the part of the jet it has entered.

The maximum vertical velocity of the foehn jet, established in our practice, is about 12 m/s, and in many cases it is 5-6 m/s. Having in mind that the average upward velocity of the sonde is 5-6 m/s, in such cases the radiosonde starts to descend. The drop can sometimes reach 1500-2000 m and pressure begins to rise. Usually the pressure rise is several tens of hPa, reaching 150 hPa in some cases. There are cases with several successive downward motions of the sonde. Temperature differences in foehn jets are of the order of several tenths to 7-8 °C . In some cases of weakly pronounced foehn these differences can be negative. Cases of sonde passing along the jet are also possible.

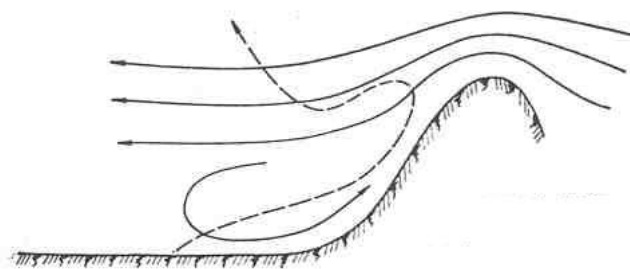


Fig.1 Scheme of the foehn (possible trace of radiosonde - - - - > )

Radiosounding data processing in foehn situations is more specific, and several problems arise in consequence, which could be generally grouped in the following way:

1. Slowing the process of sonde ascending due to decrease of the ascent rate, which normally is about 5-6 m/s, and in such case could drop down under 1 m/s. (Fig.2.);
2. Balloon return to lower height due to wind gust (3,4);
3. Cases where the lifting process is disturbed more than once (5).

These events are with different duration and are accompanied by corresponding fluctuations of values of meteorological elements, usually following the balloon movement.

Some particular cases are discussed to illustrate the behavior of balloon sonde.

Situation of slowing down of the process of lifting (group 1) is shown in Figure 2a and 2b.

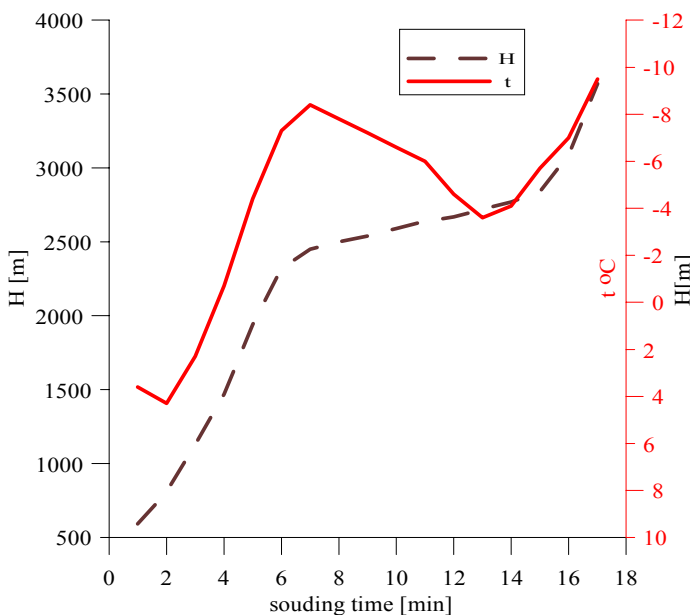


Fig.2.a. Vertical temperature profile group 1

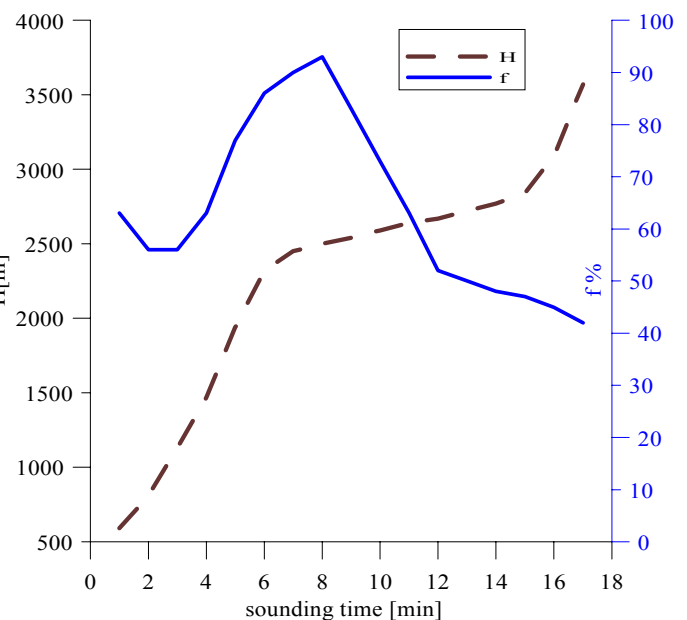


Fig.2.b. Vertical humidity profile group 1

As shown in Figure 2, from height 2450 m up to 2840 m the sonde falls in the foehn flow, resulting in the decrease of the ascent rate by some 2 m/s, i.e. the balloon ascent rate becomes 4 m/s. Temperature rise of some 5 °C is registered in this section (fig. 2.a). At the same time relative humidity decreases from 93% to about 46% (Fig. 2.b).

The reverse motion of the sonde due to foehn effect is shown in Figs 3 and 4.

As seen in Fig. 3, at height 2700 m sonde enters a strong foehn flow with descending vertical velocity of 8-9 m/s, which leads to reducing of its height to 2040 m. Air temperature increases by 7,8 °C (Fig. 3.a). Humidity also changes, decreasing by some 56% (Fig. 3.b).

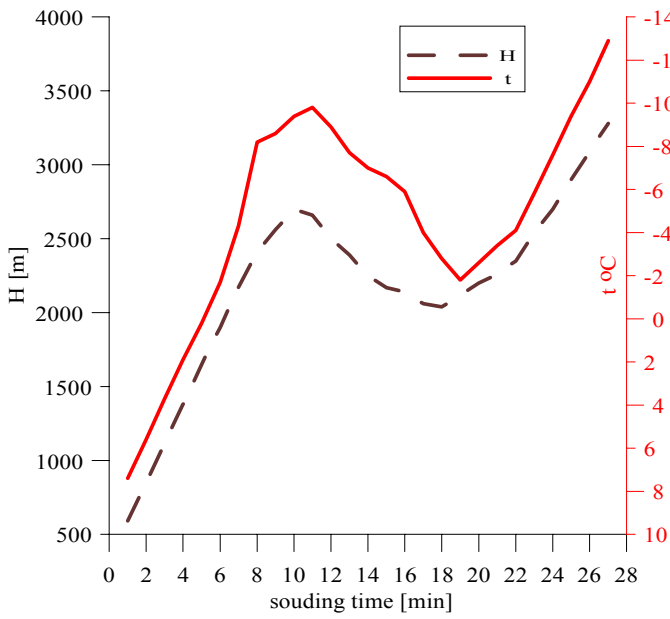


Fig.3.a. Vertical temperature profile group 2

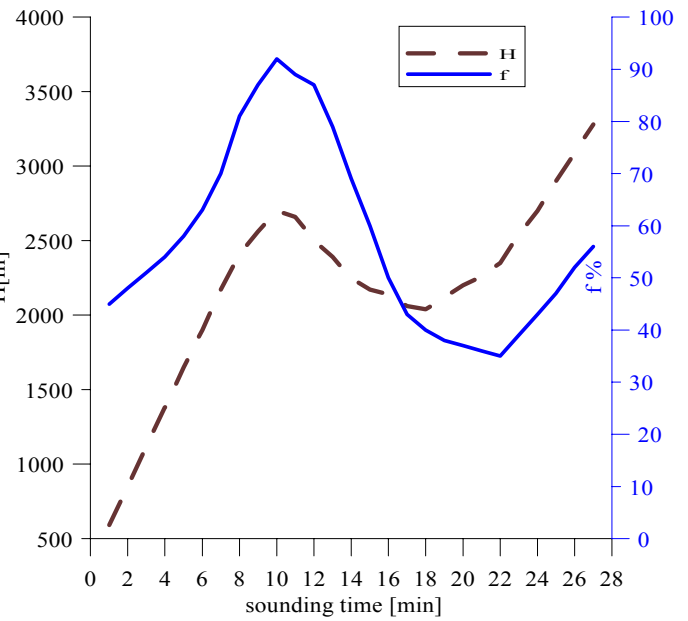


Fig.3.b. Vertical humidity profile group 2

Similar case is shown in Figure 4, where the return of the sonde commences at 1800 m and reaches 1400 m, and the vertical velocity increases from 7 m/s in the beginning to more than 9 m/s. Most probably the sonde crosses different sections of foehn flow, causing different variation of temperature and humidity in separate track sections. The general trend is of temperature increase (of about 6 °C, Fig. 4.a). Relative humidity at the same time shows a trend to decrease by some 30% (Fig. 4.b).

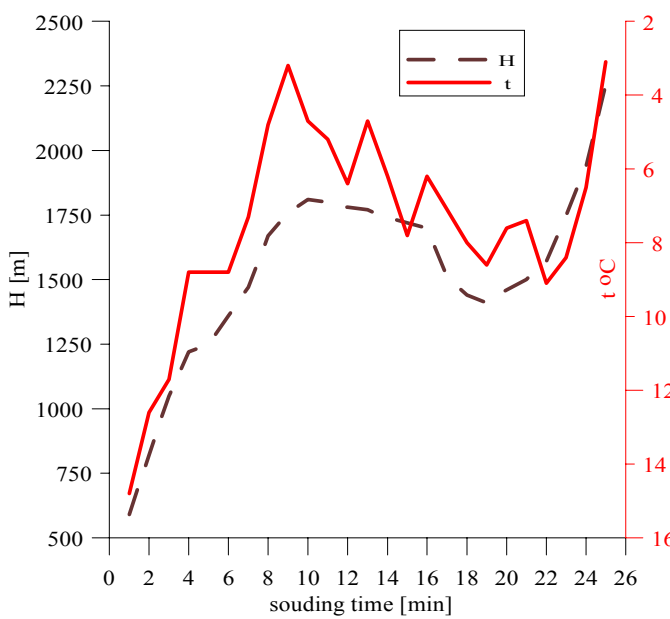


Fig.4.a. Vertical temperature profile group 2

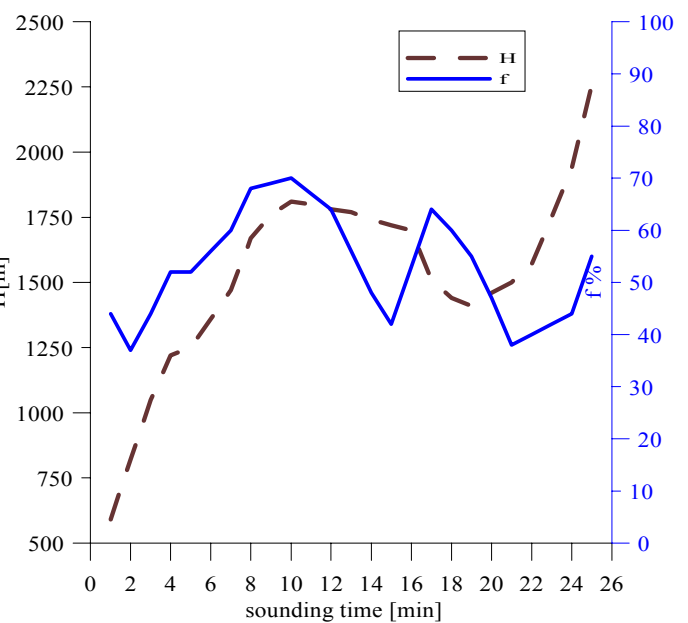


Fig.4.b. Vertical humidity profile group 2



All cases discussed so far concern the sound entry into foehn at heights about and above 200 m. Group 3 is illustrated by an instance (Fig. 5) where sonde passes various sectors of foehn rotor as shown in Fig. 1.

At height 1290 m balloon sonde enters an air flow with downward velocity of about 7 m/s, which returns the sonde down to 1240 m. This motion is accompanied by a temperature increase of some 1,5 °C, while humidity remains constant. Then balloon continues to ascend with about normal velocity up to 2200 m. At this height sonde enters the upper part of the foehn rotor and returns to about 2120 m. In these cases temperature increase of 1,4 °C is registered, while the relative humidity increases with about 10%, which could be due to entering the periphery of foehn cloud.

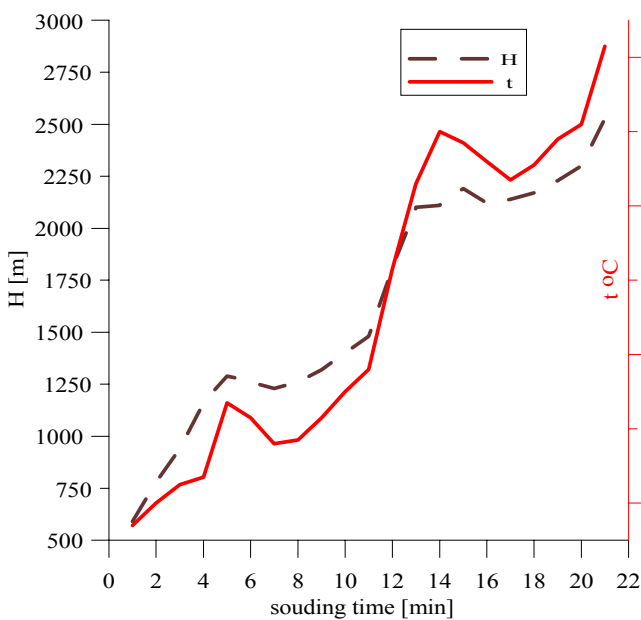


Fig.5.a. Vertical temperature profile group 3

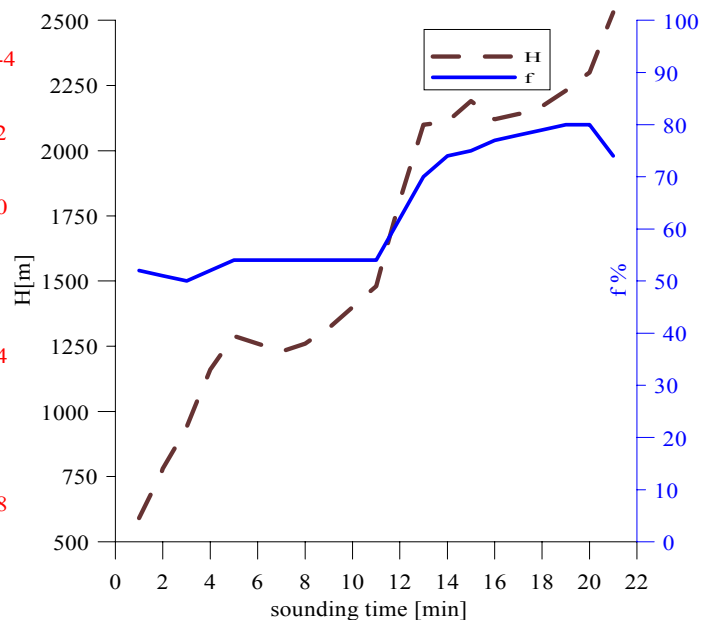


Fig.5.b. Vertical humidity profile group 3

In atmosphere radiosounding practice cases of disturbed sonde raising arouse doubt. The above discussed foehn situations are of this type. According to the conventional practice and coding requirements in these cases we have adopted following approaches of data processing:

1. In case of motion corresponding to group I data are processed as in a standard case of sonde in flight;
2. In the rest of cases (group II and III) sections where the sonde is swept along by the foehn flow are cut out from the sounding. In order to separate such foehn situations from the random errors, we assume such cases, where the decrease of height is accompanied with the corresponding variation of meteorological

elements, confirmed in several successive reports. For beginning of foehn we assume the height where the return motion of the sonde starts. The end of foehn is the level 100-200 m higher than the one where return motion starts.

This processing reduces data to convenient for international exchange kind, but reflects actually existing local phenomena. These type of phenomena are of substantial interest for a number of important for the local climate studies.

## **DISCUSSION**

All considered cases are based on soundings that used RKZ-5 radiosondes and Meteorite radar. They are processed with software developed in NIMH. Since 2001 the sounding system is replaced by Vaisala DIGICORA3 and RS90 radiosondes. In December 2001 there was a foehn situation, when the sounding was interrupted from the moment of the sonde return motion. It was an obvious foehn event, followed for some time, but was interrupted by the software as the pressure increased by 50, and a message for balloon burst was issued. The new software version, provided in 2002 has been improved for such cases. Due to decrease of Mediterranean cyclone frequency [4] we didn't observe more foehn cases during upper-air sounding. So, we didn't have a chance to test the software improvement in practice.

## **REFERENCES**

1. S. Sabev, S. Stanev, "Climate regions in Bulgaria and their climate", Zemizdat-1963, in Bulgarian
2. M. Syrakova, D. Syracov, K. Donchev, "Meteorology for everybody", Science and art-1989, in Bulgarian
3. Chapanov, A. Dragieva "On the some peculiarities of foehn in Sofia", Hydrology and Meteorology XVII, boock 5, 1968, in Bulgarian
4. Marinova, T., L. Bocheva, V. Sharov, 2003. Some Climatic Changes in the Circulation over the Mediterranean Area and Their Influence under the Meteorological Conditions in Bulgaria. Proceedings of Sixth European Conf. on Applications of Meteorology, 15–19 September, Rome, Italy (CD version)

**Applying working knowledge for well managing the Upper Air Stations Network  
in order to preserve its historical achievements and work  
on continuing its development and prosperity**

**By**

**Mostafa A. E. Amer**

**Director General of Upper Air Stations Network**

**Egyptian Meteorological Authority**

**P. O. Box 11784, Cairo, Egypt**

**Tel.: 00202-6849860, Fax: 00202-6849857**

**E-mail : [ma@idsc.gov.eg](mailto:ma@idsc.gov.eg) & [mamer1950@yahoo.com](mailto:mamer1950@yahoo.com)**

**ABSTRACT**

The main Egyptian upper air stations network had been constructed since fifty years ago by first constructing the three upper air stations in Helwan, Aswan and Matruh. At that time the upper air observations were done by the aid of using manual radars, radiotheodolites, radiosonde receivers, sliding rules and wind plotting boards. In 1995 another upper air station was constructed in Arish, and in 2002 both Farafra and Qena upper Air stations were constructed. The six upper air stations are currently equipped with modern automatic radiotheodolites and the upper air weather reports are generated by accompanied computers.

The author explains how to prepare the Electronic Technicians in the field of modern electronics, communications system and accompanied computers software and hardware to help the technicians well digest the whole upper air observing process and consequently be able to diagnose and solve various technical problems. The author also points out the difficulties faced in providing the required radiosonde and balloons in order to keep the six stations in regular continuous operation.

**1- Introduction:**

The upper air information and reports are considered the backbone of the weather analysis, forecasting and aeronautical meteorology. The costs for building a new upper air station and equipping it are very high. The daily costs for operating such station and providing it with radiosondes and balloons are also very high. The capacity building of high standard upper air technicians and observers to keep the upper air stations in regular and continuous operation for long times and to have accurate radiosonde information and reports is not an easy task. For all those reasons it is very important to well manage the upper air stations network and preserve its historical achievements and continuing its development and prosperity.

## **2- Historical survey of the upper air stations network in Egypt:**

There are six upper air stations now in Egypt located in Cairo, Aswan, Matruh, Arish, Qena and Farafra. They started work in 1959, 1962, 1965, 1995, 2003 and 2003 respectively. They all were equipped with manual radars, radiosonde receivers and manual radiotheodolites. Now all these stations are equipped with automatic radiotheodolites. The future plan aims at including another three upper air stations to be located in Siwa oasis, Oweinat and Halaib. Find in the attached map the currently implemented upper air stations as well as the stations that will be implemented in the future.

## **3- Capacity building of high standard upper air Observers and Technicians:**

Upper air Observers and Technicians should have a Diploma in electronics from a specialized technical institute after obtaining their high school general certificate, science branch. As soon as they join EMA a special training course in upper air observations for six months must be taken, that course include:

- a) Introduction to general meteorology and its branches; Physical Met., Dynamical Met, Synoptic Met. and Climatology.
- b) Manual radiosonde calculation and plotting Adiabatic and wind charts and extracting codes.
- c) Training on operating automated upper air systems equipped with personal computers including solving software problems.
- d) Field training for additional two months in one of the automated upper air stations.

After completing this training, the upper air Observers should become ready to carry out the regular work of upper air stations equipped with high technological equipment and sophisticated software programs as well as distinguishing between correct and non-correct data indicated on the PC's screen, in addition to intervening to eliminate errors. Also they should be carrying out the essential tests and adjustments for radiosondes before launching in order to isolate the faulty sondes for either repair or replacement by the manufacturers free of charge according to the contract between them and us.

## **4- Preparing the high standard Technicians:**

It is very important to have high standard electronic Technicians to perform the frequently maintenance and necessary repair of the automated upper air systems as well as having a complete set of spare parts precisely chosen by technicians themselves to preserve their regularity and continuity of operation. In this aspects those technicians should have regular specialized and advanced courses in:

- English language
- Modern electronics
- Communication systems
- Computer Engineering (Hardware)
- Advanced Software programs

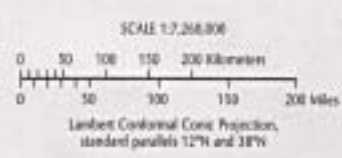
to help technicians well digest the whole upper air observing process and consequently be able to diagnose and solve various technical problems.

**5- Difficulties faced in providing the required radiosondes and balloons:**

The fact that the radiosondes and balloons are very costly, specially radiosondes that are working with GPS, which are used to avoid the problems of calculating the wind in case of low elevation angles of radiotheodolite. Consequently it is required exerting major effort to convince the authorized (non-specialized) people to dedicate the required budget for buying radiosondes and balloons. In order to reduce the cost, we sometimes have to minimize the operation program of upper air stations during summer (from first of May till end of September) which happens to be a period of weather stability. Usually Helwan, Aswan and Matruh make one observation at 11:30 GMT, whereas Arish, Farafra and Qena make one observation at 23:30 GMT. Occasionally, at first of September we have to make two observations in Helwan for environmental proposes.

**6- Conclusion:**

In conclusion, to preserve the historical achievement of those upper air stations and maintaining their regular operation plus their development and prosperity, we have to well manage the network of those stations by well preparing the observers and technicians to help solve all technical problems, in addition to providing the required radiosondes and balloons for operation.



- International boundary
- ★ National capital
- Governorate capital
- Railroad
- Expressway
- Road
- - - Track

## **A New Round the Clock Observation Technology to Measure Vertical Profiles of Visibility and Spectral Transmission in the Mixing Layer (ML)**

M. Weller, A. Knöfel, S. Weber, Met. Obs. Lindenberg, Am Observatorium 12, 15848 Tauche/OT Lindenberg, Germany, Tel.: +49 33 67 76 02 89, Michael.Weller@dwd.de

Profiles of the relative humidity measured all 6 hours by a new precision Vaisala-Radiosonde (Leiterer et al.) and hourly available humidity profiles provided by the Local Model of the Deutscher Wetterdienst serve as input of a model (Khvorostyanov & Curry) describing the growth of aerosols with the relative humidity. Assuming constant aerosol concentration in the ML simultaneously measured spectral aerosol scattering coefficients at known relative humidity (TSI nephelometer typ 3563) allow the determination of total aerosol scattering coefficients in dependence on the relative humidity in the ML at different heights. The method takes into account instrument corrections concerning the pronounced forward scattering of aerosols and the (weak) aerosol absorption in rural regions. The final product are continuously (day and night) derived vertical profiles of the visibility in the ML (applying Koschmieders formula) . Adding the total scattering coefficients within the ML yields the spectral aerosol optical depth and the transmission respectively. The presented procedure will be tested to be helpful for flying weather prediction.

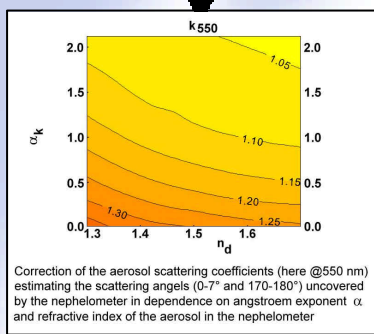
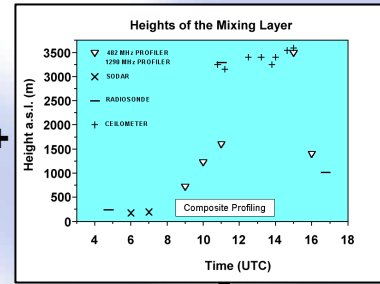
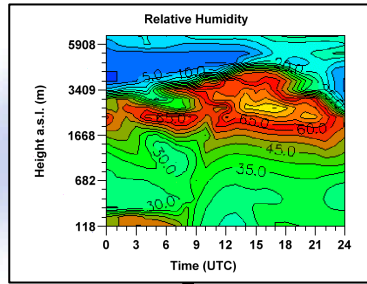
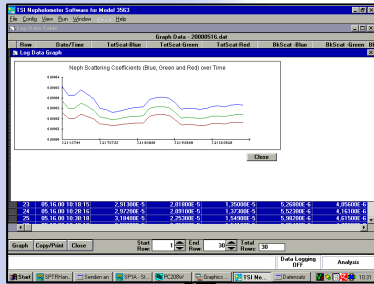
### Literature:

Khvorostyanov V. F.; Curry, J. A.; JGR Vol. 104 No. D2; 2163-2174 (1999)

U. Leiterer et al.; Journal of Atmospheric and Oceanic Technology (JTECH) Vol. 22 No. 1; 18-29 (2004)

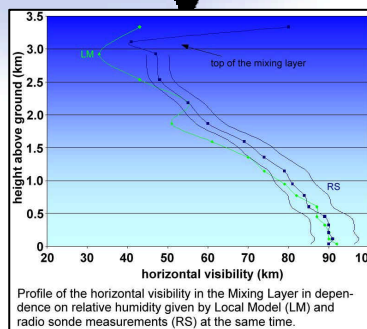
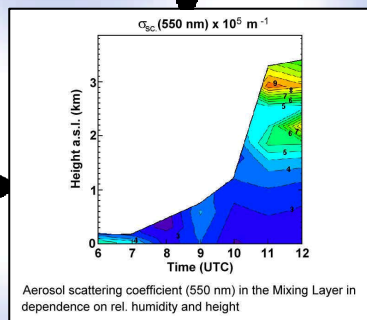
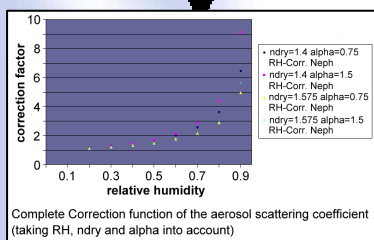
# A New Round the Clock Observation Technology to Measure Vertical Profiles of Visibility and Spectral Transmission in the Mixing Layer (ML)

M. Weller, A. Knöfel, S. Weber, Met. Obs. Lindenberg, Am Observatorium 12, 15848 Tauche/OT Lindenberg, Germany, Tel.: +49 33 67 76 02 89, Michael.Weller@dwd.de



$$\sigma_s = K(\alpha, i) \sigma_s(RH_{Neph}) \psi(RH) \alpha^{\frac{\alpha+2}{3}} \frac{(1-RH_{Neph})^{-1}}{(1-C_2(1-RH)^{-1})}$$

$K$  - from nephelometer measurement and Mie Theory  
 $\sigma_s(RH_{Neph})$ ;  $\alpha$ ;  $RH_{Neph}$  - from nephelometer measurement  
 $RH$  - from local model (LM) and radio sonde  
 $\psi$  - given by look-up-tables for dry aerosol refractive index  
**Koschmieder formula:**  $VV = \frac{3.91 \text{ km}}{\sigma_{ext}}$   
 $\sigma_{ext} = \sigma_s + \sigma_{abs}$   
 $\sigma_{abs} = 1/10 \sigma_s$



Profiles of the relative humidity measured all 6 hours by a new precision Vaisala-Radiosonde (Leiterer et al.) and hourly available humidity profiles provided by the Local Model of the Deutscher Wetterdienst serve as input of a model (Khvorostyanov & Curry) describing the growth of aerosols with the relative humidity. Assuming constant aerosol concentration in the ML simultaneously measured spectral aerosol scattering coefficients at known relative humidity (TSI nephelometer typ 3563) allow the determination of total aerosol scattering coefficients in dependence on the relative humidity in the ML at different heights. The method takes into account instrument corrections concerning the pronounced forward scattering of aerosols and the (weak) aerosol absorption in rural regions. The final product are continuously (day and night) derived vertical profiles of the visibility in the ML (applying Koschmieders formula). Adding the total scattering coefficients within the ML yields the spectral aerosol optical depth and the transmission respectively. The presented procedure will be tested to be helpful for flying weatherprediction.

## Literature:

Khvorostyanov V. F.; Curry, J. A.; JGR Vol. 104 No. D2; 2163-2174 (1999)

U. Leiterer et al.; Journal of Atmospheric and Oceanic Technology (JTECH) Vol. 22 No. 1; 18-29 (2004)



# USE OF DOPPLER RADAR IN ROMANIA FOR NOWCASTING AND WARNING

**Aurora Stan-Sion and Aurel Apostu**

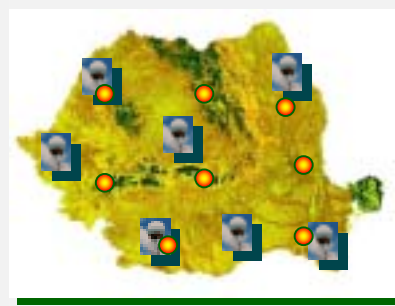
National Administration of Meteorology Bucharest, Romania

The Weather Service in Romania operates two types of weather radars. These are C and S-band Doppler radars. Immediately upon installation our forecasters faced one challenge that is the storms in Romania have never been before observed with Doppler radar.

Hence it was not known how different the fields of Doppler velocity might be comparing with those cited in literature and if the signatures of severe weather phenomena could be readily detected. After nearly 4 years of observations several of the severe storms attributes have been observed with the Doppler radars.

Although this is a short time for statistical evaluations answers to questions such as what is the prevalent storm type that causes severe weather are beginning to emerge. It is confirmed that rotating storms (mesocyclones) do occur and some have produced tornadoes. These storms are principal causes of strong winds, severe hail, flash floods, and intense electrical activity.

## FACAENI TORNADO, 12 AUGUST 2002: RADAR-BASED TORNADO SIGNATURE AND DAMAGE SURVEY



### Radar and Lightning detection Networks in Romania



S- and C-Band Doppler Radars (WSR-98D & DWSR-2000C)



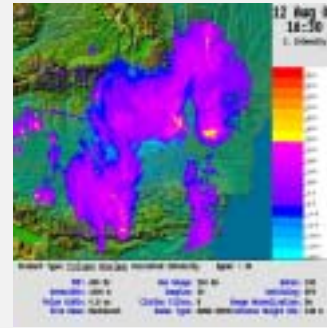
Lightning Detectors



Facaeni tornado path, black bold. Footprint produced by the fast moving tornado (about 80 km/h). Danube River in blue.



Reflectivity as measured by the ANM radar for 0.5° antenna elevation angle, 12 August 2002, 1700 UTC (top) and 1710 UTC (bottom) respectively few minutes after Facaeni village was struck.



This was the first supercell observed in Romania observed with a Doppler radar. The velocity data were not available

The storm phenomenon was responsible for at least three fatalities, a large but undetermined number of injuries, 33 home destroyed and 428 damaged.

After the event, the forecasters declared in mass-media that the damages were caused by strong winds or by a pseudo-tornado, saying that the latitude of Romania was too far north to permit tornadoes and the tornadoes are "confined to the tropics."

### Terminology

The survey of the damage path and type indicated an F3+ tornado. However, due to the fact that this phenomena is rare in Romania, it took some time for the terminology "tornado" to be accepted by the forecasters. They preferred to use the term "strong winds".



Damaged power pole within the tornado path (upper) and a destroyed commercially made red brick home in Facaeni (left hand-side) image.



Downed trees along Danube (left hand-side) and destroyed forest near Danube and Facaeni (right hand-side).

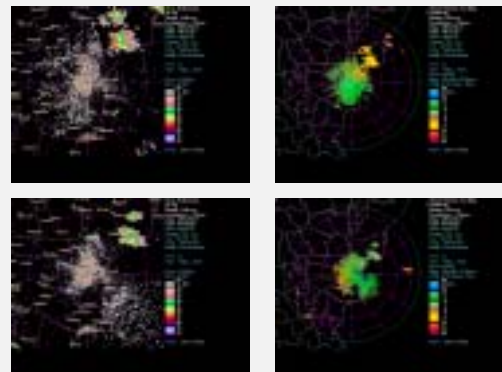
## FLASH FLOOD PRODUCED BY A HIGH-PRECIPITATION SUPERCELL, 27 AUGUST 2003

About one year after the Facaeni event another supercell was identified on S band radar image in the southeastern part of Romania. This supercell was stationary for about 5 hours in the same location producing flash floods in 2 villages. There were two fatalities.

The automatic algorithms helped in identifying the mesocyclone and the possibility of big size hail. The presence of a mesocyclone should be one of criteria for severe convective weather warning but it is not sufficient to rely on algorithms alone for its identification.

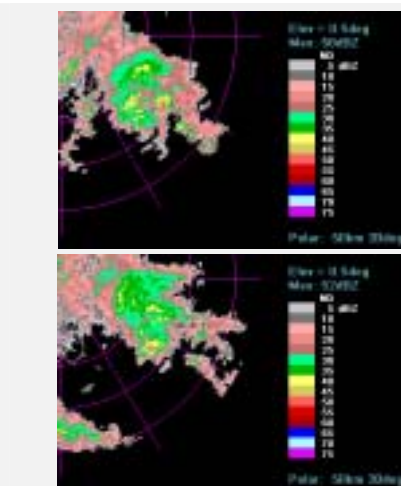


Radar data from RDMD as processed by OmniWxTrac (Baron) application identifying severe weather using automatic algorithms. The image above shows a mesovortex identified in AO location with characteristics enumerated in the Meso "AO" New legend.

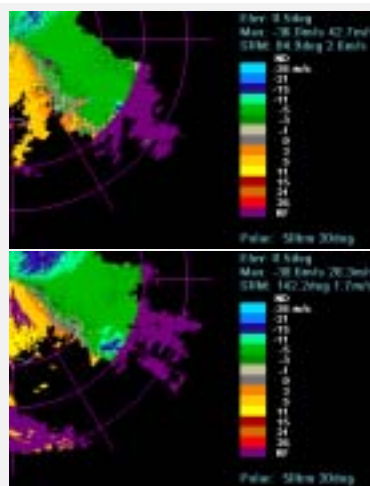


Reflectivity (top and bottom left) and Storm Relative Motion (top and bottom) data as measured by RDMD WSR-98D (located in Medgidia, nearby the Black Sea) for 0.5° antenna elevation angle, 12 September 2003, 0635 UTC (top) and 1125 UTC (bottom) respectively. The images illustrate the quasi-stationary supercell storms.

## A MEZOVORTEX OVER THE BLACK SEA, 12 SEPTEMBER 2003



Reflectivity as measured by RDMD Doppler radar for 0.5° antenna elevation angle, 12 September 2003, 0635 UTC (top) and 1125 UTC (bottom) illustrating the mezovortex over the Black Sea.



Storm relative motion as measured by RDMD Doppler radar for 0.5° antenna elevation angle, 12 September 2003, 0635 UTC (top) and 1125 UTC (bottom) illustrating the mezovortex over the Black Sea.



This event was a mezovortex that developed in the western basin of the Black-Sea; two supercells formed in the eastern and then southern part of the mezovortex. The strong winds associated with the mesocyclones produced heavy damage to the Ukrainian ship Slavutici-7 that subsequently sank.

# TIME-LAG CORRECTION OF OPERATIONAL RS80-A RADIOSONDE HUMIDITY

A. Kats, U. Leiterer<sup>\*</sup>, H. Dier<sup>\*\*</sup>

FGUP KOMET, Roshydromet,  
3, build.6, Pervomaiskaya Street, Dolgoprudny, 141700, Russian Federation  
Tel.: +(7 095) 408 6104, Fax:+(7 095) 408 6865  
E-mail: [komet.kats@mtu-net.ru](mailto:komet.kats@mtu-net.ru)

<sup>\*,\*\*</sup>) Meteorological Observatory Lindenberg, DWD  
Am Observatorium 12, Tauche/OT Lindenberg, 15848, Germany  
Tel.: +49 (33677) 60-244, Fax:+49 (33677) 60-280  
E-mail: <sup>\*</sup>) [ulrich.leiterer@dwd.de](mailto:ulrich.leiterer@dwd.de), <sup>\*\*</sup>) [horst.dier@dwd.de](mailto:horst.dier@dwd.de)

## ABSTRACT

It is described the method and results of time-lag correction of Vaisala RS80 A-Humicap radiosonde humidity sensor correction. Specially developed numeric technique and free public software for its application is presented. Results of correction have been validated by comparison of humidity profiles, obtained during ascent, with descent ones, and, as well with FN-sonde data – a special research version of Vaisala RS90 radiosonde, with faster sensors.

Since January 2003 described lag correction procedure was in operational use at Meteorological Observatory Lindenberg, Germany – GUAN and GVaP reference upper-air station, until its transition to new Vaisala RS92 radiosonde in July 2004.

---

## 1. Introduction

The work, presented here, was undertaken within the long-term activity of Meteorological Observatory Lindenberg (MOL), Germany, which is GUAN and GVaP reference upper-air station, to develop comprehensive correction of Vaisala RS80-A radiosonde humidity measurements /8/. The development of the correction was based on their regular weekly comparison with research humidity reference radiosondes using developed in Lindenberg so-called *Standardized Frequencies* (FN)-method (FN-sonde - a special research version of Vaisala RS90 radiosonde /5/).

As many of real world measurement, humidity measurements of A-HUMICAP sensor of RS80-A radiosonde suffer from sensor's inertia. As sensor requires time to reach equilibrium with ambient environment, variable in general case time delay, or lag, appears between the variations of ambient humidity and sensor's output, expressed in the units of relative humidity. Exposure the sensor from dry to moister environment results in too low measurements (and vice verse – from moist to drier conditions – in too high ones) before the sensor gets the equilibrium (if environment is stable). Corresponding error component is referred to as lag error.

Comparison of RS80-A with FN-sonde /5/ humidity has shown that lag error has rather deterministic nature and noticeable magnitude to be worth to be corrected.

## 2. Background

Basis for correction is that sensor response follows well-established equation, assuming that rate of change of sensor's output is proportional to the difference between ambient humidity and sensor's output

$$\lambda \cdot \frac{dU}{d\tau} = U^{\text{true}} - U \quad (1)$$

or, in canonic form

$$\lambda \cdot \frac{dU}{d\tau} + U - U^{\text{true}} = 0 \quad (2)$$

where

$U^{\text{true}}$  – ambient humidity, %RH

$U$  – measured sensor's output in relative humidity units, %RH

$\tau$  – time, seconds

$\lambda$  – time constant, seconds, defined as time required to sensor to reach 63% of input signal variation after its instantaneous change.

More strictly notation for time constant should be  $\lambda\{t(\tau)\}$ , where  $t$  is the ambient temperature as A-HUMICAP response is strongly temperature dependent (see Equation (9)), but for the sake of clarity we will use hereinafter  $\lambda(t)$ .

Equation (2) is the 1<sup>st</sup> order ordinary linear differential equation with general solution in form

$$U = \exp\left(\int -\frac{d\tau}{\lambda(t)}\right) \cdot \left(C + \int U^{\text{true}} \cdot \exp\left(\int \frac{d\tau}{\lambda(t)}\right) \frac{d\tau}{\lambda(t)}\right) \quad (3)$$

where  $C = (U^{\text{true}})_0$ .

An important property of solution (3) is that it is linear regarding  $U^{\text{true}}$ .

Important partial case is when input parameter varies with constant rate

$$U^{\text{true}} = u_0 + u_\tau \cdot \tau$$

Solution 3 in that case looks like

$$U = U_0 \cdot \exp\left(-\frac{\Delta\tau}{\lambda(t)}\right) + u_0 \cdot \left(1 - \exp\left(-\frac{\Delta\tau}{\lambda(t)}\right)\right) + u_\tau \cdot \tau - u_\tau \cdot \lambda \cdot \left(1 - \exp\left(-\frac{\Delta\tau}{\lambda(t)}\right)\right) \quad (4)$$

In steady state, i.e. when  $\Delta\tau \rightarrow \infty$ , we have from Equation (4)

$$U = u_0 + u_\tau \cdot \tau - u_\tau \cdot \lambda$$

or

$$U = U^{\text{true}} - u_\tau \cdot \lambda \quad (5)$$

From Equation (5) it follows that within layers with constant humidity gradients in steady state (after termination of transition processes) measured humidity has the same gradient as true humidity, and time delay between actual and measured humidity is equal to time constant regardless of gradient value itself:

$$U(\tau) = U^{\text{true}}(\tau - \lambda) \quad (6)$$

In presentation of radiosonde ascents pressure or height is used as abscissa instead of time. As well, for the analysis of ascent-descent flights (see later in section 3.2) only presentation in height or pressure domain is reasonable. For this, expressing time differential  $d\tau$  as  $s \cdot dH$ , where  $s$  is vertical (ascent or descent) velocity and  $H$  is height, we receive from Equation (1)

$$\lambda s \cdot \frac{dU}{dH} = U^{\text{true}} - U \quad (7)$$

In principle, we can also come to pressure domain using hydrostatic equation to relate height and pressure differentials but it has no practical sense. Again, for the  $s$  stricter notation should be  $s(H)$ .

Correspondingly, for the layers with constant vertical gradient of measured humidity Equation (6) is transformed under condition of constant (more-less) vertical velocity to

$$U(H) = U^{\text{true}} \cdot (H - \lambda s) \quad (8)$$

that easily characterizes vertical height shift between measured and actual profile.

### 3. RS80 A-HUMICAP time constant model

#### 3.1. Literature data

Determination of time constant for humidity sensors is quite complicated and challenging technical task. So, it's not surprising that little information is available on this matter. Actually, these are early report of Vaisala RS80 introduction /2/, results of ordered by Vaisala the NIST measurements /4/, several measurements @ 20 and -20 °C, made during the 1<sup>st</sup> Phase of WMO Radiosonde Humidity Sensor Intercomparison /3/ and more recent /7/. Results are more less consistent and indicate strong dependency of time constant from the temperature which is expressed according to /4/ as

$$\lambda = \lambda_0 \cdot e^{\lambda_t \cdot t} \quad (9)$$

where

$\lambda$  is time constant in seconds

$t$  is temperature, °C

$\lambda_0=1.7$ ,  $\lambda_t=-0.06916966$  (from the Figure 3 in /7/ there were derived values  $\lambda_0=1.0$  and  $\lambda_t=0.0743$ ).

It is really tremendous relationship - enough to say that time constant increases almost twofold ( $\ln 2=0.69314718$ ) from the temperature decrease by 10 °C.

As well, /4/ indicates that response of sensor follows exponential law and the 90% response time is 2.3 times as longer as the 63% response time, or time constant. It is to some extent confirmed by results of /3/. This allows application of model from Equation (1). Also, results of the Figure 1 from unpublished report of the Phase-I Laboratory Test of WMO Radiosonde Humidity Sensor Intercomparison prove us in adequacy of Equation (1).

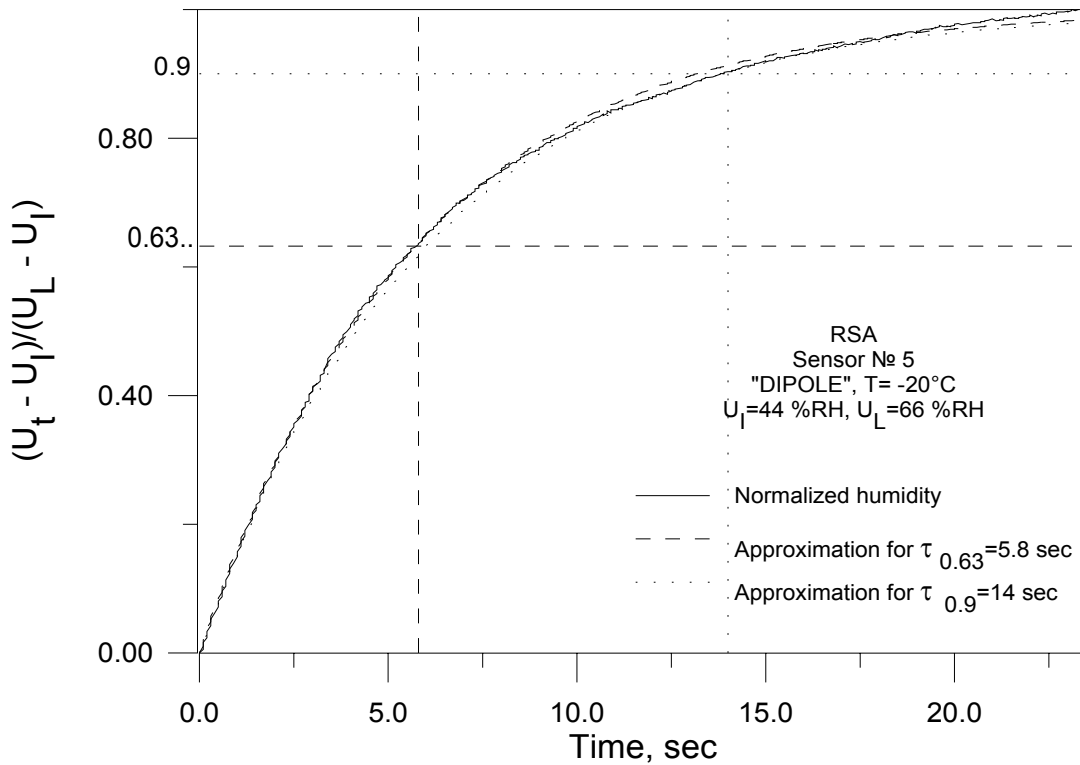


Figure 1: An example of RS80-A time constant examination from WMO Radiosonde Humidity Sensor Intercomparison (see /3/). It is shown variation of normalized relative humidity with time after step-wise change of humidity ( $U_i$  – initial,  $U_L$  – final and  $U_t$  – intermediate humidity) from  $U_i$  to  $U_L$ .

However, some measurements, made by authors of /3/ in addition to official program demonstrate that response of sensor itself, without protective cap, rather faster than usual configuration. That means possible presence of the second-order term or transport delay in more accurate than Equation (1) model.

Also /4/ declares that to curtain (although not quantified) extent time constant depends from direction of humidity variation. Other parameters, that remained beyond the scope of investigation of A-HUMICAP response and potentially could affect it, are pressure, ventilation, humidity itself and last but not least production variability.

So, present state-of-the-art knowledge of A-HUMICAP response do provide necessary background to the development of lag compensation algorithm but could not serve as solid fundament therefore empiric should be involved to reach plausible results.

### 3.2. Comparison of ascent and descent profiles

To make qualitative validation of available information on RS80-A Humicap time constant under different temperatures it was decided to analyze data of flights with radiosonde ascent followed by descent. Typically ascent data are shifted towards upper levels relative to ones of descent. Assuming that radiosonde penetrate the same air mass on both stage of the flight apparent, a vertical displacement of ascent and descent profiles results from lag error and therefore carries out information about time constant.

It's evident that comparative analysis of ascent and descent data should be made in height domain. And using Equation (11) for the layers with constant vertical gradient of humidity gives reasonable background for rough analysis as it doesn't require calculation of derivatives and gives in this case clear interpretation of vertical height displacement of ascent and descent profiles

$$\Delta H_{\text{asc-desc}} = \lambda_{\uparrow} s_{\uparrow} + \lambda_{\downarrow} s_{\downarrow} \quad (10)$$

or, assuming  $\lambda_{\uparrow} = \lambda_{\downarrow}$ , just as

$$\Delta H_{\text{asc-desc}} = \lambda (s_{\uparrow} + s_{\downarrow}) \quad (11)$$

In MOL there were specially organized 13 RS80 flights with descent data recording. In addition to routine procedure all of the flights were made with parachute although usually reflector alone is considered to be enough to provide low drop velocity nearby the surface. As PC-CORA do not provide descent data processing, PC-CORA raw data files were used as the source for analysis<sup>1</sup>. They contain conventional unedited (except in terms of plausible engineering quantities) PTU data from each telemetry cycle instead of standard edited (i.e. controlled and smoothed) 10-seconds data along with elapsed time since switching on power of receiving system. As well, release time is provided according as detected by Vaisala data processing software from variation of pressure. Unfortunately, resolution of humidity readings again is 1%RH that introduces

---

<sup>1</sup> Comparison of raw and edited data revealed one interesting typical but prominent peculiarity. The point is that routine data processing software in addition to rounding "truncates" to 1%RH all humidity below this value. In many cases this seemed unimportant feature introduce noticeable distortion into derivative resulting in symptomatic artifact in humidity profile just in place where it comes to 1%RH. In one flight the minimal raw reported humidity was -3%RH so visible bend in profile curvature in edited data brought attention and allowed to understand the reason of artifact observed. Although that ascent was an extreme case of negative reported humidity in many other flights raw data humidity minimum was <0%RH that brings an assumption about presence of slight negative dry-end bias in A-HUMICAP measurements at low temperatures.

additional unnecessary uncertainty into results. And is more pity that time resolution in output files of 1 sec is insufficient in comparison with potential capability of radiosonde (telemetry cycle is about 1.5 sec) and receiver, that makes it difficult e.g. to compare the data with FN-sondes and investigate the influence of editing and smoothing on to final 10-s output, proper calculation of vertical velocity etc.

Some experience of the processing may be of general interest itself. As it was shown earlier we need to consider humidity data versus height coordinate in comparison with ascent and descent velocity to enable evaluation of time constant. Conventional geopotential calculations were based on hydrostatic equation. And it was pressure that was used to match ascent and descent part of measured profiles. From the uppermost part of ascent with sufficient data quality it was taken on of the latest pressure level and its height was assigned to corresponding matching pressure level of descent. Lower levels' heights were calculated again from hydrostatic equation. Examinations of relative displacement of characteristic peculiarities (prominent features or variations) of ascent and descent vertical profiles proved that accuracy of relative overlay of ascent and descent profiles against height was of order about 10-20 m.

To ensure preservation of the same atmospheric situation during the whole flight, minimal time and horizontal displacement are required. Ascents with following descents usually took as long as ~9000 sec. It was found that even in cases of moderate winds with distances of drop of order about 50 km temporal and spatial variability of humidity field in mid- and lower troposphere is too large to allow evaluation of time constant. Therefore, downfall trajectory was predicted based on profile of preceding ascent (in MOL soundings are performed with 6-h intervals). When predicted maximal distance didn't exceed 25 km upper-air station staff was requested to attach a parachute to an ascent rig and record descent data. For a few ascents it was also requested registration of radar tracking data. Unfortunately, it was available only as printout, not in machine-readable form. Therefore, use of these data was limited only to general verification of calculated geopotential height and comparison of predicted and actual descent rates and radiosonde horizontal coordinates.

Unclear issue was dependence of time constant from ventilation. Laboratory experience tell us that lower than 5 m/s ventilation really deteriorate sensor performance but it's unclear is essentially higher ventilation improves sensor's response. Even with usage of parachute descent rate was about 15 m/s at 14 km and 7-8 m/s near surface with in even higher values in flights with FN-sonde participation.

Qualitative estimates of time constant (under assumption of their independence from the ventilation) could be obtained from observing vertical displacement of profiles from ascent and descent of radiosonde given the horizontal displacement and time variations are not so big. There were processed 13 such flights. Typical example is shown on the figure 2. Analysis of vertical shift, based of Equation (11), has shown that reasonable analysis could be done only at temperatures below  $-45^{\circ}\text{C}$ . At lower levels both time constant is too small and space and temporal variability are too large to make any estimates. But below  $-45\dots-50^{\circ}\text{C}$  graphical estimation reveals for the time constant more-less reasonable agreement with model of Equation (9) that is rather satisfactory for all shortcoming of this method.

Rough evaluation of ascent-descent flights was encouraging enough to open the way for the following development of lag compensation procedure. But after the first satisfaction with compatible results intention appeared to receive more quantitative results as accuracy of such graphical estimates is quite low to get quantitative estimates for the parameters of Equation (9). Taking into account the relatively large time constant at low temperatures it is required quite a long matching fragment of ascent and descent with constant gradient. And, temperature in such layers should not undergo noticeable variations as they strongly affect time constant. So, it was decided to undertake "inverse approach" – use these data later in more productive way for verification of developed lag compensation procedure by checking if corrected ascent and descent will match.

### 3.3. Empirical estimation

Unless more reliable experimental information on  $\lambda$  approximation is available the values  $\lambda_0=1$  and  $\lambda_t=-0.06916966$  (close to information of /7/) were estimated subjectively from the analysis of results of described below correction scheme (section 5) using following considerations:

- Corrected humidity profiles made during ascent and descent in the same flights should match each other
- Underestimation of time constant is safer than overestimation because using too high value leads to implausible spurious variation in corrected data
- Corrected RS80-A humidity profiles should be close to FN-sonde.

Parameters of RS80-A time constant approximation may require circumstantiation for the temperatures below  $-65^{\circ}\text{C}$ .

## 4. Obstacles to lag correction

Having deal with mathematical abstractions it looks natural frontal solution of problem – direct use of Equation (1) to obtain immediately lag correction. However, in real world when we have a deal with discrete signal of finite accuracy and resolution accurate numeric differentiation is practically impossible. Differentiation operator is known to amplify errors of input signal. And the problem is that the more significant lag errors the more sensitive lag correction to errors in derivative calculation as their amplification is proportional to time constant.

Alternative inverse solution of Equation (3) in fact suffers from the same problems because of presence measurements, quantization and sampling errors in measured humidity. Both definition of problem are ill-posed ones. As measuring system inevitably loses information there are a priori no means to separate contribution of measurement errors and smaller scale humidity variation.

As the first guess to problem's solution it was decided to concentrate on head-on approach, i.e. use of numeric differentiation and Equation (1).

### 4.1. Particular problems of A-HUMICAP humidity lag compensation

Physical definition of relative humidity and requirements of presentation in upper-air messages impose domain constraints onto range of allowable values  $1^2$ -100.

One sort of uncertainty is that all known experiments on determination of time constant dealt with humidity variations under constant pressure and temperature and more or less stable ventilation while during ascent we have combined influence of variation of these factors in time to sensor output, inevitably resulting in hysteresis-like memory effects. That is, in terms of theory of system the problem is not stationary. At least, according to information of /6/ thermal time constant of system humidity sensor – sensor boom is about 15 seconds. Transition process is a combination of establishing water vapor and temperature equilibrium.

Conventional output of Vaisala ground station provides data with 10 s resolution, i.e. Nyquist frequency is 0.05 Hz, or in terms of period 20 s. Therefore, at negative temperatures time constant is of order or larger than the Nyquist period.

Resolution of output humidity readings in 1%RH is quite insufficient in comparison with dynamic range of 1-100 %RH. This is a pity bearing in mind potential internal capabilities of radiosonde transducer and receiving system resolution of order 0.05%. That's, due to just rounding error we can have fictitious gradient 0.1%RH/sec (or, the same, error in determination of

---

<sup>2</sup> Depending from minimal allowable resolution in humidity presentation



gradient) that is directly proportional by factor of time constant to superimposed error in lag correction.

#### 4.2. Temperature correction versus lag compensation. Order of corrections

As lag compensation was developed for inclusion in RS80-A Humidity correction procedure, implemented in MOL, it is important to determine an order of application of different corrections. Mathematically, both time-lag correction and temperature dependant, or static, one are linear transformations. Therefore the final results in ideal are independent from the order of their application. This assumption was checked by applying of both corrections in different order. Results from both way of applying correction have shown good consistency with each other. However, as mentioned earlier, resulting values from both stages have to be rounded to 1%RH. So, to avoid possible bad influence of accumulation of rounding error onto calculation of derivatives, lag correction should be performed first.

### 5. Correction procedure

Mathematical sense of correction procedure is quite unpretentious and comprises numeric inversion of Equation (1) using temperature profile for estimation of time constant according (9). But to avoid severe errors in calculation of derivative, coming from finite sampling 10-s rate and 1%RH resolution, correction scheme consists in several subsequent numeric transformations of input data (only for levels with  $\lambda$  greater of 5 s that is half of 10-s sampling rate):

- Removing round-off humidity error using 5-points local polynomials least-square-fit approximation (following to idea of Savitzky-Golay smoothing filters /1/ but in application to non-evenly<sup>3</sup> spaced data). Approximation is adaptive, i.e. initial order of approximation polynomials is 3 and it increases up to 5 unless approximation error is greater of 1%RH. However, if its absolute value is greater of 0.8%RH original value is shifted only by 0.5%RH towards approximated one.
- Filtering implausible and sub-scale humidity variations (including coming from the previous stage) by means of time-constant dependent smoothing using **Gauss kernel smoothing**

$$Y_i = \sum_{j=1}^N X_j \cdot K\left(\frac{\tau_i - \tau_j}{B}\right) / \sum_{j=1}^N K\left(\frac{\tau_i - \tau_j}{B}\right) \quad (12)$$

where kernel function is

$$K(x) = \frac{1}{\sqrt{2 \cdot \pi} \cdot (0.37)} \cdot \exp\left(-\frac{x^2}{2 \cdot 0.37^2}\right) \quad (13)$$

---

<sup>3</sup> That is missing levels are allowable.

and variable time-constant dependent bandwidth is

$$B_i = B^0 + B^1 \cdot \lambda(t_i) + B^2 \cdot \lambda^2(t_i) \quad (14)$$

where

$$B^0 = 10, B^1 = 0.5, B^2 = 0.0015$$

$X_i$  – original RH at  $i$ -th level

$Y_i$  – smoothed RH at  $i$ -th level

$t_i$  – temperature at  $i$ -th level

$\tau_i$  – time of  $i$ -th level.

- Differentiation of filtered data using coefficients of 5-points 3<sup>rd</sup> order local approximating polynomials.

- Calculation of lag correction as  $\Delta U_i = \lambda_{t_i} \cdot \frac{dU_i}{d\tau}$ .

- Calculation of corrected value at levels, where time constant is larger than 5 seconds, as

$$U_i^{cor} = 0.6 \cdot U_i^{LPA} + 0.4 \cdot U_i^{GKS} + \Delta U_i \quad (15)$$

where

$U_i^{LPA}$ ,  $U_i^{GKS}$  – values at particular level from steps 1 and 2.

- Due to limitations of existing DWD data processing scheme<sup>4</sup> results are rounded to 1%RH.

Parameters of correction procedure (including parameterization of (9)) were adjusted by comparison of corrected RS80-profiles with FN-sonde having sensors with faster response. Since June of 1999 in MOL are performed regular weekly ascents of FN-sonde with time constant at least 2.5 times faster of RS80-A /7/. The basis of investigation was the use of program SPLTau (see section 7). RS80-A–FN ascents were both *simultaneous* and *parallel* (i.e. with sondes attached to the *same* and the *different* balloons). In latter case comparison was done against height.

For verification it was used comparison of ascent and descent corrected profiles. After compensation prominent features of humidity profile of ascent should shift toward the surface while ones of descent should shift towards the upper levels. Results were quite encouraging. In most ascents reconstructed profiles matched each other and only in one (06/05/2002-12UTC) the difference between corrected ascent and descent was larger (and of opposite sign) than between uncorrected data, and ascent and descent were more likely took place in different atmospheric conditions.

It's fair to say that suggested procedure is highly sensitive to case of sensor's icing and at upper levels may bring to useless results without automatic /8/ or manual icing recognition.

---

<sup>4</sup> In the program SplTau (section 7) this step is optional.

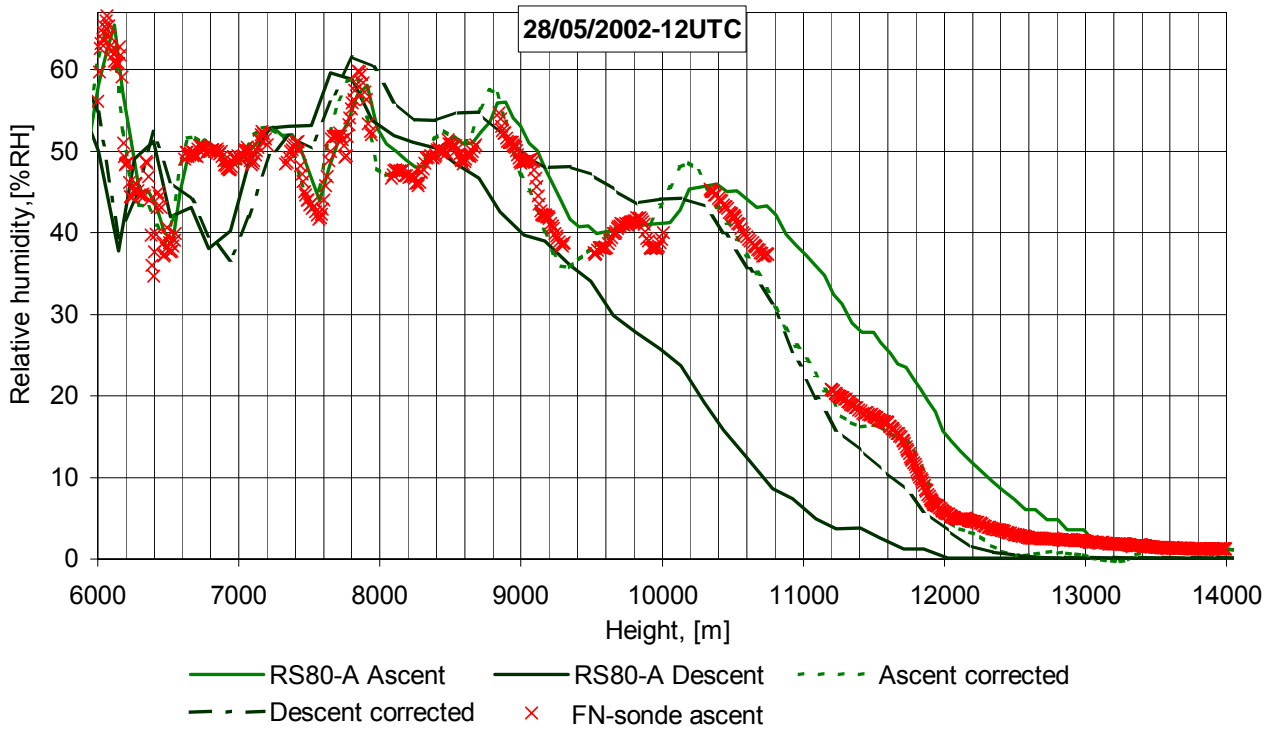


Figure 2: An example of ascent and descent humidity correction.

## 6. Statistical evaluation

For evaluation of overall impact made by proposed lag compensation algorithm, a new data set, called hereinafter RS80-A<sub>LC</sub>, was prepared for the period between June 1999 and November 2001 from RS80-A data (with temperature-dependent and ground-check corrections applied) by application of the lag correction procedure.

Statistics of *parallel* differences (for details see /8/) between RS80-A<sub>LC</sub> and RS80-A data, i.e. one reflecting lag correction, is presented on Figure 3. It is apparent presence of noticeable systematic components in differences between data sets at levels between 300 and 100 hPa, i.e. somewhere in between 9 and 16 km. These deviations look as climatological ones as they result from sensors' response to transition from moist in average tropospheric conditions to dry stratospheric ones accompanied by drastic increase of time constant due to mean temperature decrease towards tropopause. And magnitude of correction is compatible with root mean square deviation that tells about high variability of lag errors.

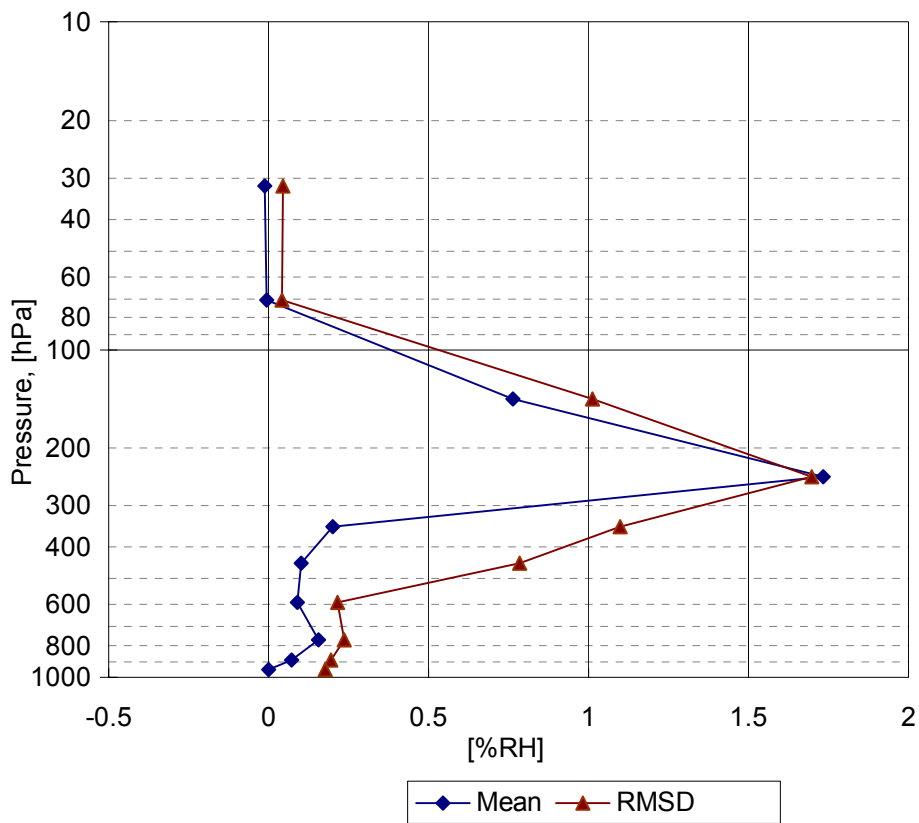
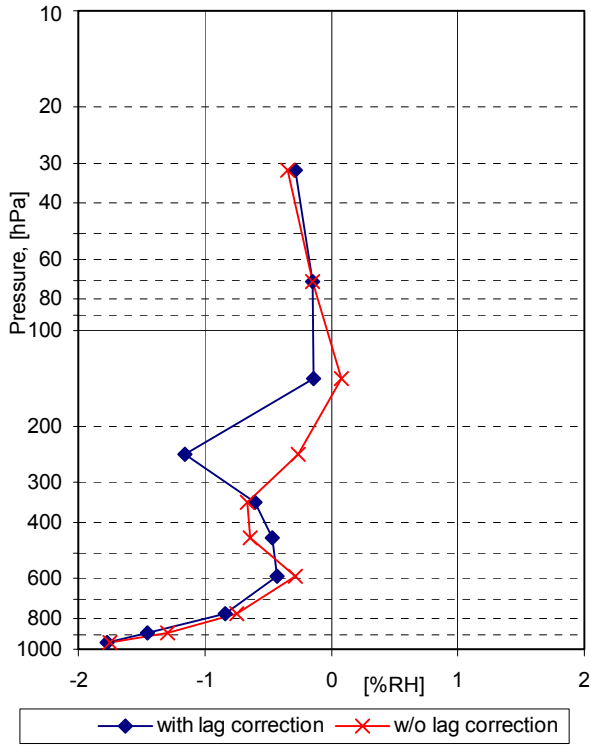
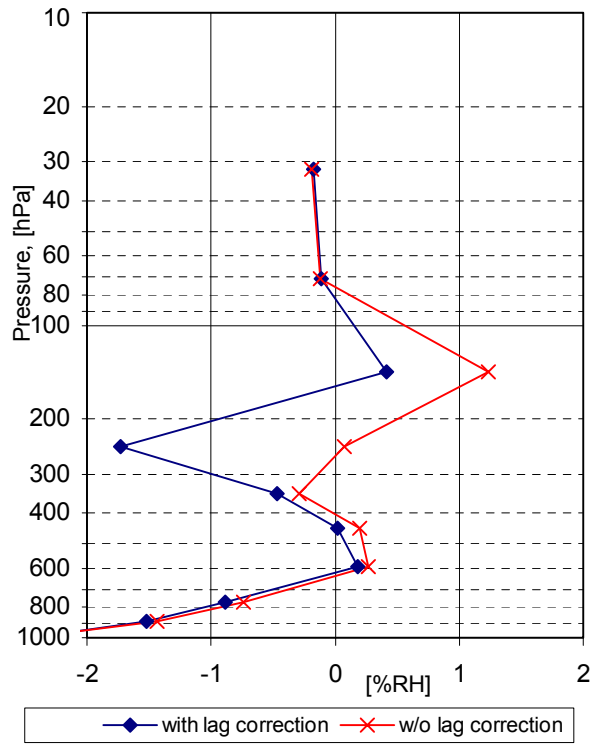


Figure 3: Statistics of “parallel” differences between original and corrected RS80-A humidity.

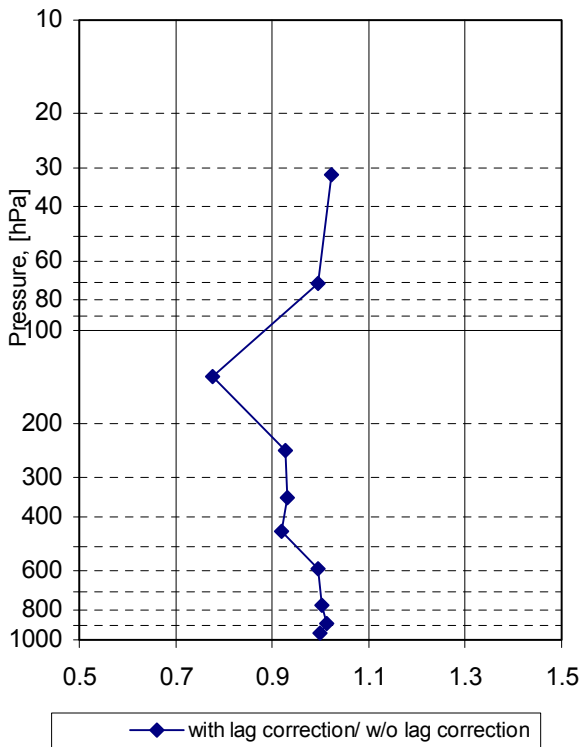
As well, for the same period it was calculated statistics of *parallel* differences between RS80-A<sub>LC</sub> and FN-sonde humidity. Results, in comparison with ones for the RS80-A data set, are presented on Figure 4 a) - d).



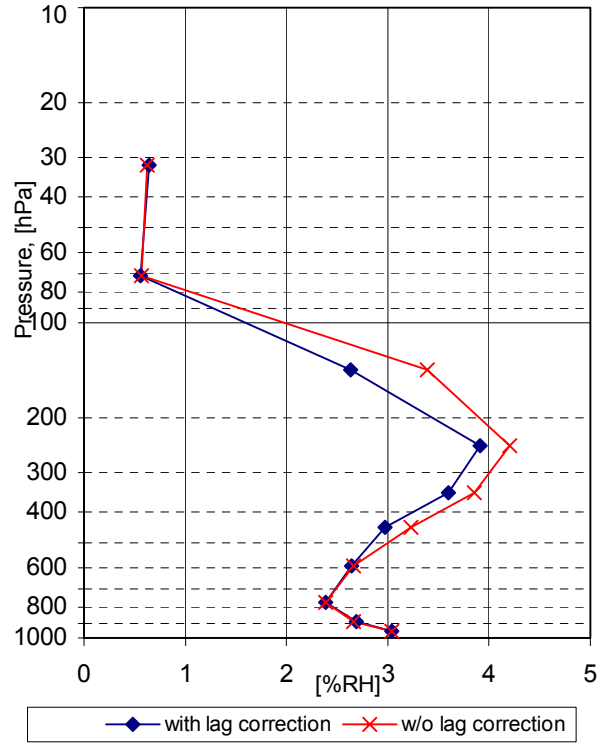
a)



b)



c)



d)

Figure 4: Statistics of RS80-A<sub>LC</sub> (with lag correction) and RS80-A (without lag correction) minus FN humidity *parallel* differences:  
a) mean differences; b) median of differences; c) standard, or root mean square, deviation;  
d) ratio of standard deviations of RS80-A<sub>LC</sub> - FN to RS80-A - FN differences.

It looks that introduction of lag correction removes positive bias at 200-100 hPa, that is just in average above tropopause where RS80-A apparently overestimates humidity and temperature-dependent correction is not so essential as humidity values are comparatively low. At lower layer, 300-200 hPa introduction of lag compensation results in negative bias as it was expected from statistics of Figure 3. It's likely, that MOL temperature dependent RS80-A correction component /8/ already contains climatological component of lag error compensation somewhere in temperature region -40...-55 °C. Therefore, in joint application of both correction procedure temperature dependent correction may require some adjustment in that temperature region. The source of this correction could be comparison RS80-A humidity data with and without lag correction in dependence from temperature. The reduction in variability of differences between corrected RS80-A and RS90FN data, characterized by standard deviation, is not so noticeable but apparent.

## 7. Software

For the application of lag correction there were developed two programs: TRAGKORR - DOS command-line utility for use in batch files within framework of routine DWD RS80-A data processing technology and SPLTau – standalone Windows menu-driven program for carrying out and presentation in time and height domain the results of lag compensation. SPLTau was developed as a versatile tool for the comprehensive investigation of influence of different variation in lag compensation algorithm on results of correction, their sensitivity to approximation of time constant from the temperature and as well for their validation by comparison with simultaneous or parallel RS90FN radiosonde. Last version of SPLTau includes now also a possibility to apply MOL ground-check and temperature dependant correction /8/ as well as correction according to /4/.

SPLTau version, able to handle RS80-A fine structure and edited data ASCII-files, produced by standard Vaisala sounding equipment family, is available from the authors for the public use.

## 8. Conclusions

It was developed an empiric algorithm for correction of lag in RS80-A humidity measurements as a part of overall humidity correction procedure /8/ including as well temperature-dependent and ground-check and recognition of icing. Applicability and parameters of algorithm were verified using RS80-A research flight with ascent followed by descent and by comparison with FN-sonde data. It was developed software for routine and research mode of application lag compensation to RS80-A data in MOL databank format and (research version) in standard Vaisala text data files.

Since January 2003 described lag correction procedure was in operational use at Meteorological Observatory Lindenberg, until its transition to new Vaisala RS92 radiosonde in July 2004.

## 9. References

1. Savitzky A., M. Golay. 1964, Analytical Chemistry, vol. 36, pp. 1627–1639.
2. Salasmaa E., P. Kostamo, 1975: New thin film humidity sensor. Preprints, Third Symp. on Meteorological Observations and Instrumentation, Washington, DC, Amer. Meteor. Soc., 33–38.

3. Balagurov A., A. Kats, N. Krestyanikova, 1998: Implementation and Results of the WMO radiosonde humidity sensors intercomparison (Phase I laboratory test). Papers presented at the WMO Technical Conference on Meteorological and Environmental Instruments and Methods of Observation (TECO-98). Casablanca, Morocco, 13-15 May 1998, WMO. INSTRUMENTS AND OBSERVING METHODS. REPORT No.70. WMO/TD - No.877.
4. Miloshevich L., H. Vömel, A. Paukkunen, A. Heymsfield, S. Oltmans, 2001: Characterization and Correction of Relative Humidity Measurements from Vaisala RS80-A Radiosondes at Cold Temperatures. *Journal of Atmospheric and Oceanic Technology*: Vol. 18, No. 2, pp. 135–156.
5. Nagel D., U. Leiterer, H. Dier, A. Kats, J. Reichardt, A. Behrendt; 2001: High Accuracy Humidity Measurements Using the Standardized Frequency Method with a Research Upper-Air Sounding System. –In: *Meteorol. Z.* 10, 5, 395-405.
6. Wang J., H. Cole, D. Carlson, E. Miller, K. Beierle, A. Paukkunen , T. Laine. 2002. Corrections of Humidity Measurement Errors from the Vaisala RS80 Radiosonde - Application to TOGA\_COARE Data. *Journal of Atmospheric and Oceanic Technology*. : Vol. 19, No. 7.
7. Antikainen V., A. Paukkunen, H. Jauhiainen; 2002: Measurement Accuracy and Repeatability of Vaisala RS90 Radiosonde. -In: *Vaisala News*, 159, pp. 11-13.
8. Leiterer, U., H. Dier, A. Kats, T. Naebert, D. Nagel, D. Althausen, K. Franke and F. Wagner; 2004: A Correction Method for RS80-A Humicap Profiles and their Validation by Lidar Backscattering Profiles in Tropical Cirrus Clouds. *Journal of Atmospheric and Oceanic Technology (JTECH)*, Vol. 22, No. 1, 18-29.

# THE IMPACT OF NEW RF95 RADIOSONDE INTRODUCTION ON UPPER-AIR DATA QUALITY IN THE NORTH-WEST REGION OF RUSSIA

A. Kats, A. Balagourov, V. Grinchenko

FGUP KOMET, Roshydromet  
3, build.6, Pervomaiskaya Street, Dolgoprudny, 141700, Russian Federation  
Tel.: +(7 095) 408 6104, Fax: +(7 095) 408 6865  
E-mail: komet.kats@mtu-net.ru

## ABSTRACT

The overall performance of geopotential measurements by Russian upper-air systems is determined by both performance of radar height measurements and performance of temperature (to much less extent - humidity) sensor of used radiosondes. Therefore, efforts aimed to improve one of the mentioned components must take into account limitations imposed on combined result by another one. The positive impact of introduction the RF95 - Russian radiosonde with Vaisala RS80 temperature and humidity sensors - onto geopotential data quality is estimated theoretically and demonstrated basing on ECMWF upper-air data quality monitoring. It is shown the apparent improvement of the upper-air geopotential data quality in the North-West Region of Russia, where RF95 was introduced since 1998. A value of using still more accurate radiosondes with existing Russian ground radars is discussed.

---

Recently a new RF95 radiosonde was introduced on some stations of the Russian upper-air network carrying out temperature and humidity sensors (without pressure capsule – see below) of Vaisala RS80-A radiosonde (more details in /5/). According to manufacturers specifications and results of WMO Radiosonde Intercomparison /1/ performance of RF95 sensors exceeds one of MRZ-3 – the radiosonde used on the vast majority of the Russian upper-air stations. However, a question all the time arises has it a practical impact onto performance of operational geopotential observations.

What benefit could be expected from introduction of more accurate sensors in the sense of performance of geopotential on standard pressure levels? Let's try to make at least a rough estimates. In Russian AVK system pressure is derived from virtual temperature  $T$  and humidity  $U$ , measured by a radiosonde, and height  $H$ , calculated from determined by a radar slant range  $D$  and elevation  $\varepsilon$  (details could be found in /1/).

Using linearization of equations used we derive following relationship between error of geopotential  $H_P$  at given pressure level  $P$  from errors of measured parameters:

$$\delta H_P = T_P \left( \int_{H_{R_0}}^{H_P} \frac{\delta T dH}{T^2} + \int_{H_{R_0}}^{H_P} \frac{\gamma d \delta \varepsilon}{T^2} dH + \int_{H_{R_0}}^{H_P} \frac{\gamma \sin \varepsilon \delta D}{T^2} dH \right)$$

where  $d$  is horizontal distance and  $\gamma$  is temperature lapse rate.

Each error source (especially, tracking errors) is actually a stochastic process and accurate evaluation of integrals in general case is very complex task, first of all due to absence of necessary information. Nevertheless, taking into account that short-period constituents are fairly well filtered



during an integration a task could be reduced to an evaluation of effect of reproducibility of each parameter upon reproducibility of geopotential in assumption of constant values of each error throughout the whole flight and neglecting the effects such as: influence of humidity upon virtual temperature<sup>1</sup>, non-linear relationship between geometric and geopotential height, uncertainty of the radiation corrections and corrections for earth curvature and radio-wave refraction. From this we receive for the quantity under consideration the following expression:

$$\sigma[\Delta_p H] = T_p \times \sqrt{\left( \int_{H_{P_0}}^{H_P} \frac{dH}{T^2} \right)^2 \sigma^2[\Delta_s T] + \left( \int_{H_{P_0}}^{H_P} \frac{\gamma d}{T^2} dH \right)^2 \sigma^2[\Delta_s \varepsilon] + \left( \int_{H_{P_0}}^{H_P} \frac{\gamma \sin \varepsilon}{T^2} dH \right)^2 \sigma^2[\Delta_s D]}$$

As one can see a great uncertainty still remains depending from actual profiles of temperature and wind. Therefore we consider a model situation with temperature stratification according to the standard atmosphere model Cospar International Reference Atmosphere (CIRA), unvarying elevation angle (i.e. constant radial wind  $f_R$ ) and permanent ascent velocity of 5.5 m/s. For characterizing measurement errors there were used the values, claimed by manufacturers for so called "sonde error" /2/. Reproducibility of temperature measurements: MRZ-3 – 0.4 °C, RS80 (RF95) – 0.2 °C below and 0.3 °C above 100 hPa, RS90/RS92 - 0.2 °C /6/, reproducibility of AVK slant range and elevation – 30 m and 0.12° (characteristics of MARL are expected to be of the same order).

Although parameterizations of CIRA allows analytical derivation of estimates in used formulation of the task it was used numerical evaluation with integration step of 1 km. Apart from resulting estimate of  $\sigma[\Delta_p H]$  there were calculated relative contribution of each component into resulting variance as  $R_x = \sigma^2[\Delta_p H(X)] / \sigma^2[\Delta_p H]$

Results of evaluation for the several fixed elevation angles are summarized in the Table 1 below for levels 16 and 31 km, nearly corresponding to levels 100 and 10 hPa (note, that below 100 hPa RS90 is considered to be equivalent to RS80).

First of all, at all considered situations at upper levels, with assumptions admitted, at the present state of temperature sensors performance tracking errors have negligible influence on  $H_P$  as in CIRA the temperature gradient is negative and therefore contribution of height error at upper levels has opposite sign to that at lower ones. Therefore, the gain in  $H_P$  performance is directly proportional to decrease in temperature error. So, RF95 is 60% (the contribution of parts below and above 100 hPa is about the same) better and RS90 is 100% better of MRZ-3. Of course, in real conditions at low angles radar tracking may seriously suffer from influence of surface. From other side, contribution of height error is proportional to temperature gradient and magnitudes of temperature gradients in stratosphere anyhow much more moderate than in troposphere. And uncertainty of radiation correction to MRZ-3 white-coated temperature sensor is larger than RS80 aluminized sensor has /2,7,8/ while RS90 temperature sensor radiation correction should have the least uncertainty.

At 100 hPa level tracking performance (within model adopted) has more significant influence, nevertheless it starts to prevail over temperature induced error of RF95 only under extremely strong winds and even under those conditions RF95 is still worth to be used as alternative to

<sup>1</sup> As contribution of humidity to virtual temperature is rather small, therefore the influence of humidity errors onto geopotential accuracy is considered to be of the second order.

MRZ-3 *ceteris paribus*. From other side, even at quite low winds (not to speak about calm when influence of distance error increases) one could not expect two-fold gain in  $H_P$  performance from the use of RF95 – the maximum possible gain is about 80%.

RS90 sensors might be worth to use in Russian system at those stations, which should provide high quality measurement at upper levels such as GUAN stations – there are twelve such stations in Russia.

Since the mid of 80-s it's already the common practice to evaluate performance of upper-air observations by comparison of observations against short-range forecast produced by the modern numeric models, valid for the time of observations. ECMWF is appointed by WMO as leading center for upper-air data quality monitoring. Produced by ECMWF OB-FG<sup>2</sup> statistics is widely recognized and for example is used by WMO Rapporteur on Radiosonde Compatibility Monitoring for overview of the quality of worldwide upper-air observations.

Usually such a statistics is produced for temperature, geopotential and wind (both for polar and Cartesian presentation). Statistics of geopotential is used more often than one for temperature, as being derived for standard pressure levels it represents an integrated indicator of radiosonde and ground station performance for temperature and height (as mentioned before – in Russian upper-air systems height is measured directly).

For the demonstration here are used diagrams of ECMWF OB-FG geopotential statistics for 1998 and 2000, kindly provided by Mr. A Garcia-Mendez (ECMWF) for the evaluation of impact of RF95-NW – project, arranged according to the Agreement between Roshydromet and Finnish Meteorological Institute (FMI), of aerological programme support during 1998-2000 on upper-air sounding stations 22113-Murmansk, 22217-Kandalaksha and 26063-St. Petersburg (Voejkovo) of the North-West Region of Russia using a new radiosonde RF95. Regular sounding with RF95 only on those stations has started since 1999.

It's necessary take into account looking at OB-FG geopotential statistics that the lower is the level under consideration the more strict are requirements to performance. As measure of magnitude it may serve WMO guidelines for selection of suspected (i.e. producing useless data) stations according to root-mean-square OB-FG deviations<sup>3</sup>: 45, 100 and 125 m for 500, 100 and 50 hPa respectively. On other edge of ruler could be placed neighboring station 2836, which shows quite typical performance for RS80-DigiCORA sounding system representing state of the art in the modern upper-air sounding /9/. For evaluation of particular station bias and standard deviation of OB-FG are equally important because they reflect average of errors and their day-to-day variability. However, for the whole network differences between biases of stations are also essential as they make inhomogeneous presentation<sup>4</sup> of atmospheric processes.

From these standpoints, one can interpret from the time series of ECMWF OB-FG geopotential statistics:

---

<sup>2</sup> As such a forecast is often used in particular as background, or first-guess, field for objective analysis of upper-air data abbreviation FG is conventionally used to denote these data. OB denotes results of observations.

<sup>3</sup> Practically could be estimated as square root from squares of bias and standard deviation

<sup>4</sup> Of course, individual scatter also reflects the extent of distortion in meteorological fields caused by observational errors

All stations under investigation showed substantial improvement especially at upper levels:

- 22113 - in 1998 the bias varied from -50 to 80 m at 50 hPa and the standard deviation reached 100 m. In 2000 the corresponding values reduced to less than 25 m at all levels.
- 22217 - in 1998 the stratospheric bias was very high, exceeding 125 m at 50 hPa, whereas it was small in the troposphere; the standard deviation remained below 50 m at all levels. In 2000 a rather noticeable positive bias still existed in the stratosphere but didn't exceed 50 m; the standard deviation also decreased from 1998 to values of less than or equal to 25 m.
- 26063 - in 1998 the bias at 00UTC varied from -25 to 40 m, while the bias at 12UTC reached even 80 m; the standard deviation was noticeable and reached almost 50 m. In 2000 the bias was less than or equal to 25 m during all months except in October, and the standard deviation was below 25 m during most months with occasional monthly extremes exceeding 25 m.

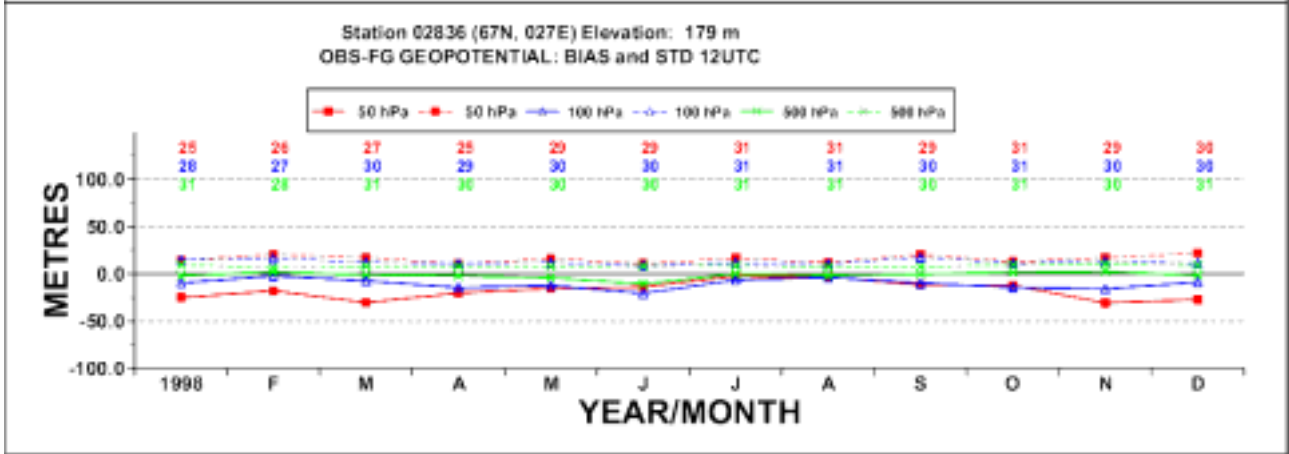
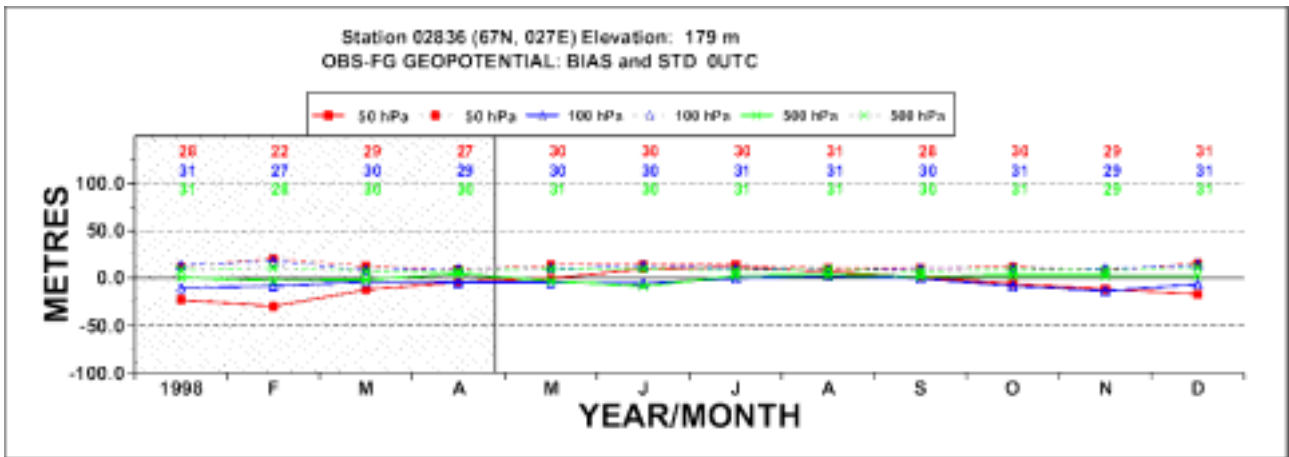
During some months in 1998 the statistics on particular levels at some stations were close to, and occasionally even exceeded, the limits for suspected stations established by WMO/CBS. In 2000 all data had acceptable quality far from such limits. As well, in some months of 1998 the absolute magnitude of systematic differences between individual stations exceeded 100 m. The examined stations were compatible in performance with the station 02836 during 2000: 22113 showed perfectly the same, while 22217 and 26063 showed a slightly inferior behavior.

#### References:

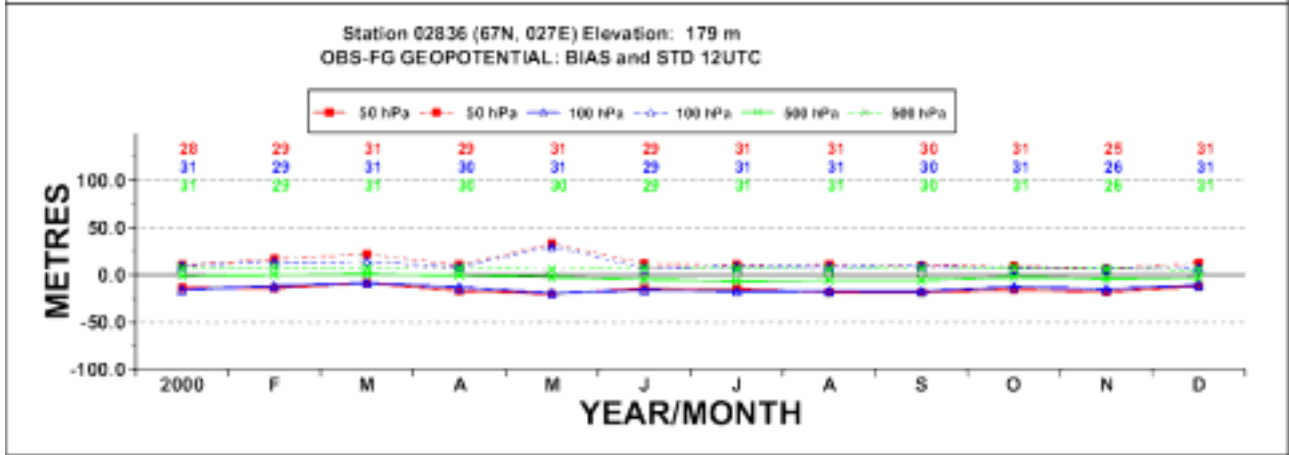
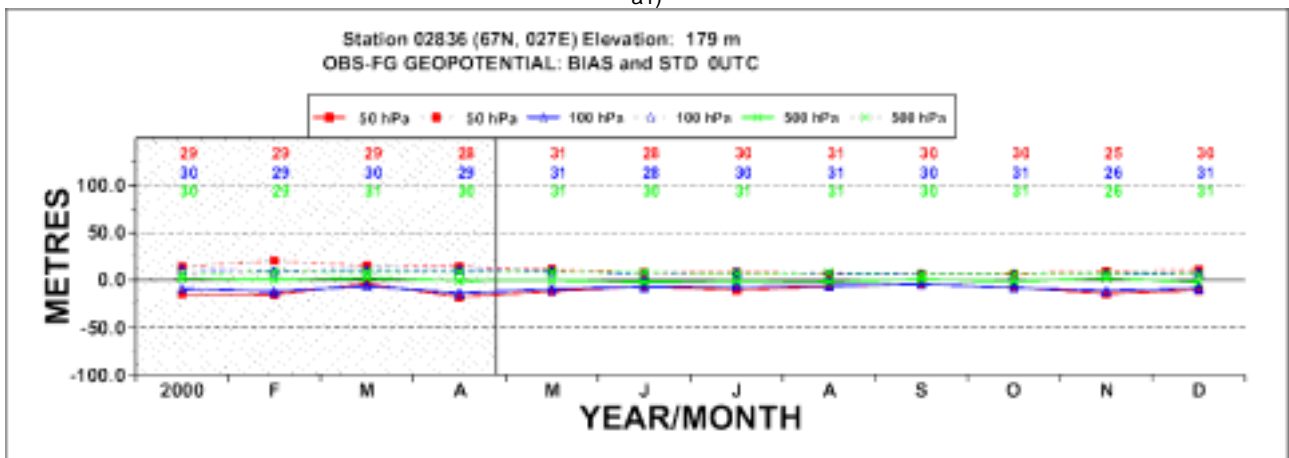
1. A. Ivanov et al, 1991. Radiosondes WMO International Radiosonde Comparison - Phase III, Dzhambul (USSR), 1989. WMO, Instruments and Obs. Methods Report No. 40.
2. WMO Guide to Meteorological Instruments and Methods of Observation, 1996: WMO-No. 8.
3. A. Balagurov, A. Kats, N. Krestyanikova. 1998. Implementation and Results of the WMO radiosonde humidity sensors intercomparison (Phase I laboratory test). TECO-98. WMO, Instruments and Obs. Methods Report. No.70.
4. F. Schmidlin. 1998. Summary of the WMO International Radiosonde relative humidity sensor comparison - September 1995 - Phase II "Field test". TECO-98. WMO, Instruments and Obs. Methods Report. No. 70.
5. A. Balagurov, V. Grinchenko, A. Kats, 2000: New Instruments for Russian Upper-air Network. Papers Presented at the WMO Technical Conference on Meteorological and Environmental Instruments and Methods of Observation (TECO-2000). Beijing, China, 23-27 October 2000. WMO, Instruments and Obs. Methods Report No. 74.
6. World meteorological instrument catalogue, 2002 Edition.
7. M.B.Fridzon et al. 1988. Radiation Corrections in Radiosonde Measurement of Temperature. Meteorologia i Gydrolgia [Soviet Meteorology and Hydrology], No. 6.
8. M.B.Fridzon. 1989. Estimation of Temperature and Humidity Radiosonde Measurements Errors on the USSR Upper-air Network. Meteorologia i Gydrolgia [Soviet Meteorology and Hydrology], No.5.
9. J. Elms, 2003: Radiosondes WMO Catalogue of Radiosondes and Upper-Air Wind Systems in use by Members in 2002; and Compatibility of Radiosonde Geopotential Measurements for the period 1998 to 2001. WMO, Instruments and Obs. Methods Report No. 80.

**Table 1.** Estimates of reproducibility of measurement of geopotential height at fixed pressure level for AVK radar with radiosondes using different temperature sensors

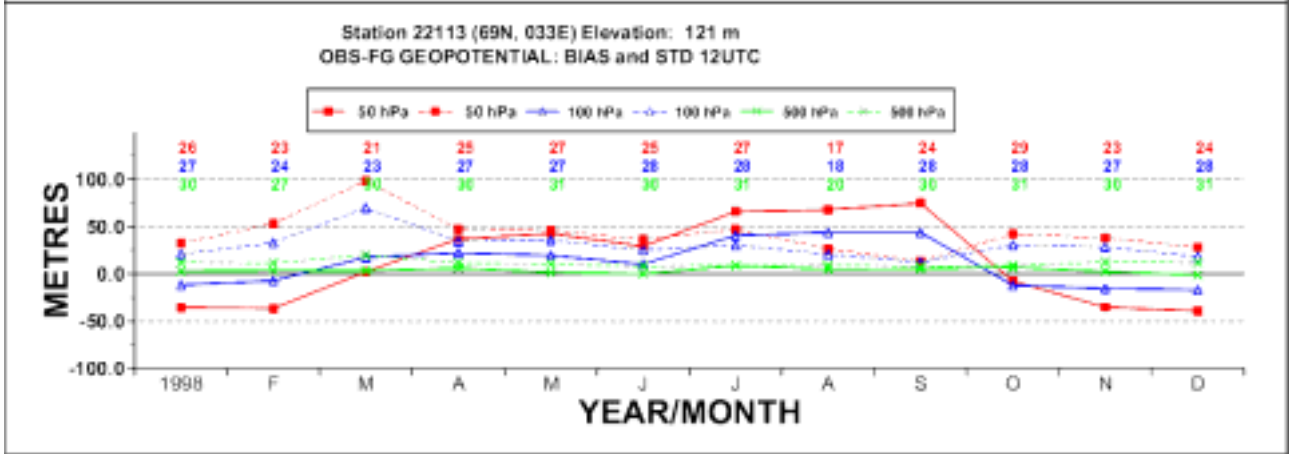
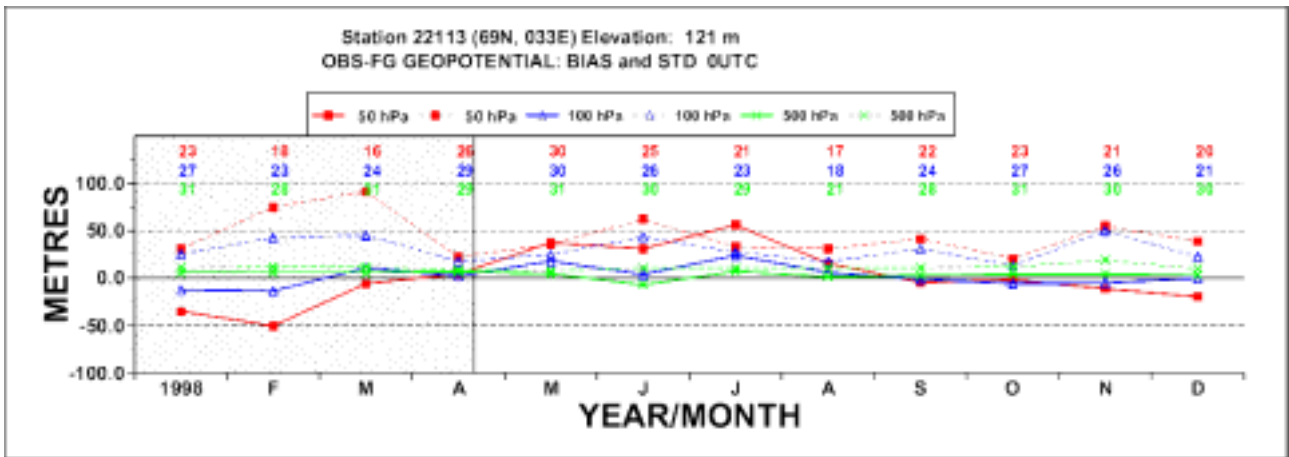
System	$\sigma[\Delta_p H]$ , m	$R_T$ , %	$R_D$ , %	$R_\varepsilon$ , %
<i>H=16 km, d=12.5 km, f<sub>R</sub>= 4.3 m/s</i>				
AVK+MRZ	25	93%	6%	1%
AVK+RF95	14	77%	20%	4%
<i>H=16 km, d=37.5 km, f<sub>R</sub>= 12.9 m/s</i>				
AVK+MRZ	26	89%	1%	10%
AVK+RF95	15	66%	4%	29%
<i>H=16 km, d=62.5 km, f<sub>R</sub>=21.5 m/s</i>				
AVK+MRZ	28	76%	0%	23%
AVK+RF95	18	44%	1%	55%
<i>H=16 km, d=100 km, f<sub>R</sub>=34.4 m/s</i>				
AVK+MRZ	33	56%	0%	44%
AVK+RF95	25	24%	0%	76%
<i>H=32 km, d=25 km, f<sub>R</sub>= 4.4 m/s</i>				
AVK+MRZ	54.1	99.0%	1.0%	0.0%
AVK+RF95	33.7	97.4%	2.5%	0.1%
AVK+"RS90"	27.4	96.1%	3.8%	0.1%
<i>H=32 km, d=75 km, f<sub>R</sub>= 13.3 m/s</i>				
AVK+MRZ	53.9	99.5%	0.2%	0.2%
AVK+RF95	33.5	98.8%	0.6%	0.6%
AVK+"RS90"	27.2	98.2%	0.9%	0.9%
<i>H=32 km, d=125 km, f<sub>R</sub>= 22.2 m/s</i>				
AVK+MRZ	54.0	99.3%	0.1%	0.6%
AVK+RF95	33.5	98.8%	0.6%	0.6%
AVK+"RS90"	27.3	97.2%	0.4%	2.4%
<i>H=32 km, d=200 km, f<sub>R</sub>= 35.5 m/s</i>				
AVK+MRZ	54.3	98.4%	0.0%	1.6%
AVK+RF95	33.5	98.8%	0.6%	0.6%
AVK+"RS90"	27.8	93.8%	0.1%	6.0%



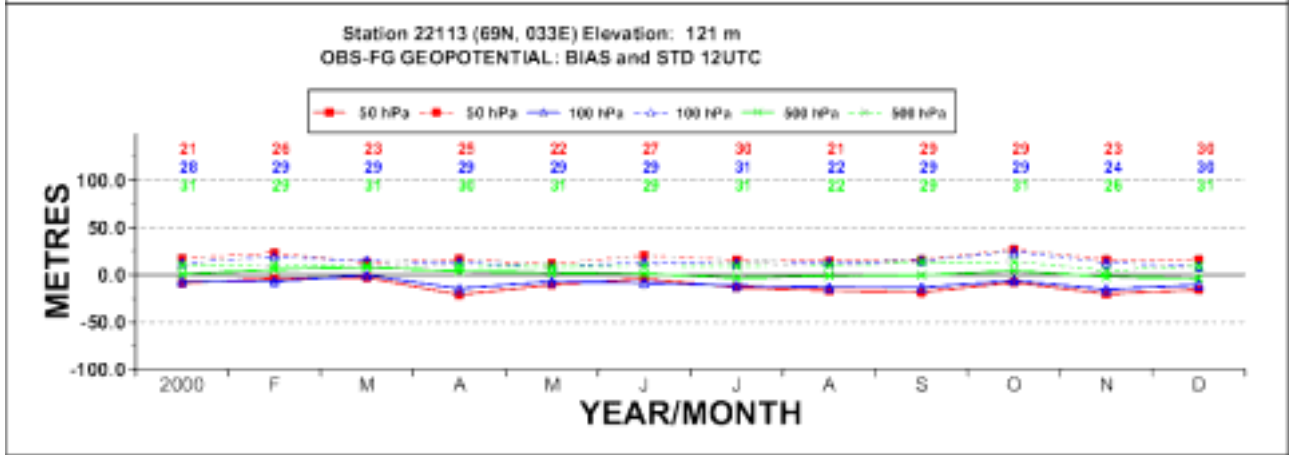
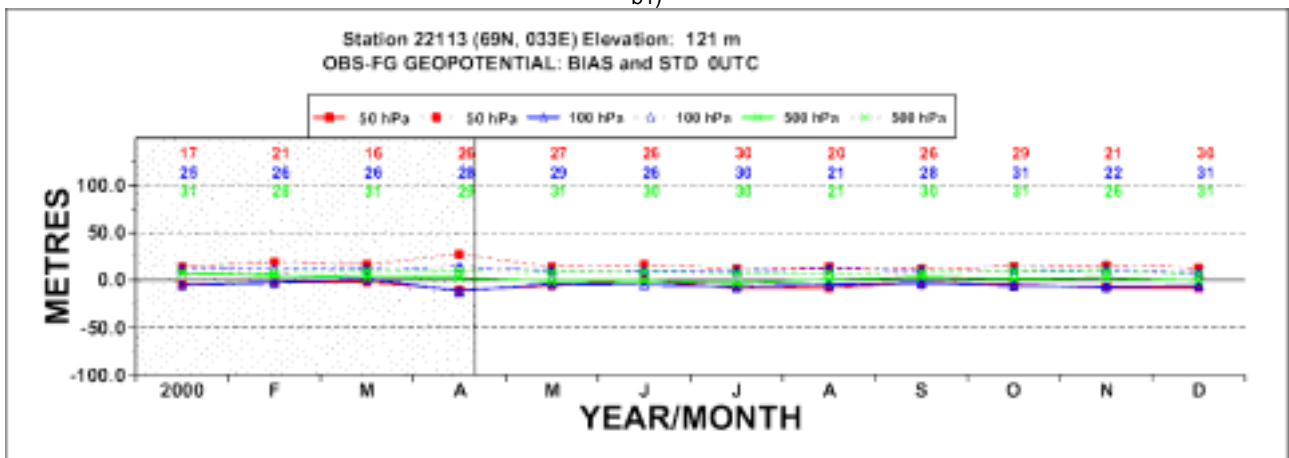
a1)



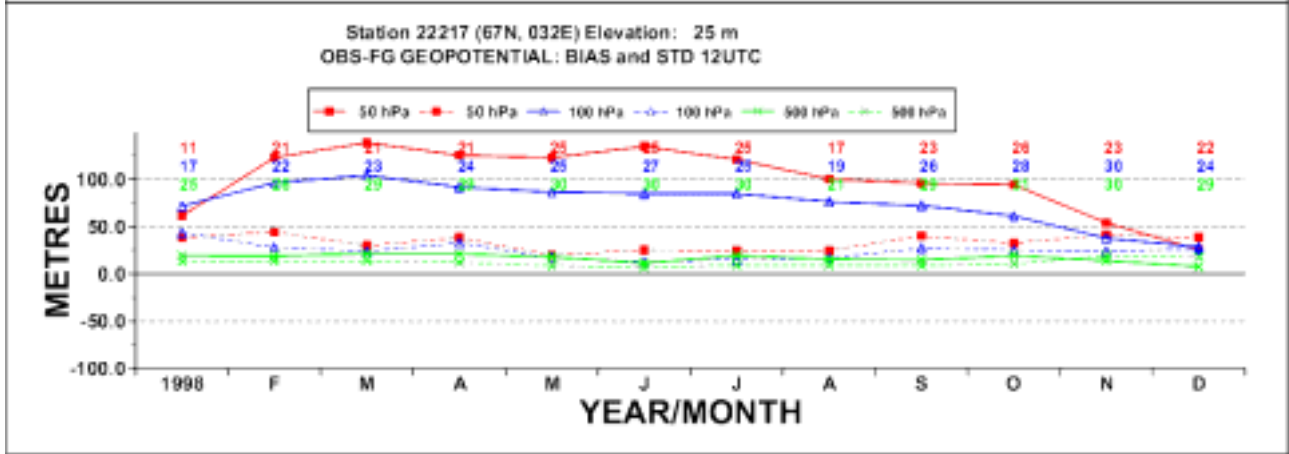
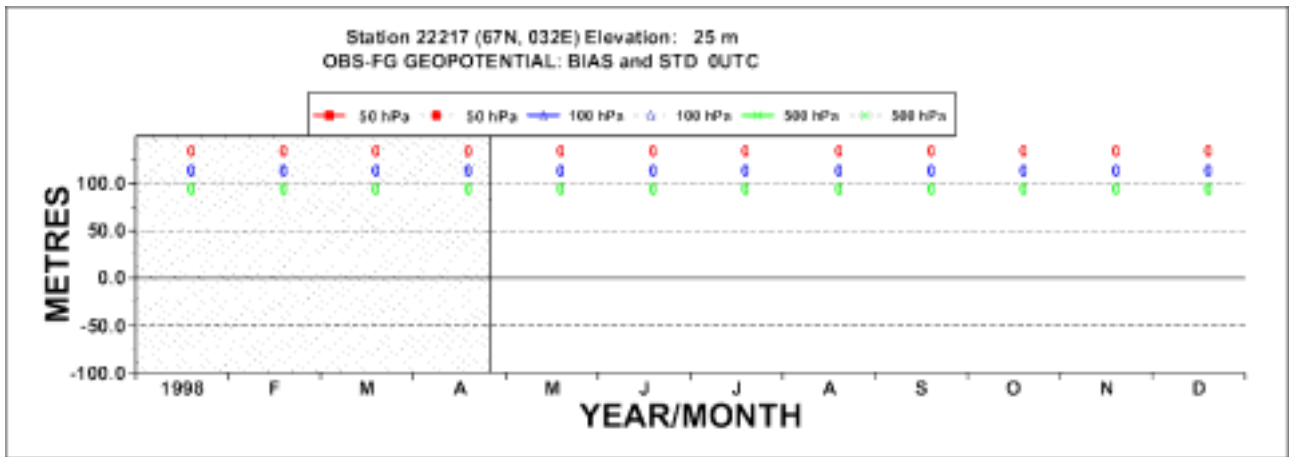
a2)



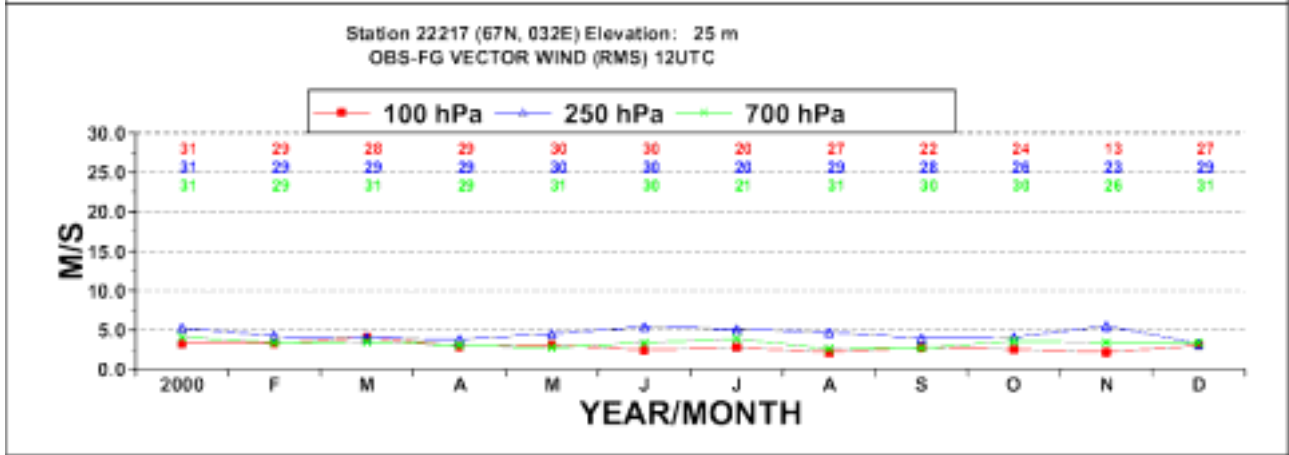
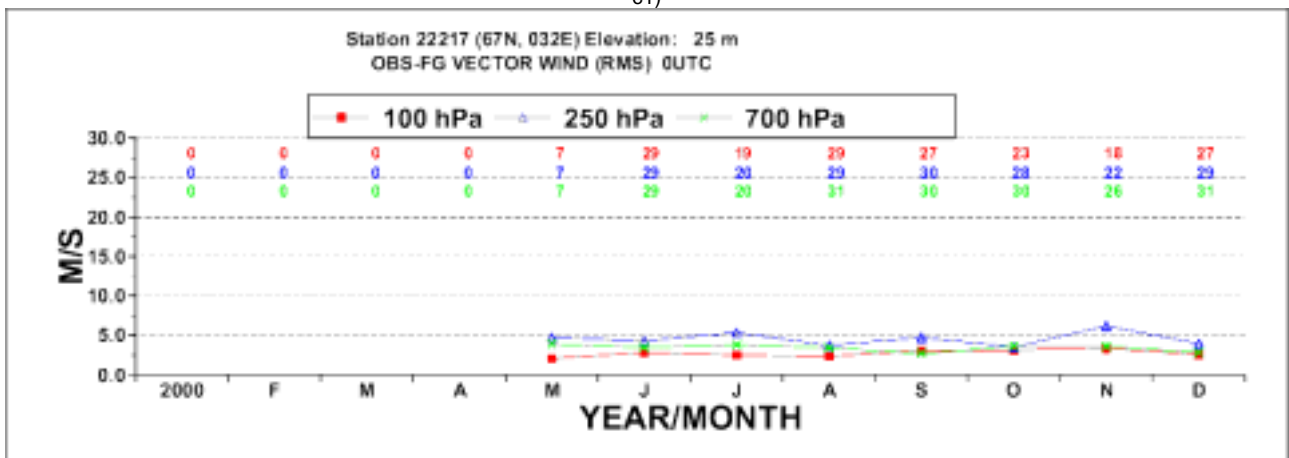
b1)



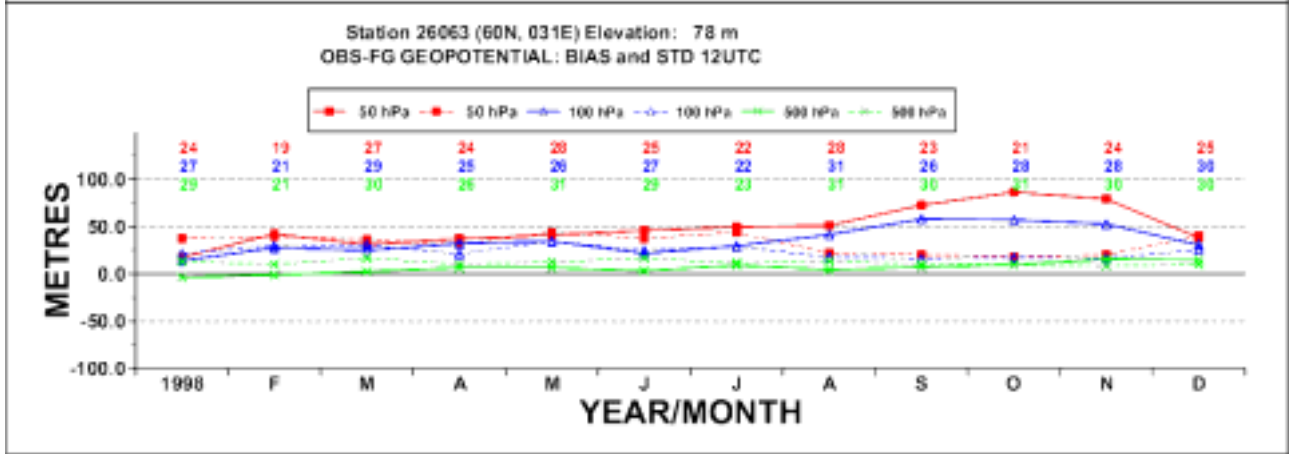
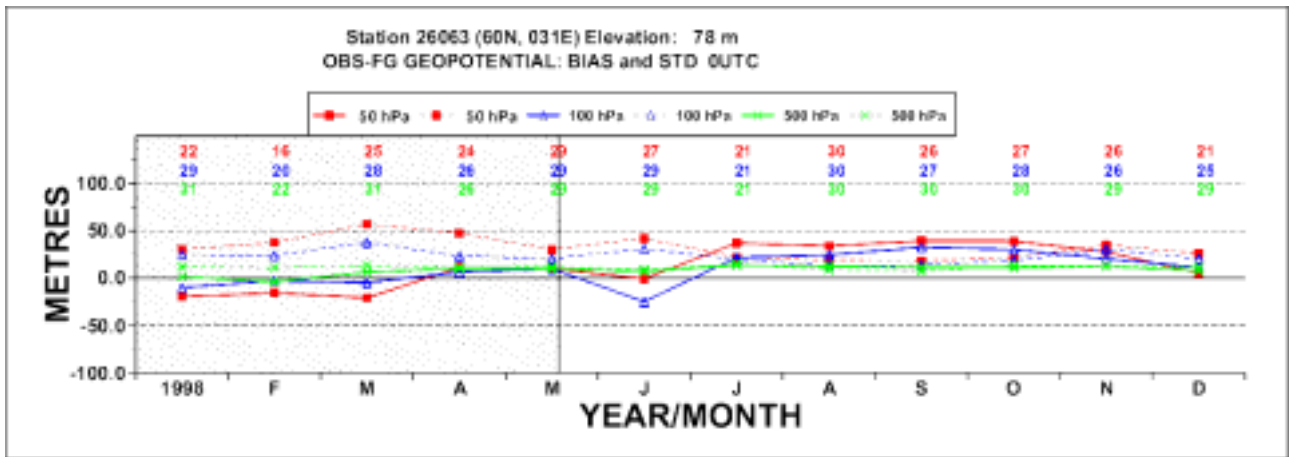
b2)



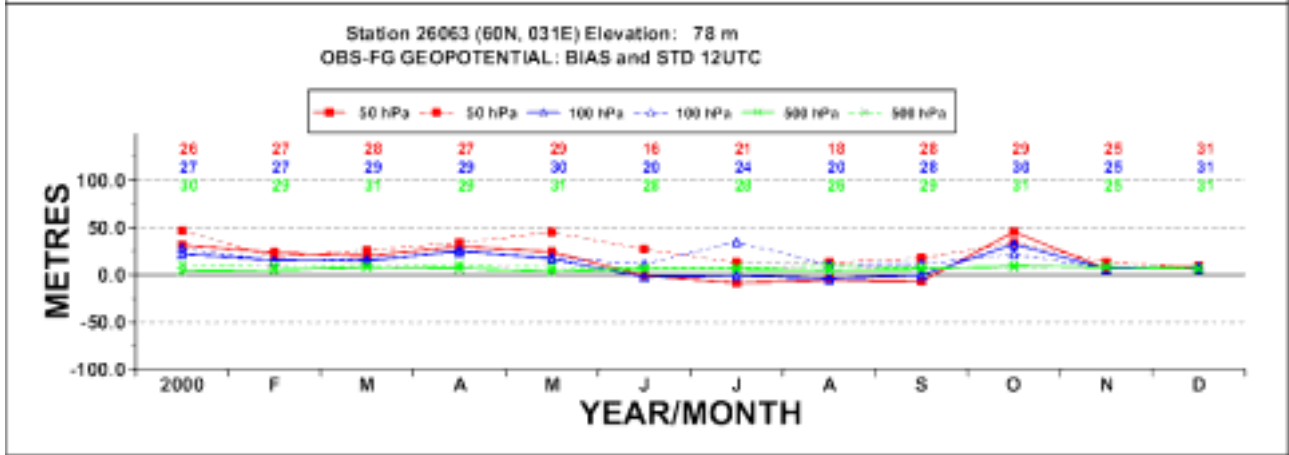
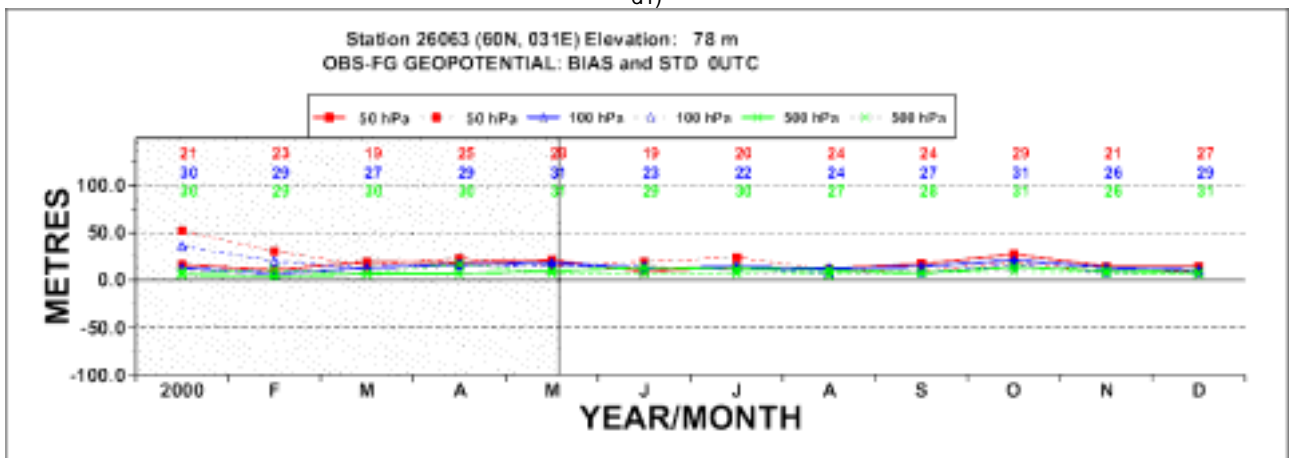
c1)



c2)



d1)



d2)

Figure 1. ECMWF geopotential statistics for stations 2836 (a), 22113 (b), 22217 (c) and 26063 (d) for 1998 (1) and 2000 (2).



# The field and laboratory intercomparison test between two different types of the sondes and the ground systems

A. Borštnik, D. Groselj, J. Knez, L. Ravnik, M. Rus  
 Environmental Agency of the Republic of Slovenia  
 Vojkova 1b, 1000 Ljubljana, Slovenia  
[ales.borstnik@gov.si](mailto:ales.borstnik@gov.si)

## Introduction

At the Environmental Agency of the Republic of Slovenia (EARS) we decided to make the intercomparison test between two sounding systems of different manufacturers and two different types of radiosondes. At EARS we had used Vaisala RS90-AL radiosondes with DigiCORA II system, but we were forced to change the ground system for the upper-air measurements and we decided to test Modem SR2K2 ground system with GPSonde M2K2. Because of the historical compatibility of the measured data, we decided to borrow Modem system first and make the intercomparison between the measured data to see what the differences are. We made the field and lab tests. First the laboratory test of each pair of sondes was made in the climatic chamber of the calibration laboratory of the EARS, and after that the field test was made with the multiple radiosounding, a balloon and the parachute.

The main goal of the intercomparison was to test the accuracy of PTU sensors in calibration laboratory and to compare PTU and wind measurements of both types of sondes in real conditions.

## Sounding equipment

In the intercomparison we used two different types of sondes with their receiver stations: VAISALA RS90-AL and MODEM M2K2 GPSonde. In the table there are the technical specifications, as they are stated by the manufacturers.

Type	Vaisala RS90-AL	Modem M2K2
Manufacturer	Vaisala Oyj, Finland	Modem, France
Wind/ Position	Loran C	GPS
<b>Temperature</b>		
Type	capacitive wire	thermistor
Range	-90 to +60°C	-90 to +50°C
Resolution	0.1 °C	0.1 °C
Response time	0.4 – 2.5 s	< 2 s
Accuracy	0.5 °C	0.5 °C
<b>Humidity</b>		
Type	thin film capacitor, heated twin-sensor design	capacitive
Range	0 to 100 % rh	0 to 100 % rh
Resolution	1 % rh	0.1 % rh
Response time	<0.5 s (at 6 m/s, 1000 hPa, +20°C)	< 2 s
Accuracy	5 % rh	5 % rh
<b>Pressure</b>		
Type	BAROCAP silicon sensor	calculated from GPS altitude
Range	3 to 1080 hPa	3 to 1050 hPa
Accuracy (at 1050 hPa)	1.5 hPa	2 hPa

VAISALA receiver station:

- **DigiCORA** II MW15 with three modules (UPP20A, MPU13P and MWV201),
- MicroCORA Radiosonde Receiver UR12 with antenna system RB 15
- Ground check (thermometer, silicagel for humidity calibration).

MODEM receiver station:

- SR2K2 receiver rack
- GPS antenna and GPS repeater system
- Omnidirectional radio 400 MHz antenna
- Built-in barometer
- Ground check (ambient temperature and humidity, with reference sensor and fan)
- Desktop PC with Modem data acquisition software

## **Data acquisition**

The data acquisition based on the hardware and software of the two tested systems. The data from both systems were stored on a PC. In laboratory tests also data from Vaisala PTU were collected. Computers clocks were synchronized to ensure the uniformity of measurements.

The frequencies of the two sondes that were measured simultaneously were kept apart to ensure the correct functioning of the two systems. The Vaisala system operated on 403 MHz and the Modem on 401 MHz radio frequency.

## **Laboratory test**

For measurements of temperature, humidity and pressure in laboratory we used the following equipment:

- Climatic chamber: Heraus HPC/S 4026
- Reference sensor in climatic chamber: Vaisala PTU 200 (**PTU**)
- Humidity generator: Thunder Scientific Corporation 2500 Humidity Generator
- Pressure chamber: Theodor Friedrich 8700.0000 BK
- Reference pressure sensor: Setra 370
- Power supplies for PTU and both type of radiosondes in laboratory test
- Personal computers (**PC**)

Due to loss of the sondes signals in both chambers, the antennas had to be extended to receive the data. Because of the duration of the laboratory measurements (several days) power supply instead of batteries was used.

### **Vaisala**

The DigiCORA unit was used for the collection of data coming from the RS90-AL sonde and transmission of gathered data to the PC through the RS232 ports. We used two outputs on DigiCORA system, one for raw and the other for filtered data. The sampling interval was one second. The start of data recording was set to manual (in operational mode is set to automatic).

The calibration of the RS90-AL sonde in ground check was not performed before laboratory tests.

## **Modem**

Changes of software settings of the system compared to operational mode were necessary during the laboratory tests. The system was in *test mode* and the option *static recording* was used to enable manual start of the recording. The data were available in raw and filtered format.

The calibration of the M2K2 sonde in ground check was not performed before laboratory tests.

### Measurements in Climatic chamber

The three sensor sets from Vaisala, Modem and PTU were kept in appropriate distance (5 cm apart) to ensure the homogeneity of the measured parameters.

Wind speed in climatic chamber was about 5m/s.

We selected 12 points with different temperature and humidity where the two sondes were tested.

-20°C, 10%	-20°C, 50%	-20°C, 80%
0°C, 10%	0°C, 50%	0°C, 95%
20°C, 10%	20°C, 50%	20°C, 98%
40°C, 10%	40°C, 50%	40°C, 98%

After the stabilization half hour interval for analysis was selected.

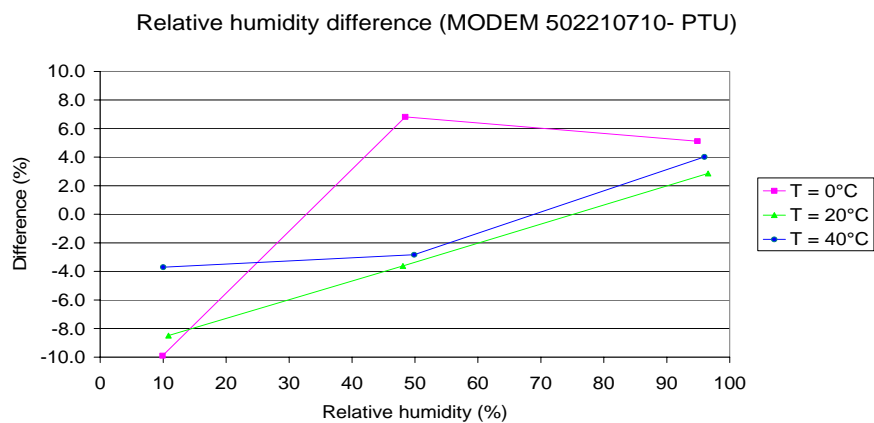
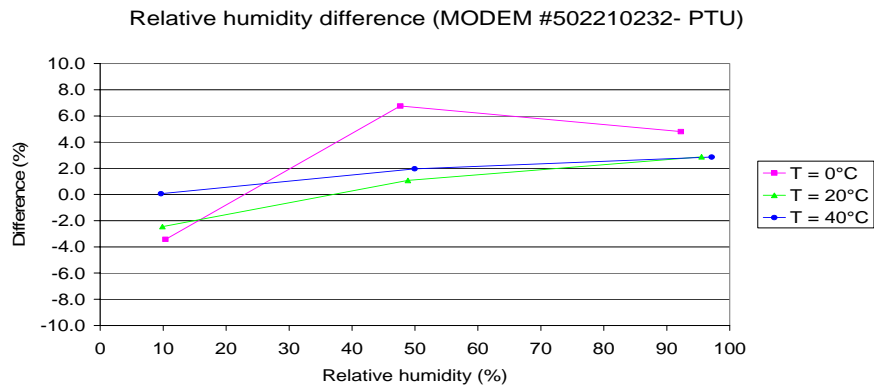
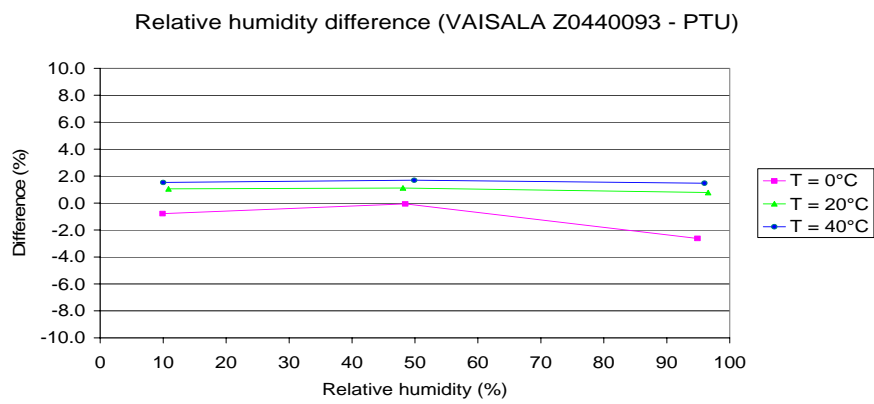
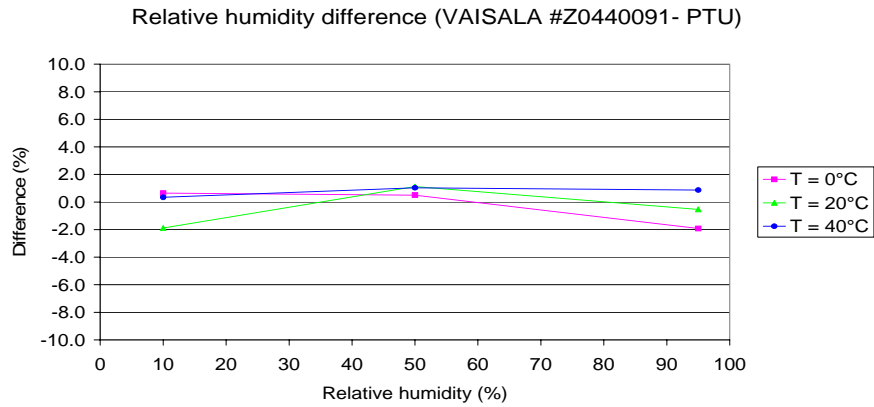
The measurements included individual disconnections of the sondes. Beside the frequency difference this procedure was necessary to avoid the possible disturbances between both sondes.

### Measurements in Pressure chamber

The chamber was used to test the RS90-AL pressure sensor. The pressure was changed in steps of 200 hPa in the range from 1100 hPa to 100 hPa. The measurements were taken during descent from 1100 hPa to 100 hPa and ascent from 100 hPa to 1100 hPa.

The data from the reference pressure sensor were collected on a PC using RS232 port.

## Results of laboratory measurements of humidity



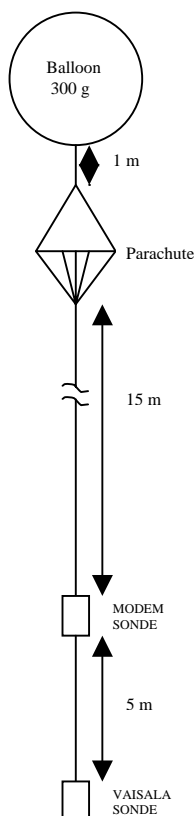
## Launching

### Flight configuration

300 g balloon was used, that carried the two sondes and a parachute.

The parachute was mounted 1 m under the balloon to ensure a safe descent during which the data could also be collected.

The sondes were attached to the parachute on a 15 m rope. The upper sonde was M2K2. The RS90-AL was attached on a rope 5 m under the M2K2.



### **Vaisala**

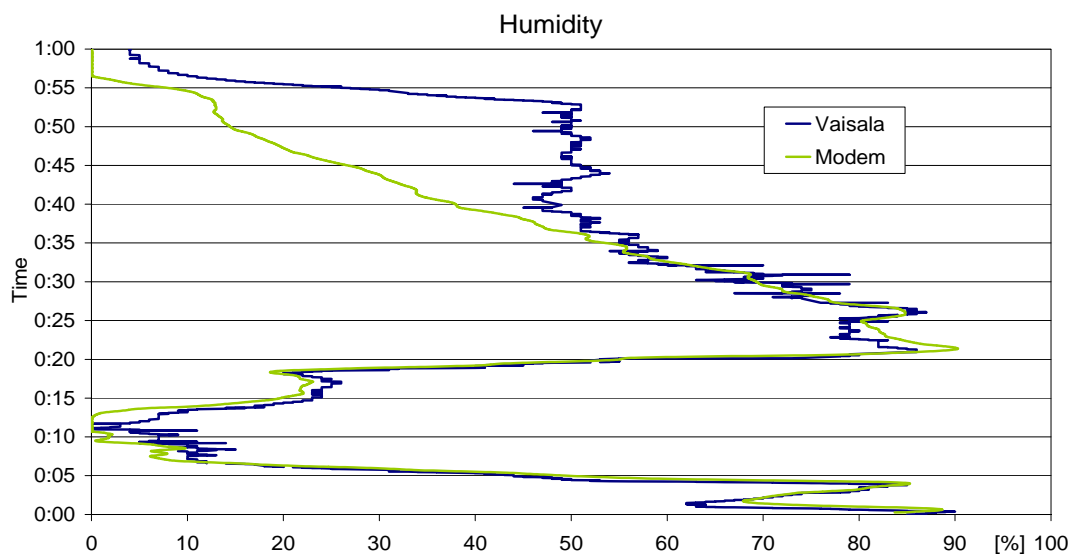
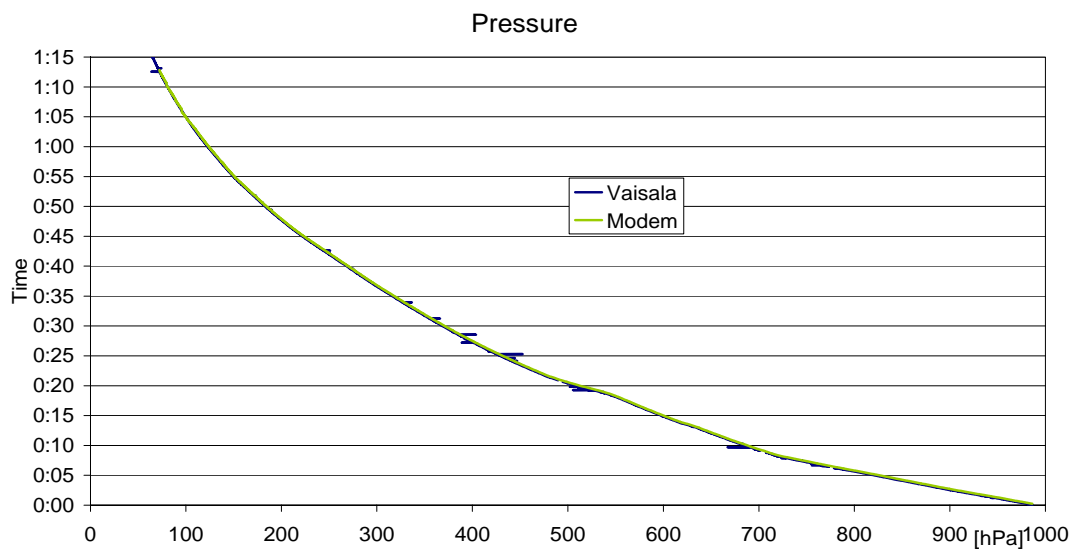
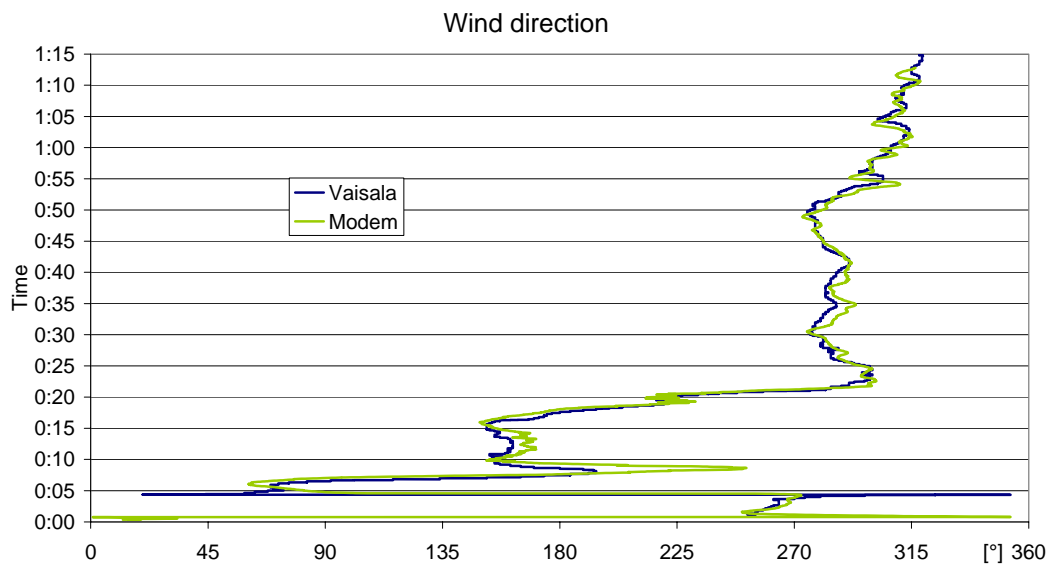
The same settings, apart from sonde calibration, remained valid during the common sounding. The sonde calibration was made in the ground check.

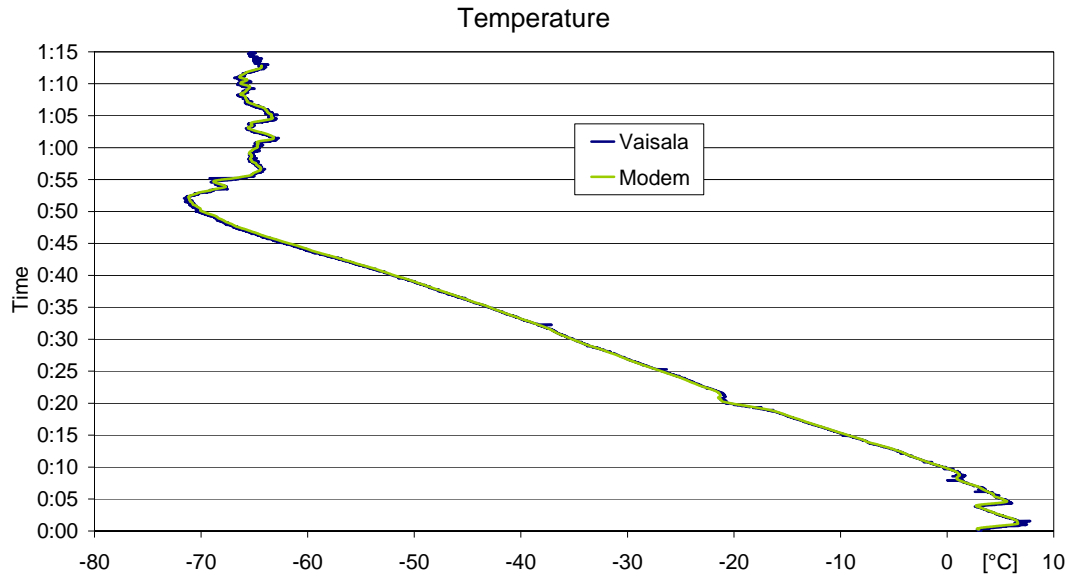
### **Modem**

During the common sounding the system was in operational mode. This means that the *test mode* and *static recording*, which were used in laboratory tests, were turned off.

The sonde was calibrated in ground check. The protocol was the same as during regular operational soundings. It included the initialization of the Modem system, calibration of the sonde and automatic start of sounding.

Examples of sounding data:





## Conclusions

Some conclusions of the intercomparison test are:

- There were small differences between measured temperatures in the climatic chamber;
- There was a difference between the measured relative humidity in the climatic chamber between Modem sondes and the reference.
- Both types of sondes have very similar pressure measurements (field test), although Modem doesn't have the pressure sensor, but it is calculated from GPS altitude.
- The differences between wind speed and direction measurements with both types of sondes in the field tests were very small.

The intercomparison test was made on a small sample of sondes, which is not enough to value the quality of the sondes. But the laboratory tests in the climatic chamber gave us very good view, how the sondes fulfill meteorological requirements.

## References

- M2K2 GPSonde; User's notice, Document No. M2K2-MUUS031001
- Vaisala Radiosonde RS90-AL: Technical Information: Ref. B210310en-B

# **On Board Processing Capability for Radiosonde Platforms Using Low Cost Processors Mixed Signal ICs and Semi-conductor Sensors**

By: Nuwan Kumarasinghe

Department of Meteorology  
Buddhaloka Mawatha, Colombo 07, Sri Lanka.  
Telephone: 94-11-2681039, Fax: 94-11-2698311  
e-mail: [nuwan1960@yahoo.com](mailto:nuwan1960@yahoo.com)

## **ABSTRACT**

Older versions of *Radiosonde* instruments with electromechanical and discrete components are still used by the meteorological community, particularly in developing countries. Within limited costs, the system can be improvised by using a mix of modern semiconductor sensors (for relative humidity and pressure), mixed signal ICs and micro-controller chips to provide more accurate, easily calibrated and on board processing capability, while reducing the weight to be carried by the balloon.

The new semi-conductor sensor platform consists of modern temperature, pressure and relative humidity sensors, where temperature sensor is in-built on one of the surface mount ICs which also has 4-channel multiplexer and 10-bit A/D converter. Hence the cost and the weight of the platform is considerably reduced. The sensor platform is controlled by 8051 compatible micro-controller provides on board processed data serially feed into an FSK modulator and the transmitter unit. The data received at the ground station can be directly fed to the computer. The computer interface software facilitates all manual calculations and graph plotting of the conventional radiosonde equipment.

|

## **1. Introduction**

The basic parameters measured in meteorological and environmental monitoring systems are temperature, relative humidity (RH), pressure, wind speed, wind direction and chemical gas particle measurement. The measurement of these parameters are required at upper atmospheric levels in addition to the measurements at the surface level for the successful environmental studies. The present system used in the Department of Meteorology, Sri Lanka for acquiring upper atmospheric information consist of basically two parts, viz;

- (a). measurements of wind speed and direction upto a height of approximately 30 Km above the sea level, using a wind finding radar.
- (b). measurements of temperature, RH and pressure upto a similar height using *radiosonde* equipment.

Meteorological Department of Sri Lanka is equipped with Indian made radiosonde system. This is entirely a analog system.

In this paper we only consider the measurements of modern I.C. based sensors of relative humidity, temperature and pressure.



The *radiosonde* which is connected to a hydrogen filled balloon and released, converts measurements obtained by the enclosed meteorological sensors (thermistor for temperature, hygistor for RH, both non linear elements) into resistance which control the blocking rate of a blocking oscillator. Consequently, the blocking oscillator modulates *radiosonde* carrier wave either in amplitude or in frequency. The rate of modulation pulses vary from 0-200 Hz, depending upon the meteorological sensor element in circuit and its resistance corresponding to prevalent temperature and RH. Each instrument is provided with a pre-calibrated data sheet in which the contact number for corresponding pressure is indicated. The aneroid capsule used as the pressure sensor performs another function by switching from temperature sensor to RH sensor. In *radiosonde* instrument a 401 MHz transmitter is used. The power required for the operation of the transmitter is obtained through water activated 22.5 V battery which is capable of giving operating voltage for approximately 90 minutes.

The objective of the present exercise confine to design and develop a prototype of a single air borne module capable of replacing the existing system. The system can measure accurately and reliably the upper atmospheric temperature, relative humidity and pressure. Somewhat complex calibration procedure is being used for the present radiosonde system. This newly designed airborne module has pre-calibrated sensors. Therefore it saves the calibration time. I.C. based sensors for the measurements of temperature, atmospheric pressure and relative humidity are being used.

## **2. Methodology**

The existing Radiosonde is used to measure upper air temperature , relative humidity and atmospheric pressure upto 25 km in analog form. The new radiosonde system is designed to measure temperature, relative humidity and pressure in digital mode, which can be directly coupled to a PC. A special I.C. is used for this particular design (AD 7817) , which has a internal temperature sensor in built and 10 –bit ADC and 5 analog channel multiplexer.

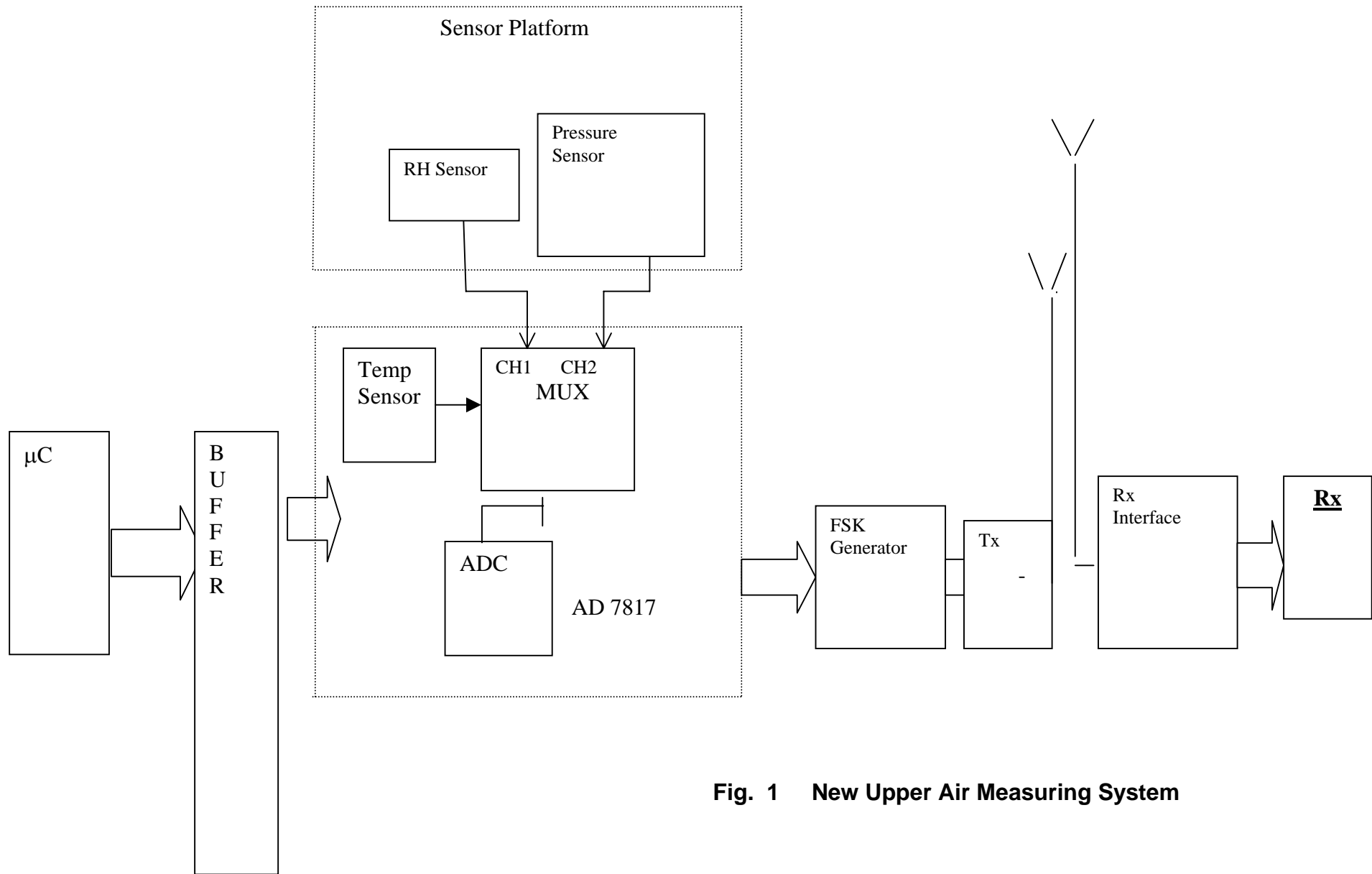


Fig. 1 New Upper Air Measuring System

The measurable temperature range is  $-55\text{ C}^0$  to  $+125\text{ C}^0$ . The temperature value is appeared as 10 – bit data at the output of ADC AD 7817 . On-chip temperature can be accessed via multiplexer channel 0 . The result of the 10 – bit conversion on channel 0 can be converted to a temperature value by using the following equation. AD 7817 contains two on-chip register. The address register and the over temperature register. These registers can be accessed by carrying out 8-bit serial write operation to the device.

$$T_{\text{AMB}} = - 103\text{ C}^0 + (\text{ADC Code}) / 4$$

In this design we have used Honeywell, IH 3602 L sensor for relative humidity measurements. IH 3602L is a high accuracy, fast response and stable sensor. It's output voltage is directly proportionate to the RH % value.

We have used Motorola MPX 5500 silicon based pressure sensor for atmospheric pressure measurements. It is a on-chip signal conditioned temperature compensated pressure sensor. It has a measuring range of 0 – 1200 millibar.

DS 87C520 high-speed micro-controller was used as the main processor. This micro-controller is an 8051 compatible processor. It has four 8-bit I/O ports, three 16-bit timer/counters and 256 bytes scratchpad RAM. It features 16 KB of EPROM with an extra 1 KB of data RAM. Besides greater speed , the micro includes a second full hardware serial port. Port 2 is used to create the control word for AD 7817 chip. Output data of AD 7817 is accessed through LSB of the Port 0.

If the five MSB's of the control byte are all logic '0' then the three LSB's are transferred to the analog input channel on which to carry out a conversion. It is also used to select the temperature sensor, which has the address of 000.

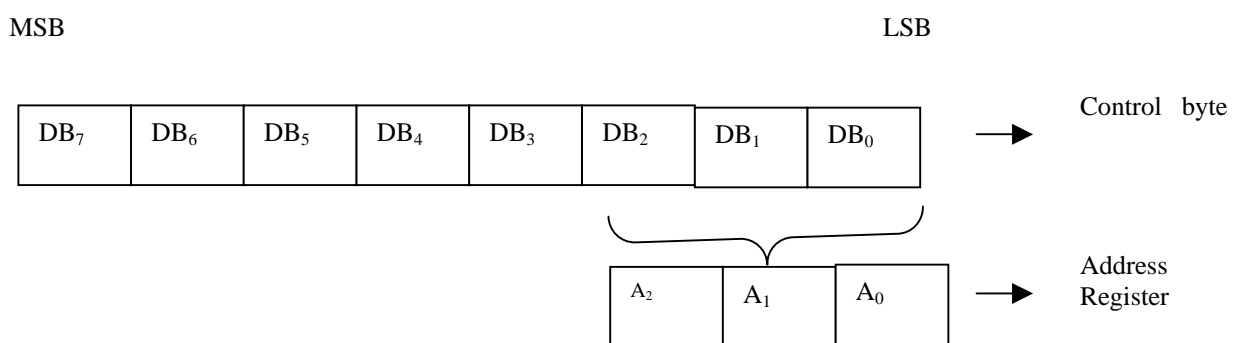


**Fig. 2 Control Byte**

The processed data is generated via Port 3 at 300 baud speed which is a compatible speed for the existing Radiosonde receiving unit. Assembly language is used to program the micro-controller DS 87C520. The corresponding flow chart is shown in Fig. 3.

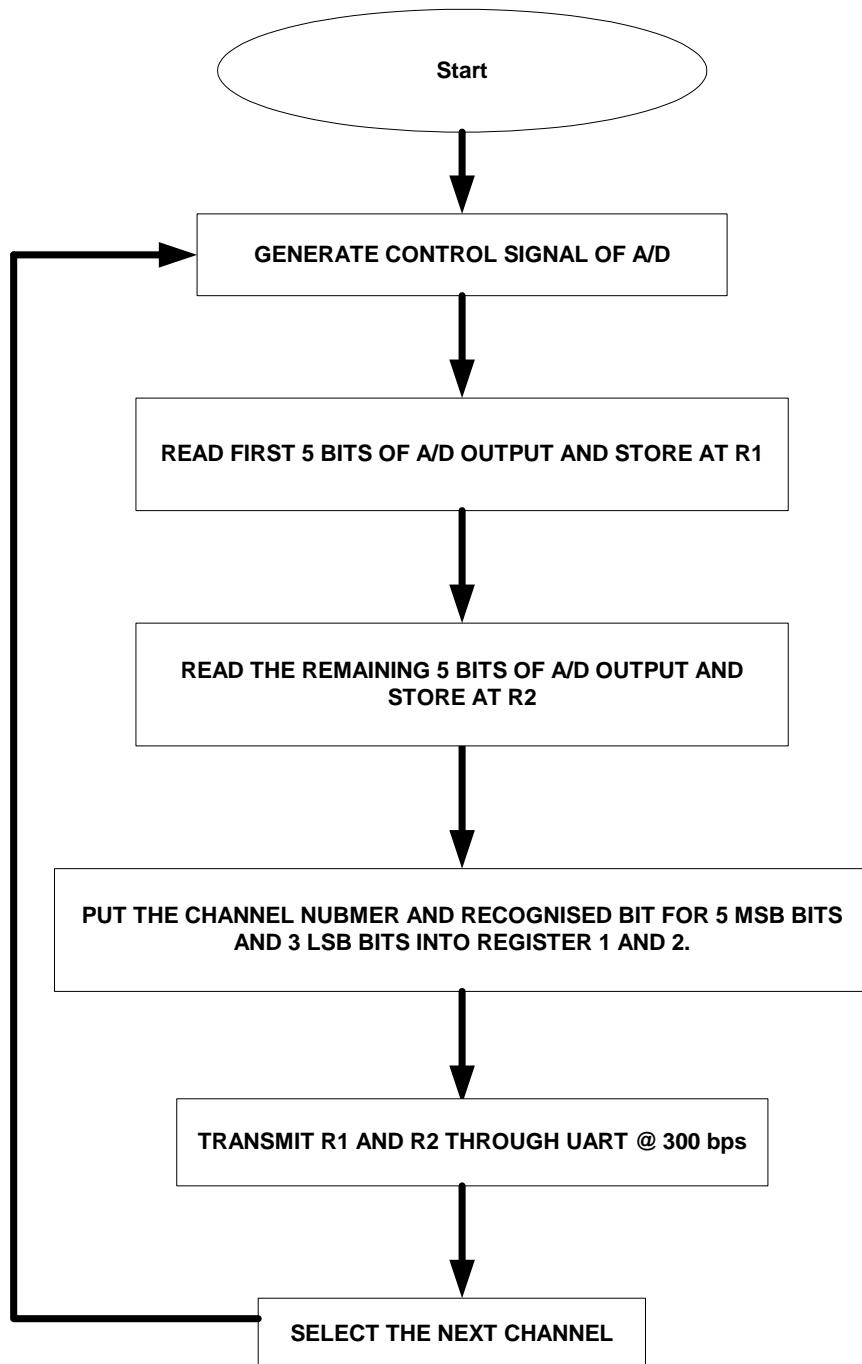


Fig. 3 Flow Chart

Output data stream of DS 87C520 micro-controller is then fed to a FSK(frequency shift keying) modulator. In this particular design, two frequencies of 1250 Hz and 625 Hz are being used for logic '1' and logic '0' respectively. The output of the FSK modulator is fed to the transmitter unit which has a center frequency of 401 MHz.

Finally the UHF receiver is used to receive the FM radiosonde signals. The frequency modulated carriers are demodulated to produce audio frequency signals.

### 3. Results and discussion

Ground level tests were conducted and the following results were obtained.

Parameter	Sensor Reading	Actual Value
Temperature (C <sup>0</sup> )	26.2	26.7
Relative Humidity (%)	73	76
Pressure ( mb)	1011	1009

Similar results were obtained in various tests. It clearly shows that the values obtained were acceptable in the ground level. Due to time limitation upper air test could not carry out.

### 4. Conclusions

Radiosonde devices normally use analog type sensors, therefore their calibration procedure is bit complex. It is somewhat troublesome to get a PC graphical output because of its analog nature. This project fulfills that need. Modern I.C. based sensors are being used for the air born module. All on board processing is done by a 8051 compatible micro-controller. PC compatible data outputs are available for any graphical outputs.

### 5. References

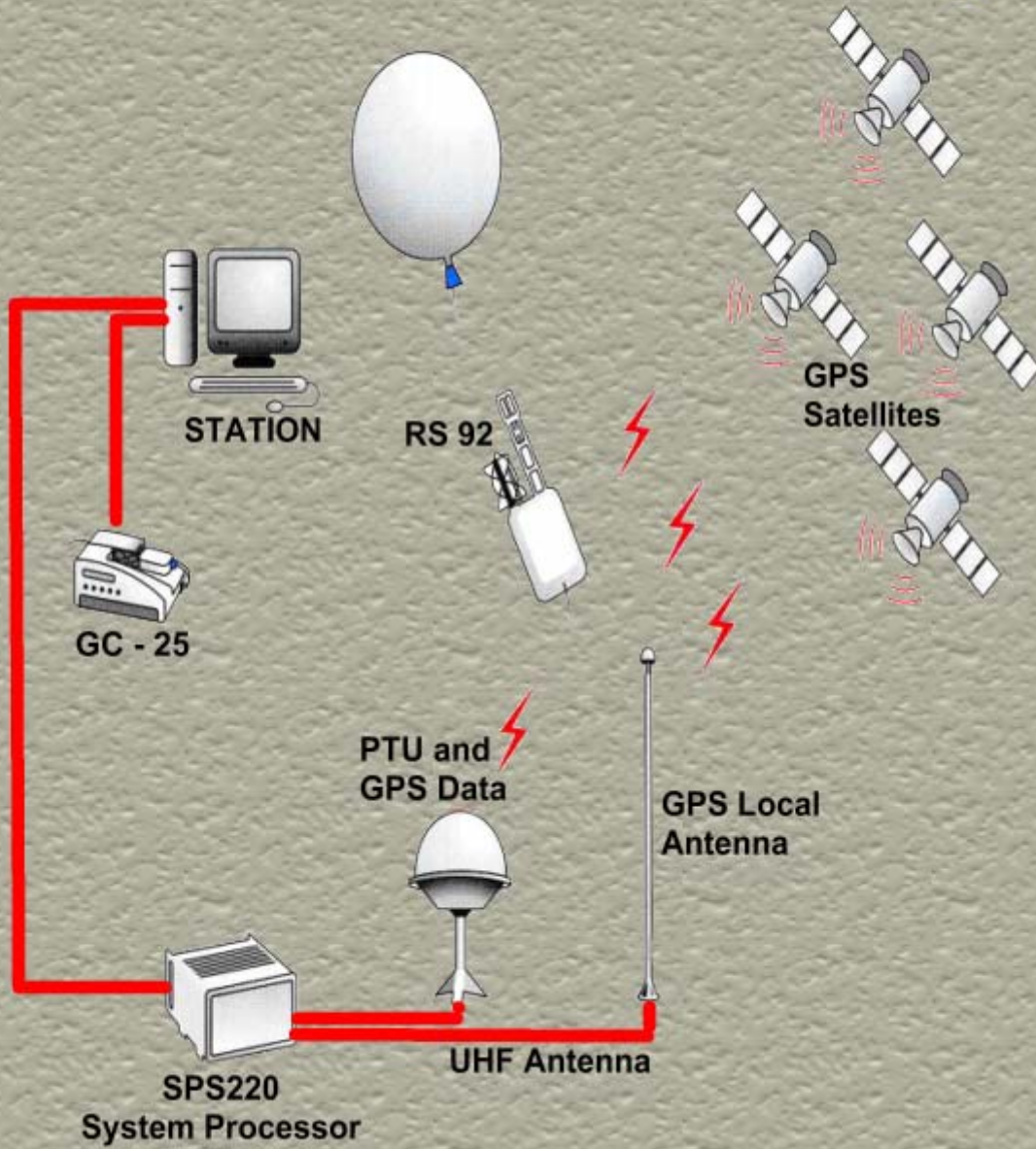
1. Hood and Linsely J. : " The Art of Linear Electronics"; Butterworth Heinemann; 1993.
2. James M.R. : " Microcontroller Cookbook"; Mike James 1997.
3. Andrews M.: " Programming Microprocessor Interfaces for Control and Instrumentation; Prentice- Hall. Inc; Englewood Cliffs 1982.

# Radio Theodolite System

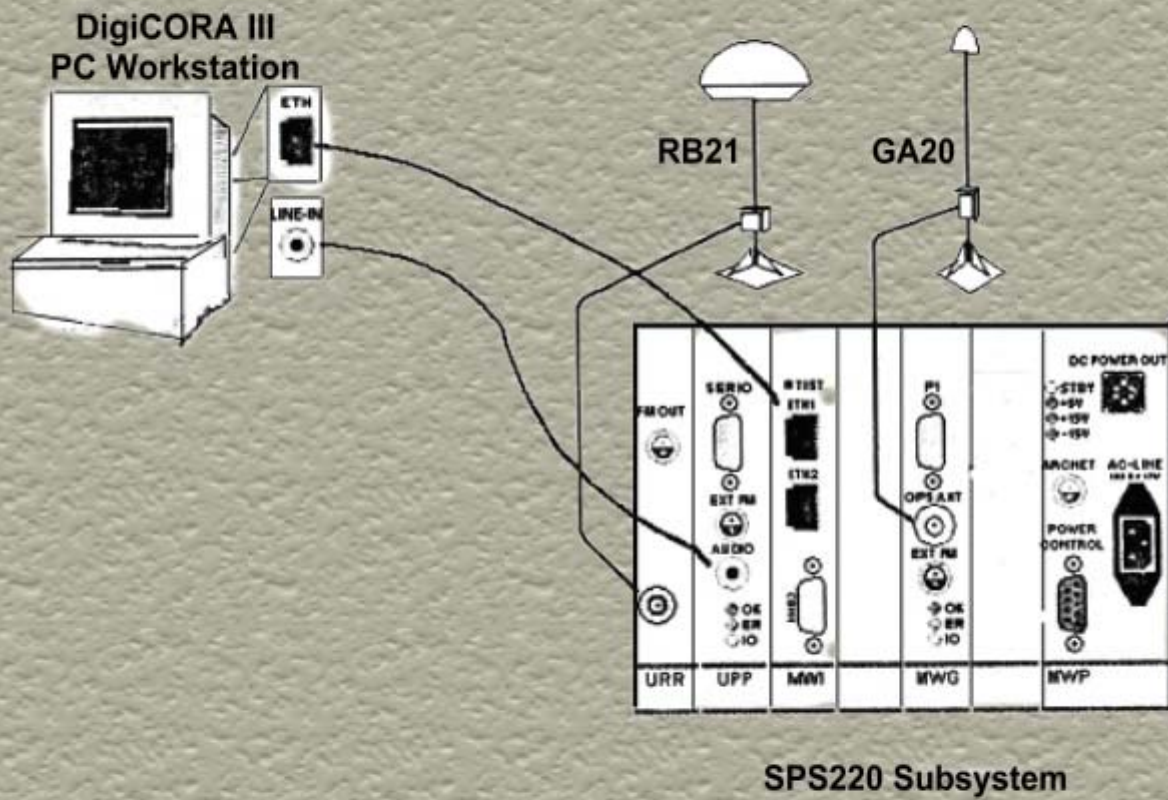


The Advantage of Radio Theodolite System is Independence

# GPS System

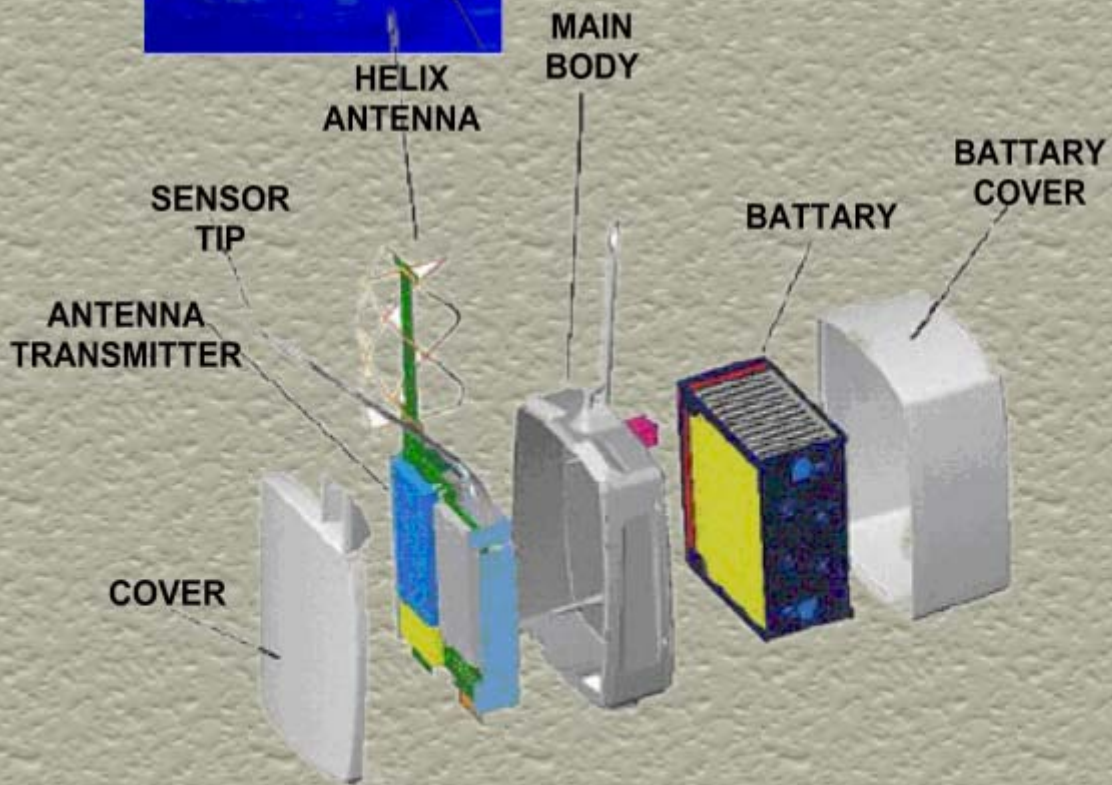


# GPS Assembly

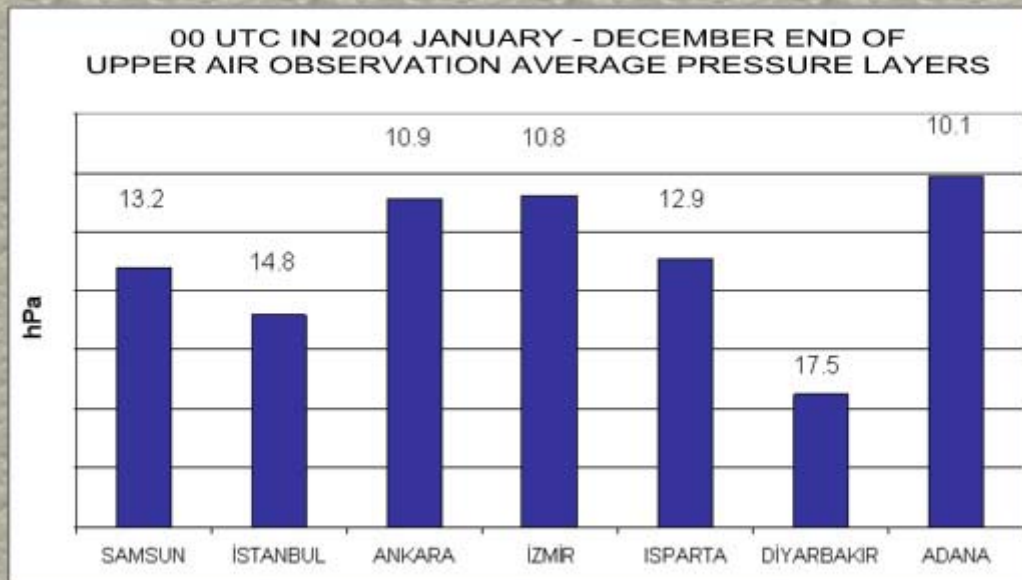
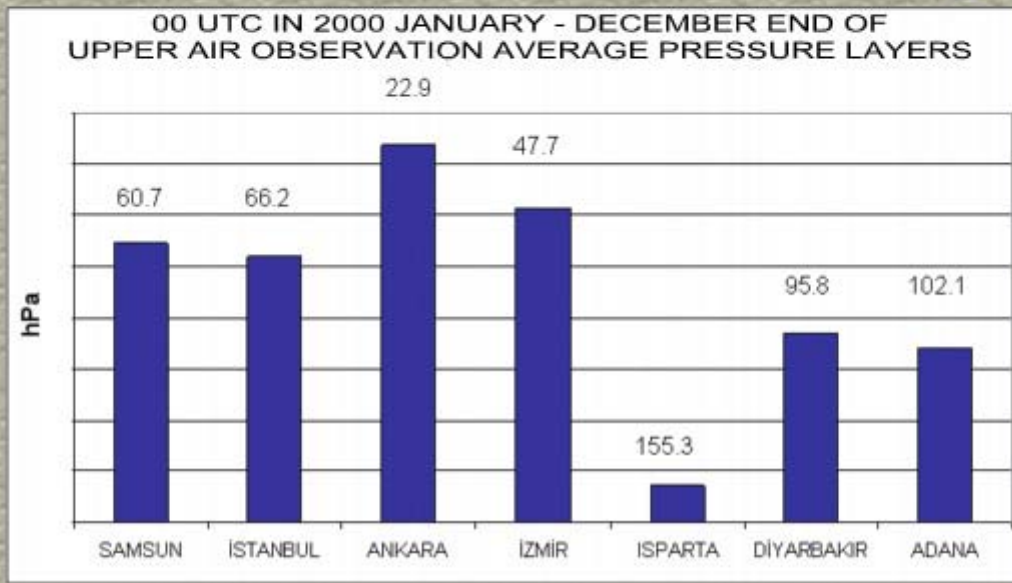




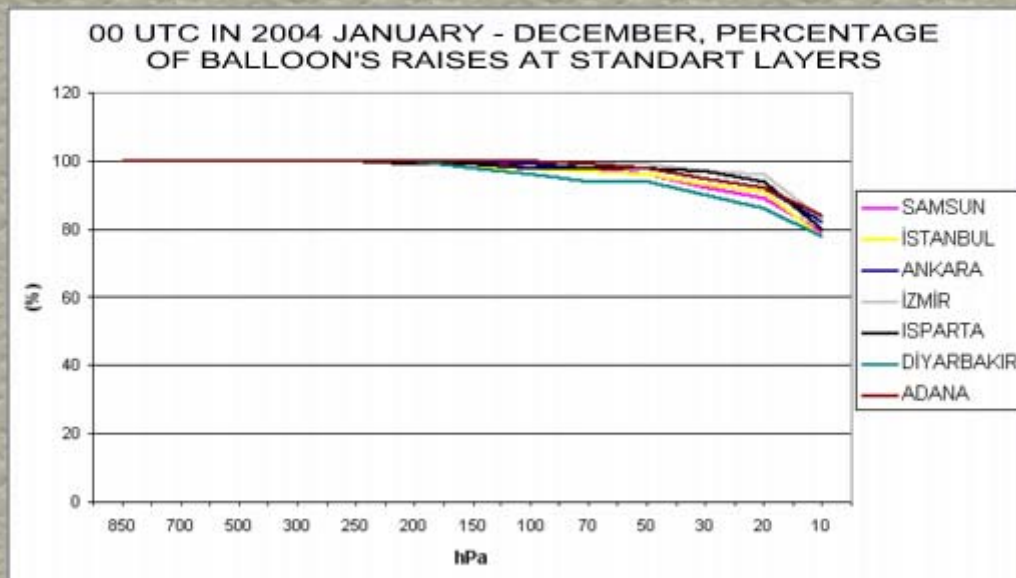
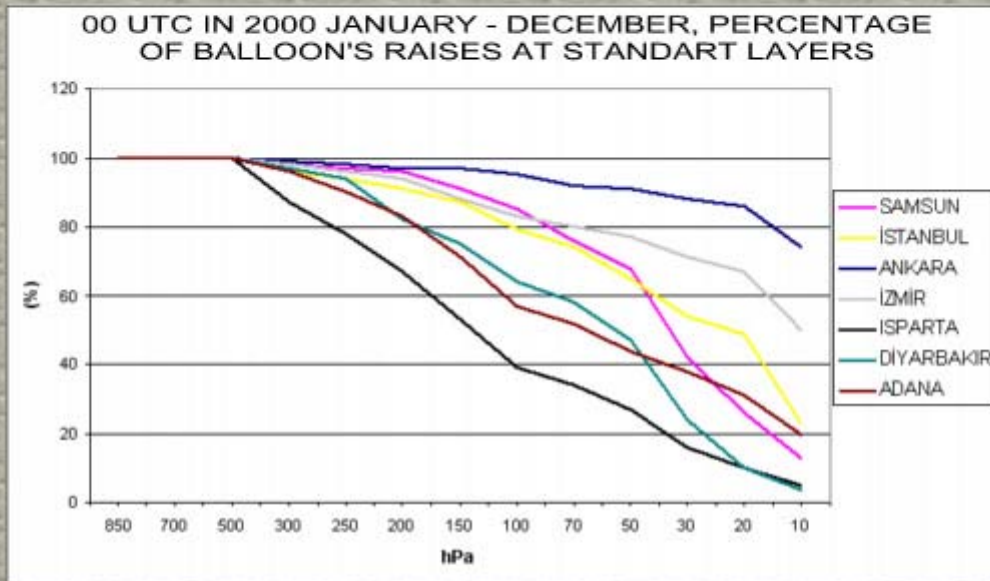
# RS - 92 - SGP



# Comparison Tables Between Before and After The Upgrade Process



# Comparison Tables Between Before and After The Upgrade Process



# Observing Fog And Low Cloud With A Combination Of 78GHz Cloud Radar And Laser Ceilometer

Met Office: Darren Lyth<sup>1</sup>, John Nash.

Rutherford Appleton Laboratory: M.Oldfield

## ABSTRACT

Results from two demonstration tests of a FMCW (Frequency Modulated Continuous Wave) 78GHz cloud radar are used to examine the radar's ability to measure low cloud and fog. The first test took place at Payerne, Switzerland (from Nov 2003 to Feb 2004), as part of the COST 720<sup>2</sup> TUC (Temperature, Humidity & Cloud Profiling) Project; and the second test took place at the Chilbolton Facility for Atmospheric and Radio Research (CFARR), UK (Aug 2004). The FMCW radar was of similar sensitivity to the pulsed cloud radars at Chilbolton and the good vertical resolution of the system allowed accurate detection of fog top and cloud top in layered clouds.

## INTRODUCTION

In partnership with the Met Office a vertically pointing 78.2GHz FMCW cloud radar has been developed by the Space Science and Technology Department of the Rutherford Appleton Laboratory (RAL), to demonstrate the potential capability of the system in cloud detection and the benefits it can offer in comparison to existing observing systems (i.e. Laser Cloud Base Recorders – LCBR). Figure 1 shows a picture of the antenna of the system along with the specification details<sup>2</sup>.



Frequency: 78.2 GHz  
Transmitted Power: 250mW  
Operated at 16km Range (30m spatial resolution) at Chilbolton  
Operated at 8km Range (15m spatial resolution at Payerne)  
Temporal Resolution: 1s  
Radiometer Sky Temperature Accuracy: +/- 1K  
Pulse duration: 800  $\mu$ s  
Pulse separation: 1.5 - 2.0 ms  
Polarisation: linear  
Total chirp excursion: 10 MHz  
Dynamic range of receiver: 50dB  
Viewing Angle: Zenith  
Beam width: ~0.5 degree (half power)

**Figure 1 – RAL 78.2GHz Cloud Radar and system specification<sup>3</sup>.**

As part of the development and assessment of this system, it has been deployed at several UK observing sites since early 2001. Major improvements to the sensitivity and data range/resolution have been added to the system through a complete redesign of the antenna and the backend processing. As such only results from the later deployments are relevant in the assessment of the systems capabilities. This paper concentrates on the results from two deployments, firstly at Chilbolton, UK ( Aug 2004) and secondly, Payerne, Switzerland ( Nov 03 to Feb 04).

## CHILBOLTON EXPERIMENT

The Chilbolton experiment was designed to provide absolute calibration of the reported cloud radar signals, which was necessary to satisfy requirements from participants in the COST TUC experiment. As well as comparing directly with the pulsed 35GHz Copernicus Cloud Radar, it was also possible to confirm that the calibration was consistent with historical records of the signals observed with the 94GHz Galileo Cloud Radar at Chilbolton.

The Vaisala 905nm CT-75K ceilometer, at Chilbolton, was used to check for low-level clouds with small drop size distributions (eg. Stratocumulus), which cloud radars find difficulty in detecting.

Figure 2 provides an example of the cloud radars performance on a day with several layers of cloud and with little precipitation. (Note Data from the FMCW radar has been range corrected.) The dashed purple line in both the cloud radar plots indicates the maximum in the ceilometer signal, which is associated with relatively thin cloud, at about 2km in height. The FMCW radar was more sensitive to the lower thin cloud, than the pulsed radar. Both cloud radar's were able to detect the higher cloud at around 5km, although due to its higher resolution, cloud structure is more evident in the FMCW profile. The ceilometer was unable to detect any of the higher cloud, due to obscuration of the signal by the lower thin cloud.

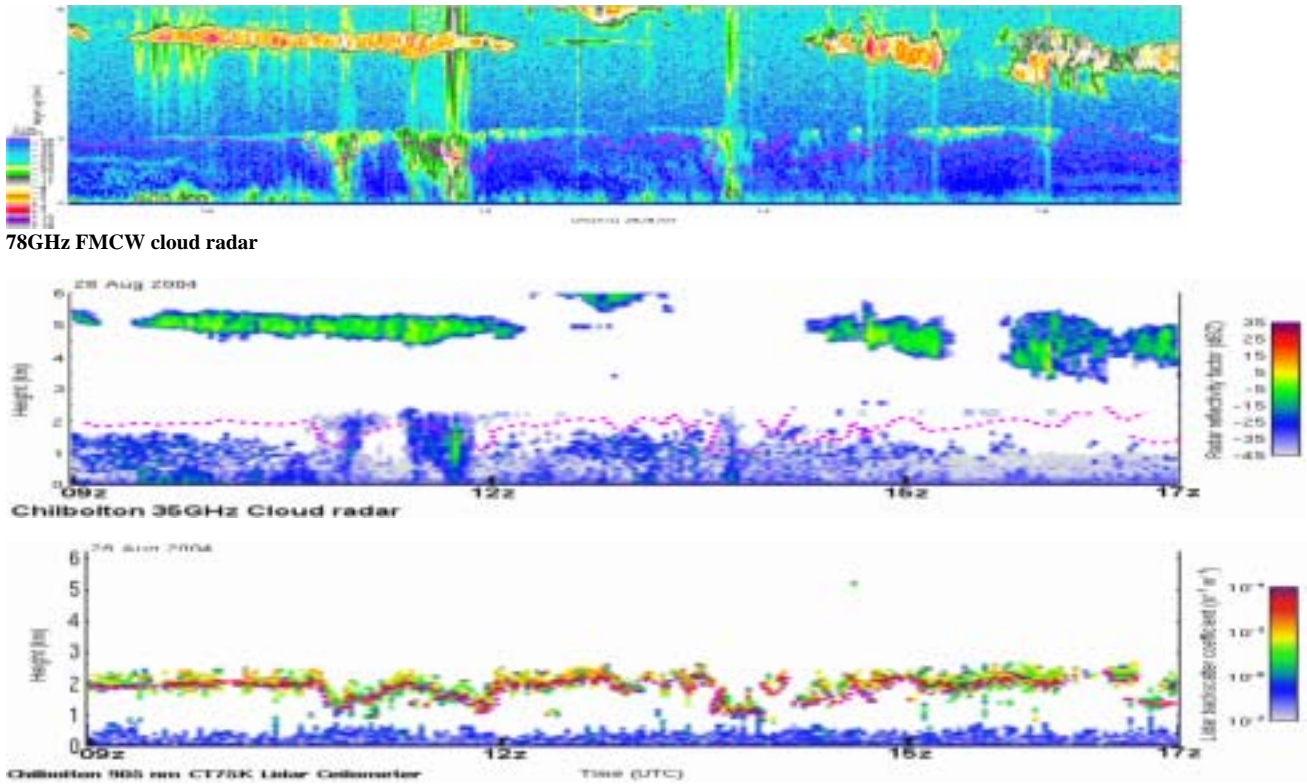


Figure 2. Time-Height cross-section plots from fmcw radar, 35GHz pulsed radar & Lidar: 28/8/04

Figure 3 illustrates the FMCW radar's ability to resolve cloud structure close to the ground, in a region where the pulsed radar is less reliable.

The dashed red line in both the cloud radar plots indicates the maximum in the ceilometer signal on this day. Note that the Chilbolton ceilometer has relatively poor resolution in the boundary layer. For these lower altitude signals the ceilometer returns are very strong, and are well matched to the cloud base from the FMCW radar. However these low level clouds were not resolved very well by the 35GHz pulsed radar.

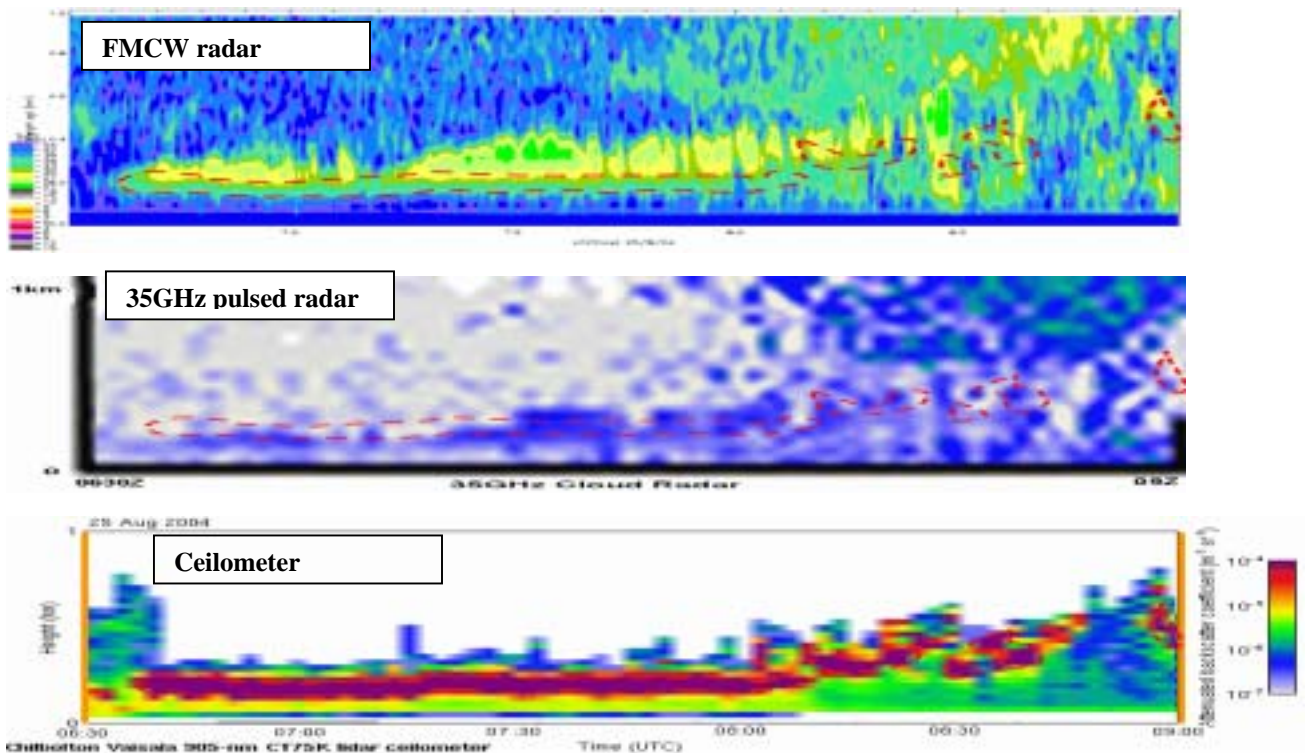


Figure 3. Time-Height cross-section plots from FMCW radar, 35GHz pulsed radar & Lidar: 25/8/04

---

## CONCLUSIONS FROM CHILBOLTON EXPERIMENT

- The results from Chilbolton indicate that the sensitivity of the 78GHz FMCW Cloud Radar was comparable to that of a modern pulsed Cloud Radar.
- The FMCW cloud radar was able to detect multiple cloud layers.
- The FMCW radar was able to detect clouds up to ~12km in height.

The testing at Chilbolton stopped after the cloud radar failed, due to the ingress of water during summer usage, which caused a short circuit. Some system degradation may have occurred before the complete failure, but this did not produce a significant shift in calibration.

---

## PAYERNE EXPERIMENT

The TUC experiment was specifically targeted on the detection of fog & cloud and thus there was a comprehensive range of ground-based remote sensing and surface measurement systems at Payerne.<sup>4</sup> Measurements from the FMCW cloud radar could be directly compared with regular Radiosondes ascents, a 1290 MHz Wind Profiler, a Vaisala CT-25K Ceilometer and surface instruments, including an Infra-Red Radiation Pyrometer, Present Weather sensor, and a total sky camera.<sup>5</sup>

Figure 4 shows an example of verification of fog top using a Radiosonde temperature profile. An increase of Temperature to ~4 deg C from the IR Pyrometer after 19utc indicated the time when this fog thickened. Low surface visibility from surface sensors at this time also indicated fog at the site, and Relative Humidity at 2m was 100%, with APCADA (Automatic Partial Cloud Amount Detection Algorithm) recording an upward jump after 19utc from 96%. The Radiosonde temperature profile (23utc launch time shown as red line) is consistent with the top of a thick fog layer at ~205m.

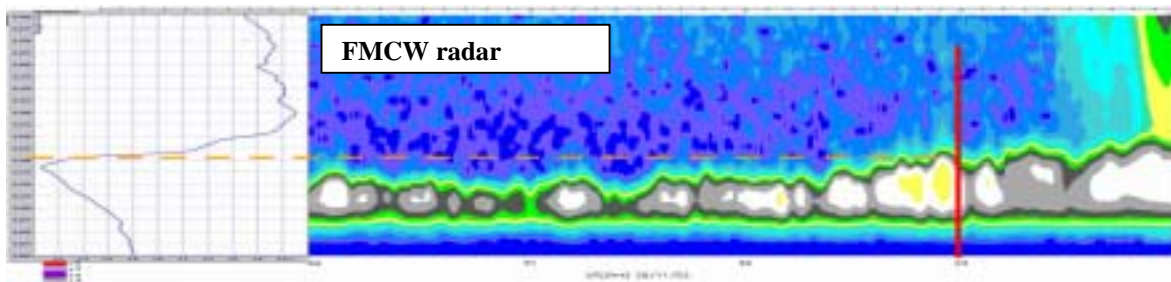


**Figure 4. Time-Height cross-section plot from FMCW radar, with 23utc Radiosonde Overlay: Fog 26/11/03**

The FMCW cloud radar plot in Figure 5 shows a day at Payerne on 6/12/03, where the fog is on the ground for part of the time, and then later lifts. The region with strong readings from the ceilometer is overlaid as a red dashed line on the FMCW radar profiles.

The fog top as deduced from the FMCW radar is superimposed as a yellow dashed line on the Wind Profiler S/N plots. In many types of cloud, especially when it is raining, the wind profiler signals in cloud are high, because of backscattering from the raindrops or ice crystals. However, in clouds or fog with low mean drop size, wind profiler signals become very low. This is because small cloud or fog droplets have very low scattering at 1GHz. In addition for this type of cloud there is very little backscattering from refractive index variations due to changes in relative humidity. In this example taken at night, the increase in wind profiler signal above the cloud/ fog correlates reasonably well with the top of the fog indicated by the cloud radar.

The S/N ratio from the Wind Profiler can be used to check on fog top. The ceilometer plot shows that the fog lifts to form an elevated layer after 0200utc, this can be seen as an increase in surface visibility. Surface measurements also showed decrease in Relative Humidity at 2m from 99% at the start of the period, to 95% at 0400utc. The S/N ratio values on the Wind Profiler plot are very low under the deduced fog top, and above the fog top rise to a relative maximum in signal power.

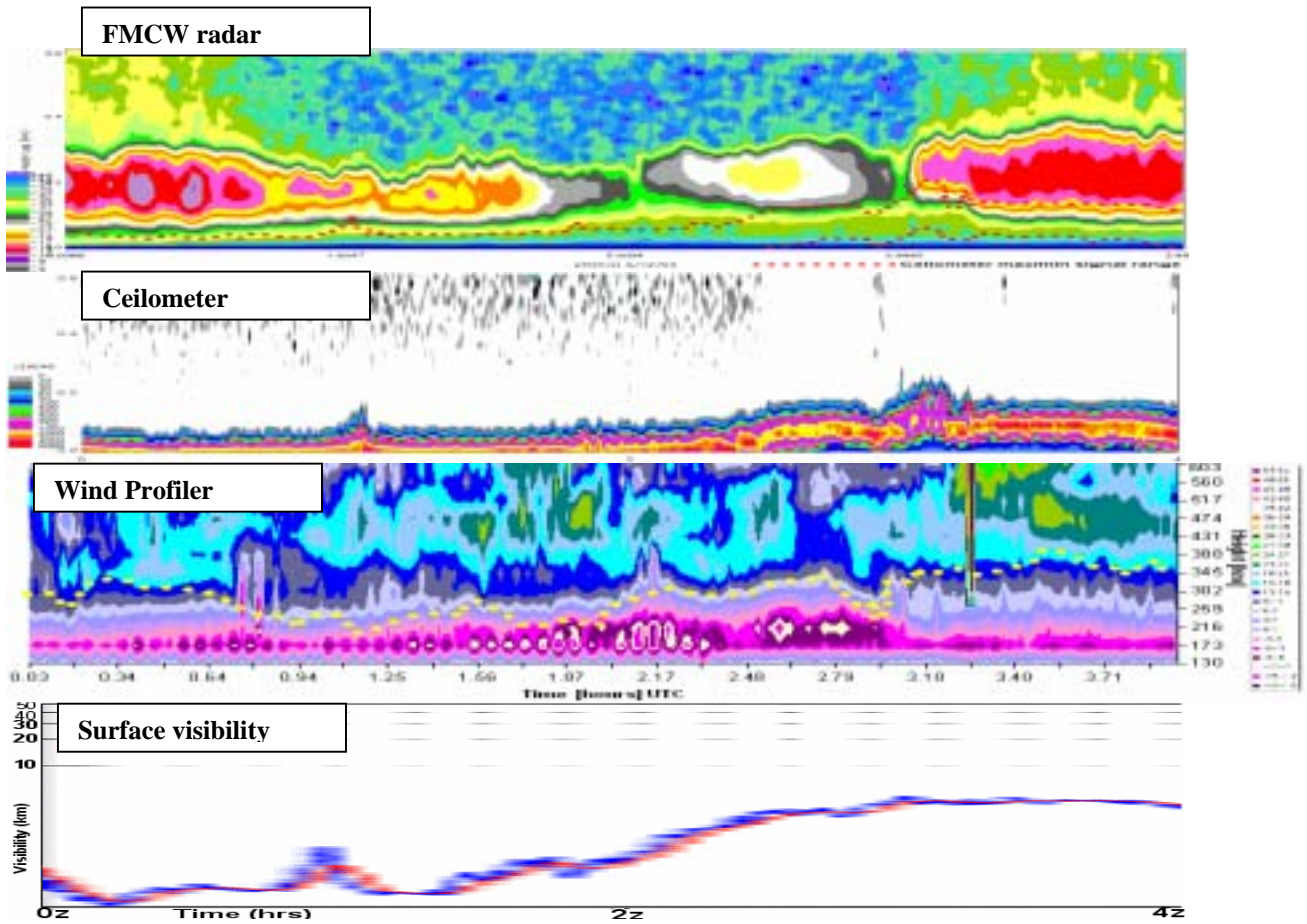


Figure 5. Time-Height cross-section plots from FMCW Radar, Lidar & Wind Profiler S/N, and Time-Distance Surface Visibility plot: 6/12/03 0000-0400utc

Later in the day, low cloud persisted at Payerne. The elevated layer evident in the latter part of Figure 5 is continuous during the period shown in Figure 6. The cloud base in the FMCW radar plots in Fig 5 & Fig 6, shows good agreement with the ceilometer signal, and tracks changes in altitude of the base. This only happens when there is negligible precipitation falling to the ground.

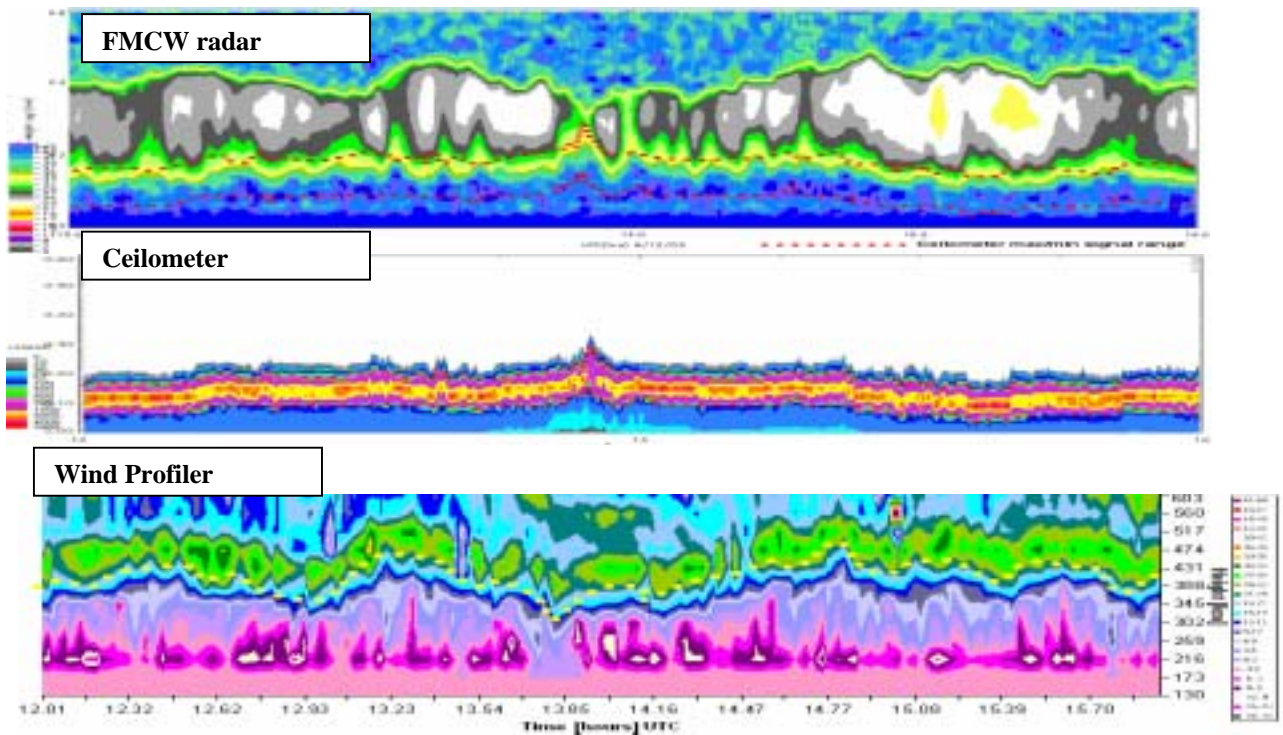
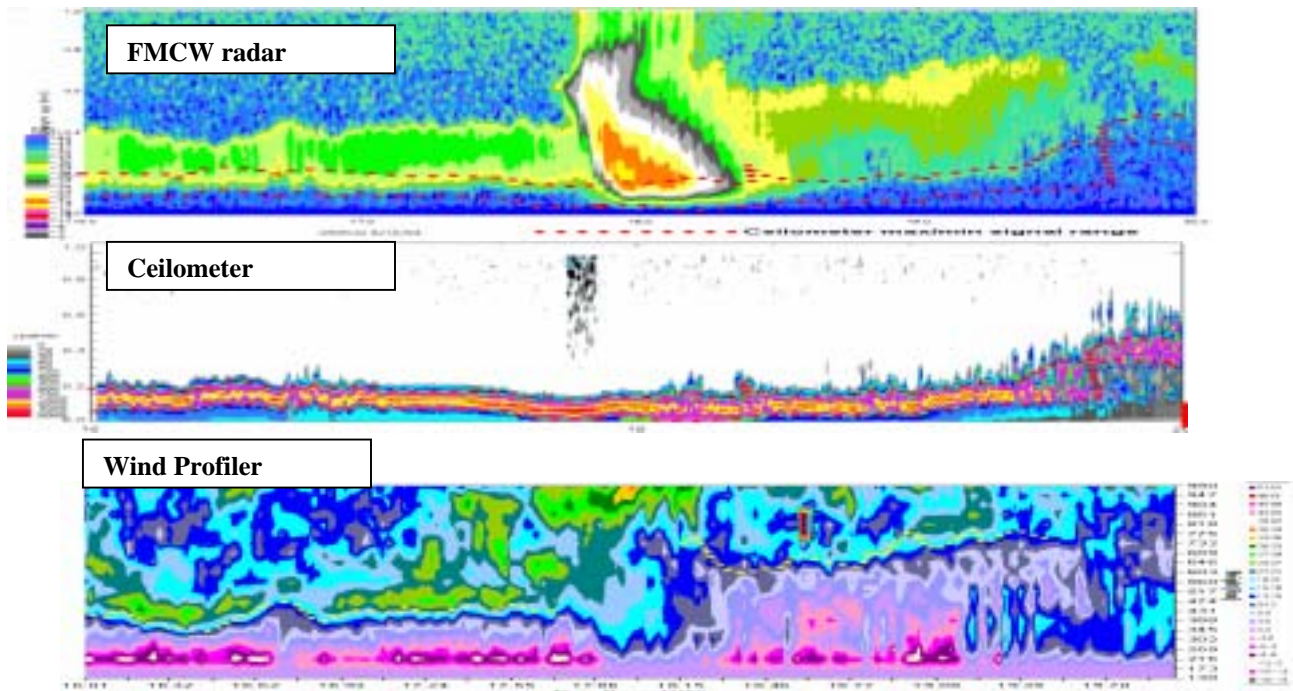


Figure 6. Time-Height cross-section FMCW Radar, Lidar & Wind Profiler S/N plots: 6/12/03 1200-1600utc

The cloud top from the FMCW Radar plots (overlain as the yellow dashed line in the Wind Profiler S/N plots) coincides, in this case, with an increase in Wind Profiler signal. The relative maximum above the cloud top, is even more pronounced in daytime (dark green area: ~30dB) than in Figure 6, a period at night when there is little mixing.

Figure 7 shows the continuing cloud radar, ceilometer and wind profiler SNR measurements for the evening of 6/12/03 (1600-2000utc). At 1800utc, when there was precipitation, the cloud radar signals extended towards the ground, but there was no major shift in cloud base recorded by the ceilometer. This can be explained by the FMCW radar being sensitive to the falling droplets from the cloud, and locking onto them. Although precipitation was reaching the surface, the radar showed a weakening of the signal at lower altitudes, giving a false indication of cloud base. This drop in signal on the FMCW cloud radar plot, is due to insensitivity in the bottom range gates, and the calibration not being optimised to compensate for this.



**Figure 7. Time-Height cross-section FMCW Radar, Lidar & Wind Profiler S/N plots: 6/12/03 1600-2000utc**

Figure 8 shows the development of hill fog at Payerne on 26/11/03. The FMCW radar and ceilometer both show a lowering of the cloud base from 1015utc, to a minimum at ~1030utc, corroborated in a lowering of surface visibility from 5km down to 500m during this period. The sky camera view also showed a deterioration in visibility (although the pole in the distance can still be seen). By 1130utc, the FMCW radar showed the cloud top had lowered to an extent where the top was too low to be reliably detected, due to insensitivity in the lowest range gates. As the cloud base also lay in this insensitive region, the cloud had appeared to dissipate on the FMCW radar plot. The sloping red line on the FMCW radar plot indicates the height of the cloud top. The ceilometer and surface visibility plots showed that the low cloud base persisted until 1140utc. Note that the ceilometer also showed insensitivity in its lowest range gates, as the strongest signal returns occur where the cloud base has lifted above a height of ~40m (as shown by the short black horizontal lines on the ceilometer plot which signify cloud base estimation). After 1140utc, the surface visibility increased, and the ceilometer showed stronger signals (yellow backscatter colour), as the cloud base lifted out of the lowest insensitive range gates. The lifting can also be seen in the sky camera view for 1153utc. At midday, the FMCW radar shows the development of another layer of hill fog, elevated at first, and undetected by surface visibility measurements. The layer gradually lowers on both the FMCW and ceilometer plots, and at ~1210utc, the fog makes ground contact, as the surface visibility suddenly lowers to a minimum, which continues for the duration of the plot. The sky camera view shows a thick ground fog, with the pole now invisible. The ceilometer records it's lowest cloud base, and again, signal strength is subdued (orange –red backscatter colour) due to insensitivity near the ground. The FMCW radar plot displayed a well-defined fog top after this time, but fog base is shown at a higher altitude than the ceilometer, again due to insensitivity near the ground.



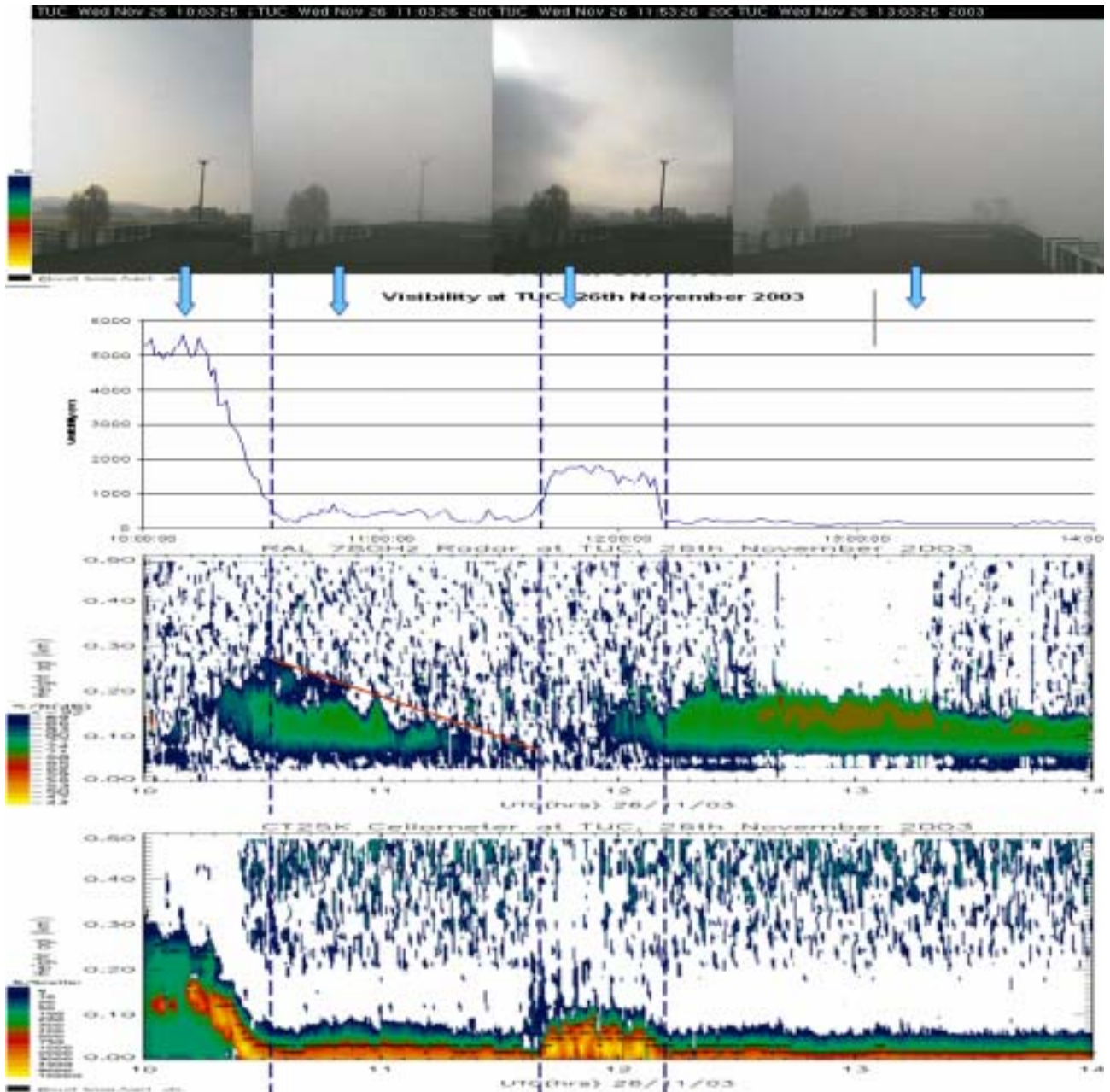


Figure 8. Sky Camera view, Time-Distance surface visibility, and Time-Height cross-section fmcw radar & lidar plots: 26/11/03 1000-1400utc

---

## CONCLUSIONS FROM PAYERNE EXPERIMENT

On many days, the FMCW cloud radar was able to detect clouds reliably. On some occasions the cloud base is also detected, but a ceilometer is needed in conjunction with the cloud radar to identify cloud properties. This is due to insensitivity of the radar in its lowest range gates.

Sometimes in very thin fog the cloud radar only records weak signals, due to the radar's inability to detect scattering from small water droplets. This was apparent in only a small proportion of cases.

---

## OVERALL CONCLUSIONS

The FMCW cloud radar has shown to be a useful system for detecting; (a) the tops of low cloud, mist and fog (at a minimum height above the radar of ~25m); (b) multiple cloud layers; and (c) upper cloud (cloud measured at >12km height).

The radar is also useful in identifying the precipitation conditions beneath cloud, in combination with a ceilometer.

Fog measurements require a combination of laser ceilometer and cloud radar measurements.

---

## ACKNOWLEDGEMENTS

1. **B.Ellison, M.Oldfield, P.Huggard** of **Rutherford Appleton Laboratory (RAL)** for collaboration in the ongoing development and maintenance of the 78GHz fmcw Cloud Radar.
2. **D.Ruffieux** and staff (MeteoSwiss) at the Aerological Station, Payerne, Switzerland, for their organization of the TUC Experiment, and their invaluable assistance during the period of Cloud Radar deployment.
3. **C.Wrench, E.Slack, D.Ladd, J.Agnew, D.King** of Chilbolton Observatory, UK, for their assistance during the Chilbolton Comparison.
4. **T.Butcher** of Met Office, UK, for permission to reproduce Fig.9

---

## REFERENCES

- <sup>1</sup> Darren Lyth, e-mail: [darren.lyth@metoffice.gov.uk](mailto:darren.lyth@metoffice.gov.uk) Phone: +44 1392 885635, Fax: +44 1392 885681
- <sup>2</sup>COST is an intergovernmental framework for European CO-operation in the field of Scientific and Technical research, allowing the co-ordination of nationally funded research on a European level. The COST720 Action is concerned with the "Integrated Ground-based Remote-Sensing Stations For Atmospheric Profiling".
- <sup>3</sup> Ellison, B.N., Oldfield, M. and Bradford, W.J., "Millimetre wave cloud radar", poster presentation at 9th International Workshop on the technical and scientific aspects of MST radar – MST9, Toulouse, 13-18 March 2000.
- <sup>4</sup> D.Ruffieux, **T.J.Hewison**, C.Gaffard, R.Nater, B.Andrade, M.Perroud, H.Berger and P.Overney, The COST720 Temperature, Humidity and Cloud Campaign: TUC, Proceedings of microRad, Rome, 24-27 Febraury 2004
- <sup>5</sup> COST720 WG2 "Integrated Ground-based Remote-Sensing Stations For Atmospheric Profiling" TUC Experiment Database, available by ftp from Dominique Ruffieux, MeteoSwiss, Payerne, Switzerland.  
Phone: +41 26 662 6247 Fax: +41 26 662 6212 email: [Dominique.Ruffieux@meteoswiss.ch](mailto:Dominique.Ruffieux@meteoswiss.ch)  
<http://www.meteoswiss.ch>

# **Demonstration of the new InterMet radiosondes system installed at the Tanzania Meteorological Agency, Dar-es-Salaam**

J. Nash , R. Smout, M. Smees      Met Office , Exeter ,UK  
C. Bower    NOAA-NWS, Silver Spring, Md, USA  
S. Mbuya, L. Mganga and S. Ndonde Tanzania Meteorological Agency

## **1. Introduction**

An IMS 1600 upper air sounding system was installed by the manufacturer in Dar-es-Salaam, Tanzania in August 2004. The upper air station is located at Dar-es-Salaam airport. The IMS 1500 radiotheodolite, see Fig.2, was installed on the top of an observatory building, as advised by WMO representatives (see Fig.1), with the ground station computers located in the upper floor of the building.



Fig.1 View of observing station at Dar-es-Salaam Airport from the balloon shed.

A contract was placed with the UK Met Office to provide a demonstration test of this system, with reports to be generated for the US donors supporting the regeneration of radiosonde stations within the GCOS network. The test took place from 18 to 30 October 2004, with a lot of help from Carl Bower of NOAA and from a wide range of staff from the Tanzania Meteorological Agency.

## 2. Structure of demonstration test

Plans for the test had to be revised daily, once it was realised that the Tanzanian staff needed more instruction in operational radiosonde procedures than had been provided by the Internet engineers responsible for the installation. Thus, the completed demonstration test consisted of:-

- 14 individual Vaisala RS92 flights, used to train TMA staff in procedures. (These flights were processed by DigiCora III software using equipment brought to Tanzania by the UK team. Measurements were usually performed by TMA staff. The radiosonde were ground checked as recommended by the manufacturer, so the humidity sensors should have been regenerated from contamination before launch.)

- individual Sippican MKII training flights.
- nighttime simultaneous comparisons between Sippican and Vaisala,
- 5 daytime simultaneous comparisons between Sippican and Vaisala ,
- nighttime simultaneous comparisons between MODEM and Vaisala
- 2 daytime simultaneous comparisons between MODEM and Vaisala.

The limited number of simultaneous flights were sufficient to identify areas where more work was needed on the system. It was found that the IMS system was not really ready for a larger scale quantitative test.

Fig.2 shows a Sippican radiosonde prepared for launch, with the chip thermistor deployed facing upwards and the wire support bent to hold the thermistor well above the top of the radiosonde. Earlier radiosonde testing in 2004 at Camborne, UK had shown that this mode of sensor deployment gave reproducible results with the Sippican MkII.



Fig.2 Sippican MKII Radiosonde and Internet IMS 1500 radiotheodolite.

The radiosondes in the twin flights were suspended under each end of a length of plastic water pipe. See Fig.3. Launching a twin flight is shown in Fig.4. The night time measurements were usually launched as the sun was setting, so the end of the flights was in the dark.



Fig.3 Preparing to launch a Sippican / Vaisala RS92 twin flight, Dar-es-Salaam.

The balloons used for the testing were a mixture of Pawan and Totex 350g balloons with burst heights typically between 19 and 23 km respectively. Six Totex 1200g balloons lifted radiosondes to heights above 30 km. The 1200g balloons were a little large for the balloon shed. However, the hydrogen generator was easily able to supply sufficient gas for this type of balloon. The large balloons performed best in the nighttime flights. Working arrangements for balloon filling were improved during the trial with the installation of an automatic balloon filler and a table on which balloons were prepared, see Fig.5.

#### Results of the test

The IMS 1600 system clearly needed more testing than had occurred before it was deployed in Tanzania. A lot of the system outputs were inconsistent within the various modules of the software.

Temperature corrections applied to radiosonde measurements were not made with the correct local time. The origin of corrections applied was not well documented and there appeared to be a significant lack of cooperation between the radiosonde supplier and the IMS software engineers. Operational measurements should be made uncorrected until reliable correction schemes can be implemented.



Fig. 4 Launch of twin flight at Dar-es-Salaam



Fig.5 Use of automatic balloon filler during the test.

A computational error for the pressure derived from geometric heights by IMS prevented operational use of the MODEM GPS radiosondes. e.g. the 100 hPa geopotential height was in error by more than 2 km.

The tracking of the radiotheodolite appeared good and able to meet user requirements for wind in the tropics, but the algorithms used for generating winds were not computing values at the resolution needed [or indicated by the software settings], i.e. 1 minute near the ground and 1 to 4 minutes in the stratosphere, see the results from the twin flight comparison in Fig.6.



Fig.6 Simultaneous measurements of wind from Vaisala (SGP) and IMS (MKII4) from flight 32 on 28.10.04

Mounting the radiotheodolite on the roof in Dar-es-Salaam hinders the automatic tracking of the radiosonde at launch. Launch routines would probably be easier if the radiotheodolite were mounted on the ground. Then, the person who launched the balloon could be responsible for checking that it was tracking on the main beam.

## General conclusions

1. Further action is required to provide a more reliable method of communicating data from Dar-es-Salaam onto the GTS. Message generations needs to be made more reliable, see Fig.7 where a considerable manual effort was required to generate the TEMP message in a suitable format.
2. Re-establishing radiosonde measurements in a location such as Dar-es-Salaam where radiosonde ascents had not been made for more than 10 years requires a concerted training effort with staff present from both the manufacturer and from a National Meteorological Service with the necessary experience in radiosonde operations.
3. It would be beneficial if a suitable expert was sent to Tanzania to complete the training started during the demonstration test and to implement improved message communications. This should be considered once IMS are ready to upgrade the system software.
4. The hydrogen generator installation worked well and is clearly capable of supporting the use of 800 or 1000g balloons on a regular basis. It is recommended that suitable funding be provided for the use of the larger balloons at Dar-es-Salaam in the long term.
5. Met Office staff were grateful for the help and enthusiasm of the staff from the Tanzania Meteorological Agency, who made the test successful.



Fig.7 Working together to generate a satisfactory TEMP message.

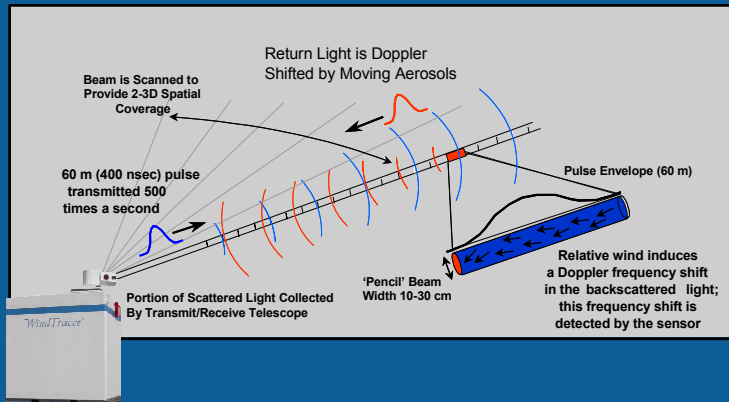


# Maturation and Application of Operational Doppler Lidar for Meteorological Applications

Stephen Hannon, James Roby  
 CLR Photonics, Inc., a division of Coherent Technologies, Inc.

## How Doppler Lidar Works

Doppler Lidar = Infrared Doppler Radar



**Infrared:** Instead of raindrops, we use natural particulates (one millionth of a meter in size)

**Doppler:** velocity/wind sensing (strength)

**Radar:** accurate position information

## Hong Kong International Airport

Installed June 2002

Windshear system works best in least needed times

ANGELA LI

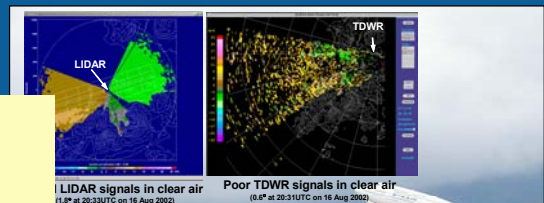
Eighty-three per cent of pilot reports of windshear at Chek Lap Kok

are associated with dry weather, it has emerged.

Eighty-three per cent of pilot reports of windshear at Chek Lap Kok are associated with dry weather, it has emerged.

Pre-WT installation article

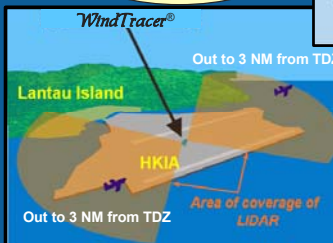
WindTracer® installed to address 83% of HKIA windshear conditions



the WindTracer® and the TDWR], in combination, will enable comprehensive detection of wind shear in all weather conditions."

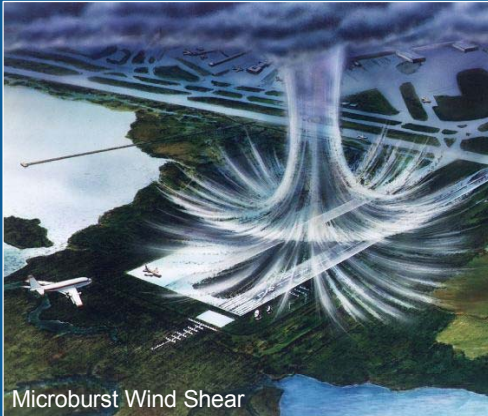
"[The WindTracer®] issued an accurate wind shear alert an hour before it happened."

Dr. H.K. Lam, Director HKO  
 13 November 2002, South China Morning Post



# Wind Shear and Turbulence Alerting

Microbursts, gust fronts, sea breezes, and terrain-induced wind shear and turbulence pose hazards to aircraft in the terminal area



Microburst Wind Shear

Pulsed Doppler Lidar scans and collects distributions of radial velocity measurements

These measurements are processed to map the hazard - strength and location

Key benefits provided by pulsed Doppler Lidar:

- negligible clutter – no side lobes
- high spatial resolution, high accuracy
- zero land acquisition costs
- similar data formats provide for ease of integration with existing radar data streams (e.g., TDWR, ITWS)

## Sample Event: 3 September 2004 Microburst at JeffCo Airport

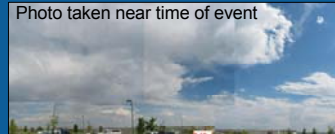
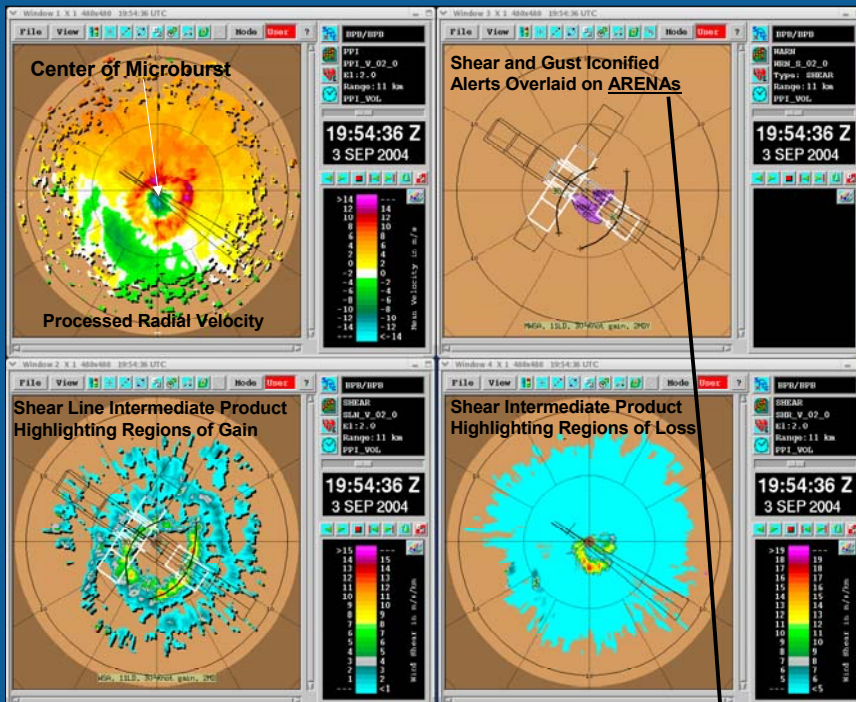


Photo taken near time of event



Graphical Situation & Virtual Ribbon Displays

“Runway 11 right departure: microburst alert, 50 knot loss, 1 mile departure”

## Automated Hazard Alerting

```

File Size
CF999 99G99 0826 ALM ON
11LA MBA 50K- RWY 999 99
11RA WSA 30K+ RWY 999 99
11TD MRA 50K- RWY 999 99
11RD MBA 50K- IMD 999 99
02-A MBA 50K- IMF 999 99
02-D MBA 50K- RWY 999 99
    
```

# Wake Vortex Sensing Supports FAA Pursuit of Capacity Enhancing Procedures

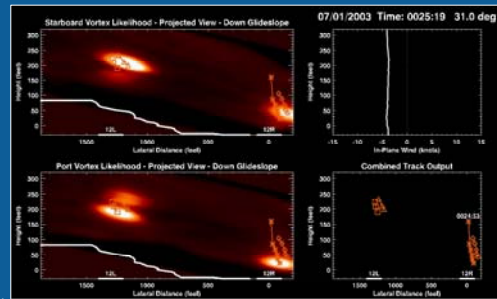
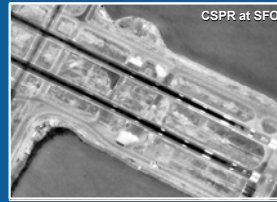
- Closely Spaced Parallel Runways
- Departures
  - Intersecting Runways
  - In-Trail Arrivals

Beneficial, phased solutions for specific problems within 3-7 yrs

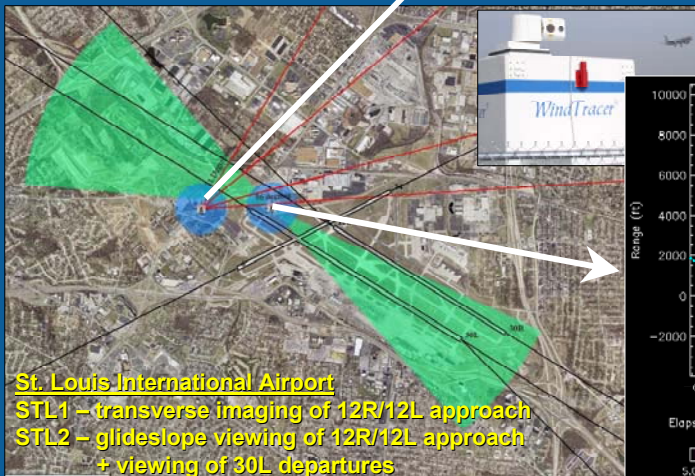
Joint program with NASA

Procedure development  
Data gathering and evaluation  
Integrated operational solutions

**Pulsed Lidar being used now to gather necessary wake safety data at STL**

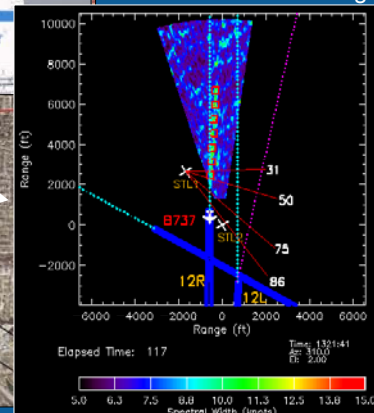


STL1 Transverse View  
Detection and Tracking



St. Louis International Airport  
STL1 – transverse imaging of 12R/12L approach  
STL2 – glideslope viewing of 12R/12L approach  
+ viewing of 30L departures

STL2 Glideslope View  
Detection and Tracking



## Summary

### Pulsed Doppler Lidar offers key & unique benefits

- Dry air (low dBZ) capability with clutter-free hazard detection
- High-density, glide-slope coverage and zero land acquisition costs
- Same sensor detects and tracks aircraft wakes

### Improved terminal area wind hazard situation awareness

- International airports adopting the technology: HKIA installed mid 2002
- SIGMET/IRIS integration demonstrates capability for automated alerting
- Airports benefit significantly with an integrated solution, especially those with limited/no wind hazard alerting infrastructure

### Wake turbulence research program relying on Doppler Lidar

- Joint FAA/NASA program: safe capacity-enhancing procedures
- STL WindTracer® installations March 2003, August 2004

# Recent Application of the Accurate Temperature Measuring (ATM) Radiosonde

F. J. Schmidlin  
NASA/Goddard Space Flight Center/Wallops Flight Facility  
Wallops Island, Virginia 23337 USA  
Tel: 1 757 824 1618; Fax: 1 757 824 1036  
E-mail: [fjs@osb.wff.nasa.gov](mailto:fjs@osb.wff.nasa.gov)

## Abstract

The Accurate Temperature Measuring (ATM) radiosonde developed at NASA's Wallops Flight Facility is now being in more applications than originally intended. A description of the method and results of new, small bead thermistors (2.5 mm diameter) fast response thermistors are presented. Results are given of recent comparisons with extremely small chip thermistors now used with the Sippican, Inc., MK-IIa and with thermistors used with the Modem, Inc. radiosonde. Comparisons indicate unexplained variations in temperature profiles that require explanation. However, temperature profile-mean-differences between the ATM radiosonde and other radiosondes, while smaller than in the past, are not yet consistent between different radiosonde instruments.

## Introduction

In this day of improved radiosonde instruments the question often asked is: have upper air instrument measurements (accuracy) really improved? The National Aeronautics and Space Administration (NASA) emphasizes measurement quality for all of its satellite data. This is especially true for *in situ* measurements since, for upper air, radiosondes often are the standard used for validation. Considerable resources are expended for validation of data related to different disciplines, yet, questions continue to be raised about radiosonde accuracy, precision, and reproducibility, especially for temperature measurements. Thermistor accuracy suffers from many influences: sensor exposure on the radiosonde; sensor calibration; sensor time constant; cloud cover; albedo; surface (earth) temperature; vertical temperature structure; processing method; and method of reporting. These influences will lead to measurement error.

World Meteorological Organization sponsored radiosonde comparisons conducted during the last two decades have identified temperature errors as the major source of radiosonde inaccuracy (Hooper, 1986; Nash and Schmidlin, 1987; Schmidlin, 1988; Ivanov et al, 1991; and Yagi et al, 1997; da Silveira, to be published). These, and other comparisons carried out in the United States (US) and United Kingdom, showed that measurement differences ranged from  $\pm 1^{\circ}\text{C}$  at 100 hPa to approximately  $\pm 2^{\circ}\text{C}$  to  $\pm 4^{\circ}\text{C}$  at 10 hPa. The scientific literature contains many citations pertaining to the evaluation of temperature measurement accuracy. Badgley, (1957) reported that at 11 hPa the radiative error of the rod thermistor, used extensively in the US, was negative during both day ( $-0.9^{\circ}\text{C}$ ) and night ( $-2.0^{\circ}\text{C}$ ). According to Ballard and Rubio (1968), the daytime error would reach  $1.8^{\circ}\text{C}$  at 10 hPa. Teweles and Finger (1960) in an effort to improve the consistency of upper air charts, examined many sets of day-night radiosonde temperatures resulting in adjustments to global radiosonde temperatures (McInturff et al, 1979). Obviously, there was considerable concern about radiosonde errors over 50 years ago. Hence, these early reports were very important catalysts for initiating radiosonde comparisons.

Other US laboratories and agencies that expend a considerable part of their budgets to obtain reliable measurements share NASA's concern about measurement quality. In particular, the US National Weather Service, US Department of Energy, US Air Force, and others, have in place programs to evaluate radiosonde temperature measurement. Data quality is a concern of weather services of all nations and, in particular, the continual carrying out of radiosonde comparisons sponsored by the World Meteorological Organization (WMO) testifies to their importance. Recognizing the lack of suitable temperature measurement standards, NASA introduced the Accurate Temperature Measuring ATM radiosonde (Schmidlin et al, 1986) and demonstrated its accuracy of  $0.2^{\circ}\text{C}$ - $0.3^{\circ}\text{C}$ .

## Descriptive Examples

Thermistors continuously try to reach equilibrium with their surroundings. Consequently, the temperature of the thermistor is reported, not the ambient temperature. The sources of radiation impinging on the thermistor include direct and indirect solar radiation; long-wave emission from the ground, clouds, the atmosphere from below and from above the thermistor. As the thermistor absorbs long-wave radiation from its surrounding environment it simultaneously emits long-wave radiation from its surface. Solar radiation reaches the thermistor directly, from reflection, and from

scattering by the atmosphere. In order to overcome the radiative influence and other thermal forces, corrections are necessary.

Using three thermistors each of a different color is necessary to characterize the emissivity and absorptivity of each, three heat balance equations are simultaneously solved. Such as

$$-HA(\Delta T) + \epsilon R + \alpha S - \epsilon\sigma AT^4 + 2\pi r_{wi}^2 k_{wi} (dT_{wi}/dl)_{l=0} = CdT/dt \quad [1]$$

Where,

H	=	convective heat transfer coefficient
A	=	thermistor surface area
$\Delta T$	=	thermistor error (T - T <sub>air</sub> )
$\epsilon$	=	emissivity of thermistor coating
R	=	long-wave radiation impinging on the thermistor
$\alpha$	=	absorptivity of thermistor coating
S	=	short-wave radiation impinging on the thermistor
$\sigma$	=	Stefan-Boltzmann constant
T	=	thermistor temperature (K)
T <sub>air</sub>	=	ambient temperature (K)
l	=	length of lead wires
r <sub>wi</sub>	=	radius of lead wires
k <sub>wi</sub>	=	thermal conductivity of lead wires
C	=	conduction
DT <sub>wi</sub> /dl	=	temperature gradients of lead wires at thermistor junction, and
dT/dt	=	thermistor temperature time/rate of change.

The two terms on the right of Eq [1], provide adjustments for conduction and thermal lag. The long- and short-wave incident radiation R and S irradiating the thermistor equals the radiative energy absorbed by the thermistor as if it were a perfect black body. When only a single thermistor is used the thermistor error  $\Delta T$  is difficult to determine unless the parameters  $\epsilon$ ,  $\alpha$ , R and S in Eq [1] are known. Laboratory measurements of  $\epsilon$  and  $\alpha$  usually are available but accurate estimates of R and S are not possible. During day and night, the incident long-wave radiation actually absorbed is proportional to the term  $\epsilon R$  and during daytime, the short-wave incident radiation absorbed is proportional to the term  $\alpha S$ . The thermistor's long-wave emission  $\epsilon\sigma AT^4$  maintains the thermistor temperature at a value lower than the ambient temperature at night while tending to reduce the size of the error during the day. The result is mostly negative thermistor errors during nighttime and at high altitudes during the day. The figures below of daytime and nighttime thermistor errors show that the radiation effect is not constant for any given thermistor but differs with the environmental background. Thermistors, other than the Sippican rod thermistor, will experience different radiative exchange, conduction, and lag; but all will have errors. This implies that a single correction (adjustment) will not be adequate under all conditions.

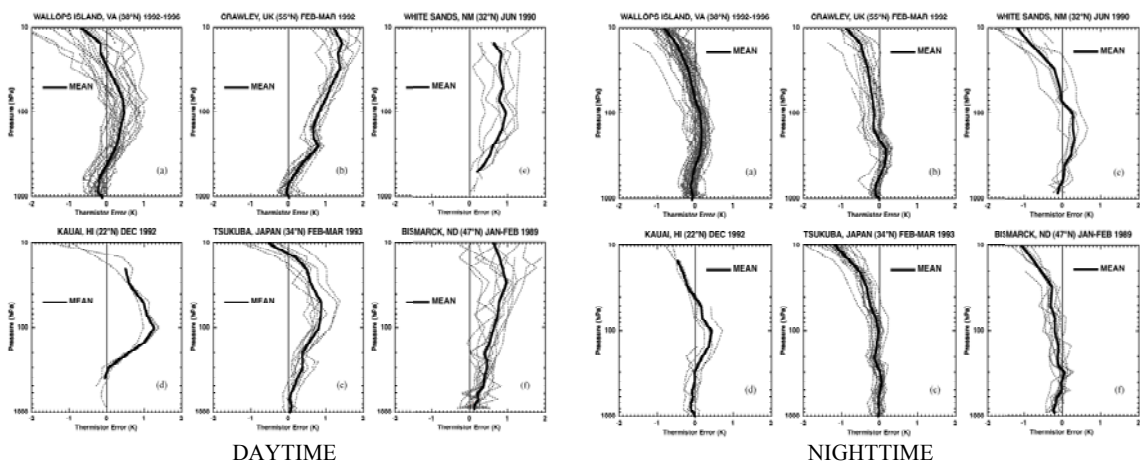


Figure 1. Describes thermistor errors resulting from different environmental backgrounds at six sites during both day and night. Nighttime results appear more stable. These examples are for the rod thermistor of early VIZ radiosondes; different radiosondes with different thermistors will experience different radiative error.

## COMPARISON BETWEEN ATM AND RS-80 TEMPERATURES

22 April 1994 1253 UTC

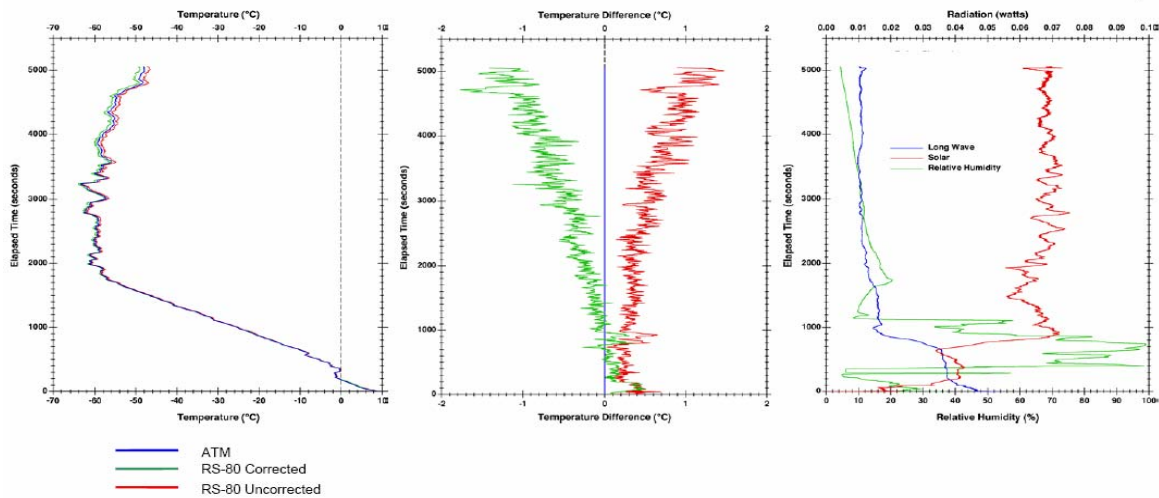


Figure 2. Comparison is shown between ATM radiosonde temperatures with the Vaisala RS-80 temperatures. This comparison was conducted at the US National Weather Service Test and Evaluation Facility, Sterling Virginia. Both instruments flew on the same balloon. Time is used as the common parameter since the pressure measurements disagreed. The Vaisala correction Table RSN-86 indicates a radiation correction at 10 hPa (in the figure at about 5100 seconds after release of the instruments) of  $-2.1^{\circ}\text{C}$ , the sun angle is approximately 35 degrees. At 100 hPa ( $\sim 2700$  seconds) the Vaisala radiation correction is given in the Table as  $-0.8^{\circ}\text{C}$ . The study suggests that the Vaisala correction is about  $1^{\circ}\text{C}$  too large at 10 hPa and  $0.4^{\circ}\text{C}$  at 100 hPa. The red curve compares the measured RS-80 temperature vs the ATM temperature and the green curve after the standard RS-80 correction is applied. The ATM radiosonde method also permits backward calculation to determine the long- and short-wave heat flux, R and S respectively. The right hand panel shows a significant increase in the short-wave flux at the top of the cloud indicated by the RH profile; long-wave decreases, and the figure also suggests that the long-wave flux in clouds is relatively constant.



Figure 3. Illustrates comparison between ATM temperature (green line) and uncorrected chip temperature (light red line) and corrected chip temperature (dark red line). The correction applied to the chip thermistor is in the proper direction, but in this example the amount of the correction is not considered to be large enough.

It has been suggested many times that radiosonde thermistors should be smaller and respond faster. Experience with the multi-thermistor ATM radiosonde indicates that the ATM method of determining the true temperature will work regardless of the thermistor size. In fact, the rod thermistor will perform as well as the new chip thermistors now adopted by Sippican. In Figure 3 an example of the ATM radiosonde temperature with the uncorrected “raw” chip

temperature and the corrected chip temperature. This example is courtesy of the US National Weather Service. The Weather Service uses ATM radiosonde results to qualify the chip thermistor for use in the radiosonde network. The example shown indicates reasonably good agreement after correction, but should not be considered a final result since many comparison observations are still needed. The use of rod thermistors should not be discounted since the atmospheric structure given by the chip thermistor is comparable to that given by the rod, as Figure 3 indicates. The time of response of the chip thermistor allows significant 'noise' to appear in the profile, nonetheless, the major atmospheric features are present in both measurements.

### **Summary**

The ATM radiosonde method has been used by NASA for a number of years. Because of its ability to provide the true atmospheric temperature it also has been used in WMO radiosonde intercomparisons, for special satellite validation requirements, more recently by the US National Weather Service, and it is proposed for use in other national tests. In this poster we have given three examples (of many available) to demonstrate the usefulness of the ATM radiosonde as a measurement standard. Work is continuing to provide a more promising radiosonde tool. New analysis methods are under investigation; one is the use of bead thermistors.

### **References**

- Badgley, F. I., 1957: Response of radiosonde thermistors. *Rev. Sci. Instr.*, 28, pp 1079-1084.
- Ballard, H. N. and R. Rubio, 1968: Corrections to observed rocketsonde and balloonsonde temperatures. *J. Appl. Meteor.*, 7, pp 919-928.
- da Silveira, R. B., G. F. Fisch, L. Machado, A. M. Dall'Antonia Jr, LK. F. Supucci, D. Fernandes, R. Marques, 200?: Report of the WMO RSO Intercomparison Experiment – Brazil. In Draft, to be published.
- McInturff, R. M., F. G. Finger, K. W. Johnson, and J. D. Laver. 1979: Day-night differences in radiosonde observations of the stratosphere and troposphere. NOAA Tech. Memo. NWS NMC 63. 47 pp.
- Hooper, A. H., 1986: WMO international radiosonde comparison Phase I, Beaufort Park, UK, 1984, WMO Instruments and Observing Methods Report No. 28, 118 pp.
- Nash, J. and F. J. Schmidlin, 1987: Final report of the WMO International Radiosonde Intercomparison. WMO Report No. 30, 123 pp.
- Schmidlin, F. J., 1988: WMO International Radiosonde Intercomparison, Phase II, 1985: Wallops Island, Virginia USA. WMO Instruments and Observing Methods Report No. 29. 113 pages.
- Ivanov, A., A. Kats, S. Kurnosenko, J. Nash, and N. Zeitseva, 1991: WMO international radiosonde comparison, Phase 3. Instruments and Observing Methods Report No. 40, WMO/TD-No. 451, 135 pp.
- Schmidlin, F. J., J. K. Luers, and P. D. Hoffman, 1986: Preliminary estimates of radiosonde thermistor errors. NASA Tech. Paper 2637. 15pp.
- Yagi, S., A. Mita, and N. Inoue, 1996: WMO International Radiosonde Comparison - Phase IV - Tsukuba, Japan, 15 February - 12 March 1993, Final Report, Instruments and Observing Methods Report No. 59, 130 pages.
- Teweles, S. and F. G. Finger, 1960: Reduction of diurnal variation in the reported temperatures and heights of stratospheric constant-pressure surfaces. *J. Meteor.*, 17, 177-193.

# INTERMET 403 MHZ RADIOSONDE SYSTEM

Rodney D. Wierenga\*, Joe Parini  
International Met Systems, Grand Rapids, Michigan

## 1. INTRODUCTION

InterMet has developed a new, digital, high-accuracy upper-air 403 MHz radiosonde with a portable ground station that is applicable to synoptic as well as military applications. The ground station is small and light weight and is easily moved to a new site. It can be set up by one person in less than 10 minutes. For non-military applications, a C/A code GPS receiver is used, while, for military applications, a P(Y)-code SAASM compliant GPS receiver is used. The radiosonde uses the same high accuracy pressure, temperature and humidity sensors used on the InterMet radiosonde developed for the U.S. National Weather Service.

Setup of the radiosonde before launch is exceptionally easy. Radiosonde unique calibration coefficients are stored in the radiosonde, power is provided by dry cell batteries, and calibration before launch is not required. This paper presents details of the design and performance of the system.

## 2. iMet 1 403 MHZ RADIOSONDE

Figure 1 shows the iMet 1 403 MHz radiosonde. It has a polystyrene case, a non-hygroscopic wrapper, a temperature-humidity boom and an elastic string for attachment to a balloon. It has four electronics boards and a 4 AA dry-cell battery pack, which has enough power to last 3 hours.

The first board is the main board with the processor and interfaces to the other boards. The second board has the pressure sensor and its electronics. The third board has the 403 MHz transmitter with its antenna. The fourth board has the C/A code receiver for non-military users, an LNA, and a GPS antenna. The GPS board is replaced by a GPS front end for military users.

To prepare the radiosonde for flight, the user removes the radiosonde from the shipping bag and opens the top of the wrapper. This allows the

user to bend the boom out to a 45 degree angle and feed the elastic string with a ring through the top of the wrapper for attachment to the balloon string. A Styrofoam door inside of the wrapper is raised to access two switches, via a hole in the wrapper, that are used to turn the power on and to set the transmitter to one of 8 frequencies in the 400.15-406 MHz range. There is no need to insert a battery pack, connect the battery pack or fill a battery with water. The mail back bag is accessible from the open flap so the user can write the launch data on the bag. A flap is provided to access the mail back bag for someone who may find the radiosonde after a flight.



**Figure 1: InterMet iMet 1 Radiosonde**

\*Corresponding author address:

Rodney D. Wierenga, PhD, InterMet Systems,  
4460 40<sup>th</sup> St SE, Grand Rapids, MI 49512; e-mail:  
[rwierenga@intermetsystems.com](mailto:rwierenga@intermetsystems.com).



The size of the radiosonde is 150 mm high by 90 mm by 90 mm and it weighs 260 grams.

While in storage, the temperature-humidity boom is bent down over the top of the radiosonde and protected by the top flap of the wrapper.

### 3. C/A CODE GPS RECEIVER

The C/A code receiver is a single chip low-power, high-quality miniature C/A code receiver. It has 12 channels with continuous tracking capability. C/A code receivers use the L1 frequency (1575.42 MHz). A hot start of the receiver can be done in 2 seconds (90%) using information from the ground station. A cold start is done in 84 seconds (90%). Outputs of GPS position and velocity are provided at a 1 Hz rate. A right-hand circular polarized micropatch GPS antenna is used which is mounted just inside the Styrofoam on top of the radiosonde. The accuracy is 8 m (90%) horizontal and 16 m (90%) altitude and 0.06 m/s (RMS per axis) with selective availability (SA) off. Smoothing of the received data is done on the ground to remove the motion of the radiosonde swinging below the balloon with a resultant wind accuracy of 1 m/s (2-sigma).

### 4. P(Y) CODE GPS RECEIVER

The P(Y) code receiver is split into two parts. A P(Y) code front end replaces the single chip GPS receiver in the radiosonde. The front end collects GPS data over a 5 to 10 msec period for each position fix. The data is transmitted by the 403 MHz transmitter down to the ground part of the GPS receiver. This data is used by a P(Y) code processor in the ground equipment to determine position and velocity of the radiosonde. With this approach, the P(Y) code is only located in the ground equipment and no classified hardware or software is in the radiosonde. There is no concern that the radiosonde may be lost and get into the wrong hands. The P(Y) code is handled in the ground receiver using the U.S. military SAASM approach. The P(Y) GPS antenna is also mounted on top of the package and is a right-hand circular polarized micropatch antenna. The position accuracy is 16 m (3-D SEP) and the velocity accuracy is 0.1 m/s (RMS per axis).

### 5. 403 MHZ TRANSMITTER

The transmitter has a crystal controlled oscillator that controls the selected channel frequency. It has a linearly polarized dipole antenna and transmits FM modulated signal containing digital PTU and GPS data. For P(Y) code GPS, the bandwidth of the transmitter is increased to

accommodate the larger amount of GPS data that is transmitted to the ground.

### 6. TEMPERATURE-HUMIDITY BOOM

The temperature-humidity boom is shown in Figure 2. It is a one-piece assembly. A high reflectance (88%) vacuum deposited aluminum coating with very low emittance (0.02) covers the thermistor, thermistor wires, and surrounding mounting structure. The humidity sensor is placed under a white cap to protect it from direct contact with water and ice.

### 7. TEMPERATURE SENSOR

The temperature sensor is a very small glass bead. Its small size allows a fast response time (<3.6 sec at sea level with 5 m/s ventilation). The aluminum coating minimizes solar and infrared heating.

### 8. HUMIDITY SENSOR

The humidity sensor is a variable capacitance device. It has a polymer dielectric insulator with a permittivity that varies with relative humidity. Due to its small size it has a fast response time (2 seconds at sea level and 20 deg C). There is very little performance degradation after long-term saturation with nearly instantaneous de-saturation. There is no performance degradation after immersion and thawing.



**Figure 2: Temperature-Humidity Boom**

## 9. PRESSURE SENSOR

The pressure sensor is a compensated piezo-resistive silicon device. It is very small and has excellent long-term stability. It is an outgrowth of the medical and automotive instrumentation industries. It has a resolution of better than 1 part in 100,000.

## 10. DATA PROCESSING

The radiosonde microprocessor manages the PTU and GPS data. The PTU data is A-to-D converted and the PTU and GPS data are transmitted in digital format. The ground station down converts the telemetered data to a baseband signal. It also performs calculations to recover the PTU and GPS data. With a C/A code receiver, a ground station GPS receiver is used to correct the position and velocity measured by the GPS receiver in the radiosonde. With a P(Y) code receiver, the data transmitted from the radiosonde is processed to determine radiosonde position and velocity.

## 11. PERFORMANCE

The performance characteristics are listed in Table 1. These are 2-sigma numbers, meaning that 95.5% of the errors in the measurements are within the listed numbers.

## 12. GROUND EQUIPMENT

The ground station is housed in an unbreakable, watertight, dustproof, chemical resistant and corrosion proof case. It has a 403 MHz receiver, a decoder, a processor, a GPS receiver, a laptop computer, and rechargeable batteries. In the C/A code case, for non-military applications, the GPS consists of a GPS receiver, similar to that in the radiosonde, for differential corrections. In the P(Y) code case, for military applications, the GPS receiver consists of a SAASM compliant receiver for processing GPS data from the radiosonde. A notebook computer is included to process P(Y)-code receiver data, for military applications, and to process and display weather data. The size of the case is 48.6 cm by 39.2 cm by 19.2 cm and it weighs 9.1 kg (20 pounds).

A second case of the same type is used to carry the antennas and antenna cables. Enough cable can be carried to allow for remotely locating the GPS and 403 MHz antennas up to 100 meters away from the ground station. Several different antennas options are available.

**Table 1: Performance**

<b>Pressure</b>	
Range	2 to 1070 hPa
Resolution	0.01 hPa
Accuracy	±1.8 hPa (> 400 hPa, -80 to +40 Deg C) ±0.5 hPa (< 400 hPa to 4 hPa, -80 to +40 Deg C)
Response Time	1 sec
<b>Temperature</b>	
Range	-95 to +50 deg C
Resolution	0.01 deg C
Accuracy	±0.3 deg C (-80 to +40 deg C)
Response Time	3.6 sec (1013 hPa, -80 to +40 deg C, ventilation speed of 4.5 to 5.0 m/s)
<b>Humidity</b>	
Range	RH: 0% to saturation
Resolution	0.1%
Accuracy	±5% (-60 to +50 deg C) ±2% change after near saturation
Response Time	2 s (5 m/s vent speed, 1013 hPa, +25 deg C) 60 s (5 m/s vent speed, 1013 hPa, -35 deg C)
<b>GPS Velocity</b>	
Range	±150 m/s (north & east)
Resolution	0.1 m/s
Accuracy	±0.06 m/s instantaneous, ±1 m/s smoothed (estimated wind)
<b>GPS Position</b>	
Range	lat, lon: any alt: -50 m to 42 km
Resolution	lat, lon: 0.01 arc sec alt: 0.1 m
Accuracy	lat, lon: ±10 m alt: ±30 m

### 13. CONCLUSIONS

This InterMet 403 MHz upper-air system is light weight, portable, rugged and has excellent accuracy. It can be used for either military or non-military applications. For non-military application, a commercially available GPS receiver is utilized, while for military applications, a SAASM compliant GPS receiver is used.

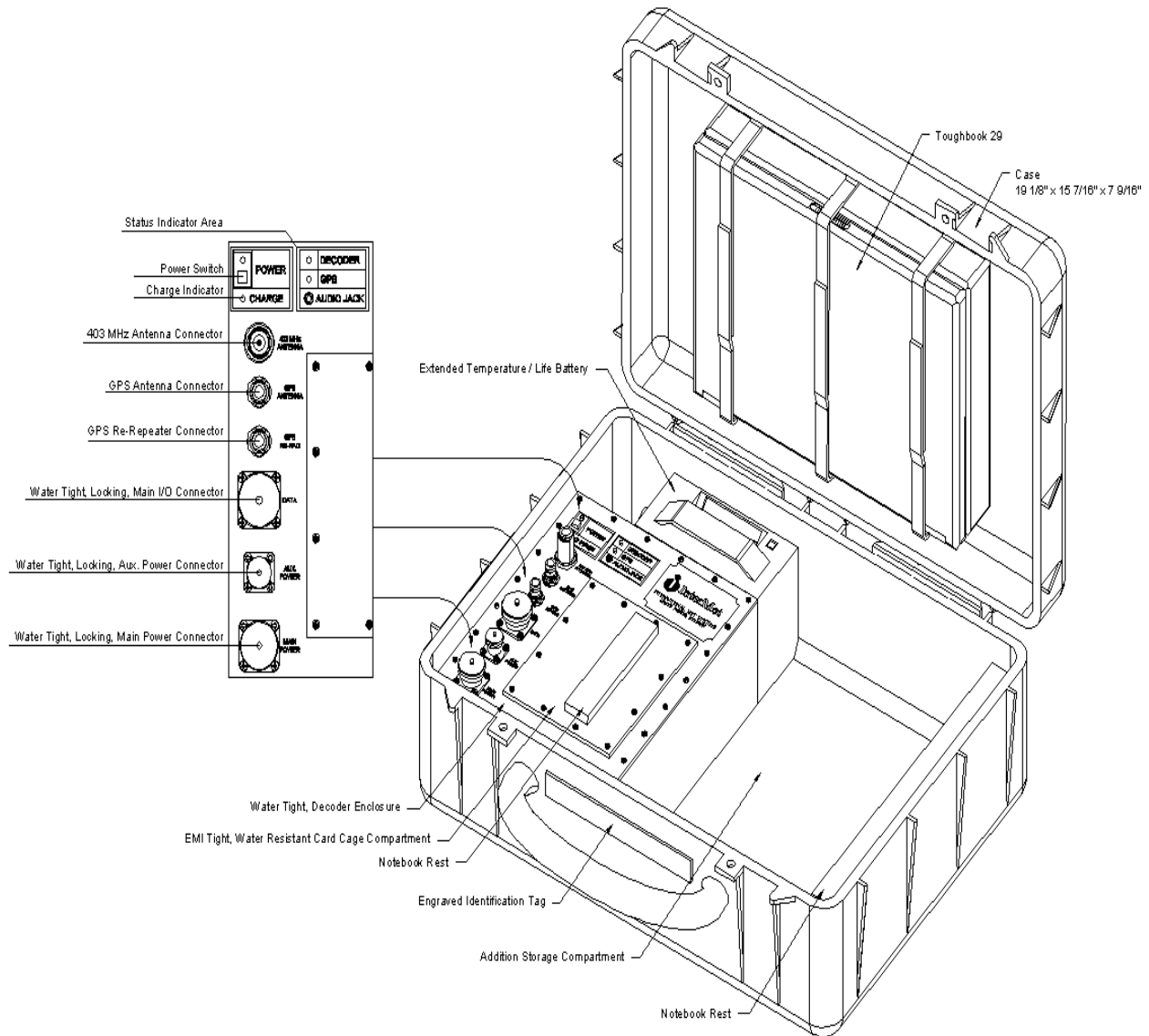


**Figure 3: Portable 403 MHz Radiosonde System Ground Station**

# Polarization Diversity for the National Weather Service (NWS), WSR-88D radars

Dusan S. Zrnica  
National Severe Storm Laboratory  
Norman, OK 73069, USA

In the early eighties the NOAA's National Severe Storms Laboratory (NSSL part of National Ocean and Atmospheric Administration) initiated a study to determine utility of polarization diversity for weather observations. This study culminated with completion of the Joint POLarization Experiment (JPOLE) which unequivocally demonstrated great potential of polarimetric diversity radar.

Common polarization bases are linear and circular. Because most hydrometeors are horizontally oriented the largest contrast in polarization measurements occurs between horizontal and vertical backscattered electric fields. Therefore, and for other practical reasons the chosen scheme employs simultaneous transmission and reception of horizontally and vertically polarized waves. With this scheme all current data acquisition modes and scanning strategies on the WSR-88D (Weather Surveillance Radar-1988 Doppler) remain as is, and the impact of polarimetric implementation on the existing algorithms and products is minimal. The National Weather Service in the US intends to implement this scheme for polarimetric measurements at the end of this decade.

Intense analysis of the outcome of JPOLE experiment proved that polarimetry can address a variety of problems in operational meteorology, like:

- C Improve quantitative precipitation estimation
- C Discriminate hail from rain, possibly gauge hail size
- C Identify precipitation type in winter storms
- C Measure precipitation in the presence of ground clutter
- C Identify electrically active storms
- C Identify presence of insects, birds, and chaff
- C Improve the accuracy of VAD winds
- C Provide initial conditions and constraints to numerical models
- C Identify aircraft icing conditions

Tested were the following polarimetric rainfall estimators:

$$R(Z) = 1.70 \cdot 10^{-2} Z^{0.714} \quad (Z = 300 R^{1.4})$$

$$R(K_{DP}) = 44.0 |K_{DP}|^{0.822} \text{sign}(K_{DP})$$

$$R(Z, Z_{DR}) = 1.42 \cdot 10^{-2} Z^{0.770} Z_{dr}^{-1.67}$$

$$R(K_{DP}, Z_{DR}) = 136 |K_{DP}|^{0.968} Z_{dr}^{-2.86}$$

where

$$[R] = \text{mm} / \text{h} \quad [Z] = \text{mm}^6 \text{m}^{-3} \quad [K_{DP}] = \text{deg} / \text{km} \quad Z_{dr} = 10^{0.1 Z_{DR}(\text{dB})}$$

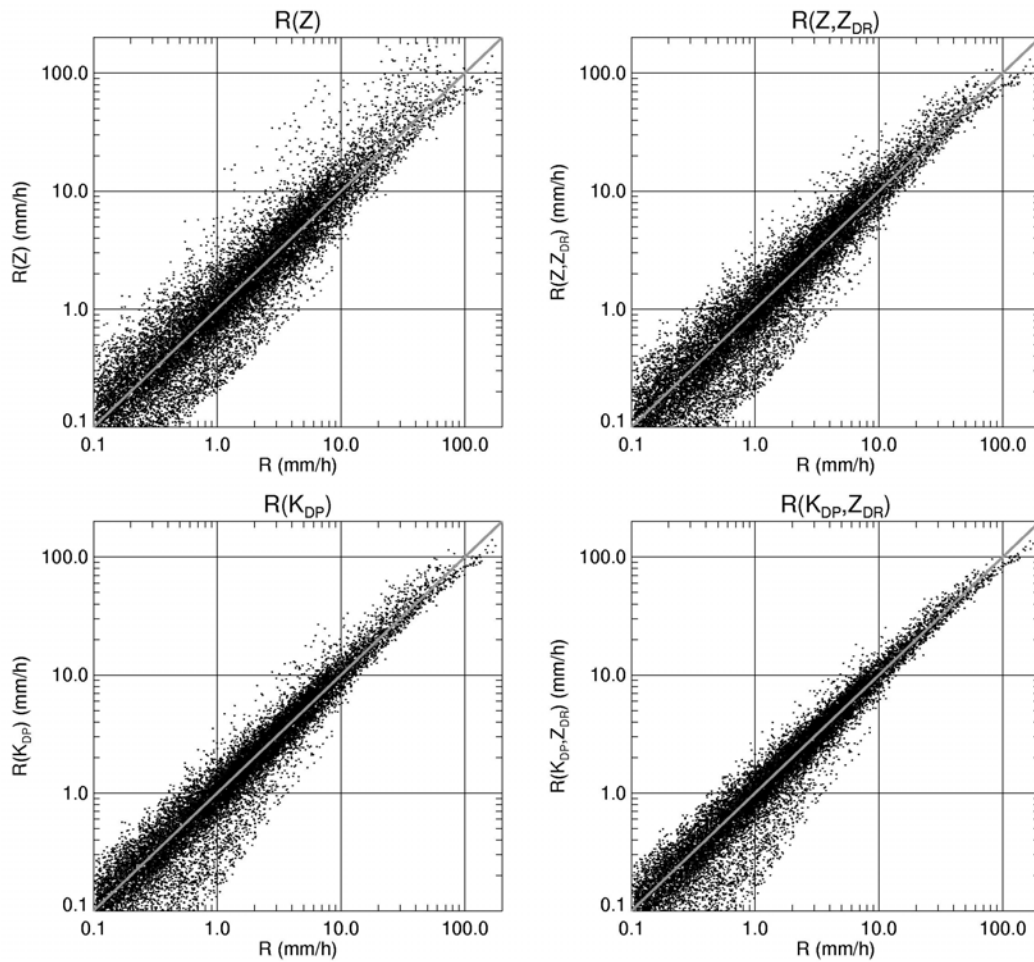


Fig. 1 Sensitivity of different rainfall estimators. Both the actual rain and polarimetric estimates were computed from disdrometer measurements.

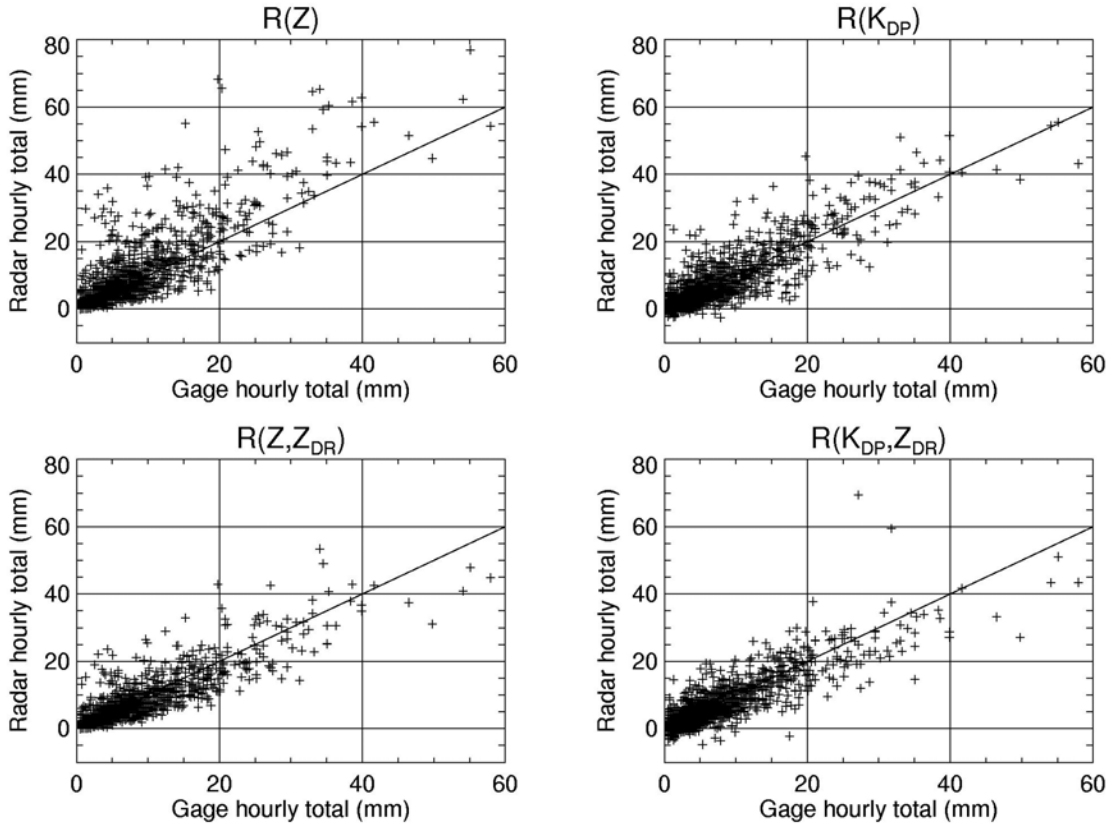


Fig. 2 Sensitivity of different rainfall estimators. The actual rain total is from gages and polarimetric estimates were measured with the radar at 40 to 90 km from the gages (Fig. 3).

Further the following synthetic rainfall estimator was also evaluated:

$$R = R(Z) / f_1(Z_{DR}) \quad \text{if } R(Z) < 6 \text{ mm} / h$$

$$R = R(K_{DP}) / f_2(Z_{DR}) \quad \text{if } 6 < R(Z) < 50 \text{ mm} / h$$

$$R = R(K_{DP}) \quad \text{if } R(Z) > 50 \text{ mm} / h$$

with

$$R(Z) = 1.7010^{-2} Z^{0.714}$$

$$f_1(Z_{DR}) = 0.4 + 5.0 |Z_{dr} - 1|^{1.3}$$

$$R(K_{DP}) = 44.0 |K_{DP}|^{0.822} \text{sign}(K_{DP})$$

$$f_2(Z_{DR}) = 0.4 + 3.5 |Z_{dr} - 1|^{1.7}$$

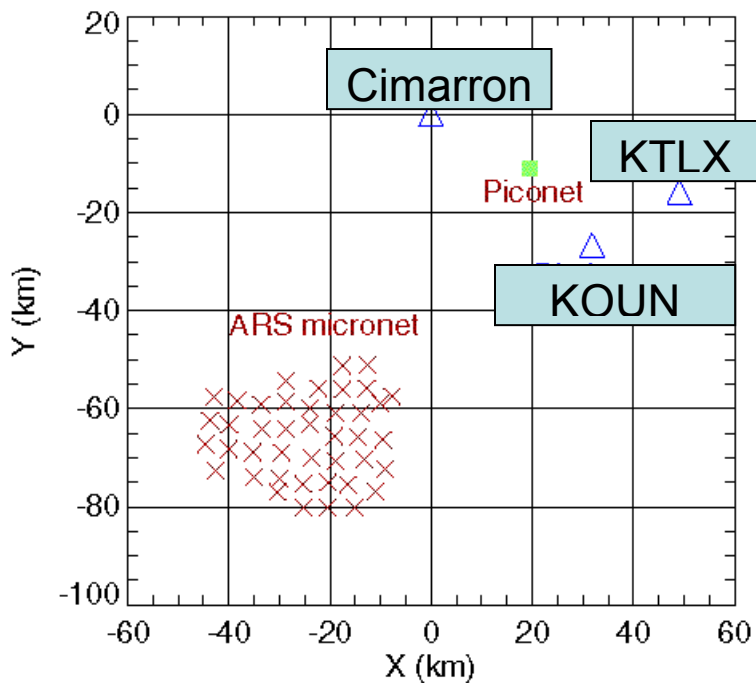


Fig. 3 Location of gages (ARS) and polarimetric radar KOUN.

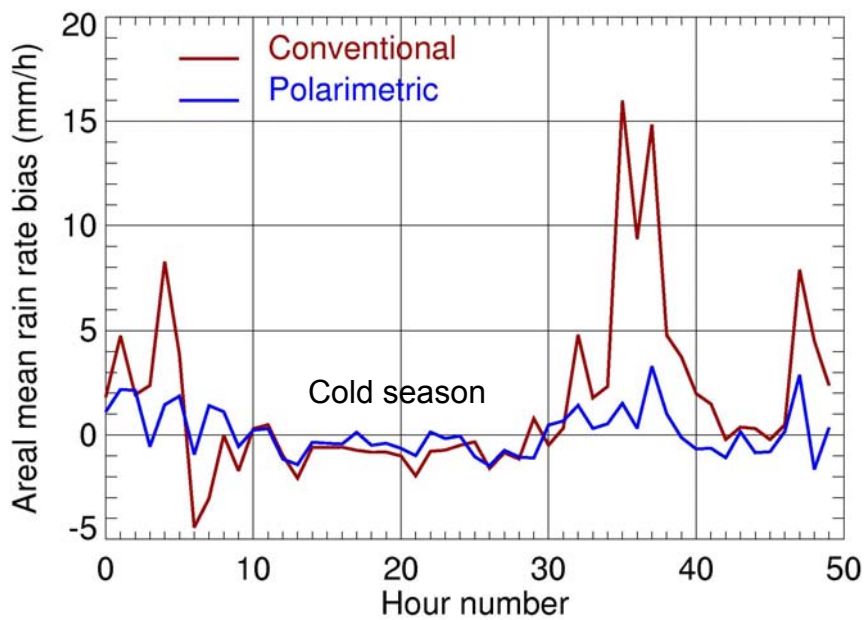


Fig. 4 Mean bias for conventional R(Z) and synthetic polarimetric measurements. Hourly accumulations are from events over two years.

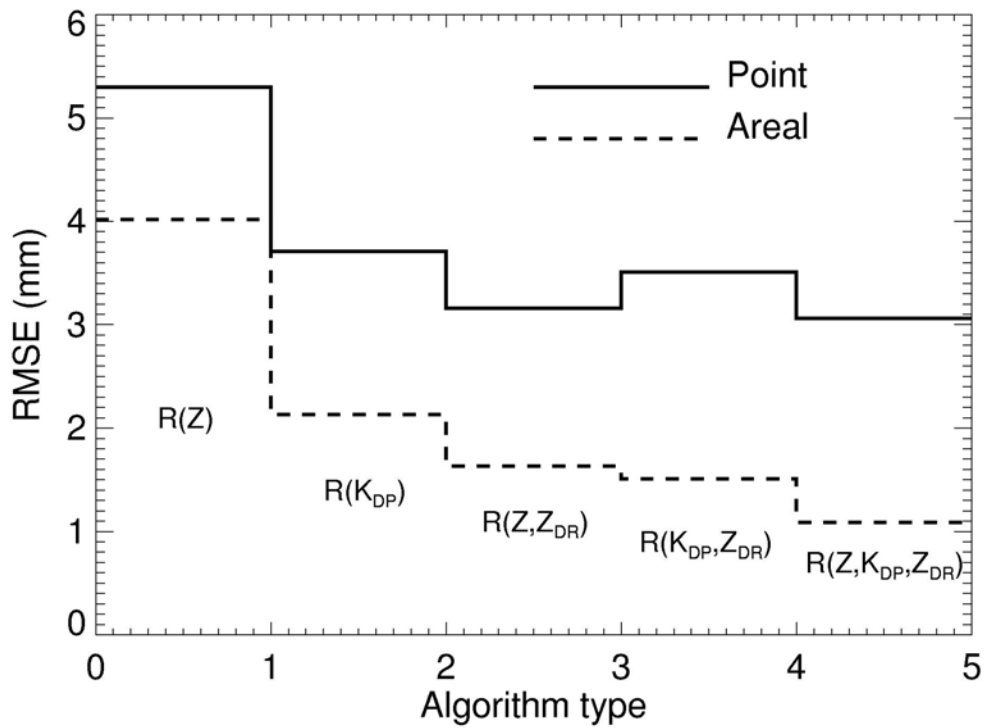


Fig. 5 RMS difference between gages and radar estimates of rain accumulations for areal and point comparison.

### Rain Measurement in the Bright Band with $R(Z)$ and $R(K_{DP})$

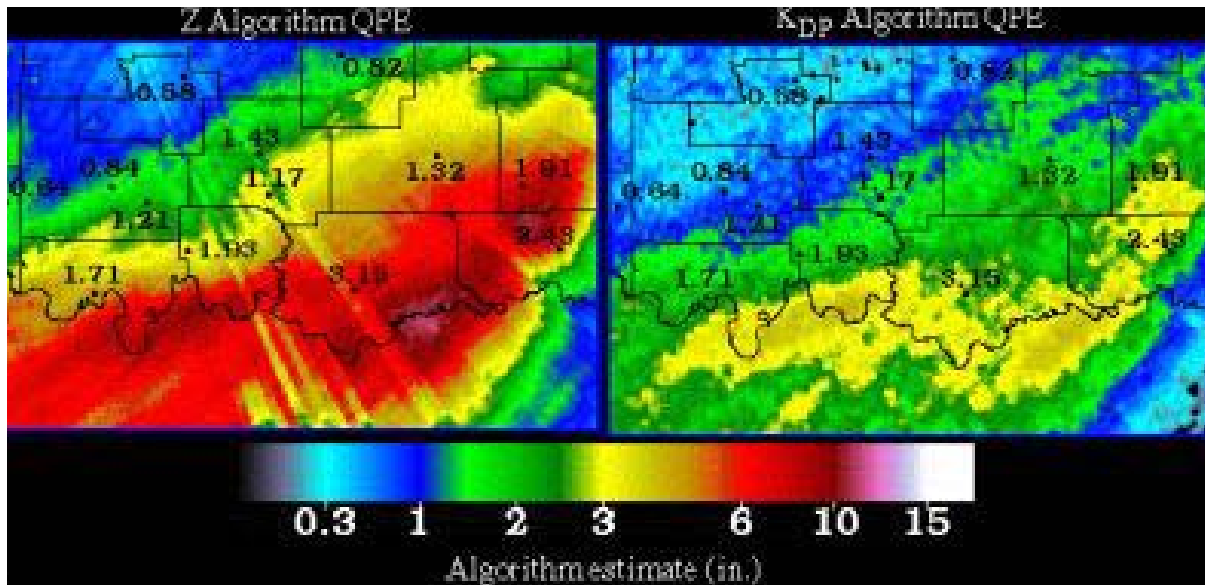


Fig. 6 Two day accumulation of rain (Oct 2002); gage estimates are superposed.



## Classification of Hydrometeors

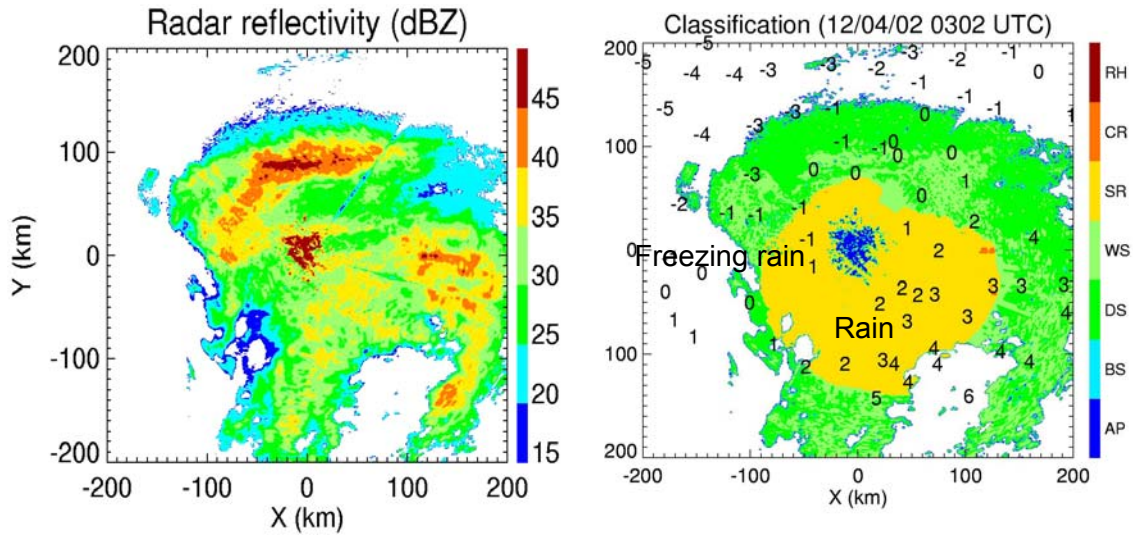


Fig. 7 Discrimination between rain, freezing rain, and snow. Temperature on the ground is superposed.

Transition between rain and snow can be detected, but for identifying freezing rain temperature on the ground is needed.

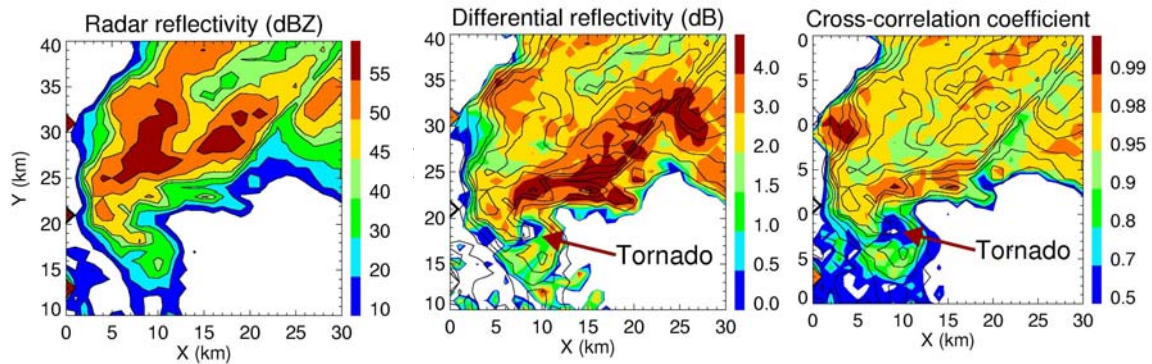


Fig.8 Tornado identification in the fields of differential reflectivity and cross-correlation coefficient.

Once tornado is on the ground it lofts debris which can be detected. Therefore polarimetric signature can confirm tornado on the ground; it can also confirm tornado demise. But it offers no lead time.

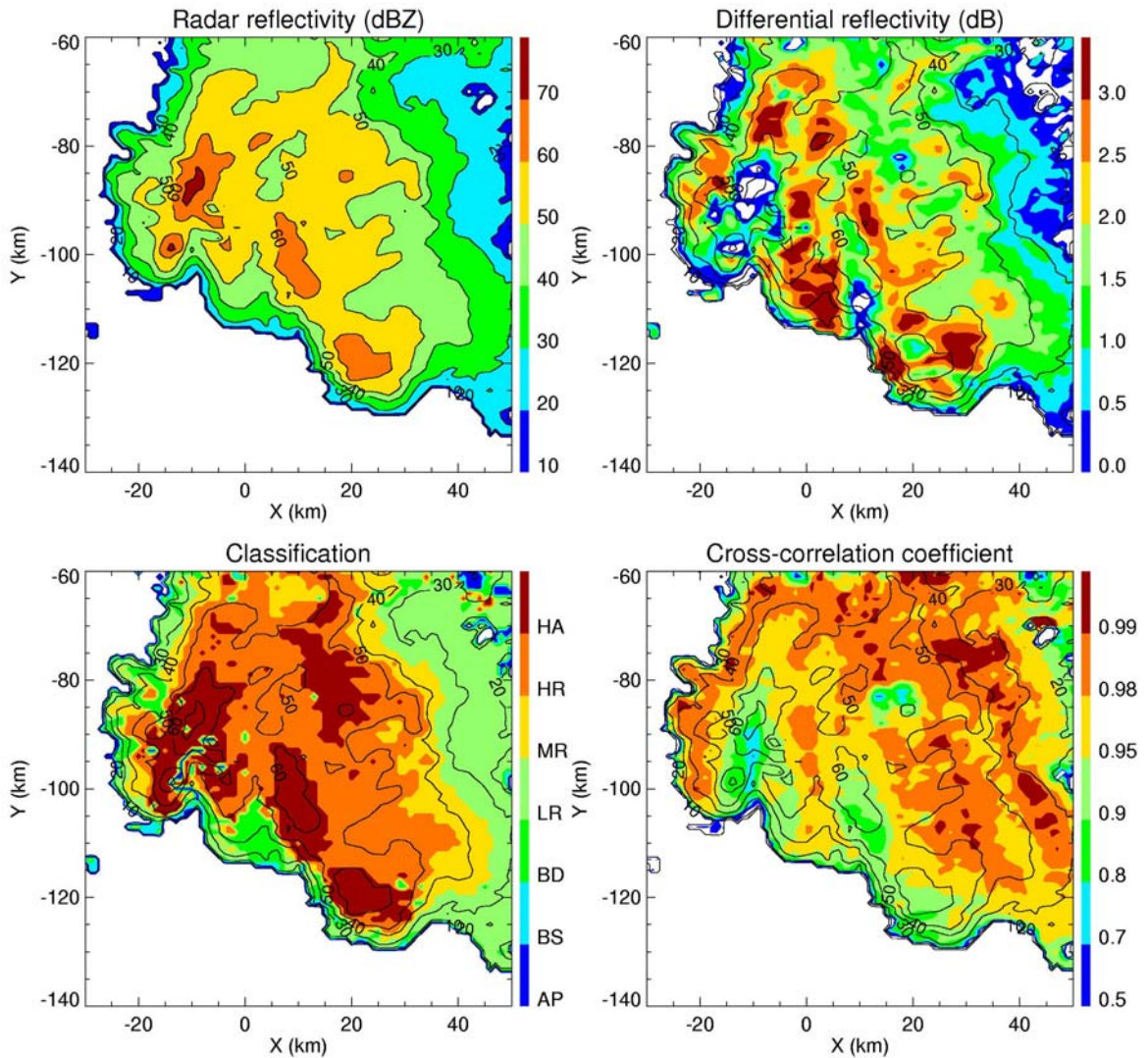


Fig. 9 Detection of Hail. Reflectivity, differential reflectivity and cross correlation fields in a hail storm. HA=hail and rain, HR=heavy rain, MR=moderate rain, LR=light rain, BD=rain with large drops, BS=biological scatterers, and AP=ground clutter (ordinary of seen via anomalous propagation).

Hail detection is direct, based on the values of differential reflectivity (small) and reflectivity (large).

#### Hail Detection Statistics

Polarimetric method	Conventional method
POD = 88%; FAR=39%; CSI=0.56	POD=100%; FAR=11%; CSI=0.89

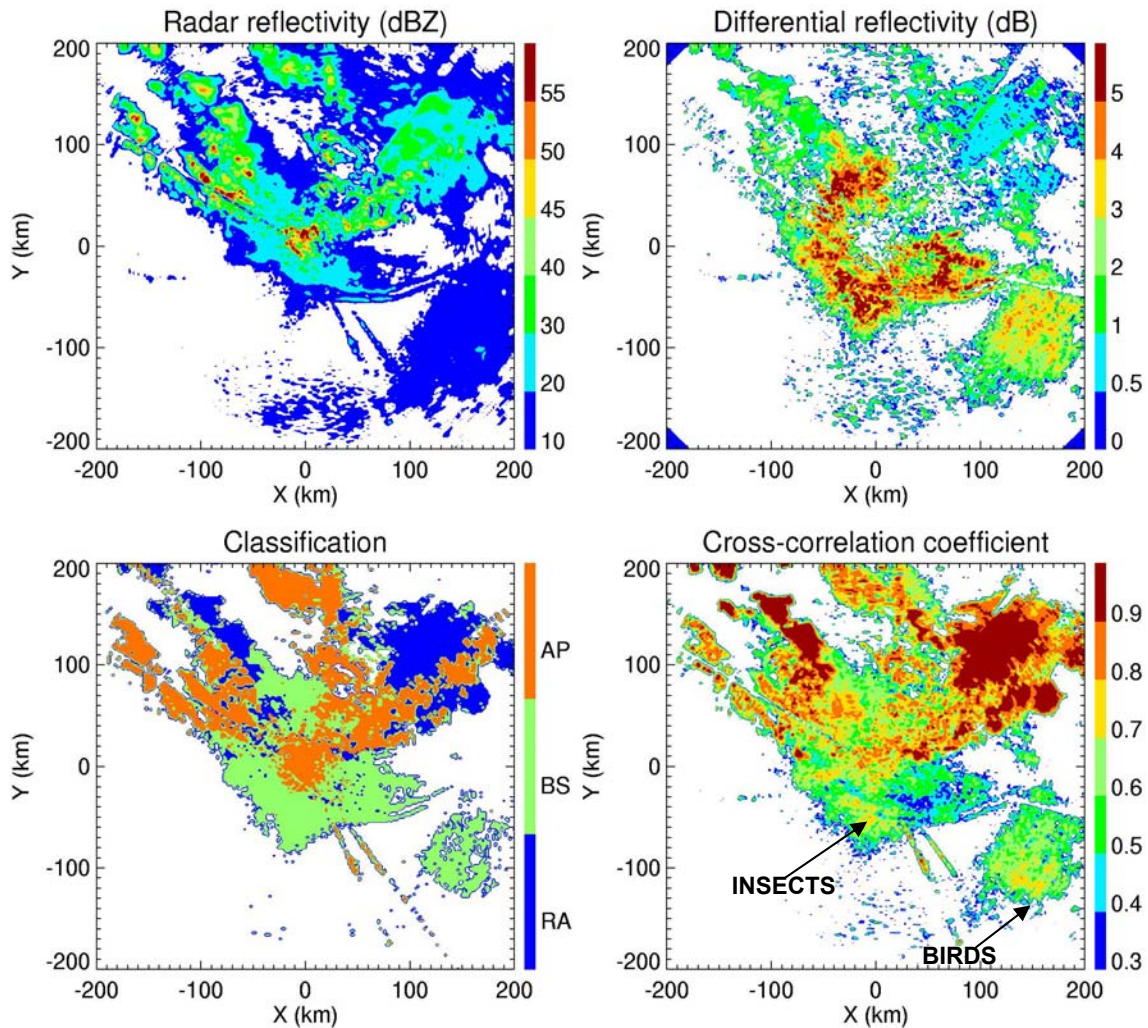


Fig. 10 Discrimination between rain (RA blue), biological scatterers (insects and birds BS green) and ground clutter (including returns via anomalous propagation AP orange).

Several significant improvements in quantitative measurements, data quality, and classification of hydrometeors have been proven, this lead to a decision for polarimetric upgrade of the network. Other less obvious improvements are under investigation.

# **Radar technique for the study of structure and dynamics of the hail-storm processes**

**Kh.A.Imamdjanov**

Centre of Hydrometeorological Service at the  
Cabinet of Ministers of the Republic of Uzbekistan

Complex of atmospheric phenomena (as stormy winds, gusts, hail, thunderstorms, etc.) is related to convection. The most dangerous of them are the hail and showers which cause the floods and wash out of soils from agricultural fields. Since 60s of XXc. in Uzbekistan the measures against the hail began to be introduced. The radar stations (RS) were used for those measures and demonstrated the possibilities of the investigation of structure and dynamics of the convective cloud.

The radar equipment as a measuring system has a fixed range of linear dimensions being detected by the clouds (cells). The working out of the inner structure in detail makes the overall area of the detection of the cloud system and thickness of the atmospheric layer narrower. The other contradictions in the demands to the measuring techniques are also revealed in the use of the hail processes. The process of development is rather short (30-90 min.). For the study of the processes dynamics it is needed to have at least 5-7 moments of the “instant” survey of clouds with the linear dimension of 20-150 km and volume of  $10^7 - 10^{10} \text{ m}^3$ .

In this concern, the main task of the radar observations is to get the three-dimension pattern of the cellular structure of the hail-storm clouds and its temporal evolution.

For this the photographic registration of the radar echo pattern was made with the indicator of circular view (ICV) and indicator of “distance – attitude” (IDA) with the different angles of aerial incline and different azimuth. The angle of the aerial incline was selected with the purpose to get the pseudo-horizontal sections of the strongest convective cells or of the centre of the hail-storm process at 1, 3, 6, 9 and 12-km atmospheric layers a.s.l. After the photo-survey of the radar echo on ICV the photographic registration of radar echo pattern was made on IDA in the azimuth of the maximum radar echo of convective cells and zone of the weak radar echo which corresponds to the zone of updrafts feeding the strong convective cells. The photographic survey on ICV and IDA was carried out within the iso-contours of the radar intensity by the step-by-step regulation of intensification of ULF of the radar receiver or by the introducing of attenuation in VHF-tract in the output of the receiver every 12db. Afterwards the measurements of the maximum radar characteristics of the convective cells: radar reflectivity ( $\eta \text{ cm}^{-1}$ ), height of the position of the radar echo maximum ( $H_{\max}$ , km), elevation of the zone of the intensified radar echo ( $H$ , km) and height of the upper limit of the radar echo ( $H$ , km) was made.

The photographic registration of the radar echo pattern on ICV, IDA as well as the measurement of the maximum radar characteristics compiled one series. (Fig.1) After the completion of one series the next one began immediately. The duration of one series of observations was about 7 – 10 min. Such time interval provides for the more or less successive pattern of radar echo from one series to another. Then it makes it possible to follow the transformation of their structure and dynamics of their development when analyzing the temporal evolution of the hail clouds and separate convective cells. The observations were conducted during the whole period of development of the hail-storm processes within 100km radius. 10 – 40 series of observations were made during the period of the hail-storm processes development.

On the base of results of photographic registration on ICV the patterns of radar echo of the hail-storm processes were made in a form of pseudo-horizontal cross-sections at the height of 1, 3, 6, 9 and 12 km a.s.l. at one scale of the multi-contour iso-echo every 12 db. The radar-echo patterns for the different height were created using the superimposing of their spatial position in such a way which allows to follow the tilt of the cells and change of their configuration with elevation. Under the radar-echo pattern the characteristic structure of it on IDA was placed on ICV also in a form of a multi-contours iso-echo, every 12 db.

Similarly, the radar-echo pattern resulted during the observations of the successive series were adjusted one with another taking into account the spatial position of the convective cells to provide a visual understanding of the direction of displacement of the whole hail-storm process and its separate convective cells.

Using the information about the successive positions of the cloud system and convective cells the pattern of trajectories of the whole process and of its separate convective cells was created. The vector of the leading flow revealed as the vector of the medium wind at 700 and 500 hPa surfaces was defined. The analysis of such patterns makes it possible to study the joint positions of the leading flow vectors and movements of the hail-storm clouds in a whole and its separate convective cells. It also gives an idea about the behaviour of as spatial extension of the precipitation-forming process (permanently, discretely-permanently and discretely). Besides, the possibility is given to follow the regularity and location of origination of radar-echoes of new convective cells, etc.

Automatic meteorological radar MRL-5 is designed on the obtained results. It fulfils the following operations:

- identification of the weather phenomena
- forecasting the dynamics of the weather phenomena development during 5, 10, 15 and 20 minutes
- showing the spatial pattern of the cloud and precipitation fields on the background of the locality map at the distance up to 240 km
- chart of the severe weather phenomena (gusts, thunderstorm, hail, shower, etc.) on the background of the map of administrative borders, regions, etc.
- evolution of the cloud processes, direction and speed of the cloud movement, cloud systems and severe weather phenomena
- chart of the fields of precipitation intensity and quantity at the distance up to 150 km
- measurement of the cloud parameters at the distance up to 150 km
- controlling the operations on the weather modification
- distinguishing between the objects of modification
- controlling the results and evaluation of the effectiveness of the weather modification
- print out the information by the user request
- archiving and representing of all collected information
- transfer of the received information to all interested users

Using the radar data, the parametric model of cloudiness of a hail cloud was developed which gives the possibility to detect the evolution of cloudiness and cells, phases of their development, age and dissipation, cloud types, etc.

Finally we would like to mention that the developed radar technique of the hail-storm processes observation is successfully being used at the hail-suppression teams of Uzbekistan, Tajikistan and Northern Caucasus.

# **RADAR TECHNIQUES OF METEOROLOGICAL EVENTS DETECTION BY POLARIZATION CHARACTERISTICS OF SIGNAL**

**Askamov F., Imamjanov Kh.**

Centre of Hydrometeorological Service at the  
Cabinet of Ministers of the Republic of Uzbekistan

During the flights in the severe meteorological conditions the thunderstorm clouds, zone of the increased turbulence, hail and intensive precipitation are the most dangerous phenomena. Up to present considerable theoretical and experimental materials related to the investigation of possible means of the detection of the listed meteorological phenomena using radar equipment are collected.

In the meteorological radar operation the technique of the detection of the thunderstorm clouds danger is applied basing on variation of the vertical profile of the radar reflectivity.

This technique is based on the fact that in the profile of the vertical reflectance a well-marked maximum is revealed in the field beneath zero isotherm, i.e.

$$Y = H_{\max} I_g Z - \text{criterion of thunderstorm danger}$$

Polarization technique has a significant advantage comparing with the above mentioned techniques.

First, the hail processes are always accompanied by the electric discharges. That is why any of the technique of the detection of thunderstorm clouds danger allows to identify the clouds which are dangerous due to their electric activity.

Second, the polarization characteristics of the electrically active clouds have peculiar features which distinct them from the common cumulo-nimbus. These peculiarities are related to the orientation of the ice crystals or deformation of drops cause by the electric field. First time this effect was detected in experimental way in optical band by different changes of the solar light reflected from the cloud crystals during the thunderstorm discharges. Later it was detected with the radar signal by the change of depolarization value on circular polarization which occurred simultaneously with the lightning discharge. However, in average, the value of polarization was near the polarization value in non-thunderstorm cloud.

In cumulo-nimbus the differential reflectivity in the layer above zero isotherm is near 0 dB. With the occurrence of electric field the differential reflectivity for the clouds producing discharges of the cloud – ground type is negative and is -0.4 – 0.6dB, while for the discharges between the clouds the value of differential reflectivity is more than zero and is 1,5 – 2,5 dB. The typical features of the temporal trend of differential reflectivity during cloud – ground discharges are sudden changes from 0.4 to 0.6 dB simultaneously with the electric discharge.

During the measurement of the turbulence in clouds and precipitation the difference between the Doppler radar frequencies of the adjacent resolvable volumes when using non-coherent radar station is used. The signal received from radar station after the amplitude limitation is transmitted to the first input of the phase detector, while the same signal is transmitted to the second input with 3,3 microsecond delay. With this, in the output of the phase detector a signal appears which is proportional to the difference between the phases of signals from the reflecting volumes shifted along

the radar beam 500 m one from another. The difference between phases is saved until the next impulse when it is subtracted and similar difference on the next impulse.

If the relative velocity on the two mentioned volumes equals zero, then the mentioned phase difference is zero, too. The fields with the increased phase difference can be identified as the areas with the increased turbulence.

If the clouds are of the mixed character, then the echo is formed both by the drops and crystals, and its depolarization differs from the depolarization of the homogeneous clouds.

The value of depolarization in the mixed cloud can be calculated by summation of echoes reflected from the both cloud components separately for each orthogonal plane. Thus, we derive the following formula for the estimation of depolarization from the mixed cloud:

$$\Delta P_{mixed} = \Delta P_{1cr} \{ (\eta II_{drops} / \eta II_{cry}) + 1 \} - 1 \quad (2)$$

Here  $\Delta P_{1cry}$  - is the polarization value which can give the purely crystal cloud;  $\eta II_{drops} / \eta II_{cry} = m$  - is the relationship between the share of drops in the radar reflectivity of the drops and crystals. Fig. 1 shows that when the drop contribution to the radar reflectivity is much more (10-15 times), than the crystal contribution, then the impact of the last ones is almost negligible, i.e. the depolarization component is sensitive to a small number of crystals.

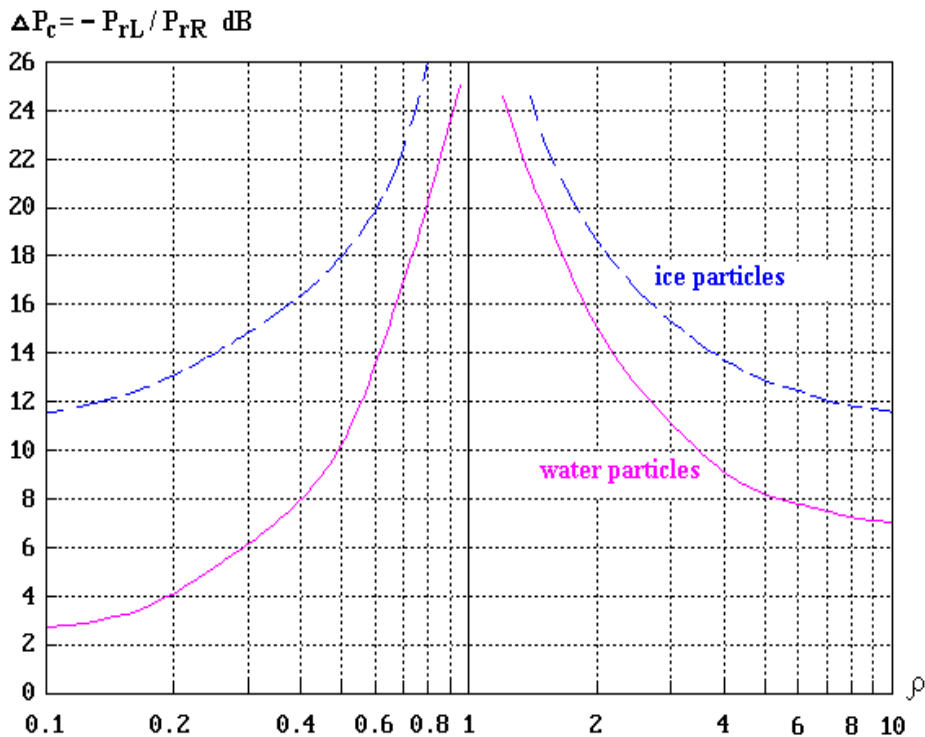


Fig.1 Relationship between the factor of circle depolarization and the particles form

The simultaneous changes of depolarization and differential reflectivity extend the possibilities of polarization techniques in the definition and study of microphysical and integral characteristics of the clouds and precipitation significantly.

Let's consider the results of computed values of differential reflectivity of crystal clouds using the horizontal radar sounding at different elevation levels.

The most probable shape and form of the crystals is given vis the air temperature. Calculation for the needles (cylinders) is made at their arbitrary orientation in horizontal plane while for the plates (disks) it is given in the vertical plane (Table 1).

Table 1

**Table of calculated values of differential reflectivity of crystal clouds at the horizontal radar sounding at different elevation**

Air temperature, °C	Type of crystals, shape	ZdR
-2 ÷ -5	Thin plates 1:50, 1:100	9.1 ÷ 9.7
-5 ÷ -7	Needles 1:10, 1:50	3.4 ÷ 4.8
-7 ÷ -10	Thin plates 1:50	9.1
-10 ÷ -16	Thick plates 1:10	7.7
-16 ÷ -20	Columns 1:5, 1:10	2.7 ÷ 3.4
-20 ÷ -30	Columns and three-dimensional form 1:5, 1:3	2.0 ÷ 2.7
-30 ÷ -35	Columns 1:5, 1:10	2.7 ÷ 3.4

As ZdR does not depend on the concentration of dissipative particles, then comparing the obtained ZdR values with the table values it is possible to estimate the relative contribution of drops and crystals separately to the reflectivity, i.e., to get the value characterizing the mixture.

With the known relationships between the drops and crystals in the cloud or its zones it is possible to determine the probability of icing.

Polarization technique of detection of possibility of hail fall from the cloud was based on the measurements of depolarization value.

During the measurements with the radar it was found out that the hail was falling from the cloud in the cloud zone where the depolarization was more then 10 ... 12 dB.

The application of differential reflectivity in the radars with the double polarization allows not only more accurate detection of hail presence in a cloud, but also to decrease the reflectivity level to such extent when the hail presence definition is possible since 32-35 dB using only depolarization and up to 27-28 dB with the differential reflectivity.

Finally, it should be noted that polarization techniques provide for the detection of the dangerous meteorological formations, to identify the reflection sources, to monitor the environment and to apply them in the solution of the applied problems on the atmospheric studies and relevant processes.



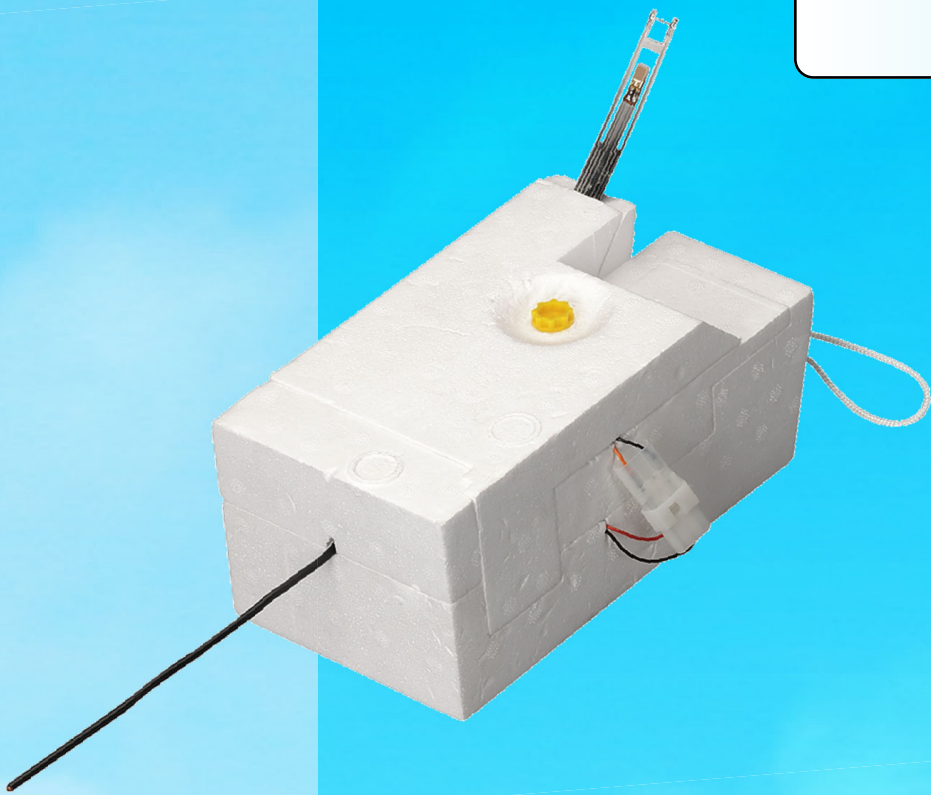
# Development of a Mean Intensity Radiometer for GRAW Radiosondes

Important applications of the new Radiosonde-based Mean Intensity Radiometer:

It offers the possibility to correct temperature measurements which are affected by solar radiation with real - measured - data (Note that the sensor has about the same dimension and shape as the temperature sensor).

The mean intensity is proportional to the atmospheric heating rate caused by solar radiation. Hence this radiative quantity measured with radiosondes can play an importance role in climatologic research.

The mean intensity which is also know as "actinic flux" is proportional to the photodissociation rate of chemical components, such as  $\text{NO}_2$  ( $\text{NO}_2$  -(UV radiation)->  $\text{NO} + \text{O}$ )



GRAW Radiosondes GmbH & Co and Kipp & Zonen BV started recently the development of a new miniature "Mean Intensity Radiometer" for balloon sounding applications. The glass fiber based Mean Intensity Radiometer has a diameter of only 3 mm and a (nearly) isotropic sensitivity, shown in Figure 1.

On 21st of December 2004 a prototype Mean Intensity Radiometer was launched with an adapted GRAW radiosonde. Results of this test sounding are depicted in Figure 2. It shows the typical curved profile of the mean intensity which increases with decreasing height due to multiple scattering before it eventually decreases again as a consequence of extinction.

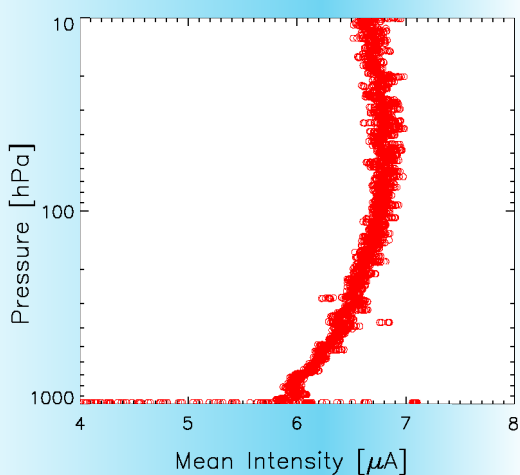


**Figure 2:** Mean intensity profile as measured with the prototype Mean Intensity Radiometer on 21st of December 2004. It shows the typical curved profile of the solar mean intensity in a cloud-free atmosphere. The maximum height of this sounding was about 50 hPa.

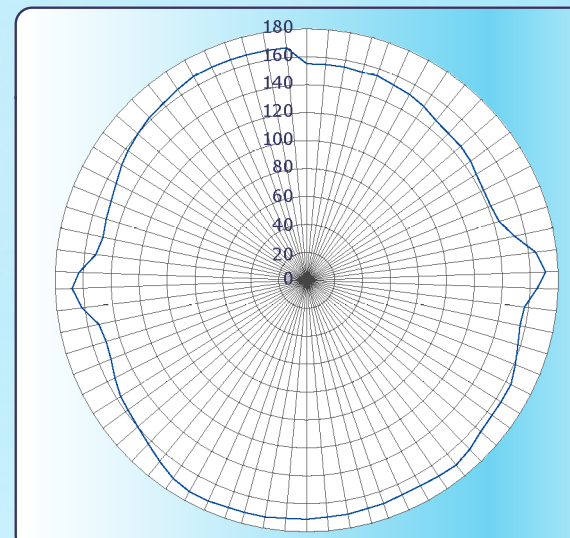
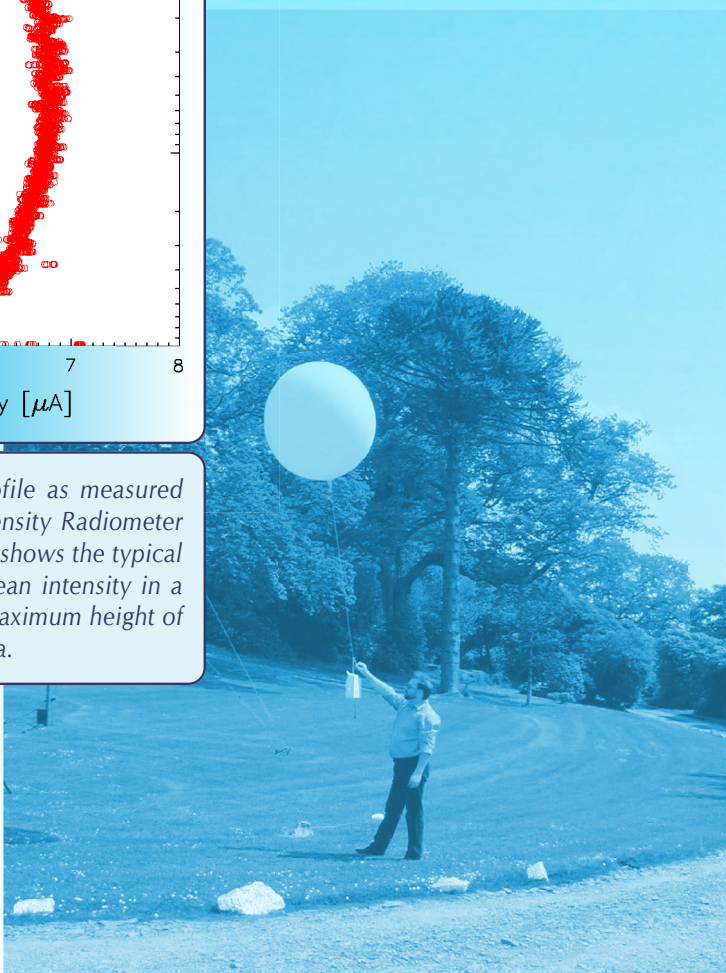


**Figure 1:** Sensitivity (or isotropy) of the prototype Mean Intensity Radiometer. The isolines are arbitrary units. The anisotropy of about +/- 12% (min/max) of this detector is not unacceptably high as detectors measuring irradiances can have even larger cosine-response errors.



[www.graw.de](http://www.graw.de)



[www.kippzonen.com](http://www.kippzonen.com)

## SESSION 3

QUALITY MANAGEMENT, CALIBRATION, TESTING AND  
COMPARISON OF INSTRUMENTS AND OBSERVING SYSTEMS

Session 3

POSTERS

# The experiment and analysis on available data rate of wind profiler radar

He Ping, Wu Lei, Ma Shuqing, Zhao Zhiqiang

Chinese Academy of Meteorological of Science

(CAMS, 100081, Beijing, China)

[heping@cma.cma.gov.cn](mailto:heping@cma.cma.gov.cn)

## Abstract

In this paper, the available data rate (ADR) of wind profiler radar (WPR) has been analyzed. The primary analysis shows that ADR has a strong relationship with seasons. In wet season, the ADR is obviously higher than its in dry season. And in the same weather conditions, ADR has relative to WPR parameters. Reasonable choice of radar parameters has effect to improve the available data rate of wind profiler radar.

**Keywords:** wind profiler radar, available data rate

## Introduction

A field experiment to measure wind structure by using wind profiler radar (WPR) has been conducted from July to November 2004, in Beijing. The data from the experiment has been analyzed to compare with Radio Sounding Systems and to estimate the observing capability of the WPR. The main technique parameters of the WPR, made in China, are shown in table 1.

**Table 1: wind profiler radar parameters**

Radar parameters	
Frequency	445 MHz
Pulse width	0.8 $\mu$ s
Maximum height	8 Km
Minimum height	300 m
Height resolution	240 m
Time resolution	9 minute

The ADR is defined as the ratio between the number of available data and the total number of data. It is an available index to show the observing capability of the WPR. Because ADR is a function of height, it is calculated from 300m up to 9km in 240m intervals. And to explore the monthly change of ADR, it is calculated month by month.

## Result

The result of ADR is shown in Fig.1. Horizontal refers to per cent, vertical refers to height, and the lines in different colors stand for ADR of different month.

Fig.1 shows that ADR is the highest between 1-3km. It decreases both at low and high level. And it drops more rapidly in winter season than its in summer season above 3km. It is smaller than 60% in most months under 500m.

ADR of wind profiler radar is affected by water vapor in atmosphere. ADR in Jul. is clearly higher than ADR in Nov. And because it is much more foggy days in Nov. 2004 in experiment area; the ADR in Nov. is even bigger than ADR in summer season at 500-2500m high level.

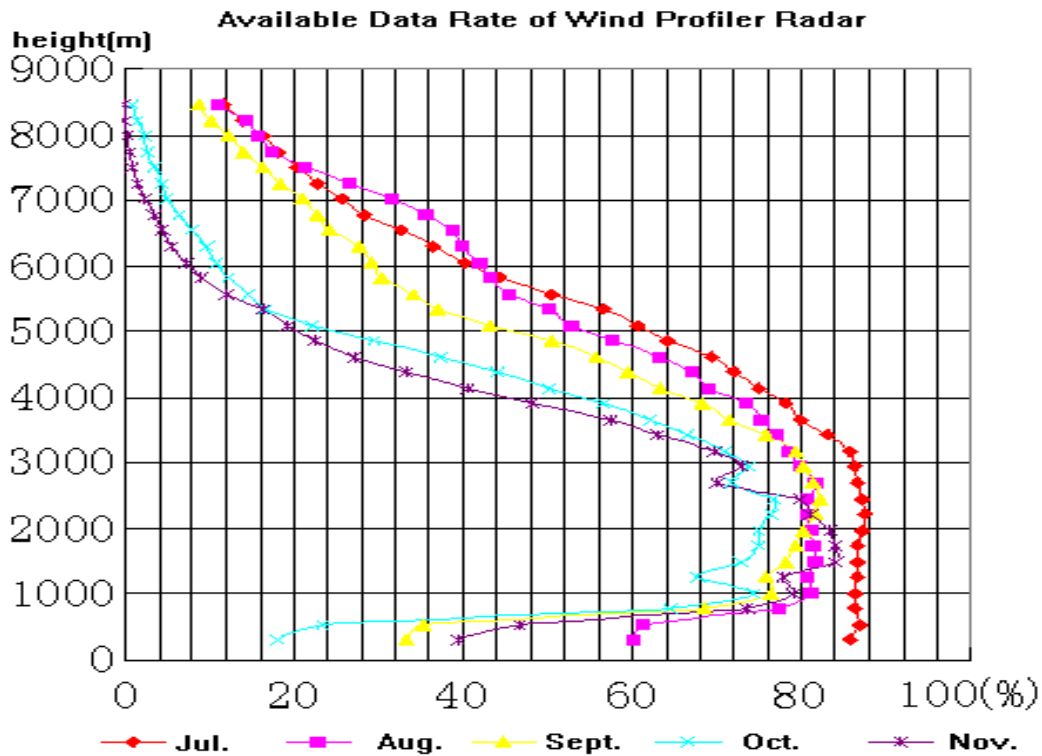


Fig.1 Available Data Rate of Wind Profiler Radar

## Conclusion

ADR is one of important index to estimate the WPR system. That can help us to improve system design and the choice of observing parameters. Better choice of observing parameters, such as coherent integral times, is benefit to increase the value of ADR.

ADR of wind profiler radar is affected by water vapor in atmosphere. The water vapor condition in some area should be considered, when we choice some type of WPR to observe.

# PERFORMANCE EVALUATION FOR NET PYRRADIOMETERS

LU Wenhua, MO Yueqin and YANG Yun

Atmospheric Observation Technology Center, China Meteorological Administration

46 Zhongguancun Nandajie, Beijing 100081, China

Tel: 0086 10 68406866 Fax: 0086 10 68400936 E-mail: [lwh@cma.gov.cn](mailto:lwh@cma.gov.cn)

## ABSTRACT

The performance of two models Net Pyrradiometer (model DFY5 and model TBB-1) made in China has been tested. We have mainly studied the long-term stability of sensitivity, nonlinearity, temperature dependence, directional response (cosine and azimuth), response time and influence of dome-shape. Sensitivity, response time and influence of dome-shape are tested in outdoor exposure and others are tested on the laboratory test facility. Main error of Net Pyrradiometer is given according to a great of test data and analysis.

## 1. INTRODUCTION

The net pyrradiometer is intended for the analysis of the radiation balance of Solar and Far infrared radiation, i.e. the net pyrradiometer is used to measure the differences of irradiance between downward and upward radiation including downward short-wave radiation, downward long-wave radiation, upward short-wave radiation and long-wave radiation. There are 50 radiation observation stations used two models Net Pyrradiometer (model DFY5 and model TBB-1) made in China to measure the net irradiance since 1990. The principle of instrument is a thermopile detector equipped with polyethylene domes and the voltage output is divided by the sensitivity to obtain irradiance. In order to evaluate the net pyrradiometers performance we have tested the main specifications. Main error for net pyrradiometers are concluded according to a great of test data and analysis.

## 2. PERFORMANCE TEST

Nine instruments are tested, which serial numbers are 007, 008, 015, 047 for model DFY5 and 9606, 9607, 9608, 9609, 9610 for model TBB-1. In the measurements we use a PC in conjunction with data logger and output of instrument can be measured and processed automatically.

### 2.1 Sensitivity and Long-term Stability

Net pyrradiometer No.84001 ( model CN-11, from EKO Japan) is used as a reference instrument. The test and reference instruments are put on the platform of roof. Data are collected every two minutes. Sensitivity is tested in different seasons and weather condition (clear day, nebulous, cloudy and less than 5 m/s wind speed). From the measurements we have got two sensitivity for the net pyrradiometer. That is daytime sensitivity (total-wave sensitivity) and nighttime sensitivity (longwave sensitivity).

The experiment is covered 8 months and the results are given in Fig.1, Fig2,

Fig3 and Fig4. It shows that the daytime sensitivity is very dispersed which occurs at the condition of lower solar elevation angle (less than  $30^\circ$ ) and lower temperature (less than  $0^\circ\text{C}$ ). The maximum relative error is about 16% for model TBB-1 at the daytime. This is a combined error caused by nonlinearity, temperature dependence, directional response, zero drift of the instrument and et al.

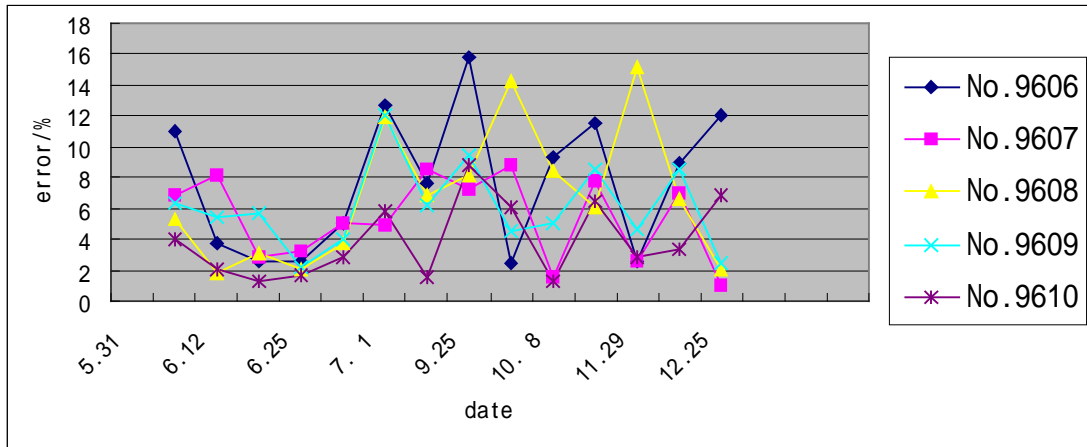


**Fig 1. Daytime Sensitivity Change for Model TBB-1 Net Pyrradiometer**

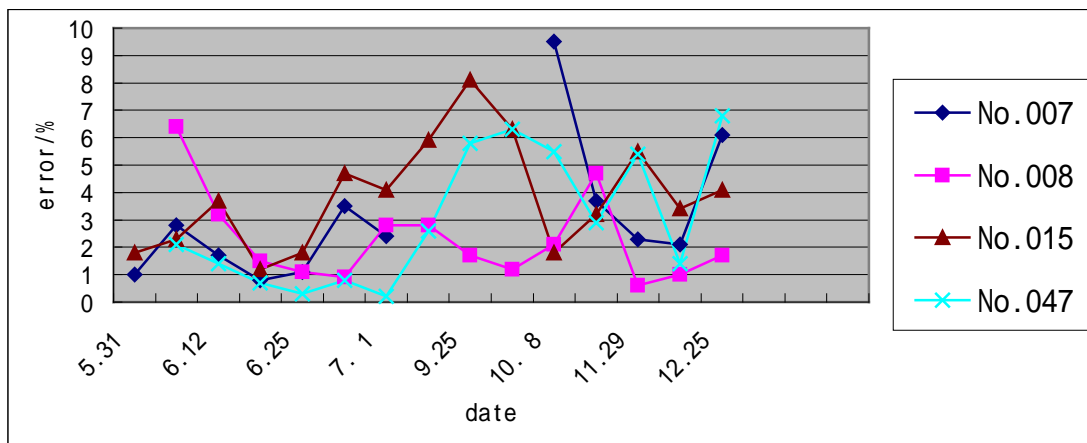


**Fig2. Daytime Sensitivity Change for Model DFY5 Net Pyrradiometer**

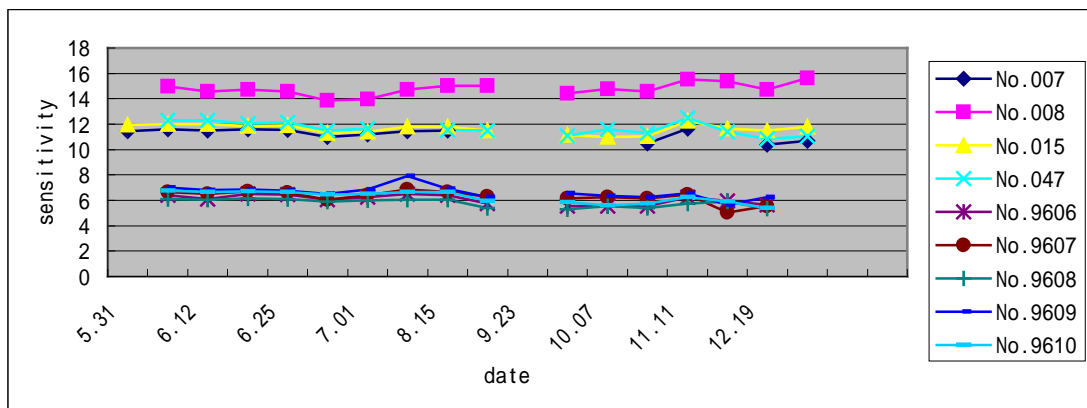


**Fig 3. Long-term Stability of Daytime Sensitivity over 8 Months**

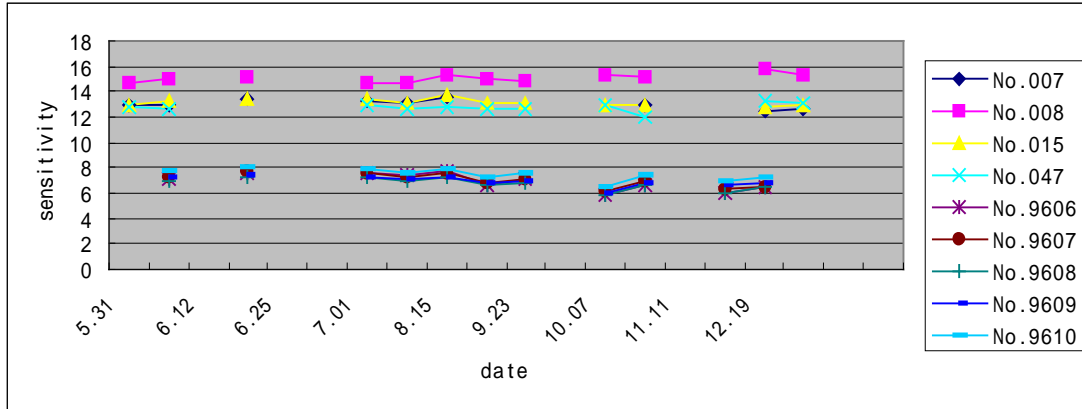


**Fig 4. Long-term Stability of Nighttime Sensitivity over 8 Months**

Nonlinearity is tested in the laboratory. The test facility consists of mechanism and a solar simulator that the spectrum components do not change with irradiance. Test point is respectively at irradiance of 250, 500, 750 and 1000 W/m<sup>2</sup>. Nonlinearity is given by  $\delta_L = (V/V_{500} - 1) \times 100\%$ . In the formula V is the output of net pyrradiometer and V<sub>500</sub> is the output of net pyrradiometer when the irradiance is 500W/m<sup>2</sup>. From the results we know that the maximum nonlinearity error is 2.3% and is in the lower irradiance.

### 2.3 Temperature Dependence

Temperature dependence is tested on the laboratory test facility with a temperature chamber. We change the temperature in the chamber while the irradiance is unchanged and then the output of instrument is measured. The temperature test point is respectively at -20°C, 0°C, 20°C, 40°C while the irradiance is 1000W/m<sup>2</sup>. Temperature error is given by  $\delta_T = (V_T/V_{20} - 1) \times 100\%$ . In the formula V<sub>T</sub>, V<sub>20</sub> is respectively output of instrument when the temperature is T and 20°C. From the results the temperature error is within  $\pm 5\%$ .

### 2.4 Directional Response

Directional response can be divided into cosine response and azimuth response

#### 2.4.1 Cosine Response

Cosine response test is made use of studying the directional character of incident beam. The irradiance is adjusted to 1000 W/m<sup>2</sup> on the laboratory test facility. First the output of instrument (V<sub>0</sub>) is tested in  $\theta = 0^\circ$  ( $\theta$  is zenith angle), namely solar elevation angle  $h = 90^\circ$ , then the solar elevation angle  $h$  is adjusted to  $80^\circ$  to measure the output of instrument. Each angle of measurement is at  $90^\circ$ ,  $80^\circ$ ,  $70^\circ$ ,  $60^\circ$ ,  $50^\circ$ ,  $40^\circ$ ,  $30^\circ$ ,  $20^\circ$ ,  $10^\circ$ . The output of instrument for solar elevation angle  $90^\circ$  ( $\theta = 0^\circ$ ) is tested again.

Cosine response error is calculated by formula  $\delta_\theta = (V_\theta/V_i - 1) \times 100\%$ . In the formula the relation between  $\theta$  and  $h$  is  $h = 90^\circ - \theta$ , V<sub>θ</sub> is the output of instrument at  $\theta$ , and V<sub>i</sub> = V<sub>0</sub> · cos  $\theta$  is an ideal value at  $\theta$  and V<sub>0</sub> is the average of two outputs of



instrument at  $\theta=0^\circ$  . The results are listed in the table 1. The maximum error is 15.65% at solar elevation angle  $10^\circ$  .

**Table 1. The Relative Error for Cosine Response ( % )**

No.	Model	$10^\circ$	$20^\circ$	$30^\circ$	$40^\circ$	$50^\circ$	$60^\circ$	$70^\circ$	$80^\circ$
007	DFY5	-15.65	-9.02	-4.67	-2.96	-1.88	-1.33	-0.01	0.29
008	DFY5	-15.62	-7.80	-4.29	-1.35	-0.41	0.21	0.47	0.41
015	DFY5	-3.93	-0.43	0.57	0.80	0.29	-0.02	0.25	0.57
047	DFY5	-7.53	-2.98	0.42	0.37	0.14	-0.08	0.86	0.70
9606	TBB-1	0.39	-0.39	0.06	-0.51	-0.35	-1.17	-1.98	-1.88
9607	TBB-1	-1.62	-3.39	-3.79	-2.42	1.34	2.38	1.77	0.63
9608	TBB-1	5.19	2.85	1.57	-0.51	-0.43	-0.24	-0.81	-0.87
9609	TBB-1	-7.68	-3.71	2.27	-1.48	-0.45	-0.79	-0.90	-1.14
9610	TBB-1	2.33	-2.25	-0.16	-0.39	-0.01	0.19	0.19	-0.63

#### 2.4.2 Azimuth Response

The method of azimuth response test is similar to the cosine response test. The output is measured at solar elevation angle  $10^\circ$  . The test point is at intervals of  $30^\circ$  within directional  $60^\circ \sim 300^\circ$  . The cable of net pyrradiometer points to north which is  $0^\circ$  .

**Table 2. The Relative Error for Azimuth Response ( % )**

No	Model	$300^\circ$	$270^\circ$	$240^\circ$	$210^\circ$	$180^\circ$	$150^\circ$	$120^\circ$	$90^\circ$	$60^\circ$
007	DFY5	-7.63	1.78	0.63	5.65	-4.96	5.94	3.07	1.12	-5.60
008	DFY5	5.34	5.16	-14.52	5.30	2.41	1.26	-4.95	3.85	5.90
015	DFY5	8.81	10.98	0.71	3.72	-20.07	-4.10	0.74	1.32	-2.11
047	DFY5	1.96	4.32	2.56	3.87	-19.70	4.86	-0.08	4.01	2.42
9607	TBB-1	-1.25	0.34	-3.39	-2.03	-0.67	-1.08	5.85	6.53	4.31
9608	TBB-1	-10.43	2.97	11.42	10.92	2.74	-0.38	-5.45	-11.72	-10.50
9609	TBB-1	-2.52	2.40	-1.68	-4.32	1.94	1.11	-0.88	14.92	-10.97
9610	TBB-1	-9.21	-3.63	0.31	-0.85	4.08	6.91	1.99	2.21	-1.82

Azimuth response error is given by the formula  $\delta_A=(V_Z/V_M-1)\times 100\%$  .  $V_Z$  is the output of each azimuth and  $V_M$  is an average of outpoints for all azimuth. The results are given in the table 2. It shows that the error of azimuth response is in  $-20,07\% \sim 14.92\%$  . According to the observation condition in use we should test 6 points, namely  $60^\circ$  ,  $90^\circ$  ,  $120^\circ$  ,  $240^\circ$  ,  $270^\circ$  ,  $300^\circ$  and its error should be less than 15%. Pay attention to that the direction of net pyrradiometer must be the same

whether in the test or in the observation, i.e. the cable of net pyrradiometer points to north.

### **2.5 Response Time**

The response time is tested in both indoor and outdoor. The results are less than 90 second (99% response).

### **2.6 Influence of Dome-shape**

The Influence of Dome-shape is tested on the laboratory test facility which the irradiance is adjusted to 500 W/m<sup>2</sup>. According to the results maximum relative error of dome-shape is about 3%.

## **3.CONCLUSION**

Based on our test study, we conclude that for net pyrradiometers of model DFY-5 and TBB-1, there are daytime sensitivity and night sensitivity which is within 5~16  $\mu\text{V} \cdot \text{W}^{-1} \cdot \text{m}^2$ , nonlinearity error is less than 2.3%, temperature error is within  $\pm 5\%$  in the range of  $-20^\circ\text{C} \sim 40^\circ\text{C}$ , maximum cosine error is less than 16% and maximum azimuth error is less than 15% at solar elevation angle  $10^\circ$ , response time is less than 90 second (99% response) and maximum relative error of dome-shape is about 3%. Last, we want to stress that the cable of net pyrradiometer points to north and the polyethylene domes must be full of air in the observation in order to get a more accurate net radiation.

## **REFERENCES**

- WMO. Guide to Meteorological Instruments and methods of Observation. Six Edition. WMO No.8, 1996
- LU Wenhua, et al. A Laboratory Test Facility for Solar Radiation Instruments and Its Application. WMO/TD No.877, 361-364,1998.
- LU Wenhua, et al. Performance Evaluation for Pyranometers. WMO/TD No.1028, 124-127, 2000.
- LU Wenhua, et al. Study on the Calibration of net Pyrradiometer. WMO/TD No.1123, 2002.
- China Meteorological Standardization. Net Pyrradiometer QX/T 19 — 2003, Standards Press of China, 2004.

# SOME STEP OF QUALITY CONTROL OF UPPER-AIR NETWORK DATA IN CHINA

Zhiqiang Zhao

China Meteorological Administration (CMA)

46, Zhongguancun Nandajie, Beijing, 100081, China

Tel: 8610-68407362, Fax: 8610-62179786, E-mail: gkyg@rays.cma.gov.cn

Bingxun Huang

Chinese Academy of Meteorological Sciences

46, Zhongguancun Nandajie, Beijing, 100081, China

Tel: 8610-68407276, E-mail: bxhuang@126.com

## Abstract

Some step of quality control of upper-air data have been made by China Meteorological Administration (CMA) recent years. The routine monitoring of daily TEMP and analysis of the upper-air network data set by reference to WMO method is conducted and special emphasis is given to the questionable and erroneous TEMP records. Various error resources from flight operation at station or communication department have been identified and informed to related stations or community to overcome. Preliminary analysis results of the monthly mean bias are presented. China is carrying on a program of replacement of the upper-air sounding system. The overlapping radiosonde flights for a period of one month are conducted at each replacement station. The preliminary comparison results of a total of 24 stations are also presented.

## 1 Introduction

It is well known that the WMO's evaluation report of the compatibility of radiosonde geopotential height observations based on comparisons with the First Guess field of the ECMWF model (T. Oakley, 1998; J. Elms, 2002) is very useful for the monitoring of long-term system performance of all upper-air stations in the Global Observing System. We obtain much valuable information of the performance of our network from the reports. However the evaluation reports are published just for quarterly results and the statistics are only generated for the 100hPa geopotential height and the (100-30hPa) geopotential height increment. Further more, they cannot be searched from the website in time, for example the next quarter. Therefore, the CMA has arranged the National Meteorological Center (NMC) and the Chinese Academy of Meteorological Sciences (CAMS) to take on the routine monitoring of Chinese upper-air TEMP reports by reference to the WMO method. The NWS is responsible to provide differences between observed values (OB) and the First Guess (FG) field of the NWS model. The CAMS takes charge for further analysis of the upper-air network data set. The statistics for differences are generated not only for geopotential height and temperature but also for wind speed and wind direction for each standard pressure levels. Some results of the analyses are presented in this paper.

There are a total of 124 upper-air stations operated in China to satisfy the requirements in synoptic scale meteorological analysis. Recent year, the L-band digital radiosonde GTS1 (Li Jiming and Feng Deli, 2000) and modernized secondary wind-finding radar GFE(L) system is being deployed to replace the obsolete mechanical radiosonde GZZ2 (Guo Yatian and Huang Bingxun *et al*, 2002) and

P-band secondary wind-finding radar (type 701) system. By the end of 2004, 36 stations have completed the replacement program. And about 32 stations will also be equipped by the new system before the end of 2005. Prior to the application of the new system at network, some function tests and field tests including the inter-comparison with Vaisala's RS80 system had been conducted at Beijing several years ago. To assess the impact of the replacement to the continuity of upper-air meteorological records, the comparison flights lasted one month between the new and the old upper-air sounding systems at all related station are conducted according to the special arrangement by the CMA. The preliminary comparison results are informed.

## 2 Quality monitoring of the TEMP report

### 2.1 Graphic display of the bias and checking on unwanted report

Generally, we draw bias curves on monthly base to show the differences between each TEMP report and the First Guess field. From the figures, we can find out intuitively the general situation of each station on the bias and deviation from the First Guess field. Especially, any particular unwanted bias curve can allure your attention. In some time, we can immediately estimate the origin of the questionable TEMP report from the graphic display of the bias curves.

The following Fig.2.1 shows the monitoring statistics of the geopotential height (in the left) and the temperature (in the right) on September 2004 for the station.52652 as an example. This station has been equipped with the new sounding system. The broad red curve represents the mean bias of the month. The narrow chromatic curves represent the bias of each day. And the two broad pink curves are the borderlines of the normal bias. The borderline is defined by the averaged standard deviation of whole Chinese stations applied the same type of radiosonde. Usually, the bias curve is within the borderlines. Once a curve is outside of the borderlines, it is affirmative that some mistake had happened. For example, at 00Z September 25, the geopotential height is 90gpm lower than the First Guess field and in parallel with the monthly mean bias but the temperature is not off normal. It can be estimated that the instant pressure value of the flight was keyed-in falsely.

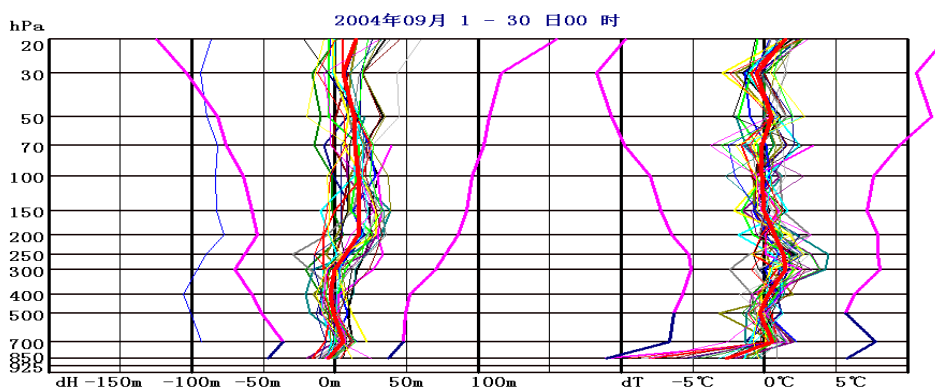


Fig.2.1, Monthly bias display with an unwanted geopotential bias.

Fig.2.2 shows a very unwanted bias of the geopotential height and the temperature at the height lower than 70hPa at 12Z January 12 for the station.52681, which is still operated with the old sounding system. The bias of the geopotential height is very correlative with the bias of the temperature. After

searching the former TEMP reports, we found that the TTAA report for 12Z January 12, 2004 is the same for 12Z December 12, 2003. Then it was found out that the mistake had happened in transmission of TEMP report.

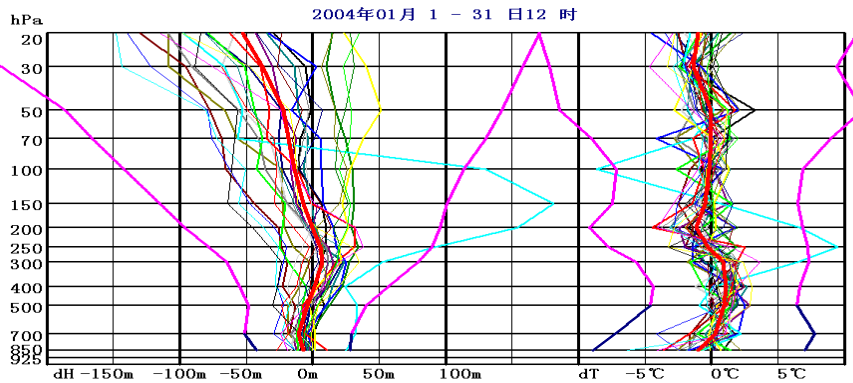


Fig.2.1, Monthly bias display with unwanted geopotential and temperature bias.

We have found various unwanted TEMP reports induced from miss-operation at station or communication department since 2003. In order to attract attention of observers in station and supervisors of all levels, our monthly monitoring reports are issued on the website. The main content of our monthly monitoring report is the bias graphics and analysis on the unwanted TEMP report. A station rank in the light of the quality of TEMP report is also included in the monthly monitoring report. The quality of TEMP report has been digitized according to the quantity of the unwanted TEMP reports.

## 2.2 Monthly and annual mean bias and deviation

Now a total of 36 stations have been equipped with the new upper-air measuring system operating at 1675MHz until December 2004. It is concerned about that if there is a notable systematic difference between the data sets provided by the new and old system. Fig.2.3 and Fig.2.4 show the monthly mean bias of geopotential height and temperature for station 54857 at the east coast of China and 51656 at the west desert area respectively. The darkish curves are denoted to the monthly average of the old system and the azury one to the new system. The bright red and navy blue curves are denoted to the annual average of the old system and new system respectively. In average, there is no notable systematic difference of geopotential height and temperature between the new and old system for station 54857. However, there is some fewer systematic bias of geopotential height and temperature of the new system than the old one for station 51656.

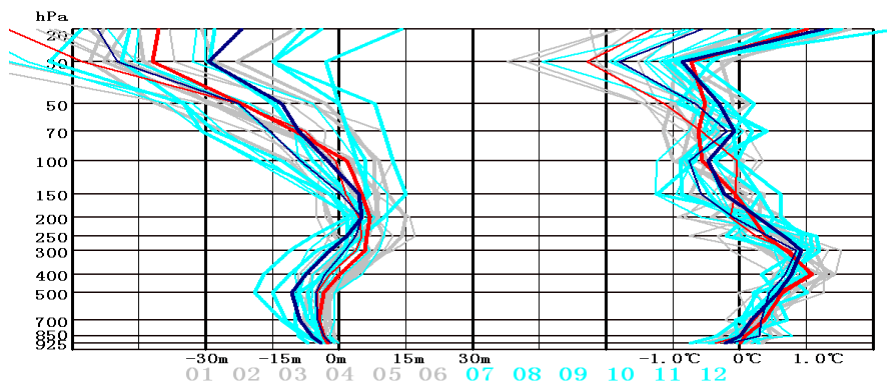


Fig.2.3, Monthly mean bias of geopotential height and temperature for station 54857

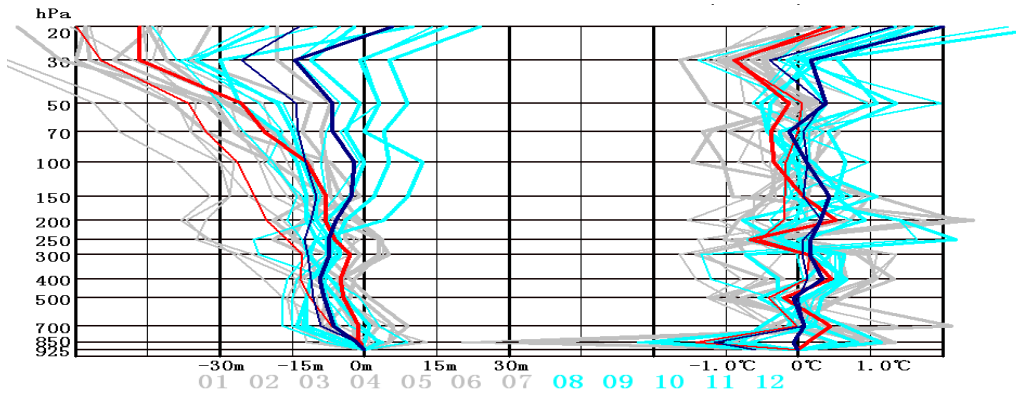


Fig.2.4, Monthly mean bias of geopotential height and temperature for station 51656

From Fig.2.5, it is apparent that the mean standard deviation of geopotential height bias from new system is much smaller than the old one. Above the height of 100hPa, the mean standard deviation of geopotential height bias of new system is only about 50% of the old system. The mean standard deviations of the temperature, wind speed and wind direction bias (see Fig.2.6.) of the new system are also improved in some degree

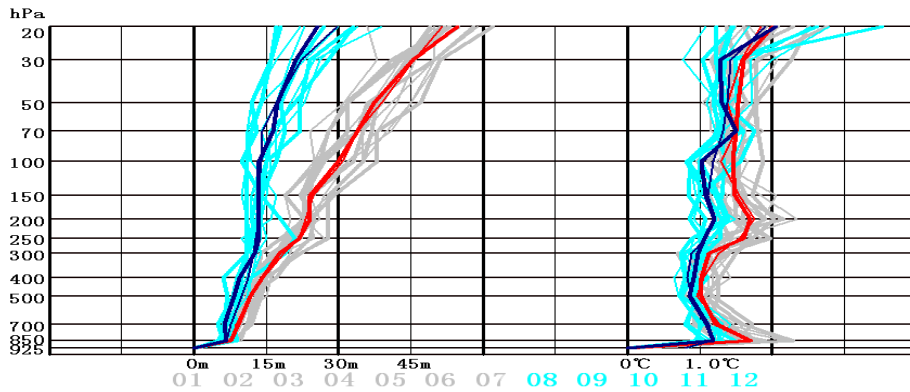


Fig.2.5, Monthly mean standard deviation of geopotential height and temperature bias

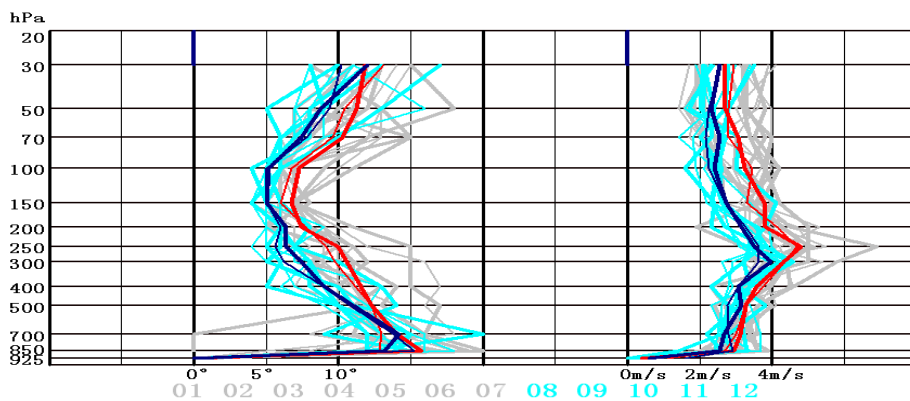


Fig.2.6, Monthly mean standard deviation of wind speed and wind direction bias

Fig.2.7 shows the overall monthly mean biases (narrow chromatic curves) and overall annual mean biases (broad chromatic curves) of the 78 old radiosonde stations in 2003. We can see that the overall monthly mean biases are different in some degree in different month and at different time of the day. In warm season and at the daytime, the temperature is in somewhat higher than that in cold season and at nighttime.

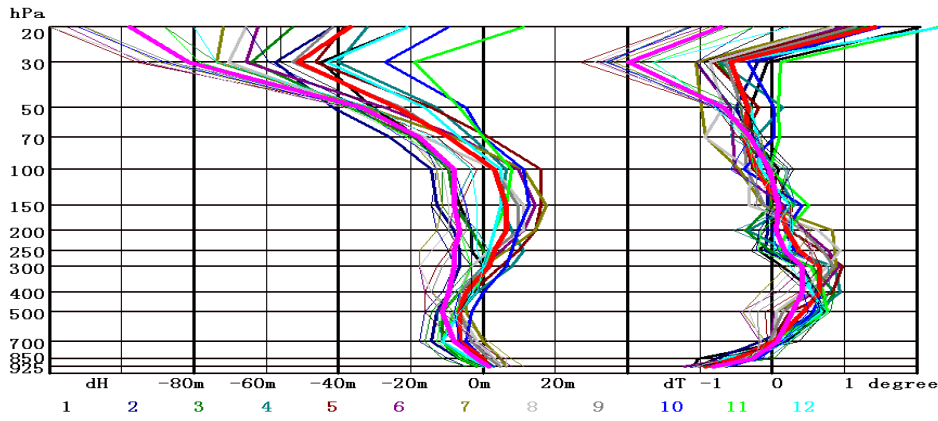


Fig.2.7, Overall monthly mean biases and annual mean biases of the 78 old radiosonde stations in 2003.

Fig.2.8 indicates that the overall annual mean biases of the old sonde stations in 2004 are nearly completely the same with that in 2003, especially at 12Z, because most of the radiosonde flight is in local nighttime after 12Z in China.

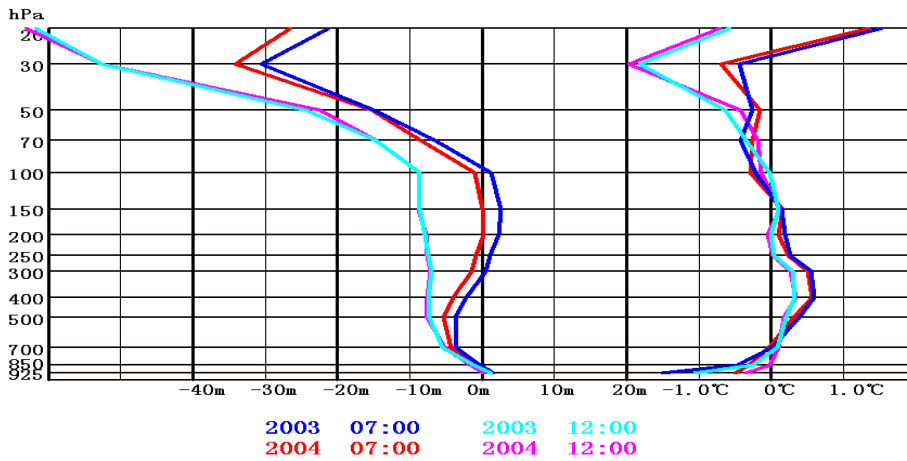


Fig.2.8, Overall annual mean biases of the old radiosonde station in 2004 and in 2003

Fig.2.9 shows the overall monthly mean biases of the 24 new sonde stations in 2004. The results are also different in some degree in different month and at different time of the day. In warm season and at the daytime, the temperature is in somewhat high.

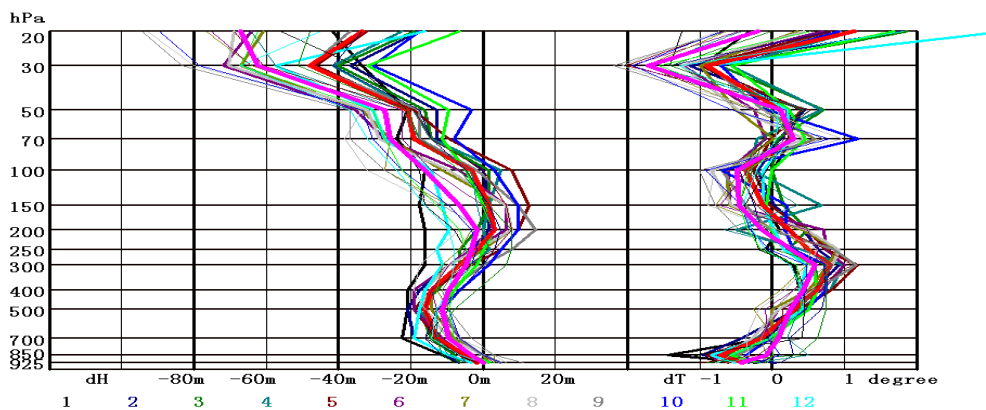


Fig.2.9, Overall monthly mean biases of the 24 new radiosonde stations in 2004

Fig.2.9 gives the compare of overall annual mean bias between the 78 stations equipped with old system and the 24 stations equipped with new system in 2004. Below the height of 50hPa, the temperature difference is less than 0.5°C and the geopotential difference is less than 10gpm.

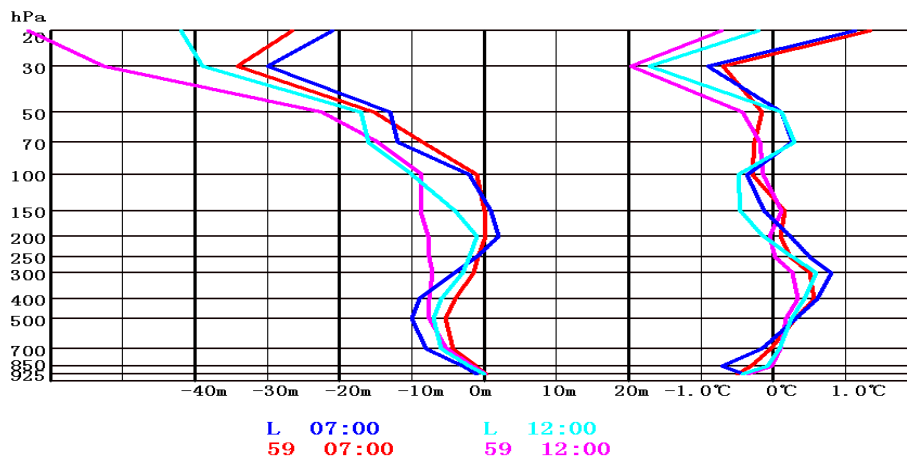


Fig.2.9, Comparing of overall annual mean bias between the old and new system in 2004.

Fig.2.10 shows the difference of overall annual mean bias between the station 45004 equipped with the Vaisala's radiosonde system and 24 stations equipped with the new system in 2004. Below the height of 100hPa, the temperature difference is less than 0.5°C. And below the height of 200hPa, the geopotential difference is less than 10gpm. However, the geopotential difference reaches 20gpm when the height higher than 200hPa.

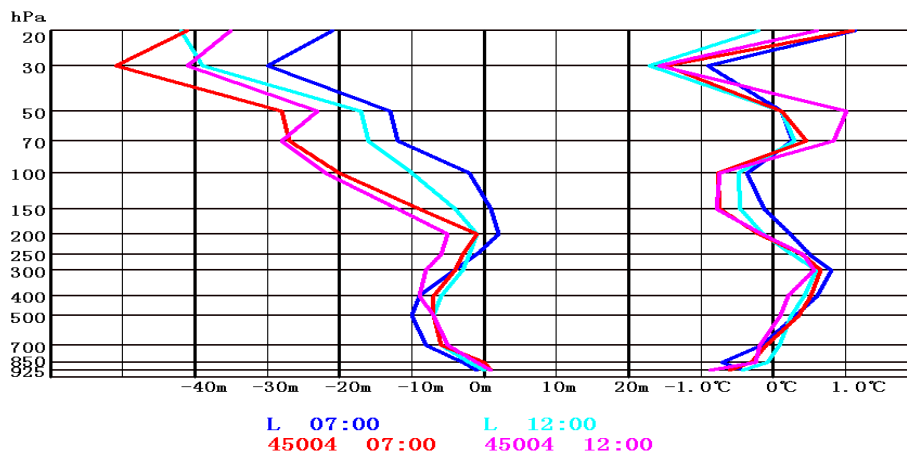


Fig.2.10, Difference of overall annual mean bias between the station 45004 and the 24 new systems in 2004.

Fig.2.11 shows the difference of overall annual mean bias between the station 45004 and its 4 neighborhood stations equipped with old system in 2004. The geopotential and temperature differences are in somewhat degree bigger than that in Fig.2.10.



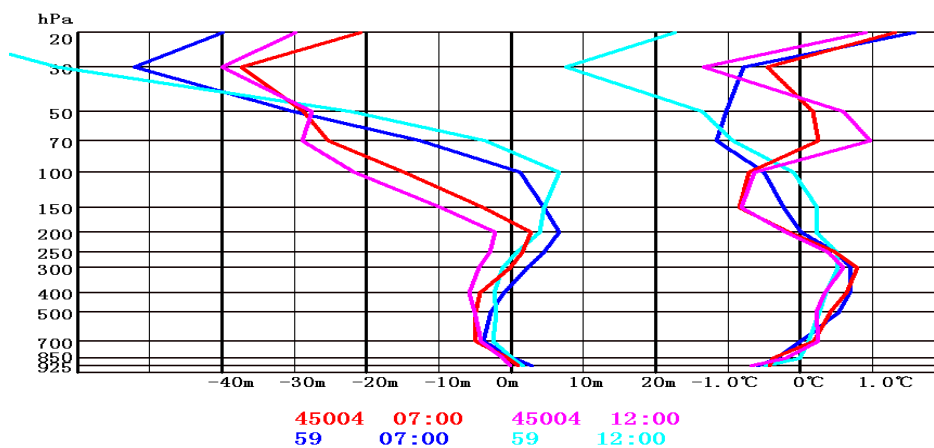


Fig.2.11, Difference of overall annual mean bias between the station 45004 and its 4 old system in 2004

It must be explained as supplement that the processing method of correcting the systematic error for the old GZZ2 sonde had been changed (Guo Yatian and Huang Bingxun *et al*, 2002) since July 2000 and the NWS model and its related initial meteorological parameter database are replaced since January 2003. In general, as discussed in this paragraph, the initial database is compatible with the in-situ observations from the upper-air network of China.

### 3 Flight comparison between the new and the old radiosonde

The first guess field offers usually a relatively stable reference for evaluating observation quality of network stations. However, it is not assumed that the FG fields have zero systematic error in each region and in any time. This implies that the direct flight comparison is still required for identify the quality performance and differences of the records between the new and the old observation systems.

Although the radiosonde network is established for short-term weather forecasting rather than long-term environmental monitoring, it has the potential to be an extremely useful tool for climate analysis and forms a foundation for calibrating and validating many satellite measurements.

The replacement of upper-air network often brings useful improvements in precision and accuracy, but they also result in the problems in continuity of the records from the perspective of climate change analysis. Data continuity is defined as the compatibility of past, present, and future data such that the observational record is free of in-homogeneities caused by instrument changes, launch and sampling procedure changes and data processing changes. Instrument biases can vary with altitude, atmospheric and ground conditions, solar elevation, time of day, and other changes. In the absence of overlapping observations, the adjusting temperature data provide by the radiosonde to remove in-homogeneities is a very complex task. Thus multi-season, multi-location comparison is necessary to understand all instrument-induced differences.

The more comparison flights, the lower the error will be in the calculations of continuity adjustments. But also the more comparison flights, the higher the costs will be. How many comparison flights are enough? It is still a strategy under discussed. However, to save the payout, CMA has decided to conduct the dual sonde flights in the train period of observers of replacement station. In order to avoid to

influence the flight state of the sonde, the comparison radiosondes ascent independently, but synchronously or with short times between their launches. The comparison flights last usually for one month and a total of 60 pairs of comparison records can be obtained. The data from the comparison flights will be used to calculate the mean difference between the old and new sondes. Until preparing of this paper, preliminarily analysis of the differences from the 24 replacement stations has been completed

Fig. 3.1 shows the mean differences of geopotentials and temperature between the old and the new radiosondes for the 24 stations (azury curves) and the overall average of the 24 stations (red). In general, the overall average below the height of 100hPa is not obvious although the comparison results for the 24 stations are differ obviously. The overall temperature average is less than 0.3°C and the overall geopotential average is less than 5gpm. But the overall temperature average reaches 1°C and the overall geopotential average reaches 30gpm at the heights of 70-50hPa.

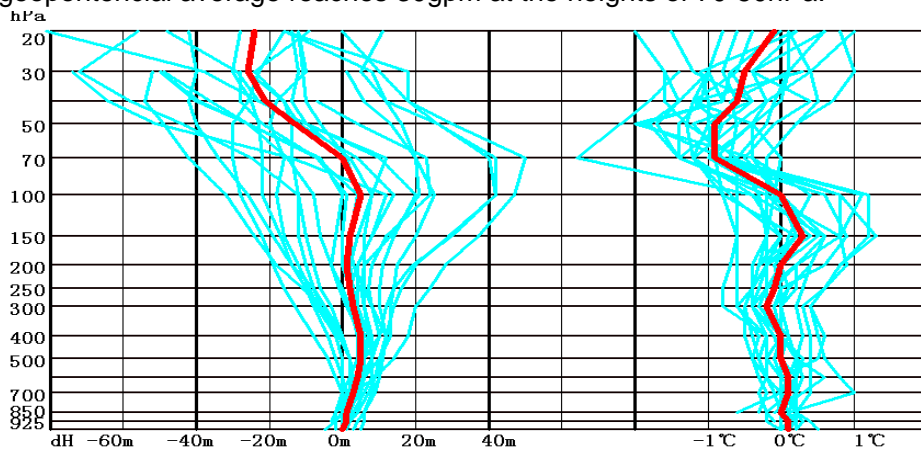


Fig.3.1, Mean differences of geopotentials and temperature between old and new radiosondes

The farther analysis has revealed that the biggest positive difference from 56187,57957 and 57972, see Fig.3.2, is related to the radiosondes produced by the factory in ShanXi province, but others produced by the factory in Shanghai with the same drawing.

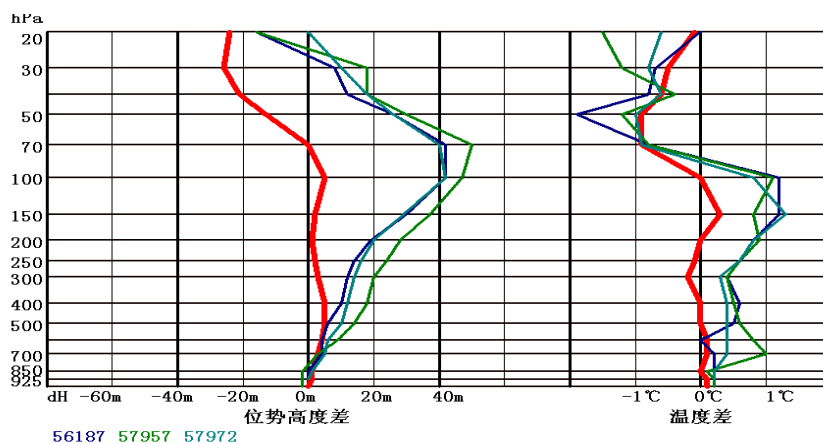


Fig.3.2, The biggest positive difference from 56187,57957 and 57972

The fact can also be validated by the analysis of the monthly monitoring (OB-FG) bias. For example, Fig.3.3 shows large negative variation of the monthly mean bias from July when old sonde was released to August when new sonde was released for station 57972. Fig.3.4 shows farther large negative variation of the monthly mean bias from the month before July to that after August for station 57972.

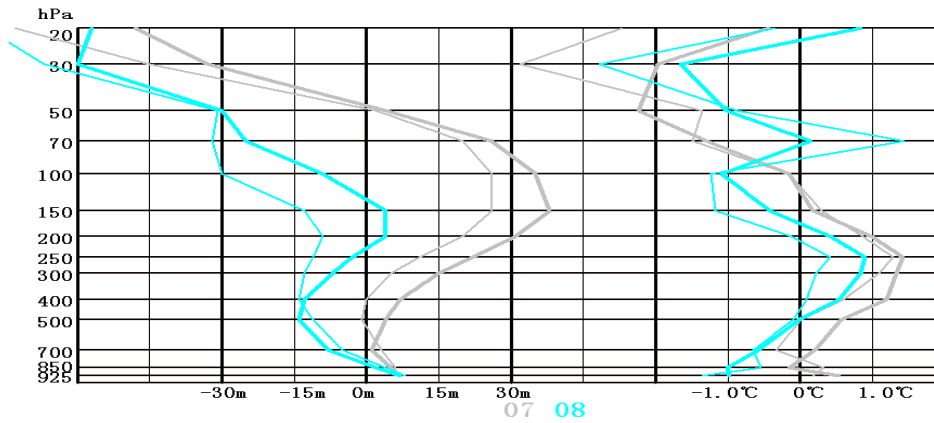


Fig.3.3, Large negative variation of the monthly mean bias from July to August for station 57972

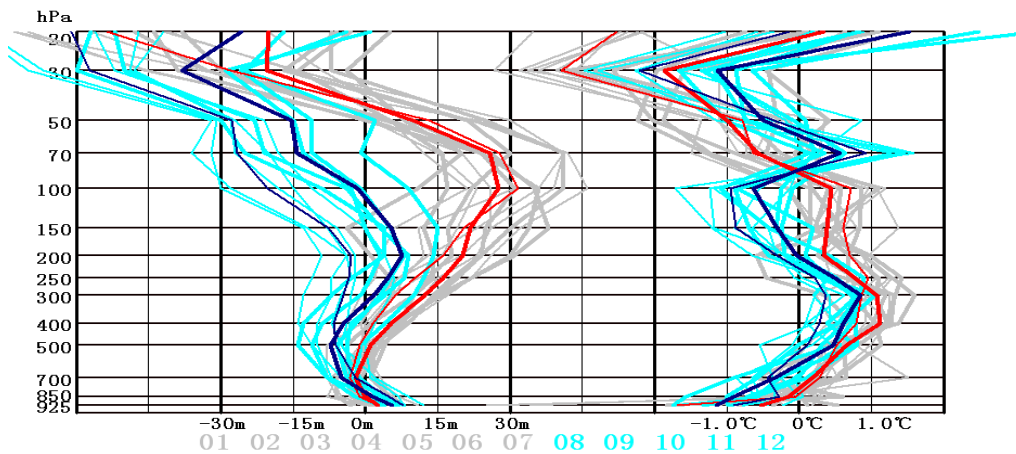


Fig.3.4, Large negative variation of the monthly mean bias from the month before July to that after August for station 57972.

The farther analysis has still revealed that the negative geopotential differences showed in Fig.3.5 are from stations 51656 to 53614 in the west China.

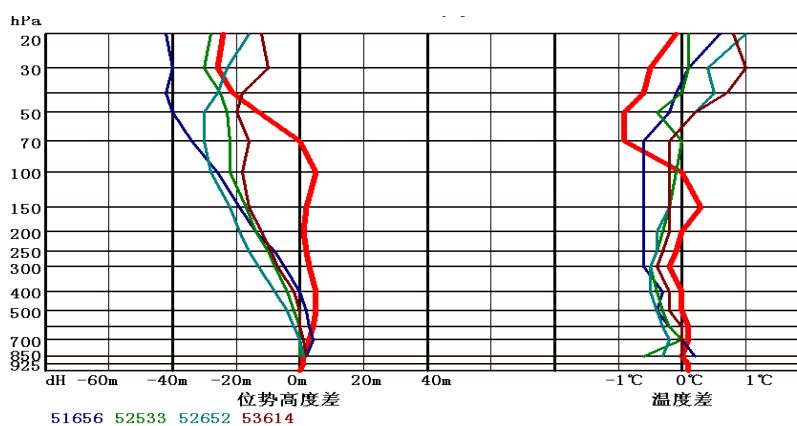


Fig.3.5, Negative geopotential differences from stations 51656 to 53614 in the west China

The fact can also be made sure by the analysis of the monthly monitoring (OB-FG) bias. For example, Fig.3.6 shows large positive variation of the monthly mean bias from July when old sonde was released to August when new sonde was released for station 51656. Fig.3.7 shows farther large positive variation of the monthly mean bias from the month before July to that after August for station 51656.

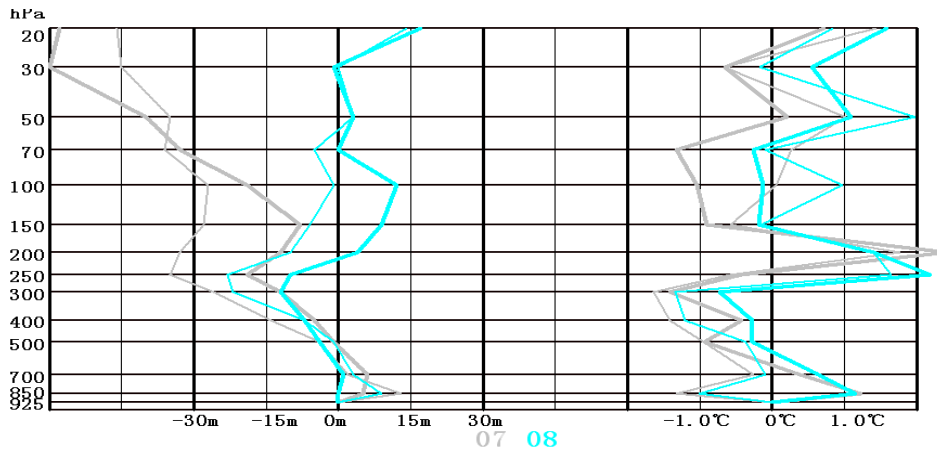


Fig.3.6, Large positive variation of the monthly mean bias from July to August for station 51656

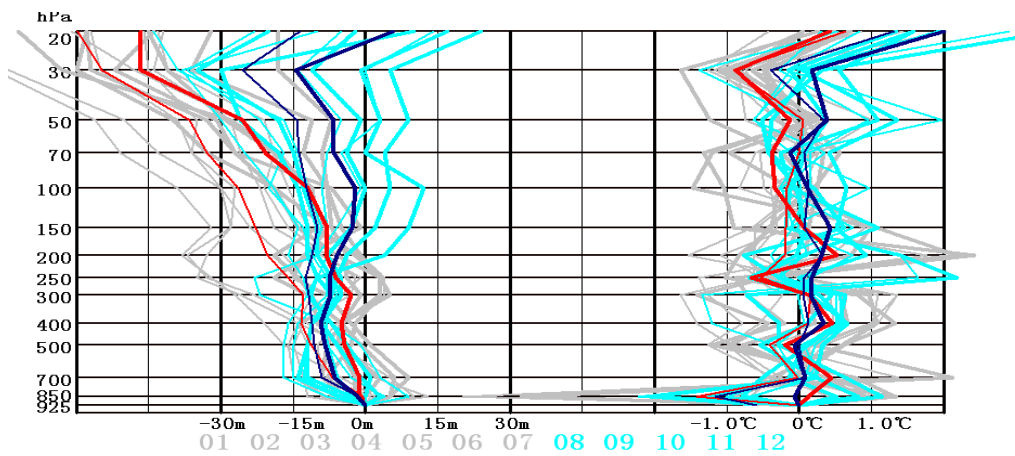


Fig.3.7, Large positive variation of the monthly mean bias from the month before July to that after August for the station 51656

It is clearly that the preliminary results are very rough to identify the systematic differences between the old and the new radiosondes mainly due to the different manufactory of the old sonde, different area of the country, different local time of the day, different cloud cover and physiognomy and *et al.* However, we will obtain useful evidence from this widely conducted comparison flights to design cost-effective comparison flights at definite stations in the different climate area and for a definite long time. And after that we hope reach the goal to obtain the mean values that could be applied to adjust the earlier data sets to make them homogeneous with the new data sets.

## 4 Conclusion

Conducting monthly evaluation of the compatibility of geopotential height, temperature, wind speed and wind direction observations based on comparisons with the First Guess field of the NWS model is very useful for the monitoring of long-term system performance of all Chinese upper-air stations. Due to the evaluation, various unwonted TEMP reports had been discovered and then are being overcome through some administrative and/or technical measures. Based on the monthly evaluation of the compatibility of upper-air records from various station, different launch time of the day, different producing factory and different radiosonde type, we hope to reveal some performance of the sonde that is difficult to be discovered in laboratory conditions.

However, direct dual flight comparison is still required to calculate the systematic differences between the new and the old network radiosondes and then to keep the continuity of the network records. Utilizing the opportunity of operational train of the new observing system for observer, to conducting comparison flight last such as one month at numerous replacement stations is a cost-effective measure. Nevertheless, much more strict dual flight comparison at some stations having some representations is certainly necessary to obtain adjusting values of the old record to the new record, especially for GCOS stations.

## References

Guo Yatian, Huang Bingxun *et al*, 2002: Correction for bias of Chinese upper-air measurements, *Papers Presented at the TECO2002*, 1.2(7).

J. Elms, 2002: Compatibility on Radiosonde Geopotential Measurements for the Period 1998 to 2001, WMO/TD-No.1197.

Li jiming and Feng Deli, 2000: New radiosonde for Chinese ground equipments, *Papers Presented at the TECO2000*, pp 191-194.

T. Oakley, 1998: Report by the Rapporteur on Radiosonde Compatibility Monitoring, WMO/TD-No.886.

# THE IN SITU PRESSURE CALIBRATION SYSTEM IN MÉTÉO FRANCE

**J. Duvernoy, A. Dubois**

Météo France, Direction des Systèmes d'Observation, Laboratoire de Métrologie

7, rue Teisserenc de Bort

78195 TRAPPES Cédex

☎ 01.30.13.63.50

✉ [jerome.duvernoy@meteo.fr](mailto:jerome.duvernoy@meteo.fr)

✉ [aurelie.dubois@meteo.fr](mailto:aurelie.dubois@meteo.fr)

[www.meteo.fr](http://www.meteo.fr)

---

## **ABSTRACT :**

Surveying and forecasting the atmosphere's behaviour is the first vocation of Météo France. The responsibility of the observation in Météo France has been entrusted to the Direction of Observation's Systems (DSO), which manages, in consequence, a network of 600 automatic weather stations. On these 600 stations, more than 300 barometers are installed.

In order to ensure the accordance of the barometers with metrological specifications, they are calibrated every 2 years in the Laboratory of Metrology of the DSO and are controlled in situ once per year. For that, the DSO developed its own in situ pressure calibration system, which is composed of a portable generator and a special software, called LEON SITE. It enables them to easily guarantee the traceability chain.

In a first part, we will describe the generator's running, which was achieved by EFFA. The running is based on the creation into two gasholders of high and low pressure (compared to the ambient pressure). The barometers to compare are connected with the mixer gasholder. The plateau are generated between 800 and 1060 hPa with a stability of 0.03 hPa.

In a second part, we will study the opportunities of the software LEON for the data acquisition and processing. The system enables us to use as reference either the inner barometer or an other reference standard, on condition that it should be calibrated before and after.

Finally, we will present the operational use of this system for Météo France's network and the usual uncertainty of measurement. For example, countries such as Cuba, Libya or Madagascar or the Asecna organization require the Meteo-France's support as Regional Instrumentation Center (RIC) to check their barometers in situ with this system.

Next step will be a LEON Software update to take into account the in-situ accreditation criteria and a Multilanguage interface.

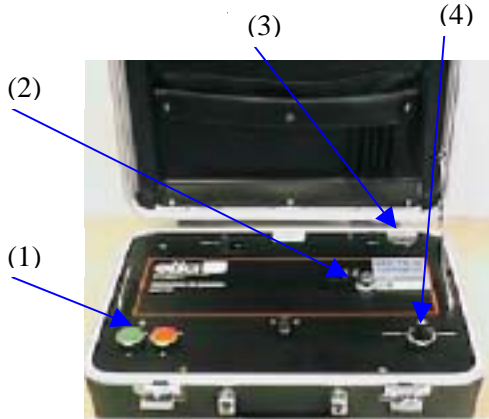
---

**TEXT :**

**1. Specifications**

**1.1. Description**

The whole generator is embedded in a small suitcase in order to make it easy to use and transport.



- Weight : 8 kG
- Size : 170 x 410 x 300 mm
- Power supply :
  - 220 V
  - inside lead-acid battery 12V (for an autonomy of 5 hours)

*fig.1 : Photo of the generator*

The electrical system and the circuit of gas generation are inside. On the outside, there are impulsive buttons for generation (1), pressure socket (2) and serial interface RS 232 (3) to connect a computer. The switch (4) is used to select the loading, measuring or stop mode.

Every kind of barometers equipped with external pressure fittings can be used.

The generator is also equipped with an internal capacitive barometer, as travelling standard.

**1.2. Generation**

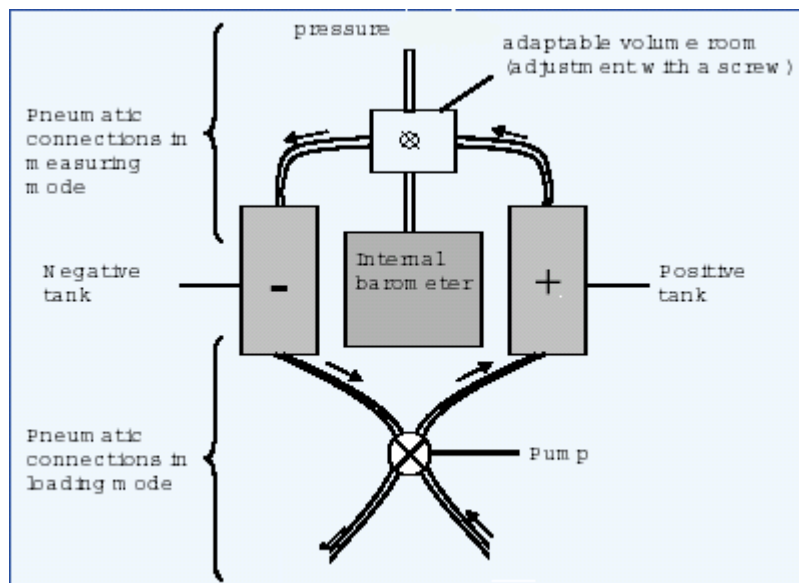


*fig.2 : Inside the generator*

An electric pump creates in two air tanks high (+400 hPa) and low (-600 hPa) pressure, compared to the ambient pressure. In loading mode, filtered air is pumped to fill the positive tank and some air is expelled from the negative. In measuring mode, the tanks are driven by electrovalves in order to fill and empty the air circuit. An accurate adjustment of the level of pressure is obtained by changing the volume adjusted by a specific screw. The maximum speed of variation is limited to 4 hPa per second through the pressure range of 600 hPa to 1100 hPa.

## 2. Calibration principle

### 2.1. Operating principle



*fig.3 : Complete calibration system*

Calibrated barometers are connected with the generator by the pressure socket (fig.1-(2)). The data acquisition and processing is done by a computer, thanks to a calibration software, called LEON.

LEON is a french acronym for Logiciel d'Etalonnage en pressiON. That means Pressure Calibration Software. Figure 3 shows the whole calibration system. The travelling standard is the internal barometer but the software enables the use as standard of either the internal or an other barometer standard.

The operating barometers are checked by a cycle calibration at fourteen pressure values from 1060 hPa down to 800 hPa.

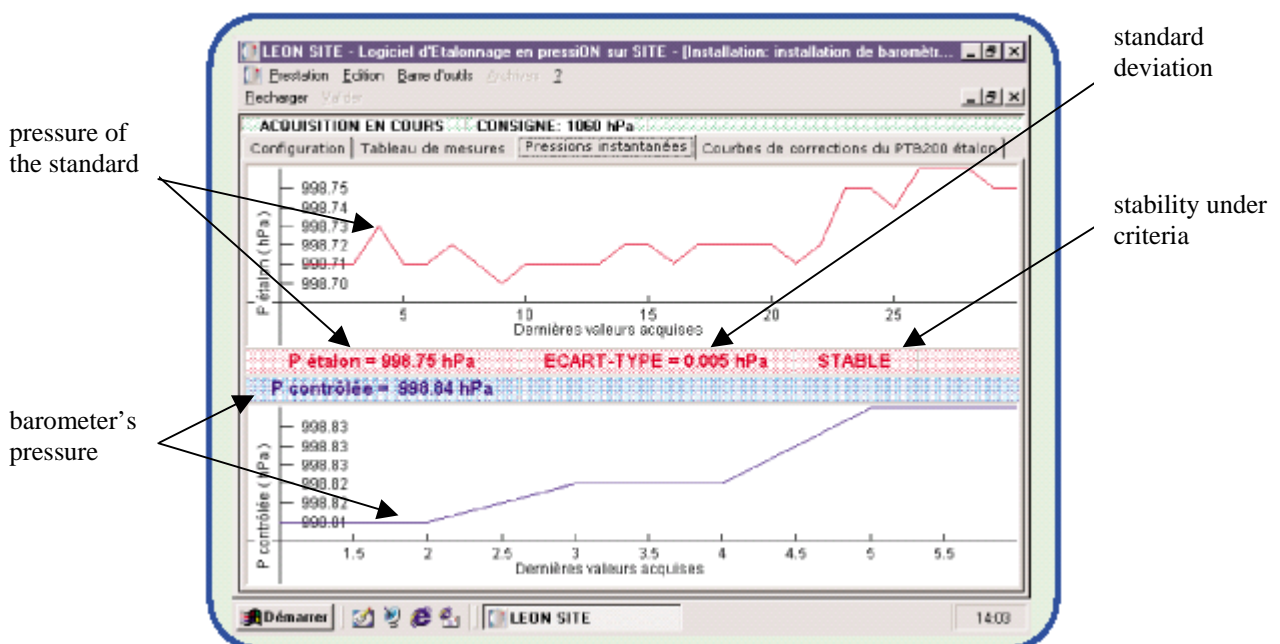


*fig.4 : Software LEON*



The calibration software, programmed in Delphi® (Pascal), uses serial RS 232 communication but there are manual calibration options too. This software is very useful for the calibration operator. The management of raw and corrected data, reference barometer, working standard and calibrated barometer is simplified.

### 2.2. Validation of the calibration

This system fulfills the needs of the traceability chain when there is no permanent installations to calibrate automatic weather station network barometers.

To validate in situ measurement, the travelling standard is calibrated before the travel and after the return (The tolerated criteria is 0.03 hPa). That means that the difference between both calibrations must be less than 0.03 hPa This criteria is part of the uncertainty balance.

## 3. Performance

### 3.1. Stability

The stability of the generator belonging to the Laboratory of Metrology was studied in July, 2004, to characterize its response time and its range of generation.

The study was led in the laboratory, at the ambient temperature, with an external standard (one of the working standard of the Laboratory of Metrology) at 20 %, 50 % and 80 % of the whole common range (1060 hPa-800 hPa). So the generator was studied from 850 hPa to 1010 hPa down first and from 1010 hPa to 850 hPa up after. Two blank cycles were made before testing.

Once the established working obtained (the standard deviation on the last five measurements is below than 0.01 hPa), one measurement was taken every 5 seconds during one minute.

Here, results are shown:

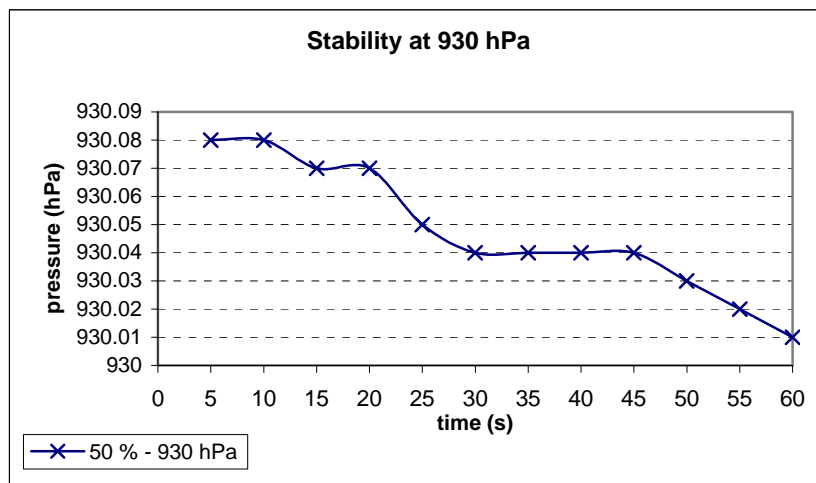


*fig.5 : Stability from 1010 hPa to 850 hPa down*

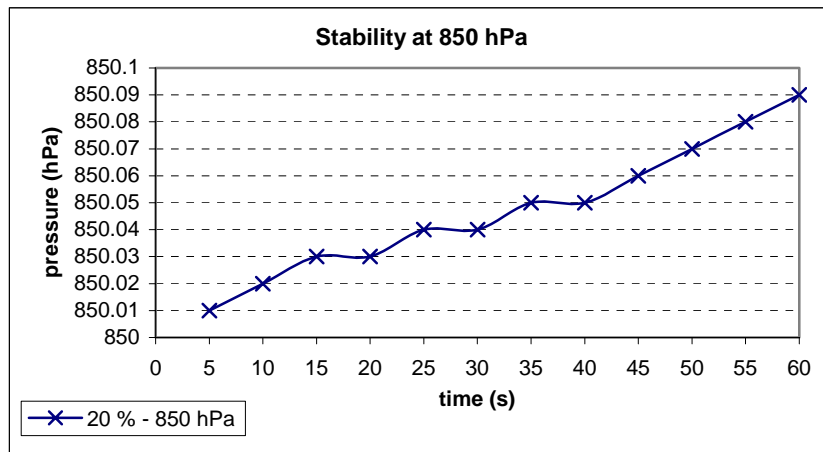


*fig.6 : Stability from 1010 hPa to 850 hPa up*

During one minute, the generation range is 0.08 hPa in the two cases. The diagrams shows the hysteresis of the generation. It contributes to the uncertainty balance with a component of 2.3 Pa considering a normal distribution law.

### 3.2. Intercomparison

To study the efficiency of our in situ calibration in pressure, an intercomparison was made with the calibration in laboratory. In our laboratory, we use a PPC 1 generator, with an external standard and special software for data acquisition.

We chose two parascientific-sensor based barometers among our standards : n°1331, our reference standard, which was considered as the standard, and the n°1332, a working standard, which was considered as the calibrated barometer .

N°1331 was calibrated in October, 2003.

N°1332 was calibrated with LEON in January, 2004, compared to n°1331, in our laboratory. Then, it was calibrated also in our laboratory with our fixed means, in March, 2004, by the same operator and according to the same measurement procedure : two blank cycles, one cycle from 1060 hPa to 800 hPa down, hence fourteen points.

Here the calibration diagram :

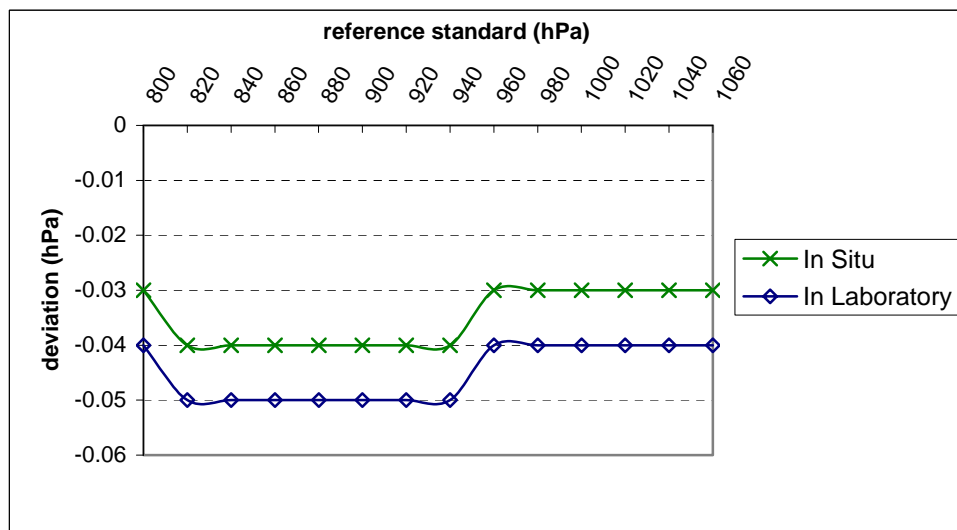


*fig.7 : Intercomparison between in situ and in laboratory*

The two calibration diagrams are similar on figure 7. The normalised deviation is :  $0.08 \ll 1$  so the two calibrations are very coherent.

To conclude, this in situ calibration system is a reliable one, which fulfills the needs of the traceability chain, provided the requirements are satisfied.

It is used by Météo France to check the drift of the french synoptical network operating pressure transmitters in addition to the calibration in the Laboratory of Metrology. This equipment is also used by Asecna, french nuclear plants network or when some countries require Météo France's support as Regional Instrument Center (RIC) to check their reference barometers (recently Egypt and Algeria).

Next step will be a LEON Software update to take into account the in-situ accreditation criteria.

This step will also include a multiple language setup (French, English, Spanish, Italian and Czech in the first step).

# UNCERTAINTIES OF MEASUREMENTS IN METEO-FRANCE' S MONITORING OF THE CHEMICAL COMPOSITION OF PRECIPITATION

A. Mezdour, J. Duvernoy, C. Thibord, A. Dubois

Météo France, Direction des Systèmes d'Observation, Laboratoire de Métrologie  
7, rue Teisserenc de Bort  
78195 TRAPPES Cédex  
☎ 01.30.13.63.50

✉ [abdelkrim.mezdour@meteo.fr](mailto:abdelkrim.mezdour@meteo.fr)  
✉ [corinne.thibord@meteo.fr](mailto:corinne.thibord@meteo.fr)  
✉ [jerome.duvernoy@meteo.fr](mailto:jerome.duvernoy@meteo.fr)  
✉ [aurelie.dubois@meteo.fr](mailto:aurelie.dubois@meteo.fr)  
[www.meteo.fr](http://www.meteo.fr)

---

## **ABSTRACT :**

The World Meteorological Organization created in the sixties, several networks of pollution's survey including a worldwide network: BAPMoN, Background Air Pollution Monitoring Network.

In 1977, Météo France in association with a chemical analysis laboratory, decided to participate in this network with six stations of precipitation sampling. Nowadays, three stations are measuring pH, conductivity and chemical composition in principal mineral ions, through weekly samples. The Météo France's network was integrated into the WMO's program Global Atmosphere Watch (GAW) in 1989. Météo France developed a quality assurance plan, according to the GAW's requirements, which has been managing the Météo France's activities since 1993.

Today, the database is 25 years old.

In a first part, the results of chemical composition of precipitation in France of the last 25 years and the methods of chemical analysis are presented. Then, different problems concerning sampling, sample's storage, handling and transporting are analyzed.

In a second part, we will deal with the protocols chosen by Météo France in order to fulfill GAW's requirements concerning:

- internal controls of the samples (visual, pH and conductivity);
  - monitoring of our measuring apparatus, control of material;
  - methods of analysis and the associated uncertainties;
  - intercomparisons organized by the WMO twice a year to evaluate the fiability of the measurements;
  - "testing samples";
  - reanalysis according some selection criteria to test some methods.
-

## **INTRODUCTION:**

In front of the increase of pollution in the world, the WMO decided to create in the sixties several networks of pollution survey, among them BAPMoN (Background Air Pollution Monitoring Network). The WMO combined them to form the GAW (Global Atmosphere Watch) in 1989. Nowadays, there are 400 GAW stations in the world, global and regional sites. The GAW programme ([www.wmo.ch](http://www.wmo.ch)) coordinates global monitoring of aerosols, ozone, greenhouse gases, ultraviolet radiation, selected reactive gases and precipitation chemistry.

Our French network for the GAW dedicated to monitor the chemical composition of precipitation began in 1977 with six regional stations. Today only three of them are still working (see figure 1).

The stations in Abbeville and Gourdon are under oceanic influence, whereas Carpentras is under Mediterranean influence.

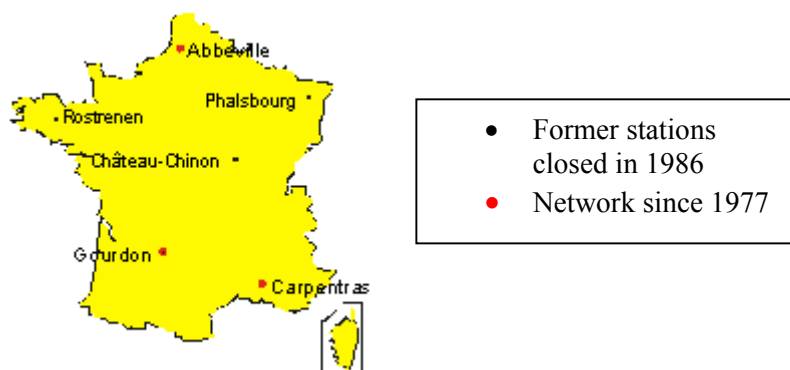
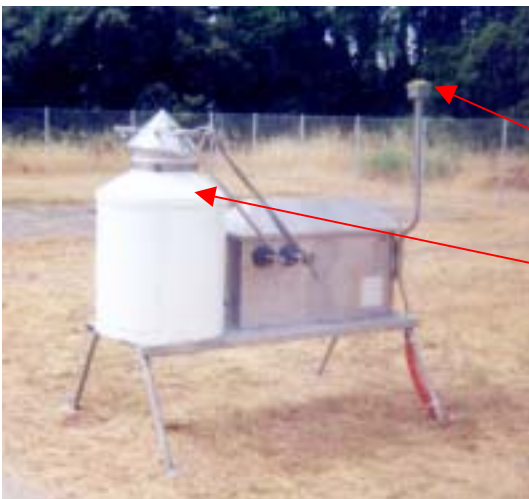


*Fig.1: GAW French network*

In a first part, we will deal with the sample collection and the chemical analysis, which are the main uncertainty components. In a second part, the main results obtained by Météo France for France over the last 25 years are presented. Finally, in a last part, the uncertainty balance is presented.

## 1. Sample collection

### 1.1. Rain Gauge



Sampling collection is made by a special rain gauge developed in the DSO (Direction des Systèmes d'Observation/Direction of Observing Systems) for Météo France. Main technical characteristics are:

- a precipitation sensor for the beginning and end of precipitation;
- a reception cone (area=580 cm<sup>2</sup>) with a lid driven by the precipitation sensor and a motorized mechanism;
- lead acid battery of 24 V for the power supply;
- height of sample collection: 1,30 m.

*Fig. 2: new rain gauge (since the end of 2004)*

A lid opens and closes over the sample container orifice. So, only the constituents of precipitation are collected. The precipitation measurements made by the rain gauge are then representative.

Precipitation sample container is chemically inert for the constituents measured and is decontaminated before each use.

## **1.2. Sample collection**

The weekly sample collection is made each Tuesday morning, according to a rigorous protocol, based on the GAW's requirements. As a matter of fact, precipitation samples are characterized by low ionic concentrations and are very susceptible to contamination.

The most important steps are:

- sample handling, for example only one sweat droplet may double the NaCl concentration;
- sample storage, because of the potential for chemical changes, especially because of temperature. The storage is also made in a fridge and the samples are transported in isothermal boxes as quickly as possible.

## **2. Chemical analysis**

Before being sent to an external laboratory to achieve all the chemical analysis, the samples are firstly analyzed by Météo France at DSO.

### **2.1. Analysis in the DSO**

Samples are first sent to the DSO where:

- aspect;
- weight;
- pH and conductivity (if there is enough precipitation >200 ml or 3.5 mm of rain) are checked.

Our pH and conductivity measurements follow of course a rigorous protocol based on the WMO requirements. Certified reference materials of pH = 4 or 7 and of conductivity = 20, 50 or 100  $\mu\text{S}\cdot\text{cm}^{-1}$  are used to calibrate our pH-meter and conductimeter.

### **2.2. Analysis in the subcontractor laboratory**

DSO has been subcontracting the measurements of pH, conductivity and main ions to the same laboratory of chemical analysis since 1977.

Their protocols follow the WMO requirements according to a quality assurance plan, which describes the sample handling and storage, the analytical measurements and the results supplied to Météo France.

Besides, the laboratory is checked by:

- comparison with our pH and conductivity measurements;
- blind samples;
- replicate analysis;
- intercomparisons planned by the WMO twice a year.

The analytical precision ( $S_i$ ) of the laboratory can be calculated from duplicate analysis of the same precipitation samples to estimate the contribution of analytical variability:

$$S_i = \left( \frac{\sum di^2}{2.N_i} \right)^{1/2}$$

where  $di$  is the difference between the two analyses and  $N_i$  the number of sample pairs.

Recently, we use the methodology *M.MAD* (Modified Median Absolute Difference) developed in the last GAW Report to calculate the precision of measurements made by our laboratory (see [1], Appendix A p91).

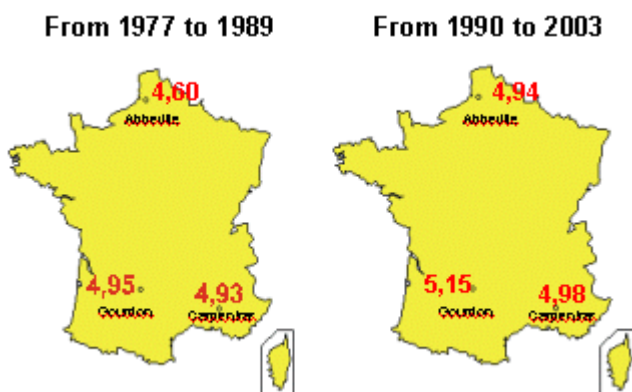
$$M.MAD = \frac{1}{0.6745} \times Median(|xi - Median(xi)|)$$

where  $xi$  is the variable of interest (in our case, the sampler error for each set of paired concentration data obtained from replicate analysis).

The different intercomparisons give the laboratory accuracy and assess the inter-laboratory bias.

### 3. Major results in France over the last 25 years

#### 3.1. pH



The comparison between the two maps on figure 3 shows a real increase of pH for the three stations especially for the North of France, in Abbeville, where the pH is also the lowest.

*Fig.3: Average pH<sup>l</sup> in France*

Cumulative distributions of pH frequency are shown on fig.4. Period of three years have been chosen to demonstrate the pH evolution.

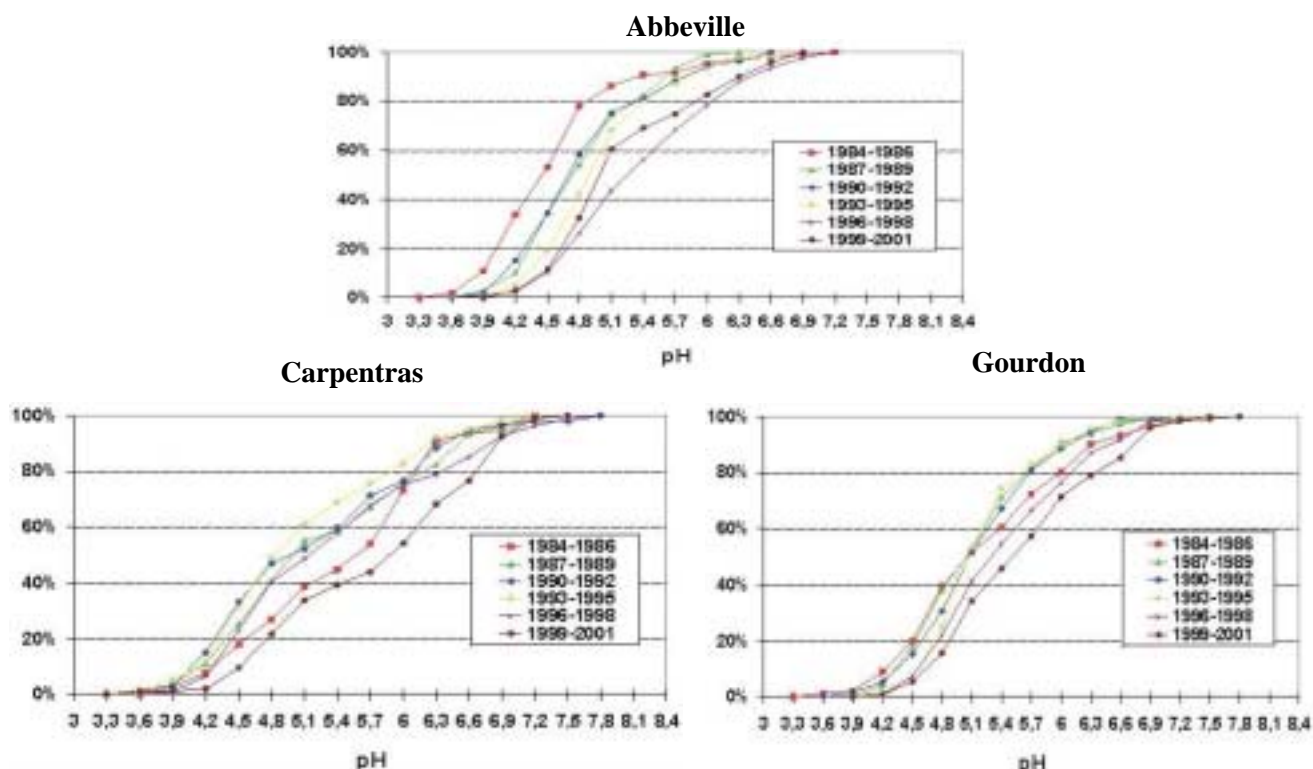


*Fig. 4: Cumulative distributions of pH-frequency in Abbeville, Carpentras and Gourdon from 1984 to 2001*

In Abbeville, between 1990-1992 and 1999-2001, the 50<sup>th</sup> percentile (median) increased of 0.4 pH-unit, in spite of an acidification between the two last periods 1996-1998 and 1999-2001, probably due to a deposit of sulphate.

We also observe for the two others stations, between 1990-1992 and 1999-2001, an increase of pH, with more intensity in Carpentras.

The difference of pH between Abbeville and Carpentras was nearly 1.1 pH-unit for the period 1984-1986 and decreased to 0.3 pH-unit in 1990-1992 until 1993-1995. Then, this difference increased and for the period 1999-2001, this difference was nearly about 0.6 pH-unit.

In Gourdon, pH has been remaining at a constant level since 1984; the little acidification of precipitation with pH > 5 observed between the periods 1984-1986 and 1990-1992 (see [3]) stopped in 1995.



Nowadays, the average pH in France is 5.13 pH-unit.

### 3.2. Ratio $\frac{NO_3^-}{SO_4^{2-}}$

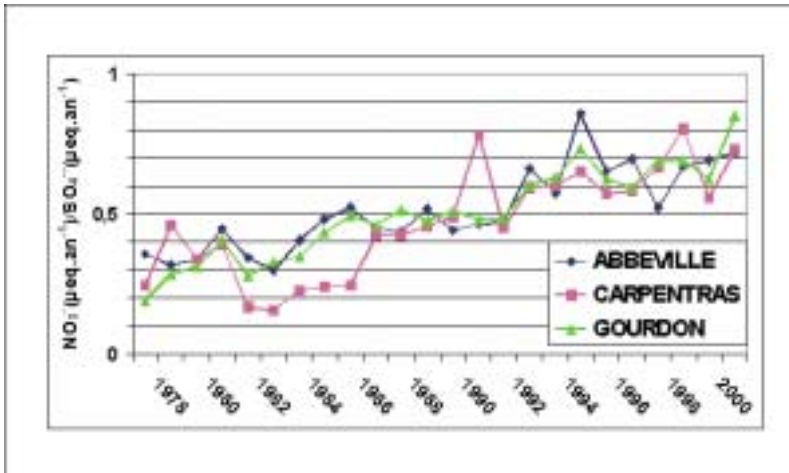


*Fig. 5: Ratio nitrogen/sulphur*

The ratio  $\frac{NO_3^-}{SO_4^{2-}}$  on the figure 5 tends to increase in the same extent for the three stations. An explanation could be that nitrogenous pollution, mainly from cars, is becoming more important.

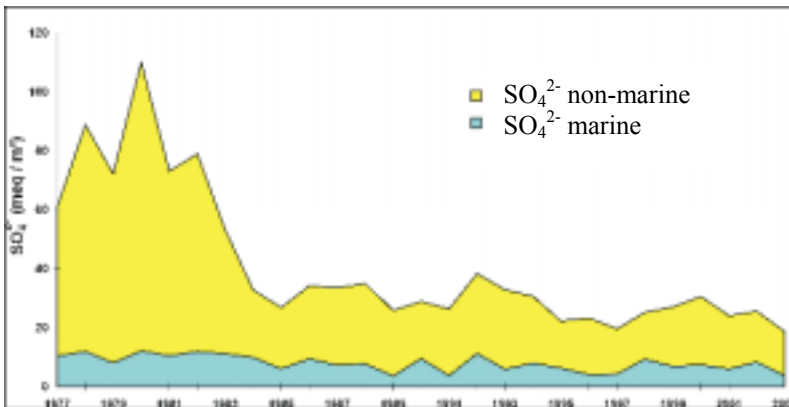


*Fig. 6: Non-marine versus marine sulphates in Abbeville*

Whereas the ratio of marine sulphates is almost at a constant level, the ratio of non-marine sulphates has been decreasing for 25 years, because of the closing down of a lot of heavy industries in the North of France and because of the stop of the thermal power stations. The decrease of non-marine sulphates is the more significant in Abbeville than in the other towns.

## 4. Measurements uncertainties

### 4.1. General description

The main components of the uncertainties for the monitoring of the chemical composition of precipitation are linked with:

- sample collection;
- analysis.

The sampling collection uncertainties are very difficult to estimate; however the precision of the whole precipitation chemistry measurement system (*overall precision*) may be determined by comparing the results obtained by two rain gauges located in the same place and working together during one year. The laboratory precision, which refers to the precision of the analytical measurements made by GAW Laboratories, could also be estimated. This calculation has been demonstrated by Sirois and Vet. Their publication in 1999 [4] was concerning the network CAPMoN (Canadian Air Pollution Monitoring Network). Then GAW fixed the Data Quality Objectives (DQO) (see [1], Appendix A p99).

The uncertainties of the laboratory that achieves the analysis are divided into:

- uncertainty of the measurement protocol;
- uncertainty of the sample matrix, which is quite difficult to determine because it depends on each sample. The only solution is to deal with the sample: replicate analysis, comparison with other measurement protocols...This solution is too expensive and so it is impossible to do it for each analysis.

### 4.2. Laboratory performance

The laboratory uncertainty\* linked to the measurement protocol has been established for stable synthetic samples and is summarized for each component of precipitation in the following worksheet 1.

In this worksheet, the precision  $Li^{**}$  of the analytical measurements made by our laboratory was calculated from precipitation samples of 2002 and 2003, which are composed of blind samples and of about 10% of routinely analyzed samples (see [2], p23).

					DQO
COMPONENT (UNIT)	MEASUREMENT PROTOCOL	RANGE	LABORATORY UNCERTAINTY*	LI**	LABORATORY PRECISION***
pH (pH-unit)	Glass electrode	3 -7.5	±0.05	±0.34 at pH >5 ± 0.13 at pH < 5	± 0.04 at pH >5 ± 0.02 at pH < 5
γ (μS/cm)	Conductivity cell	0-150	<5%	/	/
Cl <sup>-</sup> mg.l <sup>-1</sup>	Ion Chromatography	0.02-50	<5%	0.05	0.02
SO <sub>4</sub> <sup>2-</sup> mg.l <sup>-1</sup>	Ion Chromatography	0.02-30	<5%	0.03	0.03
NO <sub>3</sub> <sup>-</sup> mg.l <sup>-1</sup>	Ion Chromatography	0.02-30	<5%	0.04	0.03
NH <sub>4</sub> <sup>+</sup> mg.l <sup>-1</sup>	Automatic Colorimetry	0.01-20	<10%	0.12	0.01
Ca <sup>2+</sup> mg.l <sup>-1</sup>	Inductively Coupled Plasma	0.01-10	<10%	0.07	0.01
K <sup>+</sup> mg.l <sup>-1</sup>	Inductively Coupled Plasma	0.01-10	<10%	0.01	0.01
Na <sup>+</sup> mg.l <sup>-1</sup>	Inductively Coupled Plasma	0.01-20	<10%	0.06	0.01
Mg <sup>2+</sup> mg.l <sup>-1</sup>	Inductively Coupled Plasma	0.01-5	<10%	0.01	0.01
Acidity/Alcalinity (μeq/l)	Titration	±200	/	/	/

*Worksheet 1: Uncertainties, precision of laboratory, and DQO*

The precision of our laboratory was calculated here in 2002-2003 for 35 samples, which 16 had a pH<5. Over these 35 samples, 9 had a high conductivity (>30 μS.cm<sup>-1</sup>): six of them were collected in Abbeville, a station under marine influence.

Some analytical precision exceeds the Data Quality Objectives (pH, Cl<sup>-</sup>, NO<sub>3</sub><sup>-</sup>, NH<sub>4</sub><sup>+</sup>, Ca<sup>2+</sup> and Na<sup>+</sup>). In fact, the laboratory precision \*\*\* is calculated over more than 30 samples, as usual, but they cover the whole measurement range.

### 4.3. Intercomparisons

Twice a year, the WMO organizes an intercomparison for all the GAW members. It enables the laboratories to check if they meet the Data Quality Objectives (DQO) fixed by WMO, according to the laboratory bias:

$$bias = 100 \times \frac{Clab - MedianC}{MedianC}$$

where *Clab* is the laboratory's reported concentration and *MedianC* is the median concentration of all laboratories.

The worksheet 3 sums up the results obtained by Météo France in the intercomparisons organized by the WMO in 2003 (28<sup>th</sup> and 29<sup>th</sup>). For the two intercomparisons in 2003, our measurement bias is calculated and compared with the inter-laboratory bias:

		SAMPLE 1	SAMPLE 2	SAMPLE 3	DQO
pH	29th	O	O	O	± 0.07 pH-unit
	28th	N (0.1 pH-unit)	O	O	
γ	29th	O	O	O	± 7 %
	28th	O	O	O	
Cl <sup>-</sup>	29th	O	N (-27.54%)	O	± 10 %
	28th	O	O	O	
SO <sub>4</sub> <sup>2-</sup>	29th	O	O	O	± 7 %
	28th	O	O	O	
NO <sub>3</sub> <sup>-</sup>	29th	O	O	O	± 7 %
	28th	O	O	O	
NH <sub>4</sub> <sup>+</sup>	29th	N (-7.21%)	N (-14.63%)	O	± 7 %
	28th	N (-10.83%)	O	N (-10.15%)	
Ca <sup>2+</sup>	29th	N (19.04%)	N (56.86%)	O	± 15 %
	28th	O	N (-18.92%)	O	
K <sup>+</sup>	29th	O	N (57.89%)	O	± 20 %
	28th	O	N <sup>(1)</sup>	O	
Na <sup>+</sup>	29th	O	O	O	± 10 %
	28th	O	O	O	
Mg <sup>+</sup>	29th	O	N (-37.5%)	O	± 10 %
	28th	N (11.11%)	O	N (11.57%)	
Acidity-Alcalinity	29th	N (88.03%)	N (116.98%)	O	± 25 %
	28th	O	N (29.41%)	O	

N<sup>(1)</sup>: value was below the detection limit (<0.01mg.l<sup>-1</sup>)

O: bias meets the DQO

N: bias doesn't meet the DQO

Worksheet : Intercomparisons in 2003

In one hand, the results for pH and anions meet the quality objectives most of the time. On the other hand, results do not match for the cations, which exceeded the objectives, particularly for  $\text{Ca}^{2+}$  and  $\text{Mg}^+$  and  $\text{NH}_4^+$ . So we are working about the measurement protocol with the laboratory, to choose between chromatography and ICP (Inductively Coupled Plasma).

**To conclude**, to improve the measurement system of chemical composition of precipitation, we have to take care about:

- sampling collection, starting point of the measurement chain, in order not to provide contaminated samples;
- measurement protocols in the laboratory, especially traceability, calibration.

Thanks to the use of new rain gauges at the end of 2004, the DSO would be able to calculate the uncertainty of sample collection according to the WMO protocol (see [1], Appendix A p91-98).

### **BIBLIOGRAPHY:**

- [1] GAW Precipitation Chemistry Science Advisory Group, GAW: Manual for the GAW Precipitation Chemistry Programme, *Report No. 160*, 2004
- [2] Dr Jaroslav Santroch: Chemical Analysis of Precipitation for GAW: Laboratory Analytical Methods and Sample Collection Standards, *GAW Report No. 85*
- [3] Nadine Cenac et al., 1995: Précipitations Acides en France : Bilan et Tendances après 15 ans de mesures -10ème Congrès Mondial sur l'Air Pur, Espoo, Finlande (28 Mai- 2 Juin 1995), *IUAPPA & FAPPS*, vol.2, p.269
- [4] Sirois, A. and Vet. R. (1999): The precision of precipitation chemistry measurements in Canadian Air and Precipitation Monitoring Network (CAPMon). *Environ. Monitor and Assess.* 57, 301-329.

# Measuring Air Temperature by using an Ultrasonic Anemometer

*Eckhard Lanzinger<sup>1</sup>, Hans Langmack<sup>2</sup>*

<sup>1</sup>Deutscher Wetterdienst (DWD)  
TI23 b : Measuring Systems  
Frahmredder 95  
D-22393 Hamburg  
Germany  
ph: +40-6690-2455, fax: +40-6690-2499  
email: eckhard.lanzinger@dwd.de

<sup>2</sup>University of Hamburg  
Meteorological Institute  
Bundesstraße 55  
D-20146 Hamburg  
Germany  
ph. : +40-42838-5078, fax.: +40-42838-5452

## Abstract

This paper describes the basics for using a standard ultrasonic anemometer for measuring the air temperature. Under zero-wind conditions an uncertainty of measurement of  $< 0.1$  K was achieved in the temperature range from  $-25^{\circ}\text{C}$  to  $+25^{\circ}\text{C}$ . At wind speeds up to 14 m/s the measurement accuracy is better than 0.2 K. Future potential of acoustic temperature measurements and necessary improvements are presented.

## Introduction

Measurement of air temperature by using contact thermometers in weather screens of various designs is state of the art in meteorological measurements. However many screen intercomparisons have identified numerous sources of measurement errors that are inherent in all these systems, e.g. radiative heating, insufficient ventilation, psychrometric cooling, ageing effects and time constants.

To quantify these errors there is a need for a reference sensor, capable of measuring the true ambient air temperature with high accuracy. Measurement of the temperature dependant sound propagation has the potential for building such an "ideal" sensor as it offers a contactless temperature measurement and hence avoids most of the above mentioned error sources.

Moreover the accuracy of acoustic temperature measurements is best at low absolute air humidity conditions, e.g. at mountain sites. Therefore some ultrasonic anemometers that have already proven to perform well even under severe icing conditions [3] could be a future option for temperature measurements at automatic weather stations.

## Theory

The temperature dependence of the speed of sound  $c$  in humid air is given by [1]

$$c = \sqrt{\gamma_d R_d T \cdot \left( 1 + \left( \frac{\gamma_v}{\gamma_d} - \frac{M_v}{M_d} \right) \cdot \frac{e}{p - \left( 1 - \frac{M_v}{M_d} \right) \cdot e} \right)} \quad (1)$$

where  $\gamma_d$  and  $\gamma_v$  are the ratios of specific heats for dry air and water vapour,  $R_d$  is the gas constant of dry air,  $T$  is the air temperature,  $M_v$  and  $M_d$  are the molar masses for water vapour and dry air,  $e$  is the partial water vapour pressure and  $p$  the total air pressure.

It is important to note that the acoustic virtual temperature

$$T_{av} = T \cdot \left( 1 + \left( \frac{\gamma_v}{\gamma_d} - \frac{M_v}{M_d} \right) \cdot \frac{e}{p - \left( 1 - \frac{M_v}{M_d} \right) \cdot e} \right) \quad (2)$$

measured by an ultrasonic anemometer is not equal to the virtual temperature  $T_v$  used in meteorology [1], where the ratio of specific heats  $\gamma_v/\gamma_d$  in equation (2) has to be replaced by 1.

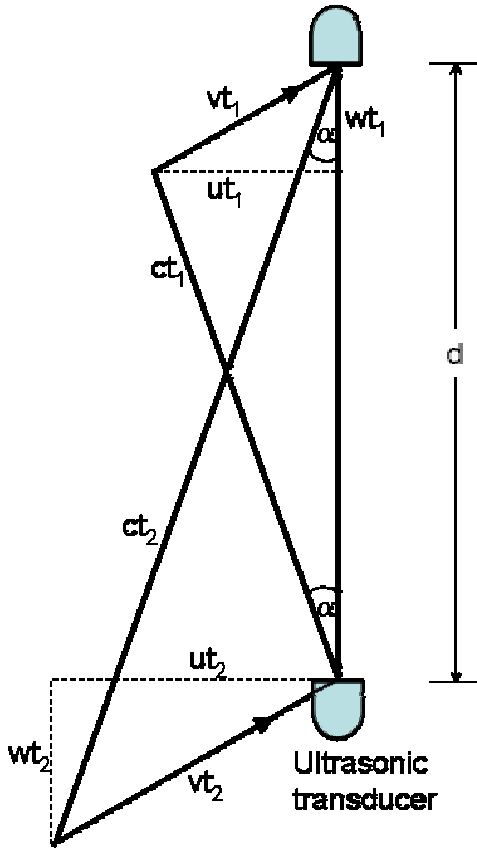


Figure 0: Schematic function principle of an Ultrasonic Anemometer (after Coppin and Taylor [4])

Unlike the wind measurement which is based on a differential measurement sonic thermometry uses an absolute measurement of the transit times

$$t_1 = \frac{d}{c \cdot \cos(\alpha) + w} \quad \text{and} \quad t_2 = \frac{d}{c \cdot \cos(\alpha) - w} \quad (3)$$

These are the times a sound wave needs to propagate from the lower transducer in Figure 0 to the upper one and back. Adding their reciprocals [2] we get

$$\frac{1}{t_1} + \frac{1}{t_2} = \frac{2 \cdot c \cdot \cos(\alpha)}{d} = \frac{2}{d} \sqrt{c^2 - u^2} \quad (4)$$

In this equation  $u$  is the wind component perpendicular to the measuring section between the transducers. Using eq. 3 and eq. 2 leads to

$$T_{av} = \frac{1}{\gamma_d R_d} \cdot \left[ \left( \frac{d}{2} \right)^2 \cdot \left( \frac{1}{t_1} + \frac{1}{t_2} \right)^2 + u^2 \right] \quad (5)$$

In ultrasonic anemometers the measurement of transit times  $t_1$  and  $t_2$  is done by counting the numbers  $n_1$  and  $n_2$  of clock cycles with duration  $t_0$  between the transmission and the reception of a sound signal. Due to processing times in the electronics some offset cycle counts  $n_0$  have to be added so that e.g.  $t_1 = (n_1 + n_0) \cdot t_0$ . Replacing these terms in eq. 5 leads to a final equation which has been used in these experiments to calculate  $T_{av}$  from the anemometers "raw data"  $n_1$  and  $n_2$ :

$$T_{av} = \frac{1}{\gamma_d R_d} \cdot \left[ \left( \frac{d}{2} \right)^2 \cdot \left( \frac{1}{(n_1 + n_0) \cdot t_0} + \frac{1}{(n_2 + n_0) \cdot t_0} \right)^2 + u^2 \right]. \quad (6)$$

Because it is an absolute measurement the geometric distance  $d$  of the sonic transducers has to be known very precisely if a precise temperature measurement is required. A deviation of 0.1 mm will result in a temperature deviation of about 0.3 K. Eq. 6 is used for calibration of  $d$  where  $T_{av}$  has to be determined by eq. 2 using precise reference measurements of  $T$ ,  $e$  and  $p$ .

## Experiment

In the following experiments two 2D ultrasonic anemometers (Thies Model 4.3810.20.340, Germany) have been investigated. Before using them for temperature measurements it is necessary to determine their actual measuring sections  $d_{NS}$  and  $d_{WE}$  of both sonic paths in a temperature controlled chamber.

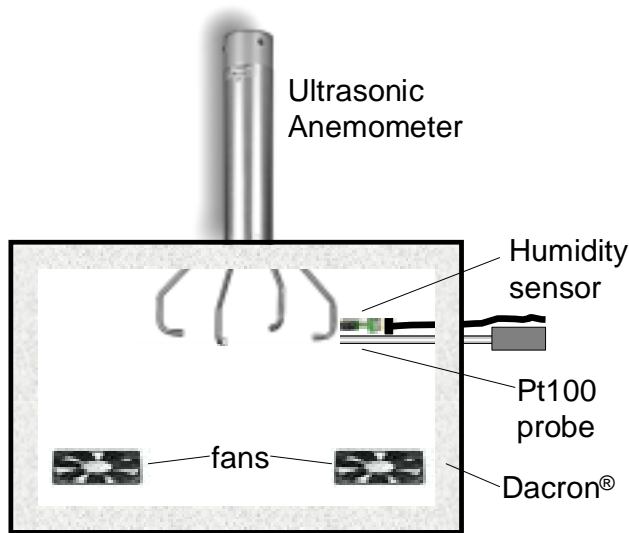


Figure 0: Temperature calibration box with ultrasonic anemometer mounted upside down, reference sensors for temperature and humidity and two fans providing vertical air circulation.

of  $T = -25^\circ\text{C}$ ,  $-15^\circ\text{C}$ ,  $-5^\circ\text{C}$ , ...,  $+25^\circ\text{C}$ . The insulated and closed box itself had a time constant of about 25 minutes which allowed the temperature inside to stabilise to a final temperature with an accuracy of  $< \pm 0.02$  K after about 4 hrs.

It was also important to avoid any heat source inside the calibration box. In our first experiments the ultrasonic anemometer was mounted completely inside the calibration box and its consumption power of 3 W induced a permanent temperature drift. In an improved setup we therefore mounted the sensor body outside the calibration box (see Figure 0), leaving only the sensor arms inside. The sensor's built-in heating was also switched off during calibration.

After calibration the influence of wind speed and direction on the acoustic temperature measurement has been investigated. In the wind tunnel of DWD in Hamburg the ultrasonic anemometer was slowly turned from  $135^\circ$  to  $315^\circ$  while applying stepwise wind speeds of 5 m/s to 45 m/s.

To avoid echoes of the sonic signals we placed the anemometer inside a wooden calibration box lined with a 5 cm layer of Dacron wadding. The reference thermometer (Pt100, 1/5 DIN class B, manufacturer: Heraeus) and a digital humidity sensor (Sensirion SHT75) were also mounted inside this box and at the same height as the ultrasonic transducers in order to avoid temperature differences by possible thermal layering. In a later experiment two small fans have been added to reduce this effect by circulating the air vertically. Air pressure was measured by a separate barometer.

The calibration box was placed inside a two-level controlled temperature chamber. Because of different time constants of the used sensors it was necessary to measure in stationary conditions, i.e. various fixed temperature levels



## Results

When determining the measuring sections  $d$  in the calibration box, we soon could see that  $d$  seems to be temperature dependent (see Figure 1) and apparently the arms of the anemometer bend slightly inward at low temperatures making the transducers coming closer. We measured a change of  $\Delta d \approx 0.4 \text{ mm}/50\text{K}$  corresponding to a temperature error of about 1.2 K if it would not be corrected. All sensors of this type we have calibrated so far show the same general behaviour but with different parameters. This means, every sensor has to be calibrated individually. To plot the temperature characteristic in Figure 1 the data for both measuring sections (North-South and East-West) were fitted by 4<sup>th</sup> order polynomials. It turned out that the data at  $T \approx +25^\circ\text{C}$  could not be used for the fit because the temperature had not stabilised enough inside the calibration box.

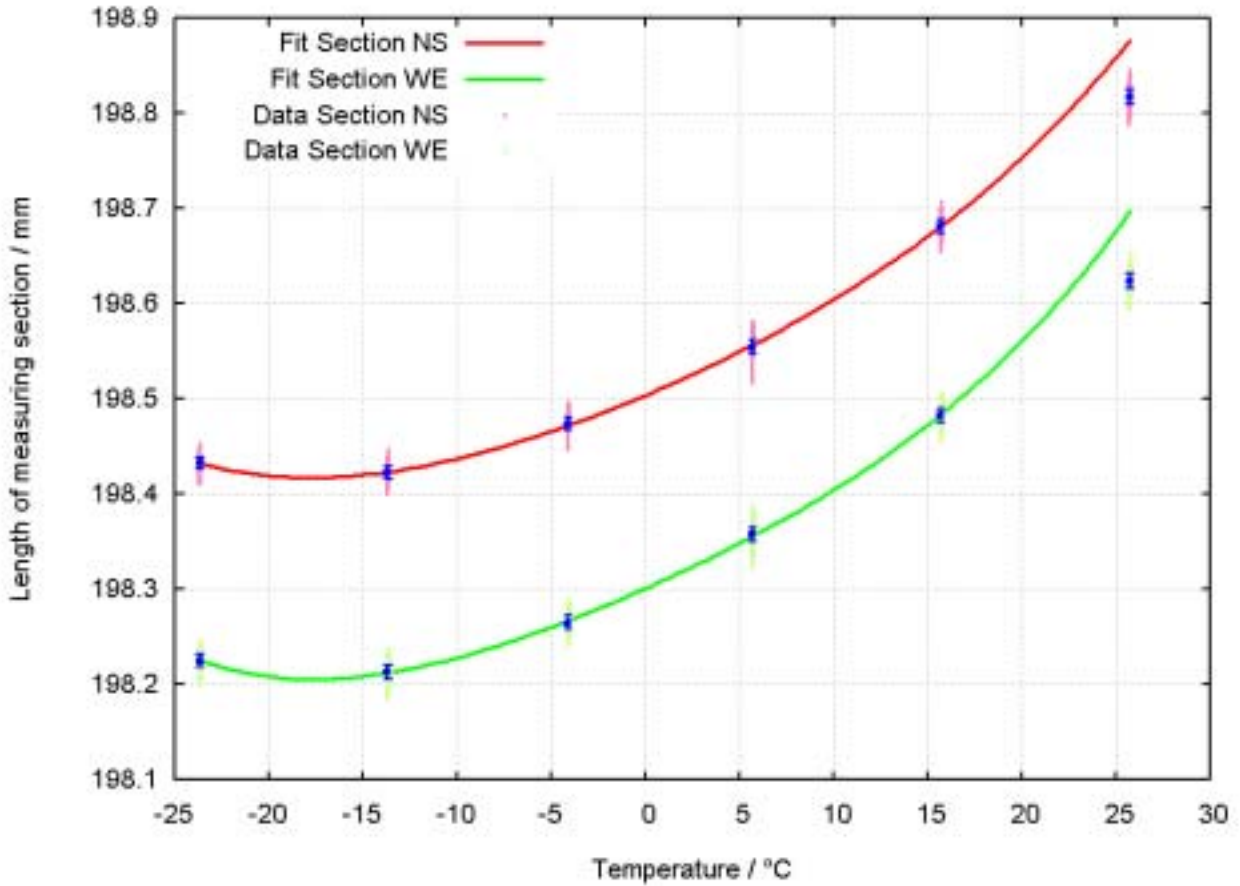


**Figure 1:** Calibration of both measuring section (NS and WE) of the ultrasonic anemometer. A 4<sup>th</sup> order polynomial was fitted to measured data. Each calibration point contains at least 1500 data whose vertical spread, mean values and standard deviation are indicated in the graph.

To confirm our suspicion that a mechanical deformation is the source of the temperature dependence we plan to carry out a direct distance measurement (e.g. interferometric), but generally any component in the signal path (transducers, protection caps) could cause this temperature effect.

Air temperatures can now be determined by an iterative calculation using eq. 2 resolved for  $T$ :

$$T = \frac{T_{av}}{\left( 1 + \left( \frac{\gamma_v}{\gamma_d} - \frac{M_v}{M_d} \right) \cdot \frac{e}{p - \left( 1 - \frac{M_v}{M_d} \right) \cdot e} \right)} \quad (7)$$

in which  $T=f(T_{av}, e, p)$ . The acoustic virtual temperature is derived by eq. 6 where  $T_{av}=f(d, n_1, n_2, u)$ , and in turn  $d=f(T)$ . In the first step of the iteration a fixed value for  $d$  was chosen, e.g.  $d$  at  $T=20^{\circ}\text{C}$ , resulting in a first guess for the air temperature which is used in  $d=f(T)$  for the next iteration step. After the third iteration the results converged and are shown in Figure 2.

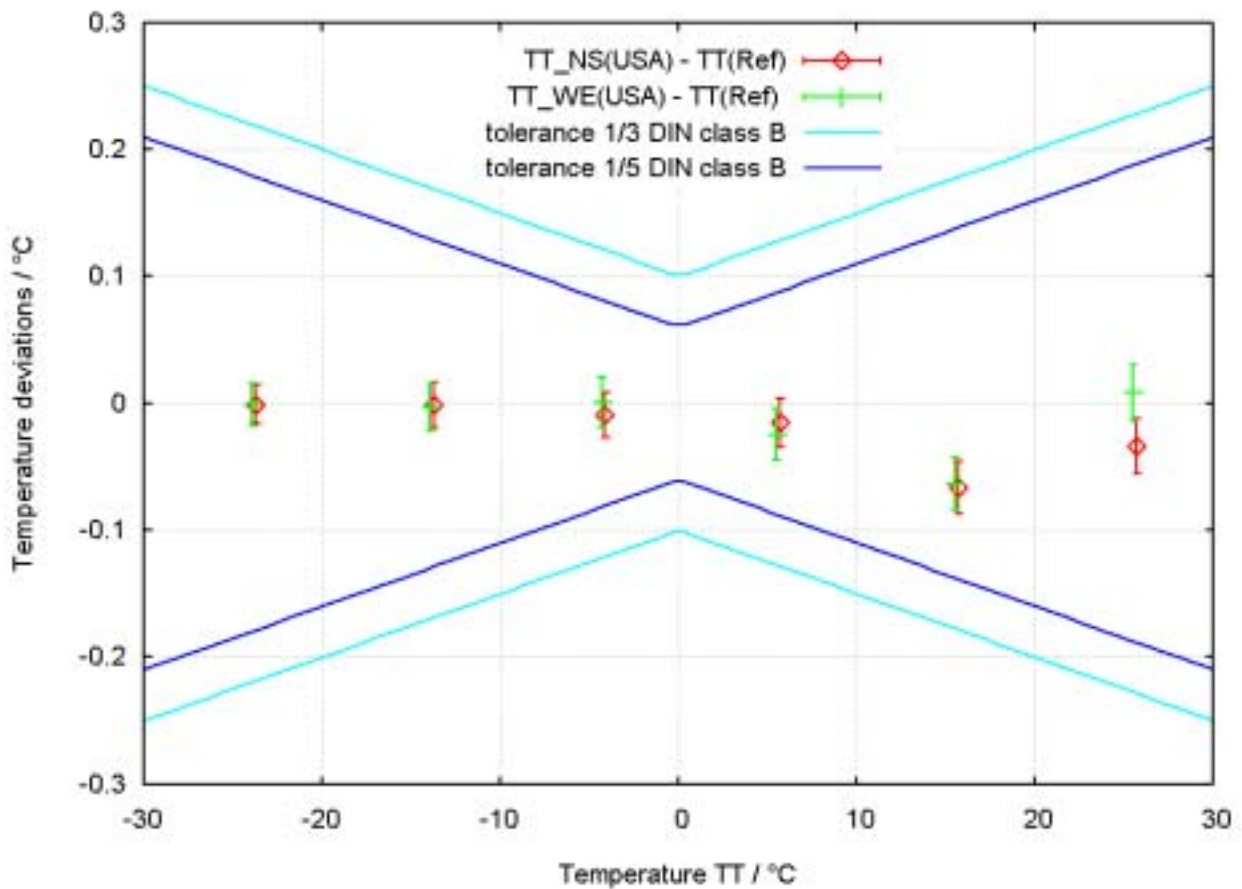


**Figure 2: Plot of Mean values and standard deviations of the sonic thermometer comparison with a reference Pt100 sensor (1/5 DIN class B). The air temperatures derived from the sonic thermometer are within the specifications of a good Pt100 sensor (under laboratory conditions).**

The mean values and standard deviations of all measurements are well inside the 1/5 DIN tolerance over the whole temperature range from  $-25^{\circ}\text{C}$  to  $+25^{\circ}\text{C}$ . The 1/3 DIN specification for operational pt100 thermometers is easily fulfilled.

The numeric results of this comparison are summarised in Table 1. The achieved accuracy is thus better than 0.1 K for the used temperature range.

It must be stated that this test has been performed under favourable conditions, i.e. stationary conditions, medium (indoor) humidity and no wind. As soon as the temperatures are drifting, larger differences between the sonic and the reference thermometer can be observed.

The measurement displayed in Figure 3 was also performed in the calibration box but a rapid temperature drop was applied. The lag free sonic thermometer (green curve) reacts immediately to the temperature change whereas the reference Pt100 (red curve) follows with a time constant of about 80s.

**Table 1: Results from the laboratory comparison of the sonic thermometer with a reference Pt100 sensor (see Figure 3).**

Reference temperature	Mean $TT_{USA} - TT_{Re}$ (NS) <sub>f</sub>	of Standard deviation	Mean $TT_{USA} - TT_{Ref}$ (WE)	of Standard deviation
-23.70	-0.001	0.016	-0.002	0.017
-13.72	-0.002	0.017	-0.004	0.019
-4.16	-0.009	0.018	0.000	0.020
5.66	-0.015	0.019	-0.025	0.020
15.66	-0.066	0.021	-0.064	0.021
25.68	-0.034	0.022	0.008	0.022

The differences (orange curve) add up to -1.5 K. If the sonic data are post processed (blue curve) with the same time constant as the reference (about 80 s) the deviations (light green curve) become less than 0.3 K. The remaining differences observed might be due to imperfect ventilation during the cooling process leading to real temperature differences on a cm scale inside the calibration box.

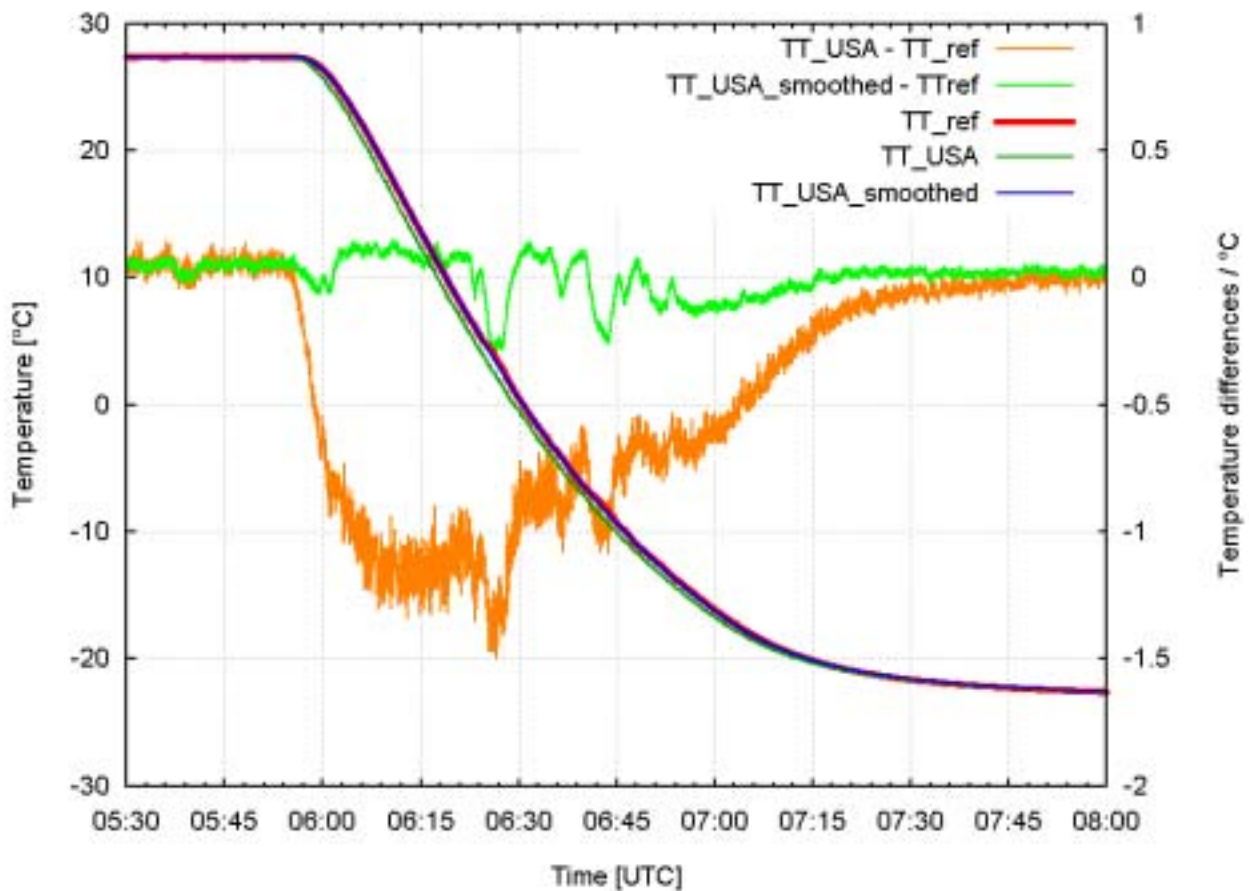


**Figure 3: Comparison of the sonic thermometer and the reference during a rapid cooling process from +27°C to -22°C (left axis) within 1.5 hrs. Obviously the sonic thermometer (green curve) reacts faster and the reference thermometer (red curve) follows with delay. For the blue curves the sonic data have been smoothed with a time constant  $T_c=80s$ , resulting in much smaller differences (light green curve).**

In order to examine the influence of the crosswind component, perpendicular to a respective measuring section, the ultrasonic anemometer was exposed to various wind speeds in a wind tunnel.

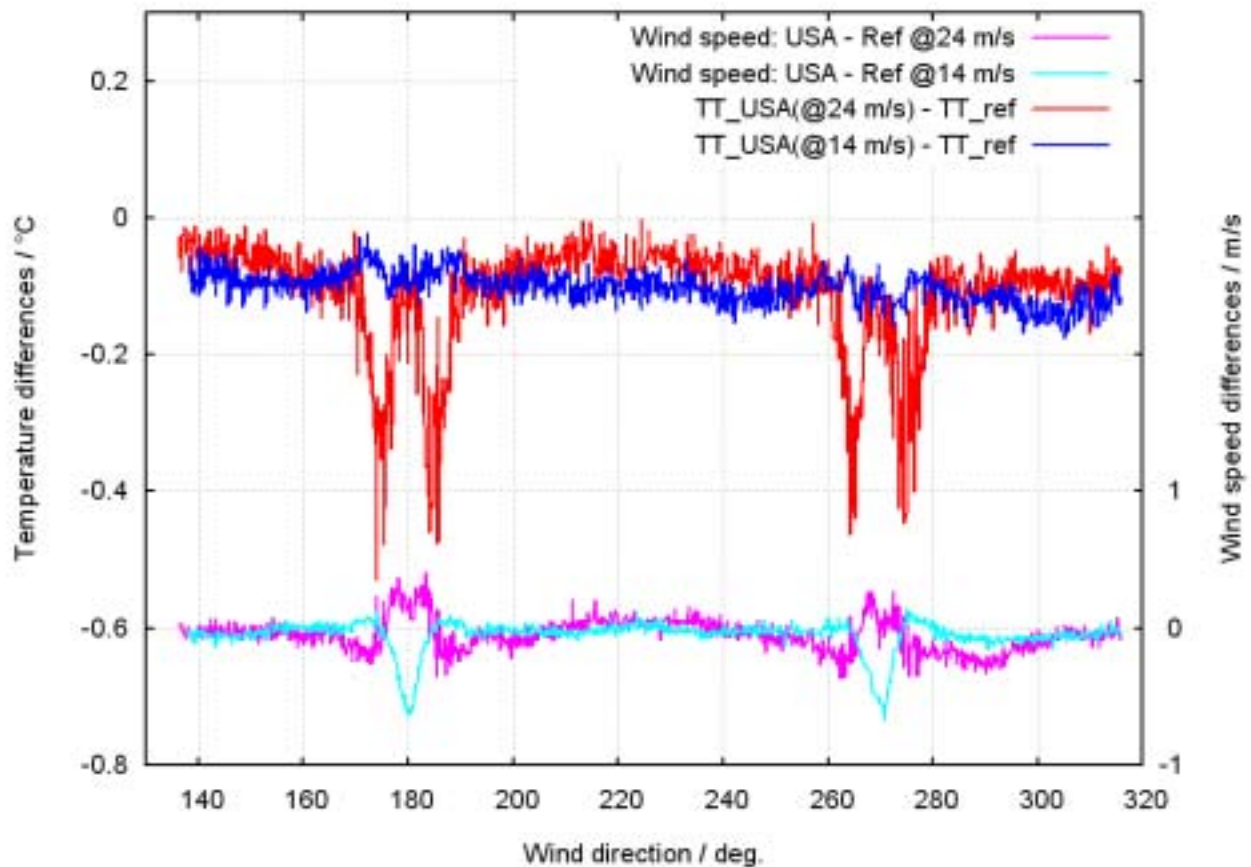


**Figure 4: Temperature differences between the ultrasonic anemometer and the Pt100 reference at 20°C and wind speeds of 14 m/s and 24 m/s (upper curves) plotted against wind direction. The lower curves show the corresponding wind speed deviations of the ultrasonic anemometer.**

According to equation 6 the crosswind component causes a temperature deviation of  $u^2/(\gamma_a R_d)$ , which amounts e.g. to 0.5 K at 14 m/s and 1.4 K at 24 m/s. In the plot in Figure 4 this correction has been applied and it is shown that the compensation generally works well. The sonic temperatures deviate only by - 0.1 K from the reference which is partly due to imperfect calibration of the measuring sections at temperatures around 20°C (see Figure 2). Figure 4 shows that the largest deviations in acoustic temperature (approx. 0.5 K at 24 m/s) and wind speed coincide at wind directions of 180° and 270° where the ultrasonic transducers are mounted. Thus these deviations originate from the transducers disturbing the wind field at higher wind speeds. For precise sonic temperature measurements it is therefore essential to correct these wind speed errors.

## Conclusions

For precise sonic temperature measurements the measuring sections of a sonic anemometer have to be calibrated with respect to its temperature dependance inside a zero-wind calibration box. By means of the resulting temperature characteristic an accuracy of less than 0.1 K can be achieved in zero wind speed conditions. The source of the observed temperature dependence of the Thies anemometer has to be further investigated and sonic anemometers of other manufacturers should be tested as well.

It has been shown that the influence of the crosswind component can be compensated very well for wind speeds up to 14 m/s. At higher wind speeds turbulences originating from the ultrasonic transducers disturb the measurements of wind speed and acoustic temperature. A sophisticated correction algorithm for the wind speed as a function of wind direction and speed has to be

developed to provide precise temperature measurements under all conditions. Further comprehensive wind tunnel experiments are necessary to establish an effective method.

The results encourage us to use a temperature calibrated ultrasonic anemometer as a temperature reference for an analysis of the measurement errors caused by a weather screen. Knowing the time lag of a thermometer-screen system as a function of wind speed it is possible to apply the respective time constants to the sonic temperature data that are virtually free of any time lag. Thereby it should be possible to separate the intrinsic lag effects from “real” screen errors like radiative heating, psychrometric cooling and others.

Application of ultrasonic anemometers for measuring temperature at mountain sites benefits from lower temperatures resulting in a reduced influence of water vapour on the acoustic temperature. On the other hand an accurate wind correction is indispensable and the influence of the automatic heating for deicing the sensor on the temperature has to be investigated.

## Acknowledgements

The authors wish to thank Manfred Theel from DWD in Hamburg for his valuable contributions to these measurements and also for assisting the evaluation by fruitful discussions. Special thanks go to Horst Niemand for building the calibration box in a very short time.

## References

- [1] Miller, D.C.: Sound Waves – Their Shape and Speed. *The Macmillan Co., New York*, (1937).
- [2] Hanafusa, T., T. Fujitani, Y. Korobi, Y. Matsuta: A New Type Sonic Anemometer / Thermometer for Field Operation. *Papers in Meteor. and Geophys.*, **33**, (1982).
- [3] Tammelin, B. et al.: Improvements of Severe Weather Measurements and Sensors – EUMETNET SWS II Project (Final Report). *Finnish Meteorological Institute, Helsinki*, (2003).
- [4] Coppin, P.A., Taylor, K.J.: A Three-Component Sonic Anemometer/Thermometer System for General Micrometeorological Research. *Boundary-Layer Meteorology*, **27**, pp. 27-42, (1983).

# **AUTOMATIC TECHNICAL SELF CHECK SYSTEM FOR THE DWD WEATHER RADAR NETWORK**

**Theodor Mammen**, Bertram Lange  
German Meteorological Service  
Frahmredder 95 22393 Hamburg  
Germany

Tel.: ++49 (0) 6690 2417

Fax.: ++49 (0) 6690 2499

Email: theodor.mammen@dwd.de, bertram.lange@dwd.de

## **Abstract**

The German Meteorological Service (DWD) operates a network of 16 operational C-Band weather radars. Approx. 36.000 products are generated and disseminated fully automatic per day.

The technical status of the radars is recorded by a Built-In-Test-Equipment (BITE) while the status of the software and data processing system is gathered by SW-daemons. This includes the production and dissemination time for every product. All information is packed every 15 minutes and sent as standard radar product to the radar operation center in Hamburg.

Here the actual parameters (approx. 600 per station) are compared with reference values. The results are shown in HTML-pages with a color coding, depending on severity of differences. The availability of products is given in detail and as percentages. The parameters are grouped and the lowest status of each group is shown on a nationwide map.

Servicemen use this utility to see problems as soon as possible and for failure analysis. The tool is simple to implement and helps to improve the system and product availability.

## **1. Introduction**

The German Meteorological Service (DWD) operates a network of 16 fully automatic weather radars. The systems are computer controlled and the operating mode can be configured widely without changes in source code. So the software on all systems is the same and only parameters may vary from site to site. To achieve optimum homogeneity throughout the network, the variance is restricted to device dependant values.

Beside the software parameters also the hardware, i.e. transmitter, receiver, server etc, must run in proper mode. Because all stations are unmanned they are serviced every 4 weeks and diverse HW-parameters are recorded by the software for technical monitoring.

The main goals for the automatic self check system in the DWD radar network is to alert the servicemen as soon as malfunction occurs and to provide information for quality management or data interpretation (metadata). The "Technical-Monitoring-Radar" (TeMonRa) started in 2000 and is continuously improved. Since the software on the radar computers (RMV from SIGMET/Lassen/EEC) will be replaced in 2005 by MURAN from GAMIC a major change is showing up, while the basic principle will be the same.

## 2. The radar system

The radar systems in DWD are standard C-band radars with well defined interfaces inside. Today two types are in operation: 5 DWSR-88 (EEC / DRS) and 11+1 METEOR 360 (Gematronik / AMS). The 12th METEOR is a research radar at Hohenpeissenberg. The 16 operational systems are evenly distributed over Germany, so that full coverage is achieved with 150 km radar range.

The general structure of both systems is given in Fig.1. The radom-covered dish is driven by a servo system while transmitter and receiver work in single polarisation with doppler capability. The HW is mainly controlled by the radar control computer and primary data acquisition is done by a signal processor (RVP-family from SIGMET). Diverse sensors in the HW give measures like forward and reverse power, several voltages and currents etc.

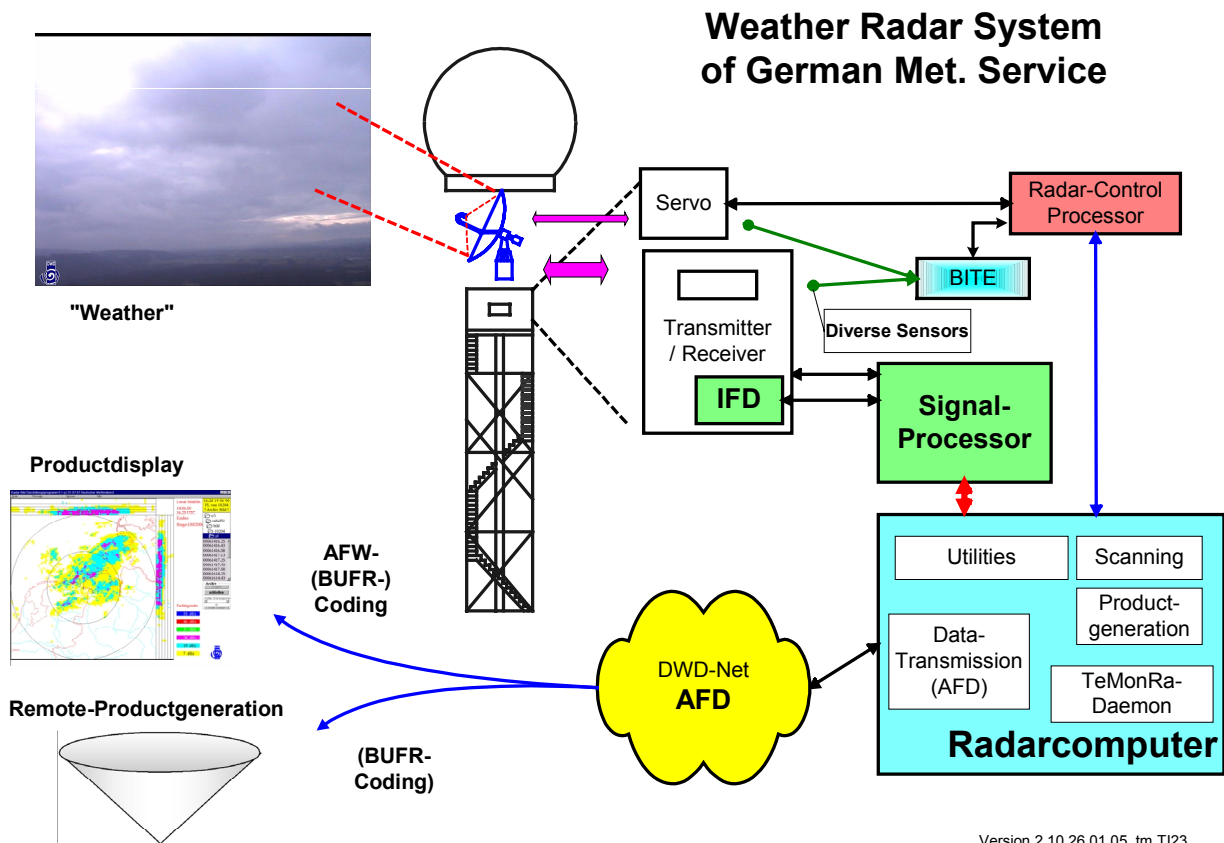


Fig. 1: General structure of the DWD weather radar system.

The radar computer holds utilities for calibration etc, software for making scans as well as products and an application for the transfer of data. Beside this typical radar software components there run some modules for the technical monitoring. The radar computers are part of the DWD-WAN (DWD-Net) and can be accessed over TCP/IP, i.e. also by cellular phone from any computer in DWD.

This year the radar computers will be switched from VAX/VMS (DEC) to Intel/Linux and run the Open Source Software AFD (Automatic File Distribution) as well as a webserver for http access. This opens more options for the technical monitoring.

## 3. Basic principle

The technical monitoring compares actual values of the parameters with a reference and displays the results as color coded HTML-tabels. It is conceived only for surveillance. The system does not allow any action on the radar, this is done by means of the radar software. TeMonRa consists of three main steps:

## A. Manual configuration

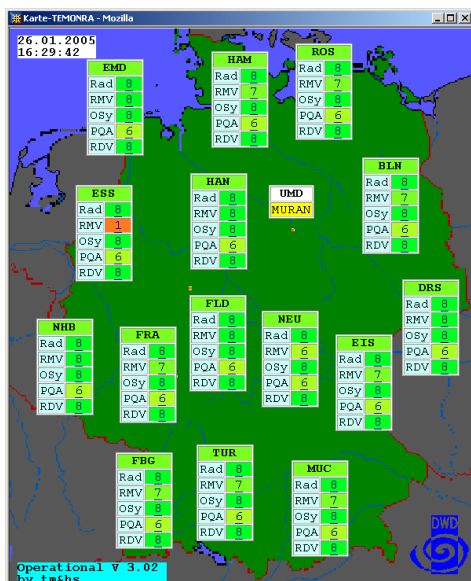
First the hard- and software is configured and calibrated manually. All parameters are set to required values, like transmit power, antenna position, pulse-repetition-frequencies or filters in the signal processor. After all (hundreds of) parameters have been checked, this gives the "reference parameter set".

## B. Recording information

On each radar computer daemons gather all available meta information and code it into files every 15 minutes. The files are sent to the radar operation center in Hamburg per AFD.

## C. Evaluation and Display

In Hamburg the actual data is compared to the "reference parameter set" from step A. The result is displayed in HTML-pages, where the state is color coded. See e.g. Figure 3. For a better overview the parameters are grouped and the bottom quality for each block is given in a nationwide overview for Germany, see Fig. 2.



Legend:

- for every radar site there is a small table
- parameters are grouped and the bottom quality of each block is shown
- the states go from 0=worst (red) to 8=best(green), with 9=no data (pink)
- each state-number is linked to a page with detailed information, see e.g. Fig 3.

Fig. 2: Nationwide overview of TeMonRa.

An example of the detailed views is shown in Fig. 3. The left frame gives links to the overview map and to the different blocks of every site. The right frame shows detailed information, here a part of the RMV scan definition. The left column gives a description of the parameter and the second column holds the actual values. The third column holds the reference values and gives differences to the actual data as color code. A severity of the parameter with respect to product quality is given as color from green, over yellow, orange to red.

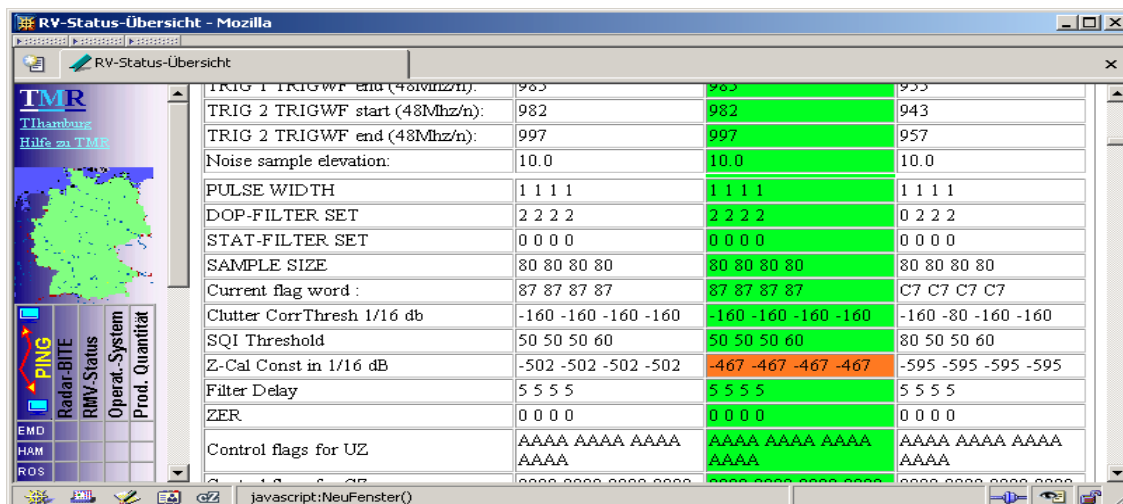


Fig. 3: Example for detailed view, here scanning parameters.



In future a comparison to the nationwide reference values in the 4th column is planned.

With the actual RMV-Software the monitoring data is gathered every 15 Minutes. As far as possible really used values are recorded, but not all parameters can be retrieved from the software after usage. Monitoring of configuration files is not included in the package.

#### 4. Future aspects

In spring of 2005 the new MURAN software will be put into operation together with packages like AFD and BigBrother. In conjunction with web servers on each radar computer the capabilities of the monitoring can be expanded while keeping the basic principles:

- substantial logging of MURAN and AFD of actions allow detailed tracing
- specialized error analysis can be done on site through dynamic HTML-pages so that only part of the local information has to be transferred to Hamburg
- monitoring on operating system level will done by BigBrother, a powerful tool, which also shows information about other components like uninterrupted power supply

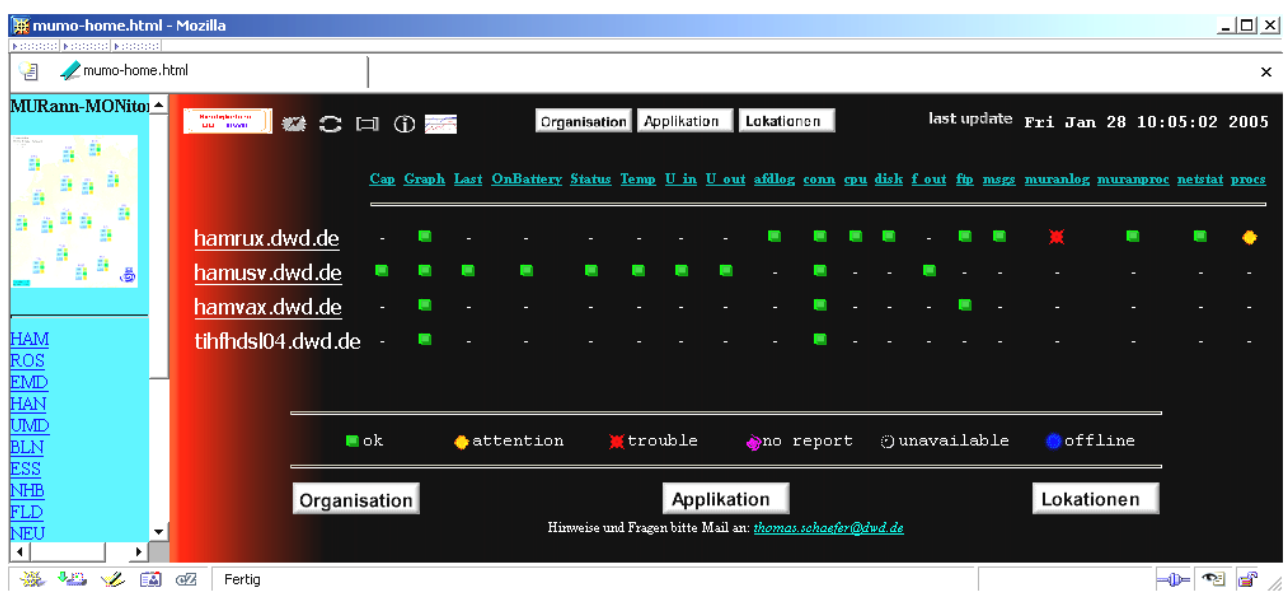


Fig. 4: BigBrother summary display of one site.

#### 6. Summary

The web based, fully automatic self check system of the DWD weather radar network is a simple but powerful tool for technical surveillance. It gives overviews and detailed views that are accessible from every browser. Rapid update rates and checking of all available parameters signal malfunctions often before they become a severe problem or before the users recognize a problem in the data.

Because HTML-pages are very small, the servicemen on standby can use them even over cellular phone. The availability of all products is computed for quality management issues and all data are archived as metadata for detailed radar data analysis.

# FAST-RESPONSE, OPEN PATH OPTICAL HYGROMETER FOR LONG-TERM MEASUREMENTS – EXPERIENCES, RESULTS, FUTURE REQUIREMENTS

Ulrich Weisensee and Jens-Peter Leps,  
Deutscher Wetterdienst, Meteorologisches Observatorium Lindenberg,

Am Observatorium 12, D-15848 Tauche / OT Lindenberg, Germany,  
Tel.: +49 (0)33677 60210, Fax.: +49 (0)33677 60280, email: ulrich.weisensee@dwd.de

## ABSTRACT

After long years of experience with Ly- $\alpha$ - and Krypton-hygrometers for flux measurements in different field campaigns, the fast response, open path optical CO<sub>2</sub>/H<sub>2</sub>O analyzer LI-7500 has been integrated into the boundary layer measurement facility of the MOL both for flux measurements and for long term monitoring of absolute humidity. The device has been found to be accurate, reliable and stable for relative fluctuation measurements in general with some problems and limitations in detail. Some teething troubles could be overcome with time.

Early devices (S/N before 0283) were found applicable for the determination of absolute humidity as well, so that no additional reference measurement appeared to be necessary for flux calculation. Moreover, reference values for QC purposes of other humidity sensors could be generated from LI-7500 measurements, a great advantage for the design of complex sensor systems and data processing algorithms. Changes in the sensor design by the manufacturer, made in order to fix a problem with CO<sub>2</sub> accuracy, negated the excellent long term specifications with respect to the H<sub>2</sub>O measurements of the devices currently sold. After a period of investigation, solutions seem to be in sight to re-approach to the original system specification.

Some of the present device specifics complicate sensor integration into complex measurement systems, which have to be modular, flexible and universal in a multivendor environment.

## INTRODUCTION

A comprehensive boundary layer measurement program has been set up at the Meteorological Observatory Lindenberg (MOL) of the German Weather Service (DWD) during the last seven years. The measurements are aimed at the investigation of atmosphere - land surface interaction processes over a heterogeneous land surface.

The experimental boundary layer facilities comprise, i.a., a special boundary layer field site (in German: Grenzschichtmessfeld, GM) at Falkenberg - equipped with a 99m tower, various measurement complexes for the determination of air ~, soil ~ and radiation parameters, and a SODAR / RASS - and a network of micrometeorological stations (energy budget measurement network- EBMN) located in an area of about 20\*20 km<sup>2</sup> around the MOL site and operated over different types of land use (Weisensee et al., 2001). In addition to a great variety of standard meteorological sensors, these facilities have been equipped with instruments for the operational determination of heat and momentum fluxes continuously throughout the year (profile mast, ultrasonic anemometer-thermometers, laser scintillometer).

The operational determination of the latent heat flux based on direct humidity fluctuation measurements has been performed during field experiments only in the past using Ly- $\alpha$ -, Krypton- or infrared hygrometers (Foken et al., 1998). A mismatch between operational requirements and sensor characteristics avoided the implementation of the LI7500 as fast response hygrometers into the operationally working systems in the 1990ies.

With the coming-up of a new commercially sold IR- hygrometer, which seemed to be more suitable for continuous, unattended operation at remote stations with low power requirements and infrequent maintenance, we saw the chance for integrating a fast response humidity sensors into these systems. After a test period we introduced the LI7500 first into the Falkenberg- facility in 2002 and later into the EBMN (Weisensee et al., 2003) at different sites.

## **FAST-RESPONSE, OPEN-PATH- HYGROMETERS**

Open path hygrometers (Ly- $\alpha$ - , Krypton- and Infrared- hygrometers) have been used for humidity fluctuation measurements (e.g.: Cerni, 1994), for more than 4 decades.

In case of Ly- $\alpha$ - hygrometers, especially the radiation sources and detectors caused a number of problems. The radiation intensity of the sources was not really stable, sources and detectors were manufactured not commercially (more or less homemade, some changes in manufacturing over the years, loss of experience), and they were very expensive. Moreover their lifetime was strongly limited.

Krypton radiation sources were not so delicate as Ly- $\alpha$ - sources, but the manufacturing dilemma and the price were problems as well. Due to the spectral characteristics the measurements were more sensitive to Oxygen. This requires a special oxygen correction, based on additional pressure measurement.

Both, the Ly- $\alpha$ - and the Krypton- hygrometer use a special window material (magnesium fluoride), which passes the far UV radiation. This material changes its transfer characteristics in humid environments by interaction of atmospheric constituents with UV photons. Windows had to be cleaned manually more or less frequent. Besides this maintenance requirements, both sensor types need accurate reference measurements of mean values of temperature and humidity as a reference.

Another disadvantage is the wide range, nonlinear output signal of both systems. This either requires special analog signal processing or the use of wide range A/D-converters for accurate calculations.

Some important advantages of both sensor types shall not be withheld. The compact sensor design, the small disturbance of wind field, the path length of a few millimeters only and the high bandwidth make the systems preferable for flux measurements, especially close to the ground. Furthermore, the low power consumption can be very advantageous in case of battery powered measuring stations.

The Lindenberg group has a long experience in using such hygrometers (Foken et al., 1998). Different types of hygrometers were used ( L-5V Buck Research ,KH20 Campbell, KOH20 Mierij Meteo), mainly during a number of field experiments over time periods not exceeding a few weeks.

Due to the special sensor characteristics and maintenance requirements in combination with some external conditions, such hygrometers were not suitable for integration into operational, more or less unattendedly working measuring facilities.

Hygrometers, using the absorption in the IR region of the spectrum, had been constructed since the early seventies of the last century. The most important advantage of these systems was that most of the stability and lifetime problems of UV- hygrometers didn't occur. IR- hygrometers have the capability to act as an absolute measuring instrument due to the physical properties of the differential absorption principle. Not all systems reach this well due to imperfect electronic or optical characteristics. Most of the IR- hygrometer were more or less special constructions, which comprise the particular interests of the developing institution.

Optical path length, flow distortion by sensor geometry, power consumption, special interfaces, temperature range and accuracy were points of discussion which over the years prevented the broad use of such a hygrometer in our long-term monitoring programs.

### **LICOR LI-7500 Open Path CO<sub>2</sub>/H<sub>2</sub>O Analyzer**

The situation seemed change with the coming-up of a modern infrared sensor, the LICOR LI-7500 Open Path CO<sub>2</sub>/H<sub>2</sub>O Analyzer at the end of 1999. At first glance, this system seemed to fulfill most of our current requirements:

- small sensor geometry for minimum flow distortion (diameter 6.5cm, length 30cm, weight 0.75 kg)
- path length comparable with that of modern sonic anemometers (12 cm)
- outdoor capability of all system components (head, control box and cables)
- low power consumption for battery powered stations (10.5 .. 16VDC, <10W after initial warm up)
- high precision
- absolute measurements
- analog and serial high speed interfaces (RS232 (20Hz), SDM (40Hz), 2x DAC16 (300Hz updated))
- additional analog inputs (2 channels for temperature and voltage)

Based on this, we decided to integrate this type of devices into our EBMN (Weisensee et al., 2003) for continuous flux measurements.

The system specifications ( a subset of which is given in table 1) promised both accurate fluctuation measurements and the determination of precise mean values of absolute humidity with one and the same sensor. This should allow to work without a second independent (slow-response) hygrometer for providing reference humidity data, and hence to avoid calculations based on sensors with different characteristics. It should give the opportunity to use the absolute humidity measurements for QC purposes (independent comparison data) of standard humidity sensors (Polymer sensors, Psychrometer). All of these different sensors have their own advantages and disadvantages. Some of them do have linearity problems, some require considerable maintenance, some of them don't work under specific conditions. But in combination, they will be able to generate an accurate data set over the whole year under a great variety of weather conditions.



Figure 1: LI-7500 sensor head



Figure 2: field installation (LI-7500, USA1)

		LI – 7500 original specification ( S/N < 0283 )	VTP6-CU ( dew point mirror )	LI – 7500 revised specification ( S/N 0283 and higher )
calibration range / measurement range		0 – 42 g/m <sup>3</sup>	-50 .. 50 °C (air temperature) -65 .. 50 °C (dew point temp.) 40K (max. depression at 20°C)	0 – 42 g/m <sup>3</sup>
zero drift with temperature (per °C)	max. typ.	± 0.01 g/m <sup>3</sup> ± 0.003 g/m <sup>3</sup>		± 0.04 g/m <sup>3</sup> ± 0.02 g/m <sup>3</sup>
accuracy of temperature measurement			± 0.15 K (-20 .. 50 °C) ± 0.25 K (-65 .. -20 °C)	
derived accuracy of absolute humidity measurements	max. typ.	± 0.750 g/m <sup>3</sup> (-25..50°C) ± 0.225 g/m <sup>3</sup> (-25..50°C)		± 3.0 g/m <sup>3</sup> (-25..50°C) ± 1.5 g/m <sup>3</sup> (-25..50°C)
accuracy of absolute humidity measurements at different air temperatures			ca. ± 0.6g/m <sup>3</sup> (50°C) ca. ± 0.2g/m <sup>3</sup> (25°C)	

Table 1: Selected specifications of the LI7500 for the humidity measurement (at 25°C and 980hPa) before and after the "solar fix" and of a dew point mirror system (VTP6) for comparison.

The accuracy of absolute humidity measurements, derived from the original system specifications given in Table 1, is comparable to the accuracy of typical dew point mirror systems for outdoor use. In conjunction with the LI-7500 data sheet statements "...Accurately measures absolute densities..." and "...Absolute ... gas analyzer ..." it could be expected, that an alternative system to large, heavy weight, power intensive dew point mirror systems was found.

## USE OF LI-7500 AT MOL

Since the end of 2000 when we bought the first two systems we have been using six LI-7500 systems. After system tests, the implementation of a sensor calibration procedure and some sensor comparisons, we realized two field experiments in 2002, including humidity fluctuations measurement as an essential part (Mauder et al., 2005).

Since the beginning of 2003, LI-7500 systems have been integrated into the different operationally working EBS- stations based on the analog coupling of the IR- hygrometer and a sonic anemometer, using the sonics capability to provide a pre-processed turbulence data set which contains all terms necessary for flux calculations. In case of GM located EBS, the acquisition of raw data was realized in parallel and it was temporarily used for special investigations. In May and June 2003 the complex field experiment LITFASS 2003 (Beyrich et al., 2004) took place at MOL. LI-7500 measurements were part of the measurement program, partially based on the operational version of the EBMN.

Quite a lot of experience could be accumulated over the years. Different problems could be solved, but, unfortunately, a number of problems still has to be solved in the future.

Some of these experiences shall be described in the following section.

## EXPERIENCES IN USE OF LI-7500

### Sensor Calibration

Calibration of the fast-response, open path absorption hygrometers has been established at MOL using some small calibration chamber, which is either put into the measuring path (LI-7500) or covers this in the case of Lyman- $\alpha$ - and Krypton-hygrometers.

Generation of a well defined humidity value is achieved by using an LI-610 dew-point generator.

Independently of the absorption hygrometer, the humidity is monitored by a precision dew point mirror system (EdgeTech- DewPrime II) additionally.

An automatic calibration procedure has been established. It covers a number of pre-defined humidity values, which are generated sequentially, first in an increasing and then in a decreasing order. An adjustment time of at least seven minutes at every calibration point was found necessary to achieve stationary and reproducible humidity conditions.

During the last years, we have been performing frequent laboratory calibrations of several of our LI-7500 sensors in order to verify their calibration stability.

Under laboratory conditions, the calibration equation of the LI-7500 were found to be linear and stable in time with very small differences in general.

Some calibration was performed after replacement of the internal chemicals. No significant deviation from previous calibrations was found.



Figure 3: Calibration facility for open path hygrometers

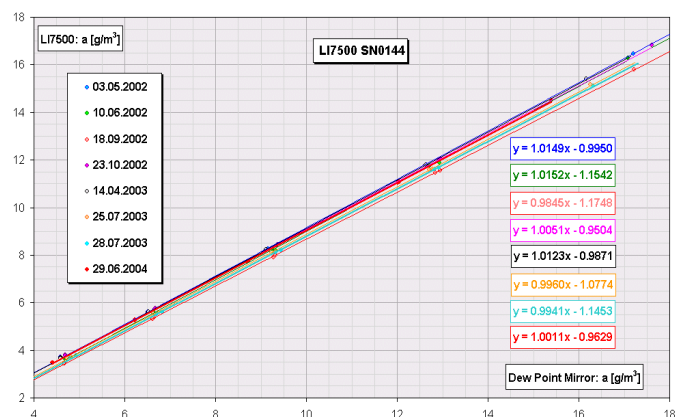


Figure 4: Result of repeated laboratory calibrations of a LI-7500 sensor over a period of two years

## Measurement Restrictions

Of course, an open path system is relatively sensitive to any disturbance within the measuring path like rain, snow, dew, ice, fog, insects. This applies to the LI-7500 as well. But, in general, the LI-7500 is less sensitive to these conditions than the Ly- $\alpha$ - and Krypton- sensors. Nevertheless, the data availability especially during winter is not yet satisfying.

From our point of view, it could be increased noticeably by implementing a window heating or a small air flushing.

## Diagnostic Information

The LI-7500 provides some diagnostic information, which only consists of a 1 byte unsigned integer. It contains information about the chopper temperature controller, the status of the chopper motor, the detector cooler and the synchronization between the embedded software, the digital signal processor and the chopper motor. This information is encoded in the highest 4 bit of the diagnostic byte. Additional information, the so called AGC- value is encoded in the lower half byte. This AGC value indicates the cleanness of the window. The bits are representing the AGC value range from 0 .. 100% in steps of 6.25%. Manufacturer tells typical clean window values of 55-65%. Higher values shall indicate the necessity to clean the windows. So, in fact, the information is available just with a resolution of 7 steps in maximum.

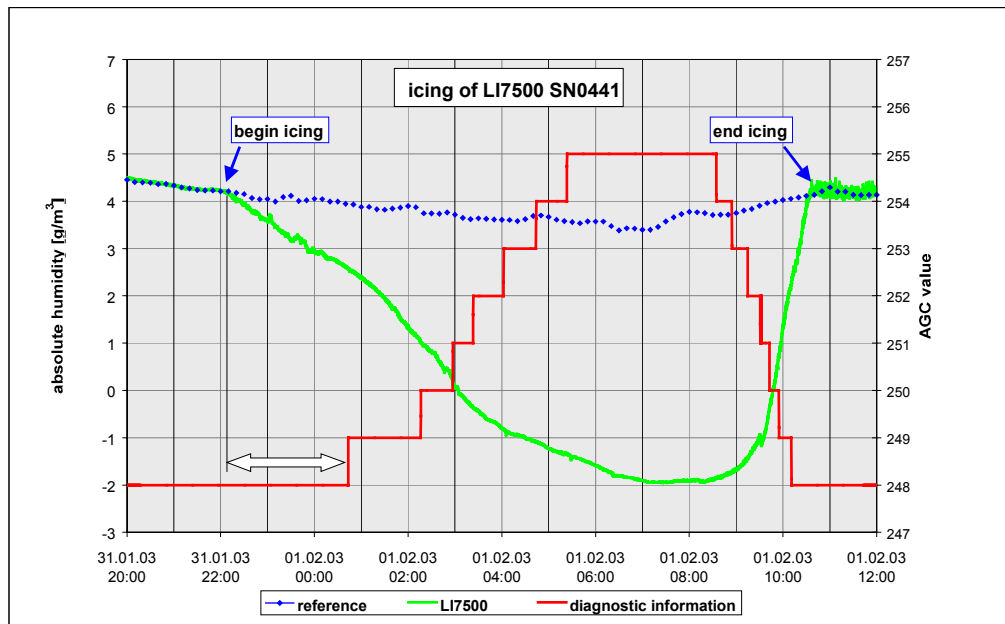


Figure 5: Diagnostic information, given by the LI-7500, during a period of sensor icing

As it can be seen in figure 5, the AGC value could be used for the QC of the data. The gradual decrease of the output absolute humidity value results from a loss of signal due to rime on the window which is indicated by the stepwise increment of the status signal. But information is not provided with the required resolution. A time period of about 3 hours with icing remains undetected in the example.

Furthermore, it is impossible to get out this diagnostic information via the analog interface, which is seen as a serious disadvantage. On the one hand, this reduces the flexibility for using the system in different measuring environments, and on the other hand, an analog AGC- output could be very helpful in realizing an automatic window cleaning device.

Unfortunately, the manufacturer does not provide a high-resolution diagnostic information over all interfaces so far.

## ***Delay Time***

Data acquisition and processing processes within the LI-7500 need a certain time. LI-7500 has a fixed throughput delay of originally 230 ms. It can be increased by the user in a limited number of 6 ms steps (see LI-7500 manual) up to about 300ms.

This shall provide the possibility to minimize the time shift between different sensors when coupling the LI-7500 with e.g. a sonic.

This time delay between the concentration measurement and the vertical wind measurement is not negligible in case of flux measurements, on contrary, it can generate quite a large error. This error depends on wind speed and wind direction. System immanent time delays can generate additional errors. Users tend to reduce the latter as far as possible.

The best way to eliminate this error generally is to acquire raw data, performing a shift between the time series and find the maximum cross correlation.

Assuming that all system delays of the combined measurements are well known, the user can reduce the fixed time delay error by compensating it through the online application of an additional time delay between the different input channels. Unfortunately, not so many data acquisition systems on the market provide such a possibility. As described in the introduction, acquisition and processing of raw data is not possible in all our applications.

Flux measurements at the Energy Balance Stations are performed using a USA1 ultrasonic anemometer-thermometer (METEK GmbH, Elmshorn). USA1 allows the synchronous sampling of analog input channels which we used to acquire the LI-7500 analog output signals. Furthermore it includes a turbulence data processor which provides a complete turbulence data set.

In a redesigned version of the Metek-USA1-Sonic, initiated by DWD and available since summer 2002, it has been possible to program an individual time delay for all the analog signal input channels of this device. In this way, constant time delays can be compensated. In addition to that, we tried to implement a kind of hardware correlator for the compensation of variable time delays.

In the middle of 2003, LI-COR company published an information on a software bug in all firmware versions before that date. Timing information, given in the manuals, had been found incorrect and not constant. Consequently, post operational correction of calculated flux data gathered before that time was possible only if raw data time series are available.

Completely new values of time delay were given in connection with a new firmware revision. Unfortunately, there are different values for DAC- and RS232/SDM- output. This further reduces the compatibility and flexibility and increases the risk of configuration errors.

This example illustrates the relevance of apparently small technical problems. The only way to avoid such problems and to become independent from manufacturers choice which pre-processed data could be of users interest seems to be the acquisition of raw data. Hopefully, the technical development soon provides this possibility even for autonomously working, battery powered stations with limited data transfer capacity.

## ***Direct Sunlight Sensitivity***

In Mai 2002, the German representative informed about a new LI-COR note, published in February 2002, announcing the recognition of a large sensitivity of the CO<sub>2</sub>- measurements to direct sunlight found for some devices.

LI-COR described a simple test to determine, whether or not a device is affected. An ad hoc procedure was suggested to reduce the effect (tilted mounting) and the manufacturer offered the possibility to send back affected devices for repair.

So far so good! Unfortunately, the manufacturer modified the LI-7500 to avoid the direct sunlight sensitivity in a way, such the system specification changed dramatically as described in the next section.

## ***Temperature Sensitivity***

The temperature sensitivity specification of the original LI-7500 design is given in Table 1. In order to solve the sunlight sensitivity problem, the manufacturer changed the optical filter combination in 2002 (S/N 0238 and higher). CO<sub>2</sub>- specification didn't change, but H<sub>2</sub>O- specification changed dramatically (see Table 1 – revised specification) as a result of this sensor modification. Especially the parameter "Zero drift with temperature" increased. Furthermore, the cross sensitivity to CO<sub>2</sub> increased.

In consequence, LI-7500 with solar fix changes are no longer suitable for absolute humidity measurements. This effect doesn't affect the usability of the LI-7500 for flux measurements.

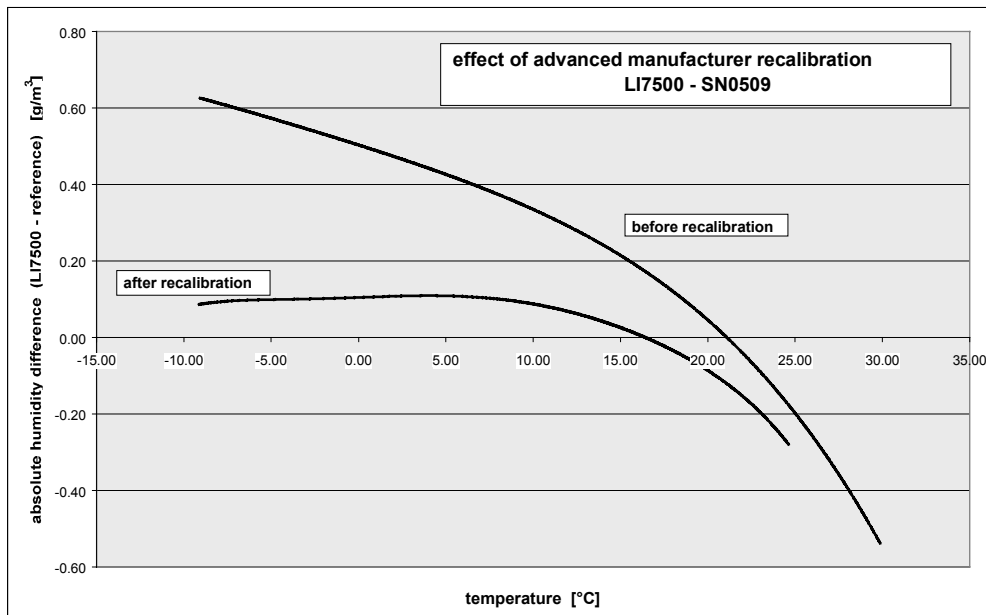


Figure 6: Effect of an advanced re-calibration of a LI-7500 (preliminary result, just for a part of the whole temperature range and just for absolute humidity values between 1 .. 3 g/m<sup>3</sup>)

An experimental re-calibration of two LI-7500 sensors was performed by the manufacturer in August 2002 in the LI-COR laboratory to achieve the original H<sub>2</sub>O-specification. A result of laboratory measurements, based on a re-calibrated sensor, can be seen in Figure 6. The first impression is, that the temperature drift significantly decreases, especially in the region of lower temperatures. For evaluation of the re-calibration effect further field measurements have to be performed, covering the whole operational temperature range and including all expected values of absolute humidity.

Nevertheless, the best way seems to eliminate the reasons for the temperature drift.

### Output Values

As mentioned in the section "diagnostic information", the AGC value would be very helpful as an analog output. Especially in conjunction with the problem of evaluating the temperature sensitivity, providing the original values of absorption at the different wavelength via the output data set would be of special interest. Currently, there are only two derived output values for CO<sub>2</sub>-absorption and for H<sub>2</sub>O-absorption. Both include a full calculation of cross correlation and zero drift.

Unfortunately, the composite of the output data set differs depending on the used interface (DAC, RS232, SDM). It seems to be, that some values are calculated only in the PC software. But this is not described anywhere.

### PC Communication Software

The LI-7500 PC Communication Software is used to transfer data and configuration files between the analyzer and the PC. It gives the possibility to edit different system parameters, to display measured data and to store data to disk. Unfortunately, not all values can be displayed (e.g. AGC) on the implemented strip chart. Any inconsistencies exist, depending on the software version. Care must be taken in case of device configuration.

### Power Supply

For battery powered stations (EBMN), a minimum power consumption is essential. The higher power consumption of the LI-7500, in comparison to Krypton- and Ly- $\alpha$ - hygrometers, has to be accepted. A real problem is the high initial current during warm up (more than three times higher than in steady state). It generates problems with overload protection circuits of DC/DC-converters. They are detecting the high current values and prevent the system working properly. This has to be kept in mind in the phase of system design. Electronic boxes with S/N 0370 and higher shall have a slightly different design, which shall give a smaller initial current. This effect is not really significant and doesn't solve the problem in general.



## REFERENCES

- Beyrich F., 2004: Verdunstung über einer heterogenen Landoberfläche - Das LITFASS-2003 Experiment – Ein Bericht, *Deutscher Wetterdienst, Forschung und Entwicklung, Arbeitsergebnisse Nr. 79, Offenbach, März 2004*
- Cerni T.A., 1994: An Infrared Hygrometer for Atmospheric Research and Routine Monitoring, *Journal of Atmospheric and Oceanic Technology, Vol. 11, No. 2, April 1994, AMS*
- LI-COR, LI-7500 CO<sub>2</sub>/H<sub>2</sub>O Analyzer, Instruction Manual, Rev. 1-4, 2001 – 2004, last Revision available on LI-COR web page
- Mauder M., C. Liebenthal, M. Göckede, J.-P. Leps, F. Beyrich, Th. Foken (2005): Processing and quality control of flux data during LITFASS-2003. *Boundary-Layer Meteorol. (submitted)*
- Weisensee U., F. Beyrich, S.-H. Richter and K. Nemeth, 2001: A Concept for Sensor Based Error Detection and Quality Assurance for a Network of Micrometeorological Stations, *Prepr.. 11<sup>th</sup> Symp. on Meteorological Observations and Instrumentation, 14 – 18 January 2001, Albuquerque, New Mexico: AMS, 275-278*
- Weisensee U., F. Beyrich and J.-P. Leps, 2003: Integration of Humidity Fluctuation Sensors into the Lindenberg Boundary Layer Measurement Facilities: Experiences, Problems and Future Requirements, *Prepr. 12<sup>th</sup> Symp. on Meteorological Observations and Instrumentation, 9 – 13 February 2003, Long Beach, California: AMS*

## Quality Management and Quality Control of the Long-Term Observing System "ZUZI" a Provider of the WMO-World Data Centre for Aerosols (WDCA)

M. Weller, S. Weber, Met. Obs. Lindenberg, Am Observatorium 12, 15848 Tauche/OT Lindenberg, Germany, Tel.: +49 33 67 76 02 89, Michael.Weller@dwd.de

Since 1986 the Meteorological Observatory Lindenberg routinely determines and analyses aerosol optical depths (AOD), a measure of the atmospheric turbidity (Weller et al.) The measurements has been expanded to "ZUZI" an observing program extending from the Zugspitze (Alps) to the peninsula Zingst (Baltic Sea) that provides the WDCA with AOD time series . The used instruments, covering the spectral channels recommended by WMO, have a dynamic range of  $10^9$  with carefully determined solid angles (about  $2.4 \times 10^{-4}$  sr) of the objectives. This allows radiance and irradiance calibrations both in laboratories (performed by the primary standard of the **Physikalisch-Technische Bundesanstalt**) and under high mountain conditions with respect to the WMO-recommended solar irradiance standard (Neckel & Labs) but also the reciprocal transfer of them. Once a year all spectrometers are simultaneously calibrated at the GAW station Izana/Tenerife applying the Langley-method to yield the extraterrestrial signals necessary to derive AOD's. Twice a year the devices are checked using high intensity sources calibrated by **PTB** and traceable also to **NIST**. Permanently the AOD-data of the "ZUZI"- observing sites Hohenpeißenberg and Lindenberg are compared with the corresponding data of the Precision Filter Radiometers (**Phys. Meteorol. Observatory Davos/World Radiation Centre**) operating here in the GAW-network. This guarantees homogeneous time series linked with the GAW- AOD- network and ensures reliable and reasonably accurate data on the AOD for the **WDCA** .

### Literature:

Neckel, H.; Labs, D.; Solar Physics 90; 205-258 (1984)

M. Weller et al.; Atmospheric Environment 34; 5107-5118 (2000)

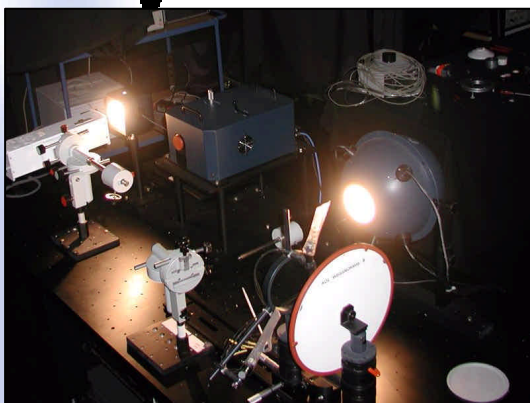
## Quality Management and Quality Control of the Long-Term Observing System "ZUZI" a Provider of the WMO-World Data Centre for Aerosols (WDCA)

M. Weller, S. Weber, Met. Obs. Lindenberg, Am Observatorium 12, 15848 Tauche/OT Lindenberg, Germany, Tel.: +49 33 67 76 02 89, Michael.Weller@dwd.de

Since 1986 the Meteorological Observatory Lindenberg routinely determines and analyses aerosol optical depths (AOD), a measure of the atmospheric turbidity (Weller et al.) The measurements has been expanded to "ZUZI" an observing program extending from the Zugspitze (Alps) to the peninsula Zingst (Baltic Sea) that provides the WDCA with AOD time series . The used instruments, covering the spectral channels recommended by WMO, have a dynamic range of  $10^9$  with solid angles (about  $2.4 \times 10^{-4}$  sr) of the objectives. This allows radiance and irradiance calibrations both in laboratories (performed by the primary standard of the **Physikalisch-Technische Bundesanstalt**) and under high mountain conditions with respect to the WMO-recommended solar irradiance standard (Neckel & Labs) but also the reciprocal transfer of them. Once a year all spectrometers are simultaneously calibrated at the GAW station Izana/Tenerife applying the Langley-method to yield the extraterrestrial signals necessary to derive AOD's. Twice a year the devices are checked using high intensity sources calibrated by **PTB** and traceable also to **NIST**. Permanently the AOD-data of the "ZUZI"- observing sites are compared with the corresponding data of the Precision Filter Radiometers (World Radiation Centre/Davos) operating here in the GAW-network. This guarantees homogeneous time series linked with the GAW- AOD-network and ensures reliable and reasonably accurate data on the AOD for the **WDCA**.

### Scheme of Quality Management and Quality Control

Determination of the solid angles of the spectrometer objectives using a point-source scanning the FOV



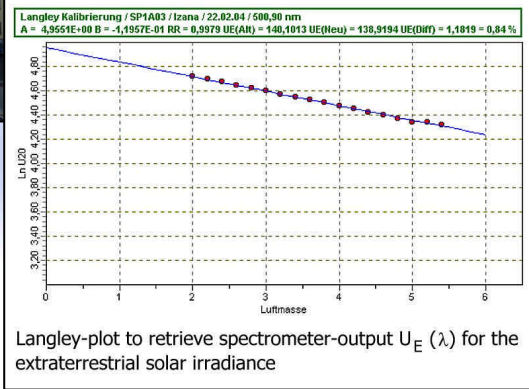
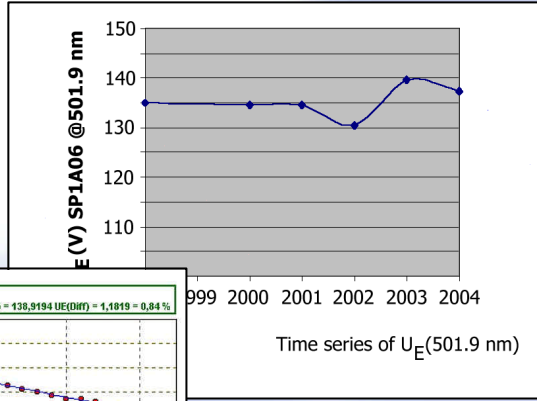
Calibration by PTB (related to the national-radiance-standard), traceable to NIST and the WMO-recommended irradiance-standard of Neckel & Labs due to Langley Calibrations

PRODUCT SELECTION CHART								LUMINANCE/RADIANCE STANDARDS
PART NUMBER	LUMINANCE RANGE	SPHERE DIAMETER (INCHES)	EXIT PORT DIAMETER (INCHES)	SPHERE COATING MATERIAL	DETECTOR	COMPUTER (CUSTOMER SUPPLIED)	OPERATING SOFTWARE	
URS-600	10-20,000 ff	6	1.25	Spectrafect	Photonic	Optional	Optional	
USS-400-Hi	>125,000 ff	4	1.25	Spectraion	N/A	N/A	N/A	
USS-600	5-600 ff	6	2	Spectrafect	Photonic	Optional	Optional	
USS-600V	5-460 ff	6	2	Spectrafect	Photonic	Required	Included	
USS-1200	2,300-9,000 ff	12	4	Spectrafect	Photonic	Optional	Optional	
USS-1200V	0-9,000 ff	12	4	Spectrafect	Photonic	Required	Included	
USS-2000	1,050-9,000 ff	20	8	Spectrafect	Photonic	Optional	Optional	
US-2000V	0-4,000 ff	20	8	Spectrafect	Photonic	Required	Included	

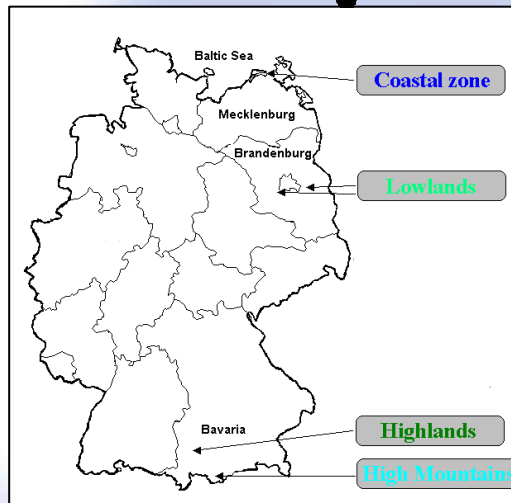
SOURCE: labSphere 1997 Catalog II

FIRST CHECK OF RADIATIVE STABILITY OVER TIME

Calibration and Re-calibration in Izana (GAW-station)



SECOND CHECK TO CONFIRM CHECK 1; CORRECTION OF  $U_E$  IF NECESSARY



COASTALZONE:  
UBA -station Zingst  
(4 m a.s.l.)

LOWLANDS:  
Meteorological  
Obs. Lindenberg  
(128 m a.s.l.)  
Comparison to  
Precision Filter  
Radiometer

HIGHMOUNTAINS:  
Weather station  
Zugspitze  
(2960 m a.s.l.)

HIGHLANDS:  
Meteorological Obs.  
Hohenpeißenberg  
(995 m a.s.l.)  
Comparison to  
Precision Filter  
Radiometer

Literature:

Neckel, H.; Labs, D.; Solar Physics 90; 205-258 (1984)

M. Weller et al.; Atmospheric Environment 34; 5107-5118 (2000)





# DEALING WITH UNCERTAINTY IN RAINFALL GAUGES CALIBRATION: THE QM-RIM METROLOGICAL VALIDATION

Molini A., Cassini G., Lanza L.G. and L. Stagi  
*DIAM - Dept. of Environmental Engineering, University of Genova*  
*Via Montallegro, 1 Genova, Italy*  
*Ph.: +39 010 3532485, FAX: +39 010 3532481*  
*E-mail: molini@diam.unige.it*

Accurate metrological validation is a crucial issue in testing the performance of any calibration apparatus. Reliability of calibration is in fact strictly connected with the capability in controlling and managing inherent calibration uncertainties. In this paper, we handle the metrological validation of the "Module for Qualification of Rainfall Intensity Measurements" (QM-RIM) developed at the Laboratory of DIAM (Dept. of Environmental Engineering of the University of Genova) and here tested in the period from March 2002 to May 2004. The laboratory is one of the three recognized laboratories involved in the WMO Intercomparison of Rainfall Intensity (RI) Gauges started in September 2004. The QM-RIM is an automatic device designed for the calibration of pluviometric instruments by means of a simply reproducible laboratory procedure and able to provide calibration curves for different types of rain gauges. Metrological analysis is here performed in terms of "a priori" error estimation (Type B errors). All the proposed standard procedures refer to the typologies of systematic and statistical errors as defined in the ISO Guide to the Expression of Uncertainty in Measurement (International Organization for Standardization, Geneva, Switzerland, 1993). We describe the methodology adopted, the main results obtained from the initial testing period, the error assessment procedures, and the uncertainty budget analyses performed on the calibration apparatus.

## 1. INTRODUCTION

The present paper focuses on the metrological validation of the QM-RIM (Qualification Module for Rainfall Intensity Measurements) developed at the Laboratory of DIAM (Dept. of Environmental Engineering of the University of Genova) in the framework of the WMO Laboratory intercomparison of rainfall intensity (RI) gauges (Lanza et al., 2005).

The QM-RIM (Figure 1a and b) is an automatic device designed for the calibration of RI gauges by means of a simply reproducible laboratory procedure and able to provide adjustment curves for different types of rain gauges. Calibration results are then expressed in terms of the coefficients of the calibration curve, which is usually assumed as a power law in the form:

$$I = \alpha \cdot I_R^\beta \quad (1)$$

with  $I$  the actual rainfall rate,  $I_R$  the rain rate measured by the gauge, and  $\alpha$  and  $\beta$  the calibration parameters. Laboratory calibration aims at the reduction of the systematic uncertainties due to the mechanics/structure/measurement principle of RI gauges, while different components of error (such as the variation of performances on different climatic conditions, the dependence from the installation, the limits of reproducibility of measurements and so on) will be the object of the second phase of the intercomparison to be performed in the field.

For a more complete explanation of issues connected with dynamic calibration and uncertainties in RI gauges measurements see Calder and Kidd (1978), Fankhauser (1997), La Barbera et al. (2002), Lanza and Stagi (2003), Molini et al. (2001), Molini et al. (2004)a and Molini et al. (2004)b.

Moreover, the effectiveness of laboratory calibration bases on the inherent precision of the calibration apparatus that, as stated in the "Quality standards for rain intensity measurements" (Lanza and Stagi, 2002) must assure a relative uncertainty lower than 1% at the very least.

The objective of this paper is to present the development of methodologies adopted in the metrological assessment of the QM-RIM uncertainty budget by means of a simple metrological validation and basing on the "ISO Guide to the Expression of Uncertainty in Measurement" (ISO, 1995).

The validation is performed in terms of "a priori" uncertainty and, in order to assure the consistency of QM-RIM with the proposed calibration standards, the principle of maximum uncertainty was applied.

The paper is essentially divided in two parts: the first dedicated to the architecture of the QM-RIM and the second to the metrological validation of different components of the apparatus.

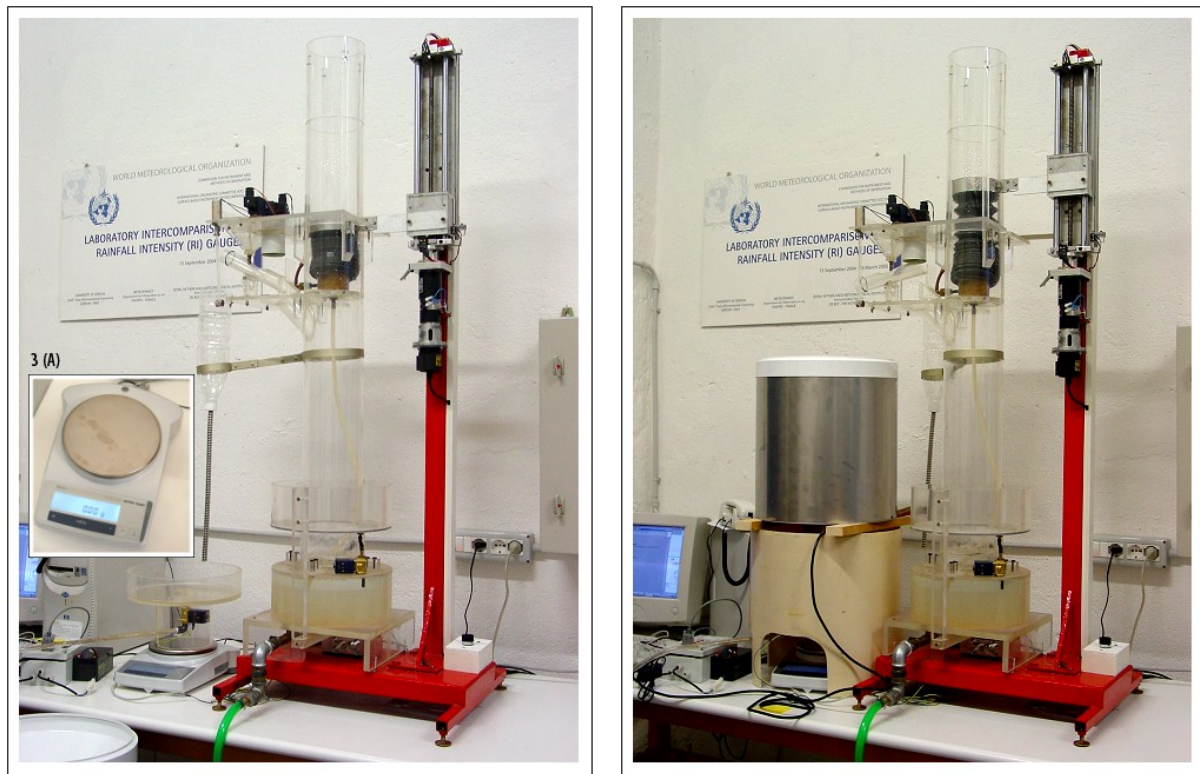


**Figure 1:** Present configuration of the QM-RIM without (a) and with (b) a RI gauge under test. The inner rectangle also shows a close view of the precision balance, while in figure 1(b) the plastic support for Rainfall Intensity gauges can be observed

In Brief, Section 2 is devoted to the description of the different phases of the QM-RIM assembly. After a concise explanation of the working principle of the module, the whole components of the system are described focusing on their particular functions in the ensemble. Also some photographic documentation is provided in order to facilitate the comprehension of the QM-RIM structure. the module presents in fact a complex structure, which can be basically decomposed in two main components; The constant water head generation component and the weighting system. Both such components are software controlled by a dedicated acquisition system, made up of a pc and an ensemble of acquisition boards. This distinction will be particularly relevant in Sections 3 and 4, where the metrological analysis and uncertainty budget inherent to QM-RIM will be addressed.

Finally, in Section 5 both the total uncertainty budget and the extended uncertainty for the QM-RI module are calculated.

## 2. THE QUALIFICATION MODULE FOR RAINFALL INTENSITY MEASUREMENTS (QM-RIM)

### 2.1. Basic Functioning Principle

The QM-RIM's calibration procedure bases on the capability of the system in producing A constant water flow. This is then provided to the RI gauge under test and both the test duration and the total weight of water flowed through the instrument are automatically recorded by the acquisition system. In particular, the weight measurement is performed by mean of the precision balance shown in Figure 1(a). During the test the ensemble precision balance/weighting tank is protected by a plastic structure (Figure 1(b)) which also supports the RI gauges under calibration.

Knowing the total water weight and the duration of the test assures to obtain, for a given collector, the value of the generated rainfall intensity ( actual intensity  $I$  ).

Accordingly, the efficiency of the QM-RIM in calibrating RI measurement instruments strictly depends on its capabilities in generating different constant flow rates. A constant synthetic flow rate is in fact a basic requirement for an accurate estimation of the actual intensity  $I$ .



The flow rate  $Q$  is simply provided by the classic equation:

$$Q = \xi \cdot \Omega \sqrt{2gH} \quad (2)$$

with  $\xi$  a suitable coefficient.

Basing on eq. 2 and assuming  $\xi$  as constant, it is possible to generate different steady flow rates by only varying the water head  $H$  and the section area of the orifice  $\Omega$ .

In the QM-RIM the water head  $H$  is varied using a cylindrical bellows (reproduced in Figure 2). The expansion of the bellows is controlled by a motor with encoder while the water flow is maintained by a submerged pump. The diameter of the bottom orifice is otherwise regulated by a set of three electro valves equipped with different nozzles (see Figure 3). The ensemble pvc bellows – motor with encoder – electro valves is represented in Figure 4. The water level and the orifice diameter are software controlled in order to generate the desired flow rates.

These are compared with the measure that is contemporary obtained by the RI gauge under consideration and dynamic calibration is possible over the full range of rain rates usually addressed by operational rain gauges (see Lanza and Stagi, 2002).

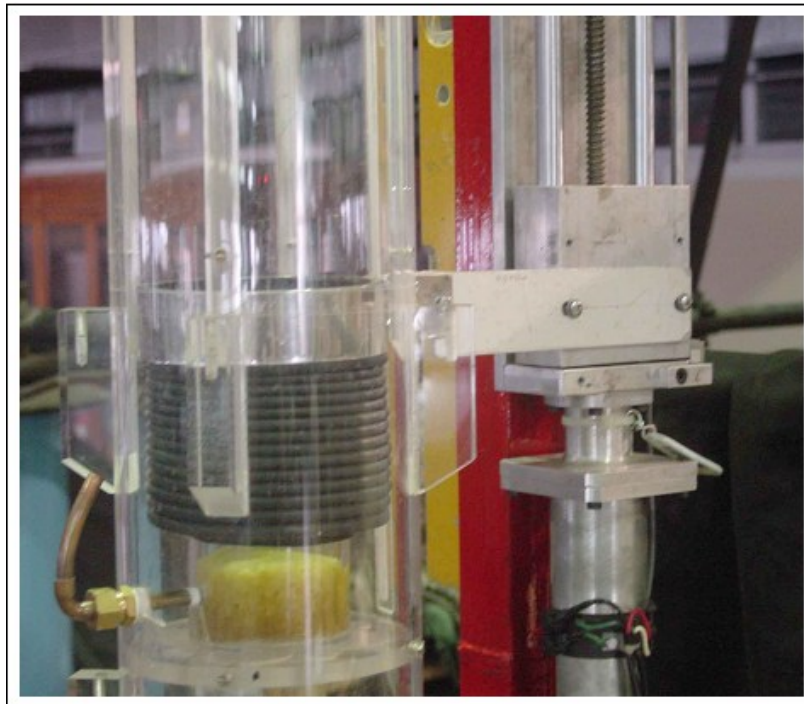


**Figure 2:** Close view of the cylindrical bellows which allows varying the water in order to produce different water heads. The top of the pvc bellows is connected to a motor with encoder controlled by software.

Moreover, since only variations of the water head  $H$  can produce variations of  $Q$ , the system has been developed to rapidly compensate  $\Delta H$  by means of a overflow control mechanism.

The spilling mechanism at the top of the bellows allows compensation of both the possible decrease and increase of the water level.

This particular features of the QM-RIM will turn out particularly relevant in the following, when the uncertainty budget for the constant flow generation apparatus will be calculated.



**Figure 3:** The three electrovalves that allow to combine different nozzles diameters in order to produce a wide range of water flow rates.

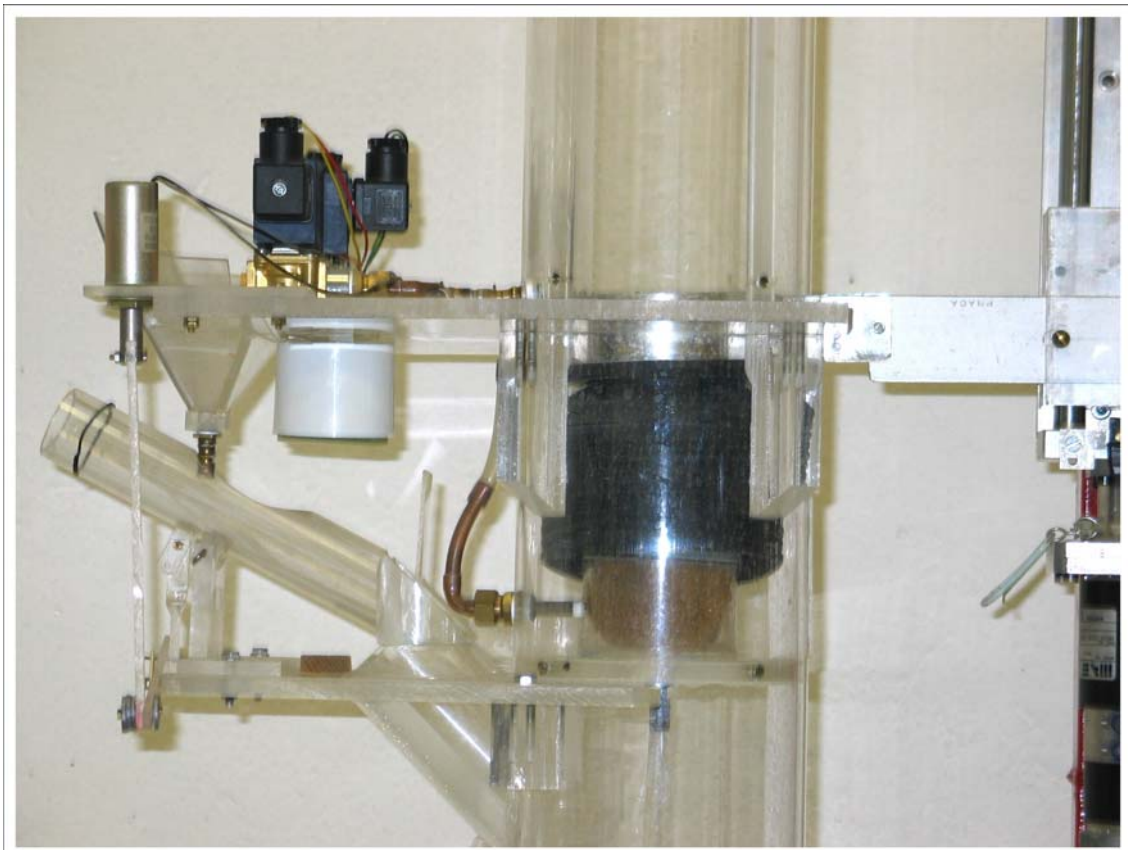


**Figure 4:** The ensemble electrovalves/pvc bellows/motor of the QM-RIM

### 3. THE QM-RIM FROM THE METROLOGICAL VALIDATION POINT OF VIEW

In the previous section we analysed the architecture of the QM-RIM and we also pointed out its specific design aimed at producing synthetic rainfall intensities in a robust way.

This section is devoted to a brief overview of basic uncertainty analysis concepts and to the explanation of the procedure adopted for metrological validation of the QM-RIM.

#### 3.1. *Uncertainty analysis in brief: type A and B error evaluations*

The uncertainty of the result of a measurement generally consists of several components which, based on the ISO *Guide to the Expression of Uncertainty in Measurement* (ISO, 1995), may be grouped in two categories according to the method used to estimate their numerical values:

- those which are evaluated by statistical methods,
- those which are evaluated by other means.

Metrological analysis is here performed in terms of “a priori” uncertainty estimation and the proposed procedure only refers to the Type B class of uncertainties.

Moreover, in the QM-RIM metrological validation we adopted the “maximum error principle”, namely, we are not interested in a precise estimation of the uncertainty of the system but simply to assess the maximum uncertainty which can derive from the calibration procedure.

#### 3.2. *Type B evaluation of standard uncertainty*

A Type B evaluation of the standard uncertainty ( $u$ ) is usually based on scientific judgment using all the relevant information available, which may include

- previous measurement data,
- experience with, or general knowledge of, the behaviour and property of relevant materials and instruments,
- manufacturer’s specifications,
- data provided in calibration and other reports, and
- uncertainties assigned to reference data taken from handbooks.

In general, Type B evaluation of standard uncertainty  $u$  can be a useful tool where, as in QM-RIM case, the objective of the metrological validation is the estimation of a maximum uncertainty and not a precise evaluation of the error.

### 4. UNCERTAINTY BUDGET OF QM-RIM

From a metrological point of view, the QM-RIM apparatus can be divided in two basic modules:

1. the synthetic rainfall intensity generation module
2. the actual rainfall intensity Measurement module

Sources of uncertainty within the QM-RIM architecture can be in fact of two main types:

1. Uncertainty on the flow steadiness deriving from possible variations in water head  $H$
2. Uncertainties due to the weighting apparatus, to delays in acquisition and to the variation of experimental conditions such as Temperature and Relative Humidity

Moreover, these two sources of uncertainty are independent one from the other and for this reason we will perform in the following a separate analysis for the two modules, later combining the results in a unique uncertainty budget in section 5.

#### 4.1. *Uncertainty budget for the RI Generation Module*

The uncertainty associated with the RI generation module essentially depends on the uncertainty on the water head  $H$ . Indeed we observed in Section 2 that the law controlling the generation of synthetic flow rates in the QM-RIM is:

$$Q = \Omega \cdot \xi \sqrt{2gH} \quad (3)$$

Since  $\Omega$  and  $\xi$  can be assumed as constant for a given configuration of the QM-RIM in standard conditions of maintenance, the evaluation of standard uncertainty on the RI Generation Module only depends on the value of  $H$ .

On the other hand, the maximum observed variation of  $H$  in RI generation module can be acceptably considered as:

$$\Delta H \leq 0.1 \text{ mm} \quad (4)$$

and so we obtain, assuming the variation of the water head  $H$  as uniformly distributed, the expression for the uncertainty on  $H$ , as:

$$u_H = \frac{\Delta H}{\sqrt{3}} \approx 0.06 \text{ mm} \quad (5)$$

The uncertainty on the synthetic flow rate  $Q$  due to the maximum observed variation of  $H$ ,  $\Delta H$ , is therefore given by:

$$u_Q^{(H)} = \sqrt{\left(\frac{\partial Q}{\partial H}\right)^2 \cdot u_H^2} = \frac{1}{2} \cdot \frac{u_H}{H} \cdot Q \quad (6)$$

In Figure 5 the relative uncertainty on  $Q$  due to the water head variation  $\Delta H$  is represented as a function of  $H$  and obviously, since  $u_Q^{(H)}$  is given as a maximum uncertainty, the relative  $u_Q^{(H)}/Q$  is maximum for the lowest water head (about 0.1%).

#### 4.2. Uncertainty Budget of the Actual RI Measurement Module

The evaluation of the standard uncertainty on the Actual RI Measurement Module depends on the value of  $u_W$  (uncertainty on weight measurement) and  $u_t$  (uncertainty on the time interval measurement).

The value of  $u_W$  is a function of the temperature variation ( $\Delta T$ ) during the experiment and of the linearity, resolution and repeatability characteristics of the precision balance.

Therefore, assuming the distribution of the weight ( $W$ ) variations due to linearity, resolution and environmental temperature as uniform and since the repeatability is just given for the QM-RIM precision balance in terms of uncertainty, we obtain:

$$\Delta W_{LIN} = 0.02 \text{ g} \quad \Rightarrow \quad u_W^{(LIN)} = \frac{\Delta W_{LIN}}{\sqrt{3}} = 0.012 \text{ g} \quad (7)$$

$$\Delta W_{RIS} = 0.01 \text{ g} \quad \Rightarrow \quad u_W^{(RIS)} = \frac{\Delta W_{RIS}}{2\sqrt{3}} = 0.003 \text{ g} \quad (8)$$

$$u_W^{(REP)} = 0.01 \text{ g} \quad (9)$$

$$u_W^{(T)} = \alpha_T \frac{\Delta T}{\sqrt{3}} \cdot W \approx 0.014 \text{ g} \quad (10)$$

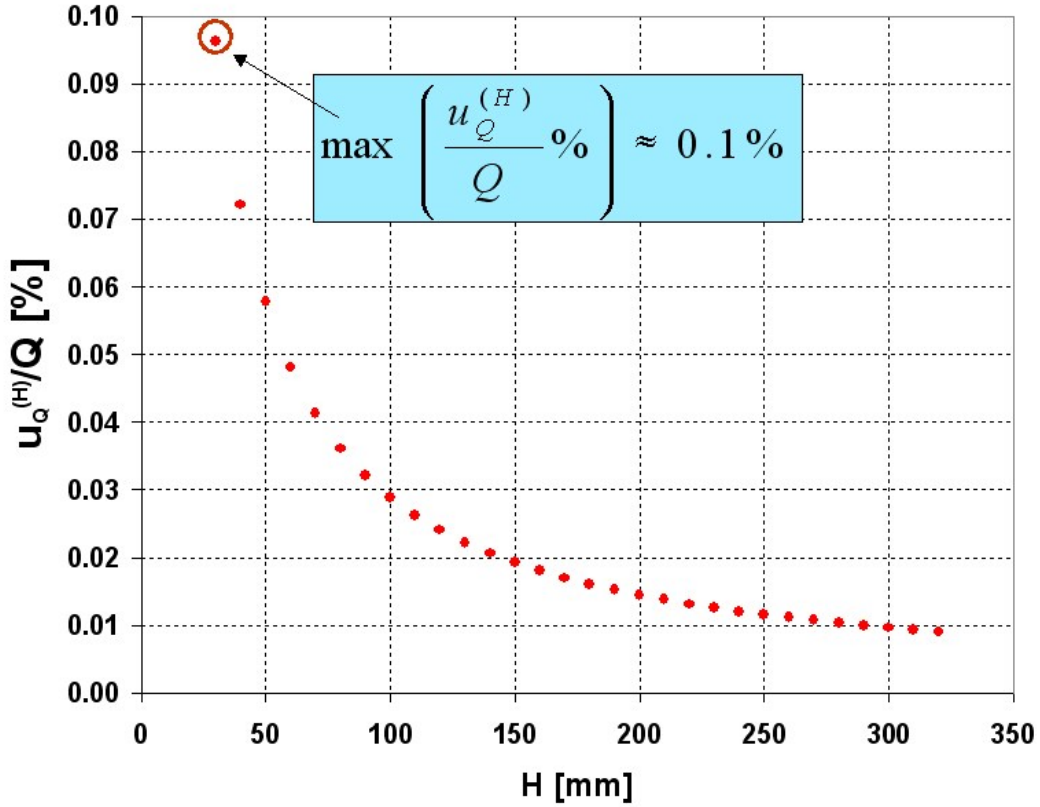


**Figure 5:** The relative uncertainty on Q (flow rate) due to H (water head) as a function of H

with  $\alpha_T=6 \times 10^{-6} \text{ }^\circ\text{C}^{-1}$  the thermal sensitivity coefficient,  $\Delta T \sim 2 \text{ }^\circ\text{C}$  the Maximum  $\Delta T$  estimation during the experiment and  $W=2000 \text{ g}$  the standard water amount provided to the RI gauge during a single test.

Equations 7-10 respectively represent the uncertainties on weight measurement (W) due to the linearity, resolution and repeatability characteristics of the precision balance and uncertainty on W deriving from environmental temperature T variations.

Then, we can obtain an overall expression for  $u_W$ , in the form:

$$u_W = \sqrt{\left(u_W^{(T)}\right)^2 + \left(u_W^{(LIN)}\right)^2 + \left(u_W^{(REP)}\right)^2 + \left(u_W^{(RES)}\right)^2} = 0.021 \text{ g} \quad (11)$$

At the same time, assuming  $\Delta t=10^{-1} \text{ s}$  (maximum deviation in the measurement of the time t), the uncertainty on the time interval estimation is:

$$u_t = \frac{\Delta t}{\sqrt{3}} \cdot \sqrt{2} \approx 0.08 \text{ s} \quad (12)$$

and we finally obtain that the standard uncertainty on the Actual RI Measurement Module is given by:

$$u_Q^{(W,t)} = \sqrt{\left(\frac{\partial Q}{\partial W}\right)^2 \cdot u_W^2 + \left(\frac{\partial Q}{\partial t}\right)^2 \cdot u_t^2} = \sqrt{t^{-2} \cdot u_W^2 + \left(\frac{W}{t^2}\right)^2 \cdot u_t^2} \quad (13)$$

## 5. Combined Standard Uncertainty and Expanded Uncertainty

The next step in the metrological validation of the QM-RIM consists in combining the uncertainties on the RI generation module and the actual RI measurement module in order to obtain the total uncertainty  $u_Q$  on the synthetic flow rate  $Q$ , in the form:

$$u_Q = \sqrt{\left(u_Q^{(W,t)}\right)^2 + \left(u_Q^{(H)}\right)^2} \quad (14)$$

From the above equation the total uncertainty on the synthetic rainfall intensity  $u_{RI}$  can be easily extracted as:

$$u_{RI} = k \cdot \sqrt{\left(u_Q^{(W,t)}\right)^2 + \left(u_Q^{(H)}\right)^2} \quad (15)$$

With:

$$k = \rho^{-1} S^{-1} = 0.01 \text{ mm g}^{-1} \quad (16)$$

where  $\rho$  is water density and  $S$  the RI gauge collector area. By calculating  $u_{RI}^{(W,t)}$  as a function of  $t$  we obtain, for the relative uncertainty on RI due to the uncertainty on weight and time measurements:

$$\frac{u_{RI}^{(W,t)}}{RI} = 2 \times 10^{-2} \div 0.15 \% \quad (17)$$

while:

$$\frac{u_{RI}^{(H)}}{RI} = 0.1 \div 0.01 \% \quad (18)$$

Since we have, for the maximum relative uncertainty on rainfall intensity:

$$\frac{u_{RI}^{\max}}{RI} \approx 0.2 \% \quad (19)$$

And assuming 2.576 as the coverage factor (corresponding to a confidence level of 99%) we obtain the expanded relative uncertainty for the actual rainfall intensity:

$$\frac{U_{RI}^{\max}}{RI} \% = 0.46 \% \quad (20)$$

## 6. CONCLUSION AND REMARKS

The QM-RIM is an experimental apparatus able to generate constant flow rates and measures the response of RI gauges under test to synthetic rain rates. The main objective of this paper is the metrological validation of the QM-RIM based on the “a priori” evaluation of total uncertainty associated with the considered calibration device.

Using the Type B uncertainty evaluation, it was possible to assign a maximum expanded relative uncertainty to the QM-RIM measurements of rainfall intensity, representing a protective estimation of the uncertainty on the actual rainfall intensity  $l$ .

Such uncertainty, calculated from overestimated values of  $H$ ,  $W$ ,  $t$  and  $T$ , is about 0.46% and is then coherent with the Laboratory Intercomparison threshold of 1% imposed for calibration devices included in the RI gauges intercomparison program of WMO.

## 7. REFERENCES

1. Calder I.R. and Kidd C.H.R. (1978). *A note on the dynamic calibration of tipping-bucket gauges*. J. Hydrology, 39, 383-386.
2. Fankhauser R. (1997). *Measurement properties of tipping bucket rain gauges and their influence on urban runoff simulation*. Wat. Sci. Techn., 36(8-9), 7-12.
3. ISO, (1995) *GUM "Guide to the Expression of Uncertainty in Measurement"*.
4. La Barbera, P., Lanza, L.G., Stagi, L., (2002) *Influence of systematic mechanical errors of tipping-bucket rain gauges on the statistics of rainfall extremes*, Water Sci. Techn., 45(2), 1-9.
5. Lanza L.G., Stagi L., (2002) *Quality standards for rain intensity measurements*, WMO Techn. Conf. On Meteorological and Environmental Instruments and Methods of Observation (TECO-2002), Bratislava, Slovakia, 23-25 September 2002. Published on CD-ROM, 4 pp.
6. Lanza L.G., Stagi L., (2003) *Sulla misura dell'intensità di pioggia con pluviometri a vaschette basculanti: errori sistematici e statistiche dei valori estremi* *Rivista di Meteorologia Aeronautica*, 63(1), 13-21 (IN ITALIAN).
7. Lanza, L.G., Leroy, M., Van Der Menlen, J. And M. Ondras, (2005) *The WMO Laboratory Intercomparison of Rainfall Intensity (RI) Gauges*. TECO 2005 (this volume).
8. Molini, A., La Barbera, P., Lanza, L. G., Stagi, L., (2001) *Rainfall intermittency and the sampling error of tipping-bucket rain gauges*, Phys. Chem. Earth (C), Vol. 26, No. 10-12, pp. 737-742.
9. Molini, P. La Barbera, L.G. Lanza, (2004) *The impact of TBRs measurement errors on design rainfall for urban-scale applications*, Hydrological Processes, in press.
10. Molini, L.G. Lanza, P. La Barbera, (2004) *Improving the accuracy of tipping-bucket rain records using disaggregation techniques*, Atmospheric Research, in press.



#### The Concept

The AWS is composed of elementary hardware/firmware modules which are commercially available off the shelf (COTS), and therefore is expandable with modularity and uses TCP/IP to transmit data from the source.

Any AWS hardware/firmware modules are scalable to fit, the expandability of the system where and when necessary.

It is able to classify and report all the AWS, software possible performances, in a basic general configuration tables. Therefore, the AWS behavior is very flexible according to the variations of this general configuration table setting.



#### Open Source, Open Architecture

The operating system used for both firmware and software is LINUX. The embedded parts of the systems are also POSIX compliant. The database used is PostgreSQL.

It must also be noted that since this is a web-based application, each element of the system software is written as an individual module to be controlled by the web-interface module. Such modularity dispenses of the idea of a single large and cumbersome application.

The system uses an Open Architecture-based concept, whereby all sensors and hardware are hot pluggable. It can therefore be called a plug- and play system and therefore it is manufacturer independent for both acquisition electronics and sensors.



#### Transmission, Protocols & Languages

ease of software maintenance while the front end interfaces use Java. The flexibility of the system enables virtually all types of transmission by changing parameters within the configuration files.

Virtually all data exchange within and outside the system uses HTTP while SOAP/XML is used for data transmission.

Perl, PHP, XML, JavaScript & Java for ease of software maintenance.

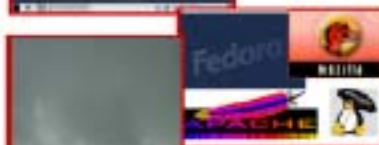
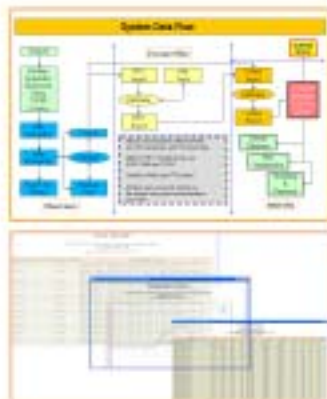
#### System In-brief

Open Source, Open Architecture, Manufacturer Independent

Modular, TCP/IP Virtually From Source

Uses Scripting Languages For A Complete Web-based Solution

Software & Hardware Configurable Using Web Applications



#### Hope for the future

It is the hope that this project inspires the advent of intelligent TCP/IP based sensors which can be connected to the WWW and the data viewed wherever an internet connection exists.





## ***QUALITY AND REPRESENTATIVITY OF WIND MEASUREMENTS***

### **Authors**

Henk Benschop, Jitze van der Meulen  
Royal Netherlands Meteorological Institute (KNMI)  
P.O.Box 201  
3730 AE De Bilt  
The Netherlands

*E-mail Benschop:* [benschop@knmi.nl](mailto:benschop@knmi.nl)  
*E-mail Van der Meulen:* [meulenvd@knmi.nl](mailto:meulenvd@knmi.nl)

*Key words: meteorology, observations, windmeasurements, guide, metadata*

### **Abstract**

Uncertainty and representativity of meteorological observations depend on the terrain roughness in the vicinity of the observation sites. The measure of representativity also depends on the wind direction. In particular at airports, where local representativity is strong requirement, it is of high importance to have a good view on the windfield at and above the runways, and also in the approach zones. The Royal Netherlands Meteorological Institute uses two methods to transform the measured windspeed to values representative for the surrounding areas, especially to the area above touch down zone. The first method is based on the influence of the roughness on the vertical wind velocity profile. The roughness around the observation site is calculated using a gust analysis as a function of wind direction. For a well qualified statistical analysis providing roughness data, a long term time series of windspeed data is required. The second method is based on a rough visual estimation of the shelter factor using a classification scheme describing the landscape. Every classification correspondends with a value of the shelter factor. These methods give the tools make it possible to present required wind information to the airtraffic. An evaluation of these methods used at several airports will be presented.

*Royal Netherlands Meteorological Institute KNMI, De Bilt, january 2005*

## 1. Derivation of potential wind speed from measured wind speed

The potential wind speed is the average wind speed (averaged out over a period  $\geq 1$  minute) that would prevail at the site of the wind mast if the immediate surroundings were flat, as per the WMO standard. In practice, completely flat surroundings for all points of the compass are rarely achievable. In order to derive a potential wind from the measured average wind speed, the average wind speed is multiplied by a factor known as the "sheltering factor", which varies for each 20 degree sector of the compass.

The sheltering factor (SF) is calculated for all average wind speed data archived in climate database KIS. This comes down to a SF for every 20-degree sector of wind directions per station\*\*. Two SFs are stored per wind direction sector for stations in a more leafy environment (i.e. where the "roughness" of the terrain varies depending on whether there are leaves on the trees), namely one SF for the summer period (1-May through 1-Oct) and one SF for the winter period (1-Oct through 1-May).

\*\* Comment:

*The 18 sectors used are 20, 40, 60... 360. The sector 20.n is the group of directions  $dd = (20.n - 10) \pm 5$  and  $dd = (20.n) \pm 5$ .*

*Example: sector = 60 actually means the range of wind directions between 45 and 65 degrees.*

To allow for possible changes in the "roughness" of the surroundings, the shelter factors are recalculated regularly (i.e. once every three years) and whenever the mast is moved.

The calculation of the shelter factor is based on the relationship between the gustiness of the wind and the roughness of the terrain,  $z_0$ . The gustiness is represented by the median value of a set of gust factors:  $\langle G \rangle$ .

In any random period of time  $\tau$ , e. g. 10 minutes or 1 hour,  $G = \{\text{maximum wind speed during } \tau\} / \{\text{average wind speed throughout } \tau\}$ .

The relationship between  $\langle G \rangle$  and  $z_0$  has been formulated by Wieringa (Wieringa, Rijkooort, 1983).

A modified version this gust model (Wieringa- Beljaars model) has been described by Verkaik (Verkaik, 2000):

$$\langle G \rangle = 1 + \frac{0,88}{\ln \frac{z}{z_0}} * \tilde{u}_p$$

- $u_p = 2.41$  for 10-minute data and 2.99 for hourly data;
- $z$ : (measurement) height (m).

In the case of 10' data, the formula becomes:

$$\langle G \rangle = 1 + \{ 2.12 / \ln (z/z_0) \}$$

This gives:  $z_0 \langle G \rangle = z \cdot \exp\{2.12 / (1 - \langle G \rangle)\}$

In the following calculation of the SF, the assumption is made that the vertical wind profile is logarithmic so that the following applies for the reduction of the average wind speed at height  $z_1$  to height  $z_2$ :

$$ff_{z_1} / ff_{z_2} = \{ \ln (z_1/z_0) / \ln (z_2/z_0) \}$$

The said assumption is correct up to 60 or 100m altitude and where atmospheric conditions are neutral (applicable where  $ff > 5$  m/s). (Wieringa and Rijkooort, 1983)

The above hypothesis is used when the average wind speed at the measurement site is converted to a "fictitious" average wind speed at  $z_0 = 0.03$  m, as is the assumption that the wind speed at 60 m (meso-altitude) is roughly the

same throughout a large surrounding area (radius = 4 km). The reduction to 60 m altitude is actually done first and then the "fictitious" situation. So, we obtain:

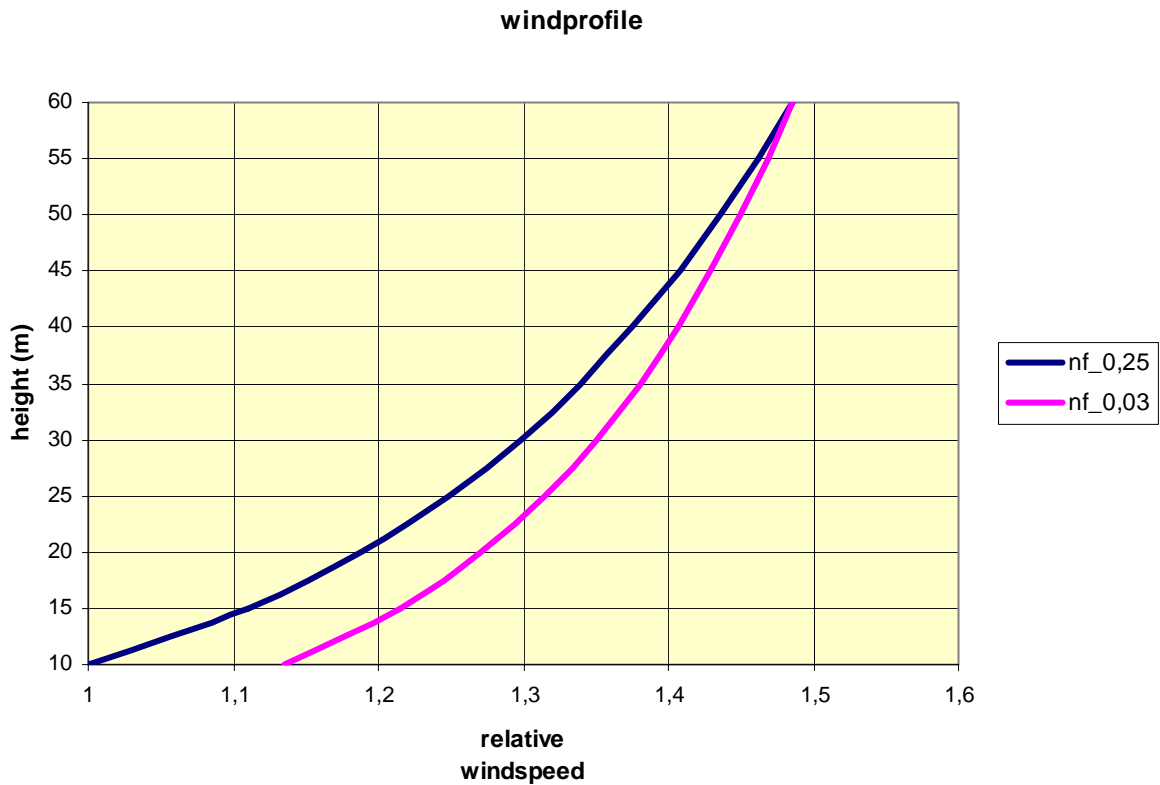


Fig.1. Profile windspeed

$$SF = ff_{pot} / ff_{met} = \{ \ln(10/z_{0p}) / \ln(60/z_{0p}) \} / \{ \ln(z/z_{0s}) / \ln(60/z_{0s}) \}$$

$z_{0p}$  = roughness for flat surroundings;

$z_{0s}$  = actual roughness at the location of the wind mast; this is calculated for every wind direction sector of 20 degrees;

$z$  = sensor height.

Filling in  $z_{0p} = 0.03$  m and  $z = 10$  m gives:

$$BF = \frac{1 + \left( \frac{1,79}{2,3 - \ln z_{0s}} \right)}{1,308}$$

Recently the shelterfactors of the 8 windstations at Amsterdam Airport Schiphol (figure 2) have been calculated per 10 directiondegrees. The results are presented herewith (table 1, figure 3).



*Fig.2. Amsterdam Airport Schiphol, location of windstations*

Direction (10bgr)	Shelterfactor							
	27	18C	18R	22	36R	36C	36L	6
0	0,99	0,98	0,97	1,01	0,96	0,96	0,96	1,01
1	1,04	1,00	1,03	1,05	1,00	0,98	0,99	1,06
2	1,06	1,01	1,04	1,07	1,00	0,98	1,01	1,06
3	1,05	1,01	1,05	1,05	1,00	1,00	1,05	1,02
4	1,06	1,02	1,06	1,04	1,04	1,01	1,05	1,00
5	1,03	1,02	1,05	1,04	1,09	1,02	1,05	0,99
6	1,04	1,02	1,05	1,05	1,11	1,00	1,05	1,00
7	1,04	1,02	1,07	1,08	1,08	1,00	1,04	1,04
8	1,03	1,02	1,08	1,06	1,13	1,01	1,04	1,06
9	1,02	0,98	1,03	1,00	1,15	1,00	0,99	1,01
10	1,02	0,98	1,07	1,03	1,15	1,04	0,98	1,02
11	1,05	1,02	1,05	1,09	1,12	1,05	1,00	1,06
12	1,07	1,02	1,11	1,08	1,07	1,04	1,02	1,05
13	1,05	1,02	1,07	1,11	1,09	1,01	1,01	1,07
14	1,02	0,99	1,04	1,09	1,07	0,99	0,99	1,10
15	1,00	0,99	1,01	1,09	1,06	0,98	0,97	1,09
16	1,00	0,98	0,99	1,11	1,04	0,98	0,98	1,09
17	0,99	0,97	0,97	1,03	1,02	0,97	0,99	1,08
18	0,98	0,94	0,96	0,98	0,99	0,95	0,98	1,05
19	0,99	0,97	0,99	1,04	1,02	0,98	1,00	1,08
20	0,99	0,99	1,00	1,02	1,01	0,98	1,00	1,05
21	1,00	1,01	1,01	0,99	1,01	1,02	1,02	1,03
22	1,01	1,04	1,03	1,00	1,03	1,04	1,04	1,03
23	1,01	1,04	1,02	1,00	1,04	1,04	1,03	1,03
24	1,02	1,03	1,03	0,99	1,04	1,04	1,03	1,01
25	1,03	1,04	1,04	1,01	1,05	1,04	1,03	1,02
26	1,01	1,02	1,03	1,01	1,04	1,03	1,03	1,02
27	0,98	0,99	1,00	0,98	1,02	1,00	1,01	1,01
28	1,00	1,03	1,05	0,99	1,04	1,03	1,03	1,07
29	1,02	1,06	1,06	1,01	1,03	1,04	1,05	1,09
30	1,03	1,07	1,07	1,02	1,07	1,03	1,06	1,09
31	1,02	1,08	1,06	1,01	1,07	1,02	1,08	1,10
32	1,04	1,09	1,05	1,04	1,08	1,02	1,09	1,11
33	1,06	1,06	1,05	1,05	1,05	1,01	1,08	1,09
34	1,06	1,03	1,03	1,05	1,01	0,99	1,05	1,08
35	1,06	1,00	1,01	1,06	0,98	0,99	1,03	1,06
36	1,01	0,98	0,99	1,02	0,96	0,95	0,96	1,02

Table 1, Calculated shelterfactors at Amsterdam Airport Schiphol

Shelterfactors 8 windobservation sites Airport Schiphol

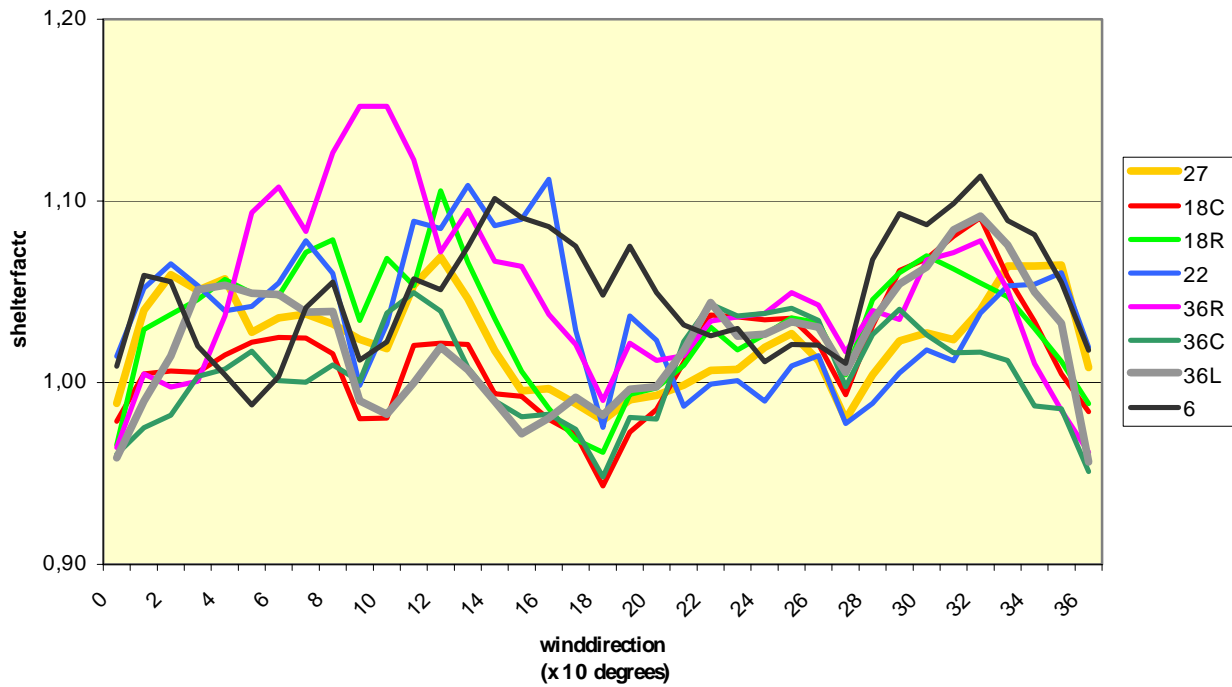


Fig.3. Calculated shelterfactors at Amsterdam Airport Schiphol

## 2. Discussion of the shelterfactor in relation to the relative obstacleheights and the roughness of the surroundings

The roughness  $Z_0$  and the shelterfactor SF can be classified using the scheme of Davenport. (Davenport 1960)

Class.	Type	$Z_0$	SF	Landscape
1	Sea	0,0002	0,89	Open sea or lake
2	Flat	0,005	0,94	Landsurface without any obstacles or vegetation, or ice surface
3	Open	0,03	1,00	Flat country with lgrass
4	Rough, open	0,1	1,06	Flat country with low vegetation and some incidental obstacles (distance between 20 x obstacle height)
5	Rough	0,25	1,14	Country with vegetation, row of trees, bigger obstacles (distance between 15 x obstacle height)
6	Very rough	0,5	1,22	Clusters of obstacles (farmhouses, trees) with open areas (distance between 10 x obstacle height)
7	Closed	1	1,36	Surface completely covered by high obstacles without any significant open area
8	City	2	1,62	Centre of city or woods

Table 2, Classification shelterfactors

A description have been made of the surroundings of windmast 22 Airport Maastricht-Aachen(table 3, figure 4)

<i>direction (degr)</i>	<i>Object</i>	<i>distance (m)</i>	<i>height (m)</i>	<i>rel.obst. height (%)</i>	<i>estimated shelter-factor</i>
0-24	Hangars	600-1480	6-20	1,35	1,01
28-37	Row of trees	1590	12	0,75	
36-43	Buildings	700	8	1,14	
44-46	Edge of building	545	16	2,94	1,03
47-52	Schreiner building	347	16	4,61	1,05
53-69	KLM-building	213	16	7,51	1,16
108	tower	3600		0,00	
118	Farm house	790	8	1,01	
118-128	Row of trees	1120	16	1,43	1,01
130	House	831	5	0,60	
133-182	Buildings	835		0,00	
153	tower	490	20	4,08	1,04
182-192	High trees	1720	20	1,16	
187	Low buildings, sheds	447		0,00	
202-212	Row of trees	540	14	2,59	1,02
213	House	1660		0,06	
232	Radar	1445		0,00	
232-245	Trees beside highway	1040		0,00	
245-272	Hangars	895		0,00	
263-271	Row of trees	770	17	2,21	1,02
272	Tower	590	27	4,58	1,05
272-285	Buildings	542	12	2,21	1,02
285-302	Law buildings	473	3	0,00	
280-303	Trees beside highway	680-570	28-15	4,12	1,05
304-305	Board commercials (vodafone)	484	18	3,72	1,04
328-330	Trees	580-611	12-18	2,95	1,03
334	Farm house	550	5-6	1,09	
334-346	Row of high trees	550	20	3,64	1,04
346-360	Hangars, sheds	600-1480	6-20	1,35	1,01

*Table 3, Surroundings windstation Airport Maastricht - Aachen*

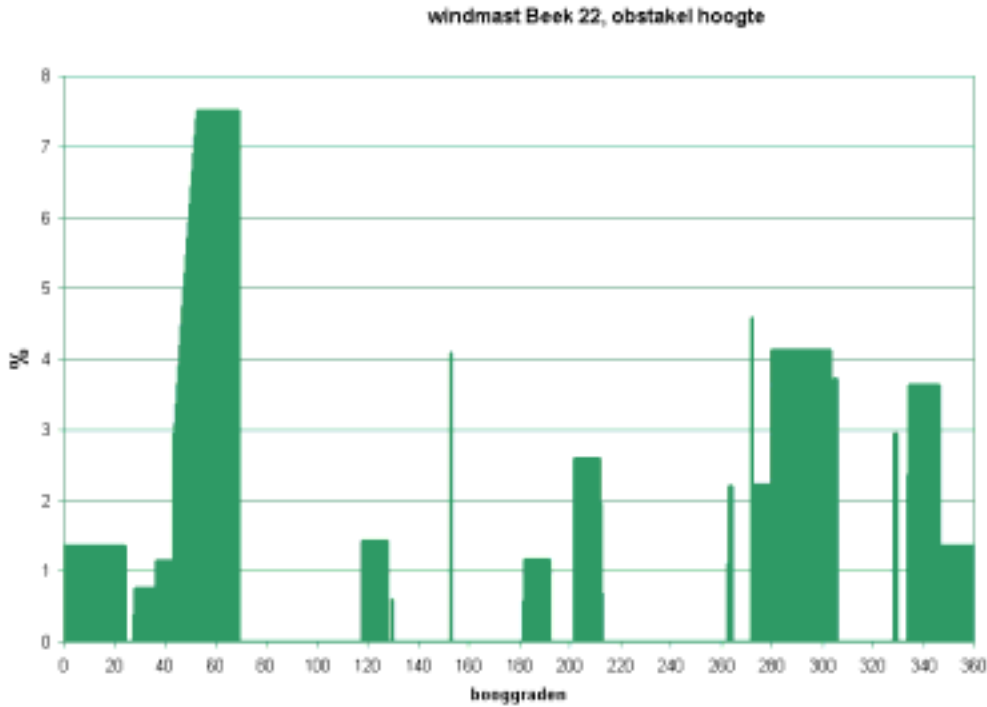


Fig. 4. Relative heights of obstacles around windmast 22 at Airport Maastricht Aachen

The calculated values of the shelterfactors and roughnesslengths per winddirectiondegree of windmast 22 at Airport Maastricht Aachen are presented in table 4 and figure 5.

dd	bf_calc_2004_summer	bf_calc_2004_winter
20	1,052	1,068
40	1,083	1,085
60	1,119	1,125
80	1,059	1,026
100	1,026	0,998
120	1,025	1,006
140	1,153	1,038
160	1,131	1,096
180	1,145	1,1
200	1,122	1,093
220	1,079	1,06
240	1,079	1,052
260	1,127	1,13
280	1,206	1,192
300	1,203	1,185
320	1,176	1,223
340	1,116	1,144
360	1,105	1,054

Table 4, Calculated shelterfactors at Airport Maastricht Aachen



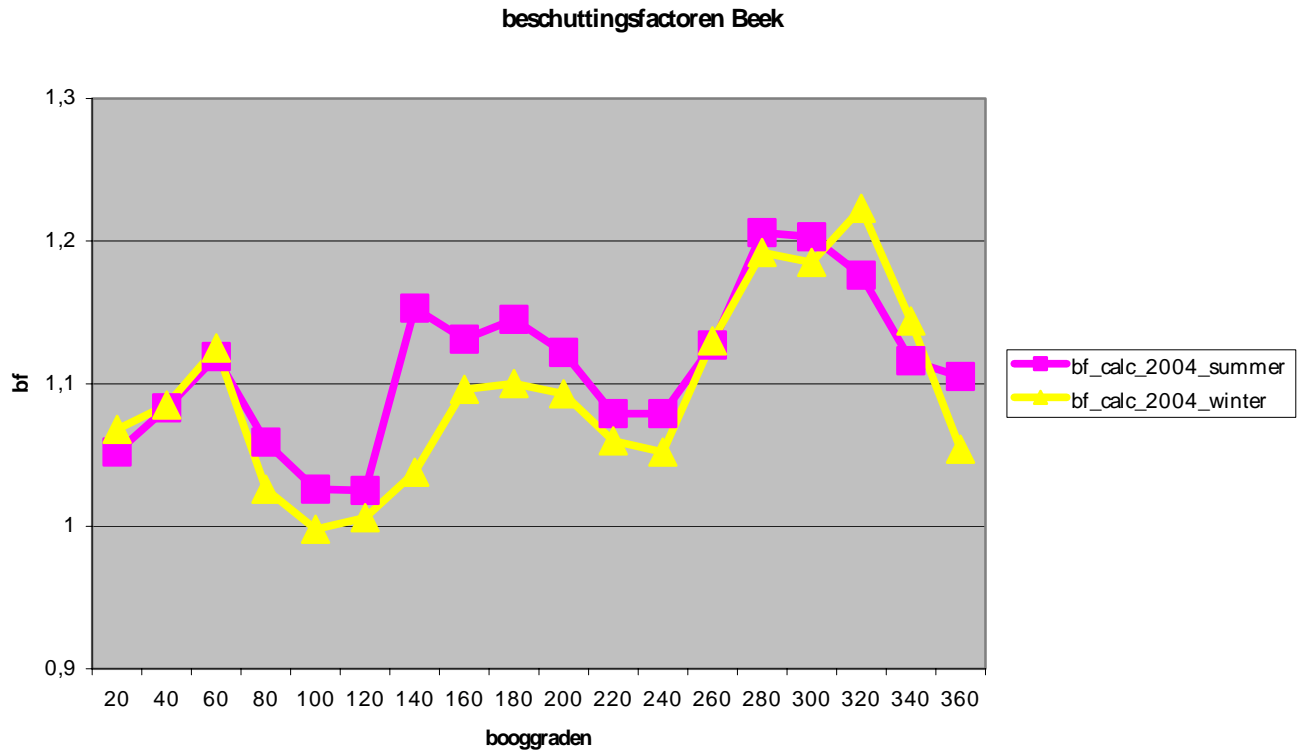


*Fig. 5. Calculated shelterfactors at Airport Maastricht Aachen*

The calculated values of the shelterfactors and roughnesslengths per winddirection degree of windmast 22 at Airport Maastricht Aachen can be compared with the description of the surroundings, and the interpretation of the Davenport scheme .

One can make the following conclusions with respect to the roughness and shelterfactor:

- a) the influence of the buildings in direction 40 – 70 degrees is consistent;
- b) the roughnesslength/ shelterfactor in directions 150 – 220 degrees and 260 – 360 degrees is much higher than one may expect because of the big distance of the objects; it means the extreme roughness outside the airport field (hills, trees, buildings) has a a long distance influence on the turbulency of the wind and in this view on the gustfactor and the corresponding shelterfactor at the windstation. It overrules the complete flatness of the airport field in the concerning direction.

### 3. Setup requirements and conditions for the surroundings

The sensors for measurement of wind speed and direction are mounted on a stable metal or plastic mast. The sensor height is 10 metres above terrain that should in principle be flat.

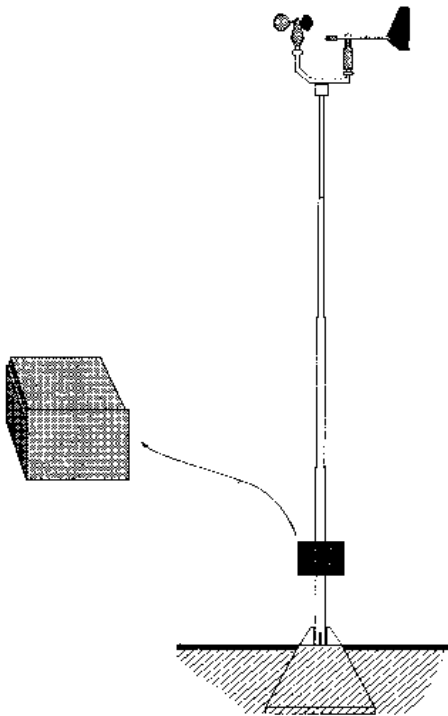


Fig.6. Windmast

#### a) Conditions relating to the surroundings and the measurement location

The roughness  $z_0$  should be  $< 0.5$  m in all directions. This condition implies a shelter factor SF of  $< 1.2$  (less than 20% reduction of the average wind speed).

The distance from the wind mast to any obstacles in the vicinity must be at least ten times and preferably twenty times the height of the obstacle (applies to all obstacles).

The terrain in the immediate vicinity of the wind mast (radius  $\geq 100$  metres around the measurement site) is flat grassland or a water surface.

#### b) Conditions relating to the surrounding and the measurement location and representativeness of the observations

The location of the wind mast is such that an observation of the wind can be performed (including any reduction using a shelter factor) that is representative for an area with a radius of 30 km around the measurement site. (NB: for wind measurements on the coast, the degree of representativeness is obviously partly dependent on the wind direction) This condition is based on statistical studies performed by J. Wieringa: "For a separation of 30km between two observation points in a homogeneous landscape, the difference in wind speed is less than 5% for 90% of the time." The density of the wind measurement network required then follows from the level of representativeness to be achieved.

#### c) specific conditions relating to the surroundings and the measurement site on an airfield

The wind observation at an airport must be representative for the wind conditions on the (adjacent) runways for take-off or landing, and in particular for the touchdown zone. In order to realize these objectives as well as possible, the following measure are taken:

- A 10-metre metal wind mast is placed 190 metres away from the centre of the runway. Closer than this to the runway is not possible, since a metal mast may not protrude through what is known as the "obstacle surface". (the obstacle surface is a plane running parallel to the centre of the runway 120 metres from it and then rising at a 1 in 7 angle)

- In the case of a so-called "frangible" plastic mast with a sensor at a height of 10 metres, the mast can be placed 115 metres from the centre-line of the runway. Closer than this is not possible, given the wingspan of NLA craft and the disruption of the wind behaviour caused by passing aircraft.
- The measurement height for wind speed and direction should preferably be 10 metres and at least 6 metres, placed above flat ground.
- The wind mast is positioned at least 120 metres from the centre of a runway for taxiing, due to the *ad hoc* effects on wind behaviour due to stationary or moving aircraft.
- The wind mast should be placed at a distance of at least 50 metres and preferably at least 100 metres behind the nearby ILS-GP antenna mast [NB: the ILS mast is an open construction approximately 1 metre in width and 9 metres in height]. When placed behind the ILS mast, disturbance of the wind measurement will only occur for wind directions that are inappropriate for use of the runway. Turbulence effects in the airflow as a result of passing a narrow, porous obstacle such as an ILS mast at a distance of 30 times the width of the obstruction will be virtually damped out anyway, and the wind profile at this distance is once again near enough identical to the profile in front of the obstacle. At a distance of 50 metres from an ILS mast, the wind as measured is in principle no longer perturbed.
- Positioning of the wind mast in front of the ILS mast is only possible if the distance is at least 100 metres, due to the possibility of the wind mast interfering with the ILS signal. Furthermore in this case, maintenance or inspection activities on the wind mast can only be carried out when the runway (and therefore the GP antenna too) is not in use.

## References

World Meteorological Organization, 1996: WMO No. 8, Guide to meteorological instruments and methods of observations, 6<sup>th</sup> edition, 1996 (in particular Chapter 5); WMO, Geneva, 1996

International Civil Aviation Organization 1998: Meteorological Service for International Air Navigation, International Standards and Recommended Practices, Annex 3 to the Convention on International Civil Aviation, 13<sup>th</sup> edition; ICAO, Montreal, Canada, 1998

Wind Climate in the Netherlands, J. Wieringa and P. J. Rijkoort, 1983\*

Rationale for determining design wind velocities, Davenport. A.G., J. Am. Soc. Civ. Engin., ST-86, pp.39 –68; 1960;

Shelter factors for wind, B. Oemraw, KNMI Technical Report TR-52, 1984\*

World Meteorological Organization, 1992: International Meteorological Vocabulary, WMO No. 182, second edition; WMO, Geneva, 1992

Aviation Regulations; Staatsuitgeverij, The Hague\*

Evaluation of Two Gustiness Models for Exposure Correction Calculations, J. W. Verkaik, Journal of Applied Meteorology, Volume 39, pp. 1613 - 1626, 2000.

Rationale windspeed measurements.... Davenport, 1960

\* in dutch

# A TEST OF THE PRECIPITATION AMOUNT AND INTENSITY MEASUREMENTS WITH THE OTT PLUVIO

Wiel M.F. Wauben,

Instrumental Department, Royal Netherlands Meteorological Institute (KNMI)

P.O. Box 201, 3730 AE De Bilt, The Netherlands

Tel. +31-30-2206-482, Fax +31-30-2210 407, e-mail: Wiel.Wauben@knmi.nl

## ABSTRACT

The Pluvio precipitation sensor of Ott has been tested at KNMI in order to find out whether it is a suitable candidate for replacing the current operational KNMI precipitation gauge. Tests performed at the calibration facilities of KNMI showed that the accuracy of the Pluvio is within the WMO requirements and proved stable after the field tests. The 1-year field test in De Bilt showed good agreement between the KNMI precipitation gauge in a pit and the Pluvio placed on the measurement field within a windscreen. The differences between Pluvio and KNMI gauge showed no evidence of a wind effect, but a dependency on precipitation intensity, ambient temperature, and the temperature gradient has been observed. A Vaisala FD12P present weather sensor showed generally the same behaviour for the differences as the Pluvio. The Pluvio did hardly report any faulty precipitation events that were not detected by the KNMI gauge or the FD12P. The Pluvio results obtained during a 1-year field test at the coastal station of De Kooy are not fully satisfactory. The observed differences for the Pluvio are generally not corroborated by the FD12P. Furthermore, the Pluvio reported isolated precipitation events that were not confirmed by the KNMI gauge or the FD12P. These faulty precipitation reports show a dependency on wind speed. It is unclear why these faulty reports were not observed at De Bilt in the same the wind speed range. The Pluvio is not suitable for operational use at KNMI due to the faulty precipitation reports observed in De Kooy although their effect on total amounts is small. Ott has currently an updated version of the Pluvio that should overcome the faulty reports. KNMI now considers an upgrade of the KNMI gauge in combination with the usage of a precipitation detector.

## 1. INTRODUCTION

The Royal Netherlands Meteorological Institute (KNMI) measures precipitation amount with an electronic precipitation gauge that has been developed indoors. The design of this sensor originates from 1991 and since then it has undergone no significant changes. The sensor is of the so-called float type and determines the precipitation intensity by the change of the water level in a reservoir as measured by a potentiometer every 12 seconds. A more detailed description of the KNMI precipitation gauge is given in Wauben (2004). The KNMI gauge has some shortcomings namely: (i) isolated faulty precipitation events up to about  $3\mu\text{m}=0.018\text{mm/h}$  sometimes occur during sunny days and are reported because the users require a high sensitivity since the sensor is also used for precipitation detection; (ii) a relatively high level of maintenance is required as a result of the sensitivity to contamination and the potentiometer is susceptible to failures; (iii) the large delay both at onset and cessation of solid precipitation that can occur since solid precipitation falling into the funnel has to be melted before the gauge can register it. The Pluvio precipitation sensor from Ott Hydrometrie is of the weighing type and hence will be less susceptible to contamination and will detect solid precipitation directly. Furthermore, tests with the Pluvio performed in other countries looked promising suggesting that the sensor could be a good alternative for the KNMI precipitation gauge. Therefore KNMI decided to test the new Pluvio precipitation sensor and to compare the results with that of the KNMI precipitation gauge. The tests are performed in the laboratory as well as during 1-year field trials performed at the KNMI test site in De Bilt and the coastal station at De Kooy. The aim of the tests was to investigate how the precipitation amount and intensity measurements of the Pluvio and the KNMI precipitation gauge compare in order to determine whether the Pluvio is suitable for being considered for operational use by KNMI.

Details of this study are reported in a KNMI technical report (Wauben 2005).

## 2. OVERVIEW OF THE PRECIPITATION SENSORS

An overview of the main sensor characteristics of both precipitation sensors is given in Table 1. The reported specifications for both sensors meet the criteria of WMO. Comparison of the main characteristics of the Pluvio precipitation sensor (Ott Hydrometrie, 2000 and 2002) and the KNMI precipitation gauge already point out some interesting differences. The Pluvio precipitation sensor will measure solid precipitation without

delay since the precipitation that has passed the orifice will directly fall into the collector bucket and will be measured. This could overcome the delays and possible evaporation losses the KNMI gauge might experience during solid precipitation. However, the filtering algorithm of the Pluvio can give a delay up to maximally 90 seconds. A further advantage of the Pluvio precipitation sensor is that the sensor is less sensitive to contamination. In case any contamination by insects, leaves, dust, bird excrements, etc. falls in the collector, it could result in a faulty precipitation event -although the sensor filters out the very low (less than 0.03mm in 20minutes) and very high (more than 50mm per minute) contributions- but it will not lead to sensor failures. Another advantage of the Pluvio is that it can easily be calibrated by using a set of reference weights whereas the KNMI precipitation gauge of the float type involves the use of fixed (weighed) amounts of water. Drawbacks of the Pluvio sensor are the lesser sensitivity compared to the KNMI precipitation gauge and the additional maintenance required for emptying the bucket and the required application of a saline solution to the collector at the start of the winter season in order to prevent deformation or damage of the collector. The reduced sensitivity of the Pluvio makes the sensor less suitable for precipitation detection and the determination of precipitation duration.

**Table 1: An overview of the general characteristics of the Pluvio precipitation sensor and the KNMI precipitation gauge.**

<i>Parameter</i>	<i>Pluvio</i>	<i>KNMI gauge</i>
Range	0 ... 10mm/min	0 ... 10mm
Accuracy	±0.04mm@10mm	±2% full scale
Reproducibility	±0.04mm@10mm	within ±1% full scale
Long-term stability (1yr)	±0.06mm@10mm	within ±2% full scale
Resolution	0.01mm/h	0.006mm/h
Sensitivity	0.03mm/20min	0.001mm/10min
Maximum intensity	600mm/h	300mm/h
Averaging time	30-90sec <sup>1</sup>	12sec
Collector content	0-200mm	1-11mm
Temperature range	-30 ... +45°C	-25 ... +40°C
MTBF	3500h	26500h
Calibration interval	+1year	36months
Maintenance	1 p.a. antifreeze 2-3 p.a. emptying	Covering of orifice during mowing
Collector area	200cm <sup>2</sup> ±0.5%	400cm <sup>2</sup> ±0.5%
Diameter sensor	210mm	226-284mm
Height sensor	570mm	610mm
Weight	6kg	19kg
Voltage sensor	12VDC	24VAC
Power usage sensor	<1.8W	3.6W
Voltage heater	24VAC	24VAC
Power usage heater	70W	115W
Communication interface	RS232/RS485	Frequency output

### 3. INDOOR TESTS

The Pluvio precipitation sensor was first subjected to some indoor tests. The Pluvio sensor that was considered at that time did not include the data logger but used a pulse output. Furthermore the sensor was equipped with the automatic emptying mechanism. Tests were performed with an adjustable pump and a balance so that the amount of water pumped into the collector of the Pluvio could be regulated and determined. The results of these tests will not be discussed here because since then changes were made to the sensor/software that resolved the problems or overcame them, whereas other findings could be explained in terms of the processing performed by the sensor. The results described in this paper are based on the Pluvio precipitation sensor without the automatic emptying mechanism, since tests showed that the emptying occurred only when the collector was almost full. Furthermore, a sensor equipped with a serial interface and a data logger was considered. A software upgrade (release 2.13) was performed in end of January 2001, after preliminary field test results indicated faulty precipitation events caused by wind effects. During the software upgrade the 2 sensors tested at KNMI were calibrated. Checks of the calibration were performed again in October 2003 after the field tests were completed. These tests showed that the addition of 1 and 2.5mm at five levels of the collector contents is accurate within ±0.01mm, i.e. the resolution of the Pluvio. The contents measurements of 0, 50, 100, 150 and 150mm give differences of about 0.00, +0.03,

<sup>1</sup> Depending on the variability of the raw weight measurements the averaging time can be as high as 400sec.

0.00, -0.05 and -0.08mm, respectively. All these differences are within the stated long-term accuracy of  $\pm 0.06$ mm when adding 10mm, and the accuracy required by WMO (1996), i.e.  $\pm 0.1$ mm for precipitation sums less than 5mm and  $\pm 2\%$  for larger amounts.

#### 4. FIELD TEST DE BILT

The field tests with the Pluvio precipitation sensor have been performed between February 1, 2001 and May 16, 2002 in De Bilt and between May 25, 2002 and August 11, 2003 in De Kooy. At both locations the Pluvio was placed on the measurement field in a windscreen, whereas the KNMI precipitation gauge was installed in the so-called English set-up. The data used in this study is the 10-minute averaged precipitation intensity of the KNMI gauge, the precipitation duration, and some additional parameters like the 10meter wind speed and direction, ambient temperature and humidity. Furthermore, precipitation intensity data from a Vaisala FD12P present weather sensor is used. The validated hourly KLIM data of the climatological department was used as a reference. Monthly sums of the precipitation amounts obtained by all 3 sensors are given in Table 2 and compared to the hourly KLIM data. Here, only those hours are considered where all 10-minute intervals of all 3 sensors have valid readings. The monthly results show that the sums for KNMI gauge and the KLIM data are quite close, i.e. within  $\pm 1$ mm or in the range -1 to 2%, as could be expected, since the KLIM data are mainly based on the sensor reading from the KNMI gauge. The large differences between the KNMI gauge and KLIM for June and July 2001 could both be ascribed to faulty sensor readings on a particular day that lasted several hours and returned to normal without any intervention. More suspicious events can be found in the raw sensor data by scanning the daily plot. The differences between Pluvio and KLIM are generally larger than those for the KNMI gauge, and range between -3 and 2mm or -4 and 3%. This could be expected when comparing the results for 2 different types of precipitation sensors during a field test. The monthly precipitation amounts for the present weather sensor show larger differences. However, KNMI does not use the PWS for the determination of precipitation amounts, but only for precipitation detection, and for the determination of precipitation type and visibility.

**Table 2: Monthly sums and differences between the precipitation amounts reported by the Vaisala PWS, the KNMI gauge, the Ott Pluvio, and the validated climatological sum for the field test in De Bilt. All hours are considered where valid precipitation data of all three sensors is available.**

Month	Sum (mm)				# valid hours	Difference (mm)		Difference (%)	
	PWS	Gauge	Pluvio	Klim		Ga-KI	Pl-KI	Ga-KI	Pl-KI
0201	89.4	87.7	84.8	88.1	592	-0.41	-3.35	-0.47	-3.80
0301	84.0	74.0	72.4	74.2	735	-0.22	-1.81	-0.29	-2.44
0401	97.2	83.7	82.3	84.3	675	-0.55	-2.05	-0.66	-2.43
0501	33.2	29.2	29.6	29.1	739	0.14	0.49	0.49	1.68
0601	53.4	61.7	56.5	52.8	705	8.87	3.66	16.80	6.93
0701	76.3	74.3	85.0	86.6	737	-12.34	-1.63	-14.25	-1.88
0801	105.6	99.0	99.8	99.2	723	-0.20	0.61	-0.20	0.61
0901	188.9	190.3	187.4	190.3	704	-0.04	-2.90	-0.02	-1.52
1001	36.5	34.8	35.3	34.3	704	0.54	0.98	1.58	2.86
1101	68.3	60.7	61.0	59.7	655	0.99	1.29	1.66	2.16
1201	109.5	93.0	95.9	93.9	743	-0.95	1.96	-1.01	2.09
0102	61.1	57.6	58.3	57.8	719	-0.15	0.53	-0.26	0.92
0202	131.8	136.8	135.7	137.2	663	-0.40	-1.46	-0.29	-1.06
0302	34.7	29.7	28.1	29.3	718	0.38	-1.18	1.29	-4.03
0402	46.6	39.8	39.0	39.5	700	0.34	-0.55	0.85	-1.39
0502	24.7	21.2	21.4	21.4	360	-0.21	0.02	-0.98	0.09
<b>Total</b>	<b>1241.0</b>	<b>1173.5</b>	<b>1172.3</b>	<b>1177.7</b>	<b>10872</b>	<b>-4.22</b>	<b>-5.38</b>	<b>-0.36</b>	<b>-0.46</b>

The differences are studied in more detail by comparing of the 10-minute precipitation data of the 3 sensors directly. A histogram of the differences between the 10-minute intensity measurements of any 2 precipitation sensors is presented in Figure 1 using a bin size of 0.03mm/h. The histogram is plotted using a logarithmic scale. The histogram roughly resembles a Gaussian distribution. Both histograms peak at a difference of 0.00mm/h, where the bin for Pluvio-Gauge contains 41% of the cases and PWS-Gauge 33%. The number of cases within  $\pm 0.1$ mm/h is 66% for Pluvio-Gauge and 68% for PWS-Gauge. The number of cases in the bins for larger differences decreases exponentially. The histogram for PWS-Gauge shows more cases with positive than negative differences leading to the larger monthly sums for PWS compared to the

KNMI gauge. The histogram for Pluvio-Gauge shows almost a constant value for differences between +0.03 and +0.18mm/h. This feature can probably be explained in terms of the reporting threshold of 0.03mm of the Pluvio. The cases with precipitation amounts of less than 0.03mm in 10 minutes, i.e. a 10-minute averaged intensity of less than 0.18mm/h, will be reported by the KNMI gauge, but not by the Pluvio. Such events add cases to the slightly negative bins of the histogram, as do faulty KNMI gauge readings. However, there are no or in any case less corresponding events adding cases to the slightly positive bins. As a result the number of cases with positive differences Pluvio-Gauge less than 0.18mm/h is reduced.

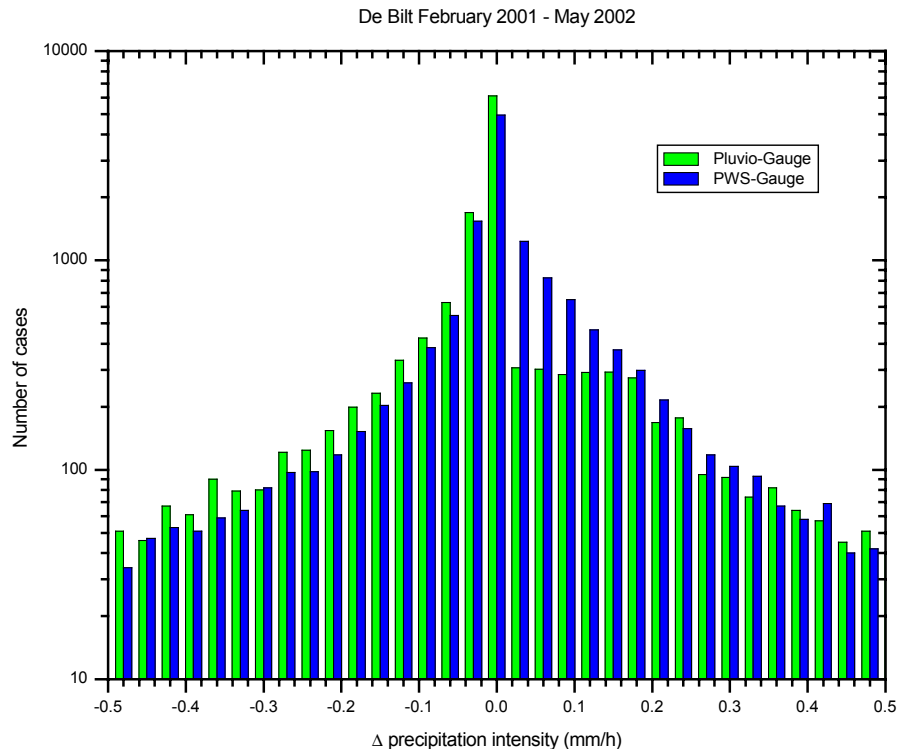


**Figure 1: Histogram of the differences between the raw 10-minute averaged precipitation intensity measurements for any combination of 2 precipitation sensors during the field test in De Bilt. The bin size is 0.03 mm/h. All cases are included where at least one of the sensors reports precipitation.**

Next the differences between the measured 10-minute precipitation intensities are studied as a function of wind speed in bins of 1m/s. The differences are calculated for different wind speed bins in order to determine any wind speed effect. The averaged differences between the 10-minute precipitation intensities for 2 precipitation sensors per wind speed interval are given in Figure 2. The results are given as the percentage of the total precipitation amount per wind speed bin as measured by the KNMI gauge. The precipitation amount measured by the KNMI gauge and the total number of cases involved is also shown per wind speed bin. In addition, the number of so-called 'faulty' sensor only cases, i.e. the cases where one precipitation sensor reports precipitation but the other 2 sensors do not report precipitation nor in the previous and in the next 10-minute interval if available, are given as the sensor only cases in Figure 2. First of all note that the behaviour of the curves for Pluvio-Gauge and PWS-Gauge are generally the same. Between 1 and 8m/s the differences Pluvio-Gauge show no wind speed effect. The results above 8m/s are not shown because statistics is poor in that region. Below 1m/s the differences Pluvio-Gauge increase up to about 12%. A similar increase can be observed for PWS-Gauge. At low wind speeds the KNMI precipitation gauge reports less precipitation compared to the Pluvio and PWS. It is unlikely that this behaviour is related to a wind effect, but it is partly the results of the relatively large number of faulty Gauge only events at low wind speeds. Any wind speed effect also depends on the type of precipitation such as solid or liquid precipitation and the droplet size since small/light particles have a smaller fall velocity, and hence are more sensitive to the wind. The under catch due to the wind effect will be larger for snow compared to rain, but it will also be larger for smaller particles. The influence of droplet size will be investigated by analysing the results as a function of the precipitation intensity, although this is not a real measure of the droplet size.

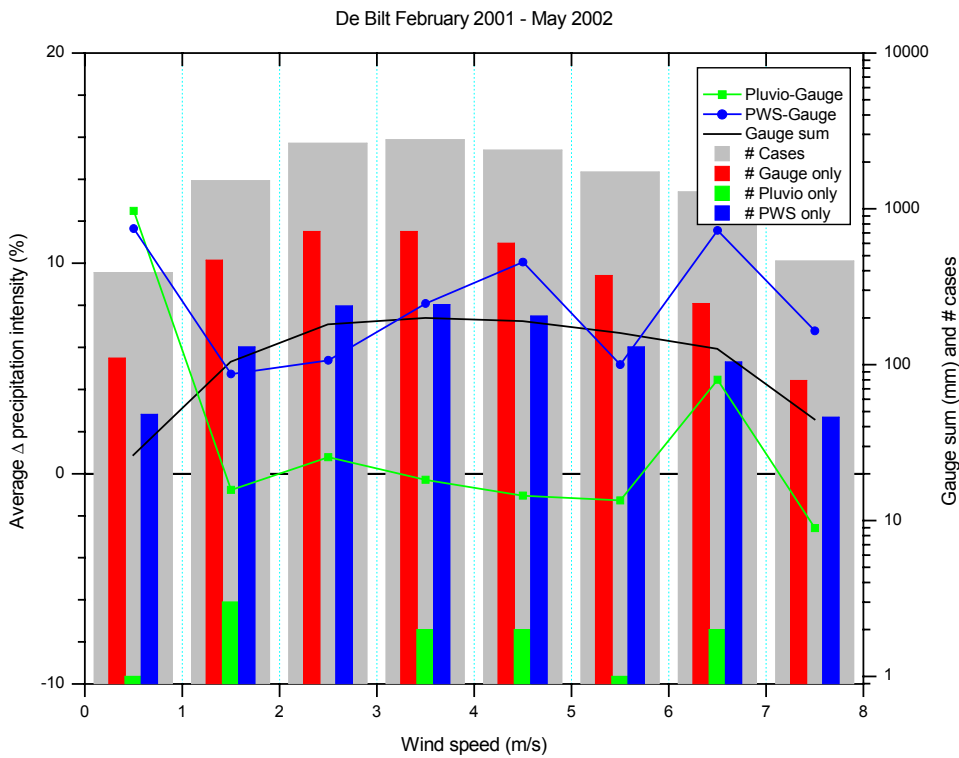


**Figure 2: Averaged relative differences between the 10-minute precipitation intensities measured by 2 precipitation sensors as a function of the wind speed in bins of 1m/s for the field test in De Bilt. The results are presented as the percentage of the total precipitation amount per wind speed bin as measured by the KNMI gauge, which is indicated by the black line. The total number of cases involved is indicated by the histogram, as is the number of ‘faulty’ sensor only events.**

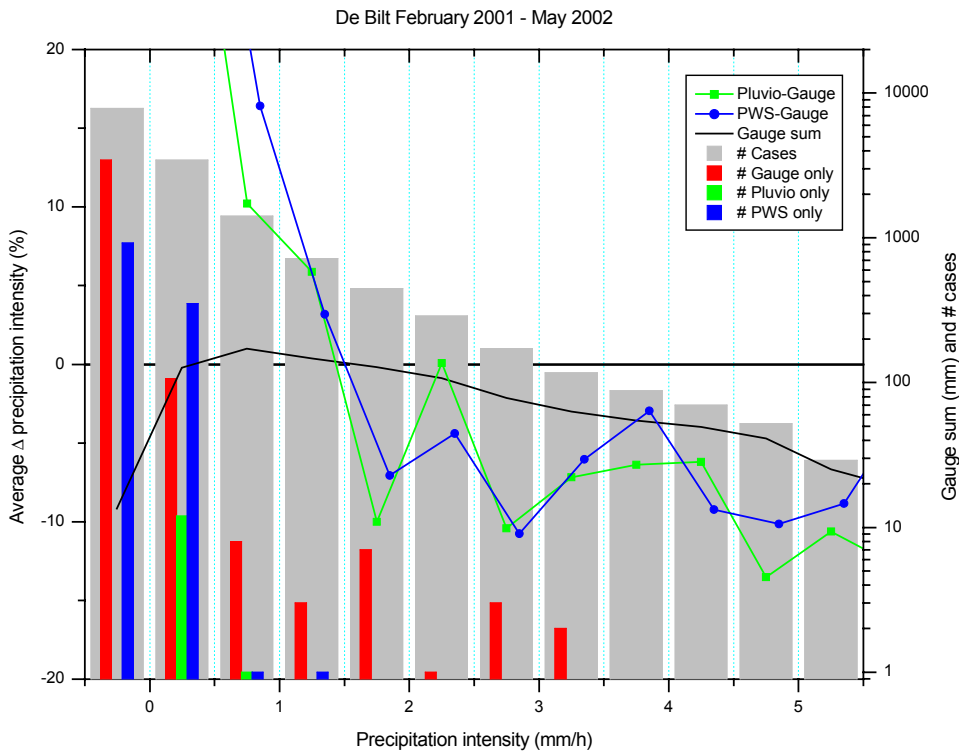


**Figure 3: As Figure 2, but now the relative differences are given as a function of the precipitation intensity. The binning in steps of 0.5mm/h is performed on the intensity measured by the KNMI gauge. The first bin contains the cases with intensity less than 0.05mm/h. The number of ‘faulty’ sensor only events is reported in the intensity bin derived from their own reported precipitation intensity.**



Figure 3 shows the relative difference between the precipitation intensity measured by 2 precipitation sensors as a function of the precipitation intensity. Again, the curves for Pluvio-Gauge and PWS-Gauge show generally the same behaviour. The first bin at zero contains the cases where the KNMI gauge reported traces of precipitation with intensities less than 0.05mm/h. This mainly consists of the ‘faulty’ cases when the KNMI gauge only reports traces of precipitation. Since the other 2 precipitation sensors report generally a higher intensity, if any, and the faulty cases of these 2 sensors are also added to this bin when calculating the relative differences, the relative difference at the first bin is large and positive. Note that Pluvio and PWS report faulty cases when the intensity of the sensor is below 1 and 1.5mm/h, respectively, whereas the KNMI gauge reports faulty cases up to 3.5mm/h. The differences Pluvio-Gauge and PWS-Gauge decrease with intensity between 0 and about 2mm/h. Above 2mm/h, the differences between Pluvio-Gauge and PWS-Gauge are generally about –5% to –10%, respectively. The behaviour of the curves resembles the curves given by Nešpor and Sevruc (1999) obtained by numerical simulations. However, the curves are such that the measurements of the KNMI gauge in the so-called English set-up seem to be affected by the wind effect. This is contrary to the results obtained by Wauben (2004) when comparing the measurements for 2 KNMI gauges, one placed in the English set-up and the other on the measurement field surrounded by a windscreen. The above results seem to indicate that the Pluvio installed on the measurement field in a windscreen is not affected by the wind effect. If such an effect does exist, it must be masked by other error sources that occur when comparing different types of precipitation gauges (cf. WMO, 1994). Since both the Pluvio and the PWS show the same general behaviour, it could be concluded that the KNMI gauge seems in general to underestimate precipitation intensities below 1.5 mm/h and to overestimate intensities above 1.5mm/h. This could be caused by wetting and evaporation losses in the collector of the KNMI precipitation gauge. These losses are relatively largest at small precipitation intensities. The Pluvio and PWS measure precipitation more directly and it is therefore expected that these instruments will be less affected by wetting and evaporation losses.

## 5. FIELD TEST DE KOOY

The results of the field test at the coastal station in De Kooy show much larger differences, although the same Pluvio sensor was used. The differences in monthly precipitation sums between Pluvio and KLIM range between –1 and 8mm. Generally the Pluvio gives higher precipitation amounts. Overall the differences between Pluvio and KLIM in De Kooy are 34mm or 4.5% compared to –5mm or –0.5% for De Bilt. In order to find the reason for these differences the 10-minute data are analysed in more detail. The averaged differences between the 10-minute precipitation intensities for 2 precipitation sensors per wind speed interval are given in Figure 4. In contrast to the corresponding results for De Bilt (cf. Figure 2) the differences Pluvio-Gauge show a wind speed effect between 1 and 8 m/s. A linear fit to the data gives a slope of about  $2.5\%/ms^{-1}$ . The results above 8m/s are not considered because statistics is poor in that region, but in that region the differences Pluvio-Gauge decrease again. Figure 4 also shows that the number of faulty Pluvio cases increases between 3 and 8 m/s. The sign of the slope suggests that the KNMI gauge in the English set-up reports less precipitation under high wind speed conditions compared to the Pluvio on the measurement field in a screen. Again this effect is opposite to the results obtained by comparing 2 KNMI precipitation gauges in a similar set-up (Wauben 2004), where the gauge on the measurement field and within a windscreen reported less precipitation with increasing wind speed. The differences PWS-Gauge show a different behaviour as a function of wind speed in the region 4 to 7 m/s. This is in contrast to the results for De Bilt, where Pluvio-Gauge and PWS-Gauge showed generally the same behaviour as a function of wind speed. The faulty Pluvio readings are a probably reason for the observed differences at De Kooy. A major difference between the faulty Pluvio readings for De Bilt and De Kooy is that the number of faulty cases is much higher for De Kooy (776 out of a total of 4226 precipitation reports) than for De Bilt (13 out of 6117). Most faulty Pluvio cases occur in the 0.05 to 0.5mm/h intensity bin. The results of the KNMI gauge also shows differences between De Kooy and De Bilt. The faulty cases for the KNMI gauge at De Kooy occur mainly for traces (1893 out of a total of 7042 precipitation reports), but some faulty cases (63) occur at the next intensity bin at 0.5mm/h, whereas for De Bilt the faulty cases occur up to 3.5mm/h. The faulty readings for the PWS (812 out of a total of 5341 precipitation reports) occur mainly in the lowest precipitation intensity bins. The total amounts of precipitation included in the faulty cases at De Kooy are 5, 34 and 6mm for KNMI gauge, Pluvio and PWS, respectively, whereas for De Bilt the corresponding values are 16, 1 and 9mm. Since the Pluvio overestimates the total precipitation amount at De Kooy as measured by the KNMI gauge by about 38mm, the exclusion of the above mentioned “faulty” cases will reduced the overall difference by 29mm.

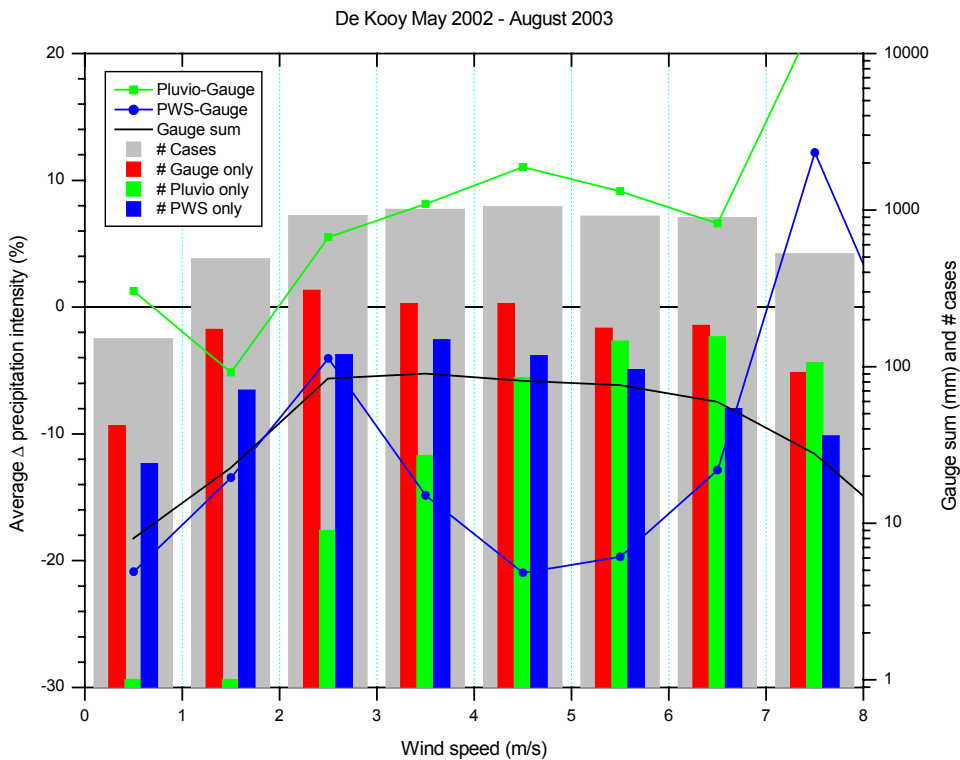


Figure 4: Averaged relative differences between the 10-minute precipitation intensities measured by 2 precipitation sensors as a function of the wind speed in bins of 1m/s for the field test in De Kooy. The results are presented as the percentage of the total precipitation amount per wind speed bin as measured by the KNMI gauge, which is indicated by the black line. The total number of cases involved is indicated by the histogram, as is the number of ‘faulty’ sensor only events.

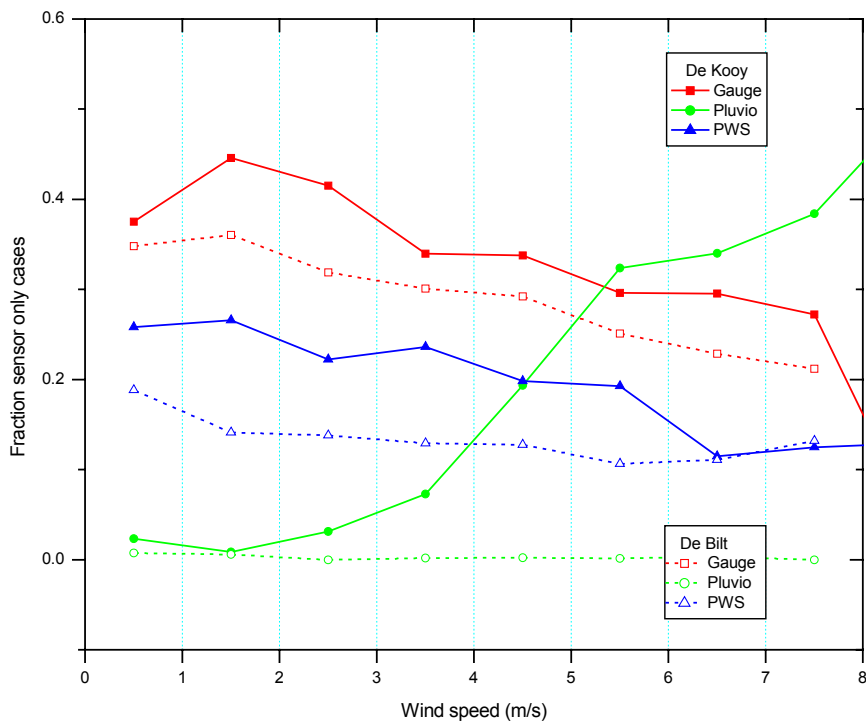


Figure 5: The ratio of the number of ‘faulty’ sensor only readings and the total number of sensor readings with precipitation as a function of the observed wind speed in bins of 1m/s. The ratios are given for the 3 precipitation sensors involved and for the field test in De Bilt and in De Kooy.

The reason for the faulty cases is studied next. Figure 5 shows details of the ratio of the number of faulty sensor readings and the total number of sensor readings with precipitation as a function of the observed wind speed. The ratios are given for each precipitation sensors and for the field tests in De Bilt and in De Kooy. In general, the faulty readings for the field test in De Bilt show no clear dependence on wind speed for all three sensors. The KNMI gauge and PWS also show no wind speed dependency at De Kooy, but the number of faulty cases is in general about 5% higher at De Kooy. The faulty Pluvio readings for De Kooy, however, show a clear dependency with wind speed, although the wind speeds considered are the same as for De Bilt. The faulty Pluvio cases in De Kooy occur mainly when the collector is nearly empty and hence more sensitive to wind induced vibrations, and are probably as a result thereof also related to the ambient temperature, relative humidity and global radiation. There is a slight dependency of the number of faulty Pluvio cases on wind direction, but this is not correlated to the gustiness of the wind. Therefore it is still unclear why the faulty Pluvio cases that occurred at De Kooy have not been observed at De Bilt. Note, however, that the wind mast in De Kooy is located at about 500m from the measurement field where the KNMI gauge and Pluvio are situated. Faulty Pluvio precipitation reports could also be observed when the sensor was placed in a climate chamber and the temperature gradient changed more than 0.5°C/min. However, during the field test in De Kooy the faulty cases occurred also at lower gradient.

## 6. CONCLUSIONS

The results obtained with the Pluvio precipitation sensor during the field test in De Bilt showed that the Pluvio agrees within WMO requirements with the current operational KNMI gauge and in case of differences the Pluvio generally shows the same behaviour as the results obtained with a present weather sensor. Based on the De Bilt results the Pluvio seemed to be a good alternative for the KNMI gauge. However, the results obtained during the field test in De Kooy showed many cases with faulty precipitation reports by the Pluvio and the observed differences between Pluvio and KNMI gauge are not corroborated by the PWS. The faulty Pluvio events are most probably induced by wind effects, although it is still unclear why these faulty reports were not observed at De Bilt in the same the wind speed conditions. The field test furthermore showed that the Pluvio is not suitable for precipitation detection. For that purpose the usage of a precipitation detector will be considered by KNMI. The use of separate sensors for the determination of precipitation amount and precipitation detection not only overcomes the compromises one has to make in the design when making an instrument for 2 different purposes including accurate overall sums and a high sensitivity, but furthermore the usage of 2 separate sensor makes it possible to perform online quality checks which is particularly useful for a meteorological parameter that shows large spatial differences.

The tested Pluvio is not suitable for operational use at KNMI due to the faulty precipitation reports observed in De Kooy although their effect on total amounts is small. Ott has currently an updated version of the Pluvio that should overcome the faulty reports. KNMI now considers usage of a precipitation sensor in combination with a precipitation detector and considers an upgrade of the current KNMI precipitation gauge.

## 7. REFERENCES

- Nešpor, V. and Sevruk, B.: Estimation of Wind-Induced Error of Rainfall Gauge Measurements Using a Numerical Simulation, *J. Atmos. Oceanic Tech.*, Vol. **16**, 450, 1999.
- Ott Hydrometrie: Pluvio Precipitation Sensor DWD-Version (in German), User Manual, Ott Hydrometrie, 2000.
- Ott Hydrometrie: Pluvio, Brochure, Ott Hydrometrie, 2002.
- Wauben, W.M.F.: Precipitation Amount and Intensity Measurements using a Windscreen, Technical Report **TR 2004-262**, KNMI, De Bilt, 2004.
- Wauben, W.M.F.: Precipitation Amount and Intensity Measurements with the Ott Pluvio, Technical Report **TR 2005-270**, KNMI, De Bilt, 2005.
- WMO: Guide to Hydrological Practices, Fifth Edition, WMO-No. **168**, WMO, Geneva, 1994.
- WMO: Guide to Meteorological Instruments and Methods of Observation, Sixth edition, WMO-No. **8**, WMO, Geneva, 1996.

# WIND TUNNEL AND FIELD TEST OF THREE 2D SONIC ANEMOMETERS

Wiel M.F. Wauben,

Instrumental Department, Royal Netherlands Meteorological Institute (KNMI),

P.O. Box 201, 3730 AE De Bilt, The Netherlands

Tel. +31-30-2206 482, Fax +31-30-2210 407, e-mail: [Wiel.Wauben@knmi.nl](mailto:Wiel.Wauben@knmi.nl)

## ABSTRACT

Three 2D sonic anemometers (so-called sonics) have been selected by KNMI and have been subjected to tests in order to establish whether they are suitable for operational use. The three sonics are the Thies 2D, the Gill Windobserver 2 and the Vaisala WAS425. The sonics have been compared to the KNMI cup anemometer and wind vane that are used operationally. After some initial tests, during which all three sensors showed some problems, all sensors were upgraded and the tests commenced. Wind tunnel tests were performed for wind speeds up to 75m/s. Overall the agreement of all sensors is within the WMO requirements, although in detail all three sensors have strong and weak points. The field test showed that all 3 sonics worked properly although the Thies showed some signs of wear and the Vaisala occasionally missed a measurement. Overall the sonics agree very well with each other. The differences between the sonics and the conventional cup and vane are larger. The differences for the 10-minute averaged wind speed show a strong directional dependence that is probably related to surface roughness. The results also show a dependency on precipitation intensity. Overall the sonics seem suitable for operational use, but the use of sonics instead of the conventional wind sensors requires the construction of transfer functions for the homogenization of the climatological measurements.

## 1. INTRODUCTION

The Royal Netherlands Meteorological Institute (KNMI) uses conventional cup anemometers and wind vanes to measure wind speed and direction. Although the KNMI cup and vane meet WMO and ICAO requirements concerning the accuracy of wind measurements, the sensors require a large amount of maintenance and occasionally some anemometer freeze during calm winter conditions. Therefore, the usage of alternative wind sensors is considered. Sonic anemometers, in this report referred to as sonics, have no moving part, which makes them robust and almost maintenance free. In addition, the sonics have virtually no detection limit and detect changes almost instantly, whereas cup and vane have a threshold speed and need some time to adjust to the prevailing conditions. Furthermore sonic anemometers can optionally be equipped with a heater in order to prevent malfunctioning due to icing. Sonic anemometers have been available for several years. These sensors are generally used for scientific research, particularly because the 3-D sonics also measure the small vertical wind component very accurately and with a high temporal resolution. In recent years new measurement techniques and especially by more advanced processing of the raw data make the measurements of new sonic anemometers more reliable under all weather conditions. Therefore KNMI considered it a good moment to perform a test of sonic anemometers in order to find out whether they are suitable for use in the operational meteorological network. The test is restricted to commercially available 2-D sonic anemometers since the more expensive 3D sensors are not required in the operational network.

In this paper some preliminary results of the data analysis will be presented. Details of this study will be reported in a forthcoming KNMI technical report (Wauben 2005).

## 2. WIND SENSORS

KNMI uses conventional cup anemometers and wind vanes that have both been developed indoors. An overview of the sensor characteristics is given in Table 1. The cup anemometer and the wind vane are both connected to a sensor interface that reads the instruments with a 4Hz-sampling rate. The sensor interface calculates running averages for wind speed (scalar) and direction (unit vector), computes the wind gust (highest 3-second averaged speed) and takes care of marked discontinuity according to WMO and ICAO regulations (WMO, 1994). The sensor interface outputs a measurement string every 12 seconds that includes the sample values, 1-minute and 10-minute averages and extremes as well as the 10-minute standard deviation. Sonic anemometers determine wind speed and direction from the travel time of sound pulses. Three 2D sonic anemometers have been selected for the test. The specifications of these sensors meet the requirements (cf. Table 1) and the sensors are already extensively used, albeit not operationally by the meteorological community, although some tests have been performed. The selected sonics are the Thies 2D ultrasonic anemometer (Thies Clima, 2001), the Gill Solent WindObserver II ultrasonic wind sensor (Gill Instruments, 2000) and the Vaisala WAS425 ultrasonic wind sensor (Vaisala, 2000).

**Table 1: An overview of the general characteristics of the wind sensors considered in this study and the WMO requirements.**

<b>General sensor characteristics</b>					
<i>Parameter</i>	<i>KNMI cup</i>	<i>KNMI vane</i>	<i>Thies</i>	<i>Vaisala</i>	<i>Gill</i>
Name	KNMI cup anemometer	KNMI wind vane	Ultrasonic Anemometer 2D	Ultrasonic wind sensor WAS 425 AH	Solent WindObserver II
Software version	4.0	4.0	1.90	6.04	2.01
Operating Frequency	N.A.	N.A.	250kHz	100kHz	± 180kHz
Output rate	1/12Hz	1/12Hz	10Hz	1Hz	1, 4 or 10Hz

<b>Wind direction</b>					
<i>Parameter</i>	<i>WMO</i>	<i>KNMI</i>	<i>Thies</i>	<i>Vaisala</i>	<i>Gill</i>
Range	360°	0 to 359.9°	1 to 360°	0 to 359°	0 to 359° or 1 to 360°
Resolution	3°	1°	1°	1°	1°
Accuracy	±5°	±3°	±1.5°	±2°	±2°
Sample rate	4Hz	4Hz	400Hz	1Hz	40Hz
Running average	3sec	3sec	0, 1, 10sec or 2min (3sec in SW upgrade end 2000)	1 to 9sec (RS232)	0 or 1 to 3600sec
Detection limit	0.5m/s	0.4m/s	0.01m/s	virtually zero	below 0.5m/s no direction reported, but u,v in 0.01m/s
Damped wavelength	< 10m	3.8m	N.A.	N.A.	N.A.
Damping ratio	0.3 to 0.7	0.36	N.A.	N.A.	N.A.
Time constant	1sec	?	meas. time 0.0025sec, response time 0.1sec	meas. time 0.2sec, response time 0.35sec	< 0.1sec

<b>Wind speed</b>					
<i>Parameter</i>	<i>WMO</i>	<i>KNMI</i>	<i>Thies</i>	<i>Vaisala</i>	<i>Gill</i>
Range	0.5 to 75m/s	0.5 to 75m/s	0 to 60m/s (above value)	0 to 65m/s	0 to 65m/s (above value or error)
Resolution	0.5m/s	0.01m/s	0.1m/s	0.1m/s	0.01m/s
Accuracy	Max of ±0.5m/s and ±10%	±0.5 m/s	Max of ±0.1m/s and ±2%	Max of ±0.135 m/s and ±3%	±2%
Sample rate	4Hz	4 Hz	400Hz	1Hz	40Hz
Running average	3sec (gust)	3 sec	0, 1, 10sec or 2min (3sec in SW upgrade end 2000)	1 to 9sec (RS232)	0 or 1 to 3600sec
Threshold speed	0.5m/s	<0.5m/s typically 0.3m/s	0.001m/s	virtually zero	0.01m/s
Response length	2 to 5m	2.9m	0.20m	0.40m	0.15m
Time constant	1sec	?	meas. time 0.0025sec, response time 0.1sec	meas. time 0.2sec, response time 0.35sec	< 0.15sec

The basic quantity, which is needed for the measurement of wind gust in particular, are running 3-seconds averages with an update frequency of 4Hz as recommended by WMO (1987). Since not all three sonic anemometers facilitate running 3 seconds averages and 4Hz updates it was decided to poll all three sensors identically with 1Hz during which the 1-second averaged wind is obtained.

The three sonic anemometers have different mounting mechanism, power and signal connectors, dimensions and alignment methods. A coupling device was developed in order to facilitate the installation of each of these sensors. This device allows the mounting of the sensor to the standard 9-pole plug of the KNMI cup anemometer and wind vane. A reference pin in this plug is used for the orientation of the sensor. Tests showed that the alignment of the sonics agreed within  $\pm 1^\circ$ .

### 3. WIND TUNNEL TESTS

Wind tunnel tests were performed in the Low Speed Tunnel (LST) of the Dutch National Aerospace Laboratory (NLR) that is operated by DNW (German-Dutch Wind Tunnels). The LST is an atmospheric, closed-circuit wind tunnel with a  $3 \times 3 \times 2.25$ m test section. The wind speed range of the tunnel is 1.5m/s to 80m/s. The absolute accuracy of the tunnel wind speed calibration is 0.11m/s at 2.0m/s, decreases to 0.05m/s at 5.0m/s, remains 0.05m/s up to 10.0m/s and increase to 0.15m/s at higher wind speeds. The blocking factors applied for the cup, Gill/Thies and Vaisala were determined to be 2.1, 2.5 and 2.7%, respectively. The variation in wind speed across the test section is less than 0.2% and turbulence is below 0.03%. The horizontal and vertical flow angularities are within  $0.1^\circ$ . The sensors are mounted on a unipod with a height of 1.1m that is equipped with a standard 9-pole plug and brings the sensor near the middle of the test section. The unipod is fixed to the centre of the turntable in the floor of the test section that can be rotated over  $360^\circ$  with accuracy well below  $0.1^\circ$ . At each of the wind speeds 2, 3, 5, 10, 20, 50, 60, 75, 70, 30, 15, 7, 5m/s azimuth scans are taken with a constant angular speed of the turntable of  $0.5^\circ/\text{sec}$ .

Some results of the azimuth scans are shown in Figure 1. For that purpose the 1-second sensor and tunnel readings are averaged over 2-degree interval of the turntable and presented as a function of the azimuth angle of the turntable. Note that a discontinuity at about  $-60^\circ$  is the result of the angular offset between the North directions of the turntable and the sonic. Also note that the full scale of the figure corresponds to the accuracy required by WMO, i.e.  $\pm 5^\circ$  for direction and the maximum of  $\pm 0.5$ m/s and  $\pm 10\%$  for the wind speed. Overall the agreement of all sensors is within the WMO requirements. The results of the Vaisala are fine at high wind speeds. For wind speeds of 50m/s and more a small disturbance caused by the transducer arms can be observed. At low wind speeds ( $< 5$ m/s) the results are bit noisy, but well within WMO limits. The results of the Thies clearly show that the sensor compensates for the disturbance caused by the transducer arms, although a small effect can still be observed at wind speeds below 15m/s. The Thies results for all wind speeds are close to the reference, but the Thies failed to give good measurements above 50m/s. Inspection of the sensor by Thies showed that this was a result of bird-inflicted damage during the field test, whereby moisture entered the sensor. The Gill measurements are very consistent even at low wind speeds. Gill does not correct for the disturbance of the transducer arms. Especially at high wind speeds ( $> 30$ m/s) the disturbance is very pronounced and above 60m/s the differences induced by the transducer arms even exceeds the WMO limits at some orientations.

All azimuth scans were used to calculate the azimuthally averaged differences in the measured wind speed. The deviations of these averaged wind speeds from the tunnel wind speed are shown in Figure 2 as a function of the tunnel wind speed. Two KNMI cup anemometers are also included in this figure. For that purpose the cups were placed in the wind tunnel and sampled for about 2 minutes at each of the tunnel speeds. During these measurement the turntable was not operated and delays were included in order to allow the tunnel and the cup anemometer to adjust to the new speed. Figure 2 shows that the azimuthally averaged wind speeds of all sensors agree with the tunnel reference speed within the accuracy of  $\pm 10\%$  required by WMO. All sensors give lower averaged wind speed values at low tunnel speeds. The cup anemometers measurements are close to the tunnel values in the middle wind speed range of 5 to 30m/s, but underestimate the wind speed at low and high wind values. The sonic anemometers generally show the largest relative differences at low wind speed values and the differences decrease for higher wind speed values. The Vaisala and Thies generally give the best results. The Vaisala slightly overestimates the wind speed above 5m/s whereas the Thies always reports slightly lower values. The Gill generally differs more from the tunnel reference values than the other 2 sonics and also shows larger fluctuations between the differences at neighboring wind speed values. Note that the successive wind speed values were measured alternatively in the upward and downward sweep through the full wind speed range.

Tests were also performed in the KNMI wind tunnel with a closed measurement section of about 0.4m and a wind speed range of 0.2m/s to about 27m/s. Due to the rather small dimensions the KNMI tunnel is not suitable for absolute calibrations of the sonics. However, tests revealed that the KNMI tunnel could be used for verification of the alignment and the azimuth response as well as for checking the wind speed although the magnitude and sign of the differences shows a different behaviour than was observed in the LST tunnel tests. The different behaviour observed in the KNMI tunnel cannot be explained by a single correction factor. However, all sensors agree within WMO limits with the KNMI tunnel over the full wind speed range.

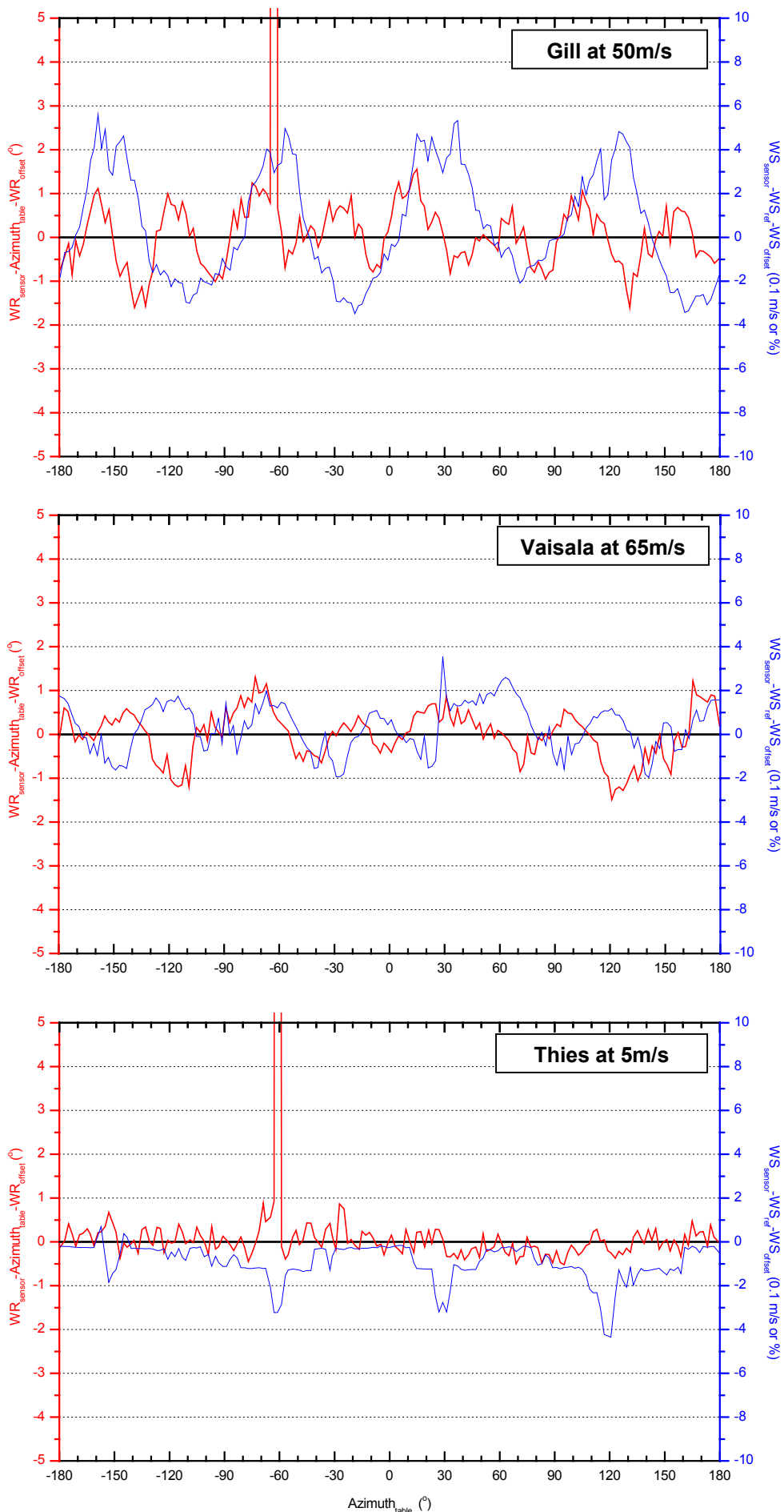
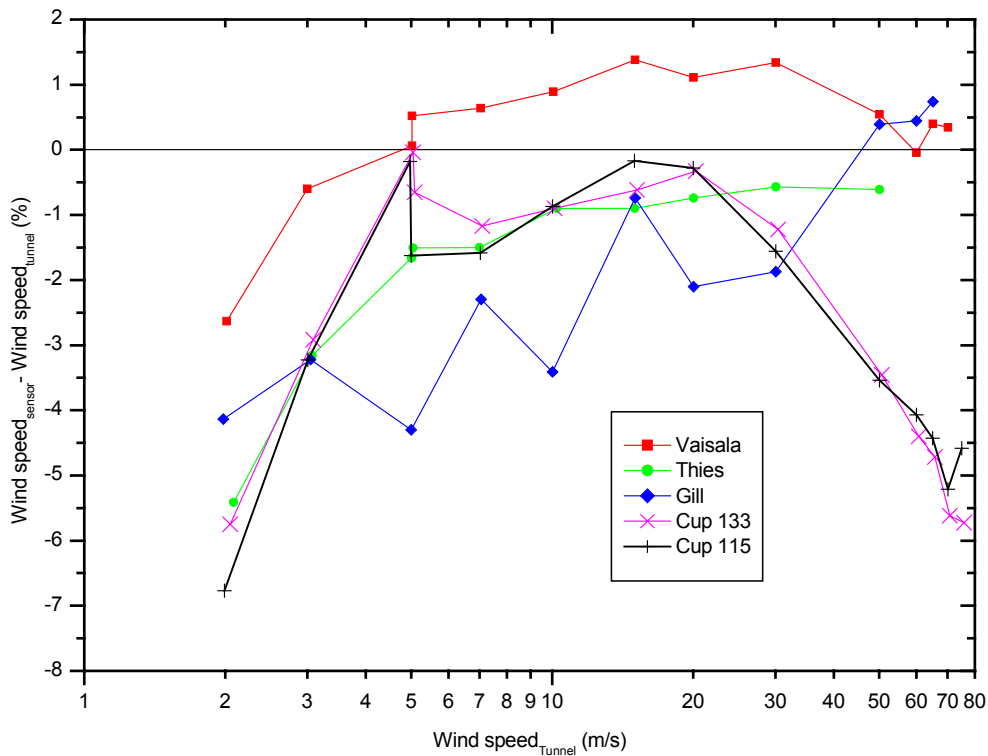


Figure 1: Differences between the LST tunnel wind speed and turntable direction and the values reported by the three sonics during azimuth scans with a fixed tunnel speed.



**Figure 2: Relative differences between the LST tunnel wind speed and the sensor speed averaged over all angles as a function of the tunnel wind speed.**

#### 4. FIELD TEST

The field test was conducted at the test site in De Bilt between June 15, 2002 and July 2003 after all three sensors were upgraded. The 3 sonics were mounted on a 10m mast using a head that separated the sonics 1m. The mast was located 20m to the south-southwest of the 10m mast containing the KNMI cup and vane. The 3 sonics Gill, Thies and Vaisala were oriented ENE to WSW. During the period of the field test 12-second data of the KNMI sensor set and 1sec values of the sonics were archived. The sonic data was later processed into running 3-second averages from which the 10-minute averaged values and extremes were derived. The analysis below is based on 10-minute data.

A histogram of the 10-minute averaged wind speed data clearly show that the cup anemometer reports more cases where the wind speed is below 0.5m/s and generally also reports more cases when the speed is above 5m/s. The first is related to the detection threshold of the cup anemometers whereas the latter is probably related to the so-called speeding. Speeding was clearly observed during a storm when the cup and sonics showed good agreement for the wind gusts up to 28m/s, whereas for the 10-minute averaged wind speed up to 12m/s the sonics generally reported lower values. A scatter plot of all 10-minute wind speed data of the cup anemometer versus a sonic have a correlation of 0.992, the slope of a linear fit is about 0.95 and the standard deviation is 0.19m/s for all three sonics. Although the overall agreement is quite good some cases with large differences that exceed WMO criteria do occur. Most striking are the cases where all 3 sonics reported wind speeds between 0.5 and 2m/s while the cup anemometer was probably frozen and reported 0m/s. Comparison between the 3 sonics shows much better agreement with a correlation of 0.999, slope of the linear fit of 0.98 and the standard deviation is 0.06. Similarly the 10-minute averaged wind direction of the vane and a sonic have a correlation coefficient of 0.94, the linear fit has a slope of 0.94 and the standard deviation is 11°. Again cases occur when the differences exceed the WMO criteria and some even reach 180°, but that is during low wind speeds. The agreement between the 3 sonics is again much better with a correlation of 0.97, a slope of 0.96 and a standard deviation of 4°.

Next only cases where the cup anemometer reports wind speeds above 0.5m/s are considered in order to overcome the large differences at low wind speeds. The observed differences in the 10-minute averaged wind speed are next studied as a function of wind direction reported by the vane in Figure 3. At all bins about 1000 cases or more are available. The figure shows larger differences near 0, 90, 180 and 270° that are probably caused by the disturbance of the transducers. Furthermore a large increase can be observed near 250° with elevated values between 210 and 360°, which is the roughly in the direction of a line of 20-25m trees at a distance of about 150m, but also coincides with the direction of the highest wind speeds. Figure 4 shows the same results, but indicates the fraction of cases were the wind speed agrees within the WMO limits. Overall in about 98% of the cases the sonics agree within the WMO limits with the cup anemometer, but at 250° this applies only for about 87% of the cases. When the sonics are compared to each other the



averaged absolute differences per wind direction bin are much less and nearly independent of wind direction. The wind speed of the sonics is in nearly 100% of the cases within the WMO limits. Figure 3 and Figure 4 show that the results of the Thies deviate slightly more from the cup anemometer than the other 2 sonics.

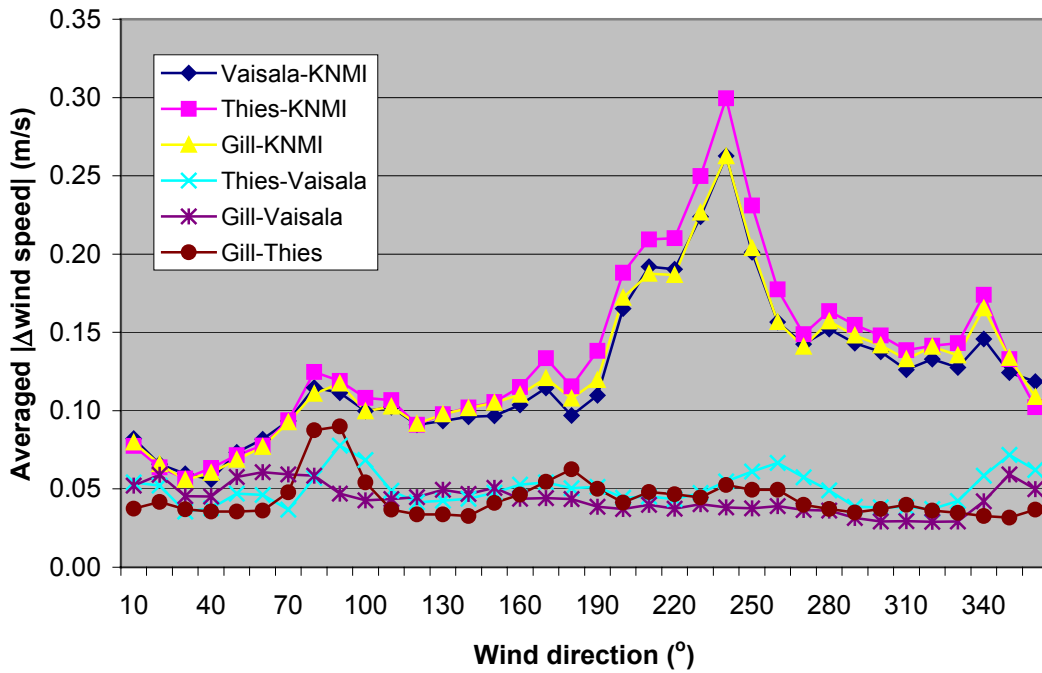


Figure 3: Averaged absolute differences in 10-minute wind speed as a function of the wind direction in bins of 10°.

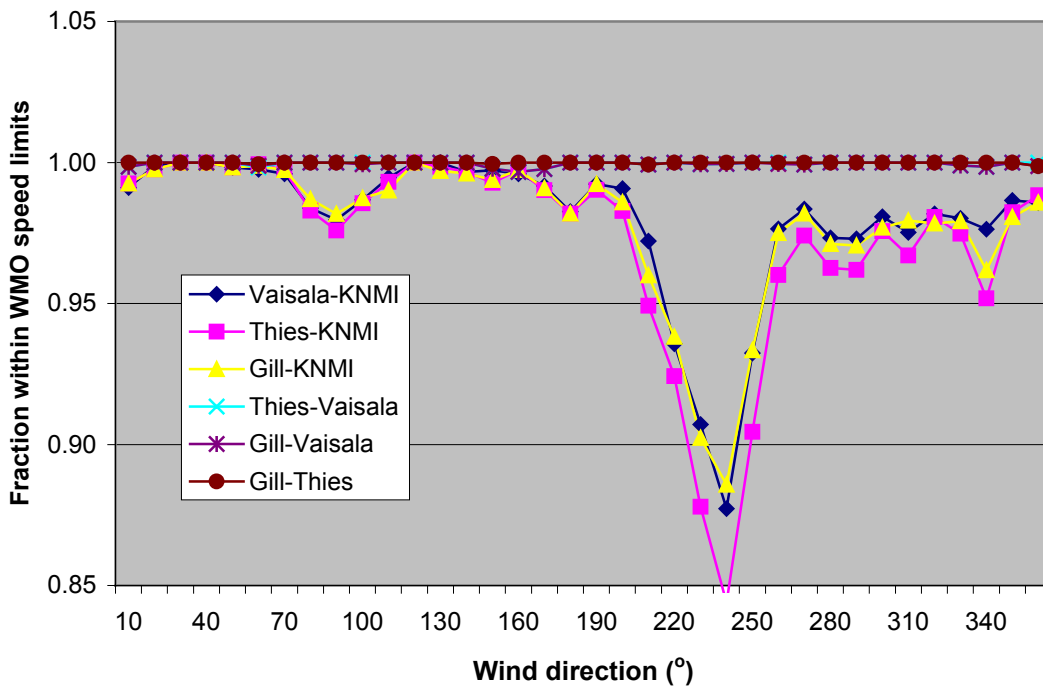


Figure 4: Fraction of the cases per wind direction bin of 10° where the wind speed agrees within the WMO limits of  $\pm 0.5\text{m/s}$  or  $\pm 10\%$ .

The differences in wind direction are shown as a function of wind speed in Figure 5. Below wind speeds of 5m/s the number of cases per wind speed bin is larger than 1000, but the number decreases rapidly with increasing wind speed and is less than 100 at 7m/s and is even less than 10 above 8.5m/s. At low wind speeds the fraction of cases where the wind direction is outside the WMO limits of the wind vane is rather large, but the agreement gets gradually better at higher wind speeds. The Gill compares better to the KNMI

wind vane than the other 2 sonics. The averaged absolute differences in wind direction shows hardly any dependency with wind speed, except a sharp increase at wind speed values below about 2m/s.

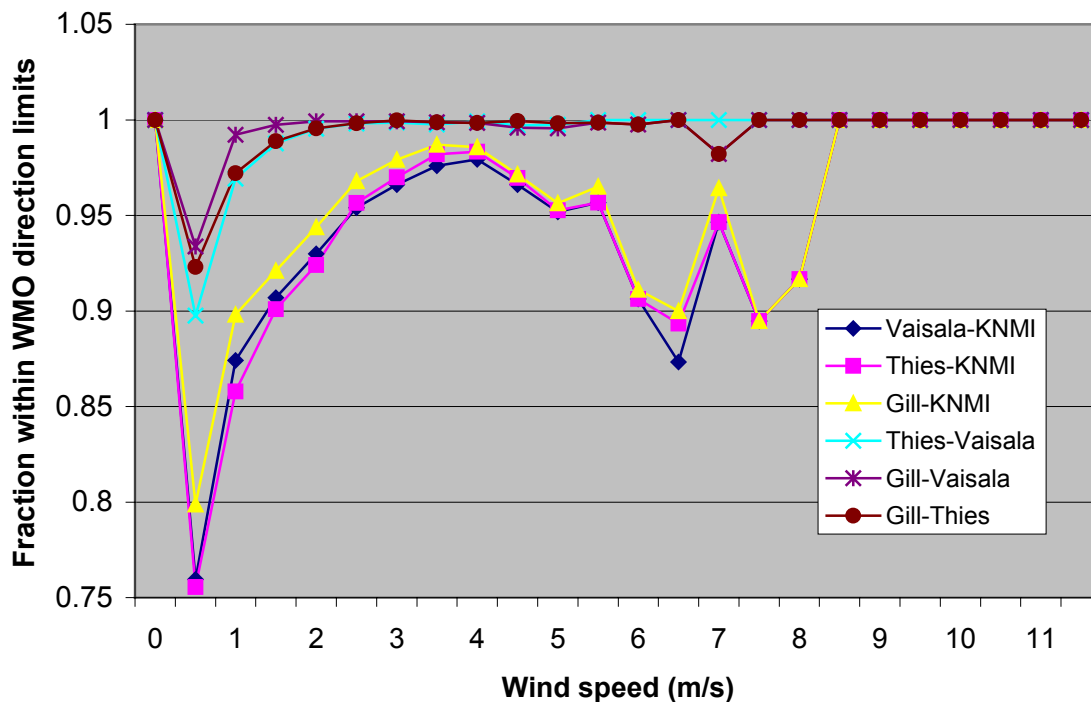


Figure 5: Fraction of the cases per wind speed bin of 0.5m/s where the wind direction agrees within the WMO limits of  $\pm 5^\circ$ .

Next the differences are studied as a function of the precipitation class. The precipitation intensity and type as measured by a FD12P present weather sensor is used for the purpose. The 10-minute averaged precipitation intensity and the ‘maximum’ precipitation type observed in the previous 10 minutes are used for that purpose. The precipitation classes considered are, respectively, no precipitation (NP), traces (TR with 10-minute averaged intensity below 0.05mm/h) and intensity classes rounded to mm/h in the range 0-10 where the last bin also contains all cases with higher intensity values. Next all cases with precipitation are summed (AP) and a distinction is made between the precipitation types liquid (LP), solid (SP) and unknown precipitation (UP). Finally the results are given independent of precipitation (All). In all classes the number of cases is above 100, except for the classes for intensity larger than 5mm/h. The averaged absolute differences of the wind direction show a dependency on precipitation class, although the statistics is poor, the averaged differences increase from about  $2^\circ$  for intensities below 3mm/h to about  $4^\circ$  at intensities of 10mm/h. The same behaviour can be observed in the fraction of cases the sonics agree within the WMO limits with the KNMI vane, which is generally above 90% and decreases below 80% at the highest intensities. The averaged differences between the three sonics and the KNMI wind vane for solid precipitation are less ( $1.5^\circ$ ) than for liquid precipitation ( $2.5^\circ$ ). The differences in wind direction between the sonics themselves show no clear dependency on precipitation class and are about  $1.5^\circ$ . The averaged absolute differences of the observed wind speed as a function of the precipitation class (cf. Figure 6) show a clear dependency on the precipitation intensity and increase from about 0.15 to 0.25m/s. The same behaviour again holds for the fraction of cases the sonics are within WMO limits from the cup anemometer which is about 95%, but decreases to about 85% at high intensity values. Again solid precipitation seems to have less effect on the differences that liquid precipitation. The results indicate that the Thies is slightly more affected by precipitation than the other 2 sonics when compared to the KNMI cup anemometer. When the sonics are compared to each other the wind speed of the Thies and Gill agree almost in 100% of the cases within the WMO limits, whereas the Vaisala shows a slightly reduced agreement of about 98% at mid and high intensity levels. It should be noted that the observed differences between the sonics and the conventional cup anemometer and wind vane during precipitation can also be the result of a deterioration of the performance of the conventional sensors since the precipitation will attach to these sensors and affects their dynamical properties.

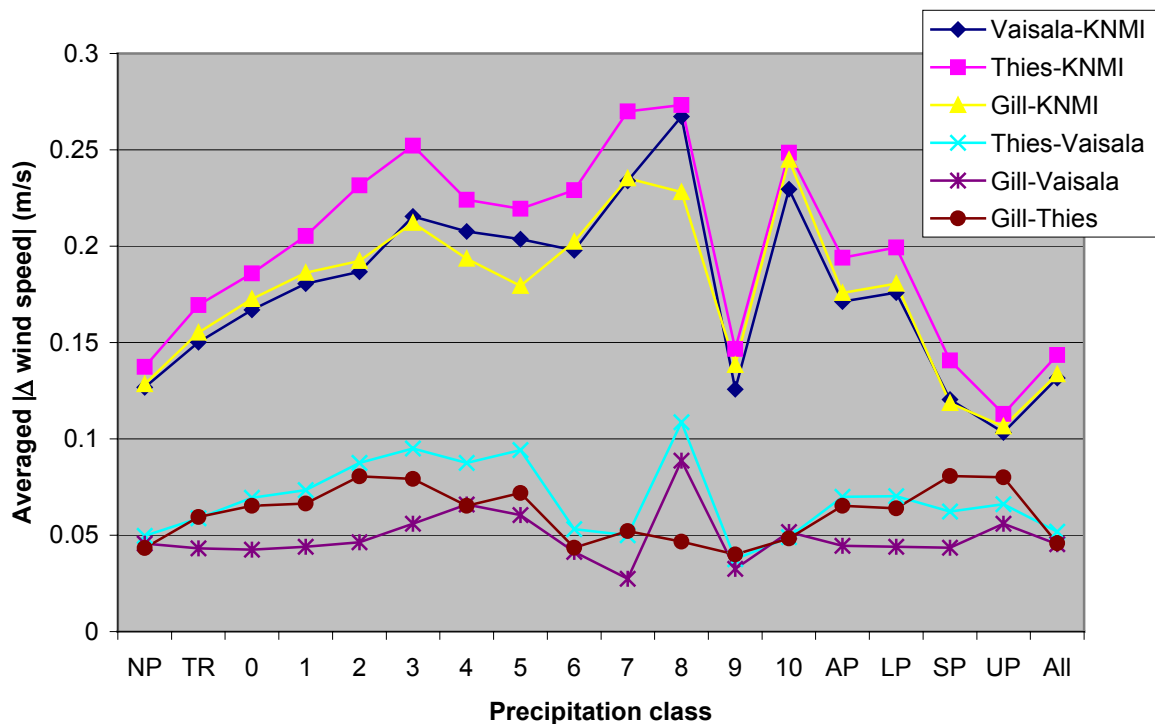


Figure 6: Averaged absolute differences in 10-minute wind speed as a function of the precipitation class.

## 5. CONCLUSIONS AND OUTLOOK

Three sonics, i.e the Thies 2D, the Gill Windobserver 2 and the Vaisala WAS425 have been compared to the KNMI cup anemometer and wind vane. Wind tunnel tests were performed for wind speeds up to 75m/s. Overall the agreement of all three sonics and the KNMI cup anemometers is within the WMO limits when compared to the tunnel reference. The Vaisala compares well with the reference over the full angular and wind speed range, although the signal is a bit noisy at low wind speeds (<5m/s). The Gill measurements are very consistent, but the differences generated by disturbances by the transducer arms, which are not corrected for in the software, exceed the WMO limits at some orientations for high wind speeds (>60m/s). Furthermore, the wind speed reported by the Gill is generally smaller than the tunnel reference, although within WMO limits. The Thies compensates for the disturbances caused by the transducer arms and is close to the reference, but it failed to give good measurements above 50m/s as a result of damage obtained during the field test. The field test showed that all 3 sonics worked properly although the Thies showed some signs of wear and the Vaisala occasionally missed a measurement. Overall the sonics agree very well with each other. The differences between the sonics and the conventional cup and vane are larger. The differences for the 10-minute averaged wind speed show a strong directional dependence that is probably related to surface roughness. The differences show a dependency on precipitation intensity. The sonics seem suitable for operational use, but the introduction of the sonics requires the construction of transfer functions for climatological purposes. A more detailed analysis of the data is required before KNMI can make a definite choice for a specific sonic anemometer. After this selection KNMI will perform further tests with some sonic anemometers in 2005 at selected locations such as airports, coastal stations, platforms and possibly at the 200m research tower, in order to get more operational experience with these sensors.

## 6. REFERENCES

- Gill Instruments: WindObserver II Ultrasonic Anemometer, User Manual, 1390-PS-0001, Issue 1, Hampshire, England, 2000
- Thies Klima: Ultrasonic Anemometer 2D, Operating Instructions 4.3800.00.xxx, Adolf Thies GmbH, Göttingen, Germany, 2001.
- Vaisala: Ultrasonic Wind Sensors WAS425, User's Guide, U428en-1.1, Helsinki, Finland, 2000.
- Wauben, W. M. F: Wind Tunnel and Field Test of Three 2-D Sonic Anemometers, To appear as a Technical Report, KNMI, De Bilt, 2005.
- WMO: The Measurement of Gustiness at Routine Wind Stations: A Review, Instruments and Observing Methods Reports No. 47, WMO, Geneva, 1987.
- WMO: Guide to Meteorological Instruments and Methods of Observation, Sixth edition, WMO-No. 8, WMO, Geneva, 1996.

# TESTING OF WINDSENSORS AND THE USEFULNESS OF VIDEO TECHNOLOGY AT MARINE STATIONS

Author: Merete H. Larre et al

The Norwegian Meteorological Institute, Niels Henrik Abels vei 40, Box 43 Blindern, 0313  
Oslo, Norway.

Tel. +4722963000, Fax. +4722963050, e-mail: merete.larre@met.no

## Abstract:

At many lighthouses along the coast of Norway observations have been carried out by lighthouse keepers. Since most of the lighthouses now are unmanned, the Norwegian Meteorological Institute (met.no) has to find other solutions for observations along the coast.

Different types of windsensors are installed for comparison at a testfield at Stavernsodden lighthouse (south east coast of Norway). The data collection from the different windsensors started October 2002. Both cupanemometers and ultrasonic sensors are compared.

The test field also includes use of video technology for registration of visibility. Some visibility points are used to decide the visibility. The camera is preprogrammed to move to the visibility points.

## Objectives

- To get experience regarding reliability of different windsensors.
- Enable selection of windsensor types that minimize maintenance, work and expenses.
- Evaluate the usefulness if video technology substituting observers.

The poster presents preliminary results.

## Windsensors

Since the measurements are used for intercomparison of sensors and not as observation data, all wind sensors are installed at a 6 m high mast instead of normally 10 m above ground.

- 1 Vaisala WA15 (cupanemometer and wind vane)
- 1 Gill Windobserver (ultrasonic)
- 1 Vaisala WS 425 (ultrasonic)

As reference we use the Vaisala WA15 sensor since that is the mostly used sensor at the Norwegian AWS. For the Vaisala WS 425 sensor there is only 1 min. average data (1 min. data) available for the analysing period in this poster, but for the VaisalaWA15 and Gill sensors also 10 min. average data (10 min. data) are available. These 1 min. data are not so good as the 10 min data for analysis, because "noise" effect the results. The data are from August to December 2003.

## Difference in wind speed

### Gill Windobserver

Figure 1 shows the 24 hour average of the windspeed (based on 1 min. data) for the Vaisala WA15 sensor and the Gill sensor. Mostly it is few differences between the two sensors. A couple of times it seems like Gill isn't reaching the same peaks as Vaisala WA15. This happens probably because Gill is in the shade of the other sensors at a few wind directions and is placed a bit lower than Vaisala WA15.

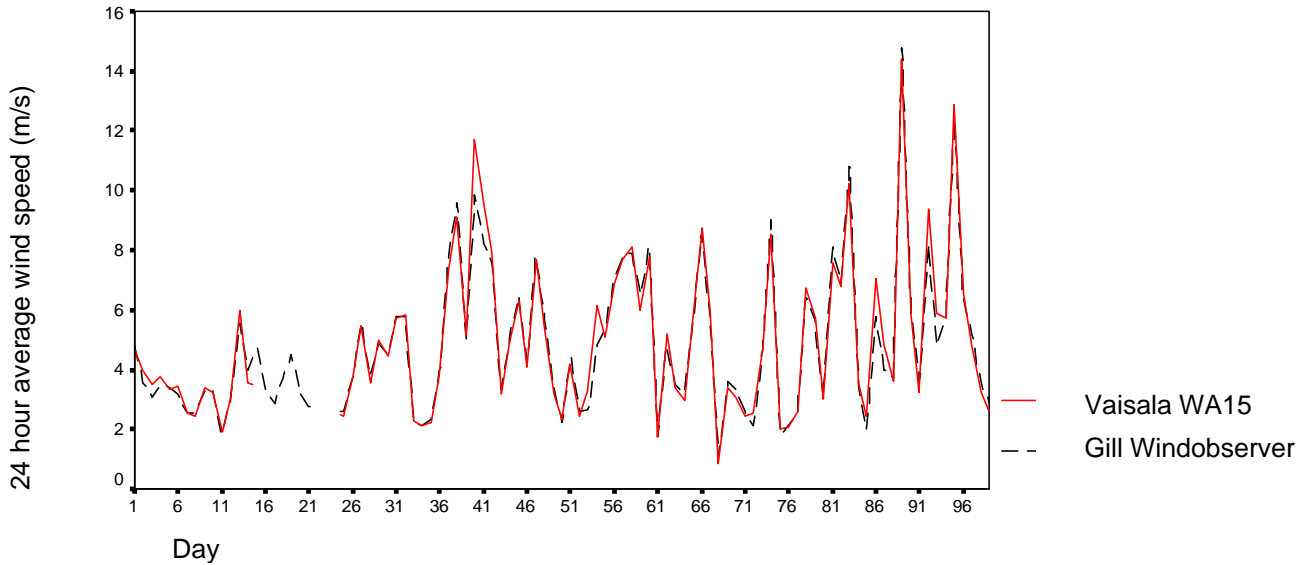


**Figure 1:** The 24 hour average of the wind speed for the Vaisala WA15 sensor and the Gill sensor based on 1 min. data (August – December 2003).

Table 1 shows the difference between Vaisala WA15 and Gill every month based on 10 min. data. The standard deviation is acceptable and the average values are close to zero. The total average is negativ (-0,06). This result suits well with the placement of the Gill sensor in the mast.

**Table 1.** Difference in wind speed between Gill and Vaisala WA15 (10 min.data)

Month	Number of measurements	Average	Minimum	Maximum	Standard deviation
August	25573	-0,10	-2,34	0,60	0,41
September	14422	-0,21	-3,56	0,97	0,89
October	20360	0,02	-2,59	0,80	0,52
November	14276	0,02	-2,85	1,37	0,59
December	40639	-0,07	-3,78	1,48	0,68
<b>Total</b>	<b>115270</b>	<b>-0,06</b>	<b>-3,78</b>	<b>1,48</b>	<b>0,63</b>

Since we only have 1 min. data available from the Vaisala WS 425 sensor, it is interesting to compare it with the 1 min. data from the Vaisala WA15 sensor and the Gill sensor too. Table 2 shows what the total values of the difference between Gill and Vaisala WA15 is, based on 1 min. data. Notice that the average is the same, but that the standard deviation is bigger as expected because of more “noise”.

**Table 2.** Difference in windspeed between Gill and Vaisala WA15 (1 min data)

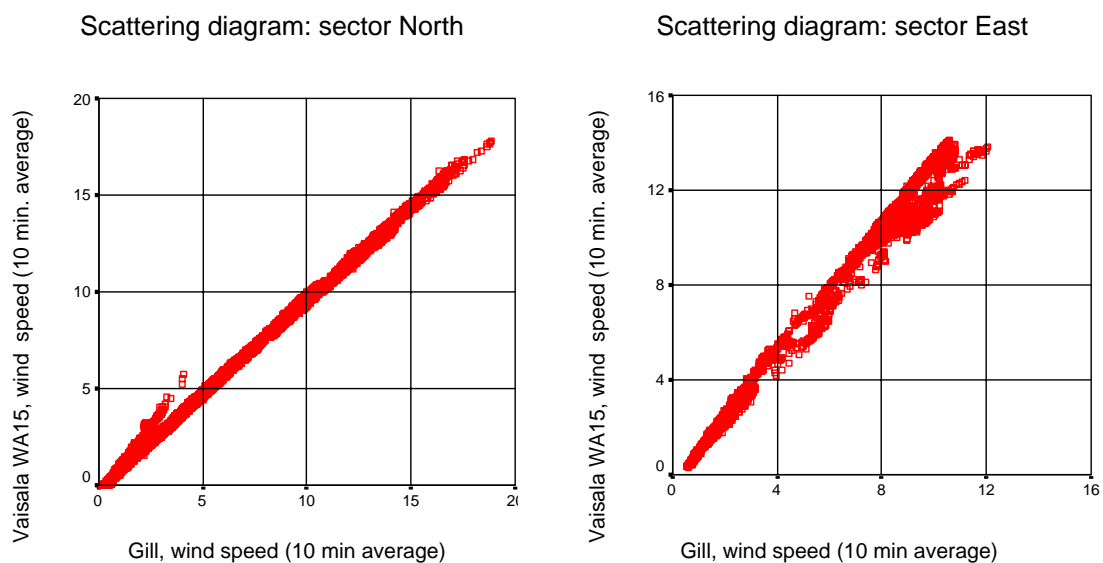
Month	Number of measurements	Average	Minimum	Maximum	Standard deviation
August-December (total)	<b>116742</b>	<b>-0,06</b>	<b>-11,16</b>	<b>11,50</b>	<b>0,99</b>

Table 3 shows the difference in windspeed between Gill and Vaisala WA15 at different wind directions (divided into 16 sectors at 22,5 degrees each) based on 10 min. data. Notice that the standard deviations are at a satisfying level, but that they are not so good for wind from east (E) and south west (SW-WSW). This is caused by how the Gill sensor is placed at the E-W pointing crossarm. The Gill sensor is placed in the shade of the other sensors and the buildings near by. Also notice that wind from north (NNW, N, NNE) gives lower standard deviation, because of less disturbances from that direction.

**Table 3.** Difference in wind speed between the Gill and Vaisala WA15 sensors for different sectors based on 10.min data in the period August-December 2003.

Sector	Number of measurements	Average	Minimum	Maximum	Standard deviation
N	19773	0,30	-1,67	1,14	0,15
NNE	18531	0,15	-2,19	0,62	0,15
NE	8701	-0,11	-2,31	0,77	0,33
ENE	8768	-0,51	-3,02	0,32	0,47
E	4020	-1,33	-3,56	0,34	1,10
ESE	2189	-0,23	-2,26	0,35	0,33
SE	1738	0,07	-2,30	0,57	0,28
SSE	3195	0,48	-1,60	1,37	0,36
S	3066	0,58	-2,90	1,48	0,43
SSW	7491	0,33	-2,98	1,30	0,38
SW	13036	-0,75	-3,78	1,04	0,59
WSW	3458	-1,02	-3,78	0,51	0,82
W	3618	-0,20	-2,50	0,51	0,31
WNW	7396	-0,13	-1,69	0,59	0,32
NW	5440	0,34	-1,49	0,99	0,22
NNW	6312	0,34	-1,18	0,95	0,18
<b>TOTALT</b>	<b>115270</b>	<b>-0,06</b>	<b>-3,78</b>	<b>1,48</b>	<b>0,63</b>

We have looked a bit closer at the "best" direction (N) and the "worst" direction (E). The scattering diagram in figure 2 shows that both the displacement and the scattering is small for wind from north (except for a few measurements for wind under 5 m/s). For wind from east there is much more scattering and a marked displacement.



**Figure 2:** Scattering diagram for the Gill sensor and the Vaisala WA15 sensor based on 10 min data from sector North (N) and East (E) for the period August - December 2003.

Figure 3 shows scattering diagram for the same directions, but based on 1 min. data. Here we really see the "noise". We also see a larger displacement for wind from east compared with wind from north.

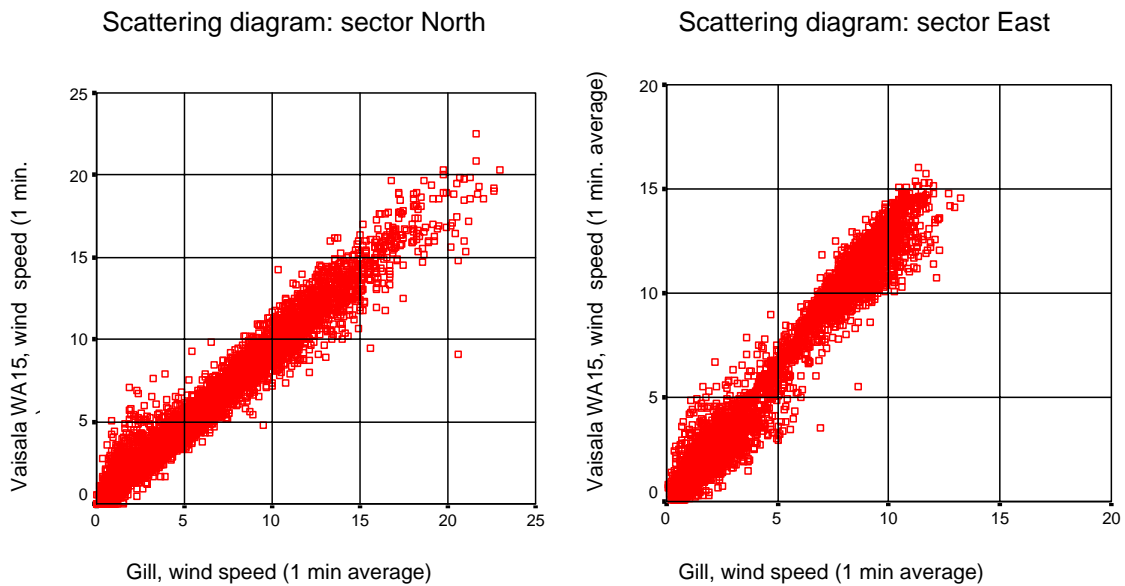


**Figure 3:** Scattering diagram for the Gill sensor and the Vaisala WA15 sensor based on 1 min data from sector North (N) and East (E) for the period August - December 2003.

### Vaisala WS 425

Figure 4 shows the 24 hour average of the wind speed for Vaisala WA15 and Vaisala WS425 based on 1 min. data for the period August – December 2003. There are periods where data is missing from Vaisala WS425. In periods with comparable data (see the figure) the difference between the two sensors is small.

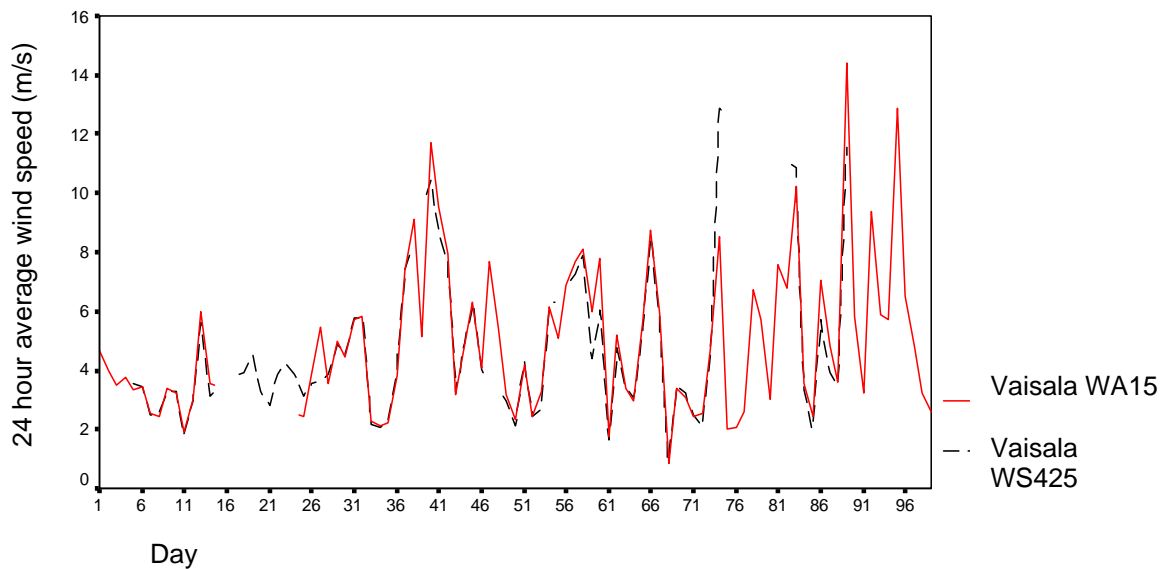


**Figure 4:** The 24 hour average of the wind speed for the Vaisala WA15 sensor and the Vaisala WS425 sensor based on 1 min. data (August – December 2003).

In table 4 is the difference in wind speed between Vaisala WS425 and Vaisala WA15 is shown for each month based on 1 min data. Notice that it is much less measurements from Vaisala WS425 than from Vaisala WA15. The total values (average: -0,17 and st. deviation: 1,17) are not so good as for the 1 min values for Gill – Vaisala WA15 (average: -0,06 and st. deviation: 0,99), but the difference is not very big.

**Table 4.** Difference in wind speed between Vaisala WS425 and Vaisala WA15 (1 min. data).

Month	Number of measurements	Average	Minimum	Maximum	Standard deviation
August	17711	-0,09	-8,80	7,04	1,00
September	10985	-0,21	-8,63	4,71	1,09
October	12646	-0,15	-10,33	7,57	1,20
November	13587	-0,11	-7,33	5,10	1,01
December	12784	-0,35	-10,50	9,34	1,52
<b>Total</b>	<b>67713</b>	<b>-0,17</b>	<b>-10,50</b>	<b>9,34</b>	<b>1,17</b>

Table 5 shows the difference in wind speed between Vaisala WS425 and Vaisala WA15 at different wind directions based on 1 min data. The standard deviations varies a bit. The lowest value is for wind from north (N) and the highest value is for wind from south-west (SW-WSW). The highest value for wind from south-west is caused by the placement of the Gill sensor in the mast.

**Table 5.** Difference in wind speed between Vaisala WS425 and Vaisala WA15 for different wind sectors based on 1 min data in the period August – December 2003.

Sector	Number of measurements	Average	Minimum	Maximum	Standard deviation
<b>N</b>	10500	0,14	-6,39	9,34	0,74
<b>NNE</b>	10805	0,06	-5,89	7,04	0,94
<b>NE</b>	5794	-0,15	-4,83	4,37	0,93
<b>ENE</b>	3599	-0,42	-7,33	6,24	0,97
<b>E</b>	3384	-1,00	-8,60	3,97	1,27
<b>ESE</b>	2358	-0,29	-6,46	5,57	0,98
<b>SE</b>	1786	-0,01	-8,63	5,70	0,85
<b>SSE</b>	2175	0,18	-4,60	5,87	0,80
<b>S</b>	1679	0,05	-4,73	6,14	1,06
<b>SSW</b>	4556	0,06	-7,90	5,00	1,11
<b>SW</b>	5962	-0,74	-10,50	7,44	1,78
<b>WSW</b>	2898	-0,99	-10,33	5,57	1,87
<b>W</b>	2020	-0,36	-5,43	5,47	1,19
<b>WNW</b>	2836	-0,32	-8,43	8,41	1,19
<b>NW</b>	3385	-0,01	-6,60	5,07	0,92
<b>NNW</b>	3976	0,11	-6,20	7,70	0,98
<b>TOTAL</b>	<b>67713</b>	<b>-0,17</b>	<b>-10,50</b>	<b>9,34</b>	<b>1,17</b>



The scattering diagrams for the differences in sector north (N) and south-west (SW) are shown in figure 5. The “noise” can be seen very well in both sectors. The scattering and the displacement are very characteristic for sector SW.

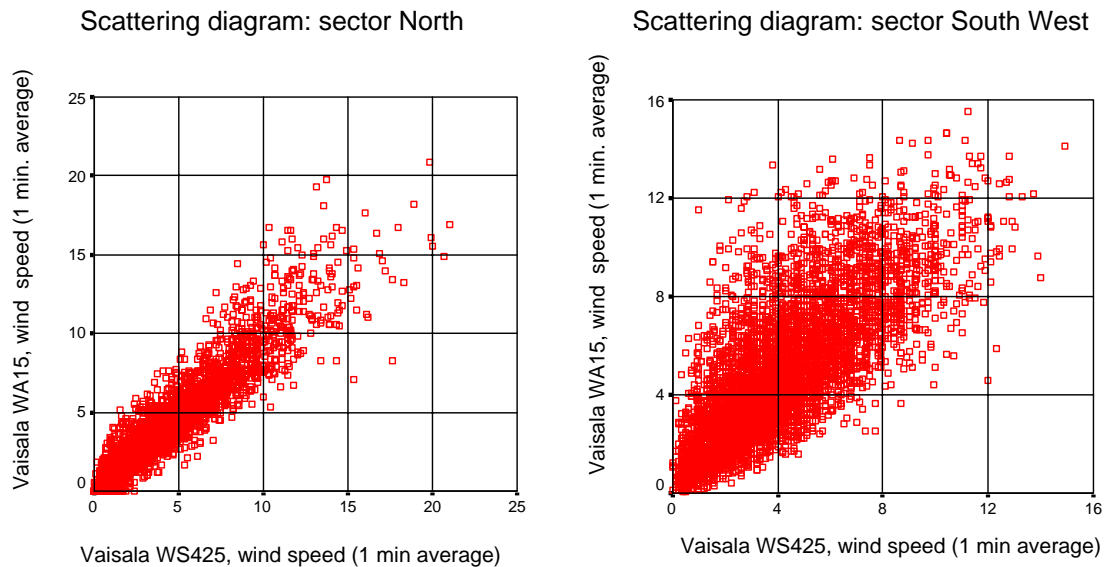


**Figure 5:** Scattering diagram For the Vaisala WS425 sensor and the Vaisala WA15 sensor base don 1 min data in sector north (N) and sector south west (SW) (august – December).

### Difference in wind direction

All the sensors measure wind direction. We use Vaisala WA15 as reference to investigate the difference in wind direction.

### Gill Windobserver

Table 6 shows the difference in wind direction between Gill and Vaisala WA15. The wind directions have been divided into 16 sectors. By looking at the average values (table 8) and the raw data (not show here) there is often a positive difference (about 10 degrees) between the two sensors. This might be because the sensors are installed 10 degrees “wrong” compared to each other. It is important to be aware of this difference in analysing the data. Notice the low standard deviation and the average values in the sector SSW/SW. This might confirm our theory that wind from a bigger area (190-270 degrees) is “pressed together” because of the buildings nearby.

**Table 6.** Difference in wind direction between Gill and Vaisala WA15 for different wind sectors based on 10 min. data in the period August – December 2003.

<b>Sector</b>	<b>Number of measurements</b>	<b>Average</b>	<b>Standard deviation</b>
<b>N</b>	19773	9,52	11,14
<b>NNE</b>	18531	11,03	6,97
<b>NE</b>	8701	11,55	8,44
<b>ENE</b>	8768	10,63	7,16
<b>E</b>	4020	12,64	6,88
<b>ESE</b>	2189	13,82	5,42
<b>SE</b>	1738	13,51	5,47
<b>SSE</b>	3195	13,40	3,97
<b>S</b>	3066	11,59	4,83
<b>SSW</b>	7491	8,68	3,55
<b>SW</b>	13036	5,57	5,24
<b>WSW</b>	3458	6,74	12,34
<b>W</b>	3618	8,58	13,25
<b>WNW</b>	7396	10,03	11,33
<b>NW</b>	5440	10,80	14,66
<b>NNW</b>	6312	8,78	15,61
<b>TOTAL</b>	<b>116732</b>	<b>9,85</b>	<b>9,54</b>

#### **Vaisala WS 425**

By looking at only 1 min. data for the difference in wind direction between Vaisala WS425 and Vaisala WA15 the effect of the "noise" can be seen very well (table 7). The average values vary a lot while the standard deviations are big. Therefore we don't get much useful information by only have 1 min. data available.

**Table 7.** Difference in wind direction between Vaisala WS425 and Vaisala WA15 for different wind sectors based on 10 min. data in the period August – December 2003.

<b>Sector</b>	<b>Number of measurements</b>	<b>Average</b>	<b>Standard deviation</b>
<b>N</b>	10500	15,41	30,98
<b>NNE</b>	10805	11,86	22,78
<b>NE</b>	5794	17,53	31,91
<b>ENE</b>	3599	25,40	39,05
<b>E</b>	3384	24,54	38,65
<b>ESE</b>	2358	28,24	40,94
<b>SE</b>	1786	31,39	43,43
<b>SSE</b>	2175	23,55	37,43
<b>S</b>	1679	32,58	45,00
<b>SSW</b>	4556	19,84	34,36
<b>SW</b>	5962	23,46	32,35
<b>WSW</b>	2898	36,20	42,26
<b>W</b>	2020	45,09	45,25
<b>WNW</b>	2836	34,58	41,32
<b>NW</b>	3385	24,85	38,59
<b>NNW</b>	3976	18,53	34,85
<b>TOTAL</b>	<b>67713</b>	<b>21,81</b>	<b>35,62</b>

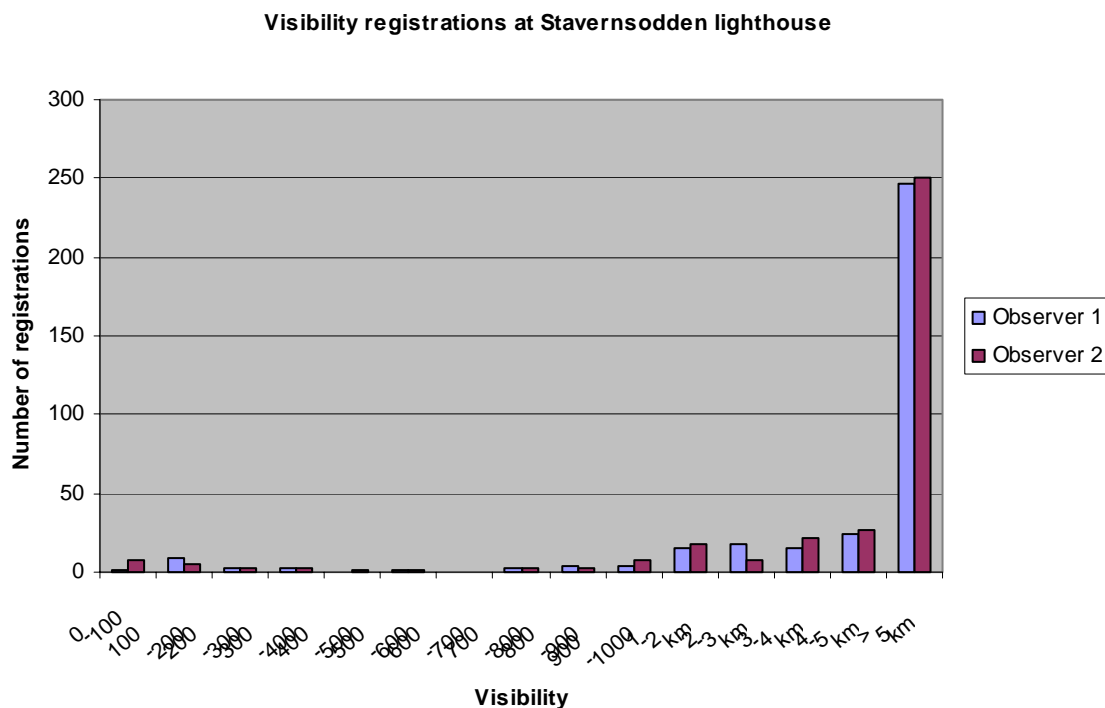
### Use of video camera

The test field also includes use of video for registration of visibility. At the top of the lighthouse a camera is installed. One can steer the camera from the Norwegian Meteorological Institute. The visibility points used to decide the visibility are at 100 m, 800 m, 1 km and 5 km. The camera was preprogrammed to move to the visibility points.

In March 2003 the registration of visibility at Stavensodden lighthouse started and went on to May 2004. Two persons have individually used the camera to decide the visibility at the same time. The visibility registrations have been done 2-4 times every day. Over 350 individual registrations of visibility have been taken during the test period. The registrations have been compared to see if there were any differences.

Comparison of the visibility registrations shows that the differences were negligible between the two observers (figure 7). The biggest/largest differences occur when there is fog and when the visibility is between 1 and 5 km. In this interval there were few visibility points.

**Figure 7.** Visibility registrations made by two observers (March 2003 – May 2004).



There have been some maintenance problems with the camera. The camera has a steering mechanism so the observers can steer the camera 360 degrees, move it up and down and zoom out and in. The problem has been that the camera's steering system has been locked so the camera couldn't be moved to the visibility points. Problems with this steering has been the most difficult to maintain since personnel from met.no are very seldom at Stavensodden lighthouse.

The camera lens must be cleaned often because in marine environment it easily come salt and dirt on it. This makes bad pictures and can make the visibility registrations difficult. Other minor problems have been rain, snow and dew on the lens, but this has never been such a huge problem that visibility registrations couldn't be done.



Norwegian  
Meteorological Institute  
*met.no*

**POSTER PRESENTATION:  
Comparison of manual precipitation  
observations with automatic observations in  
Oslo and Utsira**



- **Utsira:** An island at the western coast of Norway. Annual precipitation: 1165 mm
- **Oslo (Blindern):** In the northern end of Oslofjorden (Oslo Fiord). Annual precipitation: 763 mm

## Oslo (59° 56' N, 10° 44' E):



**Figure 1:** Picture showing the manual (to the left) and the automatic (to the right) precipitation gauges.

- The data comparison is based on data from September 2003 to July 2004.
- The automatic precipitation gauge is a Geonor T-200

**Table 1:** Monthly precipitation data from Geonor and the manual gauge

Month	No of days	Geonor	Manual	± %
September 2003	13	50.5	54.0	-6.5 %
October 2003	31	25.8	29.6	-12.8 %
November 2003	30	61.0	64.8	-5.9 %
December 2003	31	48.4	53.7	-9.9 %
January 2004	31	102.0	108.9	-6.3 %
February 2004	22	19.9	19.8	-0.5 %
March 2004	31	32.2	36.1	-10.8%
April 2004	30	51.7	54.3	-4.8%
May 2004	31	34.5	39.6	-12.8%
June 2004	30	67.0	74.7	-10.3%
July 2004	31	46.8	51.9	-9.8%
<b>Total</b>	<b>311</b>	<b>539.8</b>	<b>587.4</b>	<b>-8.1 %</b>

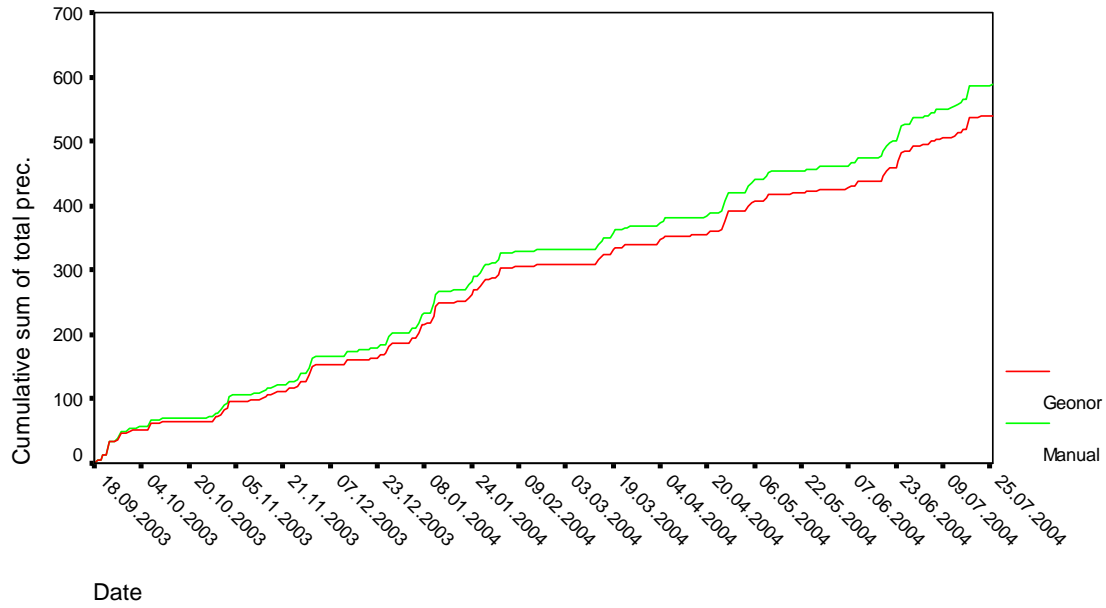


**Figure 2:** Cumulative sum of total precipitation

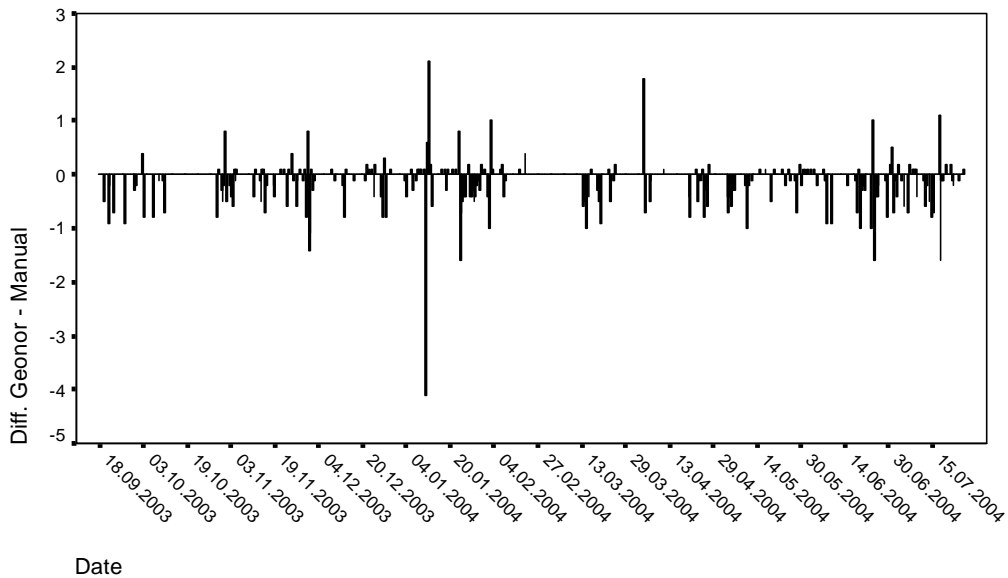


**Figure 3:** The difference (cases) between Geonor and manual gauge from Oslo.

**Table 2:** Number of cases in different precipitation intervals.

Prec. in 12-h period	Number of cases
Precipitation 0.5-1 mm	25
Precipitation 1-2 mm	33
Precipitation 2-5 mm	55
Precipitation 5-8 mm	27
Precipitation 8-10 mm	7
Precipitation > 10 mm	7

There are different reasons for the observed peaks (differences) for each case in figure 3:

- **Time of observation:** If the manual gauge is emptied and checked too early or too late from the correct observation time during a precipitation period, this could influence the differences (peaks).
- **Heavy precipitation period:** In situations with a lot of precipitation registered, the difference may seem considerable, but the percentage difference could be small.
- **Noise:** Electromagnetic disturbances, problems with the logger etc may cause lack of data or strange values from Geonor.
- **Other physical reason (exposure):** This is often the most important and most difficult factor to study.

## Exposure, physical and technical factors

Since there is an observed considerable difference of about 8 % between Geonor and the manual gauge (remembering that the two gauges are placed near each other) we would like to focus at some physical and technical factors:

- *Area of the buckets and level control*

The area at the top of the manual gauge and at the top of Geonor were measured and controlled, and we found no differences. We also checked that both Geonor and manual were in level.

- *Control of the manual measuring equipment*

All equipment being used in the observation and emptying of the manual gauge were controlled. No irregularities were discovered.

- *Volume expansion of water because of an increase in temperature*

Geonor is measuring precipitation based on weight measurements. The manual gauge is on the other hand based on volume measurements. Since water is expanding with an increase in temperature (from 4°C), we would like to find out what effect this could have on our results. Figure 4 presents a change in volume as a function of a change in temperature ( $T - T_0$ ). An increase in the water temperature from 4 to 17 °C, increases the water volume of about 0.13 % (1.3 ‰). This physical effect is obviously not significant for the accuracy to our measurements.

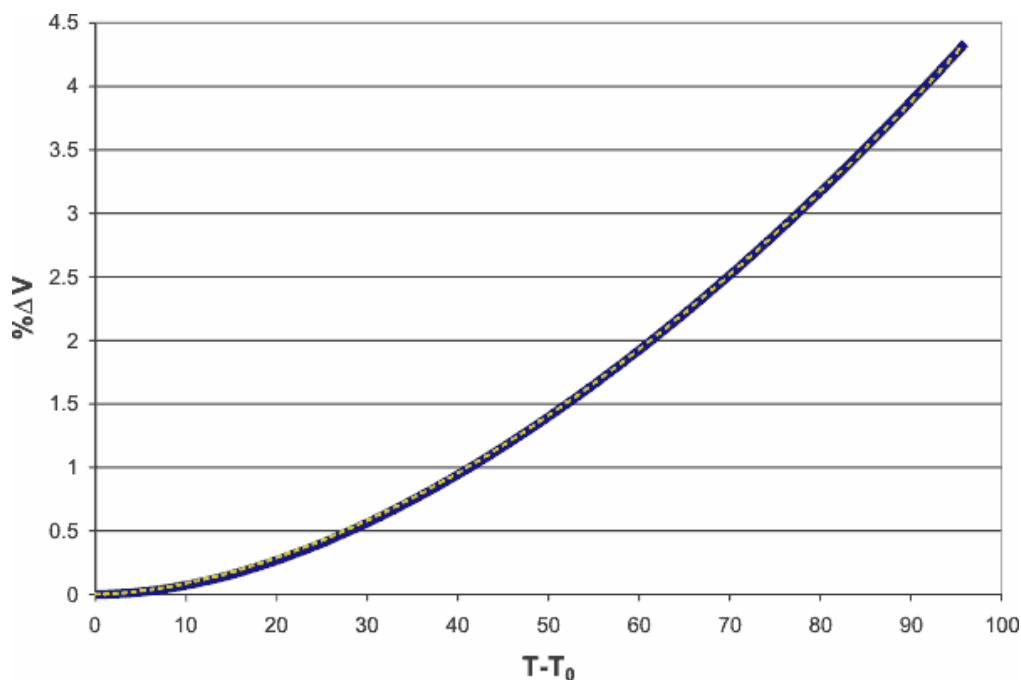


**Figure 4:** Changes in volume as a function of change in temperature.

- **Evaporation**

By studying the data from the “bucket hour-values” from Geonor we see that there is a continuously evaporation from the bucket, despite the layer of oil at the liquid surface. To have a closer look at this evaporation effect we have more closely studied data from March, April and May 2004. The method used in getting an estimate for the contribution from the evaporation is not shown here, but the estimated values are presented in table 3.

**Table 3:** Estimated evaporation from Geonor

Month	Evaporation pr. 12t	Total contribution from evap. in the prec. periods	Monthly measured prec. for Geonor	The new “corrected” monthly prec. values.
<b>Mach</b>	0.060 mm	0.7 mm	32.2 mm	32.9 mm
<b>April</b>	0.065 mm	1.3 mm	51.7 mm	53.0 mm
<b>May</b>	0.102 mm	1.8 mm	34.5 mm	36.3 mm
<b>Total</b>	-	-	<b>118.4 mm</b>	<b>122.2 mm</b>

Looking only at these 3 months and considering no evaporation from the manual bucket, we find that the total difference between Geonor and the manual gauge is -5.6% instead of -8.7%.

But, of course evaporation also is going on from the manual gauge. In most time of the year the manual gauge is equipped with a funnel, and a report (DNMI- ”Klima-desember 1979, no 2”) tells that the evaporation from a similar manual gauge on a regular summer day is under 0.1 mm pr 24h-period (under 0.05 mm pr. 12h-period). We also know that evaporation from Geonor is going on all the time, while the evaporation from the manual gauge only is happening when there is water in the bucket (for instance only the last 2 hours in the 12h-period).



Some of the negative difference between the two gauges may therefore be explained by a more considerable evaporation from Geonor than from the manual gauge (in rain situations).

- ***Test of Geonor string response (calibration values)***

We made a test at Geonor (filling controlled amount of water in bucket) and checked the response from the string frequency on a dry summer day (table 4). The bucket was in level during the test.

**Table 4:** The results from the test measurements of Geonor (Blindern, Oslo).

Amount added: ml/mm	Second value (string frequency)	Minute value (stab. meas. bucket value)	Expected value	Correction
	13311	51,80		
1000 ml /50 mm	15394	100,86	101,80	0,94
1000 ml /50 mm	17210	150,09	150,86	0,77
1000 ml /50 mm	18841	199,39	200,09	0,70
1000 ml /50 mm	20330	248,74	149,39	0,65
1000 ml /50 mm	21707	297,80	298,74	0,94
1000 ml /50 mm	22999	347,19	347,80	0,61
1000 ml /50 mm	24221	396,52	397,19	0,67
1000 ml /50 mm	25375	445,71	446,52	0,81
1000 ml /50 mm	26477	494,91	495,71	0,80
1000 ml /50 mm	27534	544,17	544,91	0,74
1000 ml /50 mm	28548	593,35	594,17	0,82
<b>Mean value (correction)</b>				<b>0,77</b>

The results indicate a correction of 0.61-0.94 mm (mean value: 0,77) pr. 50 mm added water, which means 1.5 % less registered precipitation amount than added into the bucket. These results is a bit surprising, knowing that the correct calibration values to the string is used in the logger.

- ***Wind conditions***

Oslo (Blindern) is not a very windy place. We have studied many of the difference-cases (peaks in figure 3) one by one and looked at other meteorological parameters, for instance wind, but this parameter does not seem to be significant for the observed differences in our cases. We also see that the two gauges are placed close to each other, which means that the exposure should be quite identical.

At SMHI in Sweden they are doing an extended theoretical wind study of Geonor by testing different wind shields. The idea is that the shape of the Geonor-container is creating an upward going wind field, slightly reducing the possible “caught” precipitation, especially slight rain or snow. The results from these tests are not ready.

## Utsira (59° 18' N, 4° 52' E)



**Figure 5:** Geonor T-200 is placed to the right in the picture, at the bog behind the house. The picture is taken before Geonor was mounted. The manual gauge is placed at the lawn between the houses.

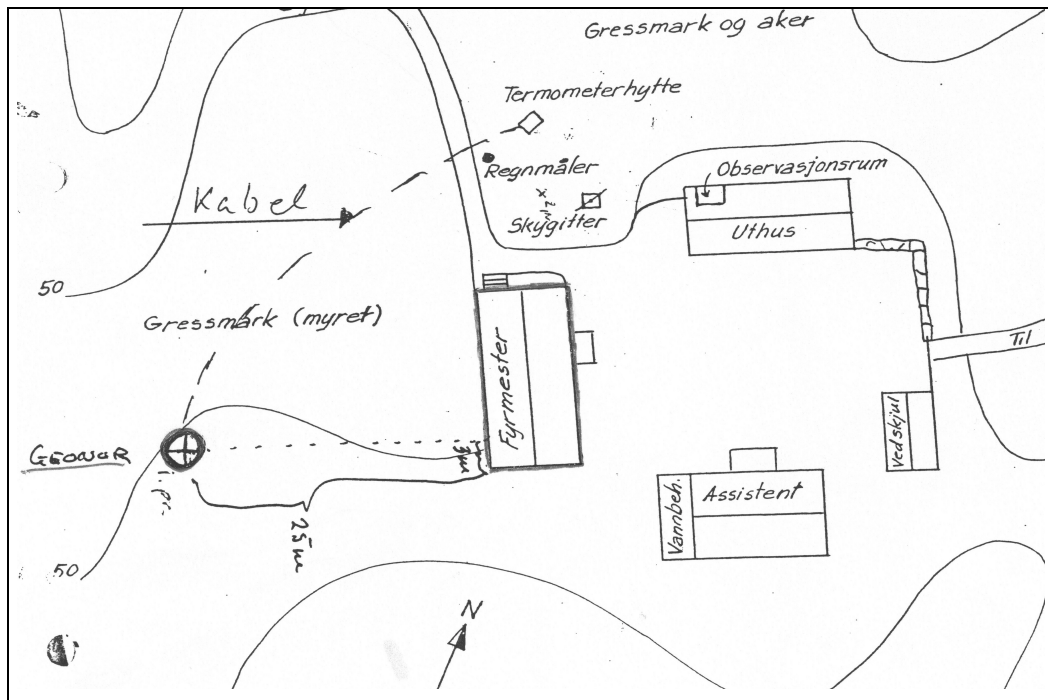


**Figure 6:** The lighthouse station. Geonor is placed to the left. The manual precipitation gauge is placed north of the “Fyrmester” house.

In figure 7 the difference between Geonor and manual gauge for the different cases is presented (period June 2003 to June 2004). Geonor is collecting 1052.6 mm precipitation during the studied period, while the manual gauge is collecting 1130.0 mm, a difference of approximately 7 % (table 5).

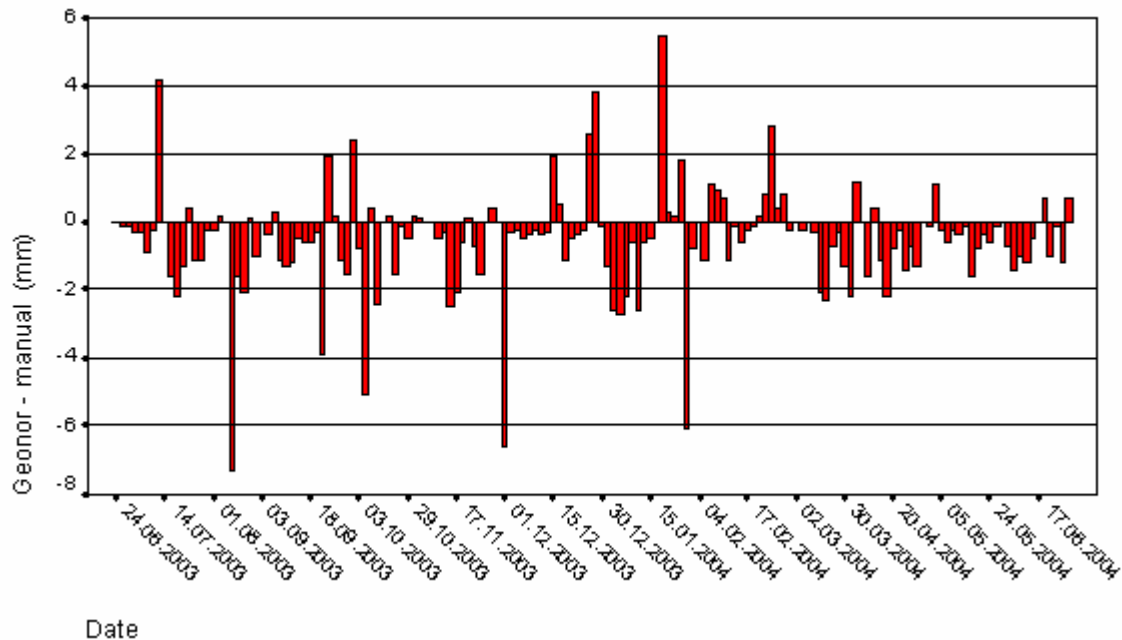


**Figure 7:** The difference (cases) between Geonor and manual gauge from Utsira

**Table 5:** The difference between Geonor and the manual gauge.

	<b>Geonor</b>	<b>Manual</b>	<b>Difference</b>
Total amount of precipitation	1052.6	1130.0	-6.85 %

At Utsira Geonor and the manual gauge are located some distance from each other, and we may expect a bit difference in the “catch” of the precipitation because of the local topography and the location to the buildings. Utsira is a very wind exposed station and in precipitation situations it is often very windy. By studying each case (peak) more closely we found that the wind direction during the precipitation periods seemed to have a considerable influence on the “catch” of precipitation at Utsira. We have studied all differences (peaks) in figure 7 greater than 2, totally 18 “negative” cases and 6 “positive” cases. The results are shown in table 6.

**Table 6:** Possible reasons for the observed differences between Geonor and manual gauge

<b>Possible reasons</b>	<b>Mainly SE-ly wind (frontal precipitation)</b>	<b>Mainly NW-ly wind (showers)</b>	<b>Wind in sector S to W</b>	<b>Snow/sleet-cases</b>	<b>Geonor-top filled with snow</b>
<b>18 negative cases</b>	13 cases	4 cases	-	-	1 case
<b>6 positive cases</b>	-	-	4 cases	2 cases	-

# **Preliminary results obtained following the intercomparison of the meteorological parameters provided by automatic and classical stations in Romania**

Madalina Baciu, Violeta Copaciu, Traian Breza, Sorin Cheval, Ion Victor Pescaru

National Meteorological Administration  
Sos. Bucuresti-Ploiesti 97, Bucharest 013686, ROMANIA  
Tel. +40-21-2303116, Fax. +40-21-2303143,  
E-mail: [madalina.baciu@meteo.inmh.ro](mailto:madalina.baciu@meteo.inmh.ro)

## ***Abstract***

*At present, 60 automatic weather stations operate in the Romanian meteorological network, two of which - of THIES CLIMA type and the rest – VAISALA (MAWS301 and MILOS). In order to compare and analyse the meteorological parameters provided by the automatic and classical stations, parallel measurements were performed at 18 weather stations, uniformly distributed over the Romanian territory.*

*There were analysed the hourly values of the following parameters, recorded in 2004: mean temperature, minimum and maximum air temperature, relative humidity and air pressure, from the considered stations.*

*The statistical parameters computed for the air temperature components showed that the mean daily values recorded by the automatic station does not differ significantly from those obtained with classical instruments, whereas the extreme values – the daily minimum and maximum – differ significantly from the statistical standpoint.*

*The statistical parameters were also computed of the differences between data yielded through the two measuring methods (classical and automatic), for relative humidity and air pressure.*

Data yielded from measurements carried out with various technical systems disclose small differences for one identical geographic environment. However, in view to analyse climate changes, it is important to compare obtained results. The factors that may intervene in the analysis of long term climate changes, resulting from the change of the “conventional” measurement system to the automated one, refer to changes in: observation terms, mediation methods, station location, apparatus design, calibration methods. Differences may be systematic or stochastic. Long-term intercomparison (1-2 years) is necessary of the two systems, in representative locations and in varied meteorological conditions, in order to test the compatibility of the two systems and establish correction algorithms.

To write this paper, there were used hourly precipitation, air pressure and humidity data, as well as extreme temperature data, recorded in parallel, in the January-September 2004 interval, at the automatic and classical stations. Inter-comparative measurements took place at 18 weather stations endowed with MAWS 301 automatic stations (except for Bucharest Baneasa, where the automatic station is a THIES one and Buzau - endowed with portable MAWS one). Stations were chosen observing the principle of major climatic areas representative features. Table 1 renders classical interests and the sensors type of MAWS 301 automatic stations for each meteorological element to be used in the intercomparison.

Table 1

Measured parameter	Classical instruments	Instrument location	MAWS 301 sensors	Sensor location
Air temperature	Mercury thermometer	In instrument screen, 2m above ground	QMH101	On station arm, 2m above ground
Air minimum temperature	Alcohol thermometer	In instrument screen, 2m above ground	QMH101	On station arm, 2m above ground
Air maximum temperature	Mercury thermometer	In instrument screen, 2m above ground	QMH101	On station arm, 2m above ground
Relative humidity	Hair hygrometer	In instrument screen, 2m above ground	QMH101	On station arm, 2m above ground
Air pressure	Mercury barometer	In station office	PMT16A	In station logger

To highlight differentiation between the two observation types and recording errors of classical and even automatic ones, comparative graphs were drawn for each parameter, day or station taken apart. Figures 1 to 5 exemplify the evolution of the hourly values of the five analysed parameters, recorded classically and automatically.

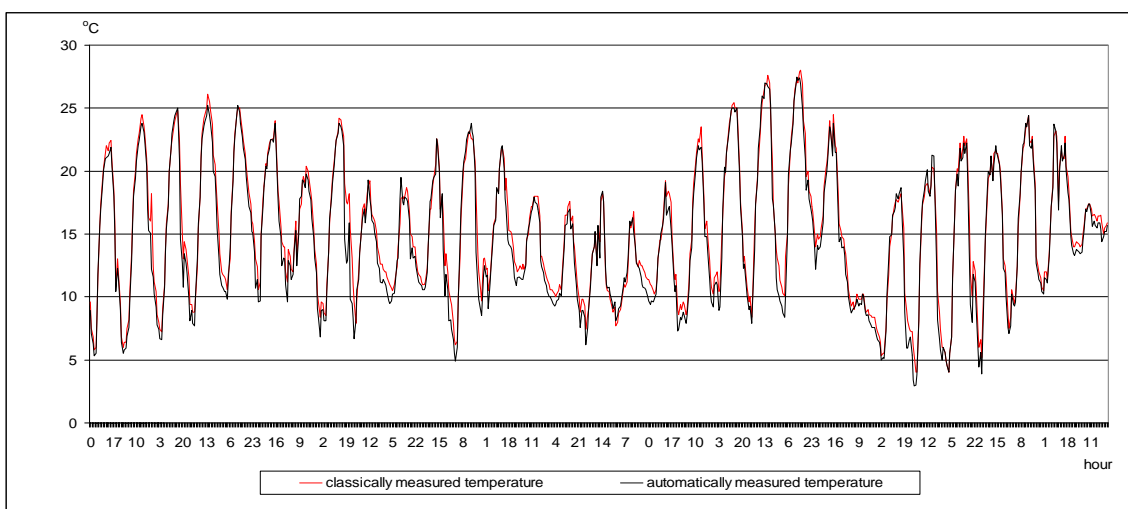


Fig. 1 Hourly variation of air temperature ( °C) at Bucharest-Baneasa weather station in May 2004

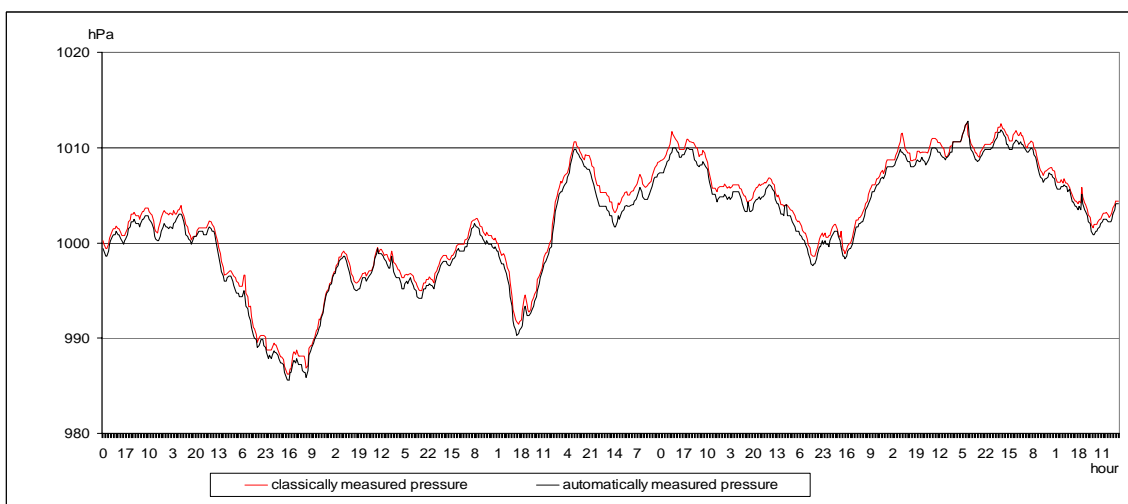


Fig. 2 Hourly variation of air pressure (hPa) at Bucharest-Baneasa weather station in May 2004

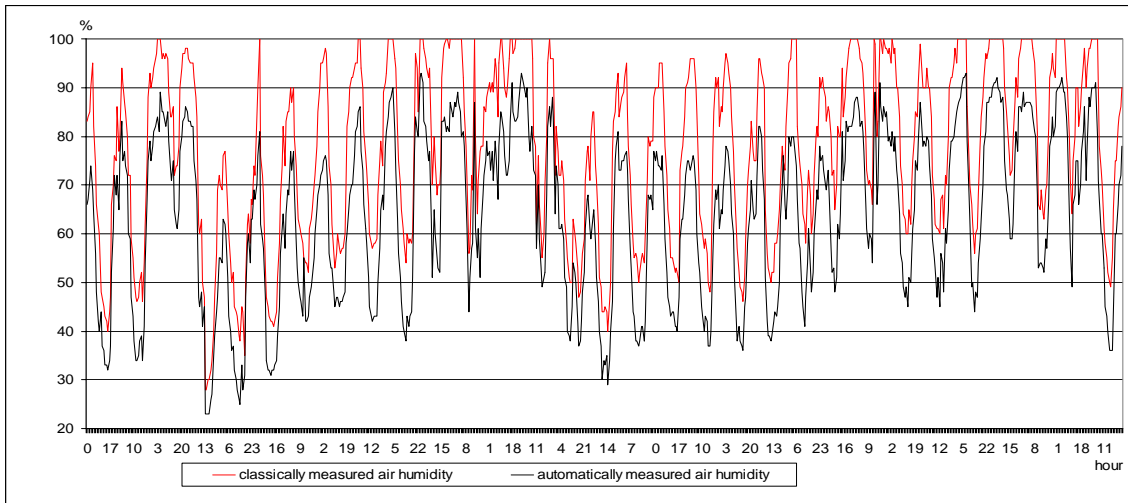


Fig. 3 Hourly variation of air humidity (%) at Buzau weather station in July 2004

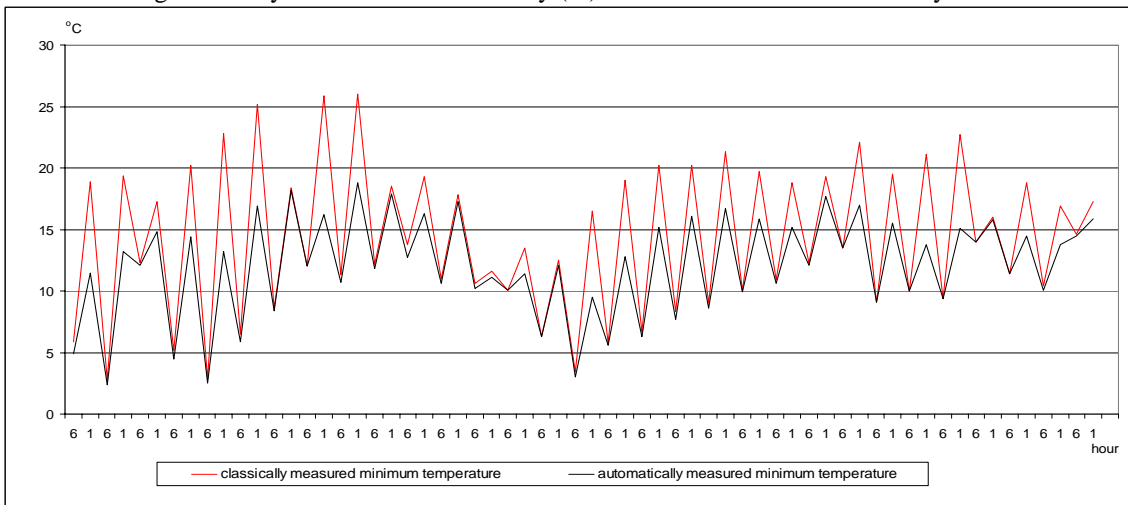


Fig. 4 Hourly variation of minimum air temperature (°C) at Miercurea Ciuc weather station in July 2004

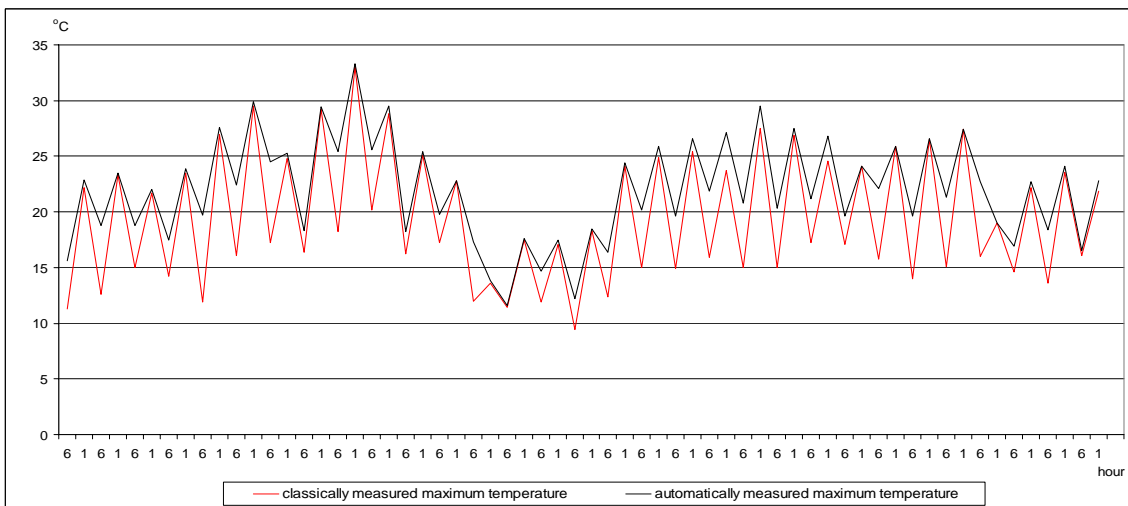


Fig. 5 Hourly variation of maximum air temperature (°C) at Miercurea Ciuc weather station in July 2004

There were also computed: the mean of the hourly data series, the mean square deviation and the correlation coefficient, whereas for the residue series (differences between classical and automatic measurement), the mean, mean square deviation and amplitude of these series were computed. In figures 6 to 15 the monthly means are rendered of the residue series for each parameter, i.e. the amplitude of these series.

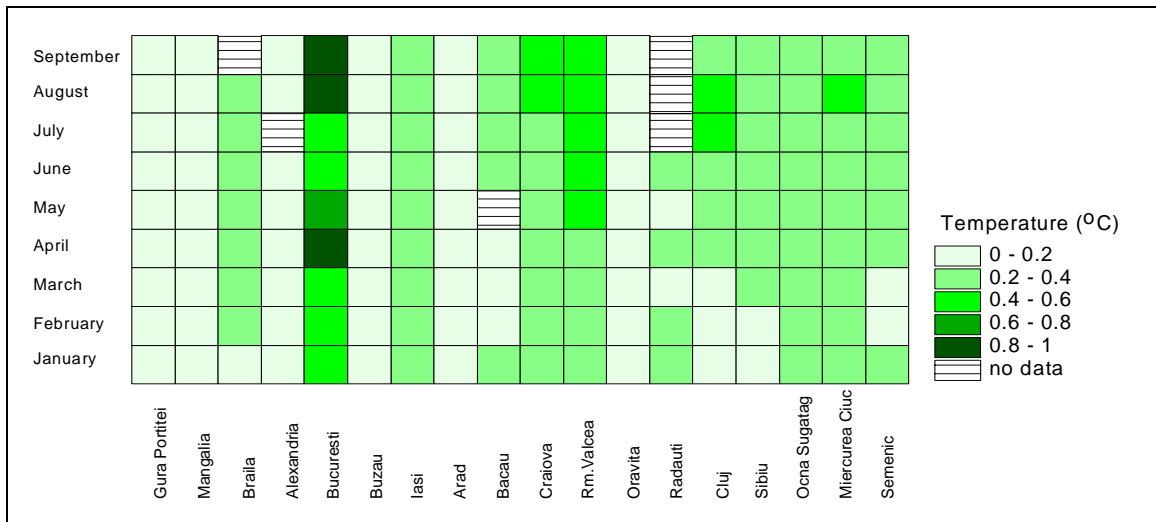


Fig. 6 – Monthly mean of differences between the classically and automatically measured hourly mean temperature

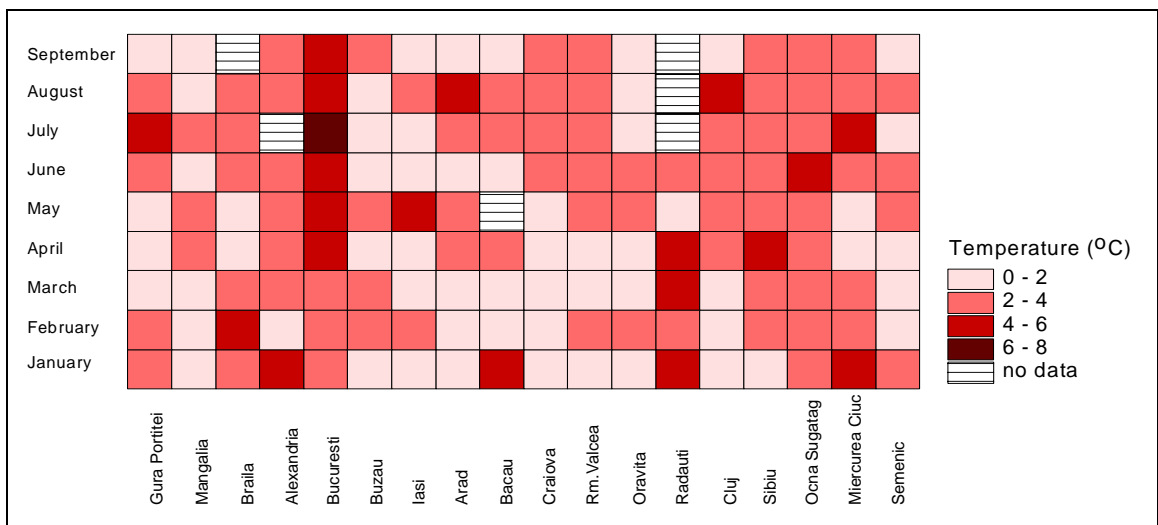


Fig. 7 Amplitude of difference series between classically and automatically measured hourly mean temperatures

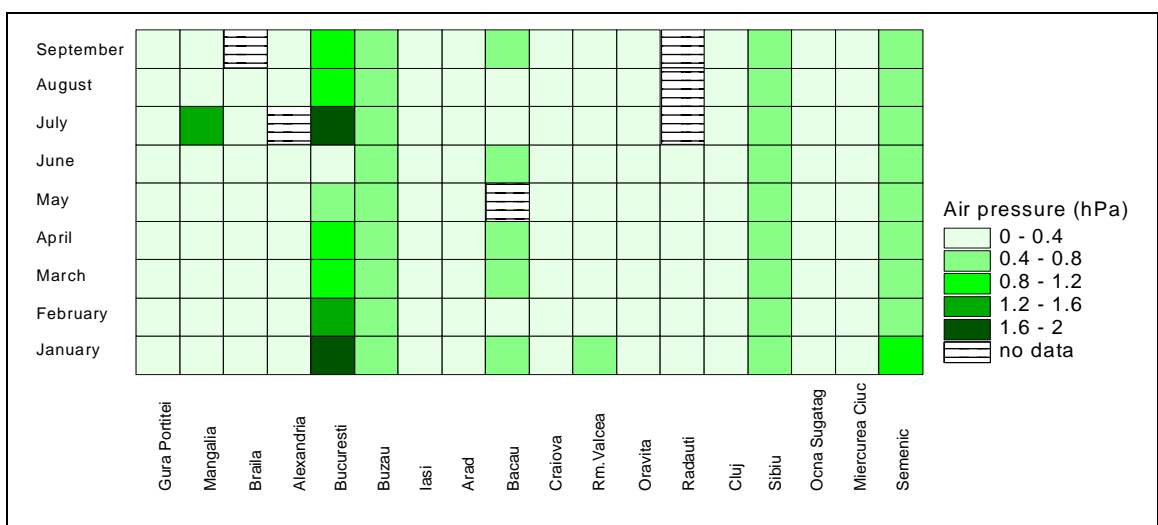


Fig. 8 Monthly mean of differences between classically and automatically measured air pressure

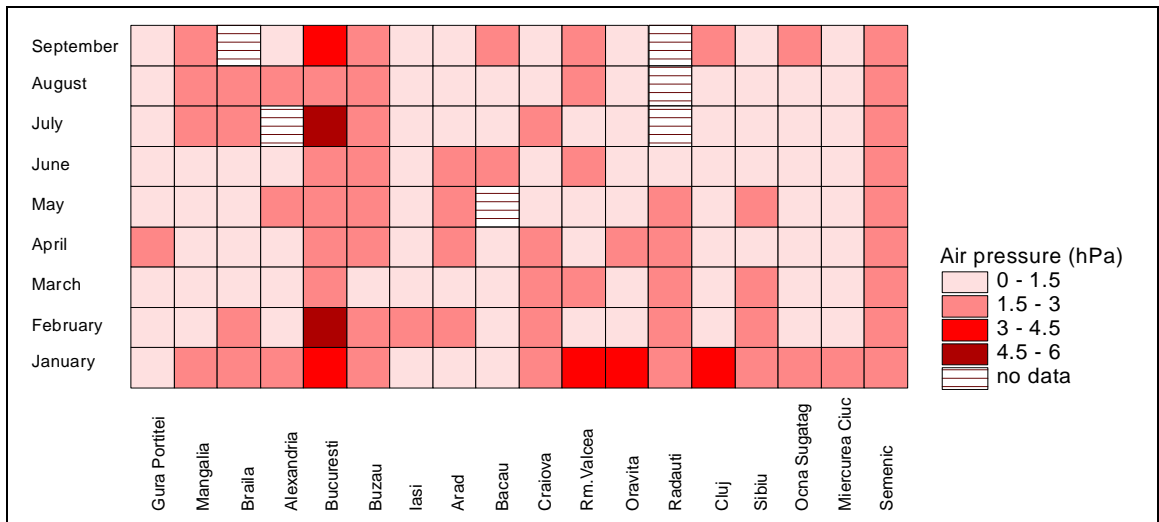


Fig. 9 Amplitude of difference series between classically and automatically measured air pressure

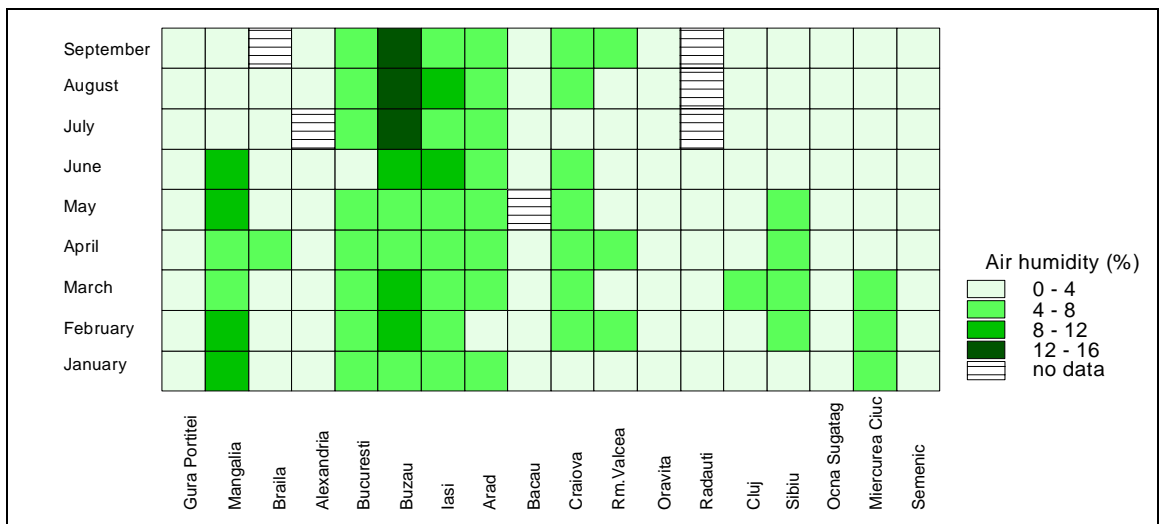


Fig. 10 Monthly mean of differences between classically and automatically measured relative humidity

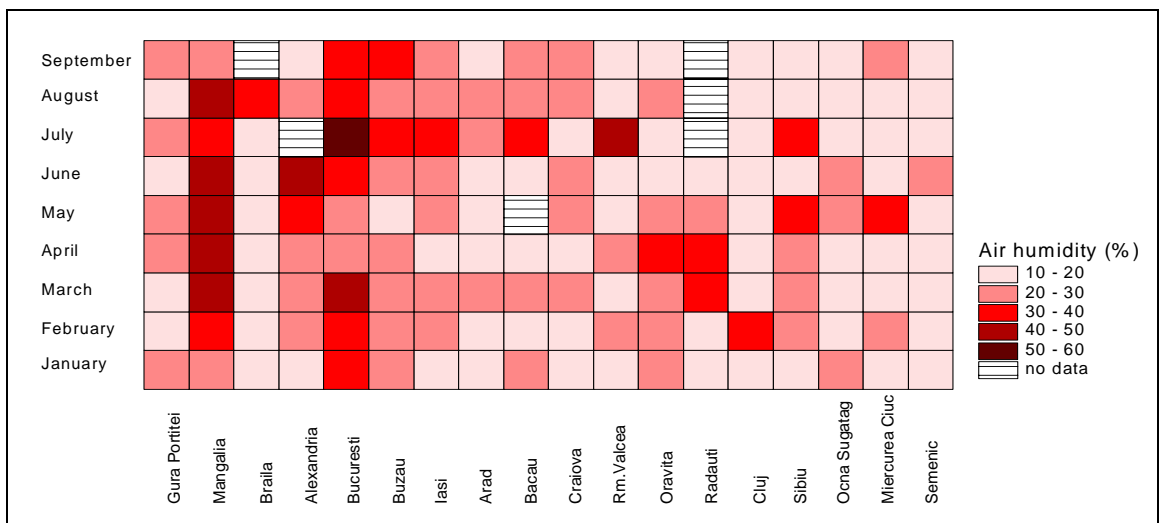


Fig. 11 Amplitude of difference series between classically and automatically measured relative humidity



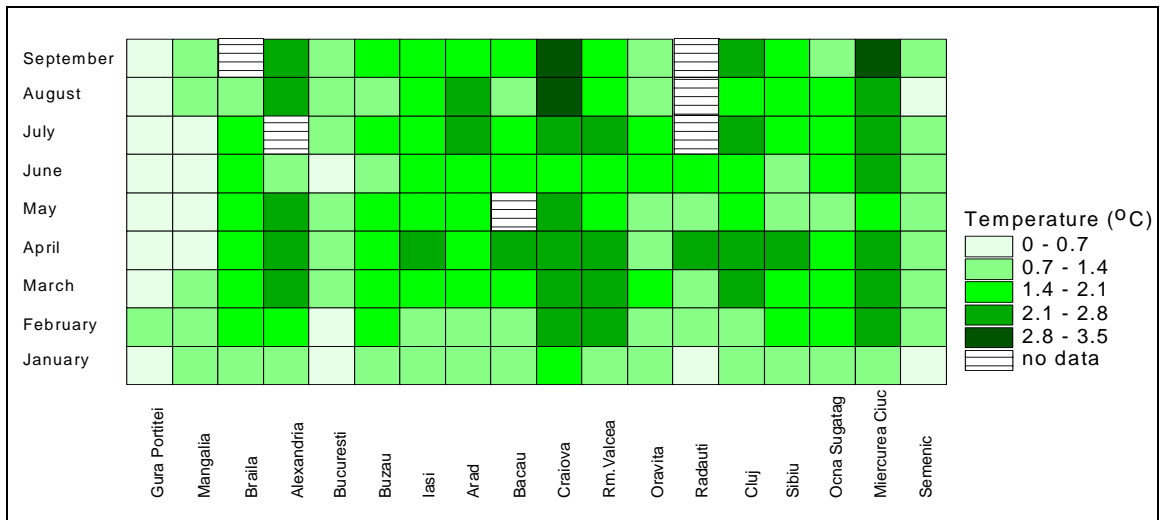


Fig. 12 Monthly mean of differences between classically and automatically measured minimum air temperature

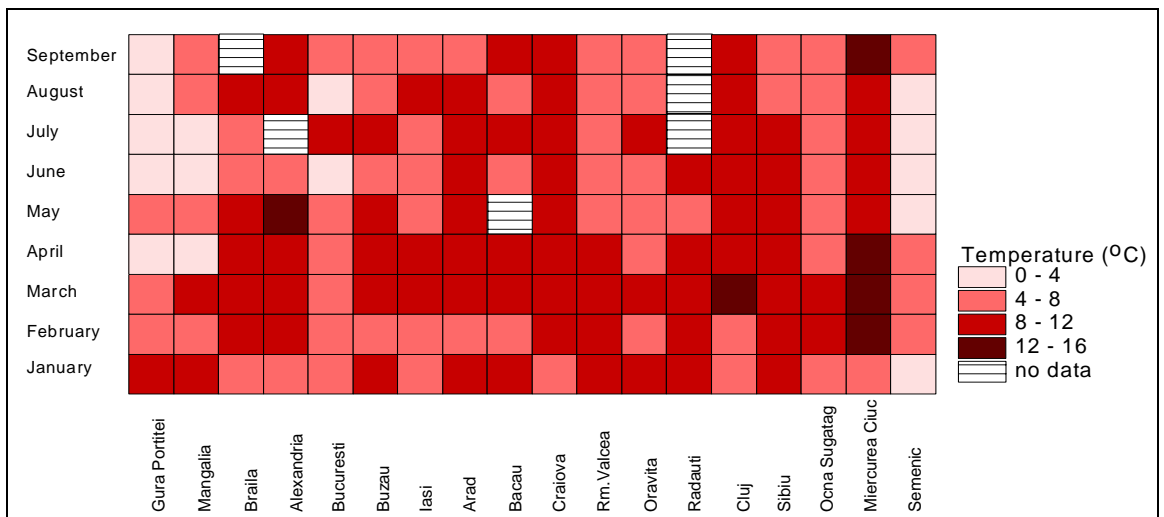


Fig. 13 – Amplitude of difference series between classically and automatically measured minimum air temperature

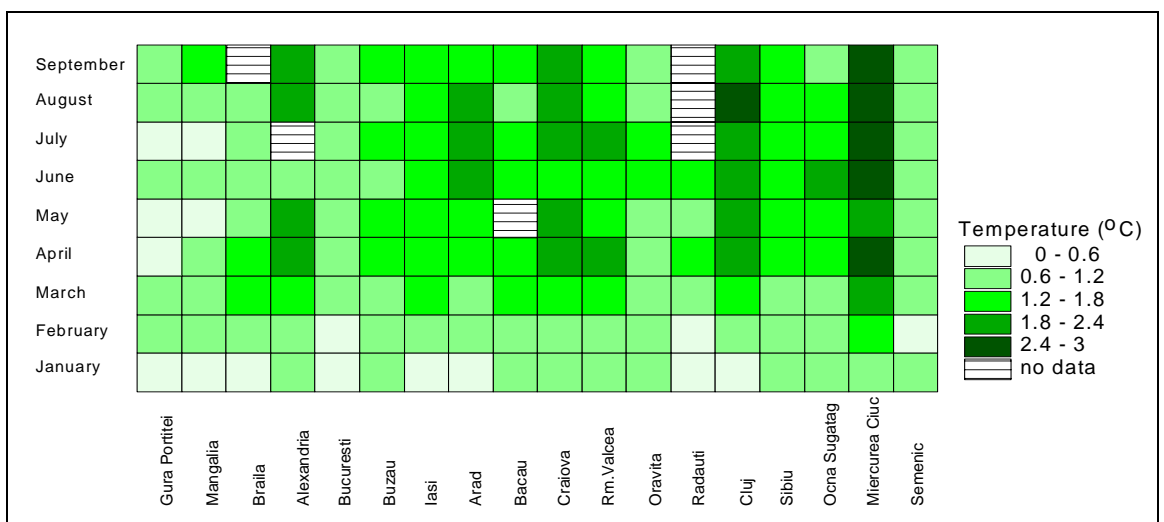


Fig. 14 – Monthly mean of differences between classically and automatically measured maximum temperature

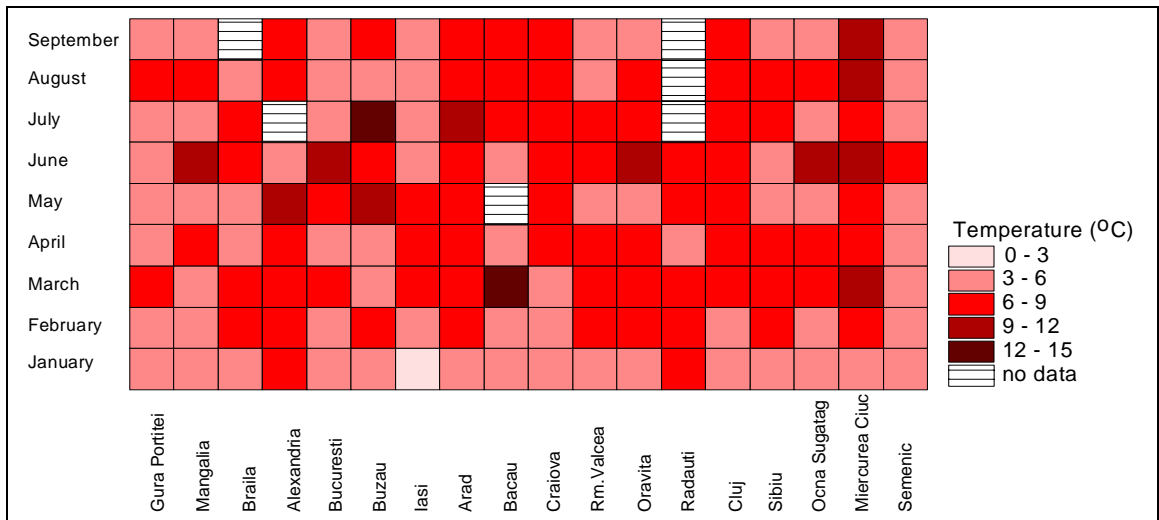


Fig. 15 Amplitude of difference series between classically and automatically measured maximum air temperature

Another statistical analysis was performed through applying the averages Student test, to check the existence of any significant difference between the values in the two series. We mention that t value in the tables is 1.96 for mean temperature, humidity and air pressure and 1.94 for extreme temperatures, both showing a confidence level of 95%. Student test results are rendered in figs 16-19.

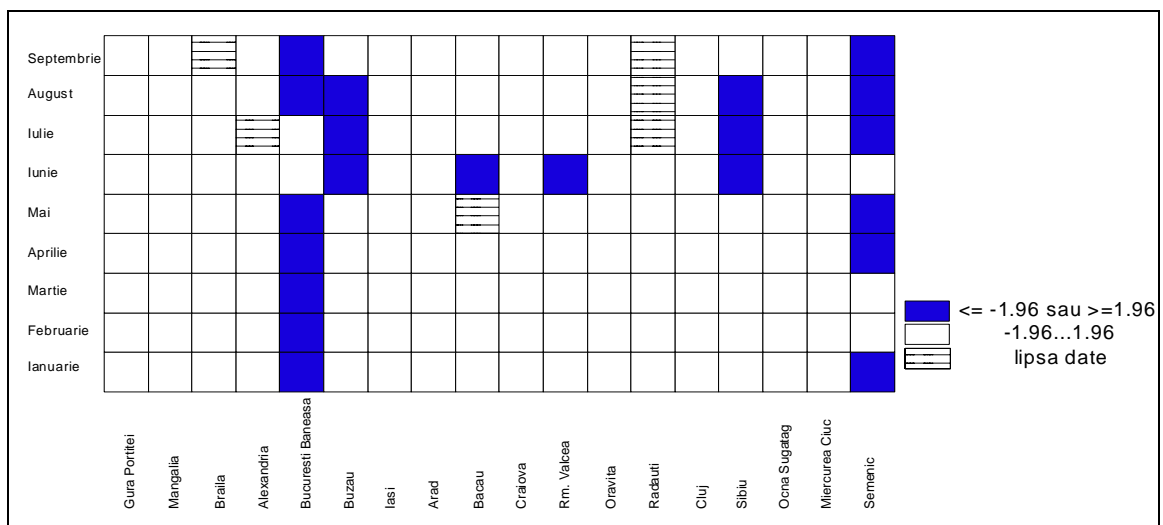


Fig. 16 Student test results for air pressure

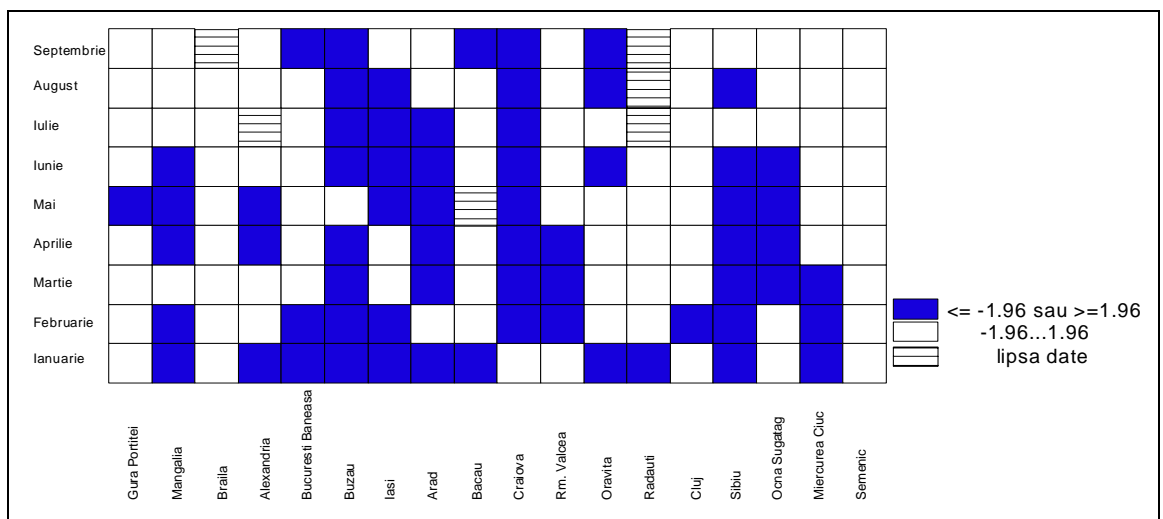


Fig. 17 Student test results for relative humidity

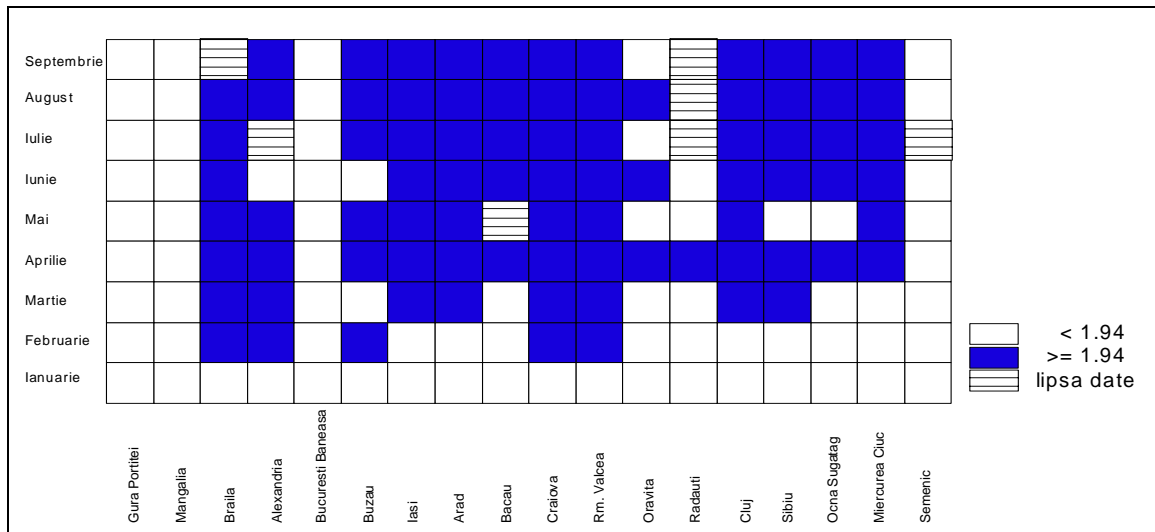


Fig. 18 Student test results for minimum temperature

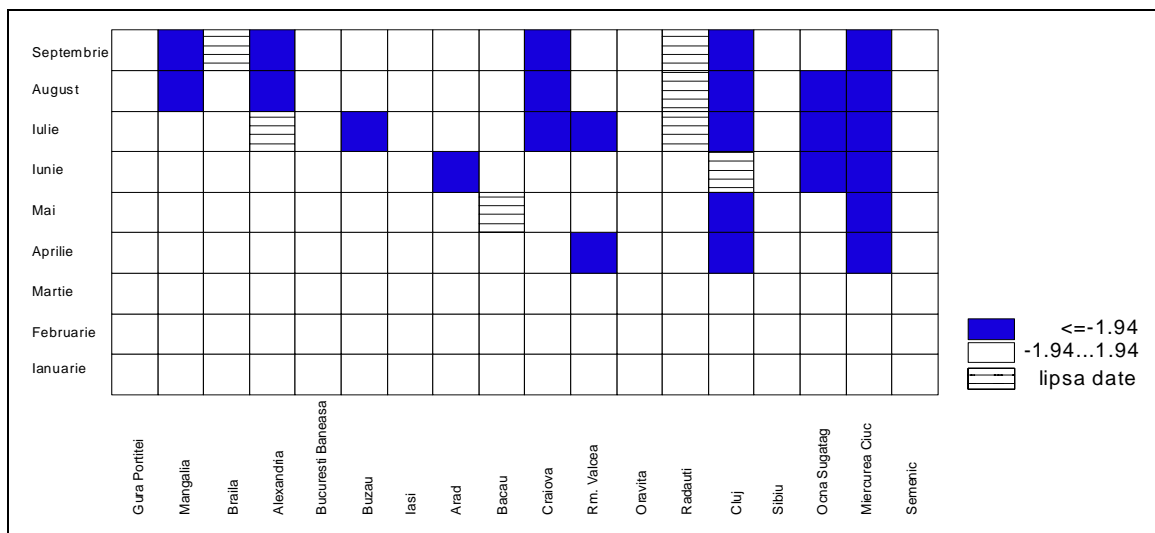


Fig. 19 Student test results for maximum temperature

The mean air temperature does not display large differences between the two series measured classically and automatically. The monthly means of the differences between the mean hourly temperature measured at the classical station and the temperature measured by the automatic one kept within 0 – 0.6°C at all analysed stations, except for Bucharest Baneasa, where the mean is higher than elsewhere, namely between 0.6 and 1°C (fig. 6). Student test results also show that the difference of the mean temperature values is significant (not accidental), with a confidence level of 95%, again at Bucharest Baneasa, in April, May, August and September. We mention that Bucharest Baneasa weather station is a THIES one, different from the other 17 MAWS - type that made measurements.

As a rule, the air pressure did not record very large differences between the classical and the automatic stations, the mean of the differences series ranging within 0-0.8 hPa in all the months. Bucharest Baneasa stands out again, with values of the differences mean reaching 2 hPa (fig. 8). Student test disclosed that at Bucharest Baneasa, Buzau, Bacau, Rm. Valcea, Sibiu and Semenic stations differences between classical and automatic measurements are significant as regards one or more months. It is remarkable that values recorded with the classical station are higher than those

recorded automatically keeping a constant difference throughout one whole month. Given the constant character with time of the monthly means of the differences between the two types of measurements at five of the 18 stations, this suggests either one apparatus failure or wrong application of temperature corrections.

The relative moisture is characterized through very large amplitudes of the series of differences between the classical and the automatic measurements, ranging from 10 to 52 % (fig. 10). Student test results (fig. 17) also prove that differences between classical and automatic measurements are significant at a quite large number of stations, with January and February standing out. Differences between the two types of measurements may be attributed to the different measurement environments (instrument screens with different inertia), to the hygrometer sensitiveness and to the variation of its indications against temperature evolution. However, the relatively small variations of the mean temperatures cannot account for the large humidity variations. As a conclusion this issue remains to be studied and hygrometers may be recalibrated in standard conditions (climatic chambers).

Extreme temperatures have a common feature: values recorded classically are always higher for the minimum temperature (fig. 4) and lower for the maximum one (fig. 5) than those recorded automatically, most remarkable at 18.00 p.m. At all stations and almost throughout the whole period, the monthly means of the series of differences between classical and automatic measurements range from 1.4 to 3.5°C as regards the minimum temperature (fig. 12) and from 1.2 to 3.0°C as regards the maximum temperature (fig. 14). The amplitude of the differences of the minimum temperatures reaches 15.7°C (March, Miercurea Ciuc), whereas that of the series of differences of the maximum temperatures reaches 14.3°C (March, Bacau).

The significant differences between the extreme temperatures are the natural consequence of the difference in the measurement environment and implicitly of the different inertia of the instrument screens.

# **THE METEOROLOGICAL DATA QUALITY MANAGEMENT OF THE ROMANIAN NATIONAL SURFACE OBSERVATION NETWORK**

**Ioan Ralita , Ancuta Manea, Doina Banciu**  
National Meteorological Administration, Romania

**Ionel Dragomirescu**  
Starkrom Technologies, Romania

## Romanian surface observation network

- **The observation network:**
  - since **1887 : 30 observation stations**
    - ... some meteorological observations even before 1884 when the Meteorological Institute was settled
- **Dynamic structure, permanently undergoing transformation, improvement and modernization processes.**
  - ✓ at present 160 meteorological stations with a relative uniform spatial distribution
  - ✓ 1995-2000 : 12 Automatic Surface Observation Stations (ASOS): Vaisala MILOS 500, Vitel 1040, Thies AWS 7800, and Thies DL 15.
  - ✓ Since 2000 : **60 ASOS from Vaisala**
    - within the **SIMIN** (National Integrated Meteorological System) project



**co-existence of two station types – manual and automatic**

**New procedure for surface observation processing (SOP)  
improving the data quality management**

## Meteorological observation programs

### **SYNOP program**

hourly measurements of the air temperature, air pressure, relative air humidity, wind direction and speed, atmospheric precipitation, snow cover depth, atmospheric phenomena, sunshine duration, clouds type, cloud base height, cloud cover, ice deposits, soil and sea temperature

### **Climatological program**

evolution of the meteorological parameters within the climatological interval

### **Agrometeorological program**

specialized measurements, performed in standardized platforms, of soil humidity, plant density and development.

### **Solar radiation program**

net solar radiation, diffused solar radiation, reflected solar radiation, global solar radiation, solar radiation balance.

### **Snow program**

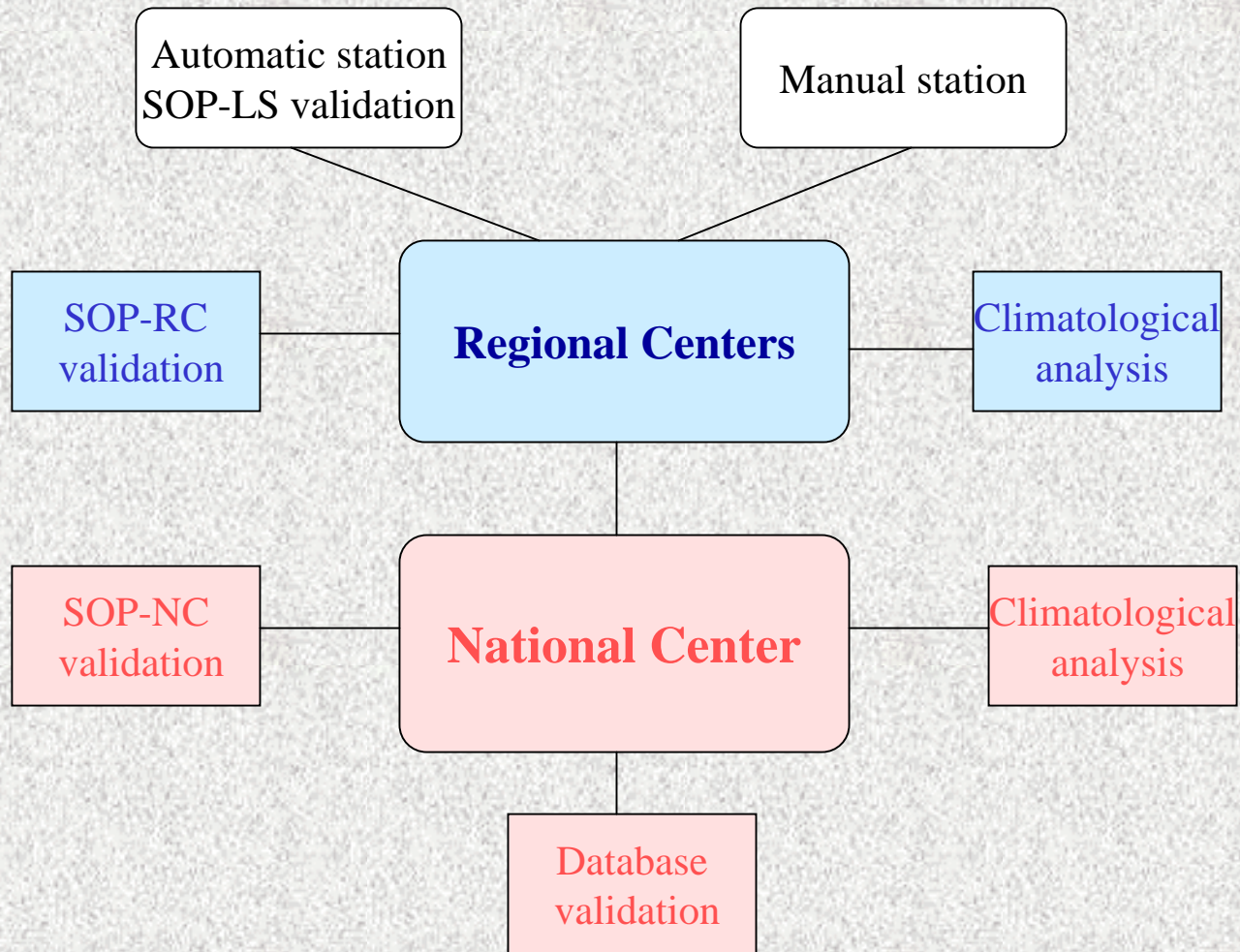
snow characteristics and layer structure

### **Alert program**





## Data quality management



## Surface observation processing (SOP) applications

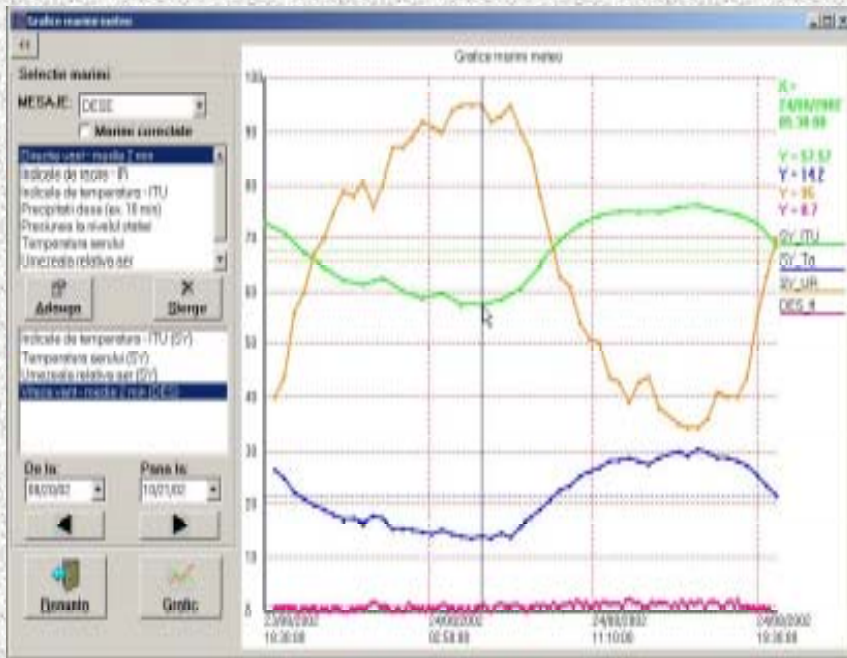
- ✓ support data collection, validation and distribution
- ✓ ensure the data processing for all observation stations (manual and automatic)
- ✓ quite similar with the old procedure, involving 3 processing levels:  
local (SOP-LS), regional (SOP-RC) and central (SOP- NC)

**but with a higher level of sophistication and capabilities:**

- flexibility in defining new message (through specific templates)
- pre-configured time schedule for generation/sending/receiving messages
- activation of the message transmission with higher frequency
- the possibility for local configuration and control of all applicable parameters and features of the sensor stations
- non standard formats (higher precision and compression for communications) between applications and standard formats
- possibility to interrogate a missing station (SOP-RC/NC)
- a more elaborate validation and parameter correction, including a tracking modification system

## Local sensor surface observation processing application SOP-LS

- ✓ data retrieval from the automatic station for further processing
- ✓ real-time display to allow the operator (at local sites) to continuously monitor the measured meteorological parameters
- ✓ automatic generation of messages from measured data and human observation in accordance with to the defined template for each specific message type
- ✓ automatic message transmission to SOP-RC, using GSM/SMS technology
- ✓ data storage in local databases; database (automatic compression and archiving)



- ✓ computations of derived parameters
- ✓ data validation and parameter correction
- ✓ data editing function
- ✓ alphanumeric and graphical visualization
- ✓ survey of sensors functioning
- ✓ log file downloading, processing and storage
- ✓ back-up transmission by PSTN, FTP, e-mail
- ✓ missing data recovery system
- ✓ supports ASOS remote management

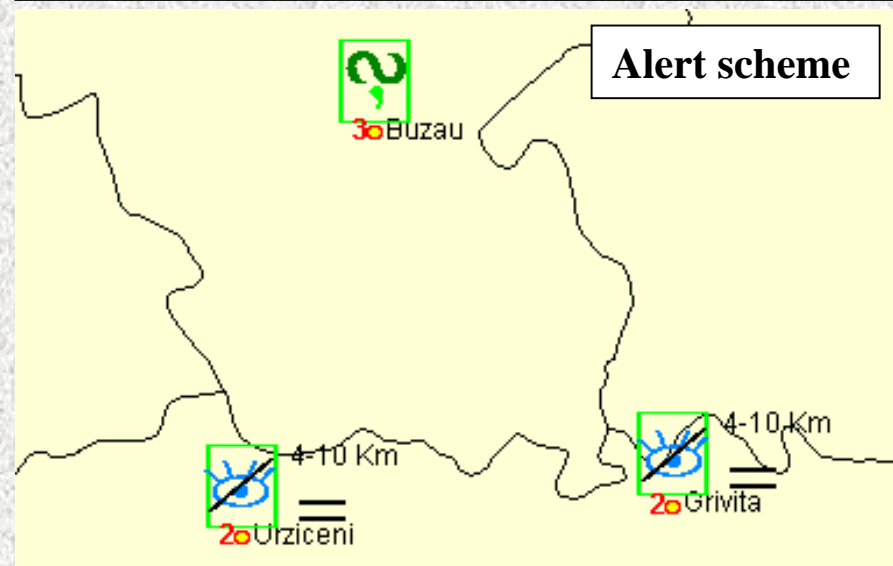
## Regional and central level SOP applications

### SOP-RC

- ✓ collection of the messages sent by automatic (through SOP-LS) and manual stations
- ✓ data decoding and storage
- ✓ computation of derived parameters
- ✓ automatic generation of individual and collective messages (standard and non standard formats)
- ✓ automatic transmission of collective messages to the National Center
- ✓ station interrogation and remote control
- ✓ data validation and editing function
- ✓ alphanumeric and graphical visualization ( full GIS interface)
- ✓ automatic database management
- ✓ printing and graphical product export

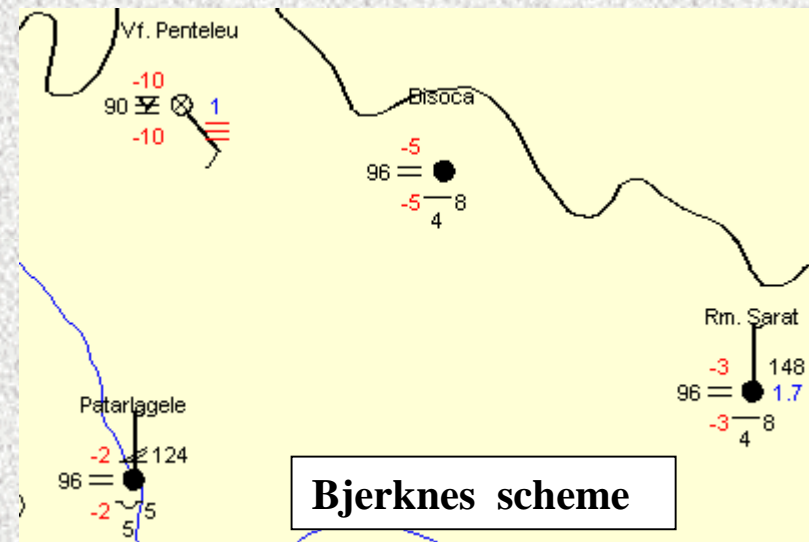
### SOP-NC

- ✓ messages collection SOP-RCs
- ✓ supports all the capabilities of SOP-LS and SOP-RC
- ✓ additional features (administrative and controlling station messages management, feeding the historical database, taking over of all RFC's functions, for a period of time, controlling of all automatic station and SOP-RCs, etc.)



## SOP Data validation

- ❖ **To all SOP application levels, depending on the level and message type**
- ❖ **Automatic validation**
  - ✓ message format structure according to specific presets (for message type, time schedule, derived parameters)
  - ✓ checking against the validity range
  - ✓ multiple correlation between measured and observed parameters
- ❖ **Manual validation**
  - ✓ temporal validation by graphical visualization of the parameter evolution for each station
  - ✓ spatial validation by visualization geographically plotted forms (one parameter, Bjerknes scheme, time differences and sums)
  - ✓ comparison with the climatological values and numerical weather prediction model output



# ADVANCED ATMOSPHERIC BOUNDARY LAYER TEMPERATURE PROFILING WITH MTP-5HE MICROWAVE SYSTEM

**E. Kadygrov\*, M. Khaikin\*, E. Miller\*, A. Shaposhnikov\*,  
A. Troitsky\*\***

**\* Central Aerological Observatory,  
Dolgoprudny, Moscow region, Russia**

**\*\* Radiophysical Research Institute,  
N. Novgorod, Russia**

**([src\\_attex@mtu-net.ru](mailto:src_attex@mtu-net.ru))**

## **1. ABSTRACT**

The MTP-5, a ground based temperature profiler, has been widely used since 1991 for investigation of the atmospheric boundary layer. The MTP-5 is an angular scanning single-channel passive microwave instrument with a frequency in the center of molecular oxygen absorption band (60 GHz). It can measure the thermal emission of the atmosphere with sensitivity 0.04 K at 1 s integration time from different zenith angles. On the basis of this measurements, it is possible to retrieve temperature profiles at the altitude range up to 600 m. But for many applications it is needed to have altitude range up to 1 km. For those applications was developed advanced MTP-5HE instrument which has a new low noise receiver, new profile retrieval algorithm and shifted central frequency. The MTP-5HE system had successful comparison with radiosondes data within the COST720 WG2. Action “Integrated Ground-based Remote Sensing Stations For Atmospheric Profiling” at aerological station Payerne, Switzerland, in March-April, 2004.

## **2. INTRODUCTION**

The investigation of atmospheric boundary layer (ABL) covers many areas: (atmospheric dynamics, radiation, turbulence, cloud physics, numerical modeling, air-sea interaction. Applications of this investigations are air pollution, urban climate, short-term meteorological forecasting. One of the important measurement parameter in ABL is temperature profile (Garrat, 1994). Temperature profiles in ABL are classified as stable, neutral and convectively unstable with a capping inversion somewhere between several meters and 2 km in height. Knowledge of ABL temperature profiles is important in many applications: e.g. forecasting pollution near big factories

and power station, regional weather forecasting, radio wave propagation etc. Last decade or so for temperature profiling in ABL were used passive microwave radiometers with the frequencies in molecular oxygen absorption band (Westwater, 1993). One of the widely used instrument was MTP-5H - a single channel an angular-scanning microwave temperature profiler (Troitsky et al, 1993). It can measure the thermal emission of the atmosphere with sensitivity 0,04K at 1 s integration time from different zenith angles (Kadygrov and Pick, 1998). On the basic of this measurements it is possible to retrieve temperature profiles at the altitude range up to 600 m (Westwater et al, 1999). But for many applications it is needed to have altitude range up to 1 km (Kadygrov et al, 2002, Kuznetsova et al, 2004). For those applications was developed advanced MTP-5HE instrument (HE – height extension).

### 3. DESCRIPTION OF ADVANCED PROFILER

Maximum altitude for ground-based microwave temperature profilers depends first of all from the central frequency. If the central frequency is in the center of molecular oxygen absorption band (about 60 GHz), the maximum measured altitude is about 600 m, for the frequency about 53 GHz (on the wings of oxygen band) the maximum measured altitude is about 5 km. For sufficient accuracy of the temperature profile retrieval in ABL it is needed to have high sensitivity of the radiometer ( $\Delta T_b$ ) which can be calculated from equation  $\Delta T_b = \frac{T \cdot k}{\sqrt{\Delta f \cdot \tau}} (K)$ , where  $T$  – noise factor of the radiometer,  $k$  – depends from radiometer type ( $k \approx 1 \div 3$  for different type of radiometer);  $\tau$  – time of integration;  $\Delta f$  – radiometer bandwidth.

MTP-5H instrument had  $\Delta T_b = 0,04$  K at 1 sec integration time and bandwidth about 4 GHz. For the frequencies in the absorption line wings impossible to use such wide bandwidth: it is needed to be about 200÷400 MHz. So, the noise – factor of MTP-5HE radiometer needed to be 2÷3 times less in contrast with MTP-5H for about the same sensitivity. Finally MTP-5HE has following main technical parameters: central frequency 56 GHz, bandwidth 400 MHz, improved receiver with sensitivity 0,08 sec at 1 sec integration time, and new improved algorithm for temperature profile retrieval. During one year MTP-5HE was in continuous operation mode at aerological station Dolgoprudny, Russia, and had successful comparison with radiosonde in aerological station Payerne, Switzerland, during COST-720 Action “Integrated Ground-based Remote Sensing Stations For Atmospheric Profiling”.

### 4. COMPARISONS IN PAYERNE

The main goals of the campaign in Payerne were:

- Test ground-based temperature and humidity profiling systems;

- Study in particular their ability to detect ABL phenomena like temperature inversion presence, formation and dissipation of fog and low clouds;
- Test cloud detection systems (passive and active ground-based systems);
- Provide a dataset for studying the possibility of system integration for improving temperature and humidity profiling with ground-based remote sensing systems.



Photo 1. MTP-5HE in Payerne, Switzerland, March 2004

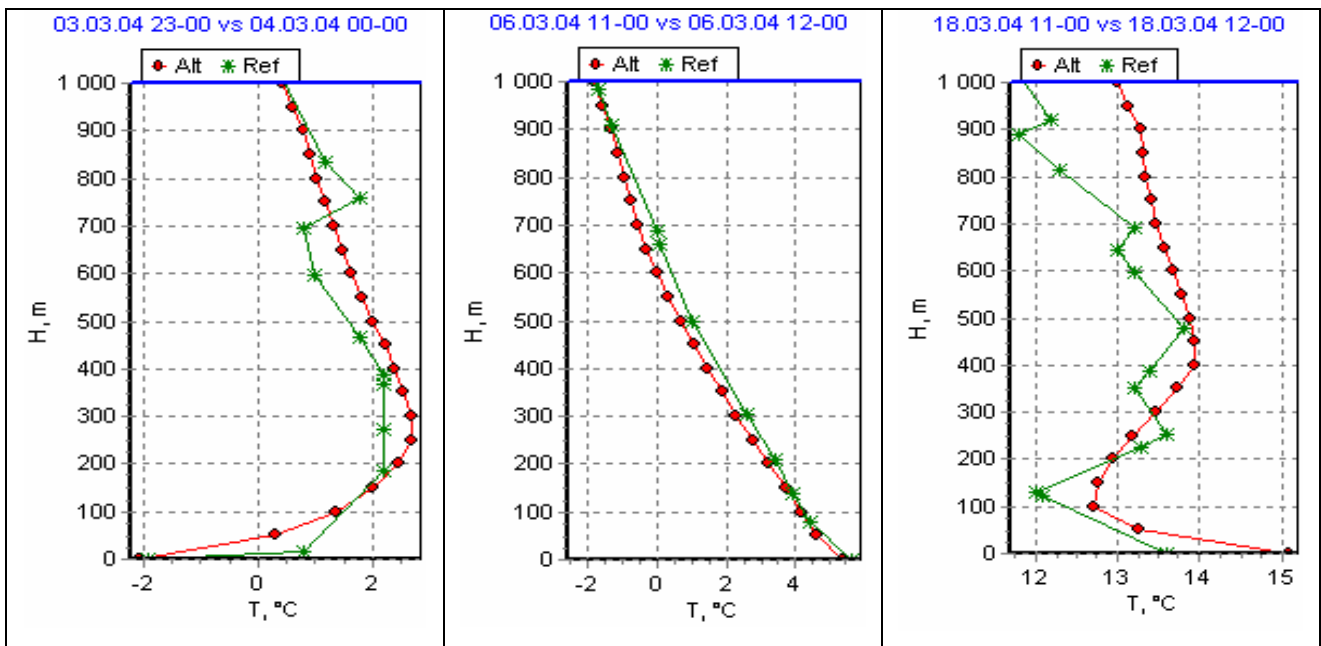


Figure 1. Results of the comparison with radiosondes.  
(Alt-MTP-5HE data; Ref- radiosondes)



Regular measurements of ABL temperature profiles were provided by MTP-5HE profiler from March, 3, 2004, up to the April, 5, 2004. The measurement cycle was 5 minutes. The MTP-5HE instrument was installed at height 8 m from the ground surface (499 m above sea level), with radiosondes site at the distance about 50 m. (Photo 1). All in all, about 63 radiosondes launches took part in comparison with 9633 profiles obtained from MTP-5HE profiler. At Fig. 1 are shown some results of comparison of remote sensing data with radiosonde ABL temperature profile data. It is possible to see that not only ground-based, but even elevated temperature inversion were retrieved with sufficient accuracy. At Fig. 2 are shown statistical results of radiosonde and MTP-5HE data comparison, and in Fig. 3 – same results, but separated for different atmosphere stratification (adiabatic or with temperature inversion), where:

$dA_v(h)$  – mean deviation for height  $h$ ;

$dA_{v\ mean}$  – mean total deviation;  $RMSD(h)$  – root mean square deviation for different  $h$ ;

$RMSD$  – root mean square deviation for all data.

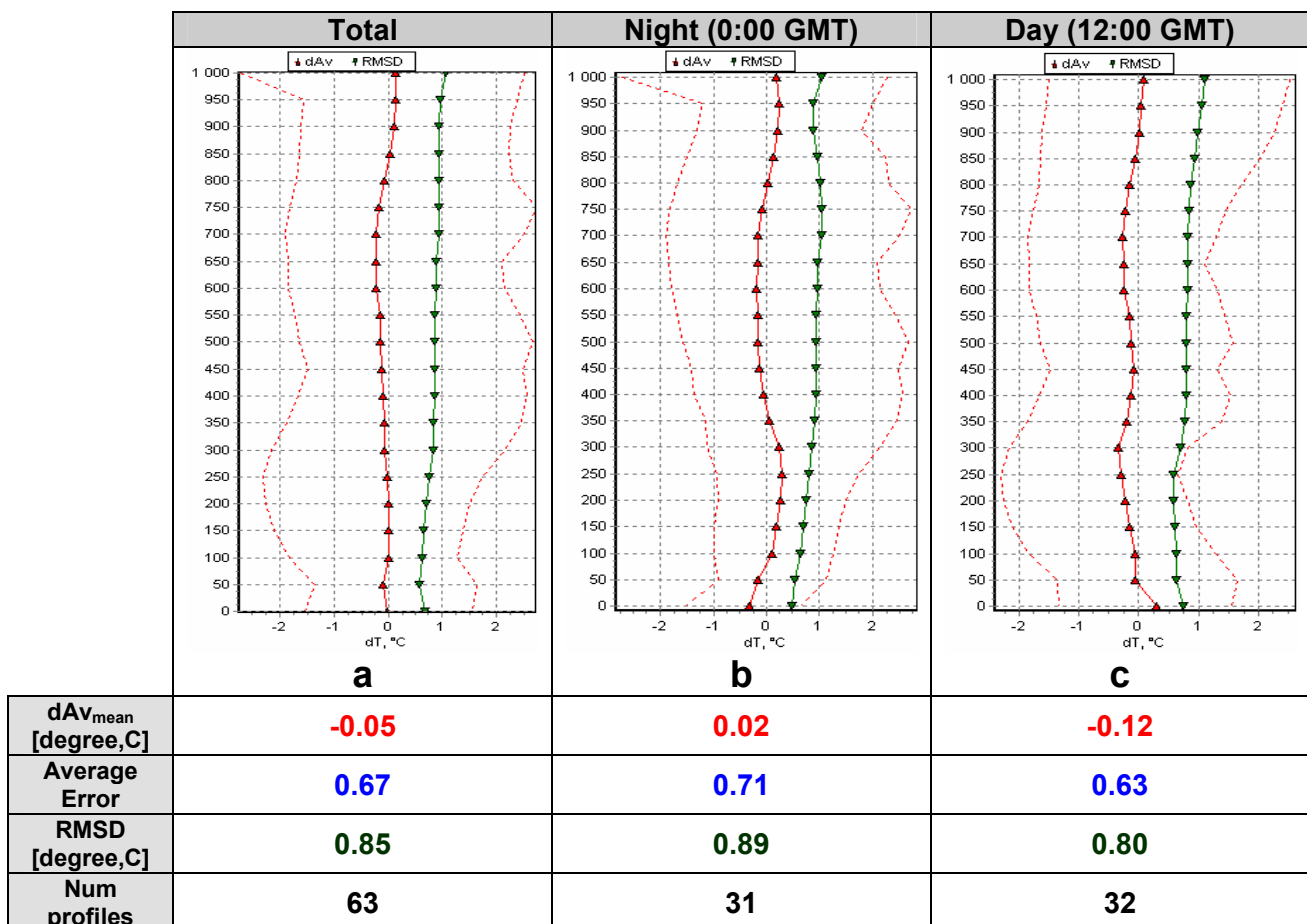


Figure 2. The results of radiosound and profiler data comparison. In figures are shown the values of  $dA_v(h)$  and  $RMSD(h)$  and maximum and minimum deviations obtained for total statistics (a), for nocturnal (b) and diurnal (c) sounds

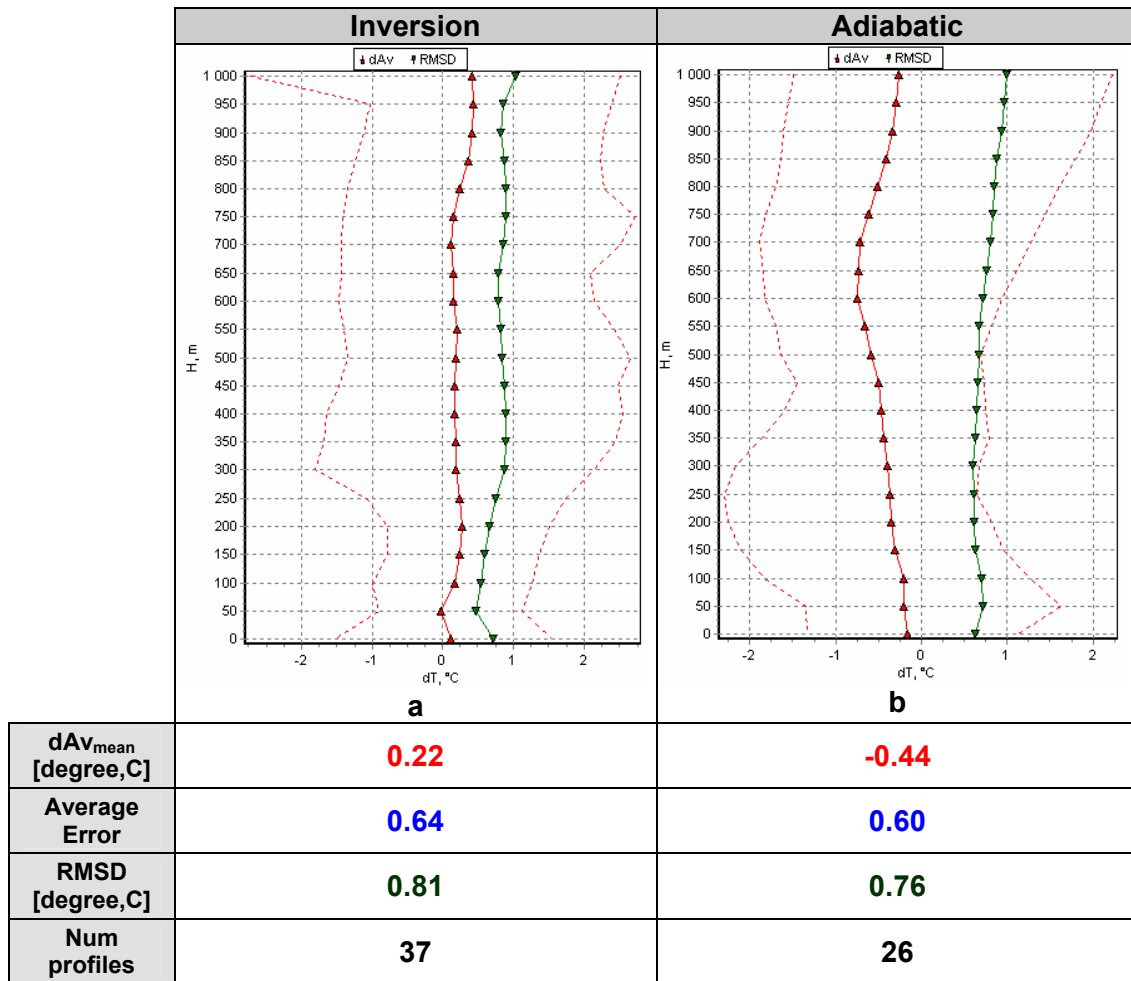


Figure 3. The results of radiosound and profiler data comparison for different stratifications. In figures are shown the values of  $dAv(h)$  and  $RMSD(h)$  and maximum and minimum deviations obtained for statistics when inversion was observed (a) and without inversions (b).

## 5. CONCLUSION

Results of testing MTP-5HE – a new modification of single-channel an angular-scanning microwave temperature profilers - and comparison with radiosondes data from aerological station Dolgoprudny (Russia) and Payerne (Switzerland) confirmed that it can provide continuous ABL temperature profiles measurement in altitude range 0÷1000 m with accuracy about 0,5-0,8°C.

## 6. ACKNOWLEDGMENTS

This work was supported by the Russian Fund for Basic Research, grant nos. 05.05-65288

## REFERENCES

1. Garrat, J.R., 1994: The atmospheric boundary layer. Cambridge Univ. Press, New York, 316.
2. Westwater, E.R., 1993: Ground-based microwave remote sensing of meteorological variables, in: Atmospheric Remote Sensing by Microwave Radiometry, edited by M.A. Janssen. John Wiley, New York.
3. Troitsky A.V., Gajkovich K.P., Gromov V.D., Kadygrov E.N., Kosov A.S. Thermal sounding of the atmospheric boundary layer in the oxygen absorption band center at 60 GHz. IEEE Trans. on Geoscience and Remote Sensing, v. 31, N 1, 1993, pp. 116-120
4. Kadygrov E.N., Pick D.R. The potential for temperature retrieval from an angular-scanning single-channel microwave radiometer and some comparisons with in situ observations. Meteorological Application, 5, 1998, pp. 393-404
5. Westwater E.R., Han Y., Irisov V.G., Lenskiy V., Kadygrov E.N., Viazankin A.S. Remote sensing of boundary layer temperature profiles by a scanning 5-mm microwave radiometer and RASS: Comparison Experiments. Journal of Atmosp., and Ocean. Techn., vol. 16, July 1999, pp. 805-818
6. Kadygrov, E.N., I.N. Kuznetsova, and G.S. Golitsyn, 2002. Heat island above Megapolicy: New results on the basis of remote sensing data. Dokl. Rus. Akad. of Sciences, v.385. No 4, pp. 1-4
7. Kuznetsova, I.N., M.N. Khaikin, and E.N. Kadygrov, 2004. Urban effect on the atmospheric boundary layer temperature from microwave measurements in Moscow and its suburbs. Physics of Atmosp. And Ocean, vol. 40, No 5, pp. 678-688

# THE OPERATIONAL WEB-BASED PRESENTATION OF THE RF UPPER-AIR NETWORK PERFORMANCE MONITORING

A. Kats, A. Naumov, A. Ivanov

Central Aerological Observatory, Roshydromet  
3 Pervomaiskaya Street, Dolgoprudny, 141700, Russian Federation  
Tel.: +(7 095) 408 6677, Fax:+(7 095) 576 3327  
E-mail: [caoaero@mail.ru](mailto:caoaero@mail.ru)

## ABSTRACT

It is presented and discussed the very first experience of regular (on the quarterly basis) publication in Web miscellaneous results of the Russian Federation (RF) upper-air network performance monitoring, covering different aspects of its operation: equipment modernization, data quality and availability, achieved height, regularity of observations. Performance marks are presented either for level of particular stations, territorial bodies of Roshydromet – Regional Administrations for Hydrometeorology and Environmental Monitoring of Roshydromet and for the whole RF network. The 1<sup>st</sup> version of quarterly updated monitoring page has started since 2004 at <http://caometeo.no-ip.org/monitor/monitorres.htm>. Some annual results for the year 2004 are presented here.

Web-based presentation proved itself as a cost-effective and efficient tool for providing operative feed-back to upper-air network from a national upper-data quality monitoring system.

---

In early 90-s under conditions of economic difficulties of the FSU countries it was urgently necessary to concentrate efforts on maintaining in working order and even preservation of upper-air network. Such activity is impossible without comprehensive information about state of network.

Therefore Central Aerological Observatory, as Roshydromet leading centre for upper-air observations, with participation of the Hydrometeorological Centre of Russia (Dr. A.N.Bagrov at al.), Main Computer Centre and Main Radio-Meteorological Centre of Roshydromet, started in 1993 organization and implementation of the national monitoring system of upper-air network operation complementary to the ECMWF (WMO CBS Lead Centres on radiosonde data quality) monitoring, enabling timely preventive and remedial actions on maintaining proper upper-air data quality and performance of upper-air network. After feasibility study since 1994 CAO under financial support of Roshydromet started an official experimental operation of monitoring system, and since 1995 - routine operation.

Source information enters to CAO everyday from the Main Computing Centre data bases as well as directly from the National meteorological telecommunication network and comprises for the FSU and neighbouring countries upper-air stations:

- 00 and 12 UTC de-coded radiosounding results from parts A, B, C and D of **TEMP** messages;
- results of upper-air data complex quality control on standard pressure levels /1/, performed operationally by the Hydrometeorological Centre of Russia data assimilation system;
- geopotential and wind first-guess (FG) field, based on 12-h forecast /2/, for several standard pressure levels, interpolated to the station's locations;
- **NIL** messages, compiled according extended national code form, encoding information on reasons of absence for each missed radiosonde observation, such as routine maintenance, lack of consumables, failure of ground equipment, absence of energy, severe weather conditions and so on.

Data are collected and processed on conventional PC which so far allows to store and analyse data bases for the whole period of operation. Different aspects of upper-air network operation under monitoring include fulfilment of program of observations, reasons of stations downtime, completeness and quality of observations. Developed software allows generation in operational mode different kinds of monthly, quarterly and annual reports for stations, regional administrations and member states of the Intergovernmental Council for Hydrometeorology of the Commonwealth of Independent States, e.g.:

- detailed monthly list of soundings and reasons of observations absence;
- statistics of program of observations fulfillment for 00 and 12 UTC and both terms;
- statistics of soundings heights;
- reasons of failure of observations statistics;
- rejected data statistics;
- (OB-FG) geopotential and wind statistics and their distributions and lists of suspected stations for geopotential and wind observations (followinging to recommendations of /3/).

Analysis of monitoring results as well as direct mutual exchange by monitoring statistics and intercomparison with ECMWF, UK Met Office and JMA proved us in skill of statistics, based on the Hydrometeorological Centre of Russia FG, to reflect the real upper-air data quality. An example of such assessment is given on Figure 1.1 - Figure 1.4 where presented are correlation between ECMWF (taken from supported by the UK Met Office radiosonde team EUMETNET radiosonde web site <http://www.metoffice.com/research/interproj/radiosonde/reports/index.html>) and Hydrometeorological Centre of Russia quarterly monitoring statistics for the year 2000: 00 and 12 UTC (OB-FG) geopotential bias and standard deviation. Despite of some apparent particular inconsistencies\*, a general agreement is evident, especially for stations with larger systematic and random deviations, i.e. for cases of the most practical significance.

The national monitoring system was successfully operated for quite a long period but its output (more or less extensive tables and reports) had rather limited distribution: monthly results were presented regularly to Roshydromet only, and limited information entered regional administrations just in emergency urgent cases (data quality problems with particular soundings or suspected operation). And only once per year annual CAO survey of RF network operation with monitoring results reached all interested bodies.

Recent progress in telecommunications made it possible to bring to public pictorial information on monitoring results in much more timely way using Internet. Almost all regional administrations have an access to Internet and about 60 upper-air stations have PC in their ground systems, i.e. they potentially are able to have off-line access to these materials.

There were developed rather plain HTML templates suitable for presentations of quarterly and annual results. Original software was developed to create maps, suitable for displaying and publishing to Web miscellaneous performance indicators for the whole network. To keep brevity, names and indices of upper-air stations are displayed using tooltips, which are displayed by browser when the users mouse pauses over the station symbol.

The very first experience with publication of annual results for the year 2003 met a good responses and in 2004 it was started regular quarterly publications. The starting page (in Russian) of the CAO upper-air network monitoring is located at <http://caometeo.no-ip.org/monitor/monitorres.htm>. English version at the moment of preparation of this paper was available only for the annual results of the year 2004 at <http://caometeo.no-ip.org/monitor/2004/index2004e.htm>.

For the illustration of published results and forms of their presentation is given as an example the information presented for the year 2004.

---

\* Some systematic inconsistency in standard deviations results from different procedure of quarterly averaging, other cases are worth of separate investigation

The first page "Network configuration and observational program" presents actual configuration of sounding equipment by the end of the period under report and program of observations actual for the reporting period (Figure 2.1 - Figure 2.2).

Next page "Data availability" reflects overall percentage of observational program fulfillment for each station, quarterly distribution of stations amount by average daily number (for 00 and 12 UTC and for both times) of ascents and quarterly distribution of average daily number of ascents (Figure 3.1 - Figure 3.3).

"Data quality marks" presents network maps and diagrams with distribution of stations for the average heights of soundings, weighted (following procedure /3/) root-mean-square 'OB-FG' geopotential differences in 1000-100 hPa layer, root-mean-square 'OB-FG' wind vector differences in 850-100 hPa layer (Figure 4.1 - Figure 4.6).

To some extent the present work was simulated by ideas, implemented by USA NWS in the National Upper-air Station Performance Ranking Program /4/. However, the Russian upper-air network is rather bulky to have all stations ranked in a compact way. The Roshydromet manage hydrometeorological service throughout the country via its territorial bodies - Regional Administration for Hydrometeorology and Environmental Monitoring (Russian acronym is UGMS). To stimulate an interest and responsibility of regional administrations to manage and control operation upper-air station, situated on their territory, on the page "Regional administrations (UGMS) ranking" average results of above mentioned statistics for regional administrations are presented ordered according to their values (Figure 5.1 - Figure 5.5).

And the final page "The results of the RF upper-air network performance monitoring" presents a summary table\* with numerical presentation of annual results for each station, regional administration and the whole network (Table 1).

The monitoring system itself should be re-designed in 2005 in connection with modernization of computers park and of Main Computer Centre and relevant changes in technology of the Hydrometeorological Centre of Russia. These changes must result in use FG, based on 6-h forecast, with all levels up to and some levels above 100 hPa, temperature FG, quality control flags, reflecting reasons for data rejection, raw TEMP messages with time of their parts receiving, direct FTP-access to source information instead of dial-up line. Therefore the amount of results to be published on regular basis is expected to substantial extension, first and foremost, in favor of monthly publications and trend representations.

Regular publication in Internet even such limited amount of information about performance the Russian upper-air network got a keen interest from staff of regional administrations, dealing with maintenance and control of upper-air stations, upper-air stations themselves and even from manufacturer of upper-air equipment. The Russian upper-air network nowadays meets new but positive challenges: in year 2005 two-times sounding must re-start on the whole network and new-generation MARL radars started recently to displace obsolete Meteorites. The national monitoring system and operational dissemination of its results are expected to support and manage these events.

#### **References:**

1. O.A. Alduchov, 1983. Meteorologia i Gidrologia [Soviet Meteorology and Hydrology], No. 12.
2. A.N. Bagrov, 1990. Meteorologia i Gidrologia [Soviet Meteorology and Hydrology], No. 2.
3. WMO No.485, 1992. Manual on the Global Data-Processing System, Edition 1992. Volume I - Global Aspects. Attachment II.10 Procedures and formats for the exchange of monitoring results
4. C. Bower, W. Blackmore, 2000. USA National Weather Service Radiosonde Upper Air Excellence Award Program. INSTRUMENTS AND OBSERVING METHODS. REPORT No. 74 (WMO/TD - No. 1028). Papers Presented at the WMO Technical Conference on Meteorological and Environmental Instruments and Methods of Observation (TECO-2000), Beijing, China, 23 - 27 October 2000.

---

\* Station symbols on each map on the previous pages are linked to the corresponding row of the summary table

Figures:

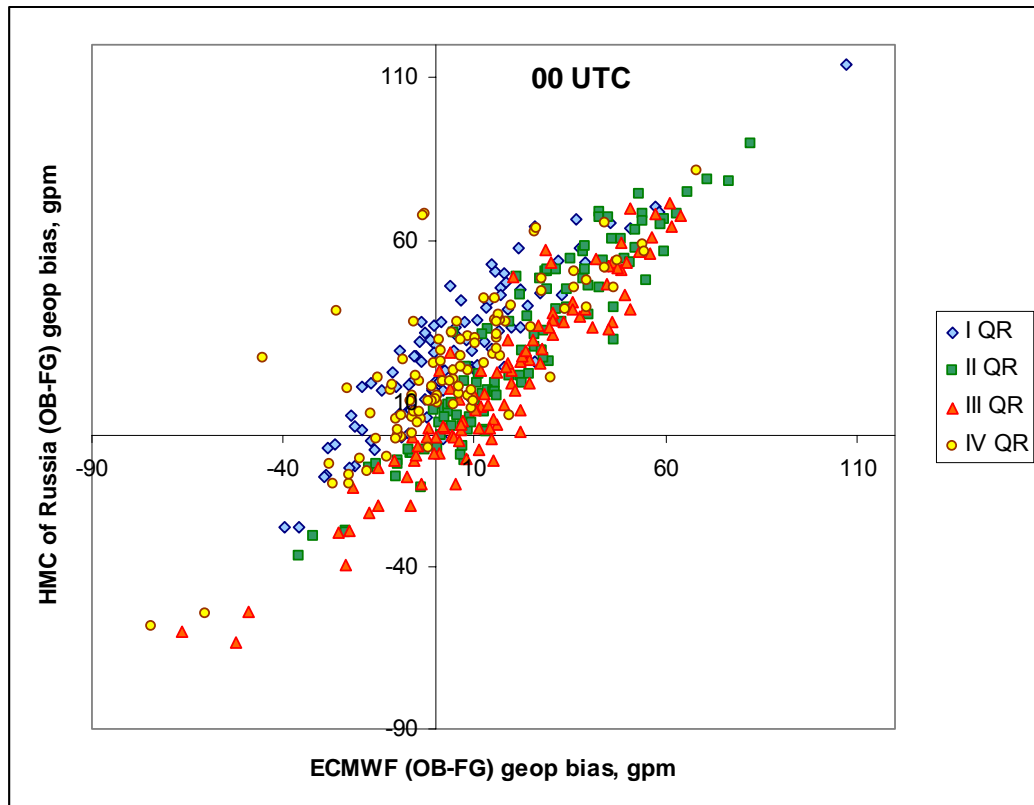


Figure 1.1. Comparison of ECMWF and Hydrometeorological Centre of Russia quarterly monitoring statistics for the year 2000: 00 UTC (OB-FG) geopotential bias.

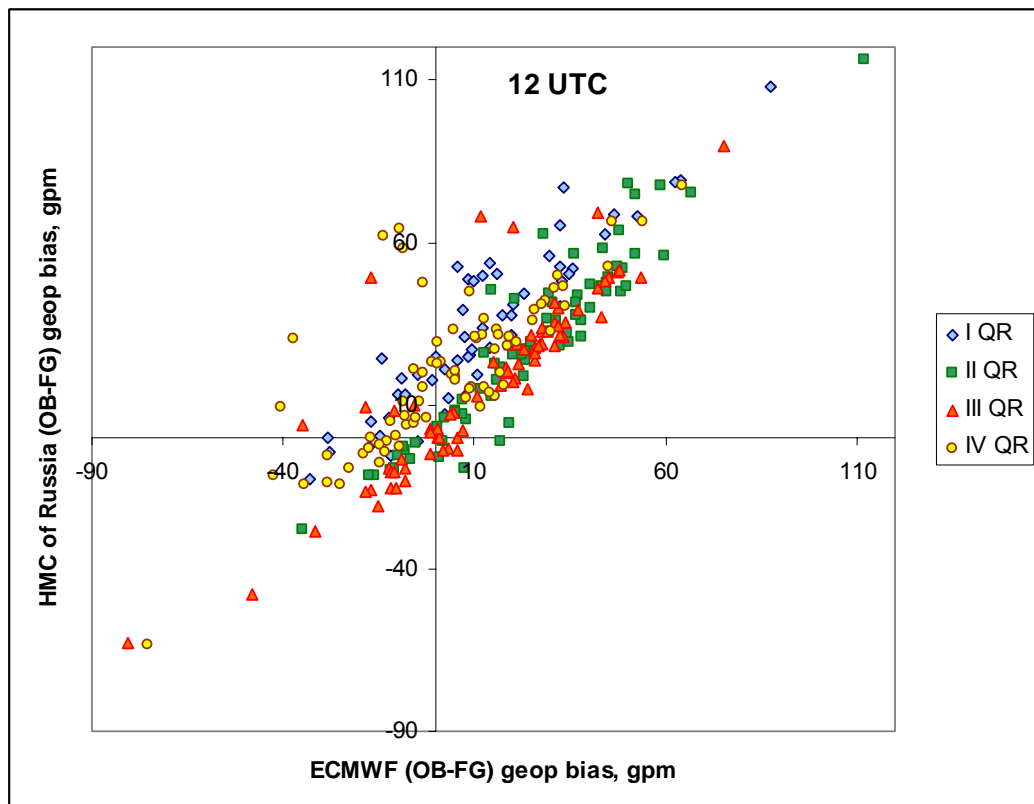


Figure 1.2. Comparison of ECMWF and Hydrometeorological Centre of Russia quarterly monitoring statistics for the year 2000: 12 UTC (OB-FG) geopotential bias.

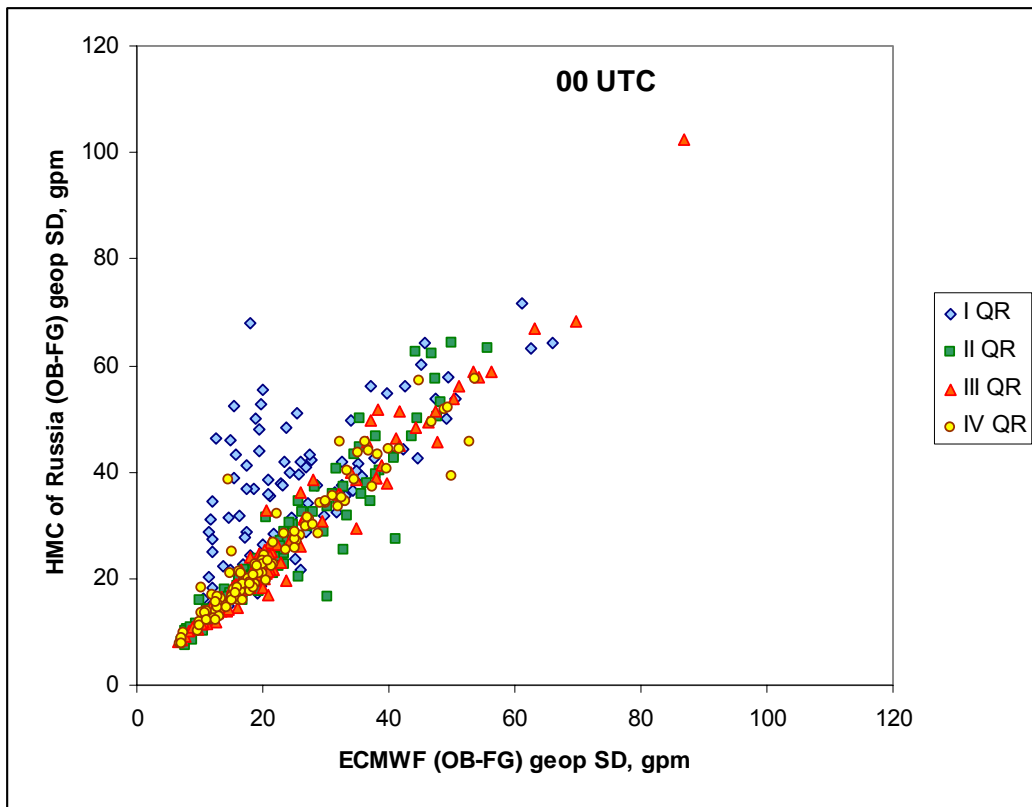


Figure 1.3. Comparison of ECMWF and Hydrometeorological Centre of Russia quarterly monitoring statistics for the year 2000: 00 UTC (OB-FG) geopotential standard deviation.

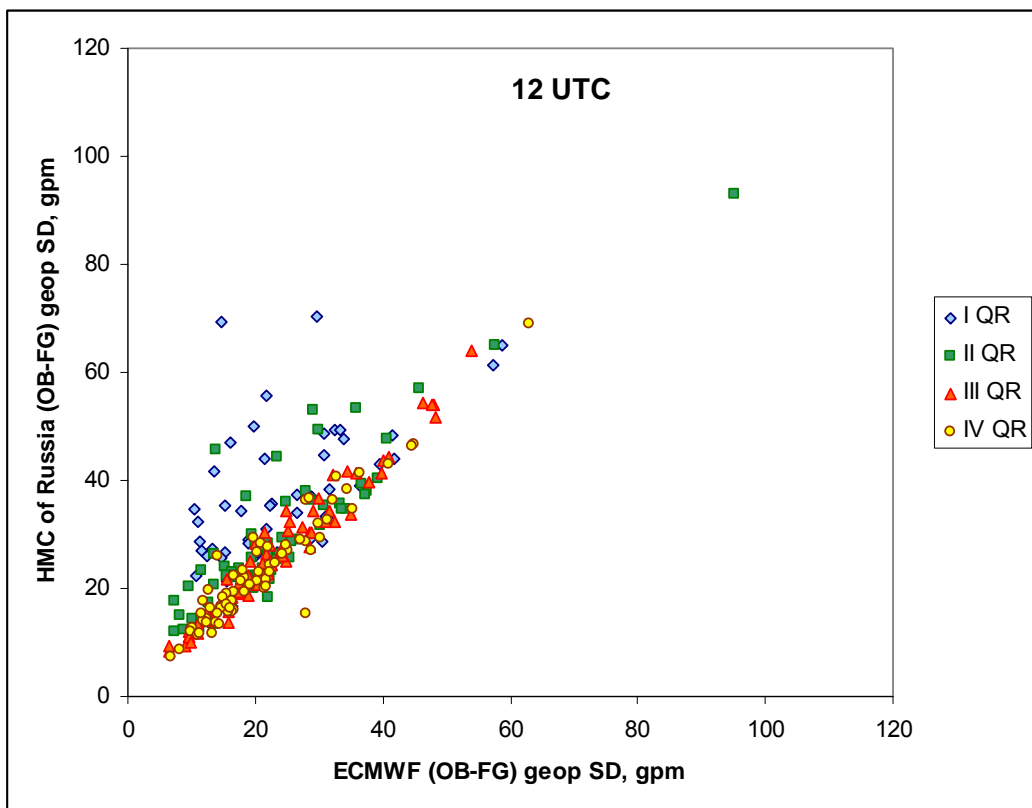


Figure 1.4. Comparison of ECMWF and Hydrometeorological Centre of Russia quarterly monitoring statistics for the year 2000: 12 UTC (OB-FG) geopotential standard deviation.



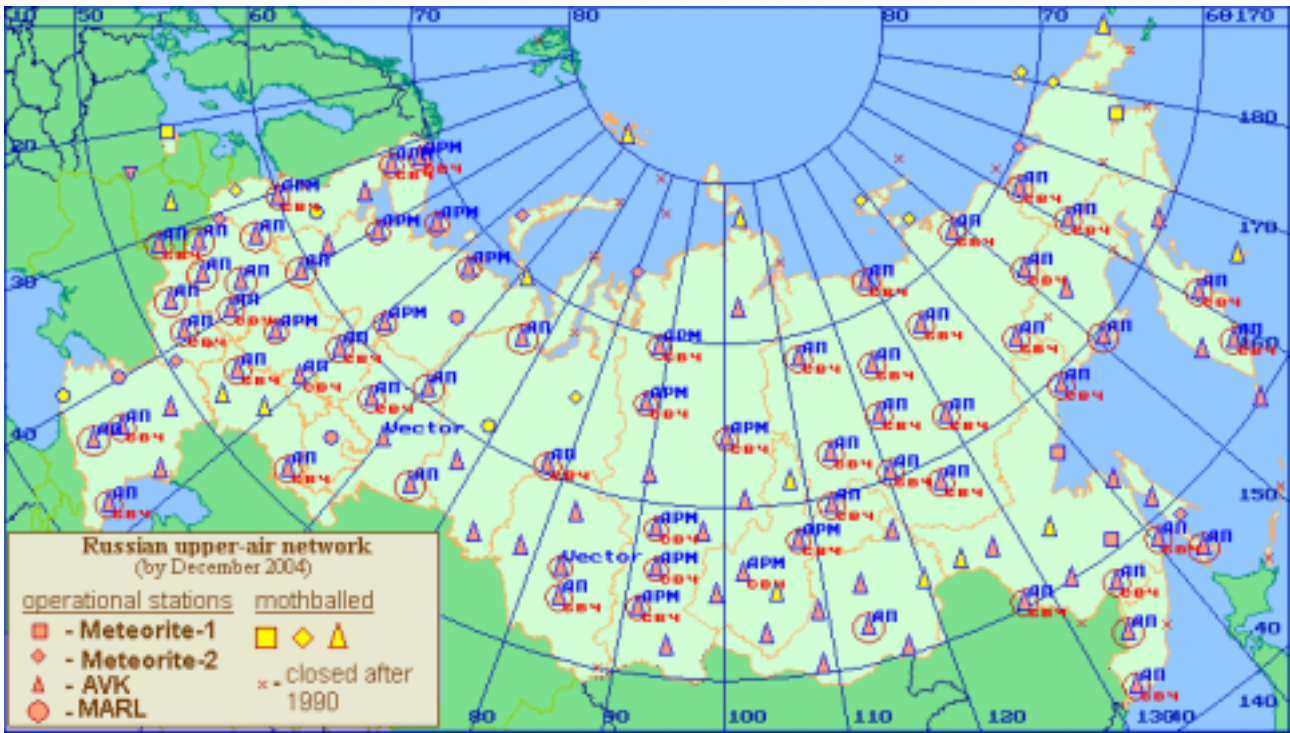


Figure 2.1. Russian upper-air network equipment (by December 2004): "CBЧ" - new solid-state microwave modules installed, which have displaced non-durable electro-vacuum devices, "АП" and "АРМ" – new PC-based data processing systems installed, which have displaced unreliable hardwired microcomputers

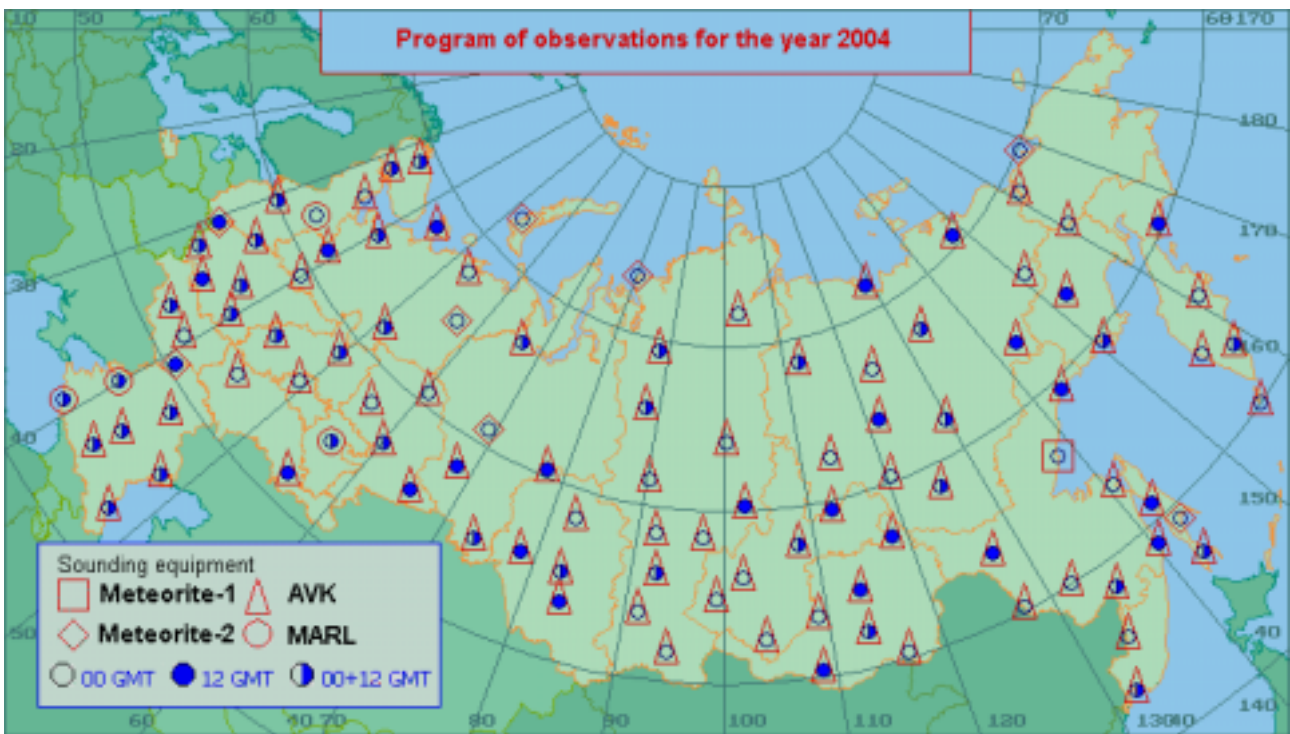


Figure 2.2. Observational program of Russian upper-air network for the year 2004.

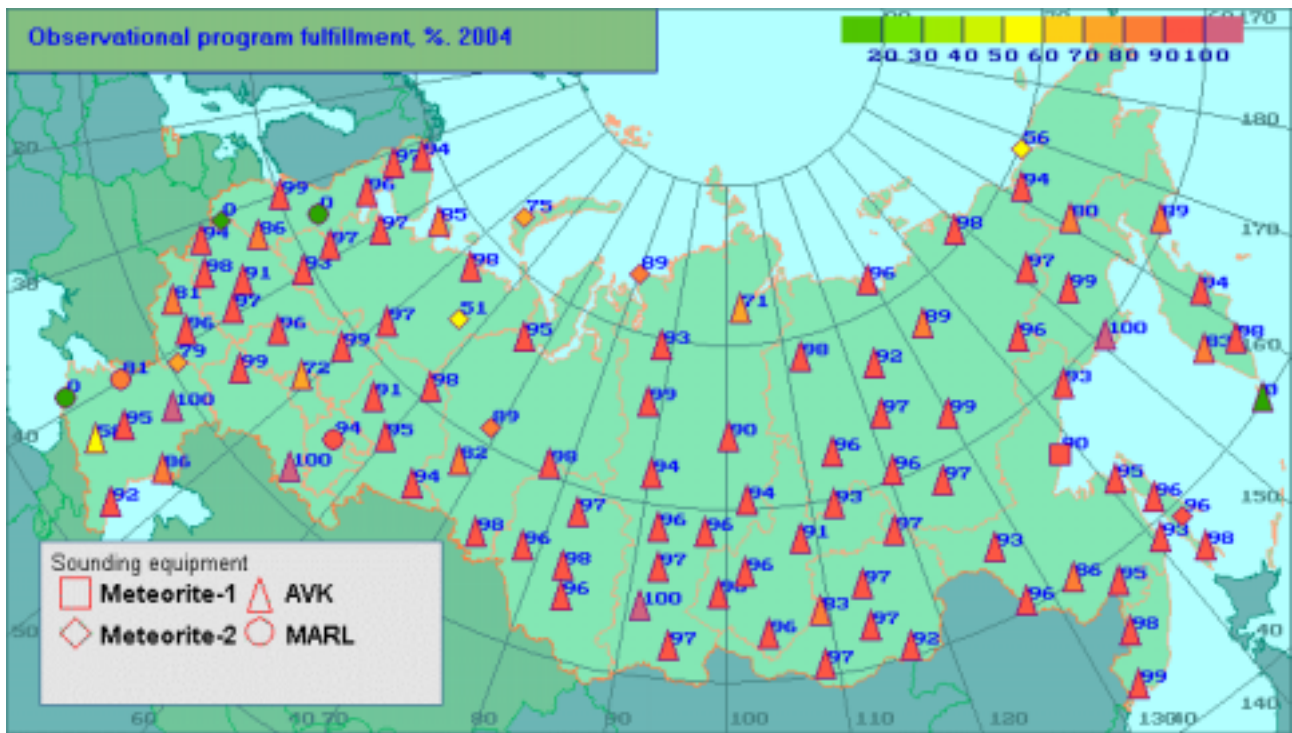


Figure 3.1. Percentage of observational program fulfillment for the year 2004.

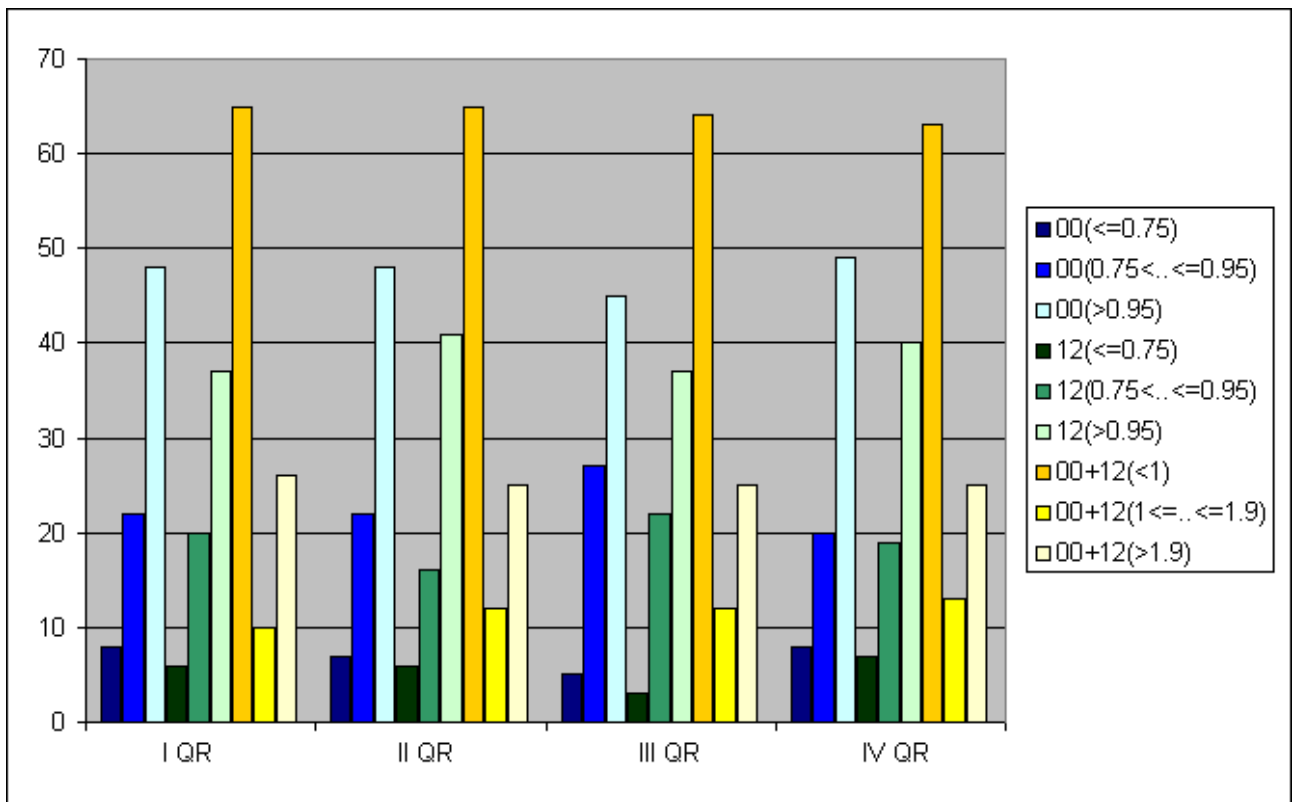


Figure 3.2. Distribution of stations amount by average number of ascents (00, 12 UTC and daily) - by the quarter. 2004.

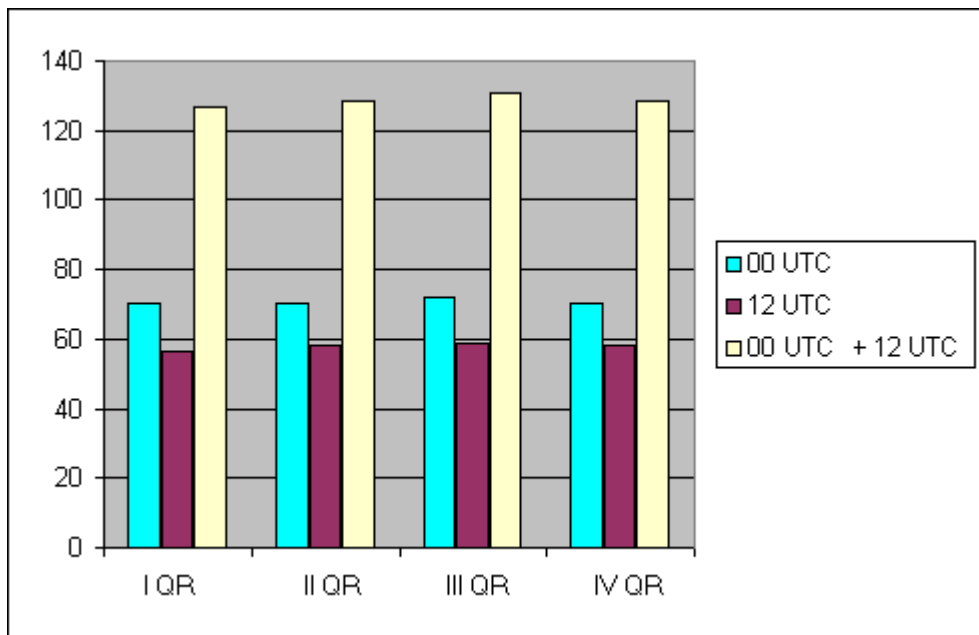


Figure 3.3. Daily amount of ascents - by the quarter. 2004.

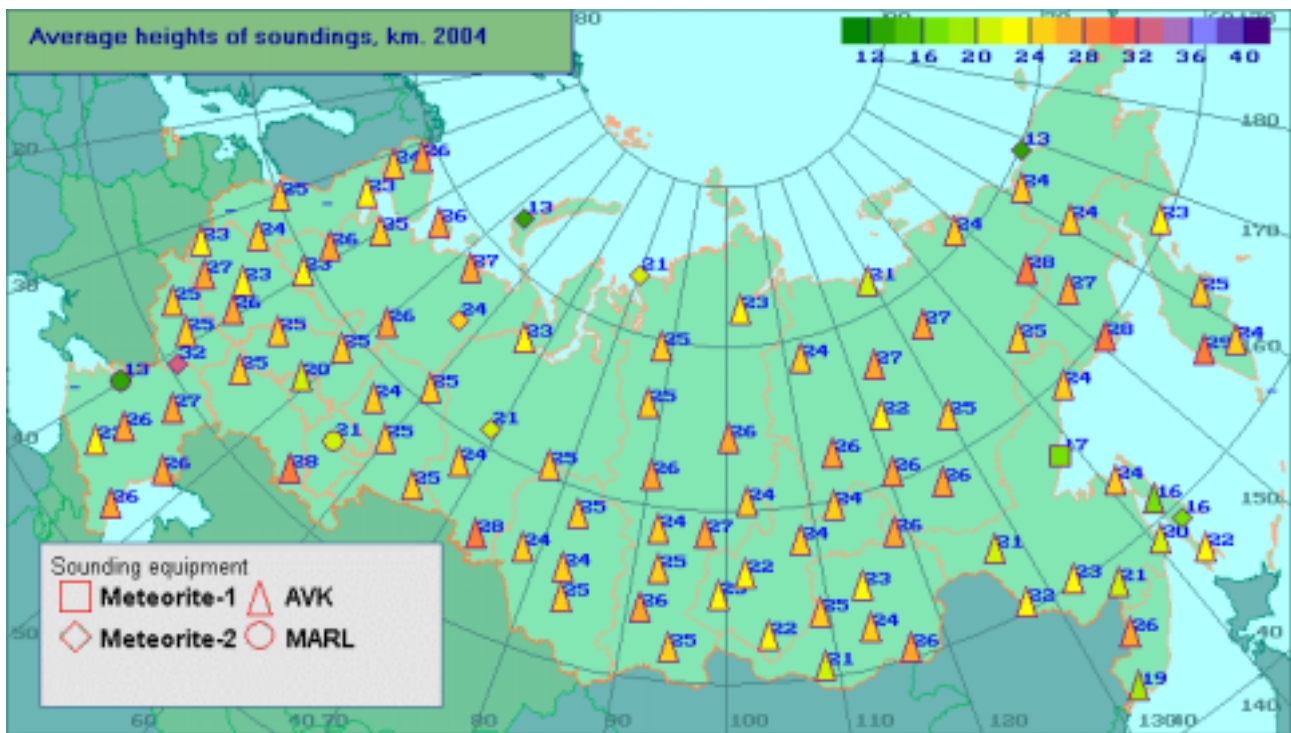


Figure 4.1. Average heights of soundings.

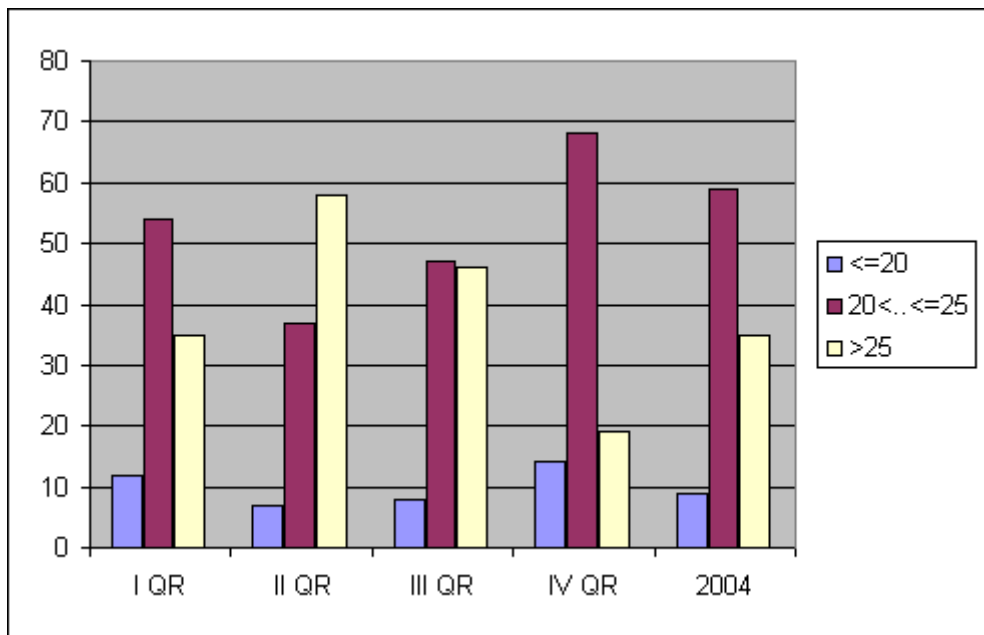


Figure 4.2. Distribution of stations amount by average heights of soundings, km. 2004.

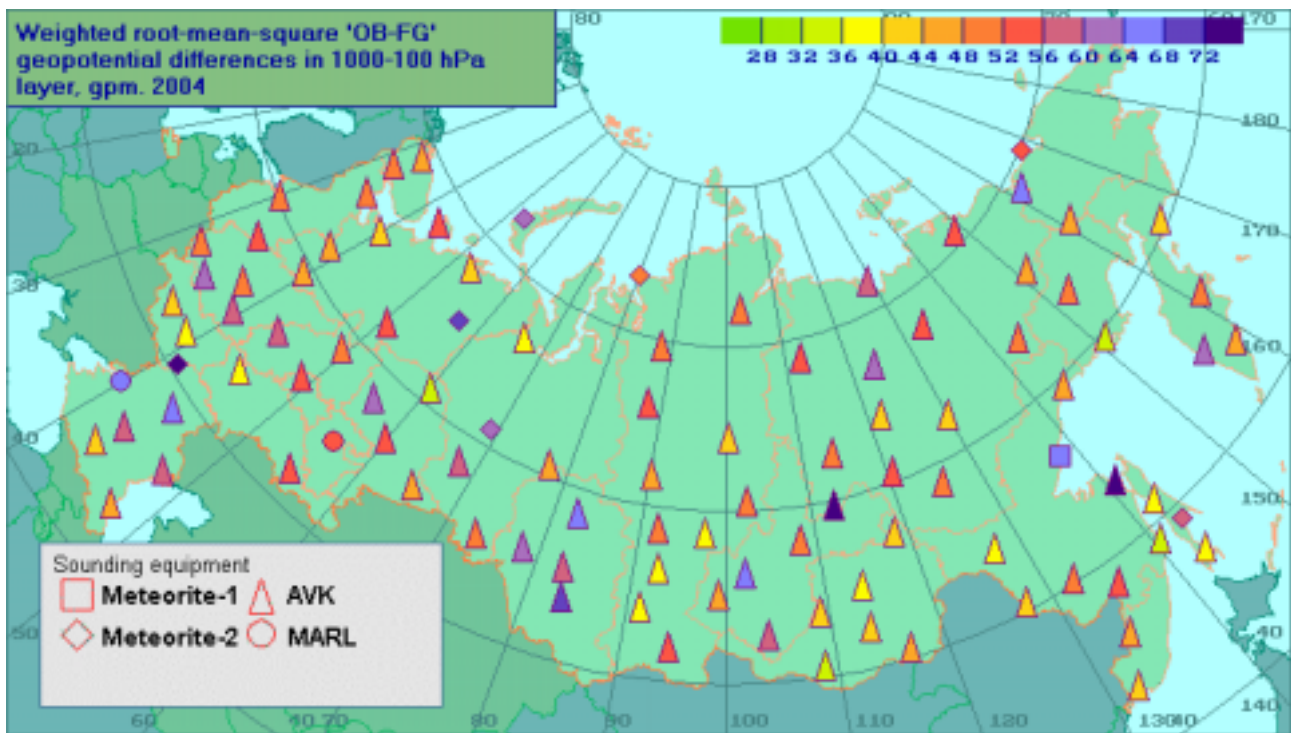


Figure 4.3. Weighted root-mean-square 'OB-FG' geopotential differences in 1000-100 hPa layer

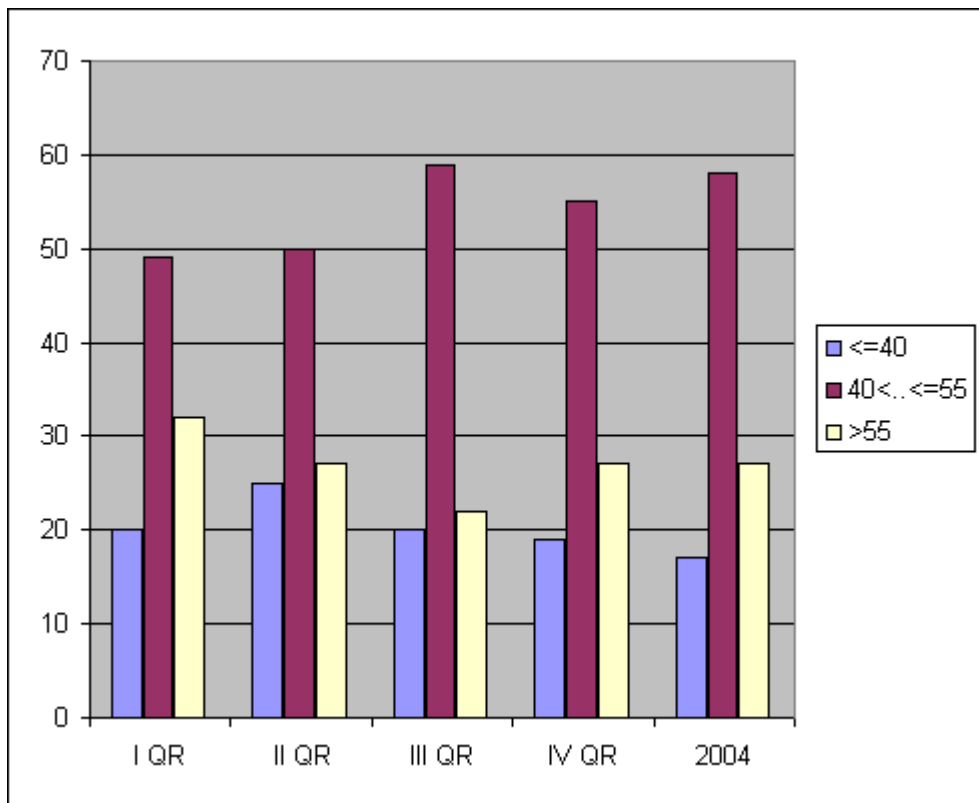


Figure 4.4. Distribution of stations amount by weighted root-mean-square 'OB-FG' geopotential differences, gpm. 2004.

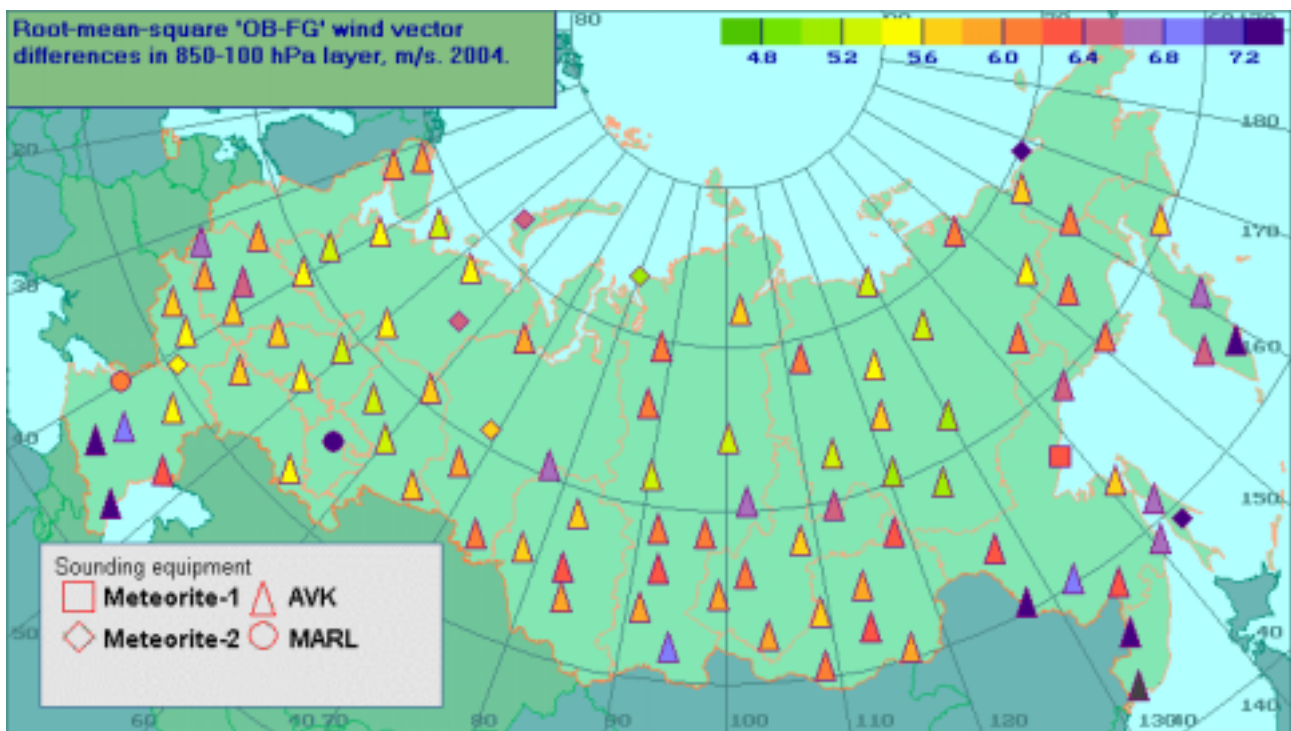


Figure 4.5. Root-mean-square 'OB-FG' wind vector differences in 850-100 hPa layer.

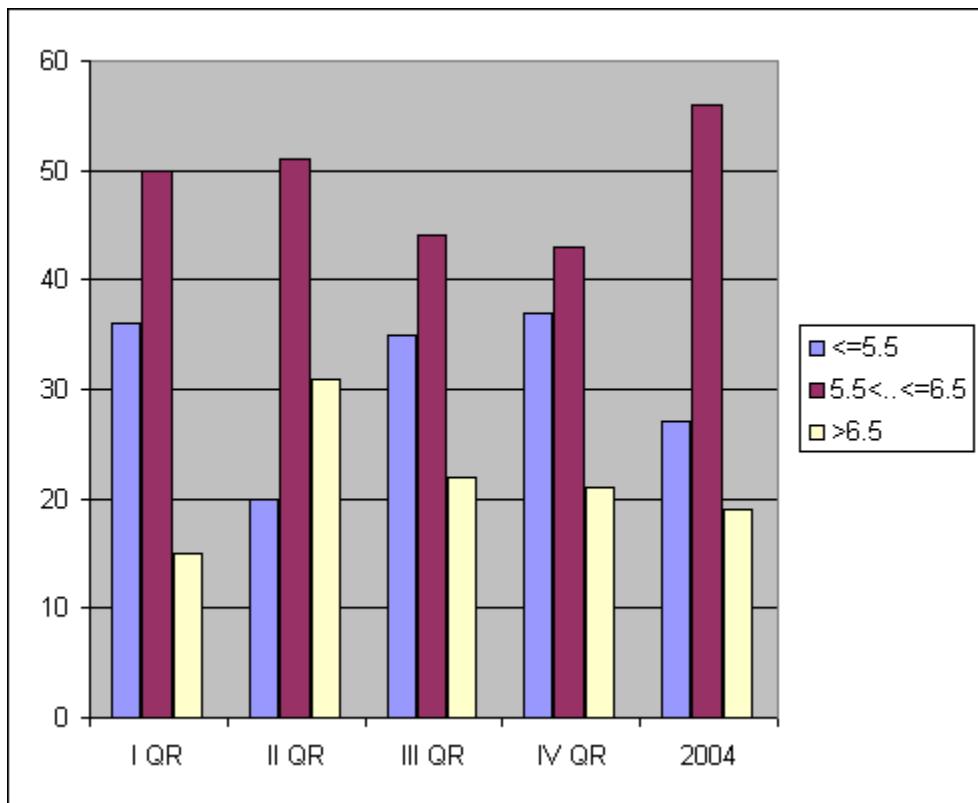


Figure 4.6. Distribution of stations amount by root-mean-square 'OB-FG' wind vector differences, m/s.2004.

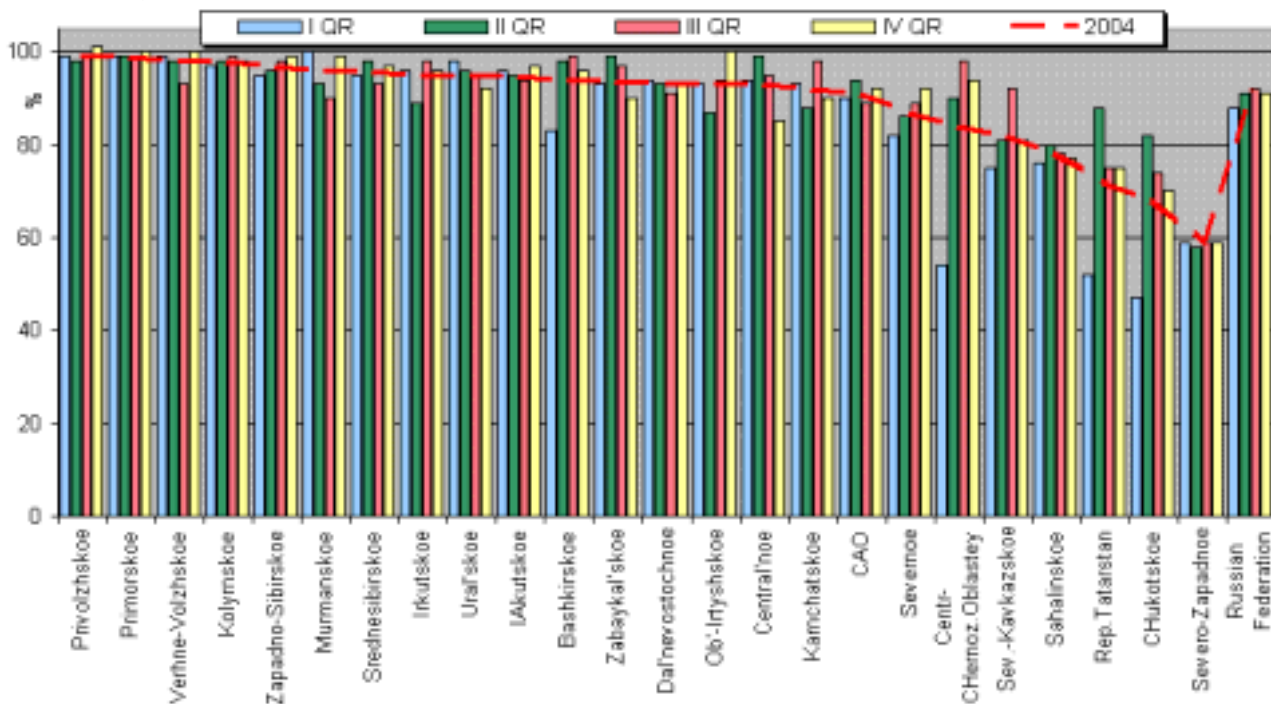


Figure 5.1. Regional administrations ranking: by upper-air observational program fulfillment.

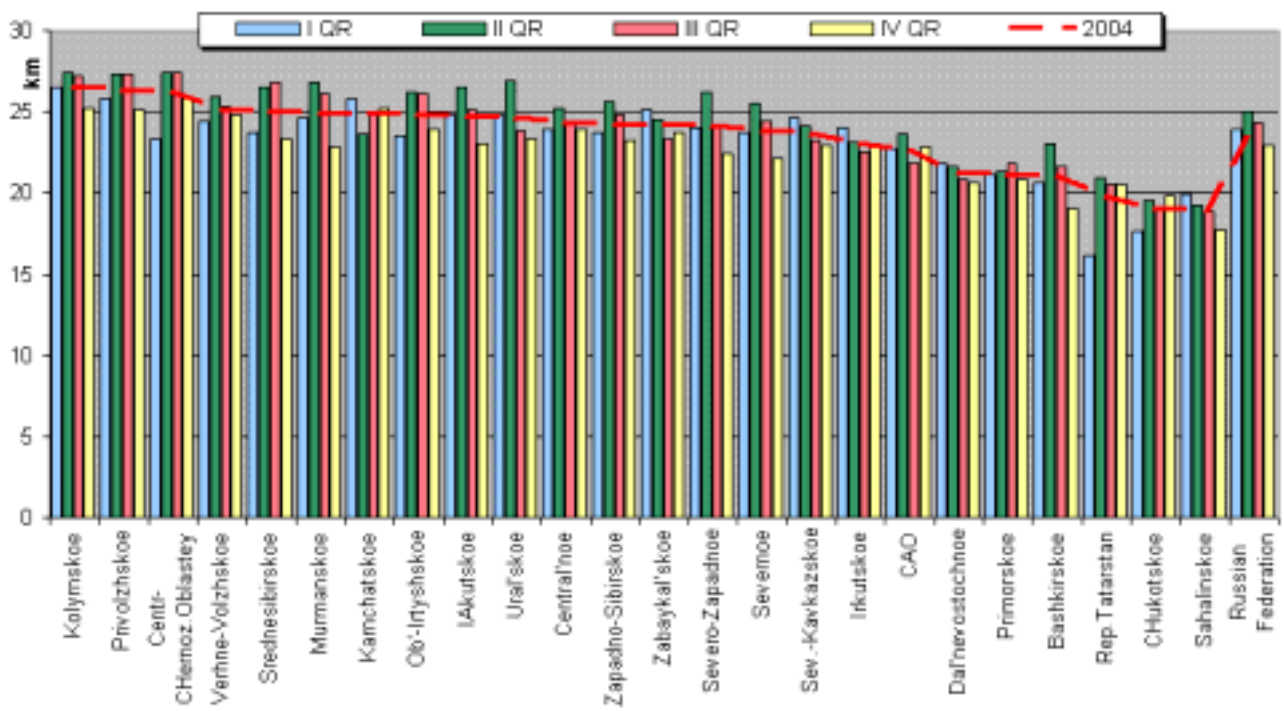


Figure 5.1. Regional administrations ranking: by upper-air observational program fulfillment.  
 .2. Regional administrations ranking: by average heights of soundings.

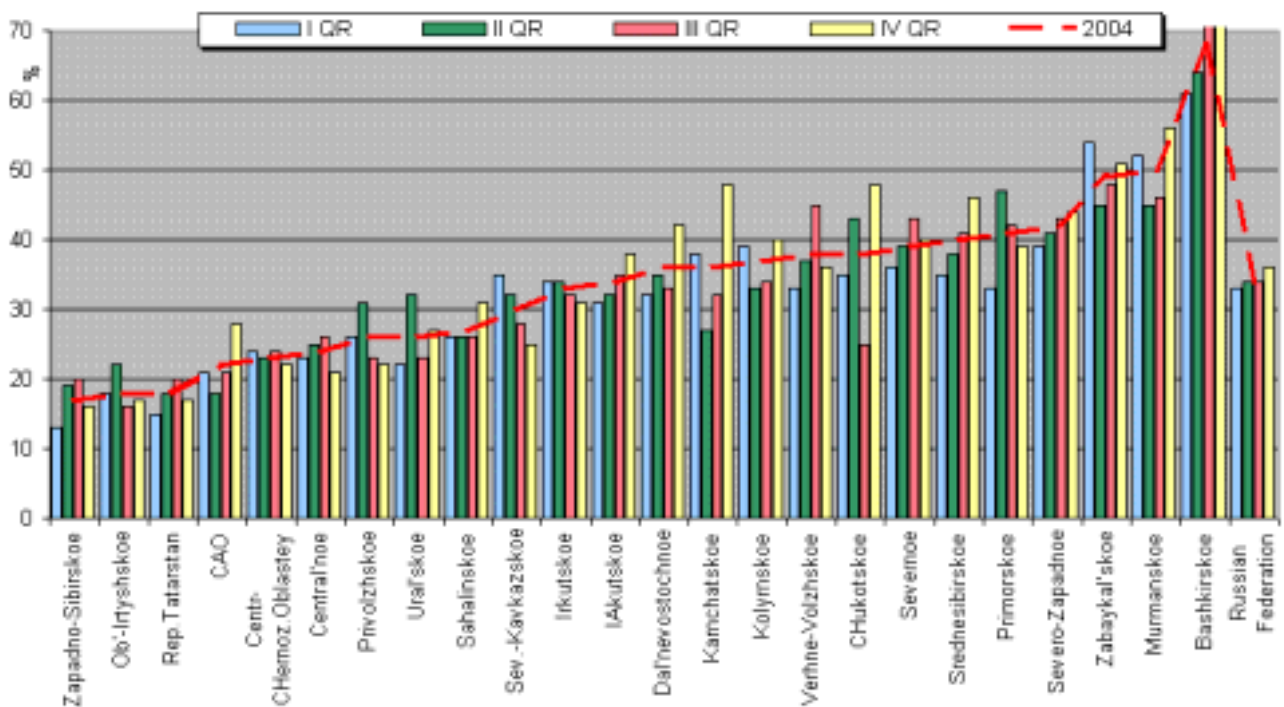


Figure 5.3. Regional administrations ranking: by percentage of soundings with rejected data.

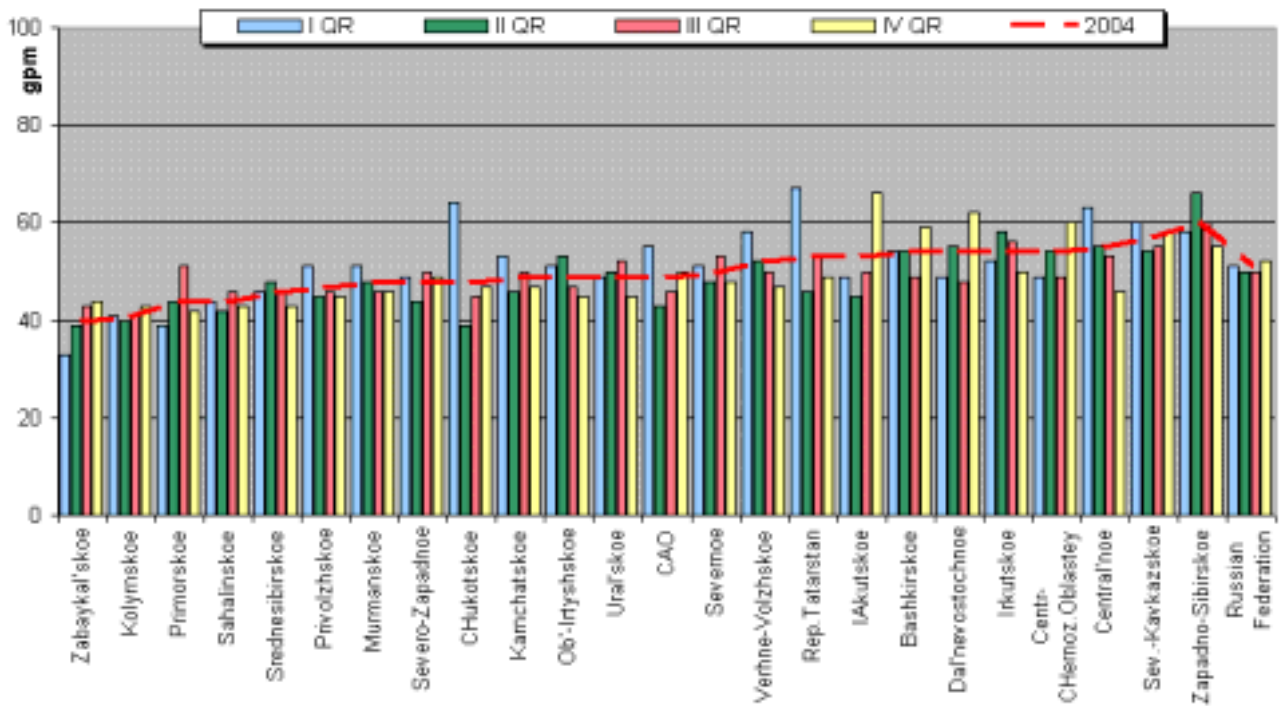


Figure 5.4. Regional administrations ranking: by weighted root-mean-square 'OB-FG' geopotential differences in 1000-100 hPa layer.

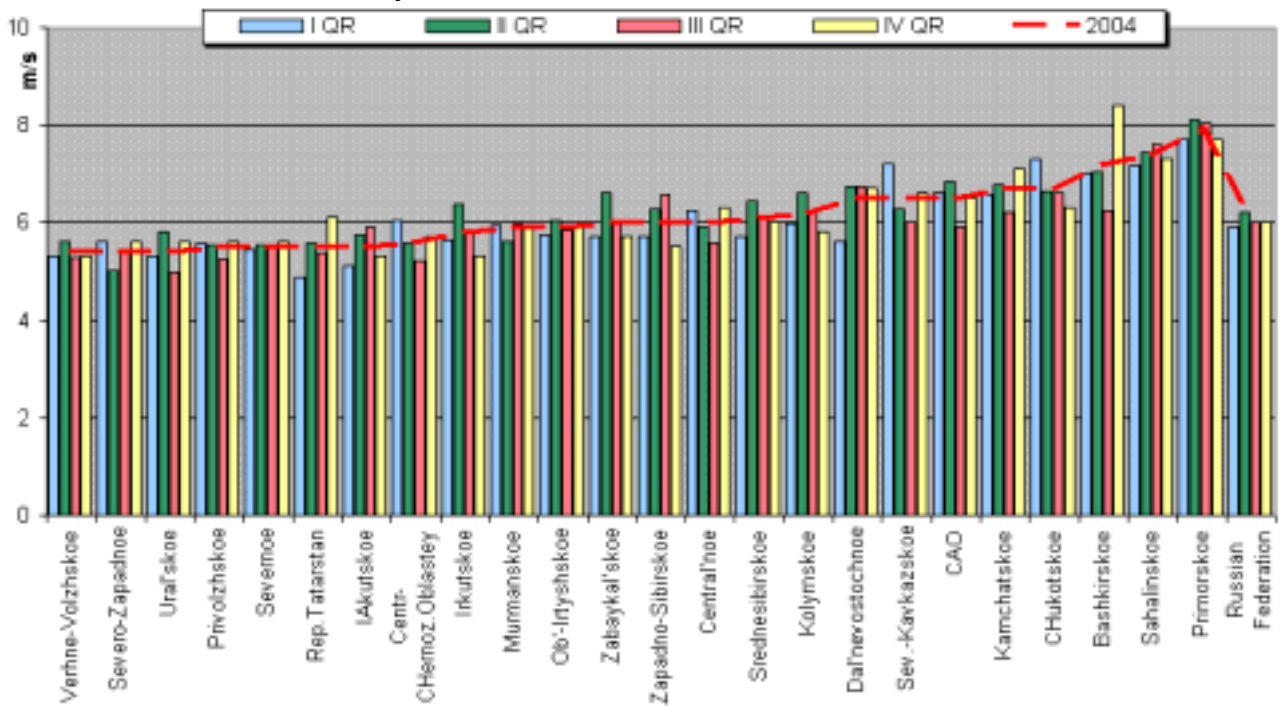


Figure 5.5. Regional administration ranking: by Root-mean-square 'OB-FG' wind vector differences in 850-100 hPa layer.



Table 1 Summary results of the RF upper-air network performance monitoring in the year 2004.

Stations/Regional administrations	a1	a2	a	b	b1	c1	c2	c3	c	d	e	f	g	h
Ufa	99	89	94	46	21.1	1	5	6	68	-	+	+	54	7.2
<b>Bashkirskoe UGMS/ 1</b>	<b>99</b>	<b>89</b>	<b>94</b>	<b>46</b>	<b>21.1</b>	<b>1</b>	<b>5</b>	<b>6</b>	<b>68</b>	<b>0</b>	<b>1</b>	<b>1</b>	<b>54</b>	<b>7.2</b>
Kirov	99	99	99	26	24.8	2	3	1	20	-	-	-	48	5.2
Nizhniy Novgorod	96	96	96	23	25.4	2	2	2	56	-	-	-	56	5.6
<b>Verhne-Volzskoe UGMS/ 2</b>	<b>97</b>	<b>98</b>	<b>98</b>	<b>25</b>	<b>25.1</b>	<b>2</b>	<b>2</b>	<b>2</b>	<b>38</b>	<b>0</b>	<b>0</b>	<b>0</b>	<b>52</b>	<b>5.4</b>
Aian	90	-	90	85	17.2	0	1	3	30	-	-	-	65	6.2
Zeia	-	93	93	47	21	1	1	2	35	-	-	-	39	6.2
Nikolaevsk	94	-	95	31	23.7	1	4	3	39	+	-	-	84	5.6
Blagoveshensk	95	-	96	37	22.4	1	1	3	38	-	+	+	42	7.4
Sutur	85	-	86	35	22.9	2	2	4	55	-	+	-	50	6.9
Habarovsk	96	95	95	44	21.4	0	0	2	27	-	+	-	52	6.2
Sovetskaia Gavan'	-	93	93	56	19.8	0	1	4	36	-	+	-	34	6.7
<b>Dal'nevostochnoe UGMS/ 7</b>	<b>92</b>	<b>95</b>	<b>93</b>	<b>45</b>	<b>21.2</b>	<b>1</b>	<b>1</b>	<b>3</b>	<b>36</b>	<b>1</b>	<b>4</b>	<b>1</b>	<b>54</b>	<b>6.5</b>
CHara	-	97	97	22	25.9	1	2	4	50	+	-	-	41	6.2
Bagdarin	-	97	97	33	23.2	1	1	3	35	-	-	-	37	5.9
Ust'-Barguzin	83	-	83	24	25.3	2	2	5	59	-	-	-	40	5.7
CHita	97	97	97	31	23.7	1	1	5	55	+	-	-	40	6.2
Krasnyy CHikoy	-	97	97	44	21.4	1	1	4	42	-	-	-	35	6
Borzia	92	-	92	21	26.2	2	2	3	50	-	-	-	46	5.8
<b>Zabaykal'skoe UGMS/ 6</b>	<b>91</b>	<b>97</b>	<b>94</b>	<b>29</b>	<b>24.2</b>	<b>1</b>	<b>1</b>	<b>4</b>	<b>49</b>	<b>2</b>	<b>0</b>	<b>0</b>	<b>40</b>	<b>6</b>
Aleksandrovsкое	-	98	98	26	24.7	0	0	1	16	-	-	-	44	6.6
Kolpashevo	96	-	97	26	24.7	0	1	1	19	-	-	-	65	5.7
Barabinsk	-	96	96	28	24.4	0	1	1	12	-	-	-	63	5.6
Novosibirsk	99	97	98	30	23.9	0	1	1	15	-	-	-	57	6.2
Barnaul	-	96	96	27	24.5	1	1	2	25	-	-	-	70	5.8
<b>Zapadno-Sibirskoe UGMS/ 5</b>	<b>98</b>	<b>97</b>	<b>97</b>	<b>28</b>	<b>24.3</b>	<b>0</b>	<b>1</b>	<b>1</b>	<b>17</b>	<b>0</b>	<b>0</b>	<b>0</b>	<b>60</b>	<b>6</b>
Nizhneudinsk	98	-	98	33	23.3	1	1	3	35	-	-	-	44	5.8
Kirensk	91	92	91	29	24	0	1	2	31	-	-	-	49	5.6
Bratsk	96	-	96	38	22.3	0	0	3	31	-	-	-	66	6
Angarsk	96	-	96	39	22.2	1	0	3	36	-	-	-	58	5.9
<b>Irkutskoe UGMS/ 4</b>	<b>95</b>	<b>92</b>	<b>95</b>	<b>34</b>	<b>23.1</b>	<b>0</b>	<b>1</b>	<b>3</b>	<b>33</b>	<b>0</b>	<b>0</b>	<b>0</b>	<b>54</b>	<b>5.8</b>
Korf	-	89	89	34	23.1	0	1	2	23	-	-	-	40	5.7
Kliuchi	94	-	94	24	25.2	1	1	3	34	-	-	-	48	6.6
Sobolevo	83	-	83	13	29.3	2	2	4	53	-	-	-	63	6.4
Petropavlovsk	96	99	98	31	23.7	0	1	3	36	-	-	-	47	7.2
<b>Kamchatskoe UGMS/ 4</b>	<b>91</b>	<b>94</b>	<b>92</b>	<b>26</b>	<b>24.9</b>	<b>1</b>	<b>1</b>	<b>3</b>	<b>36</b>	<b>0</b>	<b>0</b>	<b>0</b>	<b>49</b>	<b>6.7</b>
Seymchan	-	99	99	19	26.8	3	3	3	43	-	-	-	51	6
Magadan	100	100	100	17	27.6	0	1	3	36	-	-	-	32	6.1
Ohotsk	-	93	93	29	24.1	0	1	3	30	-	-	-	47	6.5
<b>Kolym'skoe UGMS/ 3</b>	<b>100</b>	<b>98</b>	<b>98</b>	<b>20</b>	<b>26.6</b>	<b>1</b>	<b>1</b>	<b>3</b>	<b>37</b>	<b>0</b>	<b>0</b>	<b>0</b>	<b>41</b>	<b>6.2</b>
Murmansk	95	94	94	21	26.1	3	3	2	50	+	-	-	46	5.8
Kandalaksha	97	97	97	29	24	3	3	2	50	-	-	-	50	5.9
<b>Murmanskoe UGMS/ 2</b>	<b>96</b>	<b>95</b>	<b>96</b>	<b>25</b>	<b>25</b>	<b>3</b>	<b>3</b>	<b>2</b>	<b>50</b>	<b>1</b>	<b>0</b>	<b>0</b>	<b>48</b>	<b>5.9</b>
Salehard	96	95	95	33	23.2	0	0	1	17	-	-	-	39	5.8
Hanty-Mansiysk	89	-	89	49	20.8	1	3	1	28	-	-	-	62	5.7
Tobol'sk	-	82	82	30	23.8	1	1	1	20	-	-	-	59	5.8
Omsk	98	98	98	16	27.8	0	0	1	17	-	-	-	51	6
<b>Ob'-Irtyskoe UGMS/ 4</b>	<b>95</b>	<b>91</b>	<b>93</b>	<b>26</b>	<b>24.9</b>	<b>0</b>	<b>1</b>	<b>1</b>	<b>18</b>	<b>0</b>	<b>0</b>	<b>0</b>	<b>49</b>	<b>5.9</b>
Penza	99	-	99	24	25.2	0	2	2	27	-	-	-	39	5.6

<b>Stations/Regional administrations</b>	<b>a1</b>	<b>a2</b>	<b>a</b>	<b>b</b>	<b>b1</b>	<b>c1</b>	<b>c2</b>	<b>c3</b>	<b>c</b>	<b>d</b>	<b>e</b>	<b>f</b>	<b>g</b>	<b>h</b>
Orenburg	-	99	100	17	27.5	0	1	2	24	-	-	-	53	5.4
<b>Privolzhskoe UGMS/ 2</b>	<b>99</b>	<b>99</b>	<b>99</b>	<b>20</b>	<b>26.4</b>	<b>0</b>	<b>1</b>	<b>2</b>	<b>26</b>	<b>0</b>	<b>0</b>	<b>0</b>	<b>47</b>	<b>5.5</b>
Dal'nerechensk	98	-	98	22	25.9	0	0	3	35	-	+	-	45	7.6
Sad-gorod	99	99	99	64	19	1	1	5	43	-	+	-	43	8.1
<b>Primorskoe UGMS/ 2</b>	<b>99</b>	<b>100</b>	<b>99</b>	<b>45</b>	<b>21.2</b>	<b>1</b>	<b>1</b>	<b>4</b>	<b>41</b>	<b>0</b>	<b>2</b>	<b>0</b>	<b>44</b>	<b>7.9</b>
Aleksandrovsk	-	94	96	102	16	0	1	3	28	-	+	-	39	6.7
Poronaysk	96	-	96	102	16	1	1	3	31	-	-	-	57	7.4
IUzhno-Sahalinsk	97	99	98	42	21.7	0	0	3	25	-	+	-	38	7.7
Severo-Kuril'sk	0	-	0	-	-	-	-	-	-	-	-	-	-	-
<b>Sahalinskoe UGMS/ 4</b>	<b>65</b>	<b>96</b>	<b>78</b>	<b>65</b>	<b>18.9</b>	<b>0</b>	<b>1</b>	<b>3</b>	<b>27</b>	<b>0</b>	<b>2</b>	<b>0</b>	<b>44</b>	<b>7.4</b>
O.Dikson	89	-	89	46	21.2	2	3	1	19	+	-	-	49	5.1
Malye Karmakuly	75	-	75	157	13.3	1	1	1	15	-	-	-	63	6.4
Hatanga	71	-	71	35	22.9	1	1	1	17	-	-	-	51	5.7
SHoyna	-	85	85	22	25.9	2	1	2	48	-	-	-	55	5.2
Arhangel'sk	97	97	97	26	24.7	0	1	2	51	-	-	-	41	5.4
Kargopol'	-	97	97	22	26	1	2	1	27	-	-	-	44	5.2
Nar'ian-Mar	98	-	98	18	27.3	1	2	2	52	-	-	-	43	5.5
Pechora	51	-	51	28	24.3	2	4	4	44	+	-	-	68	6.5
Syktvykar	96	97	97	23	25.6	5	5	2	57	+	-	-	55	5.5
Vologda	93	-	93	35	22.8	1	3	1	24	-	-	-	45	5.5
<b>Severnoe UGMS/10</b>	<b>84</b>	<b>94</b>	<b>87</b>	<b>30</b>	<b>23.9</b>	<b>2</b>	<b>2</b>	<b>2</b>	<b>39</b>	<b>3</b>	<b>0</b>	<b>0</b>	<b>50</b>	<b>5.5</b>
Kem'	96	-	96	34	23.1	2	3	1	27	-	-	-	48	5.2
Petrozavodsk	0	-	0	-	-	-	-	-	-	-	-	-	-	-
Voeykovo	100	99	99	26	24.7	0	1	2	49	-	-	-	48	5.5
Velikie Luki	-	0	0	-	-	-	-	-	-	-	-	-	-	-
<b>Severo-Zapadnoe UGMS/ 4</b>	<b>65</b>	<b>49</b>	<b>59</b>	<b>29</b>	<b>24.2</b>	<b>1</b>	<b>1</b>	<b>1</b>	<b>42</b>	<b>0</b>	<b>0</b>	<b>0</b>	<b>48</b>	<b>5.4</b>
Volgograd	99	100	100	17	27.4	0	1	2	23	-	-	-	66	5.4
Rostov-na-Donu	87	75	81	169	12.8	1	2	4	30	-	+	-	64	6
Divnoe	96	94	95	23	25.6	0	1	2	27	-	+	-	56	6.8
Astrahan'	87	84	86	21	26.3	0	1	2	26	-	-	-	57	6.2
Tuapse	0	0	0	-	-	-	-	-	-	-	-	-	-	-
MinVody	58	58	58	36	22.6	0	0	4	41	-	+	-	43	7.6
Mahachkala	93	92	92	22	25.8	0	1	4	38	-	+	-	47	7.4
<b>Sev.-Kavkazskoe UGMS/ 7</b>	<b>83</b>	<b>81</b>	<b>82</b>	<b>31</b>	<b>23.7</b>	<b>0</b>	<b>1</b>	<b>3</b>	<b>30</b>	<b>0</b>	<b>4</b>	<b>0</b>	<b>57</b>	<b>6.5</b>
Noril'sk	93	94	93	27	24.6	0	1	2	30	-	-	-	49	6.1
Turuhansk	99	99	99	26	24.7	0	1	1	34	-	-	-	52	6
Bor	94	-	94	22	25.9	0	1	1	20	-	-	-	44	5.3
Tura	90	-	90	23	25.6	2	2	2	43	-	-	-	43	5.3
Vanavara	-	94	94	29	24.2	1	2	2	33	-	-	+	49	6.6
Eniseysk	96	-	96	30	23.8	0	2	2	42	-	-	-	50	6
Boguchany	96	-	96	19	27	1	2	2	33	-	-	-	39	6
Emel'ianovo	98	97	97	25	25	1	1	3	55	-	-	-	37	6.3
Hakasskaia	100	-	100	20	26.3	1	1	4	56	-	-	-	39	5.8
Kyzyl	97	-	97	26	24.7	3	5	4	55	-	-	-	52	6.9
<b>Srednesibirskoe UGMS/10</b>	<b>96</b>	<b>96</b>	<b>96</b>	<b>25</b>	<b>25.1</b>	<b>1</b>	<b>1</b>	<b>2</b>	<b>40</b>	<b>0</b>	<b>0</b>	<b>1</b>	<b>46</b>	<b>6.1</b>
Kazan'	72	-	72	56	19.8	1	2	1	18	-	-	-	53	5.5
<b>Rep. Tatarstan/ 1</b>	<b>72</b>	<b>-</b>	<b>72</b>	<b>56</b>	<b>19.8</b>	<b>1</b>	<b>2</b>	<b>1</b>	<b>18</b>	<b>0</b>	<b>0</b>	<b>0</b>	<b>53</b>	<b>5.5</b>
Ivdel'	98	-	98	26	24.9	0	1	2	23	-	-	-	33	5.7
Perm'	91	-	91	30	23.8	2	2	2	32	+	-	-	63	5.2
Verhnee Dubrovo	95	96	95	25	24.9	1	1	2	25	-	-	-	52	5.3

<b>Stations/Regional administrations</b>	<b>a1</b>	<b>a2</b>	<b>a</b>	<b>b</b>	<b>b1</b>	<b>c1</b>	<b>c2</b>	<b>c3</b>	<b>c</b>	<b>d</b>	<b>e</b>	<b>f</b>	<b>g</b>	<b>h</b>
Kurgan	-	94	94	25	25	0	1	2	25	-	-	-	45	5.7
<b>Ural'skoe UGMS/ 4</b>	<b>95</b>	<b>95</b>	<b>95</b>	<b>26</b>	<b>24.7</b>	<b>1</b>	<b>1</b>	<b>2</b>	<b>26</b>	<b>1</b>	<b>0</b>	<b>0</b>	<b>49</b>	<b>5.4</b>
Moskva	99	84	91	36	22.7	3	3	1	22	-	+	-	49	6.5
<b>CAO/ 1</b>	<b>99</b>	<b>84</b>	<b>91</b>	<b>36</b>	<b>22.7</b>	<b>3</b>	<b>3</b>	<b>1</b>	<b>22</b>	<b>0</b>	<b>1</b>	<b>0</b>	<b>49</b>	<b>6.5</b>
Bologoe	87	86	86	30	23.8	3	3	2	29	-	-	-	55	5.8
Riazan'	98	97	97	23	25.7	3	3	1	22	+	-	-	56	5.7
Smolensk	93	94	94	37	22.5	1	1	1	20	-	-	-	49	6.6
Suhinichi	-	98	98	19	26.7	3	3	2	26	-	-	-	61	5.8
<b>Central'noe UGMS/ 4</b>	<b>93</b>	<b>93</b>	<b>93</b>	<b>28</b>	<b>24.4</b>	<b>2</b>	<b>2</b>	<b>2</b>	<b>24</b>	<b>1</b>	<b>0</b>	<b>0</b>	<b>55</b>	<b>6</b>
Kursk	97	65	81	26	24.8	3	3	2	26	+	-	-	42	5.7
Voronezh	96	-	96	27	24.5	0	0	1	16	-	-	-	36	5.4
Kalach	-	79	79	9	31.6	2	2	1	26	+	-	-	81	5.5
<b>Centr-CHernoz.Oblastey UGMS/ 3</b>	<b>96</b>	<b>72</b>	<b>84</b>	<b>20</b>	<b>26.3</b>	<b>2</b>	<b>2</b>	<b>1</b>	<b>23</b>	<b>2</b>	<b>0</b>	<b>0</b>	<b>54</b>	<b>5.6</b>
O.Ayon	56	-	56	161	13.2	2	2	3	33	-	-	-	52	7.7
Omolon	79	-	80	31	23.6	1	2	3	43	-	-	-	45	6
<b>CHukotskoe UGMS/ 2</b>	<b>68</b>	<b>-</b>	<b>68</b>	<b>63</b>	<b>19.1</b>	<b>2</b>	<b>2</b>	<b>3</b>	<b>38</b>	<b>0</b>	<b>0</b>	<b>0</b>	<b>48</b>	<b>6.7</b>
Tiksi	-	96	96	50	20.5	4	3	1	21	+	-	-	58	5.2
CHokurdah	-	98	98	27	24.4	1	1	1	13	+	-	-	52	6
Olenek	96	99	98	31	23.7	1	2	2	26	-	-	-	55	6
Verhoiansk	89	89	89	20	26.5	1	1	2	31	+	-	-	52	5.3
ZHigansk	92	-	92	20	26.6	2	3	1	24	+	-	-	62	5.5
Viliuysk	-	97	97	38	22.3	1	1	2	29	-	-	-	43	5.7
Oymiakon	-	90	96	26	24.7	4	5	4	88	-	-	-	48	6.1
Mirnyy	96	-	96	21	26	1	1	2	28	-	-	-	48	5.2
Olekminsk	96	-	96	22	25.8	2	2	2	27	+	-	-	52	5
IAkutsk	98	99	99	26	24.7	2	2	2	27	+	-	-	43	5
CHerskiy	94	-	94	30	23.8	1	2	1	23	+	-	-	66	5.6
Zyrianka	97	-	97	17	27.7	1	1	2	24	-	-	+	44	5.4
Vitim	-	93	93	31	23.7	12	13	3	50	+	+	-	81	6.5
Aldan	97	97	97	22	25.9	1	1	4	57	-	-	-	48	5.1
<b>IAkutskoe UGMS/14</b>	<b>96</b>	<b>95</b>	<b>95</b>	<b>26</b>	<b>24.8</b>	<b>2</b>	<b>2</b>	<b>2</b>	<b>34</b>	<b>8</b>	<b>1</b>	<b>1</b>	<b>53</b>	<b>5.5</b>
<b>Russian Federation/106</b>	<b>90</b>	<b>91</b>	<b>91</b>	<b>29</b>	<b>24</b>	<b>1</b>	<b>2</b>	<b>2</b>	<b>34</b>	<b>19</b>	<b>15</b>	<b>4</b>	<b>51</b>	<b>6.1</b>

a- Percentage of observational program fulfillment,

a1,a2 - 00 and 12 UTC

b- Average height of soundings hPa,

b1 - km

c- Percentage of soundings with rejected data,

c1 - Percentage of rejected temperature

c2 - Percentage of rejected geopotential

c3 - Percentage of rejected wind

d- suspected stations (geopotential heigh)

e- suspected stations (wind)

f- suspected stations (wind direction)

g- Weighted root-mean-square 'OB-FG' geopotential differences in 1000-100 hPa layer, gpm

h- Root-mean-square 'OB-FG' wind vector differences in 850-100 hPa layer, m/s

# INTERCOMPARISON MEASUREMENTS OF RECORDING PRECIPITATION GAUGES IN SLOVAKIA

Branislav ChvÍla<sup>1</sup>, Boris Sevrúk<sup>2</sup> and Miroslav Ondráš<sup>3</sup>

<sup>1</sup> Slovak Hydrometeorological Institute, Jeséniova 17, 833 15 Bratislava, Slovakia,  
tel. +421 2 5941 5162, fax. +421 2 5477 4419, e-mail: [branislav.chvila@shmu.sk](mailto:branislav.chvila@shmu.sk)

<sup>2</sup> Swiss Federal Institute of Technology ETH, Institute of Climate Research, Winterthurerstr. 190, CH-8057 Zurich,  
Switzerland, tel. + 41 1 635 5235, fax. + 41 1 362 5197, e-mail: [boris.sevruck@env.ethz.ch](mailto:boris.sevruck@env.ethz.ch)

<sup>3</sup> World Meteorological Organization, WWW, P.O.Box 2300, CH-1211 Geneva 2, Switzerland,  
tel. +41 22 730 8409, fax. +41 22 730 8021, e-mail: [mondras@wmo.int](mailto:mondras@wmo.int)

## Abstract

In order to check the accuracy and reliability of a new electronic weighing recording precipitation gauge with a very fine resolution of 0.001 mm, 99 precipitation measurements of liquid, mixed and solid precipitation were compared with the standard manually operated gauge and the heated tipping-bucket gauge. The results show that there are differences in the total amount and duration of precipitation as measured using these three types of gauges. The tipping-bucket gauge shows losses in the case of solid precipitation. In contrast, it overestimates the precipitation amounts in the case of long-duration precipitation events with moderate intensities, which is due to the repeated wetting of the buckets. After each emptying of the bucket a small amount of water remains in the bucket and is added by the following filling of the bucket to the precipitation. The more sensitive electronic weighing system can give some false records due to external influences like wind gusts.

## INTRODUCTION

In connection with the development of a new flood-warning system in the Slovak Republic the Slovak Hydrometeorological Institute (SHMI) is going to expand its network of automatic precipitation gauges to 250 in the next few years. The first 90 gauges have already been installed during the last year. Each gauge uses an electronic weighing system TRWS of domestic production, developed by MPS System Ltd. in Bratislava. The resolution is 0.001 mm per minute. This new type of gauge has been preferred to tipping-bucket gauges, which are considered to be not very reliable (Sevrúk, 2002). They need recalibration each year, show considerable losses in high intensity rains (Adami and Da Deppo, 1985) and due to heating in the winter season (Zweifel and Sevrúk, 2002), the buckets do not empty completely and consequently, and the tips do not correspond to the specified amount. Moreover they suffer from frequent clogging due to bird droppings and leaves falling into the gauge. The purchase price is low, but the operational cost tends to be high. The electronic weighing systems also show some specific errors such as a temperature dependence of measured values or software errors in filtering out the effects of wind shocks, vibrations and sudden changes etc. (Sevrúk and ChvÍla, 2005). These errors can result in false precipitation records.

Differences in the measurements of precipitation gauges of different design and measuring systems arise mainly due to the different magnitude of systematic errors, particularly wind induced losses, wetting and evaporation losses. The systematic errors can be minimized using appropriate corrections (Sevrúk, 1982; 2005; Nespor and Sevrúk 1999); the effect of random errors can be eliminated through the checking of precipitation records and the installation of gauges in situ (Sevrúk, 1984). All other types of errors need additional investigations. If this is not done, the

precipitation time series show inhomogeneities and hydrological computations are inaccurate. The wind-induced error of electronic weighing gauges was analyzed by Chvíla et al. (2002; 2005).

The aim of this intercomparison was to check the operational reliability and the accuracy of the new gauge, particularly the wetting and evaporation effects. Because the wind-shocks during strong winds can produce false precipitation records by the weighing gauges, this phenomenon was also investigated. It is also of interest to know how the very high resolution of 0.001 mm of the new gauges is going to expand our knowledge of the temporal precipitation distribution, particularly the precipitation amount and duration. Precipitation amounts of less than 0.1 mm and their duration, which cannot be measured using standard gauges and common tipping-bucket gauges could be important factors in the climatological, agrometeorological and hydrological applications and scientific investigations.

## METHODS

The intercomparison measurements took place at the Bratislava-Koliba meteorological station, which is located at the headquarters of SHMI, during a three months period with liquid and solid precipitation. All gauges, the recording weighing TRWS (WG), the recording heated tipping-bucket PAAR AP23 (TBG) and the manual standard gauge Metra (SG) have more or less the same catching area of 500 cm<sup>2</sup> with deviations of 0.2% for the PAAR AP23 and 0.1% for the Metra and TRWS. The Metra gauge has a thin orifice rim and the two recording gauges have thick orifice rims. The elevation height of the orifice rim was 1 m above the ground, which is standard in Slovakia. The resolution of standard and tipping-bucket gauges is 0.1 mm per minute. The standard gauge provided measurements three times per day.



*Figure 1. The experimental polygon of precipitation gauges at the Bratislava-Koliba meteorological station.*

In addition, the precipitation detector Vaisala DRD11 was also used to check the duration of precipitation measurements and, in relation to the wind speed, to separate and eliminate false precipitation records. The wind measuring instrument was elevated 10 m above the ground. The phenomena observations from SYNOP messages were used to separate between liquid, mixed and solid precipitation.

In the first step the total amounts of liquid, mixed and solid precipitation from the three gauges over the three month period were compared and differences between the precipitation events

analyzed. The precipitation events were separated from each other by at least a 10-minute precipitation-free period. This analysis has been based on the records of the more reliable weighing gauge. Non-registered precipitation events were evaluated separately.

In order to check the effects of wetting of buckets of the tipping-bucket gauge, the precipitation events were subdivided according to their duration into six sub-groups as follows: from 1 to 5 minutes; 6–15 minutes; 16–30 minutes; 31–60 minutes; 61–100 minutes and finally 101 and more minutes. In addition a special group was identified for events during which the weighing gauge does not register the precipitation as compared to the tipping-bucket. The differences in total amount between both recording gauges were computed and their dependency on the total amount, which corresponds to the number of tips was analyzed.

## RESULTS AND DISCUSSION

The results of the comparison of the total precipitation amounts measured by all three gauges are presented in *Table 1*. They show differences in precipitation amounts between the standard precipitation gauge Metra and the two recording gauges of 5%. This difference, which amounts to 4 mm, occurred in two days and can be attributed to the error made by the observer. (Metra showed 15.8 mm on one day and recording gauges 12.5 mm. On another day Metra showed 2.1 mm and recording gauges 1.1 mm.) No other explanations of such a substantial error were on hand. With the exception of these two days, the differences in precipitation amounts between the Metra and the two recording gauges were small and varied from positive to negative values. The different thickness of the gauge orifice rim can affect the wind field deformation above the gauge (Sevruk et al., 1989) and contribute to the observed differences through wind-induced losses. However these differences depend on wind speed and we estimate them to be generally small. In addition they are negative or positive between two types of gauges.

Between the weighing and tipping-bucket gauges, which have the same thickness of orifice rim, there are no significant differences in total amounts. Greater differences are obtained only in the case of mixed and solid precipitation, when the weighing gauge, WG, records more precipitation than the tipping-bucket gauge, TBG, which seems to be affected by the losses due to heating. However, the number of days with mixed or solid precipitation over the examined period was low therefore related results are not very representative.

*Table 1. The total amount of liquid, mixed and solid precipitation measured using the standard conventional gauge Metra (SG), the weighing gauge TRWS (WG) and the tipping-bucket gauge PAAR (TBG). Bratislava, Slovakia, October-December 2004.*

Precipitation form	Number of days with precipitation	Total amount of precipitation in [mm]		
		SG	WG	TBG
liquid	23	52.6	51.384	52.0
mixed	4	37.1	34.121	33.7
solid	1	0.2	0.449	0.2
Total	28	89.9	85.954	85.9

The comparison of precipitation events is presented in *Table 2*. It shows significant differences in the duration of the precipitation events. In the case of liquid precipitation, the TBG did not register roughly 50% of all events, particularly very small ones under 0.1 mm. In the total it makes 1.67 mm with a duration of nearly 1000 minutes. In the case of solid precipitation the proportion of non-registered events by the TBG is exceptional great (6 out of 8). This is primarily caused by the higher resolution of the WG. The tipping-bucket mechanism is not able to detect the low intensity precipitation events like the drizzle or very light rain even if its total amount is larger

than the gauge resolution of 0.1 mm. This is well demonstrated in the right graph of the cumulative sums in *Figure 2*. It may be due to the greater wetting losses of the gauge collector and the buckets of the TBG as compared with the WG. For the latter gauge the wetting of the collector is partly weighted and included in the amount of precipitation. Only the wetting of the orifice rim is not weighted and in this way, it contributes mostly to the wetting losses.

The start of recording solid precipitation by the TBG is also considerably delayed in relation to the WG. This is primarily due to the smaller resolution and partly to the evaporation losses of the heated catching area of the TBG. The higher wind speeds during the events with solid precipitation could also affect the magnitude of differences in measurements between the gauges due to the different wind-induced losses.

During the examined period there are 11 events with the records of the WG unrelated to the precipitation. All of them occurred during windy periods (see *Table 2*). In 7 events the wind gusts exceeded  $15 \text{ m s}^{-1}$ , which is twice the average wind speed. The force of wind shocks affects the precipitation gauge collector, which is placed directly on the weighing mechanism. Its total load can vary due to the shocks and in this way it can affect the registration, which can record some very small amounts of “precipitation” near the resolution value of 0.001 mm.

*Table 2. The total amount, duration, average wind-speed and the average delay in the start of recording precipitation events, sub-divided according to the precipitation form and the not-registered events by the tipping-bucket gauge, TBG. Bratislava, Slovakia, October-December 2004.*

Precipitation form	Number of events	Total amount		Duration		Wind speed average [m s <sup>-1</sup> ]	Delay* in beginning [min]
		WG [mm]	TBG [mm]	WG [min]	TBG [min]		
<i>All precipitation events</i>							
liquid	84	52.836	52.6	3930	1732	3.2	16
mixed	7	31.199	31.6	1372	1122	3.0	25
solid	8	1.909	1.7	327	162	3.8	26
Total	99	85.944	85.9	5629	3016	3.3	22
no precipitation**	11	0.041	0.1	34	1	6.8	-
<i>Precipitation events not registered by TBG</i>							
liquid	44	1.670	0	949	0	3.0	-
mixed	2	0.121	0	50	0	3.2	-
solid	6	0.243	0	91	0	4.1	-
Total	52	2.034	0	1090	0	3.4	-
no precipitation**	10	0.041	0	34	0	7.2	-

\* average value \*\*precipitation registered by the gauge when no precipitation occurred

*Figure 2* shows the records of liquid precipitation by WG and TBG for two different events. The left graph shows the delay in the start of recording the precipitation smaller than 0.1 mm by the TBG as compared to the WG, which is due to the different resolution of both gauges, and practically no delay at the 0.1 mm value. The TBG shows 0.05 mm precipitation less than the WG at the end of the time period. The right graph demonstrates differences in the recording of very light rain in the first 60 minutes and the following rain of higher intensity in the last 45 minutes of the record. The first part of the rainfall event was not recorded by the TBG and the second part was recorded with some delay. The difference in precipitation amount at the end of time period is 0.1 mm.

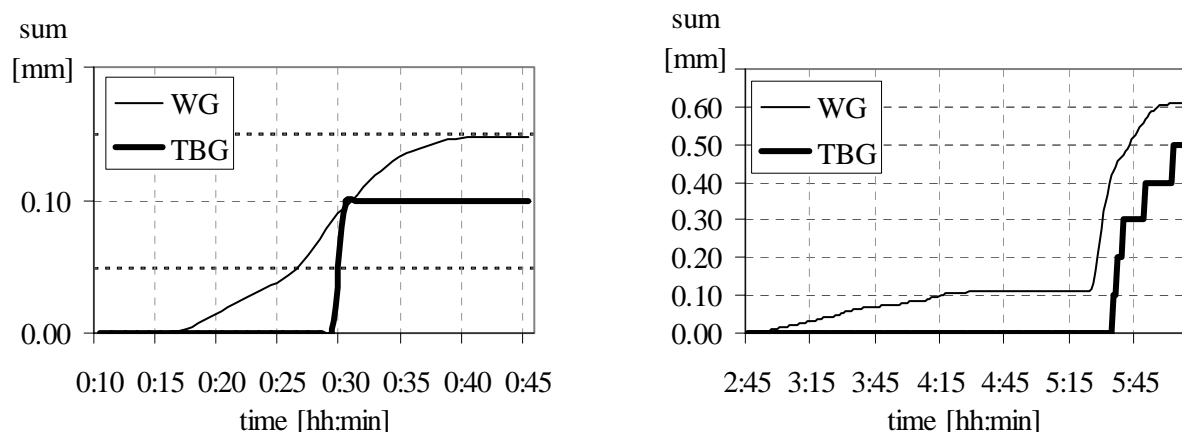


Figure 2. The cumulative sums of precipitation recorded by the weighing (WG) and tipping-bucket (TBG) precipitation gauges in two different time periods. Bratislava, 2004.

Table 3. Differences in the total amount of precipitation measured using the weighing gauge (WG) and the tipping-bucket gauge (TBG) for different forms of precipitation, sub-divided according to the duration of precipitation events into six classes and one class of precipitation events not recorded by WG.

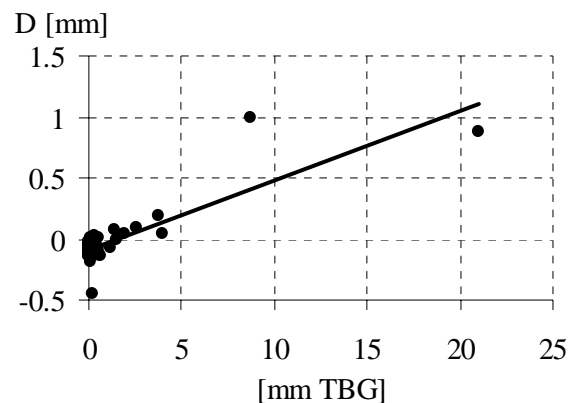
Duration of events by WG [min]	Number of events [-]	Total amount		Differences in total amount WG-TBG		Average number of tips [-]	Average duration of events		Wind speed average [m s <sup>-1</sup> ]
		WG [mm]	TBG [mm]	absolute [mm]	relative [% TBG]		WG [min]	TBG [min]	
<i>Liquid precipitation</i>									
no record by WG	3	0	0.3	-0.300	-100	1	0	1	3.6
1-5	17	0.123	0.0	0.123	100	-	3	0	3.7
6-15	17	1.168	0.9	0.268	29.8	0.5	10	1	2.7
16-30	13	1.085	0.9	0.185	20.6	0.7	21	1	2.5
31-60	13	4.206	3.3	0.906	27.4	2.5	44	13	2.8
61-100	8	2.775	2.3	0.475	20.7	2.9	71	13	2.4
101 and more	13	43.479	44.9	-1.421	-3.2	34.5	177	110	3.6
<i>Mixed and solid precipitation</i>									
1-5	1	0.001	0	0.001	100	-	1	0	4.1
6-15	4	0.084	0	0.084	100	-	9	0	2.6
16-30	2	0.331	0.2	0.131	65.5	1	23	4	5.1
31-60	4	1.634	1.8	-0.166	-9.2	4.5	43	20	3.1
61-100	0	0	0	0	0	-	0	0	0
101 and more	4	31.058	31.3	-0.242	-0.7	78.3	361	299	3.4

Table 3 confirms that in the case of precipitation events with longer duration and moderate intensities, the total amount of precipitation recorded by the TBG is slightly larger than that recorded by the WG. It is also evident, that the form of precipitation plays no role in this phenomenon at all. It agrees well with the theory of wetting of buckets. A very small part of precipitation always rests in the buckets, so the tips do not correspond to 0.1 mm amounts but count already slightly smaller amounts of precipitation as the 0.1 mm value, which explains the overestimation of the total amount. Because the wetting of buckets is very small, the number of tips should reach a certain critical value to cumulate enough water, which could be registered by the



resolution of 0.1 mm. Consequently, the number of tips greater than the critical value relates to the overestimation and to the amount of precipitation since these two variables are proportional. In calibrations curves presented by Adami and Da Deppo (1985; see also Sevruc, 2004) the overestimation is evident between precipitation intensities of less than  $50 \text{ mm h}^{-1}$ . It increases toward smaller intensities up to 4%.

The fitted line in *Figure 3* shows that the critical value corresponds to about 15 tips, when the TBG starts to record more precipitation in total than the WG. In *Table 3*, it is shown that at an average number of tips of 34.5 per event, the TBG shows already 3.2% more liquid precipitation than the WG. In contrast, the WG shows up to 30% more liquid precipitation if the average number of tips per event is less than 3. For the mixed and solid precipitation such a relationship is not so clearly evident.



*Figure 3. Relation between the total amount of precipitation measured using the tipping-bucket gauge (TBG) and the absolute difference,  $D$ , in precipitation values between the weighing gauge and the tipping-bucket gauge (TBG).*

## CONCLUSIONS

The electronic weighing principle with a very high resolution of 0.001 mm is more accurate to measure the precipitation amount and duration than the heated tipping-bucket gauge, especially in the cases of low intensity precipitation. Measurements using the recording tipping-bucket gauge are affected by evaporation and wetting. Heating losses can be considerable during the winter season. In contrast, the sensitive weighing gauge can also produce the erroneous recordings. To ensure the reliability of the gauge, it is important to use appropriate software to eliminate false records. The manual gauges are subject to observational errors and all types of precipitation gauges are subject to systematic and random errors.

## REFERENCES

- Adami, A., Da Deppo, L., 1985. On the systematic errors of tipping bucket recording rain gauges. Correction of precipitation measurements. (B. Sevruc, Ed.). World Meteorological Organization, Instruments and Observing Methods Rep., No. 24: WMO/TD-No. 104, 57-59, Geneva.
- Chvíla, B., Ondráš, M., Sevruc, B., 2002. The wind-induced loss of precipitation measurement of small time intervals as recorded in the field. In: WMO/CIMO Technical conference 2002.

- WMO Instrument and Observing Methods Rep. No. 75: WMO/TD-No. 1123, CD edition, Geneva.
- Chvíla, B., Sevruk, B., Ondráš, M., 2005. The wind-induced loss of thunderstorm precipitation measurements. *Atmos. Res.*, April 2005 (in press).
- Nespor V., Sevruk B., 1999. Estimation of wind-induced error of rainfall gauge measurements using a numerical simulation. *J. Atmos. Ocean. Techn.*, 16(4), 450-464.
- Sevruk B., 1982. Methods of correction for systematic error in point precipitation measurement for operational use: WMO-No. 589, 91 p., World Meteorol. Org., Geneva.
- Sevruk B., 1984. Comments on "Out-of-level" instruments: Error in hydrometeor spectra and precipitation measurement. *J. Clim. Appl. Meteorol.*, 23(6), 988-989.
- Sevruk, B., 2002. WMO questionnaire on recording precipitation gauges: State-of-the-art. *Water Scie. Technol.*, 2(45), 139-145.
- Sevruk, B., 2005. Rainfall measurement: gauges. In: Andersen, M. G. (Ed.), *Encyclopedia of hydrological sciences. Vol. 1, Part 2, Hydrometeorology, Chapter 40*, 8 p. John Wiley & Sons Ltd.
- Sevruk, B., Chvíla, B., 2005. Error sources of precipitation measurements using electronic weight systems. *Atmos. Res.*, April 2005 (in press).
- Sevruk B., Hertig, J.-A. and R. Spiess, 1989. Wind field deformation above precipitation gauge orifices. In: J. W. Delleur (ed.). *Atmospheric deposition. Internat. Assoc. Hydrol. Scie.*, No. 179, 65-70.
- Zweifel, A., Sevruk, B., 2002. Comparative accuracy of solid precipitation measurements using heated recording gauges in the Alps. *WCRP Workshop on Determination of Solid precipitation in cold regions. Fairbanks Alaska, June 9-14*, 9 p., (CD ROM).

# CALIBRATION OF RELATIVE HUMIDITY MEASURING INSTRUMENTS AT EARS

D.Groelj, S.Žlebir, J.Knez  
Environmental Agency of the Republic of Slovenia  
Vojkova 1b, 1000 Ljubljana, Slovenia  
Tel.:+386 1 478 4100, E-mail: drago.groelj@gov.si

## 1. Introduction

Periodical recalibration of relative humidity measuring instruments is important issue in Quality assurance system at EARS. Calibration Laboratory Service with its state-of-art equipment performs adjustments and calibration of humidity sensors in our meteorological network. Traceability scheme and an evaluation of measuring uncertainty assure traceability of calibrations to the international level. Uncertainty evaluation of the reference standard and uncertainty dissemination to comparison calibration of widely used capacitive instruments is presented.

## 2. Traceability scheme

Traceability of relative humidity instrument calibrations is maintained in the range from 10% to 95% in temperature range from -20°C to 40°C. Dew point hygrometer Mitchell S4000 as a reference standard was primarily calibrated in WYKO Calibration Service in Great Britain as shown in figure 3. In future reference standard will be calibrated in CL using temperature standards and capabilities. Thunder Scientific 2500 two pressure humidity generator is recently bought to improve efficiency and metrological capabilities. Humidity generator is nowadays in a testing and implementing mode and it is expected to improve best measurement capabilities to 1% level.

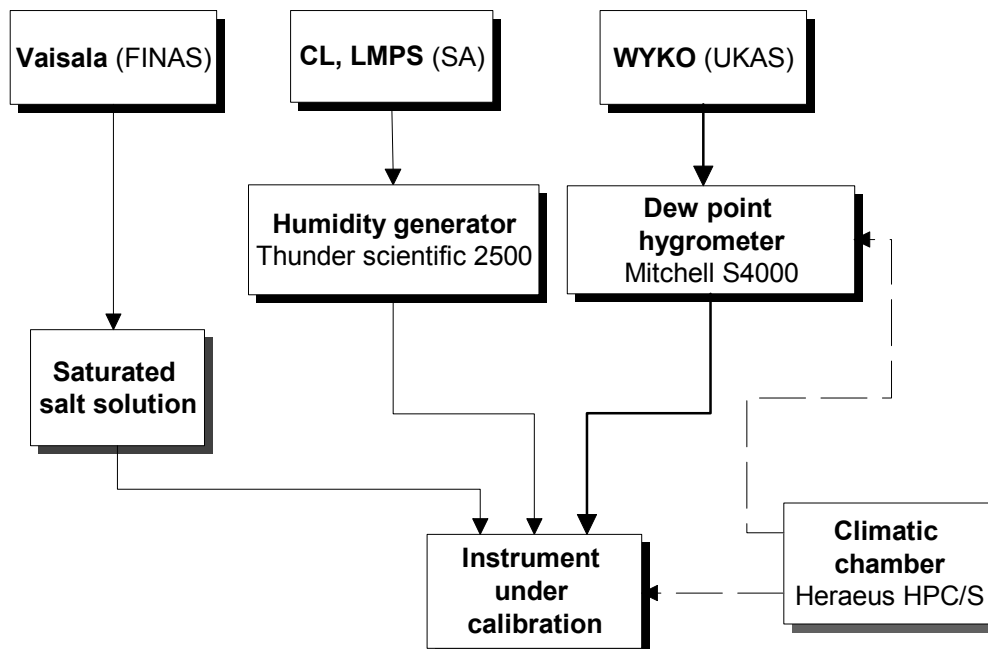


Figure 1: Traceability of calibrations of relative humidity instruments at EARS

Saturated salt solutions are used for adjustments of capacitive humidity instruments only. Climatic chamber is the main uncertainty source in comparison calibrations of field instruments (capacitive sensors, hygrographs). Reduction of time instability and spatial unhomogeneity is possible if reduced volume of climatic chamber is used. Expanded calibration uncertainty of field instruments is at present time 4%.

### 3. Reference standard

Operating principle of dew point reference standard is based on a plated copper mirror and Peltier thermoelectric device as commonly known. At a temperature determined by the moisture content of sample air, dew forms on the mirror surface as Peltier device cools the mirror. This formation of dew causes reduction in reflected light intensity from red LED light source. The control loop maintains the mirror surface at the exact dew point temperature which is accurately measured by an embedded platinum resistance thermometer as shown in figure 1.

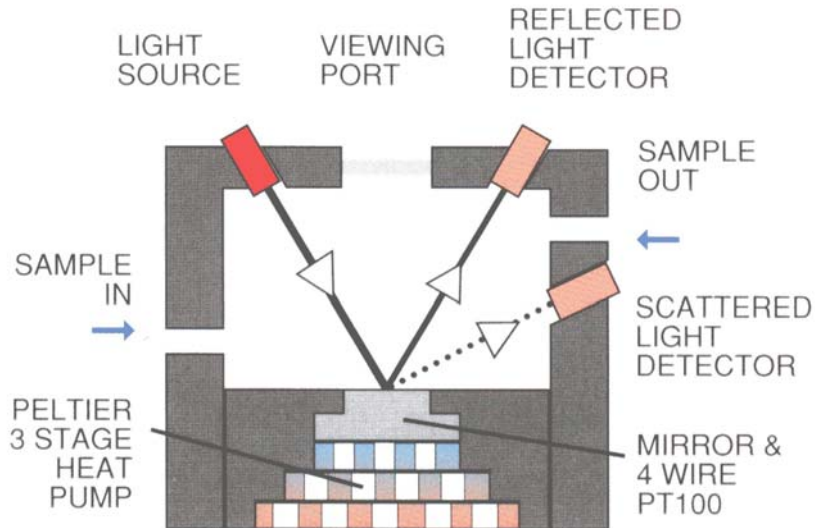


Figure 1: Dew-point sensor

Relative humidity can be calculated:

$$RH = 100 \cdot \frac{p_s(t_d) \cdot f(t_d, P)}{p_s(t_a) \cdot f(t_a, P)} \quad (1)$$

where:

$p_s(t_d)$  - calculated vapour pressure at dew/frost point temperature  $t_d$  [hPa],

$p_s(t_a)$  - calculated vapour pressure at ambient temperature  $t_a$  [hPa],

$P$  - air pressure [hPa],

$t_d$  - dew/frost point temperature  $t_d$  [°C],

$t_a$  - ambient temperature  $t_a$  [°C],

$f(t_d, P), f(t_a, P)$  - enhancement factors.

The measurement uncertainty arises from several effects on the mirror surface:

- Raout effect: soluble contaminants do not change the reflectivity of the mirror. There salts dissovle in the water layer on the surface of the mirror and couse the vapour pressure to be lowered. This result in an excess bildup of water on the mirror surface at the true dew-point. This Raoult effect can result in an error of several degrees.
- Kelvin effect: non-soluble contaminants affect the light reflective characteristics of the mirror and increase vapour pressure on the mirror and so compensation is required.
- Uncertainty of determining dew/frost point: undercooling effect of water on the mirror surface.
- Uncertainty of sampling system: dew asorption and desorption in the sample path.
- Uncertainty of dew-point temperature measurement: most important uncertainty sources are temperature gradients between mirror surface and platinum resistance thermometer and measurement uncertainty of PRT.

Some of these effects can be reduced by establishing a periodic cycle in which the hygrometer heats the mirror above dew/frost point until it is dry, looks at the reflectivity of the mirror compared to a clean, dry mirror and adjusts the bias of the optics to compensate for the contamination.

Uncertainty sources which are taken into account in analytical measurement uncertainty evaluation are:

- uncertainty of saturated vapour pressure calculation,
- ambient and dew/frost point temperature measurement uncertainty,
- uncertainty of enhancement factors calculation,
- uncertainty of air pressure measurement.

Quantity	Sensitivity coefficient	Standard uncertainty $u_i$	Probability law	Contribution $u_i$ [%]*
$p_s(t_d)$	$\frac{f(t_d, P)}{p_s(t_a) \cdot f(t_a, P)}$	$0.0001 \cdot p_s(t_d)$	normal	$2.5 \cdot 10^{-3}$
$p_s(t_a)$	$\frac{-p_s(t_d) \cdot f(t_d, P)}{p_s^2(t_a) \cdot f(t_a, P)}$	$0.0001 \cdot p_s(t_a)$	normal	$2.5 \cdot 10^{-3}$
$f(t_a, P)$	$\frac{p_s(t_d)}{p_s(t_a) \cdot f(t_a, P)}$	0.1 ppm	normal	$2.5 \cdot 10^{-6}$
$f(t_d, P)$	$\frac{-p_s(t_d) \cdot f(t_d, P)}{p_s(t_a) \cdot f^2(t_a, P)}$	0.1 ppm	normal	$2.5 \cdot 10^{-6}$
$t_d$	$\frac{f(t_d, P)}{p_s(t_a) \cdot f(t_a, P)} \cdot \frac{dp_s(t_d)}{dt_d} + \frac{p_s(t_d)}{p_s(t_a) \cdot f(t_a, P)} \cdot \frac{df(t_d, P)}{dt_d}$	0.075 °C	normal	0.222
$t_a$	$\frac{-p_s(t_d) \cdot f(t_d, P)}{p_s^2(t_a) \cdot f(t_a, P)} \cdot \frac{dp_s(t_a)}{dt_a} + \frac{p_s(t_d) \cdot f(t_d, P)}{p_s(t_a) \cdot f^2(t_a, P)} \cdot \frac{df(t_a, P)}{dt_a}$	0.1 °C	normal	0.268
$P$	$\frac{p_s(t_d)}{p_s(t_a) \cdot f(t_a, P)} \cdot \frac{df(t_a, P)}{dP} + \frac{p_s(t_d) \cdot f(t_d, P)}{p_s(t_a) \cdot f^2(t_a, P)} \cdot \frac{df(t_a, P)}{dP}$	50 Pa	normal	$1.6 \cdot 10^{-3}$
Resolution	1	0.1 %	normal	0.1
$u_A$	1	0.2 %	normal	0.2
<b>Expanded measurement uncertainty U</b>		$U = K \times \sqrt{\sum_{i=1}^{10} (u_i)^2}$		<b>U=0.69% K=2</b>

\* Ta=20 °C and 50 % relative humidity

Table 1: Evaluation of uncertainty sources

The most important contribution to the overall uncertainty of dew point hygrometer is uncertainty of measurement of ambient air temperature and dew point temperature as shown in figure 2:

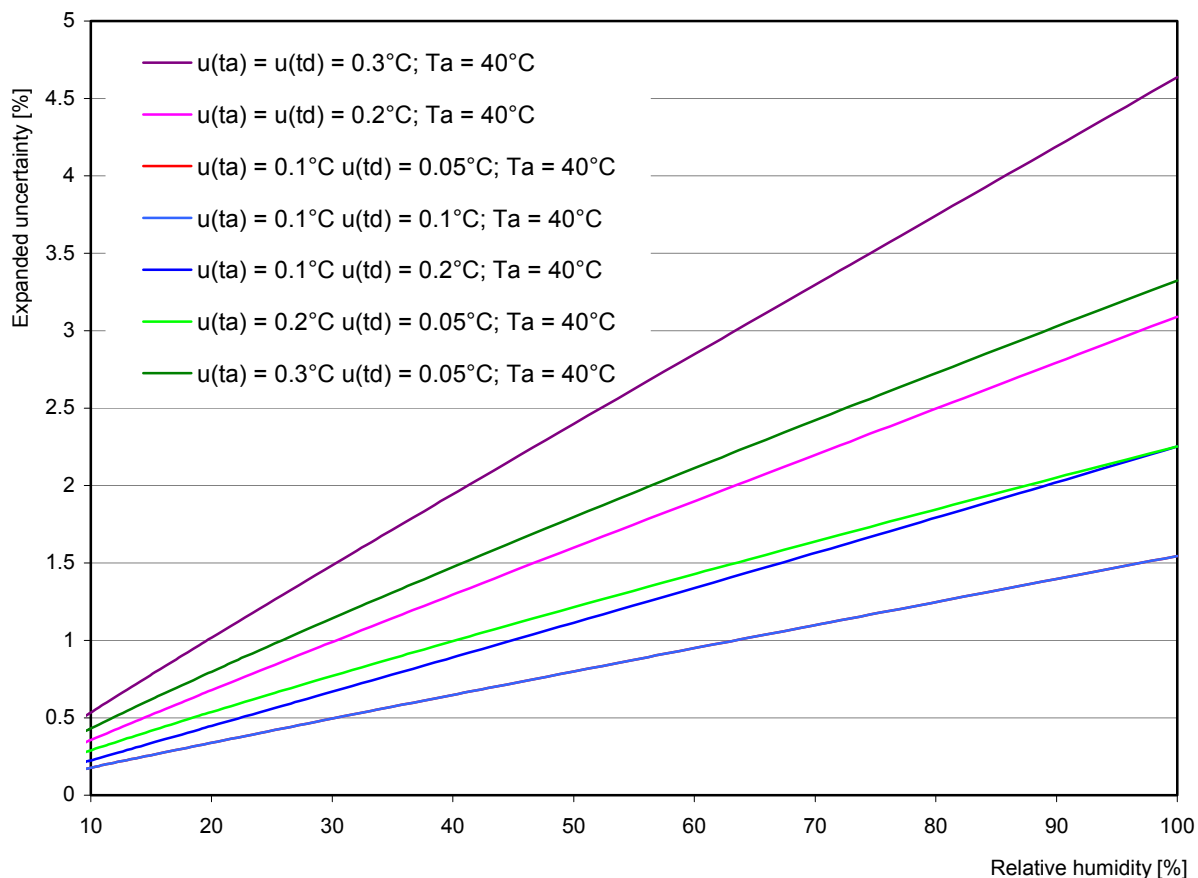


Figure 2: Temperature measurement uncertainty contribution to total uncertainty

Expanded measurement uncertainty of reference standard in the temperature range from -20 °C to 50 °C is shown in figure 3.

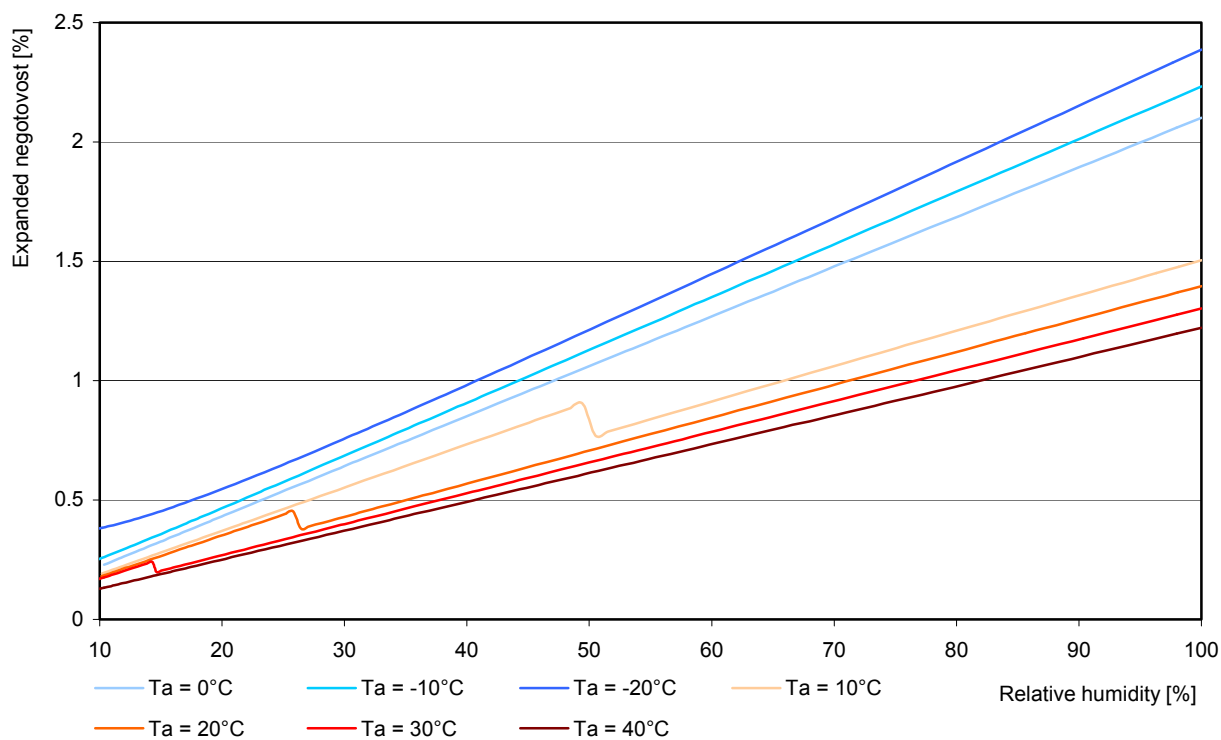


Figure 3: Expanded measurement uncertainty of reference standard in the temperature range from -20 °C to 50 °C

#### **4. Summary**

Expanded uncertainty 50% relative humidity and air temperature 40°C of Mitchell S4000 is 0.7%. Climatic chamber is the main uncertainty source in comparison calibrations of field instruments (capacitive sensors, hygrographs). Reduction of time instability and spatial unhomogeneity is possible if reduced volume of climatic chamber is used. Expanded calibration uncertainty of field instruments is at present time 4%.

Future work of Calibration Laboratory in the field of relative humidity measurements will be focused on implementation and metrological evaluation of two-pressure humidity generator to improve efficiency and metrological capabilities. Humidity generator is nowadays in a testing and implementing mode and it is expected to improve best measurement capabilities to 1% level.

#### **References**

- 1 World Meteorological Organisation, Guide to meteorological instruments and methods of observations, 6<sup>th</sup> edition, WMO No.8, 1996.
- 2 Quality Manual, Environmental Agency of the Republic of Slovenia, 3<sup>rd</sup> edition, Ljubljana, 2003.
- 3 Expression of the Uncertainty of Measurement in Calibration EA-4/02, European co-operation for Accreditation, December 1999.

# ACCREDITED CALIBRATION LABORATORY SERVICE AS A SUBJECT OF AN INTEGRAL QA SYSTEM AT EARS

D.Groselj, S.Žlebir, J.Knez  
Environmental Agency of the Republic of Slovenia  
Vojkova 1b, 1000 Ljubljana, Slovenia  
Tel.:+386 1 478 4100, E-mail: drago.groselj@gov.si

## 1. Introduction

Environmental Agency of the Republic of Slovenia (EARS) is a part of Ministry of the Environment and Spatial Planning. After integration of former Hydrometeorological Institute into EARS in year 2000, Monitoring Office was established with the intention of operating a network of automatic stations for meteorology, hydrology, ambient air-quality, water quality and ionizing radiation. At present time, there are about 60 automatic stations in our measuring networks, sending data in real time to the central database of EARS, which are quite different regarding measuring parameters and purpose. Strategic issue of EARS is quality of measured data in meteorological, hydrological and ecological network. The most important goal of Monitoring Office is to build the common integral quality assurance system for different measuring networks, which will base on ISO/IEC 17025 standard. New legislation that covers environmental monitoring, especially modern European directives in the field of air and water quality, requires that quality systems has to be established to assure technical competence, quality and international comparability of data. Meteorology, on the other hand, is bound mainly to WMO guides and recommendations, ICAO and other relevant documents. Calibration Laboratory (CL) is an important subject in an integral QA system in terms of periodical calibrations of field measuring instruments. CL perform accredited calibrations of measuring instruments in the field of temperature and air pressure. Accreditation, based on ISO/IEC 17025 standard, was achieved in 1999 in the field of temperature calibrations by joined assessment of French accreditation service - COFRAC (Comitee Francais d'Accreditation) and Slovenian Accreditation - SA. Scope of accreditation was extended in the field of air pressure in 2002. Calibration Laboratory is now preparing for accreditation assessment in the field of relative humidity and air quality quantities: carbon monoxide, sulphur dioxide, ozone, nitrogen monoxide and nitrogen dioxide.

Each accredited laboratory establishes and maintains its traceability to the national or international level. Recognition and analysis of uncertainty sources is most important subject in calibration procedure development and uncertainty evaluation. Traceability schemes and calibration procedures are further presented in the area of calibration in Calibration Laboratory.

## 2. Temperature

Calibration Laboratory performs calibrations of different type thermometers: classic liquid-in-glass thermometers, platinum resistance thermometers, self-indicated thermometers, thermistors and thermographs in a temperature range from -40°C to 50°C. We use Pt25 as a reference temperature standard which is periodically calibrated in slovenian national laboratory (LMK) with fixed point method. This external traceability links reference standard to the International temperature scale ITS-90. Internal checks of reference standard in two fixed points (water triple point and gallium melting point) are regularly performed to ensure drift and metrological stability. Intercomparison of our two fixed points assure redundant traceability to the ITS-90 in reduced temperature interval. Standard platinum resistance thermometer Pt25 is strictly used for Pt100 working standard comparison calibration in a state-of-art temperature controlled liquid bath. At present time there is not any accepted standard procedure for the metrological evaluation of the calibration baths.



Accredited laboratories have to set up their own procedures to evaluate time instability and spatial unhomogeneity of calibration baths according to available equipment of the laboratory. In the field of temperature comparison calibrations, uncertainty of reproduced quantity represents major contribution to the total uncertainty. Therefore the correct and precise characterization of calibration baths is very important.

Calibration laboratory developed its own procedures to estimate liquid bath and climatic chamber metrological characteristics. Other equipment used in calibration process (standard resistors, multimeters) are traceable to the Slovenian Institute for Quality and Metrology (SIQ) and National Research Center in Canada. Traceability scheme is shown figure 1.

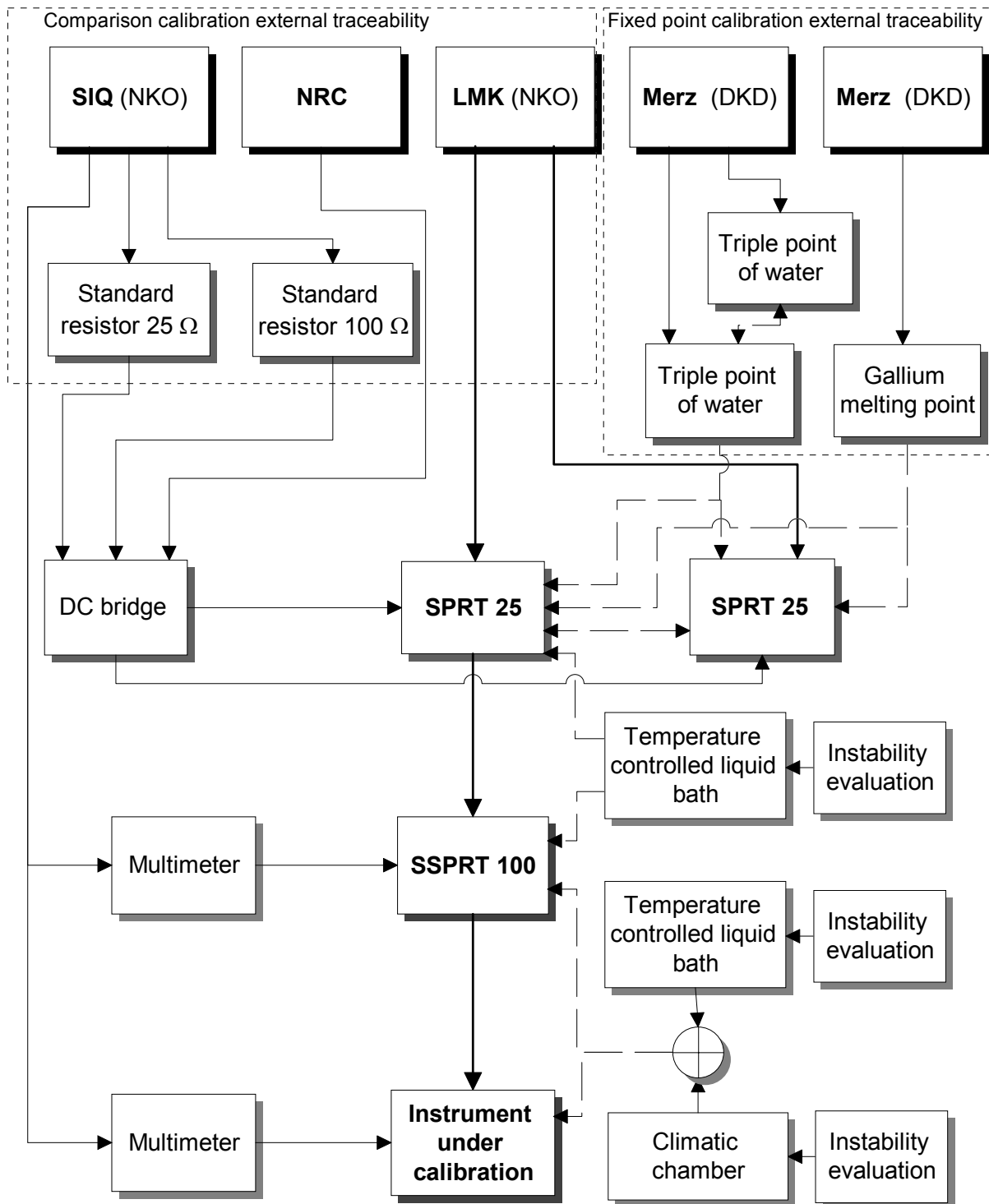


Figure 1: Traceability of temperature calibrations at EARS

Best measurement capability (BMC) for resistance thermometer comparison calibration, evaluated from uncertainty budget and accepted in accreditation assessment is 15 mK. For liquid-in-glass thermometers and other instruments under calibration the BMC is 70 mK.

### 3. Air pressure

Most instruments calibrated in Calibration Laboratory in the field of air pressure are electronic barometers, barographs and mechanical barometers in the range from 600 to 1200 hPa. For barographs and mechanical barometers the Theodore Friedrichs pressure chamber is commonly used. Degranges et Heut dead weight gauge is a pressure reference standard. Highly pure nitrogen (N5) combined with pressure regulator (DH PPC1) is used as a pressure media as shown in figure 2. Dynamometer of reference standard with piston-cylinder assembly transforms pressure into force. Special precisely defined set of masses are used to check and recalibrate dynamometer on a daily bases.

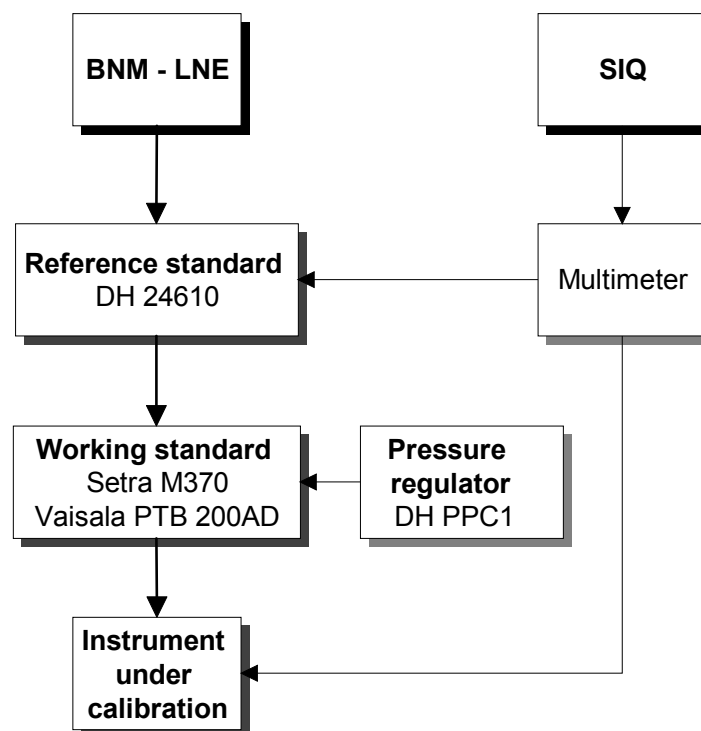


Figure 2: Traceability of calibrations of air pressure instruments

Reference standard is traceable to French BNM-LNE laboratory with expanded uncertainty 6 Pa. Two high precision barometers Setra M370 and Vaisala PTB200AD are working standards with uncertainty estimation of 17 Pa. For high precision pressure calibration reference standard can be used instead of working standards.

### 4. Relative humidity

Traceability of relative humidity instrument calibrations is maintained in the range from 10% to 95% in temperature range from -20°C to 40°C. Dew-point hygrometer Mitchell S4000 as a reference standard was primarily calibrated in WYKO Calibration Service in Great Britain as shown in figure 3. In future reference standard will be calibrated in CL using temperature standards and capabilities. Recently CL bought Thunder Scientific 2500 two pressure humidity generator to improve efficiency and metrological capabilities. Humidity generator is nowadays in a testing and implementing mode and it is expected to improve best measurement capabilities to 1% level.

Operating principle of dew-point reference standard is based on a plated copper mirror and Peltier thermoelectric device as commonly known. At a temperature determined by the moisture content of sample air, dew forms on the mirror surface as Peltier device cools the mirror. This formation of dew causes reduction in reflected light intensity from red LED light source. The control loop maintains the mirror surface at the exact dew-point temperature which is accurately measured by an embedded platinum resistance thermometer. The measurement uncertainty arises from several effects on the mirror surface (Raoult and Kelvin effect, uncertainty of determining dew/frost point, uncertainty of sampling system) and uncertainty of dew-point temperature measurement. The most important contribution to the overall uncertainty of dew-point hygrometer is uncertainty of measurement of ambient air temperature and dew-point temperature. Expanded uncertainty 50% relative humidity and air temperature 40°C of Mitchell S4000 is 0.7%.

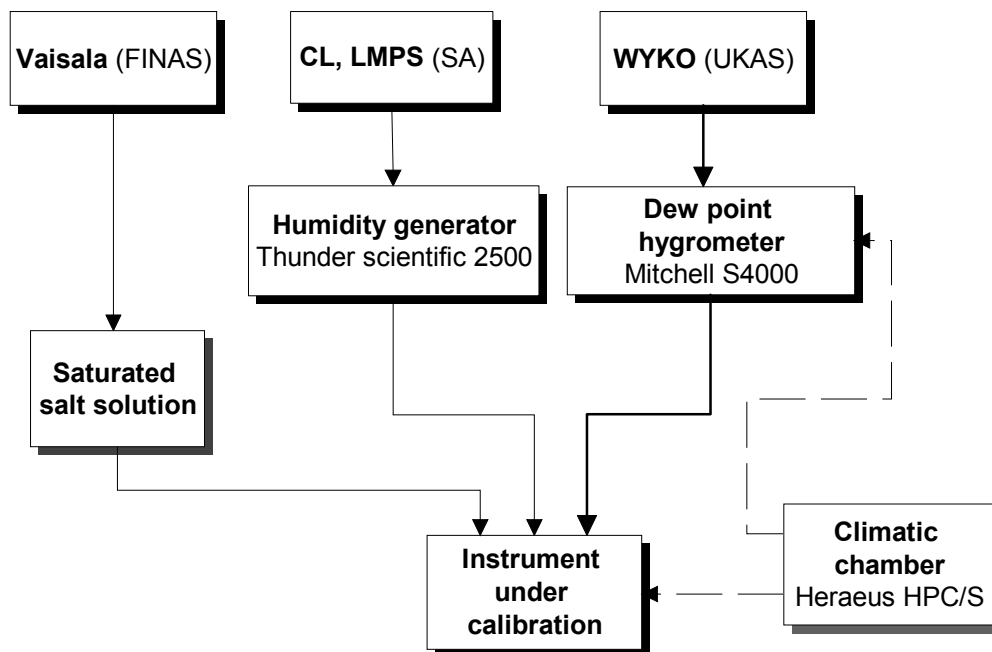


Figure 3: Traceability of calibrations of relative humidity instruments at EARS

Saturated salt solutions are used for adjustments of capacitive humidity instruments only. Climatic chamber is the main uncertainty source in comparison calibrations of field instruments (capacitive sensors, hygrogaphs). Reduction of time instability and spatial unhomogeneity is possible if reduced volume of climatic chamber is used. Expanded calibration uncertainty of field instruments is at present time 4%.

## 5. Air quality quantities

Calibration Laboratory is now preparing for accreditation assessment of air quality parameters: concentration of carbon monoxide, sulphur dioxide, ozone, nitrogen monoxide and nitrogen dioxide at ambient air concentration levels. CL uses certified reference standards (material measures held in cylinder containers or for the case of O<sub>3</sub> a TEI 49C PS O<sub>3</sub> calibrator) traceable to Czech national standards (CHMI). Our working instruments are calibrated in two points (zero air and CRM), as shown in figure 4. For customers we offer calibrations of instruments and material measures (cylinders or sample generators). In the case of instrument calibrations we offer two point calibration by zero air and CRM and multipoint calibration by comparison measurement to our working instrument. In comparison measurements between two instruments a stable but not traceable sample generator is used. In case of calibrations of material measures we offer calibrations of gas cylinders and multipoint calibrations of sample generators. For the future we plan to become an independent calibration laboratory by accrediting procedures for preparation of gas mixtures

containing above stated substances (accept ozone). Gas mixtures will be prepared by dilution of reference materials manufactured by NMI using static mixing chamber.

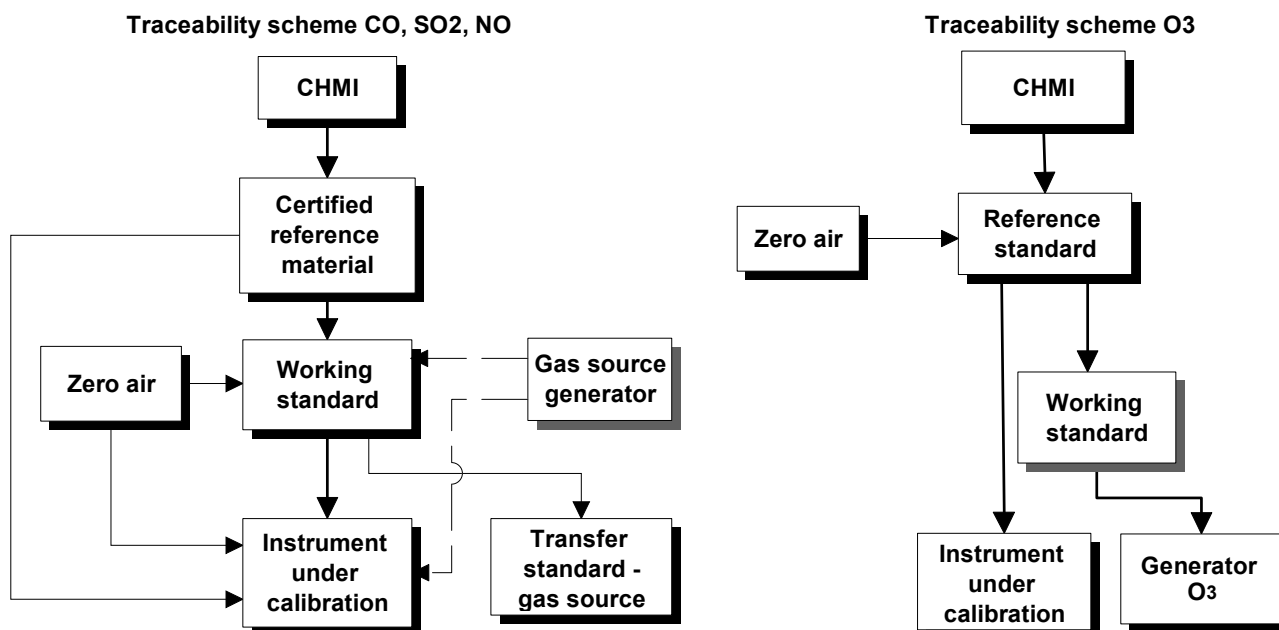


Figure 4: Traceability of calibrations of air quality quantities

## 6. Conclusion

Best measurement capabilities is a measure to compare laboratories between themselves and represent the lowest uncertainty level of calibration. BMC are shown on table 1.

Measured quantities	Range	Best measurement capability (k=2)
<b>Temperature</b>		
Resistance thermometers	-40 °C ÷ 50 °C	15 mK
Liquid-in-glass thermometers	-20 °C ÷ 50 °C	70 mK
Thermographs	-20 °C ÷ 0 °C 0 °C ÷ 50 °C	0.3 °C 0.2 °C
<b>Thermophysical properties</b>		
Water triple point	0.01 °C	1 mK
Gallium melting point	29.7646 °C	1.5 mK
<b>Relative humidity</b>		
	10 % ÷ 95 %	1%*
<b>Air pressure</b>		
	600 hPa ÷ 1200 hPa	$1.3 \cdot 10^{-5} \cdot p + 5 \text{ Pa}$
<b>Air quality quantities</b>		
CO concentration	0 - 15 ppmv	$0.07 \text{ ppm} + 0.016 \cdot c_{\text{CO}}^*$
SO <sub>2</sub> concentration	0 - 500 ppbv	$0.8 \text{ ppb} + 0.021 \cdot c_{\text{SO}_2}^*$
NO concentration	0 - 500 ppbv	$0.9 \text{ ppb} + 0.031 \cdot c_{\text{NO}}^*$
NO <sub>2</sub> concentration	0 - 500 ppbv	$1.5 \text{ ppb} + 0.02 \cdot c_{\text{NO}_2}^*$
O <sub>3</sub> concentration	0 - 500 ppbv	$2.6 \text{ ppb} + 0.024 \cdot c_{\text{O}_3}^*$

\* Expected expanded measurement uncertainty

Table 1: Best measurement capabilities of Calibration Laboratory

Other capabilities of CL include field calibration of solar radiation instruments using Sun as a light source, wind speed and wind direction instruments testing, precipitation instrument testing, calibration of water level sensors and calibration of analog inputs of automated stations.

According to the quality system of EARS Calibration Laboratory covers almost all calibration needs of our meteorological, hydrological and ecological network.

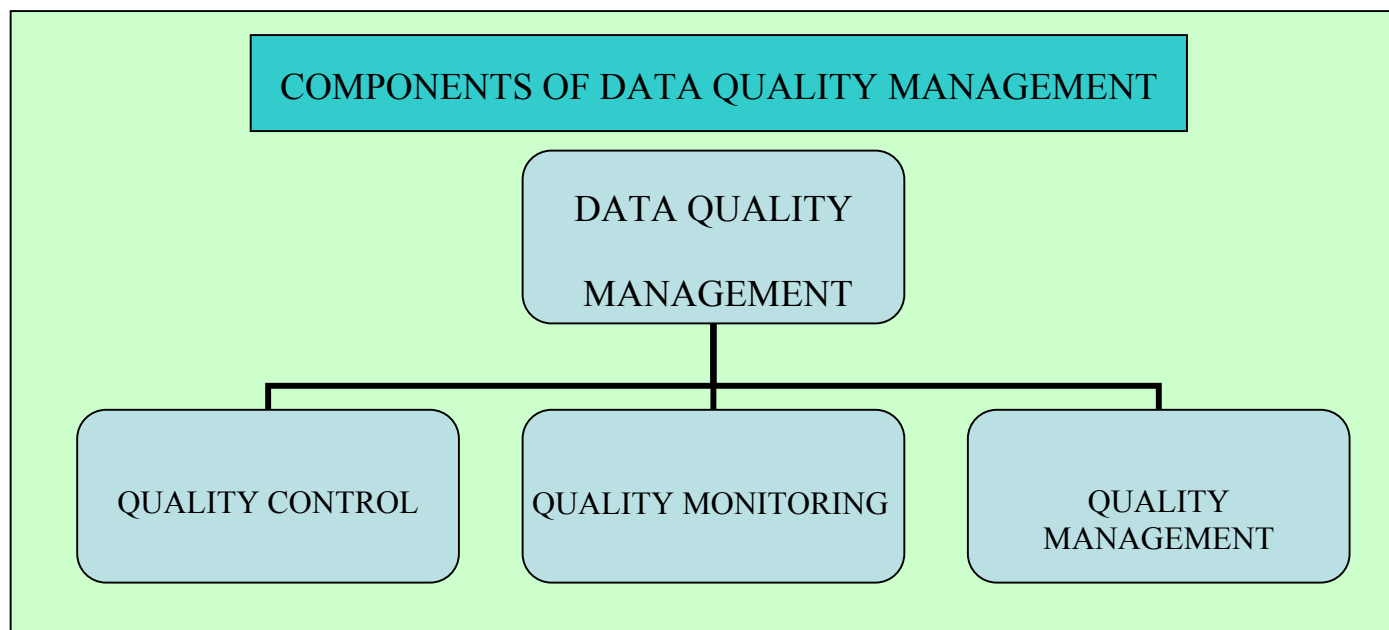
## References

- 1 World meteorological organisation, Guide to meteorological instruments and methods of observations, 6<sup>th</sup> edition, WMO No.8, 1996.
- 2 Quality Manual, Environmental Agency of the Republic of Slovenia, 3<sup>rd</sup> edition, Ljubljana, 2003.
- 3 Silvo Žlebir, Accredited Calibration Laboratory of the Hydrometeorological Institute of Slovenia, TECO 2000, Beijing.
- 4 Expression of the Uncertainty of Measurement in Calibration EA-4/02, European co-operation for Accreditation, December 1999.

# DATA QUALITY MANAGEMENT

Data are of good quality when they satisfy stated and implied needs. The purpose of quality management is to ensure that data meet requirements (for uncertainty, resolution, continuity, homogeneity, representativeness, timeliness, format, etc.) for the intended application, at a minimum practicable cost. Good data are not necessarily excellent, but it is essential that their quality is known and demonstrable.

The best quality systems operate continuously at all points in the whole observation system, from network planning and training, through installation and station operations to data transmission and archiving, and they include feedback and follow-up provisions on time-scales from near-real time to annual reviews.



**Quality control** is the best known component of quality management systems, and it is the irreducible minimum of any system. It consists of examination of data in stations and in data centres to detect errors so that the data may be either corrected or deleted. Quality control is applied in real time, but it also operates in non-real time, as delayed quality control.

Real time quality control is usually performed at the station and at meteorological analysis centres. Delayed quality control may be performed at analysis centres for compilation of a re-checked database, and at climate centres or data banks for archiving.

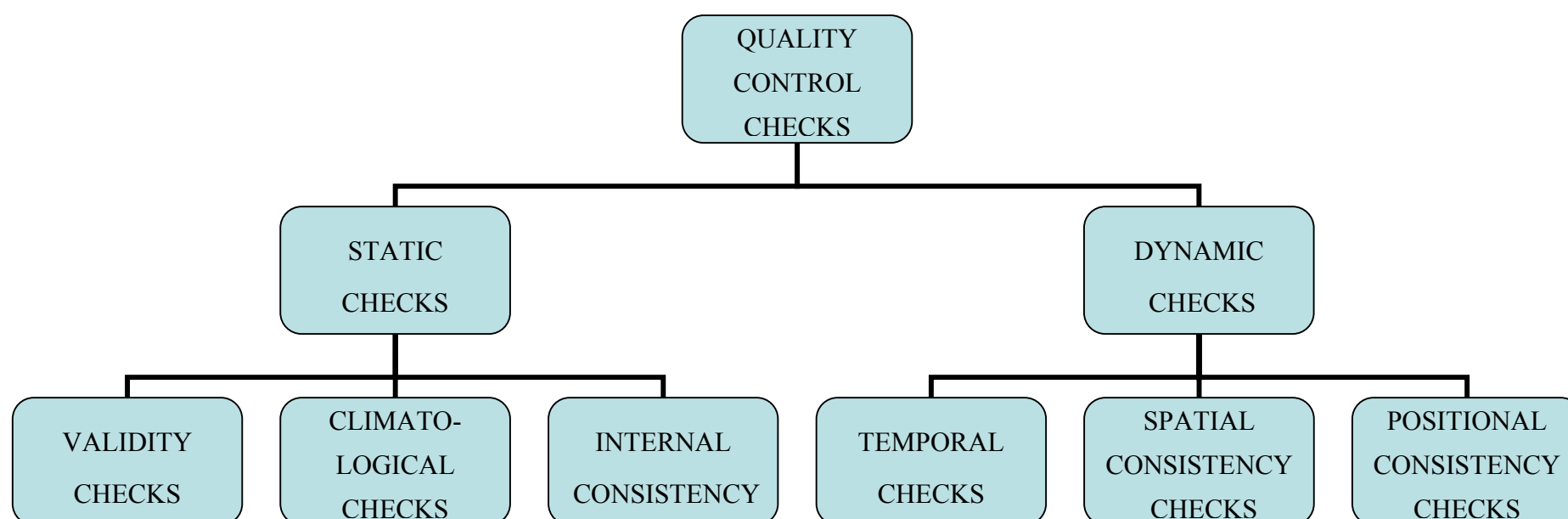
**Quality monitoring** or performance monitoring is a non-real time activity in which the performance of the network or observation system is examined for trends and systematic deficiencies.

**Quality management** includes control of the other factors that directly affect data quality, such as equipment, exposure, procedures, maintenance, inspection, data processing and training. These are usually the responsibility of the network manager, in collaboration with other specialists, where appropriate.

<b>FACTORS AFFECTING DATA QUALITY</b>	1-	Users' requirements
	2-	Functional and technical specifications:
	3-	Selection of instruments
	4-	Acceptance tests
	5-	Compatibility
	6-	Siting and exposure
	7-	Instrumental errors
	8-	Data acquisition
	9-	Data processing
	10-	Real-time quality control
	11-	Performance monitoring
	12-	Test and calibration
	13-	Maintenance
	14-	Training and education
	15-	Metadata

## QUALITY CONTROL

WMO (1981) prescribes that certain quality control procedures must be applied to all meteorological data for international exchange. WMO (1992) prescribes that quality control must be applied by meteorological data-processing centres to most kinds of weather reports exchanged internationally, to check for coding errors, internal consistency, time and space consistency, and physical and climatological limits, and it specifies the minimum frequency and times for quality control.



Two types of Quality Control checks are considered: **static checks**, which are single-station and single-time checks such as climatological checks and validity checks; and **dynamic checks** which take advantage of other information, such as temporal and spatial consistency checks.

**The Static Quality Control checks** are single-station, single-time checks which, as such, are unaware of the previous and current meteorological or hydrologic situation described by other observations and grids. Checks falling into this category include: validity, climatological, internal consistency, and vertical consistency checks.

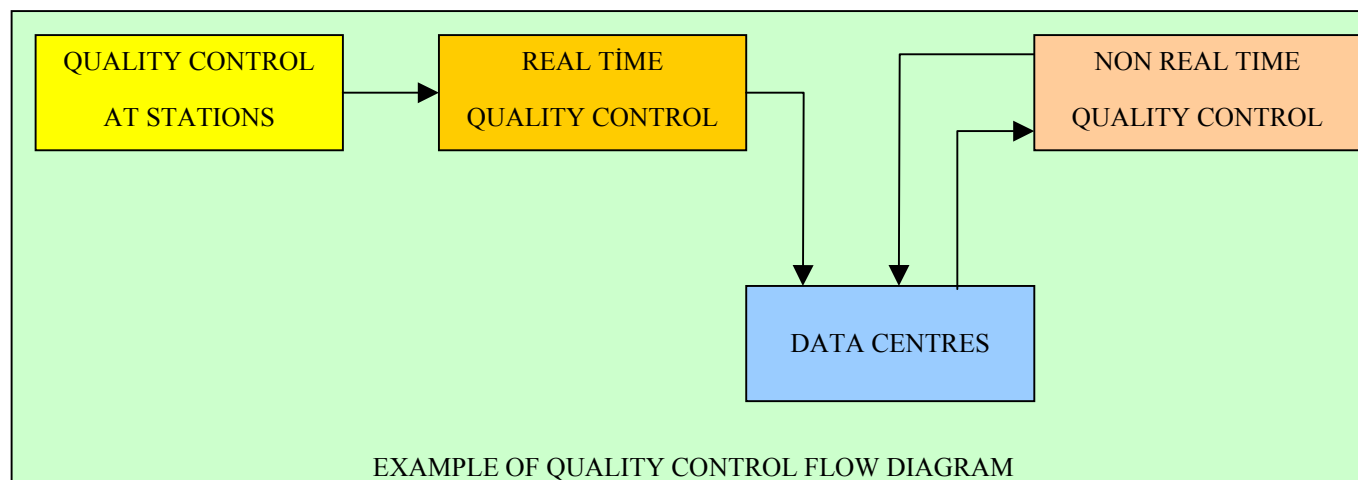
**Dynamic checks** refine the Quality Control information by taking advantage of other available information. Examples of dynamic Quality Control checks include: positional consistency, temporal consistency, spatial consistency, and model consistency checks.

**Definition of limit and step check:** In a limit or range check an observation is always compared to previously defined limit values. In a step check temporal changes are compared to step limit values. If the check implies control of one parameter only, it is a pure step check. If the check implies control of two or more parameters, it is a consistency check (of time series or instant values).

**Definition of consistency checking:** In a consistency check an observation is compared with other parameter values to see if they are physically or climatologically consistent, either instantly or for time series according to adopted observation procedures. The check always includes two or more different parameters from a single station.

**Definition of spatial checking:** In spatial checking the observation is compared with the expected value at the station which can be estimated by various methods. Spatial checks involve parameter values of neighbouring stations, either by interpolation between observations by checking against numeric prognostic values (on the basis of values from many different stations), or by comparing statistics. The checks can involve more than one parameter at one point in time, or single or multi-parameter analyses of time series.

**Definition of homogeneity checking:** Homogeneity checks consist of a variety of control methods to unveil if data series are homogeneous or not during a long period of time. Such control methods are based on statistics of different kinds (e.g. internal consistency checks, Nordli, 1997), tests for detecting change points (e.g. Pettitt test, Sneyers, 1995), comparison of statistics from neighbouring stations (e.g. Standard Normal Homogeneity Test, Alexandersson, 1986) and historical metadata checking (e.g. inspection reports from weather station).



### Quality Control For Surface data

#### MANUAL OBSERVATIONS , STAFFED STATIONS AND AUTOMATIC WEATHER STATIONS

The observer or the officer in charge at a station is expected to ensure that the data leaving the stations have been quality controlled, and should be provided with established procedures for attending to this responsibility. This is a specific function, in addition to other maintenance and record-keeping functions, including:

- (a) Internal consistency
- (b) Climatological checks
- (c) Temporal checks
- (d) All arithmetical and table look-up operations should be explicitly checked;
- (e) Messages and other records must be checked against the original data.

**Quality Control For Upper air data:** Checks should be made for internal consistency (such as lapse rates and shears), for climatological and temporal consistency, and for consistency with normal surface observations.

**Quality Control For Data centers:** The checks that have already been performed on stations are usually repeated at data centers, perhaps in more elaborate form by making use of automation. Data centers, however, usually have access to other network data, making a spatial check possible, against observations from surrounding stations or against analysed or predicted fields. This is a very powerful method, and it is the distinctive contribution of a data center.

### PERFORMANCE MONITORING

The management of a network, or of a station, is greatly strengthened by keeping continuous records of performance, typically on a daily and monthly schedule. There are several aspects to performance monitoring:

- (a) Advice from data centers should be used to record the numbers and types of errors detected by quality control;
- (b) Data from each station should be compiled into synoptic and time-section sets. Such sets should be used to identify systematic differences from neighbouring stations, both in spatial fields and in comparative time-series.
- (c) Reports should be obtained from field stations about equipment faults, or other aspects of performance.



## DATA HOMOGENEITY AND METADATA

### Causes of data inhomogeneities:

Inhomogeneities caused by changes in the observing system appear as abrupt discontinuities, gradual changes, or changes in variability. Abrupt discontinuities mostly occur due to changes in instrumentation, siting and exposure changes, station relocation, changes in calculation of averages, data reduction procedures, and application of new corrections.

### Metadata:

Data inhomogeneities should, as far as possible, be prevented by appropriate quality management. Climatologists can run appropriate statistical programs to link the previous data with the new data into homogeneous databases with a high degree of confidence. Information of this kind is commonly available in what is known as metadata — information on data — also called station histories. Metadata can be considered as an extended version of the station administrative record, containing all possible information on the initial setup, and type and times of changes that occurred during the life history of an observing system.

## NETWORK MANAGEMENT

All the factors that affect data quality are the subject of network management. In particular, network management must include corrective action in response to the network performance revealed by quality control and performance monitoring.

The manager should keep under review the procedures and outcomes associated with all the factors affecting quality including:

- (a) The quality control systems are essential operationally in any meteorological network, and usually receive priority attention by the users of the data and by network management;
- (b) Performance monitoring is commonly accepted as a network management function.
- (c) Inspection of field stations is a network management function;
- (d) Equipment maintenance may be a direct function of the network management unit.
- (e) The administrative arrangements should permit the network manager to take, or arrange for, corrective action arising from quality control, performance monitoring, the inspection programme, or any other factor affecting quality.

## REFERENCES

World Meteorological Organization, 1996: Guide to Meteorological Instruments and Methods of Observation WMO-No. 8, Geneva.

Miller, P. A. and Morone, L. L., 1993: Real-time Quality Control of Hourly Reports from the Automated Surface Observing System. Eighth Symposium on Meteorological Observations and Instrumentation, American Meteorological Society.

Quality Control And Monitoring Sysytems: [www-sdd.fsl.noaa.gov/MSAS/qcms.html](http://www-sdd.fsl.noaa.gov/MSAS/qcms.html)

Nordic Methods for Quality Control of Climate Data: [www.smhi.se/hfa\\_coord/nordklim/reports\\_task1.htm](http://www.smhi.se/hfa_coord/nordklim/reports_task1.htm)

Quality Control of Meteorological Observations : [www.smhi.se/hfa\\_coord/nordklim/reports\\_task1.htm](http://www.smhi.se/hfa_coord/nordklim/reports_task1.htm)

Manual Quality Control of Meteorological Observations : [www.smhi.se/hfa\\_coord/nordklim/reports\\_task1.htm](http://www.smhi.se/hfa_coord/nordklim/reports_task1.htm)



## Detection of Zdr Abnormalities on Operational Polarimetric Radar in Turkish Weather Radar Network

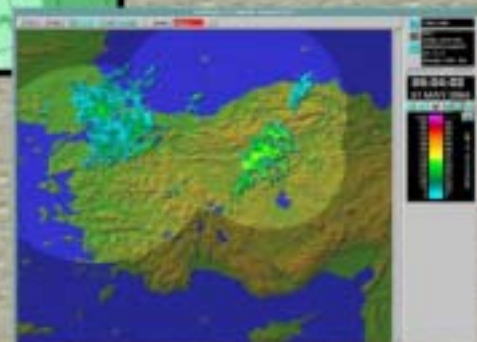
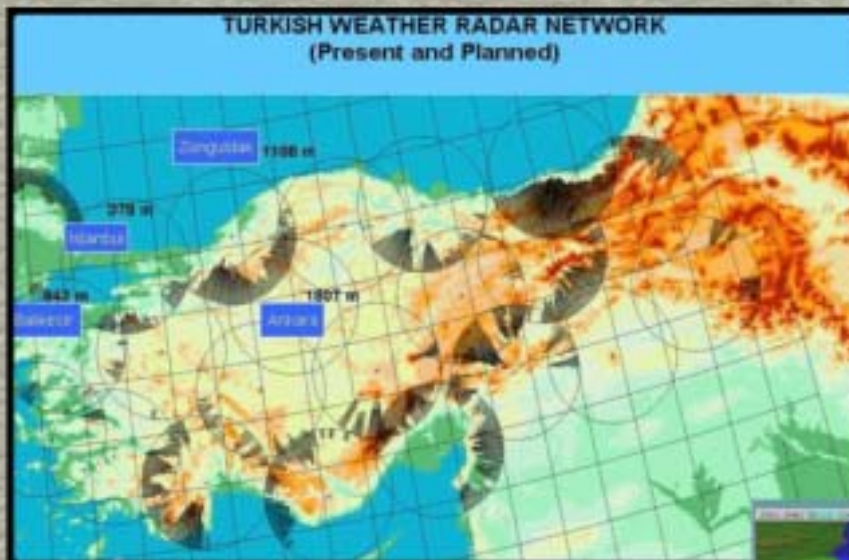


- Turkish State Meteorological Service (TSMS) has four Weather Radars
- Three radars in operation since 2003:

- C-Band, Klystron transmitter, Parabolic Antenna with a diameter of 7 m
- Sigmet Software and Mitsubishi Hardware

- Polarimetric Radar in operation since 2001:

- C-Band, Klystron transmitter, Dual Polarized with dual polarization switch, Parabolic Antenna with a diameter of 4.2 m
- Rainbow Software and Gematronik Hardware



by Oguzhan Sireci

A Composite Image from  
Turkish Weather Radar Network



## Differential reflectivity (ZDR):

Ratio between the reflectivity of a horizontal polarized pulse and the reflectivity of a vertical polarized pulse. ZDR depends on the asymmetry of the shape, the orientation and the falling behavior of the particles. ZDR is positive for oblate raindrops, zero or slightly negative for hail and graupel, and is strongly biased by differential attenuation during the passage of the radar pulse through heavy rainfall.

- Raindrops are not always spherical when they fall - especially the larger drops
  - They tend to become more oblate
  - So, the reflectivity would be larger if the wave were horizontally polarized, or  $Z_h > Z_v$
- Define,

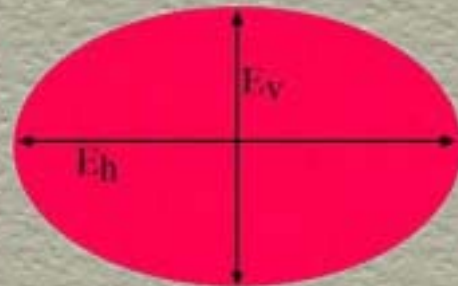
$$\text{ZDR} = \text{differential reflectivity} \\ = 10 \log(Z_h/Z_v)$$

- ZDR is great for discriminating large drops from hail - hail tumbles randomly, looks like a spherical particle.
- So, ZDR for hail is about 0.
- ZDR for ice is about 0 as well.


Table 1. Values of polarimetric variables for precipitation types (from Dostak and Zrnić 1993).


	$Z_e$ (dBZ)	$Z_{dr}$ (dB)	$\rho_w$	$K_{dr}$ ( $^{\circ}\text{km}^{-1}$ )	LDR (dB)
Drizzle	< 23	0	> 0.99	0	< -34
Rain	25 to 60	.5 to 4	> 0.97	0 to 10	-27 to -34
Dry snow	< 23	0 to 3	> 0.98	0 to 0.5	< -34
Dense snow	< 23	0 to 5	> 0.95	0 to 1	-25 to -34
Wet snow	< 43	0 to 2	0.8 to 0.95	0 to 2	-12 to -18
Dry graupel	40 to 50	-0.5 to 1	> 0.95	-0.5 to 0.5	< -20
Wet graupel	40 to 55	-0.5 to 3	> 0.90	-0.5 to 2	-20 to -25
Wet hail (< 2 cm)	50 to 60	-0.5 to 0.5	> 0.95	-0.5 to 0.5	< -20
Wet hail (> 2 cm)	55 to 70	< -0.5	> 0.90	-1 to 1	-10 to -15
Hail/hail	50 to 70	-1 to 1	> 0.90	0 to 10	-10 to -20

Bigger Rain Drops Become More Oblate



Depends on axis ratio

 oblate : ZDR > 0

 prolate : ZDR < 0

For drops: ZDR ~ drop size (0 - 4 dB)

by Oguzhan Sireci

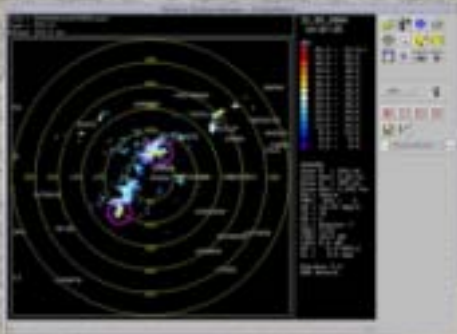
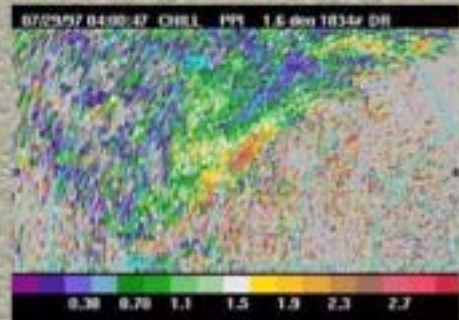


# Some Zdr samples from an operational polarimetric radar:

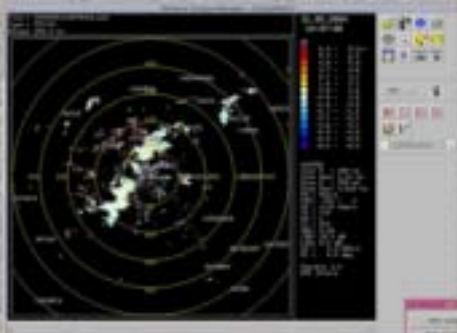


The frame shows the radar reflectivity factor (Z) in units of dBZ from a polarimetric radar. Notice that the maximum reflectivity is about 55 dBZ, a typical lower limit for hail contaminated returns. No hail was observed during the storm.

The image shows the differential reflectivity (Zdr) which is the difference between the reflectivity factors observed at horizontal polarization and vertical polarization. High values of Zdr indicate large raindrops within the pulse volume. The high differential reflectivity values (>2.5) associated with the high reflectivity regions indicate significant numbers of large raindrops.

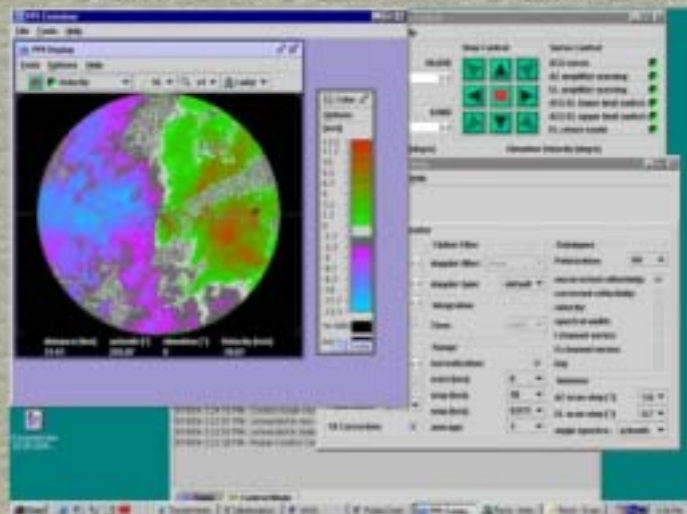


Reflectivity Image

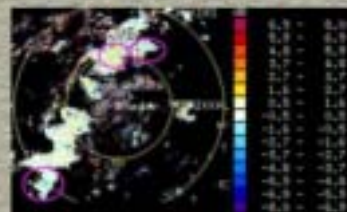


Abnormal Zdr Image

Before checking Zdr values, Velocity(V) and Reflectivity(Z) images in our Polarimetric Radar seem normal.



Velocity Image



Bigger Zdr values should have been observed in marked areas which have heavy rain

by Oguzhan Sireci

- Normally, Zdr Values should change in 0-4 dBm range in rainy areas. For small rain drops and hail, Zdr values should be ~0dBm and should be around 0-4dBm for big rain drops. This value depends on the shape of the drop. In normal conditions, Zdr becomes negative for clutter and ice crystal.



Abnormality Symptoms determined on the product

- In the area of rain echos, Zdr values changes almost randomly between -5dBm to +6 dBm.
- In received images, plus and minus values have been observed as one inside another.
- The transitions observed in Zdr values are not so logical and meaningful.
- Zdr values upper than 5dBm are almost impossible practically

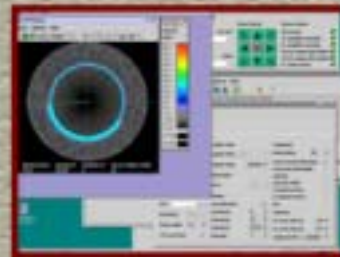
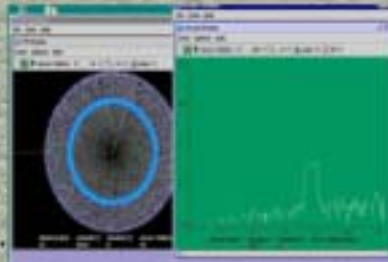


Another abnormal Zdr image

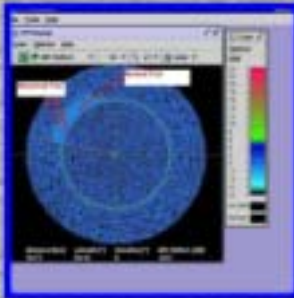
To be able to analyse problem in detail, a pulsed signal was applied to the receiver



F=5625MHz,  
Delay=100µsec (15km)  
signal was applied,  
and that signal  
was examined in  
ppi and ascope  
as reflectivity(Z).

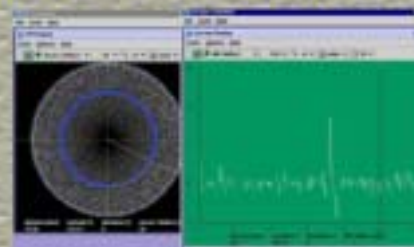
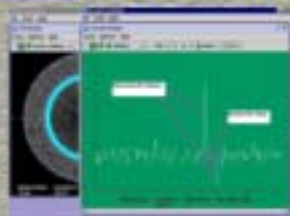


If width of the applied signal changed, it could have been observed in ppi as expected



Signal observed as -0.57dB in Differential Mode. Normally this value should have been 0 dBm. But this value was stable and caused by difference of attenuations of two separate waveguide, so it is compensated as Zdr balance from software. Fluctuates at the both side of the applied signal were very high in positive and negative side. If width of the signal getting narrow, only this abnormal signals remained.

Abnormalities at both edge of the signal could be observed more clearly in ascope



When applied pulse width decreased to 3 µsec only abnormal signals (spikes) remained.

by Oguzhan Sireci

# THE UNITED STATES NATIONAL WEATHER SERVICE (NWS) IN-SITU RADIATION TEMPERATURE CORRECTION FOR RADIOSONDE REPLACEMENT SYSTEM (RRS) GPS RADIOSONDES

Carl A. Bower, Jr

National Weather Service, 1325 East-West Highway #4312, Silver Spring, Maryland 20910  
Tel: 301 713 0722 Ext 145, Fax: 301 713 2099, E-mail: [carl.bower@noaa.gov](mailto:carl.bower@noaa.gov)

## ABSTRACT

The National Weather Service will require individual field sites to apply in-situ radiation corrections to temperature measurements from radiosondes used with the RRS. The radiation corrections will be more dynamic than current correction algorithms in use by radiosonde vendors today. Current radiation correction algorithms use solar elevation angle, balloon ascent rate, and empirical bias corrections such as differences derived from paired radiosonde flights using reference radiosonde technology such as the National Aeronautics and Space Administration (NASA) accurate temperature measurement (ATM) reference radiosonde, differences between day and night flights, and Numerical Weather Center's observation minus first guess-field differences. Improved physics and empirically-based dynamic correction techniques are being developed by NWS radiosonde providers to include the impacts of observed cloud conditions on the correction. Cloud amount, 27 cloud types, cloud base, and cloud thickness are to be considered in the in-situ radiation corrections. The required cloud information is derived from the World Meteorological Organization (WMO) coded cloud group message included with the transmission of each upper air sounding's coded message. The magnitude of the cloud impacts on the temperature correction will be shown for various cloudiness conditions. Results from NASA ATM reference radiosonde flight comparisons for corrected and uncorrected radiosonde temperature profiles will be presented. The results from the comparison flights support the determination of the radiosonde temperature sensor accuracy without correction and the assessment of the dynamic radiation correction algorithm

## 1. INTRODUCTION

The National Weather Service requires in-situ radiation corrections to be applied to radiosonde temperature measurements by individual field sites. Current radiation correction algorithms are based on solar elevation angle, balloon ascent rate, and empirical bias corrections derived from paired radiosonde flights with the National Aeronautics and Space Administration (NASA) accurate temperature measurement (ATM) three-thermistor reference radiosonde. Improved dynamic correction techniques are being developed by NWS radiosonde providers to include the impacts of 27 cloud types, cloud amount, cloud base, and cloud thickness on the in-situ radiation corrections. The cloud information is derived from the World Meteorological Organization (WMO) coded cloud group message included with the transmission of each upper air sounding. The magnitude of the cloud impacts on the temperature correction will be shown for various cloudiness conditions. Results from preliminary flight comparisons of corrected and uncorrected radiosonde temperature profiles against the NASA reference radiosonde will be presented

## 2. THERMISTOR IN-SITU BIAS EVALUATION

Successful factory tests are not good indicators of how temperature sensors will perform in the environment. Small in-situ errors over a flight can lead to large errors in geopotential heights. The inclusion of these errors and height calculations in the WMO coded message used by the National Centers for Environmental Prediction (NCEP) and International centers can lead to data rejection. Height calculations are determined from pressure, temperature, and relative humidity so the total

height error is comprised of three parts. The temperature contribution to geopotential height errors can be significant. A temperature error of 0.25 °C can lead to significant errors.

## 3. IN-SITU COMPARISONS AGAINST A STANDARD

Primary contributions to the bias error of radiosonde temperature measurements are thought to come from short and long wave radiation. A technique to determine the contribution of these biases uses three temperature sensors with different coatings. The different spectral characteristics of coatings selected provide a spread of absorptivity and emissivity values. By knowing the differences in the spectral response of the coatings, it is possible to solve a series of simultaneous equations to determine the overall radiation error. Thermistors flown at night are selected such that one is coated with a material with a low emissivity and the other with a high emissivity. The simultaneous equations solved provide the long-wave correction. The coatings used on these sensors are white and aluminum. Daytime measurements require reference sensors, one with high solar absorptivity and the other with a low solar absorptivity. These are white coated and black coated respectively (Schmidlin 1986). The above technique can be used under various cloudiness conditions and solar elevation angles to determine the temperature bias. The results from comparison measurements have been aggregated and are the basis for correction algorithms in use today. Correction tables have been generated for various solar elevation angles by the NCEP using the NASA ATM results and inclusion of data from first guess fields. While radiation corrections to thermistors are necessary, they are based on averages and, as such,

shift a bias in a given temperature reading. They may often make reasonable data worse. For this reason, every effort should be made to minimize the radiation offset required for a temperature sensor. This can be accomplished through sensor and boom designs and with better coatings to mitigate radiation on the thermistor as a function of the environment.

#### 4. PHYSICS BASED ENERGY BALANCE MODELS

Luers (1990) through the use of empirical data from three thermistor flights worked to model radiation corrections by using the heat transfer process for a rod thermistor shown Figure 1.

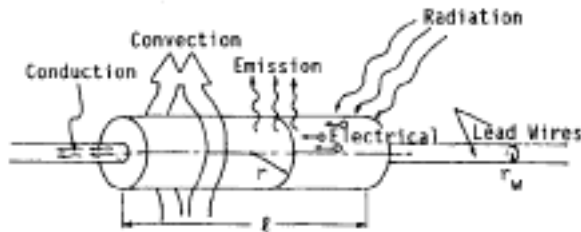


FIG. 1. Thermistor geometry and heat transfer processes.

The time rate of change of the temperature sensor of the radiosonde is shown in Equation 1 for the Figure 1 example:

$$mC(dT/dt) = q_{abs} - q_{emit} + q_{conv} + q_{elec} + q_{cond} \quad (1)$$

Equation 2 is the equation for estimating the temperature error of the radiosonde rod thermistor under different environments

$$q_{abs} = \int_{\phi=0}^{2\pi} \int_{\theta=0}^{\pi} \bar{A}_p(\theta) \int_{\lambda} \alpha(\lambda) I(\theta, \phi, \lambda) d\lambda \sin\theta d\theta d\phi \quad (2)$$

Luers (1996) in work with the National Climatic Data Center developed radiosonde correction models for enhancing historical data records. As part of the work on correction models was the use of the Air Force LOWTRAN 7 atmospheric radiance and transmission model to model the radiative fluxes a function of the environment. The model was used to generate environmental input to accommodate atmospheric conditions in the data correction solution. This included incorporating cloud information.

#### 5. NWS REQUIREMENT FOR RADIATION CORRECTION

The new GPS radiosondes that the NWS is procuring need vendor-provided radiation correction algorithms for correction of the temperature measurements before data transmission from the field sites. The algorithms are to physics-based in considering the energy balance equations. They are to be dynamic in that they will consider direct radiation under clear sky conditions as well as reflected and scattered long and short wave radiation, radiosonde ascent rate/atmospheric density, solar angle, and cloud observations (Sky cover, cloud amount, cloud height and cloud type). The cloud

information was to be extracted and derived from the WMO cloud code group.

The WMO (1995) code group used as part of the Upper Air Coded message is:  $N_h C_L h C_M C_H$

$N_h$	Amount of all the $C_L$ cloud present, or if no $C_L$ is present, the amount of all the $C_M$ cloud present.
$C_L$	Clouds of the genera Stratocumulus, Stratus, Cumulus, and Cumulonimbus.
$h$	Height above surface of the base of the lowest cloud seen. If there are no low clouds reported but middle clouds are reported, the height value is ascribed to the middle cloud.
$C_M$	Clouds of the genera Altopcumulus Altostratus, and Nimbostratus.
$C_H$	Clouds of the genera Cirrus, Cirrocumulus and Cirrostratus.

#### Limitations:

If a low cloud, middle cloud, and high cloud are reported, the cloud cover is only reported for the first layer. If the low cloud is absent (0 cloud type reported), a middle cloud (if reported with other than a 0 cloud type) is assigned the cloud cover okta amount.

Cloud cover is not ascribed to a high cloud report, even if low and middle clouds are not reported (code field populated with 0 for each cloud type).

Cloud base height information in the WMO Code Table not reported beyond 2500 meters for the low or middle cloud.

Cloud-base height information is not supplied for middle clouds above 2500 meters or for high clouds.

Cloud-layer thickness is not available from the Cloud Code Group.

Because of limitations in the WMO Cloud Code Group cloud reporting for the Low, Middle, and High clouds, empirical climatological information from work by Poore et.al., (1995) on cloud bases, thickness for various cloud types were used to complete a cloud table for all 27 types of clouds. Poore's work compiled for 10 cloud types and had to be expanded to the 27 cloud types reported in WMO code tables. Rules were also established for summing okta cover for each cloud type so that total sky cover would not exceed 8 oktas. Table 1 is the table used by the radiosonde vendors to make

Table 1. Reported and estimated cloud cover bases and thickness from WMO Cloud Code Group

Low Cloud				Middle Cloud				High Cloud			
Cloud Code	Okta Cover	Cloud Base	Cloud Depth	Cloud Code	Okta Cover	Cloud Base	Cloud depth	Cloud Code	Okta Cover	Cloud base	Cloud depth
0	0rpd			0	0	Rpd/3300 if code 9	1300	0	0	7252	1000
1	Rpd	Rpd	1000	1	Rpd/8	Rpd/3300 if code 9	1500	1	4	7572	1000
2	Rpd	Rpd	1200	2	Rpd/8	Rpd/3300 if code 9	2500	2	4	7572	1000
3	Rpd	Rpd	2000	3	Rpd/2	Rpd/3300 if code 9	1200	3	1	7252	1000
4	Rpd	Rpd	1200	4	Rpd/3	Rpd/3300 if code 9	1200	4	4	7252	1000
5	Rpd	Rpd	1200	5	Rpd/5	Rpd/3300 if code 9	1200	5	1	7252	1000
6	Rpd	Rpd	1500	6	Rpd/1	Rpd/3300 if code 9	1200	6	4	7252	1000
7	Rpd	Rpd	1500	7	Rpd/3	Rpd/3300 if code 9	1200	7	8	7252	1000
8	Rpd	Rpd	1200	8	Rpd/2	Rpd/3300 if code 9	2500	8	4	7252	1000
9	Rpd	Rpd	2000	9	Rpd/5	Rpd/3300 if code 9	1500	9	2	7252	1000
/	9			/	9			/	9		
/	/			/	/			/	/		

transformations from the WMO Cloud code group transmitted message into a form for inclusion in a thermistor radiation correction model. Data not reported in the WMO cloud message are estimated.

### 6. PRELIMINARY NWS FLIGHT TESTING

The National Weather Service uses the ATM reference radiosonde (Schmidlin et. al., 1986) to assess in situ accuracy of the radiosonde temperature sensor in day and night environments under the influence of long and short wave radiation. It is further used to verify the radiation correction algorithms employed as an evaluation standard for vendor radiosonde thermistor performance. The standard is accurate to 0.2° C in the troposphere and 0.3° C in the stratosphere (WMO, 1996). The standard is used for live radiosonde flights during daytime and nighttime. The three thermistor system enables the NWS to evaluate vendor sensor performance, including the effectiveness of the sensor coating material for both long and short wave radiation and the radiation correction algorithm the vendor is required to provide.

### 7. TEST RESULTS

The NWS flew 7-day and 4-night NASA ATM three thermistor comparison flights respectively with the Sippican MARK IIA GPS radiosonde. The purpose of this preliminary flight series was to compare how well the vendor’s sensors compared with a reference standard and to evaluate the MARK IIA radiation correction routine under development. Results from the flights are depicted. The MARK IIA temperature sensors are (small chips) aluminized.

Part of the evaluation of the prototype radiation correction model was to determine the sensitivity to cloud information on the correction to be applied to the thermistor. Figure 2 has flight information from a live flight flown under overcast conditions. The difference in temperature is shown as the difference between the NASA ATM three thermistor measurements and the vendor corrected MARK IIA temperature (MARK IIA warmer than NASA ATM). The NASA ATM is an all weather system and is not impacted by weather on measurements unless it is precipitating. As such it provides an accurate measurement in cloudy and cloud free situations. A second curve on the figure is for clear conditions. In the upper atmosphere, the difference between the correction for a clear day and an

overcast day is 0.3° C. That is, an overcast day needs a greater correction to temperature values because of reflections off the cloud tops. These values are consistent with the values of 0.5 K found in measurements in the United Kingdom (WMO 1996). Basically, the cloud cover should attenuate the short wave emissions in-cloud, diminish the correction below-cloud. Results below the cloud deck are under review and minor adjustments have been incorporated.

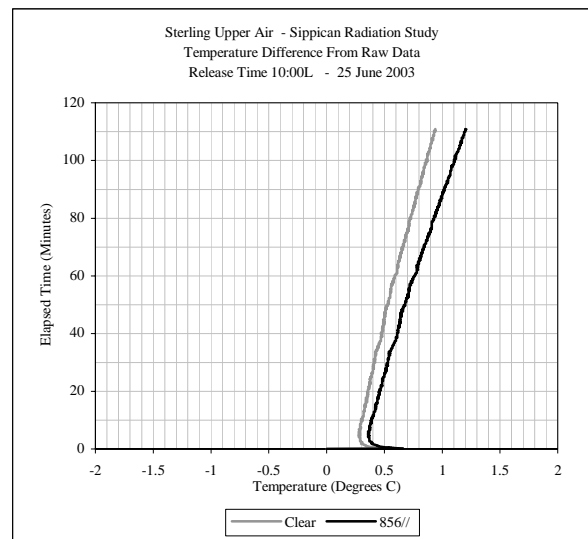


Figure 2. Temperature difference of MARK IIA minus the NASA ATM for overcast and clear conditions.

Composite corrected mean differences between the NASA ATM and the MARK IIA radiosonde for the 7 day flights are shown in Figure 3. The flights were generally during cloudy conditions and consisted of different flight times. It appears that we are over correcting near the surface and under correcting aloft. However, the values are within the worst case tolerance on the accuracy of the NASA ATM and the MARK IIA. The differences for a NASA ATM flight and corrected and uncorrected Mark IIA radiosonde data are shown in Figure 4. There is good agreement between the ATM and the corrected radiosonde data.

Means and standard deviations of the four Sippican night flights are shown in Figure 5. The night flights do not have short or long wave corrections applied by the vendor’s correction model. Although there are some long wave influences on the sensor, they are deemed small and do not receive a correction.



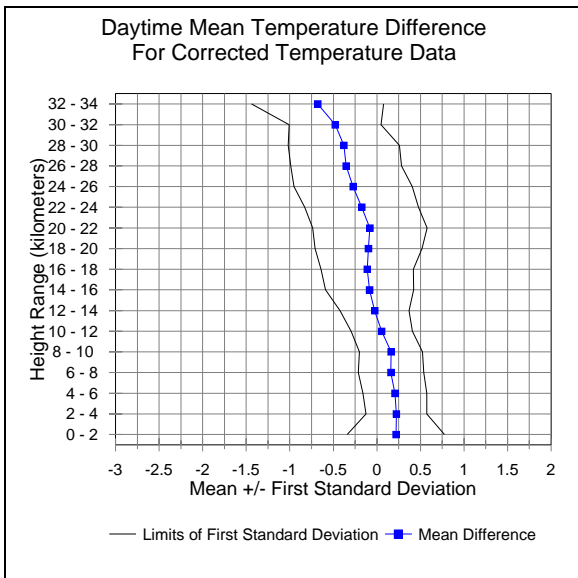


Figure 3. Composite day flight corrected difference and standard deviation NASA ATM minus MARK IIA.

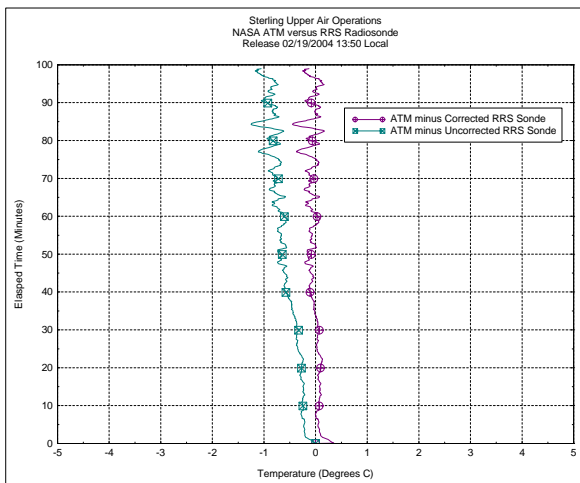


Figure 4. The difference between the ATM and Mark IIA corrected and uncorrected for radiation.

## 8. CONCLUSIONS

The NASA ATM reference radiosonde dual flight in-situ testing with standard radiosondes is critical for Determining temperature accuracy, bias, and required radiation algorithm assessment for operational radiosondes.

Preliminary results from flights of the Sippican MARK IIA radiosondes against the NASA three thermistor system are promising. The uncorrected errors are less than for previous thermistors on older radiosondes and qualitatively, the dynamic radiation correction is functioning properly. More flight testing under different solar angles and weather conditions is required.

Follow-on assessment of the radiation model and possible adjustments to more accurately account for differences between the NASA ATM all weather reference radiosonde and the MARK IIA radiosonde need to be undertaken.

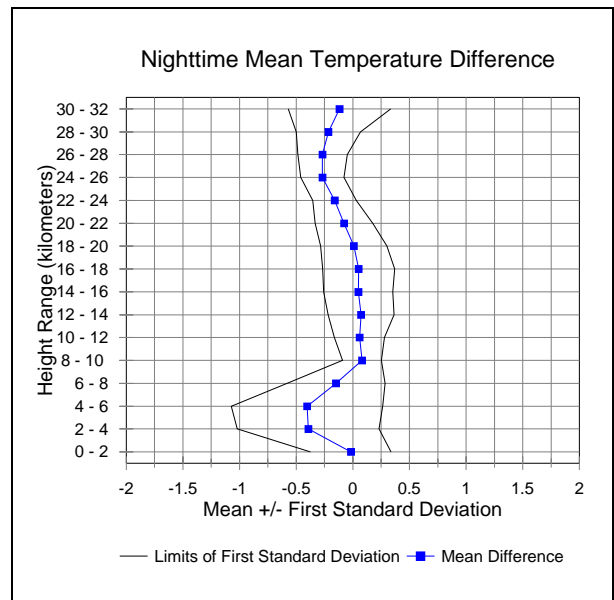


Figure 5. Night flights means and standard deviations of the difference of the NASA ATM minus the MARK IIA radiosonde.

## 9. REFERENCES

National Weather Service Specification NWS-J070-RS-SP005B, February 2002. Specification No. NWS-J070-RS-SP005B for Global Positioning System and Signal Processing System. Silver Spring, Maryland.

Schmidlin, F. J., Luers, J. K., and Huffman, P. D. 1986: Preliminary Estimates of Radiosonde Thermistor Errors. NASA Technical Paper 2637. Wallops Island, Virginia.

World Meteorological Organization, 1996: Guide to Meteorological Instruments and Methods of Observation. Sixth Edition, WMO-No. 8, Geneva.

Luers, J. K., Temperature Correction Models for the Worlds Major Radiosondes 1990-1995. Final Report, OAA Contract 50EANE-2-00077, August 1996, National Climatic Data Center, Asheville, North Carolina.

Poore, K. D. Wang, J., and Rossow, W. B. 1995: Cloud Layer Thicknesses from a Combination of Surface and Upper-air Observations, Journal of Climate, Volume 8, March 1995.

# Wind Tunnel Tests of Some Low-Cost Sonic Anemometers

Michael C. Sturgeon  
National Oceanographic and Atmospheric Administration  
National Weather Service  
National Data Buoy Center  
Sterling Test Facility  
Sterling, Virginia  
USA

## Abstract

Sonic anemometers for meteorological measurements have been around since the early 1970s. The early sonic anemometers were very expensive and did not have the high reliability, low-cost electronic components now available. Thus, early sonic anemometers had poor reliability and were mainly used for scientific research. In the last several years, manufacturers have started offering lower-cost sonic anemometers suitable for general meteorological use. The low maintenance and low electrical power requirements of these current sonic anemometers make them good candidates for remote sensing applications with solar panels. This paper presents test data for several available low-cost sonic anemometers using wind tunnel test method ISO 16622 *Meteorology – Sonic anemometers / thermometers - Acceptance test methods for mean wind measurements*. The measurement performance differences of sonic anemometers and rotating anemometers are discussed in this paper.

## 1. Background

A new generation of low cost, high performance sonic anemometers has come into the market place in the past 10 years. Prices of the latest sonic anemometers are significantly less, and the prices are now comparable to high quality cup and propeller anemometers. As an added advantage, sonic anemometers require almost no periodic maintenance since there are no moving parts to wear out. The starting threshold and response time, for both wind speed and direction, are essentially zero. These two characteristics make the sonic anemometer a good candidate for air pollution, dispersion models and other applications requiring high accuracy at very low wind speeds.

## 2. Anemometers Tested

The sonic anemometers tested were: 1) Gill WindSonic - UK; 2) R. M. Young 85000 - USA; 3) Vaisala WS425A - Finland; 4) Vaisala WXT510 - Finland. All the sensors tested were two-dimensional sonic anemometers. The Gill WindSonic and R. M. Young 85000 have a four-transducer configuration while both Vaisala sonic anemometers utilize a three-transducer configuration. All test anemometers were configured with an RS-232 serial interface and required an external dc power supply. The wind tunnel tests were conducted in the polled RS-232 mode for all the test anemometers.

---

Michael C. Sturgeon  
National Weather Service  
National Data Buoy Center  
Sterling Test Facility  
43741 Weather Service Road  
Sterling VA 20166  
USA  
E-mail: [michael.sturgeon@noaa.gov](mailto:michael.sturgeon@noaa.gov)

### 3. Test Method <sup>[1]</sup>

The tests were conducted in the NWS Sterling Wind Tunnel. The wind tunnel test section is 1.3 m x 1.3 m x 2 m long. The maximum speed of the wind tunnel is 68 m/s. The reference wind tunnel air speed measurements were made with a pitot-static tube mounted in the test section. Ambient temperature, relative humidity, and barometric pressure measurements were taken in the wind tunnel test section. These measurements were used to correct the air density in the wind tunnel test section to standard conditions of dry air at 15 °C and 1013.25 hPa. This air density correction is then applied to the pitot-static tube pressure measurement. The pitot-static tube has been calibrated at the United States' national laboratory: National Institute of Standards and Technology (NIST). All wind tunnel parameters are sampled at a 6-hertz rate and recorded in 30-second intervals, time synchronized with the test anemometer data. The wind tunnel air speed measurement uncertainty was verified by the use of a transfer standard anemometer (R. M. Young 27106DR), which had been previously calibrated at NIST. The calibration verification test was conducted over the air speed range of 6.8 to 66 m/s in approximate 8 m/s increments. Two 30-second data points were taken at each speed. The wind tunnel air speed measurement uncertainty, with a coverage factor of  $k=2$ , was 0.09 m/s over the full air speed range.

Sonic anemometers often exhibit measurement perturbations in response to the incident wind direction. These measurement perturbations are caused by the wind turbulence created by the support structure and/or the transducers themselves. A rigorous test requires that the sonic anemometer be rotated over the full 360-degree azimuth and data taken at a sufficient number of points to define the speed and direction performance characteristics. Generally, for most sonic anemometers, there seems to be little effect of the wind direction on sonic anemometer performance at speeds below 15 m/s, but as the air speed increases the performance issues often occur in the form of both wind speed and wind direction measurement accuracy.

The wind tunnel tests were conducted in accordance with section 8.3.1 of ISO16622 *Meteorology - Sonic anemometers/thermometers – Acceptance test methods for mean wind measurements*<sup>[2]</sup>. The test speeds were calculated as specified in ISO 16622. The sonic anemometers were tested at constant wind tunnel air speeds of 6, 11, 20, 36, and the maximum operational speed ( $U_{max}$ ) of the particular sonic anemometer. At each constant test speed, the sonic anemometer was rotated in five-degree increments from 0 to 360 degrees. Data was taken from the anemometer for 30 seconds at each five-degree increment. Both the wind speed and direction are averaged over the thirty-second sampling interval.

The wind direction alignment procedure was performed in two steps:

- 1) An initial visual static alignment of the test sonic anemometer to wind tunnel centerline is performed with a straight edge ruler. This results in an initial sensor alignment to within  $\pm 1$  degree.
- 2) A dynamic alignment of the sonic anemometer is performed with the wind tunnel propeller speed set to 200 rpm (~13.5 m/s) to eliminate any offset from step 1. This offset value is then entered in the rotator table controller program. This offset is then used for all wind tunnel test runs at the selected test speeds.

### 4. Test Results

The test results and manufacturers' stated specifications are summarized in Table 1. For the wind tunnel tests, all anemometers were configured to provide wind speed data in knots. The wind speed data was converted in post processing to m/s.

Manufacturer Model	Sensor Firmware Version	Vendor's Stated Current Draw @ 12.0 vdc <sup>1</sup>	Measured Current Draw @ 12.0 vdc <sup>2</sup>	Manufacturer's Stated Wind Speed Accuracy	Test Results Wind Speed Accuracy	Manufacturer's Stated Maximum Operational Speed, U <sub>max</sub>	Manufacturer's Stated Wind Direction Accuracy	Test Results Wind Direction Accuracy
Gill WindSonic sn 043116	2162-400	40 ma <sup>3</sup>	17 ma	±2% @ 12 m/s	+1% to +5% @ 11 m/s  Overall: 0% to +7%	60 m/s <sup>4</sup> (117 knots)	±3 degrees @ 20 m/s	±2 degrees @ 20 m/s  Overall: ±4 degrees
RM Young 85000 sn 00211	1.2.00	40 ma	31 ma average	±0.1 m/s (@ 3.3 m/s max)  or  ±3% whichever is greater	No test data at this speed <sup>5</sup> <i>0<sup>+</sup> to +0.3 m/s @ 6 m/s</i>  -1% to +5%	60 m/s (117 knots)	±3 degrees	-1 to +2 degrees
Vaisala WS425A sn Y1020010	6.04	25 ma	14 ma average	±0.135 m/s (@ 4.5 m/s max)  or  ±3% whichever is greater	No test data at this speed <sup>5</sup> <i>-0.1 to +0.2 m/s @ 6 m/s</i>  -5% to +4%	65 m/s (126 knots)	±2 degrees @ wind speeds greater than 1 m/s	-2 to +1 degrees
Vaisala WXT510 sn Z441004	1.03	0.07 to 13 ma  3 ma typical	4 ma average wind message only <sup>6</sup>	±0.3 m/s (@ 15 m/s max) or  ±2% whichever is greater	-0.2 m/s to +0.4 m/s @ 11m/s  -4% to +7%	60 m/s (117 knots)	±2 degrees	-4 to +8 degrees <sup>7</sup>

Table 1 - Summary of sonic anemometer wind tunnel test results and manufacturers' specifications – see notes in Appendix A

## Gill WindSonic



The measured sonic path length for the Gill WindSonic is approximately 100 mm. The WindSonic had a rather unique sonic path configuration with the sonic signals reflected off a top horizontal plate. The anemometer provided a one-second averaging time and was running at an internal sensor-sampling rate of one hertz. The one-second-averaging time is not adjustable. The Gill WindSonic User Manual accuracy statements were:  $\pm 3$  degrees at 20 m/s for wind direction and  $\pm 2\%$  at 12 m/s for wind speed. The Gill WindSonic technical brochure had the same accuracy statements ( $\pm 3$  degrees /  $\pm 2\%$ ) with no wind speed qualification statement. The WindSonic demonstrated a positive wind speed measurement bias of approximately 3 to 5% at the nominal test air speeds. The WindSonic did not reach its manufacturer's stated maximum operational speed ( $U_{max}$ ) of 60 m/s at all orientations. At an air speed of 60 m/s, the WindSonic experienced missing or anomalous data at ten azimuths: 55, 60, 65, 70, 155, 240, 245, 310, 330 and 335 degrees.

### Summary of Gill WindSonic Wind Direction Performance

Nominal Test Speed	Manufacturer's Stated Accuracy*	Results As Tested
6 m/s		$\pm 2$ degrees
11 m/s		$\pm 2$ degrees
20 m/s	$\pm 3$ degrees	$\pm 2$ degrees
36 m/s		-2 to +1 degree
60 m/s		$\pm 4$ degrees (Missing Data)

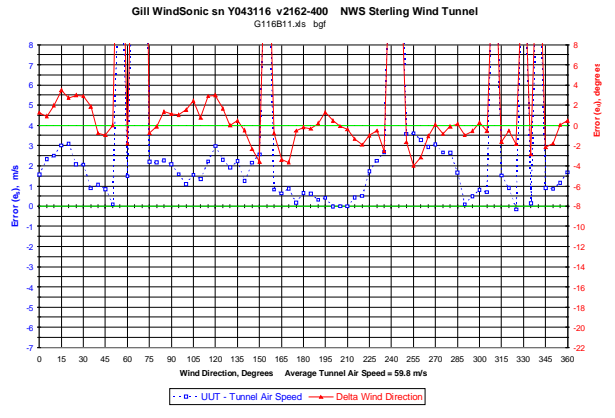
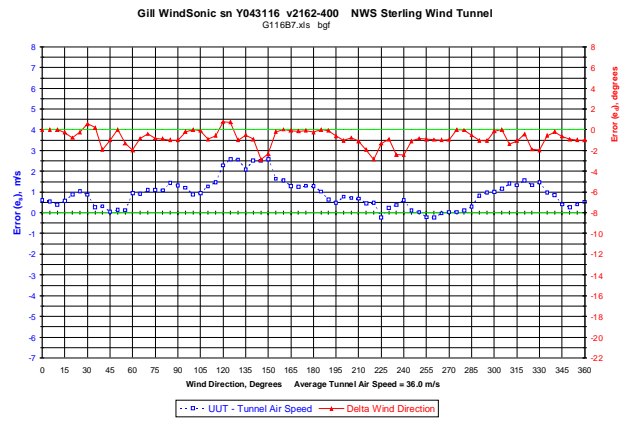
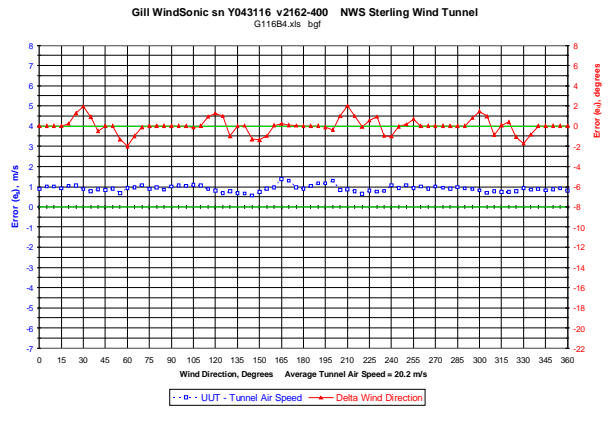
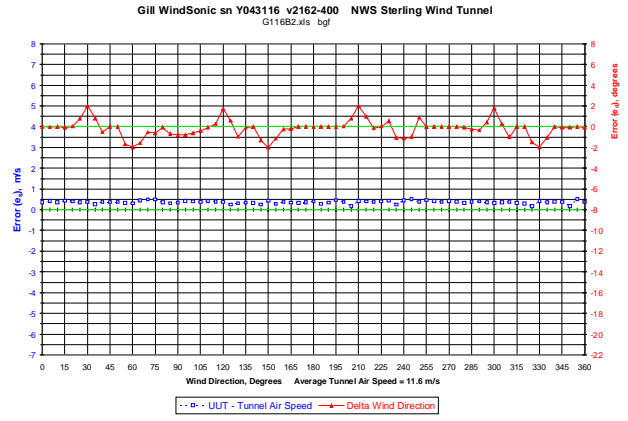
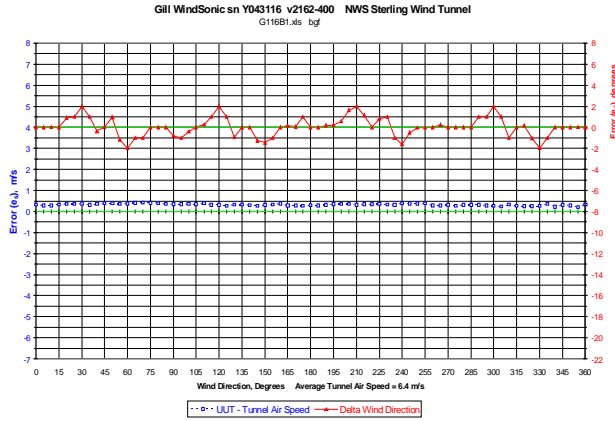
\*Manufacturer's stated accuracy is:  $\pm 3$  degrees at 20 m/s.

### Summary of Gill WindSonic Wind Speed Performance

The Gill WindSonic had missing data at its stated maximum operational speed ( $U_{max}$ ) of 60 m/s.

Nominal Test Speed	Manufacturer's Stated Accuracy*	Results As Tested
6 m/s		+3 to +7 %
11 m/s		$\pm 2$ %
20 m/s		+3 to +7 %
36 m/s		+1 to +7 %
60 m/s		0 to +6 % (Missing Data)

\*Manufacturer's stated accuracy is:  $\pm 2$  % at 12 m/s.



## Gill WindSonic wind tunnel test graphs

## R. M. Young 85000



The measured sonic path length for the R. M. Young 85000 is 141 mm. The R. M. Young 85000 was configured in software to provide three-second average wind direction and wind speed data and was running at an internal sensor-sampling rate of one hertz. The R. M. Young 85000 met the manufacturer's stated wind direction accuracy through 60 m/s. The R. M. Young 85000 demonstrated a slight positive wind speed measurement bias at all the nominal test air speeds. The average bias was approximately 1.5 %. The R. M. Young 85000 had no missing data at its stated maximum operational speed ( $U_{max}$ ) of 60 m/s.

### Summary of R. M. Young 85000 Wind Direction Performance

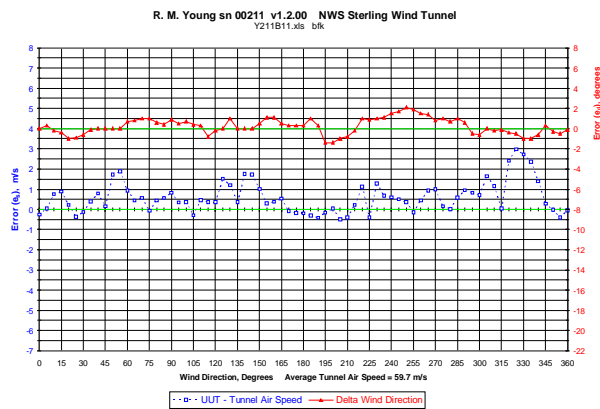
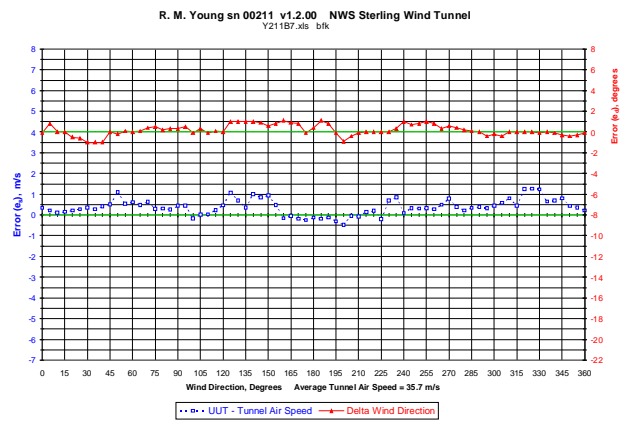
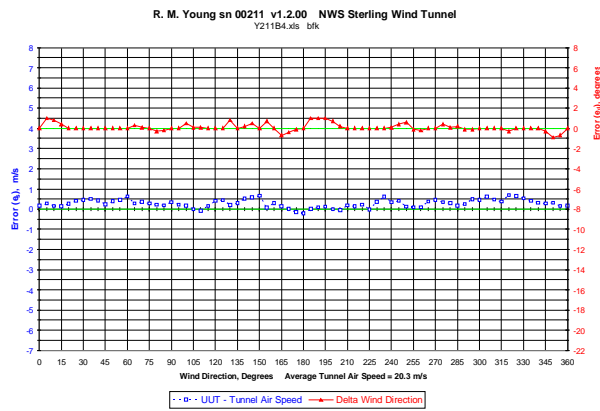
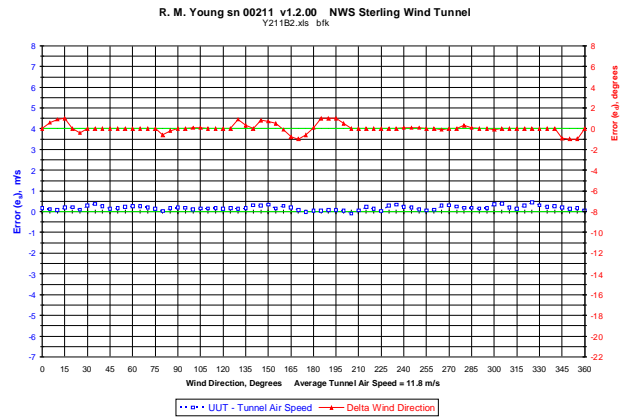
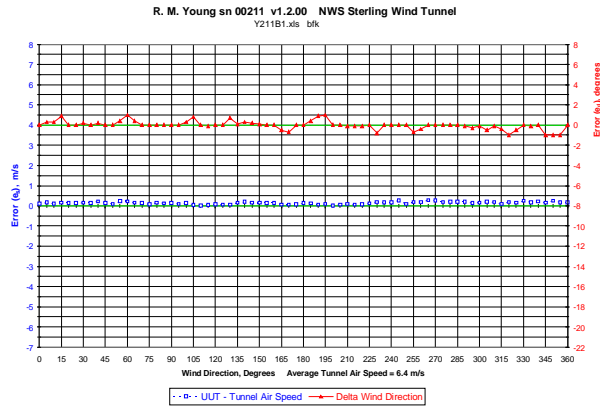
Nominal Test Speed	Manufacturer's Stated Accuracy	Results As Tested
6 m/s	±3 degrees	±1 degree
11 m/s		±1 degree
20 m/s		±1 degree
36 m/s		±1 degree
60 m/s		-1 to +2 degrees

### Summary of R. M. Young 85000 Wind Speed Performance

The R. M. Young had no missing data at its stated maximum operational speed ( $U_{max}$ ) of 60 m/s.

Nominal Test Speed	Manufacturer's Stated Accuracy*	Results As Tested
6 m/s	±3 %	0 <sup>+</sup> to +5 %
11 m/s		-1 to +4 %
20 m/s		-1 to +3 %
36 m/s		-1 to +4 %
60 m/s		-1 to +5 %

\*Manufacturer's stated accuracy is: ±0.1 m/s or ±3 %, whichever is greater.



## R. M. Young 85000 wind tunnel test graphs



## Vaisala WS425A



The measured sonic path length for the Vaisala WS425A is 217 mm. The WS425A was configured via software commands to provide three-second average wind speed and direction values and was polled every three seconds for data. With the omni-directional sonic pattern from the round transducers, it was necessary to mount the WS425A with an eight-degree side tilt in the wind tunnel to prevent disturbances in the received sonic signal due to sonic reflections off the wind tunnel sidewalls. The WS425A met the manufacturer's stated wind direction accuracy. The WS425A met the manufacturer's stated wind speed accuracy through 60 m/s but not 65 m/s.

### Summary of Vaisala WS425A Wind Direction Performance

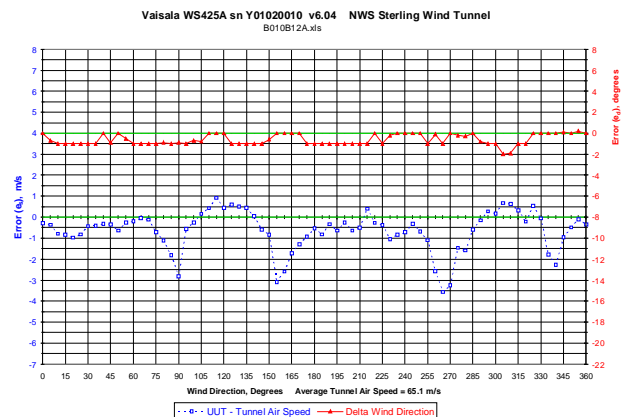
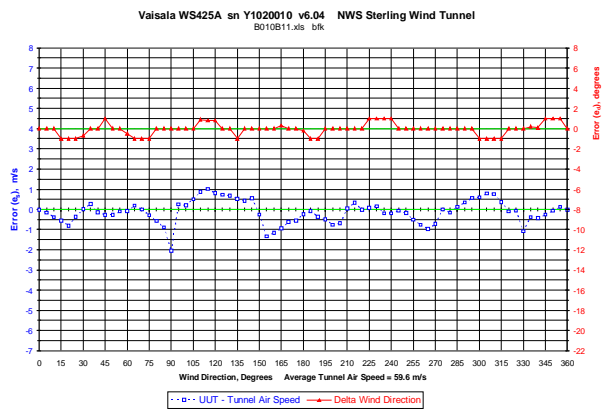
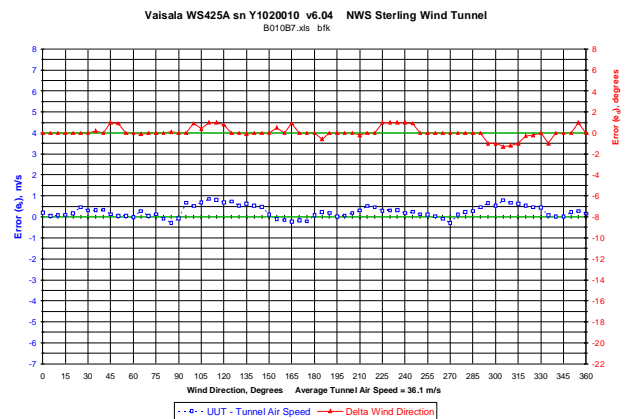
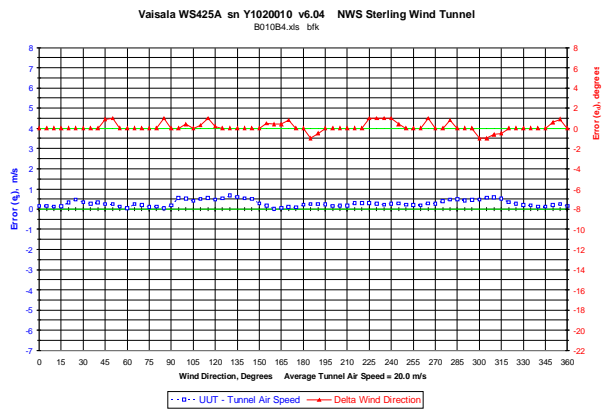
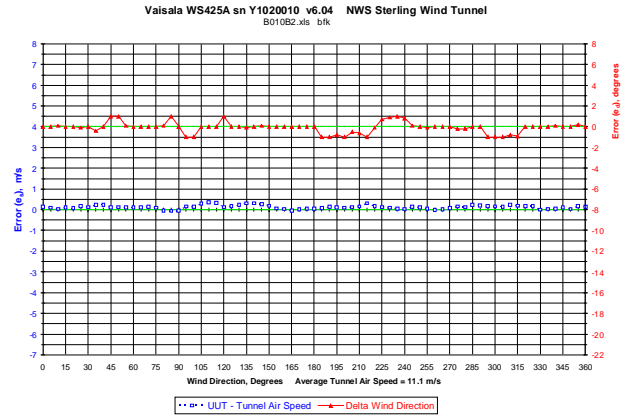
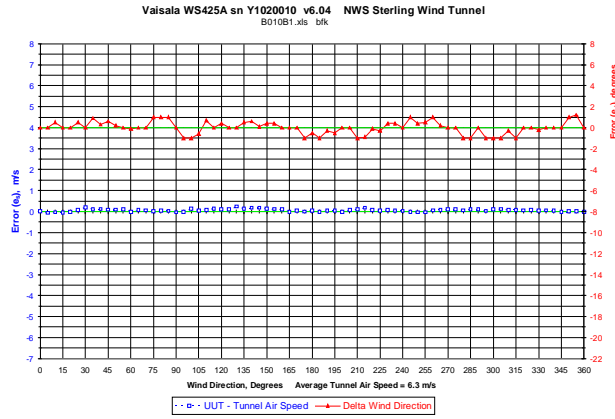
Nominal Test Speed	Manufacturer's Stated Accuracy	Results As Tested
6 m/s	±2 degrees	±1 degree
11 m/s		±1 degree
20 m/s		±1 degree
36 m/s		±1 degree
60 m/s		±1 degree
65 m/s		-2 to 0 degrees

### Summary of Vaisala WS425A Wind Speed Performance

The Vaisala WS425A had no missing data at its stated maximum operational speed ( $U_{max}$ ) of 65 m/s.

Nominal Test Speed	Manufacturer's Stated Accuracy*	Results As Tested
6 m/s	±3 %	-1 to +4 %
11 m/s		-1 to +3 %
20 m/s		0 to +3 %
36 m/s		-1 to +2 %
60 m/s		-3 to +2 %
65 m/s		-5 to +1 %

\*Manufacturer's stated accuracy is: ±0.135 m/s or ±3 %, whichever is greater.



## Vaisala WS425 Wind tunnel test graphs

## Vaisala WXT510



The measured sonic path length for the Vaisala WXT510 was 88 mm. The Vaisala WXT510 was configured via software commands to provide three-second average wind speed and direction values updated once per second. At zero degrees, the Vaisala WXT510 produced random anomalous wind direction readings of 120 and 240 degrees at all wind speeds. During some 30-second samples at zero degrees, all wind direction values were zero degrees. During other 30-second sample intervals there would be one or more anomalous wind direction values. This anomalous wind direction pattern did not occur at azimuths of 120 or 240 degrees, suggesting that the problem could be a wind direction algorithm malfunction at zero degrees.

### Summary of Vaisala WXT510 Wind Direction Performance

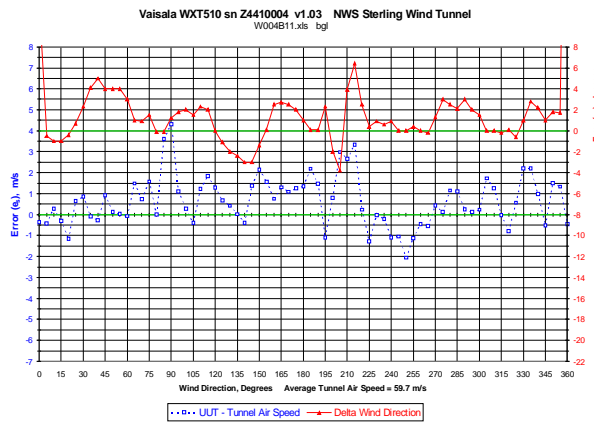
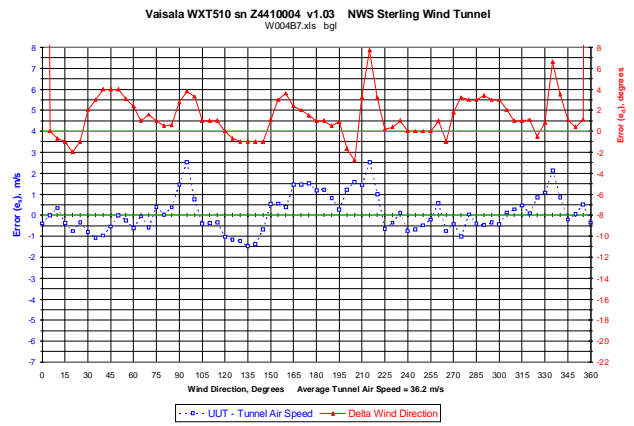
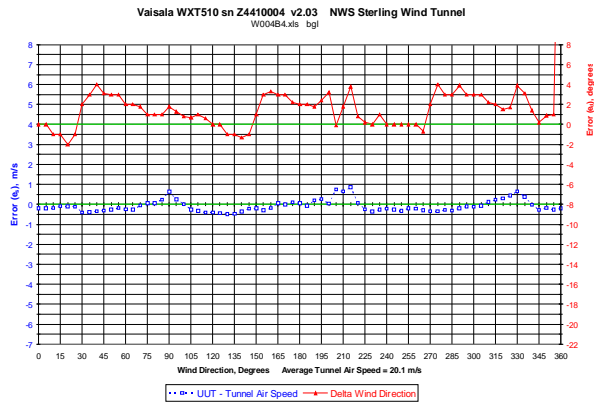
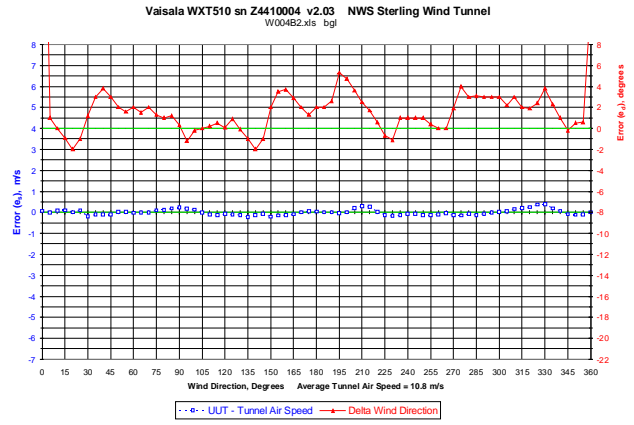
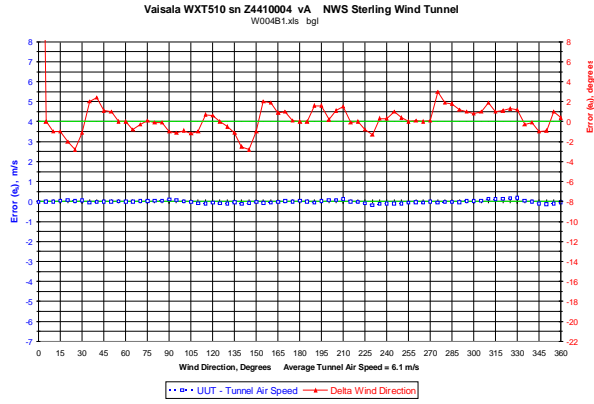
Nominal Test Speed	Manufacturer's Stated Accuracy	Results As Tested
6 m/s	±2 degrees	±3 degrees
11 m/s		-2 to +5 degrees
20 m/s		-2 to +4 degrees
36 m/s		-3 to +8 degrees
60 m/s		-4 to +6 degrees

### Summary of Vaisala WXT510 Wind Speed Performance

The Vaisala WXT510 had no missing data at its stated maximum operational speed ( $U_{max}$ ) of 60 m/s.

Nominal Test Speed	Manufacturer's Stated Accuracy*	Results As Tested
6 m/s	±0.3 m/s	±0.2 m/s
11 m/s		-0.2 to +0.4 m/s
20 m/s	±2 %	-2 to +4 %
36 m/s		-4 to +7 %
60 m/s		-3 to +7 %

\*Manufacturer's stated accuracy is: ±0.3 m/s or ±2 %, whichever is greater.

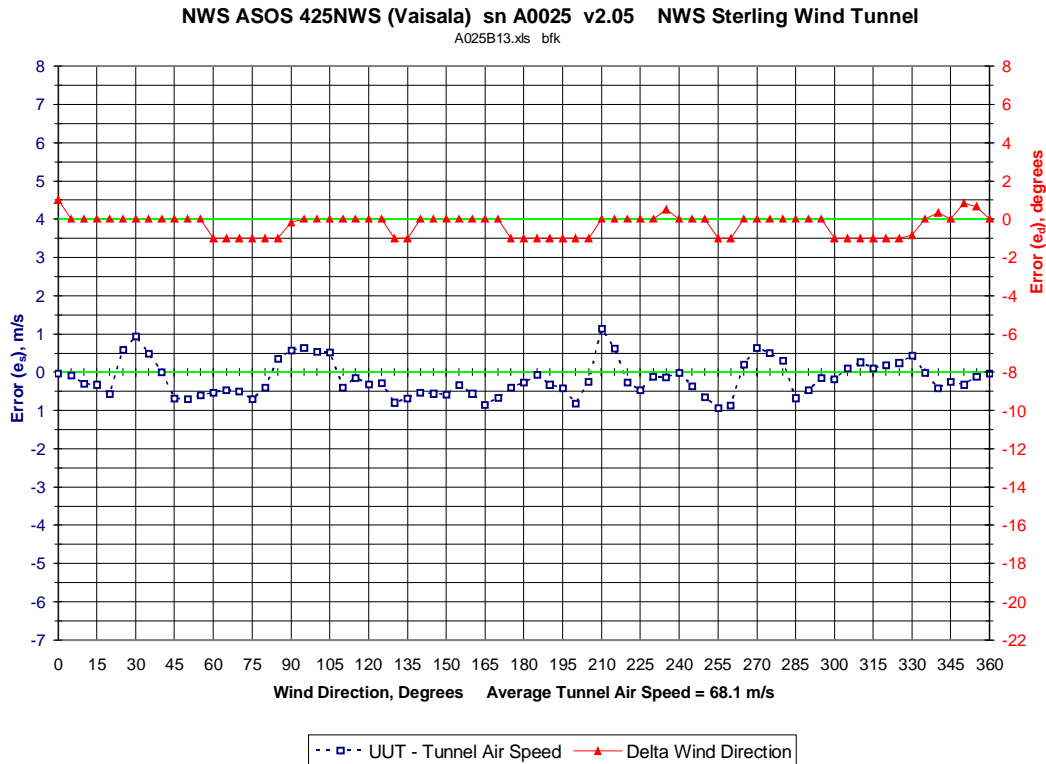


## Vaisala WXT510 wind tunnel test graphs

## 5. Conclusions

Two of the sonic anemometers, the R. M. Young 85000 and the Vaisala WS425A, met the manufacturer's stated wind direction accuracy over the full operational speed range of the anemometer.

None of the sonic anemometers met the manufacturer's stated wind speed accuracy over the full operational speed range of the anemometer. It's the author's opinion that some fine-tuning of the internal speed correction tables could improve the wind speed accuracy of these low-cost sonic anemometers to 65 m/s and beyond. The wind tunnel performance of a NWS ASOS 425NWS sonic anemometer at 68 m/s is shown below. This anemometer is not a low-cost sonic anemometer but is shown as a performance benchmark. This sonic anemometer is a modified version of the COTS Vaisala WS425A. The ASOS 425NWS wind speed accuracy was  $-1.4\%$  to  $+1.7\%$  at 68 m/s in the wind tunnel.



### NWS ASOS 425NWS sonic anemometer at 68 m/s

The author has made several observations over years concerning sonic anemometers. Is there a need to specify wind direction accuracy any better than  $\pm 3$  degrees? It's the author's opinion that a wind direction accuracy of  $\pm 3$  degrees is adequate for many applications that report wind direction to the nearest 10 degrees. In most cases, with an error allowance of  $\pm 1$  degree for a precision north alignment, a sensor accuracy of  $\pm 3$  would provide the same 10-degree wind direction-reporting bin in the database. Sonic anemometers have a definite  $U_{\max}$  when the transmitted sonic signal can no longer be discerned due to the noise created by the air turbulence of wind flowing over the transducers and support structures at high wind speeds. The analog interface on sonic anemometers may not provide the same accuracy as the digital interface. Also, the end user should test the sonic anemometer with the measurement units (knots, m/s, etc.) that are to be used in the particular application to ensure that there are no errors in the unit conversion or the internal sensor correction tables. To summarize: Test the exact model of the sonic anemometer with the sensor firmware version, interface, and with the measurement units to be used in the particular application.

## Bibliography

<sup>[1]</sup> Sturgeon, M. C., *A Wind Tunnel Acceptance Test Method For Sonic Anemometers*, presented at the 15<sup>th</sup> International Conference on Interactive Information and Processing Systems (IIPS) for Meteorology, Oceanography, and Hydrology at the 79<sup>th</sup> annual meeting of the American Meteorological Society at Dallas Texas on January 12, 1999.

<sup>[2]</sup> ISO16622: 2002, *Meteorology - Sonic anemometers/thermometers – Acceptance test methods for mean wind measurements*

## Appendix A

Notes to Table 1

<sup>1</sup>Manufacturer's stated supply voltage range:

Gill WindSonic	9 to 30 vdc
RM Young 85000	9 to 16 vdc
Vaisala WS425A	10 to 15 vdc
Vaisala WXT510	5.5 to 30 vdc

All wind tunnel tests, except for the Vaisala WS425A sonic anemometer, were conducted at 12.05±0.05 vdc. The power source used was a Tenma laboratory power supply model 72-110, sn 8705697. For the Vaisala WS425, a Vaisala model 4257006 power supply, sn 168, was used. The supply voltage was 12.15 vdc. The load current was measured with a Fluke Model 87-III True RMS multimeter, sn 69820005.

<sup>2</sup>Current draw shown for the RS-232 interface. RS-422, RS485, SDI-12, and analog interfaces are either available as a standard feature or an option depending on the particular model anemometer.

<sup>3</sup>With the newest version of sensor firmware, the manufacture's stated current draw is 14 ma @ 12 vdc.

<sup>4</sup>Missing data errors occurred at 60 m/s.

<sup>5</sup>No data was taken at the specified speed. Data shown is for closest test speed for comparison only.

<sup>6</sup>The heaters were not used during the wind tunnel tests. The heaters supply lines were jumpered at the sensor terminal board to the 12 vdc power supply ground. The sensor heaters were not energized during these wind tunnel tests. The heater supply (+) and heater supply (-) were jumpered to the power supply ground (-) terminal at the internal sensor terminal strip.

<sup>7</sup>Anomalous wind direction readings of 120 and 240 degrees occurred at zero degrees at all wind speeds.

## Acknowledgements

This paper is dedicated to the memory of Thomas J. Lockhart, whose mentoring for quality in meteorological measurements has inspired many during his lifetime.

A special thanks to: Michael Salyards, NWS, for technical suggestions and editorial review of this paper.

## Disclaimer

The opinions expressed in this paper are solely those of the author and do not represent any official position of the United States National Weather Service.

## SESSION 4

TECHNOLOGY TRANSFER, CAPACITY BUILDING,  
TRAINING AND DEVELOPMENT OF RICs

Session 4

POSTERS





## Italian Air Force Center of Aeronautic Meteorological Experimentations Technology, training, development, testing and calibration

E. Casar, L. Padellaro, P. Malaspina, P. Poli, E. Veneroli, E. Venanzoni  
Reparto Sperimentazioni di Meteorologia Aeronautica  
via Braccianese Claudia, Km 73 - 00042 - Vigna di Valle, Bracciano, Roma (Italy)

### Historical note

In 1904 the Captain of the Royal Army Maurice M. Wors undertakes the first aerostatic experiences on the Lake of Bracciano. To such purpose, in November 1907 it was projected a Military Aerologic Observatory, able to furnish meteorological support to the near yards for dirigible and to start the first systematic studies on the low and medium atmosphere. In 1910 the observatory began its activity. In 1923, passing to the dependences of the dawning Royal Aeronautics, it became Experimental Aerologic Station. The observatory continued its own activity until September 8th 1943, when it was busy from the German army. Normal activities took back in 1952 with the new denomination of "Central Observatory of Meteorology and Spatial Physics". Manifold activities have been developed by the Department during the years, among which the planning and the realization of meteorological devices and the ground and high level radioactivity measurements. From 1985 it has assumed the actual denomination of Department for Aeronautic Meteorological Experimentations (Re.S.M.A.) and since 1992 it depends from the General Office for Meteorology (UGM) and it belongs to the Command of Squares of Italian Military Aviation.



The observatory continued its own activity until September 8th 1943, when it was busy from the German army. Normal activities took back in 1952 with the new denomination of "Central Observatory of Meteorology and Spatial Physics". Manifold activities have been developed by the Department during the years, among which the planning and the realization of meteorological devices and the ground and high level radioactivity measurements. From 1985 it has assumed the actual denomination of Department for Aeronautic Meteorological Experimentations (Re.S.M.A.) and since 1992 it depends from the General Office for Meteorology (UGM) and it belongs to the Command of Squares of Italian Military Aviation.



### Disposition and expertises

The Department for Aeronautic Meteorological Experimentations (Re.S.M.A.) is placed in Vigna di Valle (surroundings of the lake of Bracciano) in an historic building where since 1902 it has been working as the first aerologic station in Italy.



HEADQUARTER

The Re.S.M.A. is covered by:

### EQUIPPED EMPLACEMENT



### METEOROLOGICAL STATION



The meteorological station works 24h, produces CLK, MET, METAR and CREX messages and makes ozone measurement and meteorological sounding.

Every emplacement are equipped of power supply, lighting, data transfer connector and real time control.

The Re.S.M.A. is responsible for instrumental tests in the field of meteorological observation. It assures the quality of measurements and observations coming from the net of the Service, by instrumentation management and testing, develops the methodologies for the control, sampling and verification of new instrumentations introduced in national area and manages the mobile support for national territory demands and out area operations.

A Meteorological Mobile Unit (uMM) is available to provide a meteorological technical support in every area of the nation. It is entirely equipped with the best portable meteorological and technical devices and it has an appropriate telecommunication system to receive and provide every kind of meteorological information. The uMM has a portable apparatus to launch sounding balloons.



### Activities and Instrumentations

Many instruments are tested and data comparison allows to know the performances of standard and experimental devices

#### Rain gauges



#### Thermo-hygrometers



The S.O.D.A.R. MFAS is one of the instruments operating at the Re.S.M.A. It's possible to study wind shear and turbulence and to have information about the wind profile up to 1000 m with resolution of 10m.



The ozone control in Vigna di Valle is one of the main activities among special meteorological observations and measurements. There are two special instruments used to analyse the atmosphere and to measure the

ozone quantity. The oldest is the DOBSON 947 and the newest is the BREWER making UV measures too.

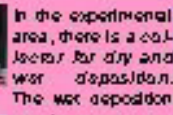


A calibration bench is used to set the pyranometer

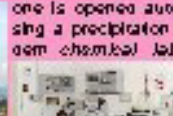
Measures of sunshine duration, global and UV radiation are effected.



In the experimental area, there is a collector for dry and wet deposition. The wet deposition



one is opened automatically by using a precipitation detector. A modern chemical laboratory makes the analysis of precipitation coming from many sampling Italian stations.



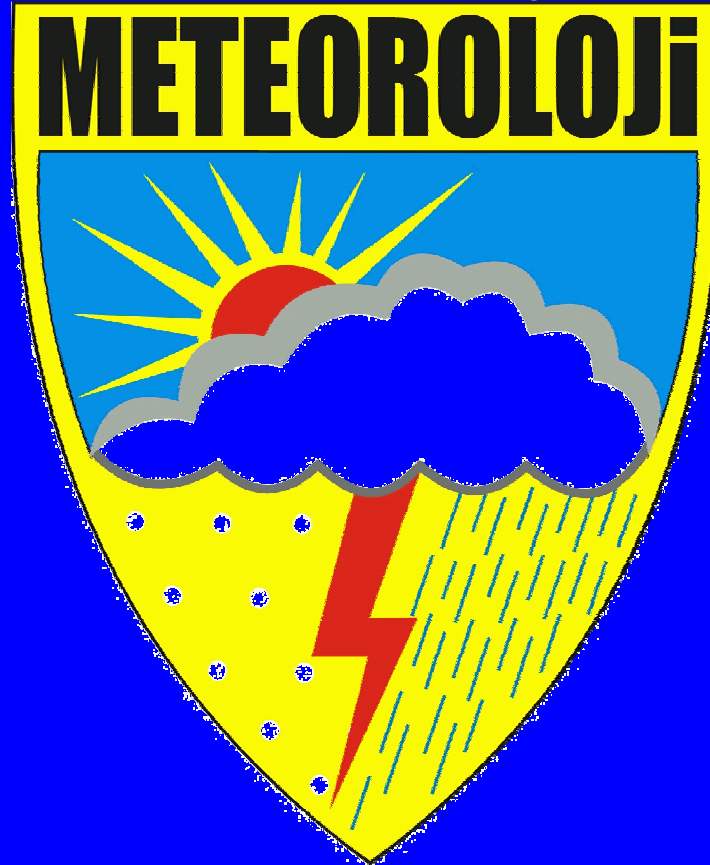
Scientific collaborations



Radio - Ozone sounding



**T.R.**  
**THE MINISTRY OF**  
**ENVIRONMENT AND FORESTRY**



**TURKISH STATE METEOROLOGICAL SERVICE**



# MODERNIZATION OF OBSERVATION NETWORK IN TURKEY

**Ercan B y kbaŐ**

**Manager**

**Electronic Observing Systems Division**



# **CONTENTS**

1. INTRODUCTION
2. OBSERVATION NETWORK
3. MODERNIZATION STUDIES
4. CONCLUSION



# 1. INTRODUCTION

In line with the increasing needs of the developing world, it has become a necessity to obtain more reliable and continuous meteorological data and transfer these data in due course to those who are concerned. Today many sectors such as aviation, transportation, agriculture, construction, tourism, health, justice, security, national defence, written and visual press, and sports are very much in need of meteorological data support.



Turkish State Meteorological Service (TSMS) started in 1997 the modernisation studies of meteorological systems, prepared investments projects of great importance and got down to execution of them at a very high speed with a view to rendering the best service to all users who demand meteorological support, and furnish the users with more reliable data continually and to put to the service of the domestic and international users the products and innovations developed by modern technology in the field of meteorology.



One of those modernisation studies is the renovation of the existing observation network and establishment of automated measuring and reporting systems, i.e. AWOS.

In general, two types of observation have been made in Turkey but this presentation covers the modernisation studies of the surface observation systems only.



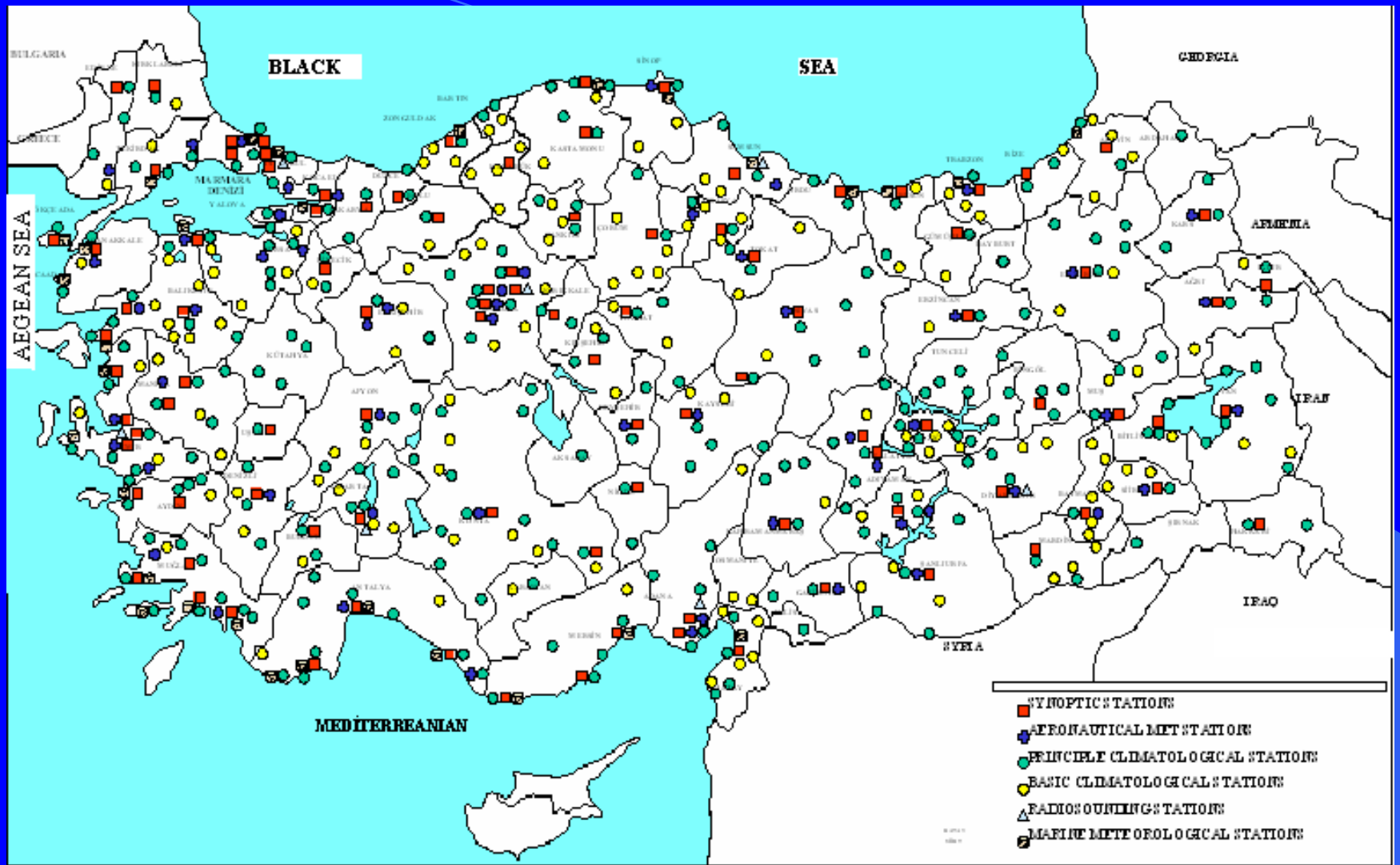
## 2. OBSERVATION NETWORK

TSMS has been operating a meteorological observation network spread all over the country consisting of:

- ★ climatologic stations – 339 (161 automated)
- ★ synoptic stations – 110 (45 automated)
- ★ airport stations – 65 ( 22 automated)
- ★ automated wind measuring and monitoring systems - 41
- ★ weather radars – 4
- ★ radiosonde stations – 7
- ★ satellite receiving system -1







The surface observation network before the implementation of modernization program;

- ❑ Mainly un-automated
- ❑ Conventional meteorological instruments
- ❑ A few automated observation instruments



### 3. MODERNIZATION STUDIES

After starting the modernization program in 1997, stations in the western part of Turkey have been equipped with automated weather observing systems, weather radars and satellite based communication system (VSAT). Those studies are still in progress and remain part of the network is planned to be equipped with automated systems by 2010.



Some of the proposed systems within the scope of modernization program have already been installed and put into the service. These are:

- C-Band Meteorological Doppler Radar (4)
- Automated Weather Observation Systems (228)
- Electronic Wind Measuring Systems (41)
- GPS based radiosonde stations (7)
- Satellite Based Communication System (VSAT-228)
- Meteorological Satellite Receiving System (1)
- Message Switching System (1)



# 3. 1. Automated Weather Observing Systems (AWOS)

Automated Weather Observation Station is a complete observing set consisting of:

- ◆ sensors and sensor interfaces
- ◆ data collection unit
- ◆ central control and processing unit
- ◆ display unit
- ◆ communication interfaces
- ◆ power supplies



## 3.2.Site selection

Determination of the correct locations to install AWOSs is the first and the most important step for overall success of the project. These locations have been determined by TSMS considering WMO recommendations. During that determination study following criteria were considered:

- types of meteorological parameters to be measured
- purpose of obtaining those parameters

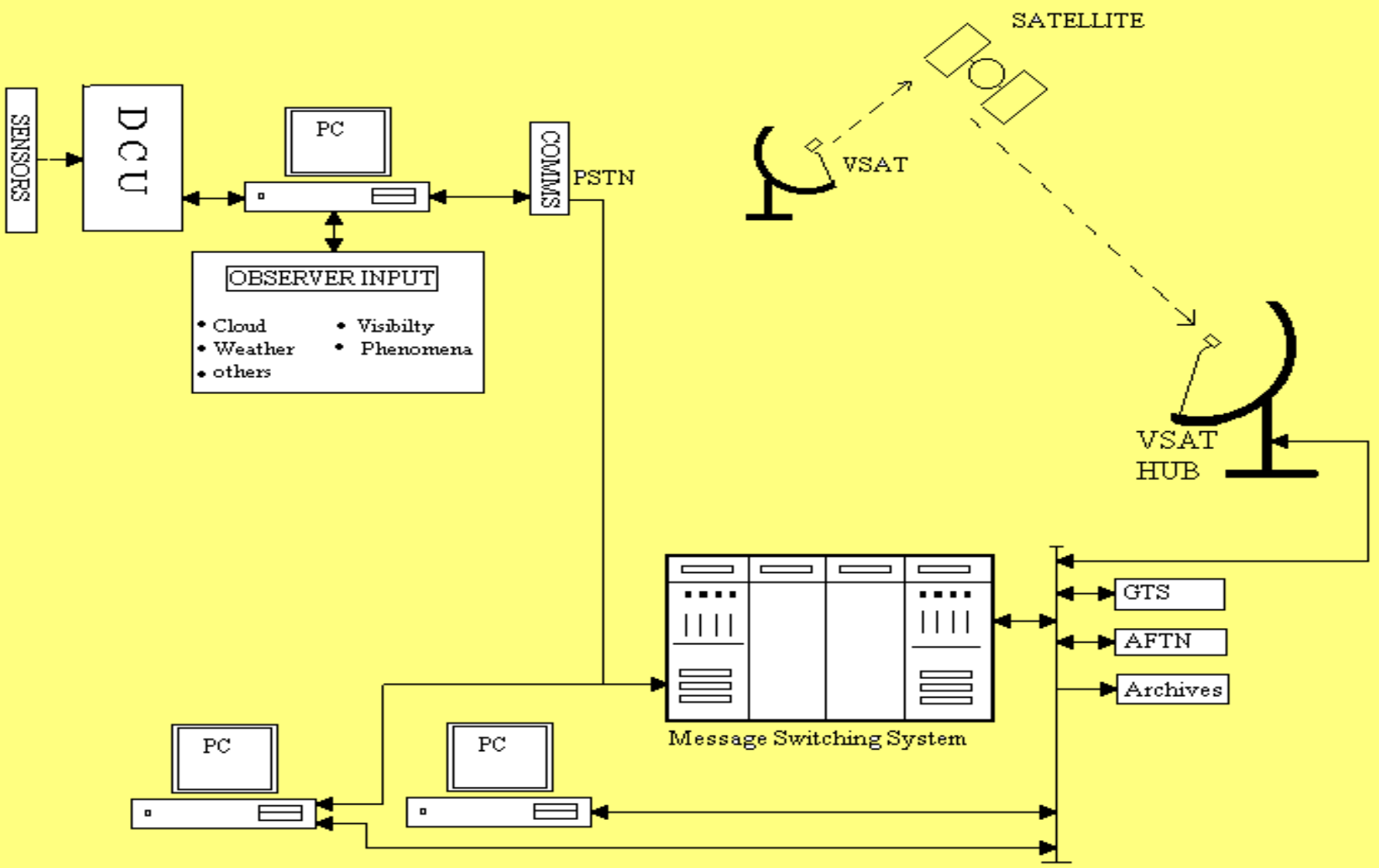


- variability of parameters according to the other places around the station
- the size of the area presented by the station
- suitability for meteorological observation
- infrastructure and communication facilities

## 3.3. General system architecture

- ◆ A general architecture and system components of AWOS network is shown below. This configuration uses the VSAT network as the primary communications medium. A secondary communication channel using PSTN is proposed for maintenance purposes as well as a backup line if the VSAT network becomes unserviceable.

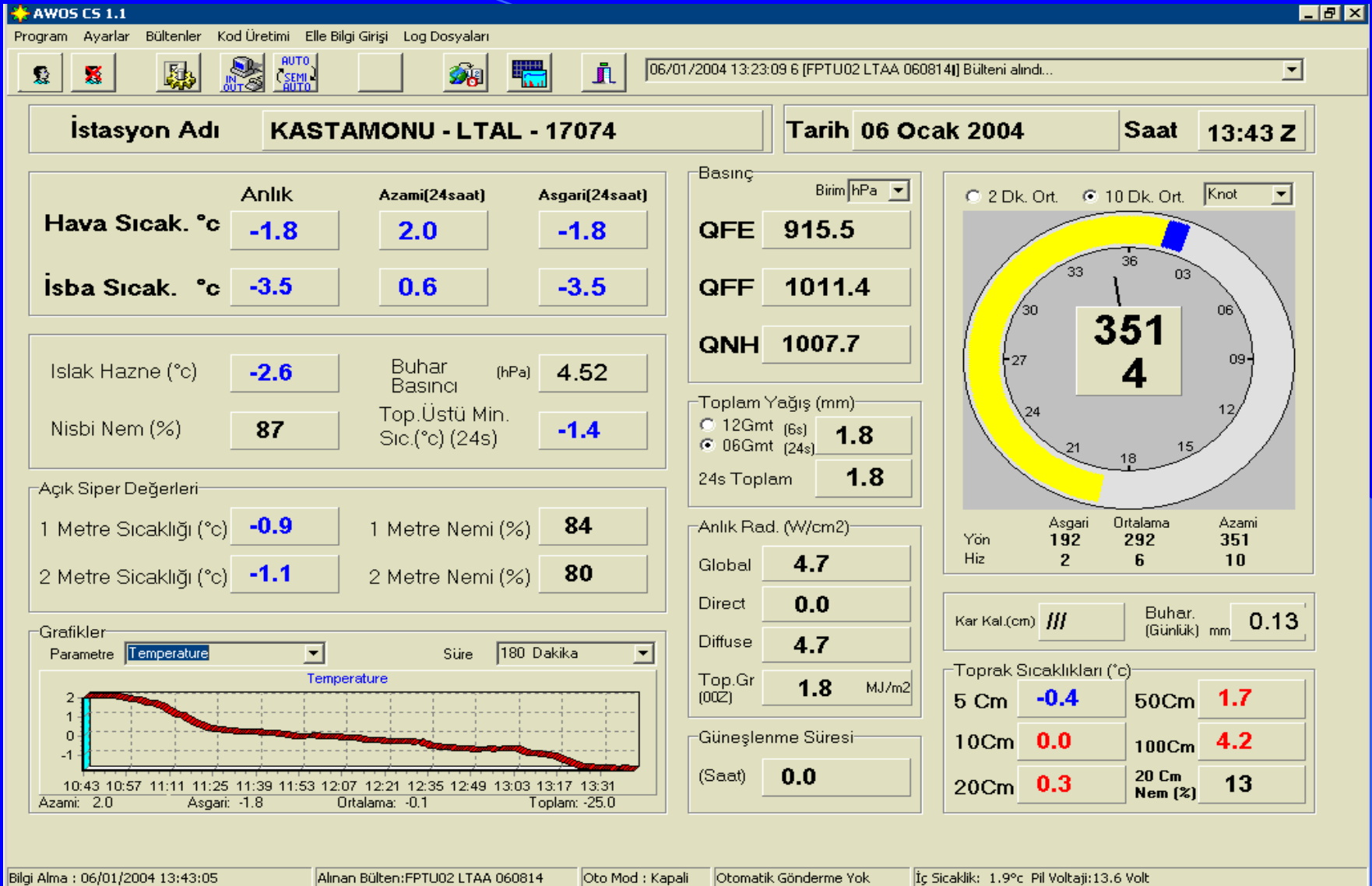




- ◆ The Observer console is a user friendly system that displays meteorological information coming from a Data Collection Unit (DCU) as well as allow an observer to manually supplement other meteorological variables such as cloud, visibility, weather, phenomena, etc. into the overall station observation process. The console automatically accepts data from a DCU and log this information in its local database.



# Observer Console Screen



- ◆ The Network Monitor Terminal is a centralised computer system used by operational staff in the forecasting centre to view and control automated surface observation network. That terminal allows the operators to interrogate a station and upload high-resolution (10 min., 1 min.) data that is logged within the Observer console or DCU in the remote station to support forecasting activities, scientific research and data management activities.



- ◆ The Network Maintenance Terminal is a centralised computer system used by the maintenance staff to assist in the maintenance of the automated surface observation network. By using this terminal, maintenance staff can analyse status and diagnostics information on the operational network. The system would also allow central connection to any observational site to perform remote first-in maintenance or further system diagnosis. The system is also used to remotely upgrade outstation software on both the Observer Console and the DCU equipment.





## 3.4. Parameters measured automatically

- Wind speed
- Wind direction
- Air temperature
- Dew point
- Relative humidity
- Precipitation
- Air pressure
- Solar radiation
- Height of Cloud base
- MOR and RVR
- Runway Surface Temperature











## 3.5. Advantages of automated weather observing systems

Advantages of automated systems can be summarised as follows:

- Standardisation of observations (both time and quality)
- Continuous measuring of parameters daytime and night-time
- More accurate
- More reliable



- Higher resolution
- Collection of data in a greater volume
- Adjustable sampling interval for different parameters
- Free from reading errors
- Free from subjectivity
- Automatic QC in both collection and reporting stages
- Automatic message generation and transmission



- Monitoring of meteorological data
- Access of archived data locally or remotely
- Data collection from harsh environments



## 3.6. Disadvantages of automated observations

Automated observations have also some disadvantages. Those systems require;

- ◆ Ongoing periodic maintenance
- ◆ Periodic test and calibration
- ◆ Well trained technicians and specialists
- ◆ Well trained operators
- ◆ High cost of instrumentation and operation

## 3.7. Features of AWOS Network

The AWOS network is capable of:

- ❖ Collecting, processing and displaying meteorological data
- ❖ Performing automated generation and transmission of meteorological reports such as SYNOP, METAR, SPECI, etc.
- ❖ Being configured to support a wide range of sensor configurations



- ❖ Supporting a vast range of data communication options
- ❖ Managing all communication protocols for the various sensors and other data communication equipment
- ❖ Storing all relevant data for subsequent retrieval as required
- ❖ Allowing for manual input of additional information unable to be automatically measured
- ❖ Providing Quality Control on both data measurements and message generation
- ❖ Allowing authorised users to access remotely for any tasks to be performed





## 3.8. Sensors in AWOS network

Following parameters are measured automatically by the sensors connected to DCU:

- ★ Wind speed
- ★ Wind direction
- ★ Air temperature
- ★ Relative humidity
- ★ Air pressure
- ★ Precipitation
- ★ Height of Cloud Base



- ★ Visibility
- ★ Soil Temperatures
- ★ Soil moisture
- ★ Global radiation
- ★ Direct radiation
- ★ Snow depth



In addition to measured parameters, some parameters are calculated by using measured data. These are:

- ◆ Wet bulb temperature
- ◆ Dew point
- ◆ Vapour pressure
- ◆ Evaporation
- ◆ Diffuse radiation
- ◆ Sunshine duration
- ◆ Runway Visual Range

## 3.9. Network Maintenance

In a very near future, TSMS will be operating a very large observation network consisting of 600 automated stations, 15 weather radars, communication equipment, etc.

The most important process after the installation of such systems is regular maintenance of the network and each sub component.



## Maintenance policy:

- -Protective maintenance
- -Corrective maintenance
- -Calibration



## 3.9.1. Protective maintenance

- Daily maintenance:
  - ◆ by local technicians and/or operators
  - ◆ general system control
  - ◆ checking data transmission, recorders, printers, etc.
  - ◆ cleaning of components
  - ◆ reporting to the centre

- Weekly-monthly maintenance:

- ◆ by local technicians

- ◆ general system control

- ◆ checking data transmission, recorders, printers, etc.

- ◆ cleaning of components

- ◆ Quality control of data

- ◆ reporting to the centre



- 6 month-and yearly maintenance:
  - ◆ By trained technicians from centre
  - ◆ general system control
  - ◆ System performance test
  - ◆ Field calibration
  - ◆ checking data transmission, recorders, printers,etc.
  - ◆ Correction of failures if any





## 3.9.2. Corrective maintenance

Any system failure can be repaired by two ways:

### ❁ Locally:

System failures in certain level shall be repaired by local technicians with remote support from maintenance centre.

## ❁ From centre:

- The failures which can not be repaired by local technicians shall be under the responsibility of system specialists and technicians in the centre.
- In case of such a failure, these specialists or technicians will reach the station as soon as possible and solve the problem.

### 3.9.3. Calibration

- ❖ It is necessary to calibrate the systems to maintain the quality of data.
- ❖ TSMS has planned to upgrade its instrument laboratory to support that network.
- ❖ This laboratory is proposed to be of sufficient standard and staffing to act as the country's national standard for meteorological observations and to possess linkages to the WMO Regional Instrument Centre , and other national laboratories.



## 4. CONCLUSION

- ✦ Using of modern observation systems seems to be a necessity to meet the requirements.
- ✦ It seems very difficult for the automated systems to replace of observers.
- ✦ While operating automated system we should also keep the manual systems in operation for a certain period as a back-up system as well for comparison.



- ✱ The observers should be trained for new systems.
- ✱ Technicians should have basic knowledge of meteorology with the knowledge of related science.
- ✱ Such systems require periodic maintenance and technical service to maintain the system in operation properly.
- ✱ Meteorological services should share their experiences.



# UNITED STATES SUPPORT FOR THE GLOBAL CLIMATE OBSERVING SYSTEM (GCOS) AND ASSOCIATED SUPPORT FOR INTERNATIONAL, REGIONAL, AND BI-LATERAL GCOS ACTIVITIES

Howard J. Diamond  
NOAA National Climatic Data Center  
1335 East-West Highway, Room 7214 Silver Spring, Maryland USA 20910  
Tel: +1-301-713-1283; Fax: +1-301-713-0819; e-mail: [howard.diamond@noaa.gov](mailto:howard.diamond@noaa.gov)

## ABSTRACT

This paper will update information on the support for GCOS provided by the U.S. Climate Change Research Initiative and how that fits in with a proactive process approach for GCOS implementation planning with the goal of obtaining a sustainable and robust GCOS observing network for international atmospheric, oceanographic, and terrestrial climate observing. The paper will describe the actions taken to date, and plans for the future regarding international, regional, bi-lateral, and U.S. national level GCOS activities. The paper will detail the continued support for GCOS that is managed by the U.S. GCOS Program Manager in NOAA. The paper will further update how that global effort for supporting GCOS in developing nations fits in with the progress that has been made in the Pacific Islands region. The progress in the Pacific has been accomplished through a solid planning process that has as its goal obtaining a sustainable and robust GCOS observing network for atmospheric, oceanographic, and terrestrial climate observing in the region. The paper will describe the actions completed to date, plans for the future, and how the establishment of a full-time Pacific GCOS Manager along with the efforts of the newly established Pacific Islands Regional GCOS Steering Committee, have combined with related efforts such as the establishment of a virtual Regional Climate Center, in order to benefit the region.

## 1. INTRODUCTION

The international Global Climate Observing System (GCOS) was established in 1992 to ensure that the observations and information needed to address climate-related issues are obtained and made available to all potential users. It is cosponsored by the World Meteorological Organization (WMO), the Intergovernmental Oceanographic Commission (IOC) of United Nations Educational Scientific and Cultural Organization (UNESCO), the U.N. Environment Program (UNEP) and the International Council of Scientific Unions (ICSU). GCOS is intended as a long-term, user-driven operational system capable of providing the comprehensive observations required for monitoring the climate system, for detecting and attributing climate change, for assessing the impacts of climate variability and change, and for supporting research toward improved understanding, modeling and prediction of the climate system. It addresses the total climate system, including physical, chemical and biological properties, and atmospheric, oceanic, hydrologic, cryospheric, and terrestrial processes. More information on the international program can be found at <http://www.wmo.ch/web/gcos/gcoshome.html>.

## 2. BACKGROUND

Meteorological surface-based networks, utilized for climate purposes, make observations of important climate factors, atmospheric profiles, and pollutant emissions, aerosols, and ozone. These surface-based networks are intended to provide the basic observational set needed to define the status and trends in climate of the world, and also to calibrate and validate satellite-based observations. Although hundreds of millions of dollars are spent each year on developing and operating space-based observation systems, surface-based meteorological networks are "under reporting" their observations in many parts of the developing world because of declining economies and the lack of understanding of how these observations contribute to the global effort to monitor climate. Consequently, these networks are operating substantially below their design standards and important observations are either not being made, or are not being communicated to users. Workshops are being conducted to define GCOS deficiencies and, during the next several years, more detailed activities to improve the networks will be identified. The implementation of a GCOS Cooperation Mechanism (GCM) was begun in 2004 as a way of identifying resources (both financial and in-kind) to aid in improving the operation of GCOS monitoring stations in developing nations.

As such, NOAA's U.S. GCOS Program Office, which represents the U.S. on the GCOS Cooperation Board, has committed to leading the way for facilitating improvements in the management and operation of GCOS and GCOS-related atmospheric networks. The U.S. GCOS Program Office has taken leadership, working with our partners at the WMO, in further GCOS improvements. This work began in Fiscal Year (FY) 2003 and plans are for continued efforts in this area for the foreseeable future. However, improvements in the various international GCOS networks cannot be done by NOAA alone, and are dependent on matching contributions from other developed nations via the GCM to aid in leveraging and implementing improvements to GCOS networks, and sustaining them. The program reflects a broad-based approach that looks at supporting observing and data management activities at the international, regional, and bi-lateral levels. In addition, support for Pacific Islands Ocean and Climate observing regional coordinators in Fiji and Samoa to aid in coordinating these observing activities among developing countries in the region has been a great boost towards capacity building in that critical region.

The support for developing nations has primarily been for retrofitting surface and upper air observing stations that have up-to-now been silent but yet are key to global climate monitoring activities. Countries that have received new equipment and expendables over the past two years include: Argentina, Armenia, Congo, Cook Islands, Costa Rica, Ecuador, Ivory Coast, Kenya, Maldives, Namibia, the Philippines, and Zimbabwe. In addition to equipment, in

cooperation with the U.S. State Department, a number of workshops for enhancing climate change monitoring in support of the Intergovernmental Panel on Climate Change (IPCC) have or are being staged in South Africa, southern South America, northern South America and Central America, Southwest Asia, and Southern Asia. These are all hands-on workshops involving seminars and hands-on work with data from the various countries in attendance. In addition, the State Department has been instrumental in aiding in the establishment of regional GCOS maintenance facilities which have been established in the Pacific and the Caribbean. Another one is being planned for Southern and Eastern Africa in order to further the sustainability of the GCOS network in the developing nations of that region.

### **3. BACKGROUND OF THE U.S. GCOS PROGRAM**

The U.S. has been involved with GCOS since its inception. Since 1992, a considerable amount of work has been done by various federal agencies. In particular, federal agencies have supported the international GCOS Steering Committee, and the work of the GCOS data, space, and science panels, as they have engaged in planning GCOS, defining its requirements, and contributing parts of the initial system. NOAA's National Climatic Data Center (NCDC) in Asheville, North Carolina, supports a number of GCOS data management activities and hosts the U.S. GCOS Program Office based in Silver Spring, Maryland.

The primary focus of this office is to coordinate the development of a national GCOS program that involves all U.S. federal agencies with a role in climate observing and monitoring. As part of this effort, the U.S. national program has taken a three-tiered approach to fostering the GCOS program. This approach involves providing support: (1) Internationally to improve and enhance monitoring stations in developing nations that require assistance as identified by the international GCOS Atmospheric Observations Panel for Climate; (2) regionally for workshops and projects such as those in the Pacific Ocean region for ensuring a robust and sustainable GCOS observing program; and (3) on a bi-lateral basis with nations that have entered into agreements with the U.S. on improving climate observing activities. The U.S. GCOS Program Office is currently involved in funding bi-lateral climate projects with Australia, China, New Zealand, and South Africa.

Like other developed nations, the U.S. was required to submit a report on the status of its systematic observations for climate. The full report is available at the U.S. National GCOS home page at [http://www.eis.noaa.gov/gcos/soc\\_long.pdf](http://www.eis.noaa.gov/gcos/soc_long.pdf).

### **4. SUPPORT ACTIVITIES FOR GCOS**

In addition to the requirements for national reports on systematic observations, the United Nations Framework Convention on Climate Change (UNFCCC) at its 1999 meeting invited the GCOS Secretariat to continue to assist with and facilitate the establishment of an appropriate intergovernmental process that would identify potential improvements in the global observing system for climate and set priorities for acting on those improvements. As such, the U.S. GCOS program has been one of the leaders in this effort.

The U.S. continues to be an active participant in and large support of the international GCOS program in a number of areas. These areas of support can be characterized in three categories: (1) Global; (2) regional; and (3) bi-lateral.

#### **4.1 Global Support**

The global support represents the overall U.S. Government's support of GCOS. In May 2002, the U.S. State Department contributed \$600K (US) in funding to the GCOS Secretariat in order to conduct the second adequacy study of GCOS on a global basis. This adequacy study was called for by the UNFCCC and is a joint GCOS/IPCC effort. This was intended to produce an adequacy report based on among other things the analysis of GCOS national reports in order to focus attention on critical gaps in the overall global climate observing in order for resources to be better directed. Published in April, 2003, *The Second Report on the Adequacy of GCOS* provides a detailed assessment on the gaps in GCOS that provides solid scientific requirements that can be used in resource mobilization towards current and future GCOS support and enhancements. It is planned to be reviewed and endorsed by Environmental and Foreign Affairs Ministers around the world, when presented to Conference of the Parties -9 (COP-9) in December 2003. A copy of *The Second Report on the Adequacy of GCOS* can be found on the GCOS home page at <http://www.wmo.ch/web/gcos/gcoshome.html>. As a follow-up to this report, the GCOS Secretariat in Geneva has developed an Implementation Plan for addressing the gaps identified and that plan is at the same address as the one noted for *The Second Report on the Adequacy of GCOS*.

As part of this global aspect of U.S. support for GCOS, and in response to a U.S. Presidential Climate Change Research Initiative (CCRI), the U.S. has formulated a Framework for International GCOS Support plan. This plan focuses on the status of GCOS, what is needed to bring GCOS to its operational-design level, and the support needed from the scientific, donor, and host communities to implement selected improvements to it.

Under the CCRI budget line for the support of atmospheric GCOS networks, NOAA has committed to selected improvements in the management and operation of GCOS and GCOS-related atmospheric networks beginning in 2003, and has taken leadership, working with the GCOS Secretariat at the WMO, in funding GCOS improvements. In line with that, the NOAA CCRI for the Global Climate Atmospheric Observing System budget for FY 2003 allocated a total of \$3.773M that begins to address the most critical needs and deficiencies of GCOS upper air observing sites in Chile, Congo, Cook Islands, Ecuador, Kenya, the Maldives, and Tanzania, as well as the establishment of new aerosol climate observing sites in the Maldives. In addition, this funding is used to: (1) Support the operations of the GCOS Secretariat; (2) stage GCOS regional workshops in developing countries; and (3) support critical GCOS data management activities

at the GCOS Lead Data Center at NCDC in Asheville, North Carolina. The FY 2004 budget of \$3.787M continued the work begun in 2003 and expanded support to observing sites in Argentina, Armenia, Congo, Cook Islands, Costa Rica, Ecuador, Ivory Coast, Kenya, the Maldives, Namibia, the Philippines, and Zimbabwe. Plans for FY 2005 are dependent on the enactment of an FY 2005 federal budget, but planning continues on working with our partners in the GCOS community to identify more sites that can be aided.

One issue that the U.S. GCOS program is addressing is the continued operation of the Global Observing System Information Center (GOSIC) located at <http://gosic.org>. The GOSIC has recently completed a second-phase 3-year development effort at the University of Delaware. The U.S. GCOS Office is one of the sponsors of GOSIC along with the NOAA Office of Global Programs. In 2004, a final 2-year transition grant to the GOSIC was awarded, and the intent at this point is for the GOSIC to transition its operation to a permanent operational status at NCDC. During this transition, NCDC will work with international organizations, particularly the IOC's Global Ocean Observing System and the Food and Agriculture Organization's Global Terrestrial Observing System in order to ensure that the data requirements for all three GCOS domains (atmospheric, oceanic, and terrestrial) are fully met during this transition and into the new operations in Asheville.

#### **4.2 Regional Support**

While the funding levels are not at the same levels as that of the U.S. global support for GCOS, it is far more focused on efforts dealing with regional workshops for developing nations, with a special emphasis on the South Pacific Island States' region.

The Regional Implementation Workshop, initiated by the GCOS in response to Decision 6/CP.5 of the UNFCCC and held in Apia, Samoa, in August 2000 with support and active participation by both Australian and U.S. experts, built on the South Pacific Regional Environment Program's (SPREP) needs analysis and has provided the basis for development of a Pacific Island-GCOS (PI-GCOS). The PI-GCOS Action Plan has identified the high priority actions, many of which can be implemented as stand alone modules that will assist in restoring and improving observing systems in the region to a level necessary to effectively monitor the climate of the region and systematically detect trends and changes in climate.

The U.S. GCOS Program Office in NOAA has been a supporter of the PI-GCOS effort since the Apia workshop and has contributed resources towards that effort. In FY 2000, the contribution to PI-GCOS was \$25K (U.S.) in support of the workshop; in FY 2001 and FY 2002 the combined contribution to PI-GCOS was an additional \$65K (U.S.) in support of the PI-GCOS Action Plan and Implementation Team meetings, and associated logistics. In FY 2003, support to SPREP amounted to \$105K; the additional funding included support for a data management workshop; as well as some support for related ocean observation work at the South Pacific Applied Geoscience Commission (SOPAC).

In FY 2004 the U.S. GCOS Program Office continued its support of the regional effort, and plans for FY 2005 are to continue this support at levels consistent with previous years. These funds continue to address the actions and proposals from the PI-GCOS Action and Implementation Plans developed over the past couple of years. The U.S. GCOS Program Office also plans to continue contributing in-kind support and facilitation of furthering the goals of PI-GCOS as it has undertaken the role as the Secretariat of the region's PI-GCOS Science and Technology (S&T) Panel. The S&T Panel is a subsidiary body established to provide advice and guidance to the PI-GCOS Steering Committee. In addition to supporting GCOS regional efforts in the Pacific, the U.S. GCOS Program Office has also provided resources to help stage other workshops, as well as in providing presenters on various topics.

In support of the PI-GCOS effort, the GOSIC has developed, in concert with the regional PI-GCOS Program Officer, a new Pacific Islands GCOS portal in order to facilitate the access to Pacific Islands GCOS datasets that may be held in a diverse group of data centers. This portal, located at <http://pi-gcos.org> has become a key tool to aid in the management of the Pacific Islands Regional GCOS Program, as well as providing an administrative tool for use by the regional program officer. That position is funded by the U.S. GCOS Program Office as part of the integrated Pacific Islands team effort of which the U.S. is an active participant along with Australia, New Zealand, and the member nations of SPREP.

#### **4.3 Bi-lateral Support**

In the past year the U.S. (via the State Department) has entered into a number of important bi-lateral climate agreements. Specifically, the U.S. GCOS Program Office is involved in funding projects with Australia, China, New Zealand, and South Africa. These bi-laterals cover a wide range of projects dealing with climate prediction, ocean observing, stratospheric detection, water vapor measurements, capacity building and training, and communication of information, and will focus the attention and resources of all these countries towards developing a more sustainable and robust GCOS program.

In conjunction with the National Institutes of Water and Atmosphere (NIWA) in New Zealand, there are now two new projects which have been implemented on a long-term basis. The first one involves the implementation of a global stratospheric water vapor measurement station in Lauder, New Zealand. Water vapor is a key climate forcing agent, and this new monitoring site will complement an existing site in Boulder, Colorado, which has been taking similar high-quality upper air water vapor measurements since 1980. A second significant project involves the implementation of a new ship track for trace gas measurements that has been implemented on a car carrier ship on a route between Nelson, New Zealand, and Nagoya, Japan. This is a brand new route and is unique in that it crosses both the Intertropical and South Pacific convergence zones; as such the principal investigators from NOAA and NIWA believe the sampling of trace gases on this route will hold great promise for new and useful data.



In conjunction with the South African Weather Service, the U.S. GCOS Program Office is also working to improve upper air observations in eastern and southern Africa via the establishment of an upper air maintenance and training facility. Joint work also continues on resurrecting the upper air station in Windhoek, Namibia, as well as in upgrading ozone measurements at the Cape Lookout Global Atmosphere Watch (GAW) station in South Africa. A similar ozone measurement enhancement project at the GAW site at Mt. Waliguan in China is also underway via the U.S./China climate bi-lateral agreement.

## 5. ENHANCED CLIMATE DATA MANAGEMENT IN THE PACIFIC

NOAA has recently taken a closer look at its data management activities in the Pacific Region. The International Pacific Research Center (IPRC) located at the University of Hawaii is a bi-lateral U.S./Japan activity that is funded by Japan, NOAA, and NASA. Specifically, NOAA funding is directed towards the operation of the IPRC's Asia Pacific Data Research Center (APDRC), and the U.S. GCOS Program Office also serves as the NOAA IPRC Program Manager. Links to the IPRC and APDRC can be found at <http://iprc.soest.hawaii.edu> and <http://apdrc.soest.hawaii.edu>

The vision of the APDRC is to link data management and preparation activities to research activities within a single center, and to provide one-stop shopping of climate data and products to local researchers and collaborators, the national climate research community, and the general public. The mission of the APDRC is to increase understanding of climate variability in the Asia-Pacific region: by developing the computational, data management, and networking infrastructure necessary to make data resources readily accessible and usable by researchers; and by undertaking data-intensive research activities that will both advance knowledge and lead to improvements in data preparation and data products. During the coming year in 2005, the APDRC will address the following activities: (1) Operate and continue the development of their Data Server System for serving data; (2) provide a global data archive and necessary data management for climate data and products; (3) conduct value-added activities that produce needed data products; (4) serve as a Global Ocean Data Assimilation Experiment (GODAE) Product Server for a broad range of research and application users with focus on satellite and model-derived products; (5) implement a high-resolution model for downscaling operational models in the Pacific Islands regions; and (6) assess and develop plans, in concert with the program manager at the Scripps Institution of Oceanography, for the data management needs of the Atmospheric Brown Cloud project (see <http://www-abc-asia.ucsd.edu>)

In September 2004 the U.S. GCOS Program Office staged a workshop in Honolulu to begin some planning for enhancing NOAA's data management efforts in the Pacific. Attendees included all NOAA line offices in the Pacific involved in environmental data management activities, the IPRC and APDRC, the East-West Center, and the U.S. Geological Survey.

The intent of the workshop was to look at how NOAA could begin to enhance its mission objectives to help meet critical regional needs for ocean, climate, and ecosystem information to protect lives and property, support economic development and enhance the resilience of Pacific Island communities in the face of changing environmental conditions by better integrating regional observations, research, assessment and services; strengthening the delivery of ocean, ocean-related, climate, ecosystem products and services to the diverse Pacific Island user community; and better supporting research and service programs in the Pacific.

This activity also fits in quite well with a Task Team which has been established by the WMO in order to provide guidance and assistance in the designation and implementation process for establishing a Regional Climate Center (RCC) within the region. Such an RCC would aid in supporting climate prediction in the region via a virtual connection of various centers across the region in order to deliver more integrated climate data products and services to users.

## 6. CONCLUSION

The U.S. has been very supportive of the overall international GCOS program effort and has provided considerable support on both a global, regional, as well as bi-lateral basis. It is believed that support for GCOS should be global in nature and the U.S. is working to be a leader in helping to make GCOS a sustainable and robust system both regionally and globally, and that can serve the needs of an improved global climate monitoring system that will be part of the Global Earth Observing System of Systems (GOESS) being planned internationally by more than 50 nations and 29 international organizations; see the following URL for more details: <http://earthobservations.org>

The progress that the U.S. GCOS Program has made over the past few years was recently recognized by the UNFCCC. In September 2004, the UNFCCC Secretariat published an In-depth Review (IDR) of the Third National communication from the U.S., entitled "U.S. Climate Action Report – 2002 (CAR3)". The IDR was performed by an independent review team on behalf of the UNFCCC and is now available on-line at <http://unfccc.int/resource/docs/idr/usa03.pdf>. The CAR3 itself can be found on-line at the following URL: <http://unfccc.int/resource/docs/natc/usnc3.pdf>. The IDR had a number of findings related to the overall CAR3; however the U.S. GCOS program was specifically identified in findings 130 and 131 on pages 28-29 of their report as follows:

*130. The United States has one of the most impressive national Global Climate Observing Systems (GCOS) for climate monitoring in five distinct yet integrated areas. The system acquires detailed local and large-scale national data, including observation of environmental variables, representing a major contribution to the Integrated Global Observing Strategy.*

131. *The review team was informed that NOAA has formulated a framework for international GCOS support. It focuses on needed improvements to meteorological surface-based networks and on the GCOS terrestrial and oceanic surface-based and satellite-based observation networks. NOAA has identified nine activities that it proposed to launch in 2003 in association with the GCOS secretariat, with a total spending of USD 4 million annually. Additional funding for rescue and digitization of long-period observational data in Africa and Asia is also provided. The provision of these datasets comprises a major contribution to the science of climate change, and is likely to enhance the Intergovernmental Panel for Climate Change (IPCC) process. The review team noted a NOAA initiative for the development of radio and Internet-based climate information dissemination tools for rural farmers in developing countries.*

In summary, the inception of the U.S. GCOS Program Office in 1999, coupled with the resources provided via the CCRI program has led to a robust and active U.S. GCOS program which has been working with a number of partners in order to provide support across a broad range of international, regional, and bi-lateral climate activities that are leading to progress for GCOS.

## Revitalization of the GCOS Surface and Upper Air Network Stations

Richard K. Thigpen  
GCOS Secretariat

7 bis, Avenue de la Paix  
PO Box 2300  
CH-1211 Geneva 2 Switzerland  
+41 (0) 22 730-8012  
[RThigpen@wmo.int](mailto:RThigpen@wmo.int)

15205 Baughman Drive  
Silver Spring, Maryland 20906  
USA  
+301-598-5683/+301-452-7669  
[thigpenr@erols.com](mailto:thigpenr@erols.com)

### Abstract

This paper presents an overview and status report of recent initiatives to revitalize the GCOS upper air and surface networks and to improve the overall performance of these important baseline networks. Almost 20 of the roughly 150 GCOS Upper Air network stations have received some benefit from these activities so far. The paper will also address the results of the first complete analysis of the GCOS surface network and describe the regional technical support projects that have been implemented to support the operation of GCOS stations.

---

### Introduction:

The GCOS Surface (GSN) and Upper air networks (GUAN) were defined in the late 1990's as baseline networks chosen from existing stations in the Global Observing System. They were selected based on a number of criteria which included good geographic location and a long history of good performance. Theoretically the Permanent Representative from the host Meteorological Service agreed that the stations would operate according to the identified criteria for climate observing stations. By 2002 almost 40% of the GSN was reported "silent" by the monitoring center at DWD and nearly the same number of GUAN stations were reported "silent" by the monitoring center in the UK Hadley Center.

The US announced its Climate Change Research Initiative and funds were made available through the US GCOS Program Office to begin actions to improve the performance of these networks. A project manager/network analyst, called the GCOS Implementation Manager/Officer was hired and the Atmospheric Observing Panel for Climate (AOPC), one of the GCOS scientific advisory panels, was asked to prioritize revitalization efforts. First priority was given to the GUAN and 5 existing stations were identified as highest priority and then 5 stations were identified as important "additional" stations.

The 5 high priority stations were:

- Nairobi, Kenya
- Lima, Peru
- Galapagos Island, Ecuador
- Easter Island, Chile
- Honiara, Solomon Islands

The 5 "additional" stations were:

- Gan, Maldives
- Kananga, Democratic Republic of Congo
- Christmas Island, Kiribati
- Pointe Noire, Congo
- Dar es Salaam, Tanzania

## **GUAN Revitalization Projects:**

The first step of course was to try to determine the reason the stations were not operating. Not surprisingly, a number of predictable reasons were encountered. Telecommunications including routing issue were found and corrected. Some stations were misidentified and this was corrected. Further the monitoring center at the Hadley Center bases its performance reports on the monthly summary report called CLIMAT TEMP and many GUAN stations operate regularly but do not prepare this format report. As a result of these first investigations, several stations were “restored” to operation and a wide variety of additional performance monitoring tools and reports were implemented. Just to illustrate, 4 of the 5 high priority stations were or are now operating to some degree without any remedial action at the site. Nairobi, Lima, and Galapagos were telecommunications problems while Chile simply did not realize that Easter Island was so important to GCOS. When contacted, they immediately began a 2- soundings- per- day operation. Honiara is indeed still silent as civil war there has prevented any remedial action.

A process was designed that took into account the technical expertise found in the WWW department, the technical and procurement expertise within the Technical Cooperation Department, the specific needs of the station, the priority of the donor as well as that of the AOPC, and whatever other cooperating WMO member countries we could enlist to assist. To illustrate, we engaged the UK Met Office to conduct the site survey for the possible activation of a new station at Gan, Maldives. The GCOS Implementation Manager conducted the site survey at Dar es Salaam, and the New Zealand Met Service was engaged to visit Honiara. Following the site surveys, detailed projects could be formulated. As a result, a WMO purchase order was issued to the UK Met Office for the implementation of the equipment at Gan. Competitive requests for tender were issued by the WMO for hydrogen generators and equipment for Dar es Salaam.

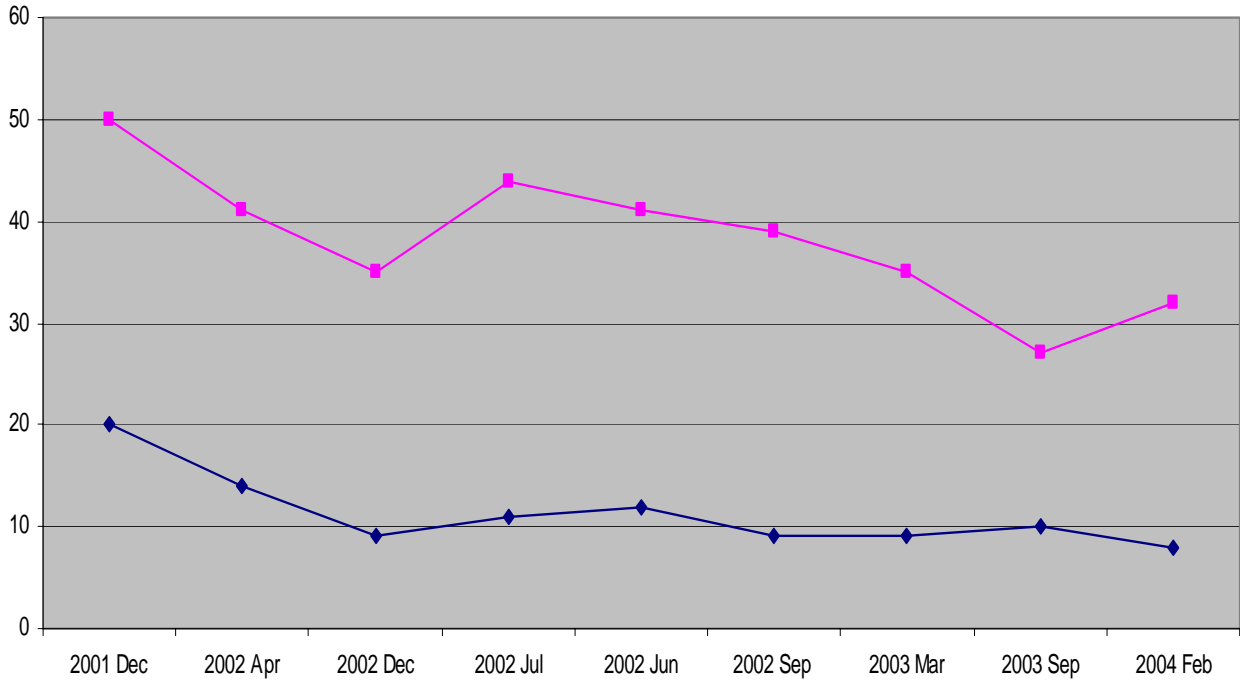
A major source of operational problems with GUAN stations is the high operating cost. Poorer countries simply cannot not afford expensive GPS radiosondes. We concluded that whenever possible we should implement radio direction finding (RDF) upper air systems. Further, as part of the initial remedial action projects, radiosondes were supplied to several stations. Several stations were found to be “silent” simply because they could not afford to purchase radiosondes. Our priorities were to get as many stations as possible up to minimum operational standards of one sounding per day. Five stations that needed nothing else were provided a year’s supply of radiosondes and balloons to restart their operation.

Another common problem was found to be the condition and age of the hydrogen generators. Many units are near the end of their useful life and are becoming difficult to maintain. Several stations were identified to receive new generators before their operation was effected.

In the first round of revitalizations, two new stations, Gan, Maldives and Dar es Salaam, Tanzania were activated and added to the GUAN. Five stations were restarted through the provision of radiosondes and balloons and two stations, Penrhyn Island and Galapagos Island received substantial equipment up-grades and renovations. Four other stations received replacement hydrogen generators. Through the analysis of station performance and direct interaction with operating staff, many other stations were returned to the “active” status.

In the second round, not yet completed, additional stations will receive generators and radiosondes while three stations, Windhoek, Namibia; Harare, Zimbabwe; and Yerevan, Armenia will receive major equipment replacements. Site surveys are also being done to prepare project plans for future years.

GUAN Poor and Silent  
 Silent=Blue  
 Poor=Red



As shown in the above chart the number of problem stations have been reduced. As this report is written, there were 7 truly silent stations at the end of 2004 and 21, including the 7 silent stations that were not meeting minimum performance specifications.

**GSN Revitalization Projects:**

Thus far the priority of funding has been directed towards the upper air network (GUAN) but substantial effort has been devoted to the analysis of the surface network (GSN). The GSN is much larger with approximately 1000 stations and the problems are much different. Whereas the operating cost is a major factor with the GUAN, the GSN performance suffers for different reasons. The monthly CLIMAT report from GSN stations is considered a mandatory requirement and over 20% of the stations currently do not prepare and send these reports. Also a substantial number, more than 50% of the stations, have not provided the historical data to the world archive center. Both of these problems must be resolved before station specific revitalization can begin.

### Performance of the GSN

	<b>Number Stations</b>	<b>Number of Silent Stations</b>	<b>Number of No CLIMAT</b>	<b>Poor</b>	<b>CLIMAT Only</b>
Reg 1	155	16	48	13	1
Reg 2	248	14	63	0	6
Reg 3	119	18	20	0	15
Reg 4	156	4	21	0	0
Reg 5	153	8	29	2	3
Reg 6	118	3	21	1	9
Reg 7	32	2	12	2	0
<b>Total</b>	<b>981</b>	65 (6.6%)	214 (21.8%)	18 (1.8%)	34 (3.5%)

As illustrated in the above chart most GSN stations are actually operating. For this analysis “poor” was defined as fewer than 30 synoptic reports per month.

To address the CLIMAT reports, the GCOS Secretariat has worked closely with the World Weather Watch and the World Climate Program of the WMO to develop a handbook on the preparation of CLIMAT and CLIMAT TEMP reports and then a computer program that may be used to automatically prepare these reports. A series of workshops teaching both the handbook and the use of the software has already started with the first held in Russia in late 2004. Also an informal training session has been conducted in Australia and the next in the workshop series is scheduled for Cairo in the first quarter of 2005.

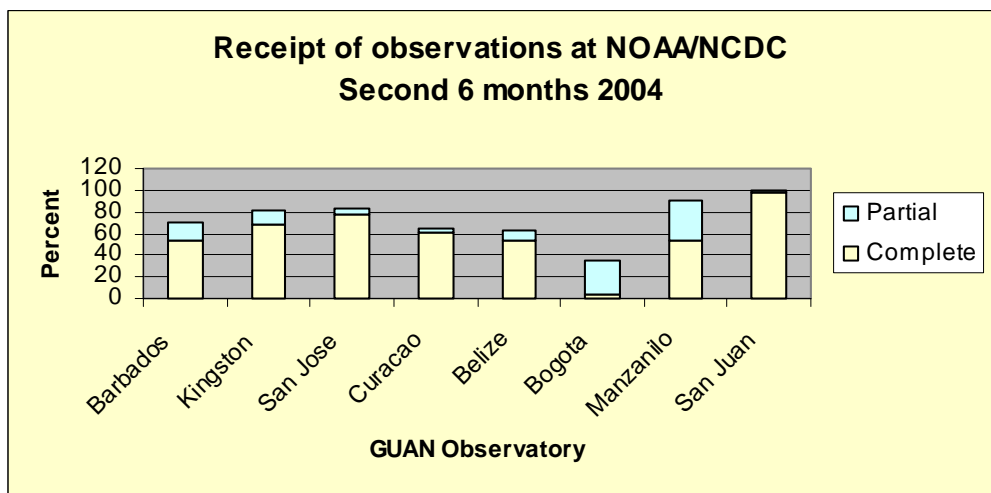
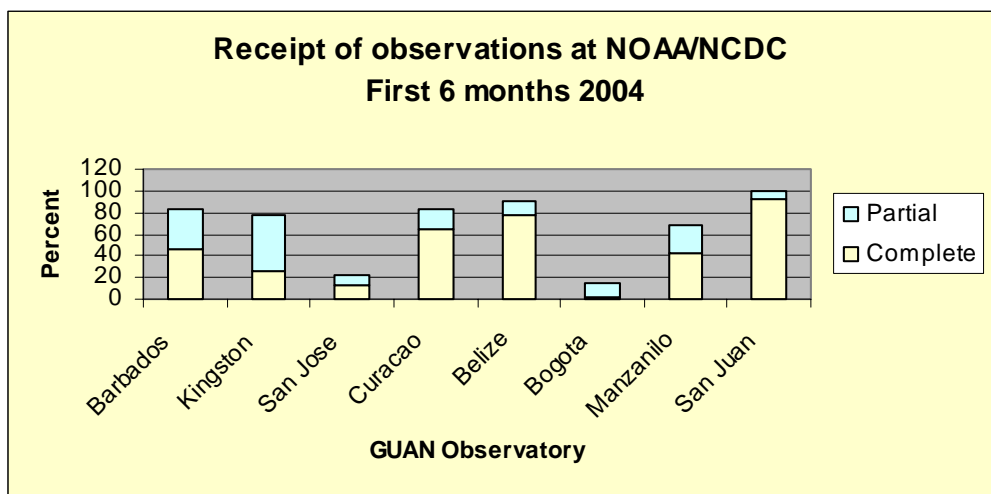
Despite being a criterion for inclusion into the GCOS baseline networks, many countries have not yet provided the historical data for inclusion into the world archive at National Climatic data Center (NCDC) in Asheville, USA. Historical data for less than half of the GSN is currently available. Substantial effort has been placed on direct contact with the member country by both the Archive center staff and the GCOS Implementation Manager. National GCOS focal points were requested by the Secretary-General of the WMO and almost all members have identified someone. These focal points provide at least a starting point for contacting someone in the country. Some progress has been made but it is not sufficient. In some cases the data must be rescued from its current state and in some cases the member country simply does not agree to share the data. It is likely that a greater emphasis through the WMO will be needed to resolve this dilemma.

#### **Regional Technical Support Projects (TSP):**

The GCOS Secretariat also received funding for the establishment of regional GCOS technical support projects in the Pacific, Caribbean, and in Africa. The support centers are to directly support the GUAN and GSN stations within their designated area. Site visits are required as is careful monitoring of the performance of stations. The site visits will include documentary photographs and station location information will be verified through the use of a GPS system. Countries within the region that need assistance will be addressed as a first priority.

The New Zealand Met Service was chosen to implement the project in the Pacific while a private company was selected for the Caribbean. The SADC part of Africa was identified as a reasonable sized area and a contract should be awarded soon. These initial projects are for one year’s duration

but certainly it is hoped that funding will be available to continue these and to add others. Initial results are an improvement in reporting frequency, an increase in the CLIMAT and CLIMAT TEMP reports, and a sharing of spare parts and technical expertise.



The above pair of charts shows the improvement in GUAN performance in the Caribbean during the first 6 months operation of the TSP there. Similar improvement is reported by the Pacific TSP. Note that San Juan is operated by the US and is not included in the scope of this TSP.

**GCOS Cooperation Mechanism:**

A GCOS Cooperation Mechanism (GCM) has been established to allow contributions from WMO members as well as any Non Government Organizations (NGO) to be applied to network revitalization. Initially several members, including the UK, Australia, US, China, and India attended the inaugural organization meeting and terms of reference have been drafted. A donor may contribute to a project of their choice or to a general fund which will be prioritized by the GCM. Donors may also contribute in non financial ways such as providing material or human resources. It is hoped that the GCM could provide the mechanism and means to address some of the more difficult data sparse areas of the globe where there is insufficient infrastructure at present to expect the host meteorological service to maintain operation.

END